

## **DISCLAIMER**

**This report was prepared as an account of work sponsored by an agency of the United States Government. Neither the United States Government nor any agency thereof, nor any of their employees, makes any warranty, express or implied, or assumes any legal liability or responsibility for the accuracy, completeness, or usefulness of any information, apparatus, product, or process disclosed, or represents that its use would not infringe privately owned rights. Reference herein to any specific commercial product, process, or service by trade name, trademark, manufacturer, or otherwise does not necessarily constitute or imply its endorsement, recommendation, or favoring by the United States Government or any agency thereof. The views and opinions of authors expressed herein do not necessarily state or reflect those of the United States Government or any agency thereof. Reference herein to any social initiative (including but not limited to Diversity, Equity, and Inclusion (DEI); Community Benefits Plans (CBP); Justice 40; etc.) is made by the Author independent of any current requirement by the United States Government and does not constitute or imply endorsement, recommendation, or support by the United States Government or any agency thereof.**

## **Verification of the REBUS Software**

---

**Nuclear Engineering Division**

### **About Argonne National Laboratory**

Argonne is a U.S. Department of Energy laboratory managed by UChicago Argonne, LLC under contract DE-AC02-06CH11357. The Laboratory's main facility is outside Chicago, at 9700 South Cass Avenue, Lemont, Illinois 60439. For information about Argonne and its pioneering science and technology programs, see [www.anl.gov](http://www.anl.gov)

### **DOCUMENT AVAILABILITY**

**Online Access:** U.S. Department of Energy (DOE) reports produced after 1991 and a growing number of pre-1991 documents are available free at OSTI.GOV (<http://www.osti.gov/>), a service of the US Dept. of Energy's Office of Scientific and Technical Information.

**Reports not in digital format may be purchased by the public from the National Technical Information Service (NTIS):**

U.S. Department of Commerce  
National Technical Information Service  
5301 Shawnee Rd  
Alexandria, VA 22312  
[www.ntis.gov](http://www.ntis.gov)  
Phone: (800) 553-NTIS (6847) or (703) 605-6000  
Fax: (703) 605-6900  
Email: [orders@ntis.gov](mailto:orders@ntis.gov)

**Reports not in digital format are available to DOE and DOE contractors from the Office of Scientific and Technical Information (OSTI):**

U.S. Department of Energy  
Office of Scientific and Technical Information  
P.O. Box 62  
Oak Ridge, TN 37831-0062  
[www.osti.gov](http://www.osti.gov)  
Phone: (865) 576-8401  
Fax: (865) 576-5728  
Email: [reports@osti.gov](mailto:reports@osti.gov)

### **Disclaimer**

This report was prepared as an account of work sponsored by an agency of the United States Government. Neither the United States Government nor any agency thereof, nor UChicago Argonne, LLC, nor any of their employees or officers, makes any warranty, express or implied, or assumes any legal liability or responsibility for the accuracy, completeness, or usefulness of any information, apparatus, product, or process disclosed, or represents that its use would not infringe privately owned rights. Reference herein to any specific commercial product, process, or service by trade name, trademark, manufacturer, or otherwise, does not necessarily constitute or imply its endorsement, recommendation, or favoring by the United States Government or any agency thereof. The views and opinions of document authors expressed herein do not necessarily state or reflect those of the United States Government or any agency thereof, Argonne National Laboratory, or UChicago Argonne, LLC.

## Verification of the REBUS Software

---

prepared by  
Micheal A. Smith  
Adam G. Nelson

Nuclear Engineering Division, Argonne National Laboratory

July 2025

(This page left intentionally blank)

## Abstract

Ongoing design activities at Argonne National Laboratory are requiring a thorough verification of the Argonne Reactor Computation codes be performed. REBUS is central to this system. The driver for this effort requires the Triangular-Z and hexagonal-Z core geometry options of REBUS to be verified.

Previous work identified the REBUS features required to be verified to support current design activities, features of which are generally applicable to hexagonal-Z fast reactor designs. The scope of this verification effort includes verifying REBUS's ability to correctly interpret the user input model, verifying that the features identified yield the intended results, and verifying the correctness of the REBUS output tables. The REBUS software verification relies heavily upon the accuracy of the embedded DIF3D software, the verification of which was completed and documented elsewhere. Given that DIF3D produces an accurate solution, the primary focus of the verification in the REBUS software is to ensure that it properly uses the DIF3D solution and that the depletion system (Bateman equations) are correctly implemented.

This manuscript reiterates the verification tasks and displays results with respect to the features needed for current design activities. Analytic solutions of the Batemen equations are displayed and the results calculated with REBUS are displayed demonstrating the accuracy. Since coupled Bateman and neutron diffusion/transport solutions are extremely difficult to obtain, much of the focus is placed on how REBUS uses a given DIF3D solution assuming the accuracy of the DIF3D solution.

The verification effort identified no issues that are debilitating or otherwise impactful to the design usage of REBUS, and thus REBUS version 11.0, release 3012 is considered verified. It is important to note that several outputs of REBUS are identified to be inaccurate, such as burnup in MWD/MT. Most of the relevant ones for VTR are generally accurate with 10-20% errors which is not impactful as all regular REBUS users are aware of this issue and know how to hand calculate the results. The REBUS manual further makes it clear that these values are consistent with the methodology being used by REBUS and thus the "errors" are more of an inconsistent definition with respect to what a user would expect given a definition in literature. Other issues that were identified included unclear documentation and software bugs all of which were inconsequential to the final results.

# Table of Contents

|  |          |
|--|----------|
| <b>Abstract .....</b>  | <b>i</b> |
| <b>1 Introduction.....</b>   | <b>1</b> |
| <b>2 VTR Specific REBUS Verification .....</b>   | <b>2</b> |
| <b>3 Verification Problems .....</b>   | <b>4</b> |
| 3.1 DIF3D Consistency Verification Test Problem .....                                    | 4        |
| 3.2 DIF3D Consistency Verification using a VTR Problem .....                             | 15       |
| 3.3 Control Rod Movement Verification.....   | 21       |
| 3.4 Depletion Chain Verification .....   | 23       |
| 3.4.1 Depletion Chain 1.....   | 25       |
| 3.4.2 Depletion Chain 2.....   | 28       |
| 3.4.3 Depletion Chain 3.....   | 30       |
| 3.4.4 Depletion Chain 4.....   | 33       |
| 3.4.5 Flux Impacted Depletion Verification.....  | 38       |
| 3.4.5.1 Flux Impacted Depletion Chain Test #1 .....                                      | 40       |
| 3.4.5.2 Flux Impacted Depletion Chain Test #2 .....                                      | 43       |
| 3.4.6 REBUS Depletion Chain Summary .....  | 49       |
| 3.5 REBUS Model Building Verification.....   | 50       |
| 3.5.1 Category 2 Input Verification.....   | 50       |
| 3.5.2 Category 3 Input Verification.....   | 58       |
| 3.5.2.1 Non-equilibrium Testing of Card Type 11.....                                     | 60       |
| 3.5.2.2 Non-equilibrium Testing of Card Type 35.....                                     | 68       |
| 3.5.2.3 Equilibrium Testing of Card Type 11 .....  | 72       |
| 3.5.2.3.1 Equilibrium Cycle Reproduction of Non-equilibrium Primary Zone Assignment..... | 72       |
| 3.5.2.3.2 Zero Power Test of the Multi-Stage Equilibrium Problem.....                    | 77       |
| 3.5.2.3.3 Full Power Test of the Multi-Stage Equilibrium Problem.....                    | 80       |
| 3.5.2.3.4 Region Assignments in Equilibrium Cycle .....                                  | 83       |
| 3.5.2.3.5 Fuel Management Group Assignments in Equilibrium Cycle.....                    | 86       |
| 3.5.2.3.6 Multi-Stage Equilibrium Cycle Fuel Shuffling Test.....                         | 88       |
| 3.5.2.4 Verification that Burnup Limits Are Applied Correctly .....                      | 92       |
| 3.5.2.5 Verification that an Equilibrium Problem is an Equilibrium State .....           | 101      |
| 3.6 Category 4 Verification .....  | 106      |
| 3.6.1.1 Verification of Fuel Fabrication .....   | 109      |
| 3.6.1.2 Detailed Verification of Card Type 12 and 13 Input.....                          | 118      |

|  |            |
|--|------------|
| 3.7 Category 5 Verification .....  | 120        |
| 3.7.1 Verification of the SFEDIT Data File.....                                  | 121        |
| 3.7.1.1 DIF3D-FD Procedure for Calculating the SFEDIT Sample Points .....        | 122        |
| 3.7.1.2 Special Nodal Procedure for Calculating the SFEDIT Sample Points .....   | 123        |
| 3.7.1.3 Simple Problem Used to Verify the SFEDIT Data .....                      | 125        |
| 3.7.1.4 Verification of the SFEDIT Data File for Triangular-Z Based DIF3D-FD ... | 126        |
| 3.7.1.5 Verification of the SFEDIT Data File for Hexagonal-Z Based DIF3D-VARIANT |            |
| 136  |            |
| 3.7.1.6 REBUS Equilibrium Problem Used to Verify the SFEDIT Data.....            | 152        |
| 3.7.1.7 REBUS Non-Equilibrium Problem Used to Verify the SFEDIT Data .....       | 157        |
| 3.7.1.8 Verification of the Mass and Power Edits.....                            | 163        |
| 3.8 SUMRY File Verification Work .....   | 167        |
| 3.8.1 SUMRY1 File Verification.....  | 167        |
| 3.8.2 SUMRY2 File Verification.....  | 169        |
| 3.8.3 SUMRY3 File Verification.....  | 170        |
| 3.8.4 SUMRY4 File Verification.....  | 171        |
| 3.8.5 SUMRY5 File Verification.....  | 172        |
| 3.8.6 SUMRY6 File Verification.....  | 172        |
| 3.8.7 SUMRY7 File Verification.....  | 173        |
| 3.8.8 SUMRY8 File Verification.....  | 174        |
| 3.8.9 SUMRY9 File Verification.....  | 175        |
| <b>4 Summary of the Preceding Verification Work.....</b>                         | <b>175</b> |
| <b>References .....</b>  | <b>177</b> |

## List of Figures

|   |    |
|---|----|
| Figure 1-1. The Argonne Reactor Code System Set of Connected Codes .....                      | 2  |
| Figure 3-1. The DIF3D Output for an Infinite Homogeneous Three Group Test Problem .....       | 5  |
| Figure 3-2. REBUS Output for Infinite Homogeneous Three Group Test Problem (Time 0.0) .....   | 6  |
| Figure 3-3. REBUS Output for Infinite Homogeneous Three Group Test Problem (Time 1.0) .....   | 7  |
| Figure 3-4. Cartesian and Hexagonal Three Group Test Problems .....                           | 7  |
| Figure 3-5. REBUS Output for the Cartesian Reactor Three Group Test Problem at 4.0 days.....  | 8  |
| Figure 3-6. DIF3D Output for the Cartesian Reactor Three Group Test Problem .....             | 9  |
| Figure 3-7. REBUS Output for the Hexagonal Reactor Three Group Test Problem at 4.0 days ..... | 11 |
| Figure 3-8. DIF3D Output for the Hexagonal Reactor Three Group Test Problem .....             | 12 |
| Figure 3-9. Binary Interface Files Created by REBUS for the Hexagonal Test Problem.....       | 13 |
| Figure 3-10. DIF3D Input when using the Binary Interface Files .....                          | 13 |
| Figure 3-11. REBUS Output for the Hexagonal Reactor Three Group Test Problem at 4 days .....  | 14 |
| Figure 3-12. DIF3D Output Using the REBUS Binaries at 4 days .....                            | 14 |
| Figure 3-13. REBUS VTR Problem BOC DIF3D Excerpt .....  | 16 |
| Figure 3-14. REBUS VTR Problem EOC DIF3D Excerpt .....  | 17 |
| Figure 3-15. REBUS VTR Problem Excerpt .....  | 18 |
| Figure 3-16. Binary Interface Files Created by REBUS for the VTR Test Problem.....            | 19 |
| Figure 3-17. DIF3D BOC Excerpt for the VTR Problem.....                                       | 19 |
| Figure 3-18. DIF3D EOC Excerpt for the VTR Problem .....                                      | 20 |
| Figure 3-19. Excerpt of the Reconstructed A.NIP3 BOC input for the VTR Problem .....          | 21 |
| Figure 3-20. DIF3D Output Excerpt for REBUS and Two Different DIF3D Approaches at 4 days..... | 23 |
| Figure 3-21. Atom Density Excerpt for REBUS for the First Test of Depletion Chain 1 .....     | 27 |
| Figure 3-22. Atom Density Excerpt for REBUS for the Second Test of Depletion Chain 1 .....    | 28 |
| Figure 3-23. Atom Density Excerpt for REBUS for the Second Test of Depletion Chain 2 .....    | 30 |
| Figure 3-24. Atom Density Excerpt for REBUS for the First Test of Depletion Chain 3 .....     | 31 |
| Figure 3-25. Atom Density Excerpt for REBUS for the First Test of Depletion Chain 3 .....     | 33 |
| Figure 3-26. Atom Density Excerpt for REBUS for the First Test of Depletion Chain 4 .....     | 36 |
| Figure 3-27. Atom Density Excerpt for REBUS for the Second Test of Depletion Chain 4 .....    | 38 |
| Figure 3-28. Atom Density Excerpt for REBUS for the Flux Impacted Depletion Chain #1 .....    | 42 |
| Figure 3-29. Atom Density Excerpt for REBUS for the Flux Impacted Depletion Chain #2 .....    | 48 |
| Figure 3-30. Depletion Chain #3 A.NIP3 and A.BURN Inputs .....                                | 51 |
| Figure 3-31. Depletion Excerpts from the Analytic Test Problems .....                         | 52 |
| Figure 3-32. Cross Section Data Input Excerpt for Depletion Chain 3 .....                     | 53 |

|  |    |
|--|----|
| Figure 3-33. Atom Density and Mass Output Excerpts for Test 2 of Depletion Chain 3 .....         | 54 |
| Figure 3-34. Select Atom Density and Mass Output Excerpts for Test 3 of Depletion Chain 3 .....  | 54 |
| Figure 3-35. Select Atom Density and Mass Output Excerpts for Test 3 of Depletion Chain 3 .....  | 55 |
| Figure 3-36. Input Excerpt of Modified Test 1 of Depletion Chain 3 .....                         | 56 |
| Figure 3-37. Base Output Excerpt for REBUS for the Modified Setup of Depletion Chain 3 .....     | 57 |
| Figure 3-38. Perturbed Output Excerpt for REBUS for the Modified Setup of Depletion Chain 3..... | 57 |
| Figure 3-39. Geometry Setup for Path Specification Verification .....                            | 59 |
| Figure 3-40. A.NIP3 Input Excerpt for Card Type 11 Testing .....                                 | 59 |
| Figure 3-41. A.BURN Input Excerpt for Card Type 11 Verification .....                            | 60 |
| Figure 3-42. REBUS Output Excerpt for the Primary Zone Assignment Option of Card Type 11 .....   | 62 |
| Figure 3-43. REBUS Output Excerpt for the Region Assignment Option of Card Type 11 .....         | 63 |
| Figure 3-44. REBUS Output Excerpt for the Fuel Management Group Option of Card Type 11 .....     | 64 |
| Figure 3-45. DIF3D Power Detail for the Region Assignment Option of Card Type 11 .....           | 67 |
| Figure 3-46. A.BURN Input Excerpt for Card Type 35 Verification .....                            | 68 |
| Figure 3-47. Modified Input Excerpt for Testing the External Storage with Card Type 35 .....     | 69 |
| Figure 3-48. Atom Output Excerpt for the External Storage Test of Card Type 35.....              | 70 |
| Figure 3-49. REBUS Input Excerpt for the First Equilibrium Test of Card Type 11 .....            | 73 |
| Figure 3-50. Atom Density Output Excerpt for the First Equilibrium Test of Card Type 11.....     | 75 |
| Figure 3-51. REBUS Region Power Differences for the First Equilibrium Test of Card Type 11.....  | 76 |
| Figure 3-52. REBUS Output Excerpt for the First Equilibrium Test of Card Type 11 .....           | 77 |
| Figure 3-53. REBUS Input Excerpt for the Zero Power Multi-stage Equilibrium Test .....           | 78 |
| Figure 3-54. Atom Density Excerpt for the Zero Power Multi-stage Equilibrium Test .....          | 79 |
| Figure 3-55. Stage Density Output Excerpt for the Multi-stage Equilibrium Test .....             | 81 |
| Figure 3-56. Region Atom Density Output Excerpt for the Multi-stage Equilibrium Test .....       | 82 |
| Figure 3-57. Region Power Output Excerpt for the Multi-stage Equilibrium Test.....               | 83 |
| Figure 3-58. REBUS Input Excerpt for the Equilibrium Fuel Shuffling Test .....                   | 83 |
| Figure 3-59. Stage Density Output Excerpt for the Equilibrium Fuel Shuffling Test .....          | 84 |
| Figure 3-60. Atom Density Output Excerpt for the Equilibrium Fuel Shuffling Test .....           | 85 |
| Figure 3-61. Total Reactor Loading Output Excerpt for the Equilibrium Fuel Shuffling Test .....  | 85 |
| Figure 3-62. REBUS Input Excerpt for the FMG Equilibrium Test.....                               | 87 |
| Figure 3-63. First Stage Density Output Excerpt for the FMG Equilibrium Test .....               | 87 |
| Figure 3-64. Total Reactor Loading Output Excerpt for the FMG Equilibrium Test .....             | 88 |
| Figure 3-65. REBUS Input Excerpt for the Three Region Equilibrium Shuffling Test.....            | 89 |
| Figure 3-66. Stage Density Excerpt for the Three Region Equilibrium Shuffling Test .....         | 90 |
| Figure 3-67. Atom Density Excerpt for the Three Region Equilibrium Shuffling Test .....          | 91 |

|   |     |
|---|-----|
| Figure 3-68. REBUS Output Excerpt for Burnup in Equilibrium Problems .....                      | 95  |
| Figure 3-69. REBUS Inputs for Applying Burnup Limits to the Equilibrium Problems.....           | 95  |
| Figure 3-70. REBUS Output Excerpt for PATH2 Burnup Limited Equilibrium Problem .....            | 96  |
| Figure 3-71. REBUS Output Excerpt for Adjusted 3.3837 Day Cycle Length Problem.....             | 96  |
| Figure 3-72. REBUS Output Excerpt for Multiple Limit Burnup Equilibrium Problem.....            | 96  |
| Figure 3-73. REBUS Output Excerpt for Single Limit Burnup Equilibrium Problem.....              | 97  |
| Figure 3-74. Geometry for Multi-stage Burnup Limited Equilibrium Problem .....                  | 98  |
| Figure 3-75. REBUS Input for the Multi-Stage Burnup Limited Equilibrium Problem .....           | 98  |
| Figure 3-76. REBUS Stage Density Output Excerpt for Multi-Stage Burnup Limited Problem.....     | 99  |
| Figure 3-77. REBUS Burnup Output Excerpt for Multi-Stage Burnup Limited Problem.....            | 100 |
| Figure 3-78. REBUS Total Loading Output Excerpt for Multi-Stage Burnup Limited Problem .....    | 101 |
| Figure 3-79. REBUS Geometry and Shuffling Setup for Equilibrium State Verification .....        | 102 |
| Figure 3-80. REBUS 6 Cycle Shuffling Input Excerpt for the Equilibrium State Verification ..... | 103 |
| Figure 3-81. Non-equilibrium $k_{eff}$ Curve for the Equilibrium State Verification.....        | 104 |
| Figure 3-82. REBUS Primary Zone Input Excerpts for the Equilibrium State Verification.....      | 104 |
| Figure 3-83. REBUS Shuffling Input Excerpt for the Equilibrium State Verification .....         | 105 |
| Figure 3-84. REBUS Input Excerpt for the Fixed Enrichment Test Case .....                       | 110 |
| Figure 3-85. REBUS Fabricated Atom Density Excerpt for the Fixed Enrichment Test .....          | 111 |
| Figure 3-86. Reprocessing Plant and External Feed Output for the Fixed Enrichment Test .....    | 115 |
| Figure 3-87. External Cycle Excerpt for the Fixed Enrichment Test.....                          | 115 |
| Figure 3-88. REBUS Input Modifications for the Search Cases .....                               | 116 |
| Figure 3-89. $k_{eff}$ Convergence Behavior for the Search Cases.....                           | 117 |
| Figure 3-90. REBUS Output Excerpt for all Three Enrichment Search Cases .....                   | 117 |
| Figure 3-91. REBUS Input Excerpt for the Multiple Fabrication Density Test Case .....           | 118 |
| Figure 3-92. REBUS Output Excerpt for the Multiple Fabrication Density Test Case .....          | 119 |
| Figure 3-93. Surface Numbering in the SFEDIT .....  | 121 |
| Figure 3-94. Test Problem Geometry Used for SFEDIT Verification.....                            | 125 |
| Figure 3-95. Power Density and Fast Flux Profiles for the SFEDIT Verification.....              | 126 |
| Figure 3-96. Output Excerpts from DIF3D-FD, the GEODST, PWDINT, and RTFLUX Binary Files .....   | 127 |
| Figure 3-97. DIF3D-FD RTFLUX and PWDINT Excerpt for COREA Surface Calculation.....              | 128 |
| Figure 3-98. SFEDIT Mesh-wise Power Output Excerpt for COREA Verification in DIF3D-FD .....     | 130 |
| Figure 3-99. SFEDIT Region-wise Power Output Excerpt for COREA Verification in DIF3D-FD .....   | 130 |
| Figure 3-100. SFEDIT Fast Flux Output Excerpt for COREA Verification in DIF3D-FD .....          | 131 |
| Figure 3-101. PWDINT Output Excerpt for COREB Verification in DIF3D-FD .....                    | 132 |
| Figure 3-102. SFEDIT Output Excerpt for COREB Verification in DIF3D-FD .....                    | 133 |

|   |     |
|---|-----|
| Figure 3-103. SFEDIT Output Excerpt for COREC Verification in DIF3D-FD.....                   | 134 |
| Figure 3-104. PWDINT and RTFLUX Output Excerpt for REFL Verification in DIF3D-FD.....         | 135 |
| Figure 3-105. SFEDIT Output Excerpt for REFL Verification in DIF3D-FD .....                   | 136 |
| Figure 3-106. NHFLUX Output Example for DIF3D-VARIANT .....                                   | 138 |
| Figure 3-107. PWDINT Output Excerpt for DIF3D-VARIANT .....                                   | 139 |
| Figure 3-108. NHFLUX Output Excerpt for COREA SFEDIT Verification with DIF3D-VARIANT .....    | 139 |
| Figure 3-109. SFEDIT Power Output Excerpt for COREA Verification in DIF3D-VARIANT .....       | 143 |
| Figure 3-110. SFEDIT Fast Flux Output Excerpt for COREA Verification in DIF3D-VARIANT .....   | 143 |
| Figure 3-111. SFEDIT Output Excerpt for COREB Verification in DIF3D-VARIANT .....             | 145 |
| Figure 3-112. SFEDIT Output Excerpt for COREC Verification in DIF3D-VARIANT .....             | 147 |
| Figure 3-113. SFEDIT Output Excerpt for REFL Verification in DIF3D-VARIANT .....              | 149 |
| Figure 3-114. DIF3D Output Excerpt for SFEDIT Verification in DIF3D-VARIANT .....             | 150 |
| Figure 3-115. EvaluateFlux.x X-Y Sample Points in Each Hexagon for DIF3D-VARIANT .....        | 150 |
| Figure 3-116. EvaluateFlux.x Versus SFEDIT Methodology for COREA DIF3D-VARIANT .....          | 151 |
| Figure 3-117. EvaluateFlux.x Versus SFEDIT Methodology for COREC DIF3D-VARIANT .....          | 152 |
| Figure 3-118. REBUS Output Excerpt of DIF3D for the Equilibrium Problem .....                 | 153 |
| Figure 3-119. BOEC DIF3D Output Excerpt for the Equilibrium Problem .....                     | 154 |
| Figure 3-120. EOEC DIF3D Output Excerpt for the Equilibrium Problem .....                     | 154 |
| Figure 3-121. DIF3D SFEDIT Output Excerpts for the Equilibrium Problem .....                  | 155 |
| Figure 3-122. REBUS Peak Burnup and Fluence Output Excerpts for the Equilibrium Problem ..... | 155 |
| Figure 3-123. REBUS Peak Burnup and Fluence Excerpts for the Non-Equilibrium Problem .....    | 158 |
| Figure 3-124. Card Type 29 and 30 Modifications to the Equilibrium Problem .....              | 163 |
| Figure 3-125. Mass Balance Output for the Equilibrium Problem .....                           | 164 |
| Figure 3-126. Instant Power Output Excerpt for the Equilibrium Problem .....                  | 165 |
| Figure 3-127. SUMRY1 Output Excerpt .....   | 168 |
| Figure 3-128. REBUS Output Excerpt to Verify SUMRY1.....                                      | 168 |
| Figure 3-129. SUMRY2 Output Excerpt .....   | 169 |
| Figure 3-130. REBUS Output Excerpt to Verify SUMRY2.....                                      | 169 |
| Figure 3-131. SUMRY3 Output Excerpt .....   | 170 |
| Figure 3-132. REBUS Output Excerpt to Verify SUMRY3.....                                      | 170 |
| Figure 3-133. SUMRY4 Output Excerpt .....   | 171 |
| Figure 3-134. REBUS Output Excerpt to Verify SUMRY4.....                                      | 171 |
| Figure 3-135. SUMRY5 Output Excerpt .....   | 172 |
| Figure 3-136. REBUS Output Excerpt to Verify SUMRY5.....                                      | 172 |
| Figure 3-137. SUMRY6 Output Excerpt .....   | 173 |

|  |     |
|--|-----|
| Figure 3-138. REBUS Output Excerpt to Verify SUMRY6..... | 173 |
| Figure 3-139. SUMRY7 Output Excerpt .....                | 174 |
| Figure 3-140. SUMRY8 Output Excerpt .....                | 174 |
| Figure 3-141. SUMRY9 Output Excerpt .....                | 175 |

## List of Tables

|   |    |
|---|----|
| Table 2-1. REBUS Identified Verification Tasks .....  | 3  |
| Table 3-1. Three Group Infinite Homogeneous Macroscopic Cross Sections.....                       | 4  |
| Table 3-2. Reproduced Table 5 from ECAR 4647.....   | 15 |
| Table 3-3. Axial Rod Positioning at Each Time Point in the Control Rod Test Problem.....          | 22 |
| Table 3-4. Control Rod $k_{eff}$ at Each Time Point in the Control Rod Test Problem.....          | 22 |
| Table 3-5. Depletion Chain Reactions Allowed in REBUS.....  | 24 |
| Table 3-6. Depletion Chains Used to Test the REBUS.....   | 25 |
| Table 3-7. MAGIC Cross Section Data. ....   | 25 |
| Table 3-8. Depletion Chain 1 Macroscopic Cross Sections and Flux Solution.....                    | 26 |
| Table 3-9. Analytical Solution to the First Test of Depletion Chain 1.....                        | 26 |
| Table 3-10. Analytical Results for the Second Test of Depletion Chain 1.....                      | 28 |
| Table 3-11. Results for the First Test of Depletion Chain 2. ....                                 | 29 |
| Table 3-12. Analytical Results for the Second Test of Depletion Chain 2.....                      | 29 |
| Table 3-13. Depletion Chain 3 Isotopic Products for the MAGIC isotope. ....                       | 31 |
| Table 3-14. Analytical Results for the First Test of Depletion Chain 3.....                       | 31 |
| Table 3-15. Analytical Results for the Second Test of Depletion Chain 3.....                      | 32 |
| Table 3-16. Test #1 of Depletion Chain 4.....   | 33 |
| Table 3-17. Analytical Results for the First Test of Depletion Chain 4.....                       | 35 |
| Table 3-18. Test #2 of Depletion Chain 4.....   | 36 |
| Table 3-19. Analytical Results for the Second Test of Depletion Chain 4.....                      | 38 |
| Table 3-20. Microscopic cross sections for the Flux Impacted Depletion Test.....                  | 40 |
| Table 3-21. Flux Impacted Depletion Chain Test #1. ....   | 40 |
| Table 3-22. Chain #1 $k_{eff}$ and Atom Density Results From the Analytic Solution.....           | 43 |
| Table 3-23. Flux Impacted Depletion Chain Test #1. ....   | 43 |
| Table 3-24. Chain #2 $k_{eff}$ and Atom Density Results From the Analytic Solution.....           | 48 |
| Table 3-25. REBUS Identified Verification Tasks for Category 3 .....                              | 58 |
| Table 3-26. REBUS A.BURN Card Type 11 and 35 Descriptions.....                                    | 58 |
| Table 3-27. $k_{eff}$ Results for the Three Non-Equilibrium Test Problems of Card Type 11 .....   | 61 |
| Table 3-28. Region Power Comparison for the Region Assignment Option of Card Type 11.....         | 67 |
| Table 3-29. Zone to Region Assignment for Testing the External Storage with Card Type 35 .....    | 69 |
| Table 3-30. Eigenvalue and Power Results for Testing the External Storage with Card Type 35 ..... | 70 |
| Table 3-31. U-235 Mass Loading in the External Storage Test of Card Type 35 .....                 | 71 |
| Table 3-32. Power Calculation Comparison for the External Storage Test of Card Type 35.....       | 71 |

|  |     |
|--|-----|
| Table 3-33. Key Input Setup Data For Fuel Fabrication For the First Equilibrium Test .....     | 73  |
| Table 3-34. $k_{eff}$ Results for the First Equilibrium Test of Card Type 11 .....             | 76  |
| Table 3-35. TRACE Isotope Results for the First Equilibrium Test of Card Type 11 .....         | 80  |
| Table 3-36. Regional Power for Multi-stage Equilibrium Test .....                              | 82  |
| Table 3-37. Criticality Results for the Equilibrium Fuel Shuffling Test .....                  | 86  |
| Table 3-38. TRACE Atom Density Results for the Equilibrium Fuel Shuffling Test .....           | 91  |
| Table 3-39. REBUS Burnup Output Comparisons Against Simple Formula .....                       | 93  |
| Table 3-40. Atom % Burnup Output Verification of Default Setup in Equilibrium Problems .....   | 95  |
| Table 3-41. Atom % Burnup Verification of Multi-Stage Burnup Limited Equilibrium Problem ..... | 100 |
| Table 3-42. TRACE Isotope Verification in Multi-Stage Burnup Limited Equilibrium Problem.....  | 101 |
| Table 3-43. REBUS $k_{eff}$ Results for the Equilibrium State Verification .....               | 105 |
| Table 3-44. REBUS Total Reactor Loading Results for the Equilibrium State Verification .....   | 106 |
| Table 3-45. REBUS Identified Verification Tasks for Category 4 .....                           | 106 |
| Table 3-46. REBUS External Feeds for Category 4 Verification Work .....                        | 107 |
| Table 3-47. REBUS External Feed Usage for Category 4 Verification Work.....                    | 107 |
| Table 3-48. REBUS Fuel Fabrication Example Calculation .....                                   | 108 |
| Table 3-49. Fabricated Atom Densities Produced by REBUS for the Fixed Enrichment Test.....     | 111 |
| Table 3-50. Fabrication Atom Densities for Each Feed .....                                     | 112 |
| Table 3-51. Mass (kg) Used in the Class 1 Feed.....  | 116 |
| Table 3-52. Mass (kg) Used in the Class 2 Feed.....  | 116 |
| Table 3-53. Fabrication Details of the Multiple Fabrication Density Test Case.....             | 119 |
| Table 3-54. Hand Calculation of the Multiple Fabrication Density Test Case .....               | 120 |
| Table 3-55. TRACE Isotope Density in the Multiple Fabrication Density Test Case .....          | 120 |
| Table 3-56. REBUS Identified Verification Tasks for Category 5 .....                           | 121 |
| Table 3-57. COMPXS Cross Section Data of Importance .....                                      | 126 |
| Table 3-58. COREA Peak Surface Power Density and Fast Flux Calculation.....                    | 129 |
| Table 3-59. COREB Peak Surface Power Density and Fast Flux Calculation.....                    | 132 |
| Table 3-60. COREC Peak Surface Power Density and Fast Flux Calculation .....                   | 133 |
| Table 3-61. REFL Peak Surface Power Density Calculation.....                                   | 135 |
| Table 3-62. REFL Peak Surface Fast Flux Calculation .....                                      | 136 |
| Table 3-63. COREA Node Volume and Surface Flux Moments.....                                    | 140 |
| Table 3-64. COREA Hand Calculation of the Axial Fitting Function and its Evaluation .....      | 140 |
| Table 3-65. COREA Power Evaluation at the Axial Sample Points .....                            | 141 |
| Table 3-66. COREA Fast Flux Evaluation at the Axial Sample Points .....                        | 142 |
| Table 3-67. COREB Node Volume and Surface Flux Moments.....                                    | 144 |

|   |     |
|---|-----|
| Table 3-68. COREB Power Evaluation at the Axial Sample Points .....                       | 144 |
| Table 3-69. COREB Fast Flux Evaluation at the Axial Sample Points.....                    | 145 |
| Table 3-70. COREC Node Volume and Surface Flux Moments.....                               | 146 |
| Table 3-71. COREC Power Evaluation at the Axial Sample Points .....                       | 146 |
| Table 3-72. COREC Fast Flux Evaluation at the Axial Sample Points .....                   | 147 |
| Table 3-73. REFL Node Volume and Surface Flux Moments .....                               | 148 |
| Table 3-74. REFL Power Evaluation at the Axial Sample Points .....                        | 148 |
| Table 3-75. REFL Fast Flux Evaluation at the Axial Sample Points .....                    | 149 |
| Table 3-76. Peak Burnup and Fluence Hand Calculation for the Equilibrium Problem .....    | 157 |
| Table 3-77. Power Peaking Factor and Average Burnup for the Non-Equilibrium Problem ..... | 160 |
| Table 3-78. Peak Burnup Calculation for the Non-Equilibrium Problem .....                 | 161 |
| Table 3-79. Peak Fast Fluence Calculation for the Non-Equilibrium Problem .....           | 162 |
| Table 3-80. U235 Micro Reaction Rate Calculation for the Equilibrium Problem .....        | 166 |
| Table 3-81. BOEC Instant Power Table Calculation for the Equilibrium Problem .....        | 166 |
| Table 3-82. REBUS Auxiliary “SUMMARY” Files.....  | 167 |
| Table 4-1. Verification Test Problems and Cross Referencing to Category and Section. .... | 176 |

# 1 Introduction

Argonne National Laboratory has maintained its own fuel cycle analysis code since the early 1960s to meet its reactor design mission. That software transitioned from the original REBUS to REBUS-2 [1] in the mid 1970s and REBUS-3 [2, 3] in the mid 1980s. Since then it has gone through many revisions and is presently at REBUS-11 using a version numbering consistent with the progression of DIF3D, the base flux solver that REBUS is built upon. The name REBUS refers to a pictorial based puzzle as the original developers were inspired by having to use six letter names to define the bookeeping that is required to track thousands of unique fuel assemblies as they are inserted into the reactor, depleted, shuffled, discharged, and reprocessed.

REBUS was designed around the DIF3D code [4-9] and thus is primarily based upon a semi-structured grid geometry using the exact same binary interface files and variable naming scheme as in DIF3D. Of particular interest to the VTR project is the ability of REBUS to perform depletion and fuel cycle operations on hexagonal 3D geometries consistent with the VTR reactor design and on Cartesian geometries consistent with the ZPPR experimental database used as part of the validation work to support the VTR design. Over its extensive history, REBUS has been applied to numerous fast and thermal spectrum reactor analysis projects, giving users the confidence needed to select this code for use with VTR.

The present REBUS capability can perform fuel cycle analysis on all of the DIF3D geometries: slab and cylindrical 1D domains, Cartesian, hexagonal, and R-Z two-dimensional domains, and Cartesian, hexagonal, triangular-Z, and R-Z- $\theta$  three-dimensional domains. By design, REBUS was intended to allow the user to simply and rapidly compute the equilibrium state of a repetitive fuel management scheme with certain approximations. This capability allows the user to search for the required fissile fuel enrichment, for a given repetitive fuel management scheme, such that the desired core criticality is met at a user specified time point. To accomplish this, the software has fuel fabrication and reprocessing plant modeling capabilities that allow multiple sources of feed materials. REBUS can also search the cycle length and adjust the enrichment to meet the specified criticality constraint. In addition to the equilibrium option, REBUS also has a conventional non-equilibrium option which allows the same type of searches as in the equilibrium option but it follows the conventional fuel cycle operation for a given reactor wherein pieces are actually moved throughout the simulated reactor.

The REBUS software is part of the ARC (Argonne Reactor Code) system [10] and is primarily used for fuel cycle analysis within the VTR project. Figure 1-1 shows the present connections of REBUS in the ARC system noting that it is an integral step necessary to define the reactor state for the PERSENT [12] and GAMSOR [13] calculations. Because DIF3D is a called subroutine of REBUS, the identical output for each time step can be reproduced via standalone DIF3D calculations given the reactor state information (depleted fuel compositions). Consequently, most of the focus of the REBUS verification is focused on the REBUS specific output which provides considerable fuel cycle performance details that are not possible with a simple steady state solver of the neutron/gamma transport and diffusion equations.

Because the ARC software has its own nomenclature which will be referred to many times in this document, the definition of that nomenclature is provided here. ARC defines subzones, zones, regions, meshes, and areas. Zones and compositions are functionally equivalent terms that effectively refer to a set of isotopes at a given temperature with stated atom densities. A subzone is equivalent to a composition in meaning but is defined by the user to be a distinguishable part of a zone (i.e. fuel

isotopes) and is only relevant for book keeping. A region is a volume of space filled with a particular zone; a zone can be assigned to multiple regions, but every region is composed of only one zone. Subzones can only be assigned to zones and subzones cannot be assigned to regions. A mesh is the computational mesh used for the numerical determination of the flux and/or eigenvalue; there is at least one mesh per region but there can be several meshes per region as defined by the analyst. Finally, an area is simply an arbitrary collection of regions that together are assigned a consistent label for convenience of output and usage by other ARC codes such as REBUS.

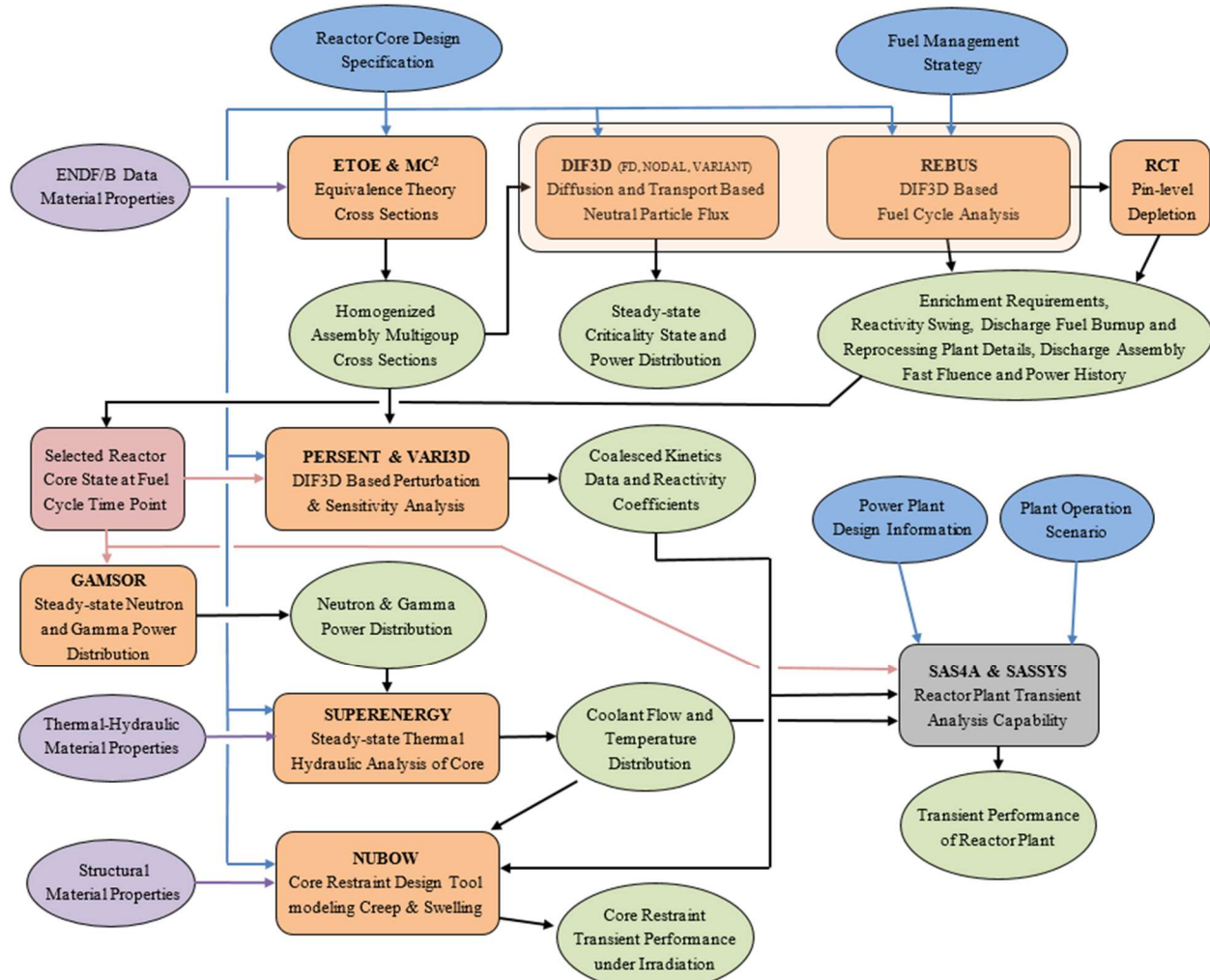


Figure 1-1. The Argonne Reactor Code System Set of Connected Codes

## 2 VTR Specific REBUS Verification

The requirements document [11] discusses the engineering outputs from REBUS used by engineers in the VTR project. This produced a set of tasks to accomplish as part of the verification work which is summarized in Table 2-1. To satisfy each task, at least one verification problem will be used regularly to test the REBUS software. Because the VTR project exclusively uses either the hexagonal or triangular-Z geometry options of REBUS, and only those geometry options need to be verified for this project.

In Table 2-1, the table has been organized into five categories according to the type of work and checking that needs to be done. In the first category, the DIF3D usage by REBUS is verified by manually reconstructing the DIF3D input at each REBUS time point and comparing the reported DIF3D output. As stated above, the DIF3D verification itself is provided elsewhere [14] thereby eliminating any need to check the accuracy of the DIF3D results in this manuscript. As part of category 1, a full VTR problem is included as part of the DIF3D usage verification. In the second category, all aspects of the user defined depletion chain are checked including how the isotopes are connected to each other through nuclear reactions, how the isotopic data provided in ISOTXS is mapped into the depletion chain, the atomic mass is for each isotope, and even Avogadro's number. In the third category, the input methodology for fuel management in REBUS is verified. This includes fuel shuffling options in non-equilibrium problems, and batch fuel operations in equilibrium problems. In the fourth category, the external feed based fuel fabrication features of the REBUS code are verified. In the final category, the peaking calculation done in DIF3D and used by REBUS is verified with regard to the reported peak region and domain burnup and the peak fast fluence of a given fuel material. Together, the set of verification test problems created from this work ensure users that the REBUS software, if used consistently with the manual, will produce accurate results for the VTR program.

**Table 2-1. REBUS Identified Verification Tasks**

| Category | Verification Tasks   |
|----------|--|
| 1        | Verify DIF3D usage in REBUS is consistent with DIF3D verification <ul style="list-style-type: none"> <li>a) Boundary condition usage</li> <li>b) Region and geometry usage</li> <li>c) Composition input</li> <li>d) Composition to region mapping input</li> <li>e) Control rod identification input is used (card 38)</li> </ul>   |
| 2        | Verify user depletion chain <ul style="list-style-type: none"> <li>a) Setup of all primary ISOTXS reactions (card 9)</li> <li>b) Decay constants are properly used (card 25)</li> <li>c) Avogadro's number declaration is used by REBUS (card 28)</li> <li>d) The ISOTXS isotope type and masses are used (card 24)</li> <li>e) The mapping of active isotopes to ISOTXS isotopes (card 10)</li> <li>f) The active isotope list used by REBUS is consistent with the input</li> <li>g) The depletion calculation is correct for a given flux distribution</li> </ul> |
| 3        | Verify the region path specification <ul style="list-style-type: none"> <li>a) The fuel paths are composed on input regions (cards 11, 35)</li> <li>b) The burnup limits specified by path are imposed (cards 5, 6, 7, 8)</li> <li>c) The equilibrium calculation is consistent with the equilibrium state of a given core</li> </ul>  |
| 4        | Verify the fuel fabrication specification <ul style="list-style-type: none"> <li>a) The external feed details (cards 19, 20, 21, 22)</li> <li>b) The enrichment modification factor usage (cards 4, 12, 18)</li> <li>c) The fuel fabrication density (card 13)</li> </ul>  |
| 5        | Verify the mass, burnup, power, and fluence edits <ul style="list-style-type: none"> <li>a) Controlled by default REBUS names or user input (cards 29, 30)</li> </ul>  |

## 3 Verification Problems

This section is focused on summarizing the verification work. The set of verification test problems is summarized at the end of this report and a table is provided linking each verification test problem to the sub-sections here to easily identify its role in the verification process.

### 3.1 DIF3D Consistency Verification Test Problem

The first verification test problem is focused on demonstrating that at each time point, the REBUS outputted DIF3D results can be identically produced by independent DIF3D calculations. This set of test problems is not concerned with the accuracy of the depletion calculation or the REBUS specific outputs.

The base of this verification test problem is a three group cross section set created in the early 1980s for use in testing the ARC software. It includes elemental data for sodium, iron, oxygen, carbon and actinide data for U-235, U-238, Pu-239, Pu-240, and Pu-241 along with the necessary LFP and DUMP isotopes needed to define a REBUS depletion chain. The first test problem is a simple infinite homogeneous test case where the macroscopic cross section data is provided in Table 3-1. The displayed data has a reference solution of 1.152400 while DIF3D reports a  $k_{\text{eff}}$  solution of 1.152283. A simple modification of the last significant digit of the total or fission cross section is sufficient to cause the observed magnitude of discrepancy and thus the difference is attributable to the round off truncation associated with the data displayed in Table 3-1 versus the data provided to DIF3D.

**Table 3-1. Three Group Infinite Homogeneous Macroscopic Cross Sections.**

| Group | Transport | Total      | Absorption | Removal           | N2N        |
|-------|-----------|------------|------------|-------------------|------------|
| 1     | 0.130893  | 0.180123   | 4.96779E-3 | 3.28752E-2        | 6.99675E-5 |
| 2     | 0.207445  | 0.233929   | 2.96165E-3 | 1.01670E-2        | 0.0        |
| 3     | 0.303421  | 0.312298   | 8.59064E-3 | 8.59064E-3        | 0.0        |
| Group | Chi       | Fission    | Nu-Fission | Scattering Matrix |            |
| 1     | 0.7811990 | 4.18979E-3 | 1.23191E-2 | 1.47248E-1        | 0.0        |
| 2     | 0.2099360 | 1.53918E-3 | 4.49207E-3 | 2.74053E-2        | 2.23762E-1 |
| 3     | 0.0088650 | 2.25853E-3 | 6.50730E-3 | 5.72039E-4        | 7.20539E-3 |
|       |           |            |            |                   | 3.03705E-1 |

As stated, the initial goal of this section is to demonstrate that the standalone DIF3D calculation will match that of the REBUS calculation at multiple time steps when there is no depletion. To begin, Figure 3-1 shows an excerpt of the DIF3D output obtained with the verified executable: dif3d.x.

```

1DIF3D 11.0 01/01/12          ADIF3D: Cartesian 3D Test Problem          PAGE 33
  NUMBER OF AXIAL INNER SWEEPS: 2
  Radial inners by group
    2 2 2
  =VARIANT|OUTER| TIME(s)|Ups| K-effective | Error |pGS| Fis Max , RMS |TCheby Vecs Dom P0 |Src(s) |j+/- (s)|Phi(s) |
  =VARIANT| 1| 0.0|001| 1.155383E+00|1.3E-01| T | 2.12E-01, 2.06E-01| T 0 0.21 0.20| 0.0| 0.0| 0.0|
  =VARIANT| 2| 0.0|001| 1.150354E+00|4.4E-03| T | 1.05E-01, 6.88E-02| T 0 0.39 0.37| 0.0| 0.0| 0.0|
  =VARIANT| 3| 0.0|001| 1.151530E+00|1.0E-03| T | 4.85E-02, 3.06E-02| T 0 0.44 0.46| 0.0| 0.0| 0.0|
  ...
  =VARIANT| 16| 0.0|001| 1.152283E+00|6.4E-08| F | 3.65E-08, 2.01E-08| T 0 0.14 0.14| 0.0| 0.0| 0.0|
  =VARIANT| 17| 0.0|001| 1.152283E+00|6.5E-08| F | 1.17E-07, 6.90E-08| T 1 3.43 3.58| 0.0| 0.0| 0.0|
  =VARIANT| 18| 0.0|001| 1.152283E+00|4.9E-09| F | 1.95E-08, 9.80E-09| T 0 0.14 0.14| 0.0| 0.0| 0.0|
  OUTER ITERATIONS COMPLETED AT ITERATION 18, ITERATIONS HAVE CONVERGED
  K-EFFECTIVE = 1.15228299
1DIF3D 11.0 01/01/12          ADIF3D: Cartesian 3D Test Problem          PAGE 34
  ...
  MAXIMUM POWER DENSITY 4.62963E-12 OCCURS AT: X-INDEX NO. 3
  Y-INDEX NO. 3
  SURFACE NO. 0
  Z-COORDINATE = 1.00000E+01
1DIF3D 11.0 01/01/12          ADIF3D: Cartesian 3D Test Problem          PAGE 35
  0 REGION AND AREA POWER INTEGRALS FOR K-EFF PROBLEM WITH ENERGY RANGE (EV) = (4.140E-01,1.000E+07)
  0
    REGION ZONE ZONE VOLUME INTEGRATION(1) POWER POWER DENSITY PEAK DENSITY PEAK TO AVG. POWER
    NO. NAME NO. NAME (CC) WEIGHT FACTOR (WATTS) (WATTS/CC) (WATTS/CC) (2) POWER DENSITY FRACTION
    1 ICORE 1 ZIFUEL 2.16000E+05 1.00000E+00 1.00000E-06 4.62963E-12 4.62963E-12 1.00000E+00 1.00000E+00
    TOTALS 2.16000E+05 0.00000E+00 1.00000E-06 4.62963E-12 4.62963E-12 1.00000E+00 1.00000E+00
  ...
1DIF3D 11.0 01/01/12          ADIF3D: Cartesian 3D Test Problem          PAGE 37
  0 REGION AND AREA REAL FLUX INTEGRALS FOR K-EFF PROBLEM WITH ENERGY RANGE (EV) = (4.140E-01,1.000E+07)
  0
    REGION ZONE ZONE VOLUME TOTAL FLUX PEAK FLUX (1) TOTAL FAST FLUX PEAK FAST FLUX(1)
    NO. NAME NO. NAME (CC) (NEUTRON-CM/SEC) (NEUTRON-CM2-SEC) (NEUTRON-CM/SEC) (NEUTRON-CM2-SEC)
    1 ICORE 1 ZIFUEL 2.16000E+05 1.38949E+07 6.43285E+01 7.65634E+06 3.54460E+01
    TOTALS 2.16000E+05 1.38949E+07 6.43285E+01 7.65634E+06 3.54460E+01
  0
    AREA AREA VOLUME TOTAL FLUX PEAK FLUX (1) TOTAL FAST FLUX PEAK FAST FLUX(1)
    NO. NAME (CC) (NEUTRON-CM/SEC) (NEUTRON-CM2-SEC) (NEUTRON-CM/SEC) (NEUTRON-CM2-SEC)
    1 CORE 2.16000E+05 1.38949E+07 6.43285E+01 7.65634E+06 3.54460E+01
  ...

```

**Figure 3-1. The DIF3D Output for an Infinite Homogeneous Three Group Test Problem**

Figure 3-2 shows the first time step result from REBUS which has the same excerpt sections displayed as those for DIF3D. The different page headers and page numbering indicate that the output is taken from REBUS as opposed to just DIF3D itself. The  $k_{eff}$ , the power and power density, and total flux, fast flux, and peak fast flux are identical to those values reported in Figure 3-1.

```

1FCC004 8.6      03/18/10          ABURN: Cartesian 3D Test Problem          PAGE  57
*****
* TIME NODE  0 DIFFUSION THEORY NEUTRONICS SOLUTION AT  0.00000E+00 DAYS FOLLOWS *
*****
1DIF3D 11.0 01/01/12          ADIF3D: Cartesian 3D Test Problem          PAGE  63
NUMBER OF AXIAL INNER SWEEPS: 2
Radial inners by group
 2 2 2
=VARIANT|OUTER| TIME(s)|Ups| K-effective | Error |pGS| Fis Max , RMS |TCheby Vecs Dom P0 |Src(s) |j+/- (s)|Phi(s) |
=VARIANT| 1| 0.0|001| 1.155383E+00|1.3E-01| T | 2.12E-01, 2.06E-01| T 0 0.21 0.20| 0.0| 0.0| 0.0| 0.0|
=VARIANT| 2| 0.0|001| 1.150354E+00|4.4E-03| T | 1.05E-01, 6.89E-02| T 0 0.39 0.37| 0.0| 0.0| 0.0| 0.0|
=VARIANT| 3| 0.0|001| 1.151530E+00|1.0E-03| T | 4.85E-02, 3.06E-02| T 0 0.44 0.46| 0.0| 0.0| 0.0| 0.0|
=VARIANT| 16| 0.0|001| 1.152283E+00|6.4E-08| F | 3.65E-08, 2.01E-08| T 0 0.14 0.14| 0.0| 0.0| 0.0| 0.0|
=VARIANT| 17| 0.0|001| 1.152283E+00|6.5E-08| F | 1.17E-07, 6.90E-08| T 1 3.43 3.58| 0.0| 0.0| 0.0| 0.0|
=VARIANT| 18| 0.0|001| 1.152283E+00|4.9E-09| F | 1.95E-08, 9.80E-09| T 0 0.14 0.14| 0.0| 0.0| 0.0| 0.0|
OUTER ITERATIONS COMPLETED AT ITERATION 18, ITERATIONS HAVE CONVERGED
K-EFFECTIVE = 1.15228299
MAXIMUM POWER DENSITY 4.62963E-12 OCCURS AT: X-INDEX NO. 3
                                         Y-INDEX NO. 3
                                         SURFACE NO. 0
                                         Z-COORDINATE = 1.00000E+01
1DIF3D 11.0 01/01/12          ADIF3D: Cartesian 3D Test Problem          PAGE  66
0 REGION AND AREA POWER INTEGRALS FOR K-EFF PROBLEM WITH ENERGY RANGE (EV) = (4.140E-01, 1.000E+07)
0
REGION ZONE ZONE VOLUME INTEGRATION(1) POWER POWER DENSITY PEAK DENSITY PEAK TO AVG. POWER
NO. NAME NO. NAME (CC) WEIGHT FACTOR (WATTS) (WATTS) (WATTS/CC) (WATTS/CC) (2) POWER DENSITY FRACTION
1 ICORE 1 ICORE 2.16000E+05 1.00000E+00 1.00000E-06 4.62963E-12 4.62963E-12 1.00000E+00 1.00000E+00
TOTALS 2.16000E+05 0.00000E+00 1.00000E-06 4.62963E-12 4.62963E-12 1.00000E+00 1.00000E+00
1DIF3D 11.0 01/01/12          ADIF3D: Cartesian 3D Test Problem          PAGE  68
0 REGION AND AREA REAL FLUX INTEGRALS FOR K-EFF PROBLEM WITH ENERGY RANGE (EV) = (4.140E-01, 1.000E+07)
0
REGION ZONE ZONE VOLUME TOTAL FLUX PEAK FLUX (1) TOTAL FAST FLUX PEAK FAST FLUX(1)
NO. NAME NO. NAME (CC) (NEUTRON-CM/SEC) (NEUTRON-CM2-SEC) (NEUTRON-CM/SEC) (NEUTRON-CM2-SEC)
1 ICORE 1 ICORE 2.16000E+05 1.38949E+07 6.43285E+01 7.65634E+06 3.54460E+01
TOTALS 2.16000E+05 1.38949E+07 6.43285E+01 7.65634E+06 3.54460E+01
0
AREA AREA VOLUME TOTAL FLUX PEAK FLUX (1) TOTAL FAST FLUX PEAK FAST FLUX(1)
NO. NAME (CC) (NEUTRON-CM/SEC) (NEUTRON-CM2-SEC) (NEUTRON-CM/SEC) (NEUTRON-CM2-SEC)
1 CORE 2.16000E+05 1.38949E+07 6.43285E+01 7.65634E+06 3.54460E+01

```

**Figure 3-2. REBUS Output for Infinite Homogeneous Three Group Test Problem (Time 0.0)**

Similar to Figure 3-2, Figure 3-3 provides the DIF3D output from REBUS at the end of the first time step. A quick comparison between the three DIF3D results in Figure 3-1, Figure 3-2, and Figure 3-3 shows that all three have identical outputs excluding the pagination related outputs. The preceding calculations were all done using a Cartesian example problem and the same result is obtained for an infinite homogeneous domain in hexagonal geometry which is not included here for brevity.

The preceding was a simplistic example with a single region. To further demonstrate that the DIF3D results are not changed when doing a zero power depletion, more complicated geometry cases were constructed in Cartesian and hexagonal geometries as shown in Figure 3-4. Each problem has typical components of a fast spectrum reactor: inner core, outer core, axial blankets above and below both core regions, radial blankets, radial and axial reflectors and shielding and five control rods at different heights. Included with the geometry pictures are power distributions to highlight the relative volume of the active core to the whole geometry and the gradients caused by the insertion of control rods. The geometric and flux details of both problems is not relevant for this test as the only interest is to verify that the DIF3D solution and its outputs are not impacted by executing through REBUS.

Because the outputs at each time point are identical, only the fourth of five time point results from REBUS are displayed and compared against the DIF3D calculated result. Figure 3-5 provides an excerpt of the DIF3D output generated in REBUS at the 4 day time point while Figure 3-6 provides the same excerpt for the standalone DIF3D calculation. The presented results are broken down into 4 tables of DIF3D output: eigenvalue, region power table, region flux integrals, region flux averages. Starting with the eigenvalue table, one can see a considerable difference between DIF3D and DIF3D in REBUS. This is primarily because REBUS does two depletion calculations to ensure convergence of

the atom densities and the provided DIF3D result is from the second depletion iteration which is a restart calculation of the first one. Thus while the eigenvalue is identical, the actual convergence history is different.

Continuing with the power tables, one finds that the ordering of the region data and the data itself is identical with the only difference being the page numbering on the pagination. Similarly, the flux integrals and average flux tables also show an identical region ordering and output data.

1FCC004 8.6 03/18/10 ABURN: Cartesian 3D Test Problem PAGE 85  
 \*\*\*\*\* THE BPOINTER DATA HAVE BEEN SAVED ON LOGICAL UNIT NO. 90 \*\*\*\*\*  
 \*\*\*\*\* TIME NODE 1 DIFFUSION THEORY NEUTRONICS SOLUTION AT 1.00000E+00 DAYS FOLLOWS \*\*\*\*\*

1DIF3D 11.0 01/01/12 ADIF3D: Cartesian 3D Test Problem PAGE 90  
 NUMBER OF AXIAL INNER SWEEPS: 2  
 Radial inners by group  
 2 2 2  
 =VARIANT|OUTER| TIME(s)|Ups| K-effective | Error |pGS| Fis Max , RMS |TCheby| Vecs| Dom| P0| Src(s)| j+/-|Phi(s)|  
 =VARIANT| 1| 0.0|001| 1.155383E+00|2.7E-03| T | 2.11E-01, 1.17E-01| T | 0| 0.12| 0.12| 0.0| 0.0| 0.0|  
 =VARIANT| 2| 0.0|001| 1.150355E+00|4.4E-03| T | 1.05E-01, 6.88E-02| T | 0| 0.59| 0.57| 0.0| 0.0| 0.0|  
 =VARIANT| 3| 0.0|001| 1.151530E+00|1.0E-03| T | 4.85E-02, 3.06E-02| T | 0| 0.44| 0.46| 0.0| 0.0| 0.0|  
 ...  
 =VARIANT| 16| 0.0|001| 1.152283E+00|6.4E-08| F | 3.65E-08, 2.01E-08| T | 0| 0.14| 0.14| 0.0| 0.0| 0.0|  
 =VARIANT| 17| 0.0|001| 1.152283E+00|6.5E-08| F | 1.17E-07, 6.90E-08| T | 1| 3.43| 3.58| 0.0| 0.0| 0.0|  
 =VARIANT| 18| 0.0|001| 1.152283E+00|4.9E-09| F | 1.95E-08, 9.79E-09| T | 0| 0.14| 0.14| 0.0| 0.0| 0.0|  
 OUTER ITERATIONS COMPLETED AT ITERATION 18, ITERATIONS HAVE CONVERGED  
 K-EFFECTIVE = 1.15228299  
 MAXIMUM POWER DENSITY 4.62963E-12 OCCURS AT: X-INDEX NO. 3  
 Y-INDEX NO. 3  
 SURFACE NO. 0  
 Z-COORDINATE = 1.00000E+01  
 1DIF3D 11.0 01/01/12 ADIF3D: Cartesian 3D Test Problem PAGE 92  
 0 REGION AND AREA POWER INTEGRALS FOR K-EFF PROBLEM WITH ENERGY RANGE (EV) = (4.140E-01, 1.000E+07)  
 0  
 REGION ZONE ZONE VOLUME INTEGRATION(1) POWER POWER DENSITY PEAK DENSITY PEAK TO AVG. POWER  
 NO. NAME NO. NAME (CC) WEIGHT FACTOR (WATTS) (WATTS/CC) (WATTS/CC) (2) POWER DENSITY FRACTION  
 1 ICORE 1 ICORE 2.16000E+05 1.00000E+00 1.00000E-06 4.62963E-12 4.62963E-12 1.00000E+00 1.00000E+00  
 TOTALS 2.16000E+05 0.00000E+00 1.00000E-06 4.62963E-12 4.62963E-12 1.00000E+00 1.00000E+00  
 ...  
 1DIF3D 11.0 01/01/12 ADIF3D: Cartesian 3D Test Problem PAGE 94  
 0 REGION AND AREA REAL FLUX INTEGRALS FOR K-EFF PROBLEM WITH ENERGY RANGE (EV) = (4.140E-01, 1.000E+07)  
 0  
 REGION ZONE ZONE VOLUME TOTAL FLUX PEAK FLUX (1) TOTAL FAST FLUX PEAK FAST FLUX(1)  
 NO. NAME NO. NAME (CC) (NEUTRON-CM/SEC) (NEUTRON-CM2-SEC) (NEUTRON-CM/SEC) (NEUTRON-CM2-SEC)  
 1 ICORE 1 ICORE 2.16000E+05 1.38949E+07 6.43285E+01 7.65634E+06 3.54460E+01  
 TOTALS 2.16000E+05 1.38949E+07 6.43285E+01 7.65634E+06 3.54460E+01  
 0  
 AREA AREA VOLUME TOTAL FLUX PEAK FLUX (1) TOTAL FAST FLUX PEAK FAST FLUX(1)  
 NO. NAME (CC) (NEUTRON-CM/SEC) (NEUTRON-CM2-SEC) (NEUTRON-CM/SEC) (NEUTRON-CM2-SEC)

**Figure 3-3. REBUS Output for Infinite Homogeneous Three Group Test Problem (Time 1.0)**

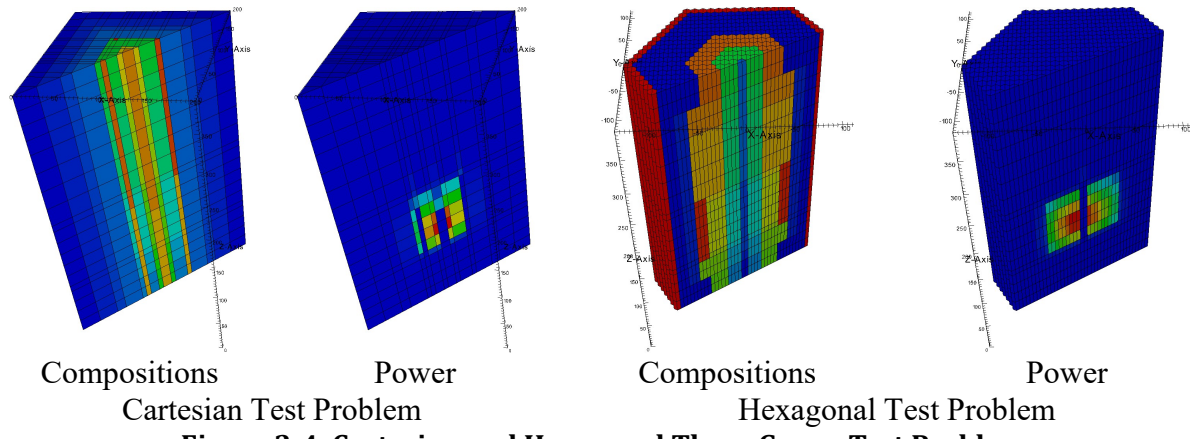


**Figure 3-4. Cartesian and Hexagonal Three Group Test Problems**

```
*****
* START OF A COMPLETE BURN CYCLE *
*****
THE BURN CYCLE TIME IS 1.00000E+00 DAYS.
THE ENRICHMENT MODIFICATION FACTOR IS 0.00000E+00.

1FCC004 8.6 03/18/10 ABURN: Cartesian 3D Test Problem PAGE 336
*****
* TIME NODE 0 DIFFUSION THEORY NEUTRONICS SOLUTION AT 4.00000E+00 DAYS FOLLOWS *
*****
.....
=VARIANT|OUTER| TIME(s)|Ups| K-effective | Error |pGS| Fis Max , RMS |TCheby Vecs Dom P0 |Src(s) |j+/- (s) |Phi(s) |
=VARIANT| 1| 0.1|001| 1.031024E+00|1.9E-08| T | 3.07E-08, 1.88E-08| T 0 0.00 0.00| 0.0| 0.0| 0.0|
=VARIANT| 2| 0.1|001| 1.031024E+00|7.0E-10| F | 1.20E-08, 2.57E-09| T 0 0.14 0.13| 0.0| 0.1| 0.0|
    OUTER ITERATIONS COMPLETED AT ITERATION 2, ITERATIONS HAVE CONVERGED
    K-EFFECTIVE = 1.03102412
1DIF3D 11.0 01/01/12 ADIF3D: Cartesian 3D Test Problem PAGE 342
.....
    MAXIMUM POWER DENSITY 4.91843E-12 OCCURS AT: X-INDEX NO. 10
                                                Y-INDEX NO. 9
                                                SURFACE NO. 0
                                                Z-COORDINATE = 1.26000E+02
(NHSREG) THE PEAK-TO-AVERAGE SEPARABILITY THRESHOLD WAS EXCEEDED IN 1268 MESH CELLS.
(NHSREG) THE PEAK-TO-AVERAGE SEPARABILITY THRESHOLD WAS EXCEEDED IN 1264 MESH CELLS.
1DIF3D 11.0 01/01/12 ADIF3D: Cartesian 3D Test Problem PAGE 343
0 REGION AND AREA POWER INTEGRALS FOR K-EFF PROBLEM WITH ENERGY RANGE (EV) =(4.140E-01,1.000E+07)
0
    REGION ZONE ZONE VOLUME INTEGRATION(1) POWER POWER DENSITY PEAK DENSITY PEAK TO AVG. POWER
    NO. NAME NO. NAME (CC) WEIGHT FACTOR (WATTS) (WATTS/CC) (WATTS/CC) (2) POWER DENSITY FRACTION
    .....
    1 SPOOL 1 SPOOL 5.61600E+06 1.00000E+00 1.11220E-12 1.98041E-19 3.14992E-18 1.59054E+01 1.11220E-06
    2 SHILD 2 SHILD 4.36800E+06 1.00000E+00 4.16755E-09 9.54108E-16 2.21644E-13 3.23205E+02 4.16755E-03
    3 RREFL 3 RREFL 1.71600E+06 1.00000E+00 7.46341E-10 4.34931E-16 5.11476E-15 1.17599E+01 7.46341E-04
    4 RBLKT 4 RBLKT 2.49600E+06 1.00000E+00 9.02455E-08 3.61516E-14 6.03896E-13 1.67025E+01 9.02455E-02
    5 OLSHD 5 OLSHD 1.26000E+05 1.00000E+00 1.70723E-10 1.35495E-15 9.40138E-14 6.93856E+01 1.70723E-04
    6 OLREF 6 OLREF 1.26000E+05 1.00000E+00 4.57977E-10 3.63473E-15 1.16758E-14 3.21229E+00 4.57977E-04
    7 OBLBK 7 OBLBK 3.15000E+04 1.00000E+00 4.38228E-09 1.39120E-13 3.02811E-13 2.17661E+00 4.38228E-03
    8 OCORE 8 OCORE 3.15000E+05 1.00000E+00 8.00567E-07 2.54148E-12 4.90171E-12 1.92868E+00 8.00567E-01
    .....
    24 CNTRL3 24 CNTRL3 5.00000E+03 1.00000E+00 8.35511E-11 1.67102E-14 1.91202E-12 1.14422E+02 8.35511E-05
    25 CNTRL4 25 CNTRL4 4.75000E+03 1.00000E+00 6.05094E-11 1.27338E-14 6.62869E-13 5.20353E+01 6.05094E-05
    26 CNTRL5 26 CNTRL5 4.75000E+03 1.00000E+00 6.05094E-11 1.27338E-14 6.62869E-13 5.20353E+01 6.05094E-05
    TOTALS 1.56000E+07 0.00000E+00 1.00000E-06 6.41026E-14 4.91843E-12 7.67276E+01 1.00000E+00
    AREA AREA VOLUME INTEGRATION(1) POWER POWER DENSITY PEAK DENSITY PEAK TO AVG. POWER
    NO. NAME (CC) WEIGHT FACTOR (WATTS) (WATTS/CC) (WATTS/CC) (2) POWER DENSITY FRACTION
    1 ABLKT 6.90000E+04 0.00000E+00 6.63467E-09 9.61546E-14 3.15093E-13 3.27694E+00 6.63467E-03
    2 CORE 3.45000E+05 0.00000E+00 8.95492E-07 2.59563E-12 4.91843E-12 1.89489E+00 8.95492E-01
    .....
1DIF3D 11.0 01/01/12 ADIF3D: Cartesian 3D Test Problem PAGE 346
0 REGION AND AREA REAL FLUX INTEGRALS FOR K-EFF PROBLEM WITH ENERGY RANGE (EV) =(4.140E-01,1.000E+07)
0
    REGION ZONE ZONE VOLUME TOTAL FLUX PEAK FLUX (1) TOTAL FAST FLUX PEAK FAST FLUX(1)
    NO. NAME NO. NAME (CC) (NEUTRON-CM/SEC) (NEUTRON/CM2-SEC) (NEUTRON-CM/SEC) (NEUTRON/CM2-SEC)
    .....
    1 SPOOL 1 SPOOL 5.61600E+06 7.71379E+03 2.18108E-02 9.23012E+02 2.56639E-03
    2 SHILD 2 SHILD 4.36800E+06 2.16687E+04 8.71829E-01 1.57903E+04 5.29793E-01
    3 RREFL 3 RREFL 1.71600E+06 6.33036E+05 4.39369E+00 2.71178E-05 1.95374E+00
    4 RBLKT 4 RBLKT 2.49600E+06 4.05669E+06 1.87935E+01 2.06050E+06 1.19680E+01
    5 OLSHD 5 OLSHD 1.26000E+05 6.64302E+02 2.81387E-01 4.00741E+02 1.26462E-01
    6 OLREF 6 OLREF 1.26000E+05 3.70142E+05 1.03728E+01 1.34015E+05 5.05094E+00
    7 OBLBK 7 OBLBK 3.15000E+04 2.86301E+05 1.57944E+01 1.52753E+05 9.67165E+00
    8 OCORE 8 OCORE 3.15000E+05 5.14480E+06 3.14973E+01 3.47945E+06 2.19620E+01
    .....
    24 CNTRL3 24 CNTRL3 5.00000E+03 1.01803E+02 2.01877E+00 7.89835E+01 1.46979E+00
    25 CNTRL4 25 CNTRL4 4.75000E+03 6.85105E+01 6.63131E-01 5.16028E+01 5.08320E-01
    26 CNTRL5 26 CNTRL5 4.75000E+03 6.85105E+01 6.63131E-01 5.16028E+01 5.08320E-01
    TOTALS 1.56000E+07 1.17042E+07 3.16257E+01 6.87929E+06 2.19621E+01
    AREA AREA VOLUME TOTAL FLUX PEAK FLUX (1) TOTAL FAST FLUX PEAK FAST FLUX(1)
    NO. NAME (CC) (NEUTRON-CM/SEC) (NEUTRON/CM2-SEC) (NEUTRON-CM/SEC) (NEUTRON/CM2-SEC)
    1 ABLKT 6.90000E+04 4.20134E+05 1.64706E+01 2.31181E+05 1.00555E+01
    2 CORE 3.45000E+05 5.75519E+06 3.16257E+01 3.90776E+06 2.19621E+01
    .....
0 REGION REAL FLUX AVERAGES FOR K-EFF PROBLEM WITH ENERGY RANGE (EV) =(4.140E-01,1.000E+07)
0
    REGION ZONE ZONE VOLUME AVG TOTAL FLUX GROUP GROUP GROUP
    NO. NAME NO. NAME (CC) (NEUTRON/CM2-SEC) 1 2 3
    .....
    1 SPOOL 1 SPOOL 5.61600E+06 1.37354E-03 7.46056E-07 1.80898E-04 1.19189E-03
    2 SHILD 2 SHILD 4.36800E+06 4.96079E-03 6.30196E-04 3.30022E-03 1.03038E-03
    3 RREFL 3 RREFL 1.71600E+06 3.68902E-01 1.72401E-02 1.55668E-01 1.95994E-01
    4 RBLKT 4 RBLKT 2.49600E+06 1.62528E+00 1.58411E-01 7.37609E-01 7.29256E-01
    5 OLSHD 5 OLSHD 1.26000E+05 5.27224E-03 2.85316E-04 3.20113E-03 1.78580E-03
    6 OLREF 6 OLREF 1.26000E+05 2.93763E+00 1.21329E-01 1.04186E+00 1.77444E+00
    7 OBLBK 7 OBLBK 3.15000E+04 9.08891E+00 1.09714E+00 4.14868E+00 3.84309E+00
    8 OCORE 8 OCORE 3.15000E+05 1.63327E+01 3.49735E+00 8.34624E+00 4.48911E+00
    .....
    24 CNTRL3 24 CNTRL3 5.00000E+03 2.03607E-02 4.95620E-03 1.19861E-02 3.41839E-03
    25 CNTRL4 25 CNTRL4 4.75000E+03 1.44233E-02 2.99461E-03 8.70074E-03 2.72791E-03
    26 CNTRL5 26 CNTRL5 4.75000E+03 1.44233E-02 2.99461E-03 8.70074E-03 2.72791E-03
    TOTALS 1.56000E+07 7.50267E-01 1.15860E-01 3.59479E-01 2.74928E-01

```

Figure 3-5. REBUS Output for the Cartesian Reactor Three Group Test Problem at 4.0 days

## Verification of the REBUS Software

July 2025

```

1DIF3D 11.0 01/01/12 ADIF3D: Cartesian 3D Test Problem PAGE 39
...
Radial inners by group
 2 2 2
=VARIANT|OUTER| TIME(s)|Ups| K-effective | Error |pGS| Fis Max , RMS |TCheby Vecs Dom P0 |Src(s) |j+/- (s)|Phi(s) |
=VARIANT| 1| 0.1|001| 7.410680E-01|3.5E-01| T | 6.08E+00, 3.86E-01| T 0 0.39 0.38| 0.0| 0.0| 0.0| 0.0|
=VARIANT| 2| 0.1|001| 9.115554E-01|1.9E-01| T | 4.19E+00, 3.90E-01| T 0 1.04 1.03| 0.0| 0.0| 0.0| 0.0|
=VARIANT| 3| 0.1|001| 9.863510E-01|7.6E-02| T | 5.42E+00, 1.39E-01| T 0 0.48 0.48| 0.0| 0.0| 0.0| 0.0|
...
=VARIANT| 39| 0.1|001| 1.031024E+00|8.1E-09| F | 1.01E-07, 1.45E-08| T 0 0.06 0.05| 0.0| 0.1| 0.0| 0.0|
=VARIANT| 40| 0.1|001| 1.031024E+00|1.5E-08| F | 4.98E-08, 1.80E-08| T 0 1.24 1.32| 0.0| 0.1| 0.0| 0.0|
  OUTER ITERATIONS COMPLETED AT ITERATION 40, ITERATIONS HAVE CONVERGED
  K-EFFECTIVE = 1.03102412
...
  MAXIMUM POWER DENSITY 4.91843E-12 OCCURS AT: X-INDEX NO. 10
  Y-INDEX NO. 9
  SURFACE NO. 0
  Z-COORDINATE = 1.26000E+02
(NHNSREG) THE PEAK-TO-AVERAGE SEPARABILITY THRESHOLD WAS EXCEEDED IN 1268 MESH CELLS.
(NHNSREG) THE PEAK-TO-AVERAGE SEPARABILITY THRESHOLD WAS EXCEEDED IN 1264 MESH CELLS.
1DIF3D 11.0 01/01/12 ADIF3D: Cartesian 3D Test Problem PAGE 41
0 REGION AND AREA POWER INTEGRALS FOR K-EFF PROBLEM WITH ENERGY RANGE (EV) = (4.140E-01, 1.000E+07)
0
  REGION ZONE ZONE VOLUME INTEGRATION(1) POWER POWER DENSITY PEAK DENSITY PEAK TO AVG. POWER
  NO. NAME NO. NAME (CC) WEIGHT FACTOR (WATTS) (WATTS/CC) (WATTS/CC) (2) POWER DENSITY FRACTION
  ...
  1 SPOOL 12 ZSPOOL 5.61600E+06 1.00000E+00 1.11220E-12 1.98041E-19 3.14992E-18 1.59054E+01 1.11220E-06
  2 SHILD 11 ZSHLD 4.36800E+06 1.00000E+00 4.16755E-09 9.54108E-16 2.21644E-13 2.32305E+02 4.16755E-03
  3 RREFL 10 ZRREF 1.71600E+06 1.00000E+00 7.46341E-10 4.34931E-16 5.11476E-15 1.17599E+01 7.46341E-04
  4 RBLKT 4 ZRBLKT 2.49600E+06 1.00000E+00 9.02455E-08 3.61561E-14 6.03896E-13 1.67025E+01 9.02455E-02
  5 OLSHD 11 ZSHLD 1.26000E+05 1.00000E+00 1.70723E-10 1.35495E-15 9.40138E-14 6.93856E+01 1.70723E-04
  6 OLREF 10 ZRREF 1.26000E+05 1.00000E+00 4.57977E-10 3.63473E-15 1.16758E-14 3.21229E+00 4.57977E-04
  7 OBLIK 3 ZABLKT 3.15000E+04 1.00000E+00 4.38228E-09 1.39120E-13 3.02811E-13 2.17661E+00 4.38228E-03
  8 OCORE 2 ZOFUEL 3.15000E+05 1.00000E+00 8.00567E-07 2.54148E-12 4.90171E-12 1.92868E+00 8.00567E-01
  ...
  24 CNTRL3 7 ZCNR3 5.00000E+03 1.00000E+00 8.35511E-11 1.67102E-14 1.91202E-12 1.14422E+02 8.35511E-05
  25 CNTRL4 8 ZCNR4 4.75000E+03 1.00000E+00 6.05094E-11 1.27388E-14 6.62869E-13 5.20353E+01 6.05094E-05
  26 CNTRL5 8 ZCNR4 4.75000E+03 1.00000E+00 6.05094E-11 1.27388E-14 6.62869E-13 5.20353E+01 6.05094E-05
  TOTALS 1.56000E+07 0.00000E+00 1.00000E-06 6.41026E-14 4.91843E-12 7.67276E+01 1.00000E+00
  AREA AREA VOLUME INTEGRATION(1) POWER POWER DENSITY PEAK DENSITY PEAK TO AVG. POWER
  NO. NAME (CC) WEIGHT FACTOR (WATTS) (WATTS/CC) (WATTS/CC) (2) POWER DENSITY FRACTION
  1 ABLKT 6.90000E+04 0.00000E+00 6.63467E-09 9.61546E-14 3.15093E-13 3.27694E+00 6.63467E-03
  2 CORE 3.45000E+05 0.00000E+00 8.95492E-07 2.59563E-12 4.91843E-12 1.89489E+00 8.95492E-01
  ...
1DIF3D 11.0 01/01/12 ADIF3D: Cartesian 3D Test Problem PAGE 44
0 REGION AND AREA REAL FLUX INTEGRALS FOR K-EFF PROBLEM WITH ENERGY RANGE (EV) = (4.140E-01, 1.000E+07)
0
  REGION ZONE ZONE VOLUME TOTAL FLUX PEAK FLUX (1) TOTAL FAST FLUX PEAK FAST FLUX(1)
  NO. NAME NO. NAME (CC) (NEUTRON-CM/SEC) (NEUTRON/CM2-SEC) (NEUTRON-CM/SEC) (NEUTRON/CM2-SEC)
  1 SPOOL 12 ZSPOOL 5.61600E+06 7.71379E+03 2.18108E-02 9.23012E+02 2.56639E-03
  2 SHILD 11 ZSHLD 4.36800E+06 2.16687E+04 8.71829E-01 1.57903E+04 5.29793E-01
  3 RREFL 10 ZRREF 1.71600E+06 6.33036E+05 4.39369E+00 2.71178E+05 1.95374E+00
  4 RBLKT 4 ZRBLKT 2.49600E+06 4.05669E+06 1.87935E+01 2.06050E+06 1.19680E+01
  5 OLSHD 11 ZSHLD 1.26000E+05 6.64302E+02 2.81387E-01 4.00741E+02 1.26462E-01
  6 OLREF 10 ZRREF 1.26000E+05 3.70142E+05 1.03728E+01 1.34015E+05 5.05094E+00
  7 OBLIK 3 ZABLKT 3.15000E+04 2.86301E+05 1.57944E+01 1.52753E+05 9.67166E+00
  8 OCORE 2 ZOFUEL 3.15000E+05 5.14480E+06 3.14973E+01 3.47945E+06 2.19620E+01
  ...
  24 CNTRL3 7 ZCNR3 5.00000E+03 1.01803E+02 2.01877E+00 7.89835E+01 1.46979E+00
  25 CNTRL4 8 ZCNR4 4.75000E+03 6.85104E+01 6.63131E-01 5.16028E+01 5.08320E-01
  26 CNTRL5 8 ZCNR4 4.75000E+03 6.85104E+01 6.63131E-01 5.16028E+01 5.08320E-01
  TOTALS 1.56000E+07 1.17042E+07 3.16257E+01 6.87929E+06 2.19621E+01
  AREA AREA VOLUME TOTAL FLUX PEAK FLUX (1) TOTAL FAST FLUX PEAK FAST FLUX(1)
  NO. NAME (CC) (NEUTRON-CM/SEC) (NEUTRON/CM2-SEC) (NEUTRON-CM/SEC) (NEUTRON/CM2-SEC)
  1 ABLKT 6.90000E+04 4.20134E+05 1.64706E+01 2.31181E+05 1.00555E+01
  2 CORE 3.45000E+05 5.75519E+06 3.16257E+01 3.90776E+06 2.19621E+01
  ...
1DIF3D 11.0 01/01/12 ADIF3D: Cartesian 3D Test Problem PAGE 46
0 REGION REAL FLUX AVERAGES FOR K-EFF PROBLEM WITH ENERGY RANGE (EV) = (4.140E-01, 1.000E+07)
0
  REGION ZONE ZONE VOLUME AVG TOTAL FLUX GROUP GROUP GROUP
  NO. NAME NO. NAME (CC) (NEUTRON/CM2-SEC) 1 2 3
  1 SPOOL 12 ZSPOOL 5.61600E+06 1.37354E+03 7.46056E-07 1.80898E-04 1.19189E-03
  2 SHILD 11 ZSHLD 4.36800E+06 4.96079E-03 6.30196E-04 3.30022E-03 1.03038E-03
  3 RREFL 10 ZRREF 1.71600E+06 3.68902E-01 1.72401E-02 1.55668E-01 1.95994E-01
  4 RBLKT 4 ZRBLKT 2.49600E+06 1.62528E+00 1.58411E-01 7.37609E-01 7.29256E-01
  5 OLSHD 11 ZSHLD 1.26000E+05 5.27224E-03 2.85316E-04 3.20113E-03 1.78580E-03
  6 OLREF 10 ZRREF 1.26000E+05 2.93763E+00 1.21329E-01 1.04186E+00 1.77444E+00
  7 OBLIK 3 ZABLKT 3.15000E+04 9.08891E+00 1.09714E+00 4.14868E+00 3.84309E+00
  8 OCORE 2 ZOFUEL 3.15000E+05 1.63327E+01 3.49735E+00 8.34624E+00 4.48911E+00
  ...
  24 CNTRL3 7 ZCNR3 5.00000E+03 2.03607E-02 4.95620E-03 1.19861E-02 3.41839E-03
  25 CNTRL4 8 ZCNR4 4.75000E+03 1.44233E-02 2.99461E-03 8.70074E-03 2.72791E-03
  26 CNTRL5 8 ZCNR4 4.75000E+03 1.44233E-02 2.99461E-03 8.70074E-03 2.72791E-03
  TOTALS 1.56000E+07 7.50267E+01 1.15860E-01 3.59479E-01 2.74928E-01
1DIF3D 11.0 01/01/12 ADIF3D: Cartesian 3D Test Problem PAGE 47

```

Figure 3-6. DIF3D Output for the Cartesian Reactor Three Group Test Problem

It is important to note that input #10 of card type 04 of A.DIF3D must be set to “2200” in order to get the message from NHSREG that matches the REBUS result. Using “1100” will invoke a different message from NHSMSH which generates the peak values based in a mesh ordered format instead of the region ordered approach that REBUS requires. While this input option does not impact any of the tables of results that users typically use, it can change this minor section of output and the “2200” input is for certain not standard as the SFEDIT file is binary in nature and is not used by any other ARC component except for REBUS.

Continuing with the hexagonal geometry example, the REBUS result at 4 days is given in Figure 3-7 while the steady state DIF3D result is given in Figure 3-8. Excerpts of the same  $k_{eff}$  convergence table and power and flux tables are provided. Because of the change in geometry, the volumes of the various regions are notably different from those in Figure 3-5 and Figure 3-6. This change in volume leads to different  $k_{eff}$ , power, and flux tables from those obtained in the Cartesian benchmark demonstrating that the two problems are inherently different. Comparing the DIF3D result to the REBUS based DIF3D result, one finds the same  $k_{eff}$  convergence table difference due again to the REBUS output being based upon a restarted DIF3D calculation. The final  $k_{eff}$  itself is of course the same to 8 significant digits. As was the case for the Cartesian benchmark, the power table, integral flux table, and average flux tables are all identical. The only significant differences from the two outputs are again the page numbers on the pagination details.

The preceding comparison relied upon a single DIF3D input to verify the accuracy at each time point of the REBUS calculation. An alternative is to use the binary files produced by REBUS at each time point which for the hexagonal problem defined by Figure 3-4. Figure 3-9 lists the files created by REBUS which have both an integer time point index and a physical time point associated with the calculation. The NDXSRF file is only created once at the beginning of the calculation for all REBUS calculations as all materials needed at all time points are added to the composition list during the initialization phase of REBUS. The GEODST, LABELS, RFILES, and ZNATDN inputs are outputted at each time point where only the ZNATDN file is generally expected to change. There is only a single time point result at 0.0 days because there is no iterative convergence associated with the depletion calculation at that time point. There should be two results at time points 1, 2, 3, 4, and 5, as it takes exactly one iteration to verify that the depletion results are converged and thus 2 flux calculations. For more difficult depletion calculations, there can be up to 5 binary files created at each time point. The reason the last point is not provided at time point 5 is because in REBUS, the binary file creation routines are only called when setting up for the start of the next time point which does not occur at the last time point of a given calculation. While this is a slight oversight for most uses of the binary files, assuming reasonable convergence error is provided by the user, the missing binary file will invariably be very close to the one that precedes it.

To run the DIF3D calculation at each time point, the four interface files GEODST, LABELS, NDXSRF, and ZNATDN are required by DIF3D as a substitute to A.NIP3 input where RFILES is the REBUS restart file and is not needed by DIF3D. To orchestrate a DIF3D calculation, the binary files listed in Figure 3-9 need to be copied to their base names and the DIF3D input seen in Figure 3-10 can be used to reproduce the REBUS reported DIF3D result at each time point, or even each iteration of each time point.

```
*****
*   START OF A COMPLETE BURN CYCLE   *
*****
THE BURN CYCLE TIME IS 1.00000E+00 DAYS.
THE ENRICHMENT MODIFICATION FACTOR IS 0.00000E+00.
1FCC004 8.6      03/18/10      ABURN: Cartesian 3D Test Problem      PAGE 338
...
*****
* TIME NODE 0 DIFFUSION THEORY NEUTRONICS SOLUTION AT 4.00000E+00 DAYS FOLLOWS *
*****
=VARIANT|OUTER| TIME(s)|Ups| K-effective | Error |pGS| Fis Max , RMS |TCheby Vecs Dom P0 |Src(s) |j+/-s|Phi(s) |
=VARIANT| 1| 0.3|001| 1.035664E+00|4.2E-08| T | 5.48E-08, 4.18E-08| T 0 0.00 0.00| 0.0| 0.1| 0.1|
=VARIANT| 2| 0.3|001| 1.035664E+00|6.3E-10| F | 1.24E-08, 4.71E-09| T 0 0.11 0.11| 0.0| 0.2| 0.1|
    OUTER ITERATIONS COMPLETED AT ITERATION 2, ITERATIONS HAVE CONVERGED
    K-EFFECTIVE = 1.03566416
1DIF3D 11.0      01/01/12      ADIF3D: Cartesian 3D Test Problem      PAGE 344
...
    MAXIMUM POWER DENSITY 2.88547E-12 OCCURS AT: RING NO. 4
    POSITION NO. 7
    SURFACE NO. 6
    Z-COORDINATE = 1.70000E+02
(NHSREG) THE PEAK-TO-AVERAGE SEPARABILITY THRESHOLD WAS EXCEEDED IN 4115 MESH CELLS.
(NHSREG) THE PEAK-TO-AVERAGE SEPARABILITY THRESHOLD WAS EXCEEDED IN 3992 MESH CELLS.
1DIF3D 11.0      01/01/12      ADIF3D: Cartesian 3D Test Problem      PAGE 345
0      REGION AND AREA POWER INTEGRALS FOR K-EFF PROBLEM WITH ENERGY RANGE (EV)      =(4.140E-01,1.000E+07)
0
    REGION ZONE ZONE VOLUME INTEGRATION(1) POWER POWER DENSITY PEAK DENSITY PEAK TO AVG. POWER
    NO. NAME NO. NAME (CC) WEIGHT FACTOR (WATTS) (WATTS) (WATTS/CC) (WATTS/CC) (2) POWER DENSITY FRACTION
...
1 SHILD 1 SHILD 6.09162E+06 1.00000E+00 2.61536E-09 4.29338E-16 8.92585E-14 2.07898E+02 2.61536E-03
2 RREFL 2 RREFL 3.06919E+06 1.00000E+00 1.20511E-09 3.92647E-16 4.21221E-15 1.07277E+01 1.20511E-03
3 EMPTY 3 EMPTY 4.67654E+04 1.00000E+00 3.79927E-11 5.12411E-16 1.53199E-15 1.88573E+00 3.79927E-05
4 CNTRL1 4 CNTRL1 1.64545E+04 1.00000E+00 1.30689E-10 7.94244E-15 2.45321E-13 3.08873E+01 1.30689E-04
5 ILSHD 5 ILSHD 1.14315E+05 1.00000E+00 1.29592E-10 1.13363E-15 8.17793E-14 7.21390E+01 1.29592E-04
6 ILREF 6 ILREF 1.14315E+05 1.00000E+00 3.82917E-10 3.34966E-15 7.64827E-15 2.28330E+00 3.82917E-04
7 ILBLK 7 ILBLK 2.85788E+04 1.00000E+00 2.61922E-09 9.16488E-14 1.47837E-13 1.61308E+00 2.61922E-03
8 ICORE 8 ICORE 2.85788E+05 1.00000E+00 3.52194E-07 1.23236E-12 1.85855E-12 1.50813E+00 3.52194E-01
...
24 CNTRL5 24 CNTRL5 2.25167E+04 1.00000E+00 4.16095E-10 1.84794E-14 1.46290E-12 7.91637E+01 4.16095E-04
25 RBLKT 25 RBLKT 9.35307E+05 1.00000E+00 4.46600E-08 4.77490E-14 2.01309E-13 4.21599E+00 4.46600E-02
26 SPOOL 26 SPOOL 2.63445E+06 1.00000E+00 2.07518E-15 7.87711E-22 8.21113E-21 1.04240E+01 2.07518E-09
TOTALS 1.84749E+07 0.00000E+00 1.00000E-06 5.41274E-14 2.88547E-12 5.33089E+01 1.00000E+00
AREA AREA VOLUME INTEGRATION(1) POWER POWER DENSITY PEAK DENSITY PEAK TO AVG. POWER
NO. NAME (CC) WEIGHT FACTOR (WATTS) (WATTS/CC) (WATTS/CC) (2) POWER DENSITY FRACTION
1 ABLKT 2.11310E+05 0.00000E+00 9.99246E-09 4.72881E-14 1.47837E-13 3.12631E+00 9.99246E-03
2 CORE 1.05655E+06 0.00000E+00 9.37491E-07 8.87313E-13 1.85855E-12 2.09459E+00 9.37491E-01
...
1DIF3D 11.0      01/01/12      ADIF3D: Cartesian 3D Test Problem      PAGE 348
0      REGION AND AREA REAL FLUX INTEGRALS FOR K-EFF PROBLEM WITH ENERGY RANGE (EV)      =(4.140E-01,1.000E+07)
0
    REGION ZONE ZONE VOLUME TOTAL FLUX PEAK FLUX (1) TOTAL FAST FLUX PEAK FAST FLUX(1)
    NO. NAME NO. NAME (CC) (NEUTRON-CM/SEC) (NEUTRON/CM2-SEC) (NEUTRON-CM/SEC) (NEUTRON-CM2-SEC)
...
1 SHILD 1 SHILD 6.09162E+06 1.13046E+04 2.84631E-01 7.39012E+03 1.42489E-01
2 RREFL 2 RREFL 3.06919E+06 9.53530E+05 3.20765E+00 3.16887E+05 9.83586E-01
3 EMPTY 3 EMPTY 4.67654E+04 3.99348E+05 1.67623E+01 2.35742E+05 1.05188E+01
4 CNTRL1 4 CNTRL1 1.64545E+04 1.36546E+03 2.09718E+00 9.91719E+02 1.34599E+00
5 ILSHD 5 ILSHD 1.14315E+05 4.53952E+02 2.24827E-01 2.48372E+02 8.77929E-02
6 ILREF 6 ILREF 1.14315E+05 2.97863E+05 6.54609E+00 9.15751E+04 2.87266E+00
7 ILBLK 7 ILBLK 2.85788E+04 1.88484E+05 8.97358E+00 9.12792E+04 4.88918E+00
8 ICORE 8 ICORE 2.85788E+05 3.23957E+06 1.70924E+01 2.05547E+06 1.09261E+01
...
24 CNTRL5 24 CNTRL5 2.25167E+04 6.13369E+02 1.96522E+00 5.07531E+02 1.58247E+00
25 RBLKT 25 RBLKT 9.35307E+05 2.11119E+06 7.25714E+00 1.01234E+06 4.20542E+00
26 SPOOL 26 SPOOL 2.63445E+06 1.37697E+01 5.46143E-05 9.71192E-01 4.32379E-06
TOTALS 1.84749E+07 1.44211E+07 1.70924E+01 7.82556E+06 1.09261E+01
...
AREA AREA VOLUME TOTAL FLUX PEAK FLUX (1) TOTAL FAST FLUX PEAK FAST FLUX(1)
NO. NAME (CC) (NEUTRON-CM/SEC) (NEUTRON/CM2-SEC) (NEUTRON-CM/SEC) (NEUTRON-CM2-SEC)
1 ABLKT 2.11310E+05 7.10623E+05 8.97358E+00 3.52119E+05 4.88918E+00
2 CORE 1.05655E+06 8.62618E+06 1.70924E+01 5.39728E+06 1.09261E+01...
0      REGION REAL FLUX AVERAGES FOR K-EFF PROBLEM WITH ENERGY RANGE (EV)      =(4.140E-01,1.000E+07)
0
    REGION ZONE ZONE VOLUME AVG TOTAL FLUX GROUP GROUP GROUP
    NO. NAME NO. NAME (CC) (NEUTRON/CM2-SEC) 1 2 3
...
1 SHILD 1 SHILD 6.09162E+06 1.85605E-03 1.40737E-04 1.18576E-03 5.29558E-04
2 RREFL 2 RREFL 3.06919E+06 3.10678E-01 8.99118E-03 1.04217E-01 1.97469E-01
3 EMPTY 3 EMPTY 4.67654E+04 8.53940E+00 1.34721E+00 4.08409E+00 3.10810E+00
4 CNTRL1 4 CNTRL1 1.64545E+04 8.29840E-02 1.41100E-02 5.10387E-02 1.78353E-02
5 ILSHD 5 ILSHD 1.14315E+05 3.97105E-03 1.32441E-04 2.25586E-03 1.58275E-03
6 ILREF 6 ILREF 1.14315E+05 2.60563E+00 8.19283E-02 7.95145E-01 1.72856E+00
7 ILBLK 7 ILBLK 2.85788E+04 6.59525E+00 6.60047E-01 2.80168E+00 3.13352E+00
8 ICORE 8 ICORE 2.85788E+05 1.13356E+01 2.06614E+00 5.66788E+00 3.60153E+00
...
24 CNTRL5 24 CNTRL5 2.25167E+04 2.72407E-02 8.81376E-03 1.51771E-02 3.24985E-03
25 RBLKT 25 RBLKT 9.35307E+05 2.25721E+00 1.97656E-01 9.78194E-01 1.08136E+00
26 SPOOL 26 SPOOL 2.63445E+06 5.22679E-06 2.49308E-07 1.31955E-07 4.84553E-06
TOTALS 1.84749E+07 7.80579E-01 1.04765E-01 3.52504E-01 3.23309E-01

```

Figure 3-7. REBUS Output for the Hexagonal Reactor Three Group Test Problem at 4.0 days

## Verification of the REBUS Software

July 2025

```

1DIF3D 11.0 01/01/12 ADIF3D: Cartesian 3D Test Problem PAGE 41
...
Radial inners by group
 2 2 2
=VARIANT|OUTER| TIME(s)|Ups| K-effective | Error |pGS| Fis Max , RMS |TCheby Vecs Dom P0 |Src(s) |j+/- (s)|Phi(s) |
=VARIANT| 1| 0.3|001| 7.887486E-01|2.7E-01| T | 6.93E+00, 3.75E-01| T 0 0.37 0.37| 0.0| 0.1| 0.1|
=VARIANT| 2| 0.3|001| 9.499702E-01|1.7E-01| T | 3.85E+00, 3.34E-01| T 0 0.88 0.88| 0.0| 0.1| 0.1|
=VARIANT| 3| 0.3|001| 1.000989E+00|5.1E-02| T | 1.77E+00, 1.17E-01| T 0 0.45 0.45| 0.0| 0.1| 0.1|
...
=VARIANT| 48| 0.4|001| 1.035664E+00|5.7E-08| F | 9.96E-08, 6.01E-08| T 1 8.50 9.89| 0.0| 0.2| 0.1|
=VARIANT| 49| 0.4|001| 1.035664E+00|3.3E-09| F | 2.40E-08, 3.51E-09| T 0 0.06 0.05| 0.0| 0.2| 0.1|
OUTER ITERATIONS COMPLETED AT ITERATION 49, ITERATIONS HAVE CONVERGED
K-EFFECTIVE = 1.03566415
...
MAXIMUM POWER DENSITY 2.88547E-12 OCCURS AT: RING NO. 4
POSITION NO. 7
SURFACE NO. 6
Z-COORDINATE = 1.70000E+02
(NHSREG) THE PEAK-TO-AVERAGE SEPARABILITY THRESHOLD WAS EXCEEDED IN 4115 MESH CELLS.
(NHSREG) THE PEAK-TO-AVERAGE SEPARABILITY THRESHOLD WAS EXCEEDED IN 3992 MESH CELLS.
1DIF3D 11.0 01/01/12 ADIF3D: Cartesian 3D Test Problem PAGE 43
0 REGION AND AREA POWER INTEGRALS FOR K-EFF PROBLEM WITH ENERGY RANGE (EV) =(4.140E-01,1.000E+07)
REGION ZONE ZONE VOLUME INTEGRATION(1) POWER POWER DENSITY PEAK DENSITY PEAK TO AVG. POWER
NO. NAME NO. NAME (CC) WEIGHT FACTOR (WATTS) (WATTS/CC) (WATTS/CC) (2) POWER DENSITY FRACTION
...
1 SHILD 11 ZSHLD 6.09162E+06 1.00000E+00 2.61536E-09 4.29338E-16 8.92585E-14 2.07898E+02 2.61536E-03
2 RREFL 10 ZRREF 3.06919E+06 1.00000E+00 1.20511E-09 3.92647E-16 4.21221E-15 1.07277E+01 1.20511E-03
3 EMPTY 12 ZSPOOL 4.67654E+04 1.00000E+00 3.79927E-11 8.12411E-16 1.53199E-15 1.88573E+00 3.79927E-05
4 CNTRL1 5 ZCNTR1 1.64545E+04 1.00000E+00 1.30689E-10 7.94244E-15 2.45321E-13 3.08873E+01 1.30689E-04
5 ILSHD 11 ZSHLD 1.14315E+05 1.00000E+00 1.29592E-10 8.13363E-15 8.17792E-14 7.21390E+01 1.29592E-04
6 ILREF 10 ZRREF 1.14315E+05 1.00000E+00 3.82917E-10 3.34966E-15 7.64827E-15 2.28330E+00 3.82917E-04
7 ILBLK 3 ZABLKT 2.85788E+04 1.00000E+00 2.61922E-09 9.16488E-14 1.47837E-13 1.61308E+00 2.61922E-03
8 ICORE 1 ZIFUEL 2.85788E+05 1.00000E+00 3.52194E-07 1.23236E-12 1.85856E-12 1.50813E+00 3.52194E-01
...
24 CNTRL5 8 ZCNTR4 2.25167E+04 1.00000E+00 4.16095E-10 1.84794E-14 1.46290E-12 7.91637E+01 4.16095E-04
25 RBLKT 4 ZRBLKT 9.35307E+05 1.00000E+00 4.46600E-08 4.77490E-14 2.01309E-13 4.21599E+00 4.46600E-02
26 SPOOL 12 ZSPOOL 2.63445E+06 1.00000E+00 2.07518E-15 7.87711E-22 8.21113E-21 1.04240E+01 2.07518E-09
TOTALS 1.84749E+07 0.00000E+00 1.00000E-06 5.41274E-14 2.88547E-12 5.33089E+01 1.00000E+00
...
AREA AREA VOLUME INTEGRATION(1) POWER POWER DENSITY PEAK DENSITY PEAK TO AVG. POWER
NO. NAME (CC) WEIGHT FACTOR (WATTS) (WATTS/CC) (WATTS/CC) (2) POWER DENSITY FRACTION
1 ABLKT 2.11310E+05 0.00000E+00 9.99246E-09 4.72881E-14 1.47837E-13 3.12631E+00 9.99246E-03
2 CORE 1.05655E+06 0.00000E+00 9.37491E-07 8.87313E-13 1.85856E-12 2.09459E+00 9.37491E-01
...
1DIF3D 11.0 01/01/12 ADIF3D: Cartesian 3D Test Problem PAGE 47
0 REGION AND AREA REAL FLUX INTEGRALS FOR K-EFF PROBLEM WITH ENERGY RANGE (EV) =(4.140E-01,1.000E+07)
REGION ZONE ZONE VOLUME TOTAL FLUX PEAK FLUX (1) TOTAL FAST FLUX PEAK FAST FLUX(1)
NO. NAME NO. NAME (CC) (NEUTRON-CM/SEC) (NEUTRON/CM2-SEC) (NEUTRON-CM/SEC) (NEUTRON/CM2-SEC)
1 SHILD 11 ZSHLD 6.09162E+06 1.13064E+04 2.84631E-01 7.39012E+03 1.42489E-01
2 RREFL 10 ZRREF 3.06919E+06 9.53530E+05 3.20765E+00 3.16887E+05 9.83586E-01
3 EMPTY 12 ZSPOOL 4.67654E+04 3.99348E+05 1.67623E+01 2.35742E+05 1.05188E+01
4 CNTRL1 5 ZCNTR1 1.64545E+04 1.36546E+03 2.09718E+00 9.91719E+02 1.34599E+00
5 ILSHD 11 ZSHLD 1.14315E+05 4.53952E+02 2.24827E-01 2.48372E+02 8.77929E-02
6 ILREF 10 ZRREF 1.14315E+05 2.97863E+05 6.54609E+00 9.15751E+04 2.87266E+00
7 ILBLK 3 ZABLKT 2.85788E+04 1.88484E+05 8.97358E+00 9.12792E+04 4.88918E+00
8 ICORE 1 ZIFUEL 2.85788E+05 3.23957E+06 1.70924E+01 2.05547E+06 1.09261E+01
...
24 CNTRL5 8 ZCNTR4 2.25167E+04 6.13369E+02 1.96522E+00 5.07531E+02 1.58247E+00
25 RBLKT 4 ZRBLKT 9.35307E+05 2.11119E+06 7.25714E+00 1.01234E+06 4.20542E+00
26 SPOOL 12 ZSPOOL 2.63445E+06 1.37697E+01 5.46142E-05 9.71193E-01 4.32379E-06
TOTALS 1.84749E+07 1.44211E+07 1.70924E+01 7.82556E+06 1.09261E+01
...
AREA AREA VOLUME TOTAL FLUX PEAK FLUX (1) TOTAL FAST FLUX PEAK FAST FLUX(1)
NO. NAME (CC) (NEUTRON-CM/SEC) (NEUTRON/CM2-SEC) (NEUTRON-CM/SEC) (NEUTRON/CM2-SEC)
1 ABLKT 2.11310E+05 7.10623E+05 8.97358E+00 3.52119E+05 4.88918E+00
2 CORE 1.05655E+06 8.62618E+06 1.70924E+01 5.39728E+06 1.09261E+01
...
1DIF3D 11.0 01/01/12 ADIF3D: Cartesian 3D Test Problem PAGE 49
0 REGION REAL FLUX AVERAGES FOR K-EFF PROBLEM WITH ENERGY RANGE (EV) =(4.140E-01,1.000E+07)
REGION ZONE ZONE VOLUME AVG TOTAL FLUX GROUP GROUP GROUP
NO. NAME NO. NAME (CC) (NEUTRON/CM2-SEC) 1 2 3
...
1 SHILD 11 ZSHLD 6.09162E+06 1.85605E-03 1.40737E-04 1.18576E-03 5.29558E-04
2 RREFL 10 ZRREF 3.06919E+06 3.10678E-01 8.99118E-03 1.04217E-01 1.97469E-01
3 EMPTY 12 ZSPOOL 4.67654E+04 8.53940E+00 1.34721E+00 4.08409E+00 3.10810E+00
4 CNTRL1 5 ZCNTR1 1.64545E+04 8.29840E-02 1.41100E-02 5.10387E-02 1.78353E-02
5 ILSHD 11 ZSHLD 1.14315E+05 3.97105E-03 1.32441E-04 2.25586E-03 1.58275E-03
6 ILREF 10 ZRREF 1.14315E+05 2.60563E+00 8.19283E-02 7.95145E-01 1.72856E+00
7 ILBLK 3 ZABLKT 2.85788E+04 6.59525E+00 6.60047E-01 2.80168E+00 3.13352E+00
8 ICORE 1 ZIFUEL 2.85788E+05 1.13356E+01 2.06614E+00 5.66788E+00 3.60153E+00
...
24 CNTRL5 8 ZCNTR4 2.25167E+04 2.72407E-02 8.81376E-03 1.51771E-02 3.24985E-03
25 RBLKT 4 ZRBLKT 9.35307E+05 2.25721E+00 1.97656E-01 9.78194E-01 1.08136E+00
26 SPOOL 12 ZSPOOL 2.63445E+06 5.22679E-06 2.49308E-07 1.31955E-07 4.84553E-06
TOTALS 1.84749E+07 7.80579E-01 1.04765E-01 3.52504E-01 3.23309E-01
...
1DIF3D 11.0 01/01/12 ADIF3D: Cartesian 3D Test Problem PAGE 50

```

Figure 3-8. DIF3D Output for the Hexagonal Reactor Three Group Test Problem

The DIF3D section of output from REBUS for the hexagonal benchmark problem at time point 4 is provided in Figure 3-11. The DIF3D output when using the binary interface files at time point are used is provided in Figure 3-12 where the DIF3D output for the A.NIP3 based input was already provided in Figure 3-8. A comparison of the DIF3D and REBUS results for this problem are all found to be identical except for the page numbering.

|             |          |             |          |
|-------------|----------|-------------|----------|
| NDXSRF_0000 | 0.000000 | NDXSRF_0000 | 0.000000 |
| GEODST_0000 | 0.000000 | RFILES_0000 | 0.000000 |
| GEODST_0001 | 1.000000 | RFILES_0001 | 1.000000 |
| GEODST_0002 | 1.000000 | RFILES_0002 | 1.000000 |
| GEODST_0003 | 2.000000 | RFILES_0003 | 2.000000 |
| GEODST_0004 | 2.000000 | RFILES_0004 | 2.000000 |
| GEODST_0005 | 3.000000 | RFILES_0005 | 3.000000 |
| GEODST_0006 | 3.000000 | RFILES_0006 | 3.000000 |
| GEODST_0007 | 4.000000 | RFILES_0007 | 4.000000 |
| GEODST_0008 | 4.000000 | RFILES_0008 | 4.000000 |
| GEODST_0009 | 5.000000 | RFILES_0009 | 5.000000 |
| LABELS_0000 | 0.000000 | ZNATDN_0000 | 0.000000 |
| LABELS_0001 | 1.000000 | ZNATDN_0001 | 1.000000 |
| LABELS_0002 | 1.000000 | ZNATDN_0002 | 1.000000 |
| LABELS_0003 | 2.000000 | ZNATDN_0003 | 2.000000 |
| LABELS_0004 | 2.000000 | ZNATDN_0004 | 2.000000 |
| LABELS_0005 | 3.000000 | ZNATDN_0005 | 3.000000 |
| LABELS_0006 | 3.000000 | ZNATDN_0006 | 3.000000 |
| LABELS_0007 | 4.000000 | ZNATDN_0007 | 4.000000 |
| LABELS_0008 | 4.000000 | ZNATDN_0008 | 4.000000 |
| LABELS_0009 | 5.000000 | ZNATDN_0009 | 5.000000 |

**Figure 3-9. Binary Interface Files Created by REBUS for the Hexagonal Test Problem**

```
BLOCK=OLD
DATASET=NDXSRF
DATASET=LABELS
DATASET=GEODST
DATASET=ZNATDN
BLOCK=STP021,3
UNFORM=A.SUMMAR
01          10    0    0    0    0    0    1
UNFORM=A.DIF3D
01  ADIF3D: Cartesian 3D Test Problem
02  1000000 1000000    0
03    0    0    0    0    99    0    0    5    0    0    0
04    0    0    0    0    00    00    10    100    0    1    0    0
05    5.0E-8    1.0E-7    1.0E-6
06    1.0    .001    .005    1.0E-6
12  60601    11    0    0    0    0    0    0    0    0    0
UNFORM=A.HMG4C
01  HMG4C: Cartesian 3D Test Problem
02  999999    1    0    0    0    1    1    0
```

**Figure 3-10. DIF3D Input when using the Binary Interface Files**

The requirements state that we must demonstrate that the boundary conditions and general input (region, composition, and mapping between them) is consistent with regard to DIF3D usage within REBUS. The preceding verification test problem demonstrates all of these aspects as the input with DIF3D and REBUS are identical except for the addition of the A.STP027 and A.BURN input necessary for REBUS to execute. The preceding work demonstrates that the DIF3D section of output at each time point is not impacted by REBUS and thus the DIF3D output does not have to be verified again. The preceding work also demonstrates that the binary files generated by REBUS are consistent with the DIF3D calculations at each given time point and are the correct translation of the ascii based input.

## Verification of the REBUS Software

July 2025

```

=VARIANT|OUTER| TIME(s)|Ups| K-effective | Error |pGS| Fis Max , RMS |TCheby Vecs Dom P0 |Src(s) |j+/- (s)|Phi(s) |
=VARIANT| 1| 0.3|001| 1.035664E+00|4.2E-08| T | 5.48E-08, 4.18E-08| T 0 0.00 0.00| 0.0| 0.1| 0.1|
=VARIANT| 2| 0.3|001| 1.035664E+00|6.3E-10| F | 1.24E-08, 4.71E-09| T 0 0.11 0.11| 0.0| 0.2| 0.1|
    OUTER ITERATIONS COMPLETED AT ITERATION 2, ITERATIONS HAVE CONVERGED
    K-EFFECTIVE = 1.03566416
1DIF3D 11.0 01/01/12 ADIF3D: Hexagonal 3D Test Problem PAGE 344
...
    REGION ZONE ZONE VOLUME INTEGRATION(1) POWER POWER DENSITY PEAK DENSITY PEAK TO AVG. POWER
    NO. NAME NO. NAME (CC) WEIGHT FACTOR (WATTS) (WATTS/CC) (WATTS/CC) (2) POWER DENSITY FRACTION
    1 SHILD 1 SHILD 6.09162E+06 1.00000E+00 2.61536E-09 4.29338E-16 8.92585E-14 2.07898E+02 2.61536E-03
    2 RREFL 2 RREFL 3.06919E+06 1.00000E+00 1.20511E-09 3.92647E-16 4.21221E-15 1.07277E+01 1.20511E-03
    3 EMPTY 3 EMPTY 4.67654E+04 1.00000E+00 3.79927E-11 8.12411E-16 1.53199E-15 1.88573E+00 3.79927E-05
    4 CNTRL1 4 CNTRL1 1.64545E+04 1.00000E+00 1.30689E-10 7.94244E-15 2.45321E-13 3.08873E+01 1.30689E-04
    5 ILSHD 5 ILSHD 1.14315E+05 1.00000E+00 1.29592E-10 1.13363E-15 8.17793E-14 7.21390E+01 1.29592E-04
    6 ILREF 6 ILREF 1.14315E+05 1.00000E+00 3.82917E-10 3.34966E-15 7.64827E-15 2.28330E+00 3.82917E-04
...
1DIF3D 11.0 01/01/12 ADIF3D: Hexagonal 3D Test Problem PAGE 348
0 REGION AND AREA REAL FLUX INTEGRALS FOR K-EFF PROBLEM WITH ENERGY RANGE (EV) =(4.140E-01,1.000E+07)
    REGION ZONE ZONE VOLUME TOTAL FLUX PEAK FLUX (1) TOTAL FAST FLUX PEAK FAST FLUX(1)
    NO. NAME NO. NAME (CC) (NEUTRON-CM/SEC) (NEUTRON-CM2-SEC) (NEUTRON-CM/SEC) (NEUTRON-CM2-SEC)
    1 SHILD 1 SHILD 6.09162E+06 1.13064E+04 2.84631E-01 7.39012E+03 1.42489E-01
    2 RREFL 2 RREFL 3.06919E+06 9.53530E+05 3.20765E+00 3.16887E+05 9.83586E-01
    3 EMPTY 3 EMPTY 4.67654E+04 3.99348E+05 1.67623E+01 2.35742E+05 1.05188E+01
    4 CNTRL1 4 CNTRL1 1.64545E+04 1.36546E+03 2.09718E+00 9.91719E+02 1.34599E+00
    5 ILSHD 5 ILSHD 1.14315E+05 4.53952E+02 2.24827E-01 2.48372E+02 8.77929E-02
    6 ILREF 6 ILREF 1.14315E+05 2.97863E+05 6.54609E+00 9.15751E+04 2.87266E+00
...
0 ENTERING ROUTINE TO WRITE REACTION SUMMARY
...
0 K EFFECTIVE 1.035664201
OPOWER(WATTS) 1.00000E-06
PEAK/AV. POWER IN CORE 2.09460E+00
PEAK/AV. FISSION RATE IN CORE 2.02027E+00
PERCENT FISS IN FERTILE MATL 1.54207E+01
FUEL ABSORP./FISS IN CORE 1.89972E+00
MEDIAN ENERGIES IN CORE
    SOURCE 2.08580E+05
    ABSORPTION 3.68688E+04
    FLUX 1.79180E+05
...
1STP027 8.1 04/30/08 PAGE 352

```

Figure 3-11. REBUS Output for the Hexagonal Reactor Three Group Test Problem at 4 days

```

Radial inners by group
2 2 2
=VARIANT|OUTER| TIME(s)|Ups| K-effective | Error |pGS| Fis Max , RMS |TCheby Vecs Dom P0 |Src(s) |j+/- (s)|Phi(s) |
=VARIANT| 1| 0.3|001| 7.887486E-01|2.7E-01| T | 6.93E+00, 3.75E-01| T 0 0.37 0.37| 0.0| 0.1| 0.1|
=VARIANT| 2| 0.3|001| 9.499702E-01|1.7E-01| T | 3.85E+00, 3.34E-01| T 0 0.88 0.88| 0.0| 0.1| 0.1|
=VARIANT| 3| 0.3|001| 1.000989E+00|5.1E-02| T | 1.77E+00, 1.17E-01| T 0 0.45 0.45| 0.0| 0.1| 0.1|
...
=VARIANT| 47| 0.4|001| 1.035664E+00|5.9E-08| F | 7.31E-08, 7.07E-09| T 0 0.12 0.10| 0.0| 0.2| 0.1|
=VARIANT| 48| 0.4|001| 1.035664E+00|5.7E-08| F | 9.96E-08, 6.01E-08| T 1 8.50 0.89| 0.0| 0.2| 0.1|
=VARIANT| 49| 0.4|001| 1.035664E+00|3.3E-09| F | 2.40E-08, 3.51E-09| T 0 0.06 0.05| 0.0| 0.2| 0.1|
    OUTER ITERATIONS COMPLETED AT ITERATION 49, ITERATIONS HAVE CONVERGED
    K-EFFECTIVE = 1.03566415
1DIF3D 11.0 01/01/12 ADIF3D: Cartesian 3D Test Problem PAGE 15
...
    REGION ZONE ZONE VOLUME INTEGRATION(1) POWER POWER DENSITY PEAK DENSITY PEAK TO AVG. POWER
    NO. NAME NO. NAME (CC) WEIGHT FACTOR (WATTS) (WATTS/CC) (WATTS/CC) (2) POWER DENSITY FRACTION
    1 SHILD 1 SHILD 6.09162E+06 1.00000E+00 2.61536E-09 4.29338E-16 8.92585E-14 2.07898E+02 2.61536E-03
    2 RREFL 2 RREFL 3.06919E+06 1.00000E+00 1.20511E-09 3.92647E-16 4.21221E-15 1.07277E+01 1.20511E-03
    3 EMPTY 3 EMPTY 4.67654E+04 1.00000E+00 3.79927E-11 8.12411E-16 1.53199E-15 1.88573E+00 3.79927E-05
    4 CNTRL1 4 CNTRL1 1.64545E+04 1.00000E+00 1.30689E-10 7.94244E-15 2.45321E-13 3.08873E+01 1.30689E-04
    5 ILSHD 5 ILSHD 1.14315E+05 1.00000E+00 1.29592E-10 1.13363E-15 8.17792E-14 7.21390E+01 1.29592E-04
    6 ILREF 6 ILREF 1.14315E+05 1.00000E+00 3.82917E-10 3.34966E-15 7.64827E-15 2.28330E+00 3.82917E-04
...
1DIF3D 11.0 01/01/12 ADIF3D: Cartesian 3D Test Problem PAGE 19
    REGION ZONE ZONE VOLUME TOTAL FLUX PEAK FLUX (1) TOTAL FAST FLUX PEAK FAST FLUX(1)
    NO. NAME NO. NAME (CC) (NEUTRON-CM/SEC) (NEUTRON-CM2-SEC) (NEUTRON-CM/SEC) (NEUTRON-CM2-SEC)
    1 SHILD 1 SHILD 6.09162E+06 1.13064E+04 2.84631E-01 7.39012E+03 1.42489E-01
    2 RREFL 2 RREFL 3.06919E+06 9.53530E+05 3.20765E+00 3.16887E+05 9.83586E-01
    3 EMPTY 3 EMPTY 4.67654E+04 3.99348E+05 1.67623E+01 2.35742E+05 1.05188E+01
    4 CNTRL1 4 CNTRL1 1.64545E+04 1.36546E+03 2.09718E+00 9.91719E+02 1.34599E+00
    5 ILSHD 5 ILSHD 1.14315E+05 4.53952E+02 2.24827E-01 2.48372E+02 8.77929E-02
    6 ILREF 6 ILREF 1.14315E+05 2.97863E+05 6.54609E+00 9.15751E+04 2.87266E+00
...
0 ENTERING ROUTINE TO WRITE REACTION SUMMARY
...
0 K EFFECTIVE 1.035664201
OPOWER(WATTS) 1.00000E-06
PEAK/AV. POWER IN CORE 2.09460E+00
PEAK/AV. FISSION RATE IN CORE 2.02027E+00
PERCENT FISS IN FERTILE MATL 1.54207E+01
FUEL ABSORP./FISS IN CORE 1.89972E+00
MEDIAN ENERGIES IN CORE
    SOURCE 2.08580E+05
    ABSORPTION 3.68688E+04
    FLUX 1.79180E+05

```

Figure 3-12. DIF3D Output Using the REBUS Binaries at 4 days

## 3.2 DIF3D Consistency Verification using a VTR Problem

The VTR geometry is taken from reference [15]. The REBUS model chosen is an equilibrium cycle calculation where fuel is fabricated at BOC for four equilibrium regions: I1FUE, I2FUE, O1FUE, and O2FUE. These regions have 3, 4, 5, and 6 batches, respectively, which means the fuel mixture placed in each region contains fuel at BOC between freshly fabricated and up to 5 cycles of residence. The cycle time is 100 days with 75 days of shutdown between cycles. Table 3-2 is the reproduced reactor characteristics detail created for the VTR design work.

**Table 3-2. Reproduced Table 5 from ECAR 4647.**

| Characteristic                                | Unit                                  | Homogeneous | Discrete      |
|---|---------------------------------------|-------------|---------------|
| Core power                                    | MW <sub>th</sub>                      | 300         |               |
| Cycle length                                  | EFPD                                  | 100         |               |
| Number of batches                             | -                                     | 3 to 6      |               |
| Plutonium concentration                       | wt.%                                  | 20.14%      |               |
| Uranium enrichment                            | at.%                                  | 5%          |               |
| Maximum excess reactivity                     | pcm                                   | 2186        | 2270          |
| Burnup reactivity swing                       | pcm                                   | 2186        | 2180-2188     |
|   |                                       |             |               |
| Test peak fast flux at BOC                    | $\times 10^{15}$ n/cm <sup>2</sup> -s | 4.34        | 4.33-4.34     |
| Test peak fast flux at EOC                    | $\times 10^{15}$ n/cm <sup>2</sup> -s | 4.23        | 4.24-4.25     |
| Absolute peak fast flux at BOC                | $\times 10^{15}$ n/cm <sup>2</sup> -s | 4.54        | 4.54-4.56     |
| Absolute peak fast flux at EOC                | $\times 10^{15}$ n/cm <sup>2</sup> -s | 4.43        | 4.43-4.45     |
| Average assembly power                        | MW <sub>th</sub>                      | 4.55        |               |
| Maximum assembly power at BOC                 | MW <sub>th</sub>                      | 6.45        | 6.70-6.74     |
| Maximum assembly power at EOC                 | MW <sub>th</sub>                      | 6.17        | 6.41-6.44     |
| Maximum absolute power variation              | MW <sub>th</sub>                      | 0.28        | 0.30-0.30     |
| Maximum relative power variation <sup>a</sup> | -                                     | 7.1%        | 7.2%-7.4%     |
|   |                                       |             |               |
| Fuel assemblies/cycle                         | -                                     | 14.9        | 14-16         |
| Heavy metal charge/cycle                      | kg/cycle                              | 596.2       | 560.1-640.2   |
| Uranium required/cycle                        | kg/cycle                              | 462.8       | 434.8-496.9   |
| Plutonium required/cycle                      | kg/cycle                              | 133.4       | 125.4-143.3   |
| Fuel assemblies/year                          | -                                     | 44.7        | 44-46         |
| Heavy metal charge/year                       | kg/year                               | 1788.7      | 1760.5-1840.5 |
| Uranium required/year                         | kg/year                               | 1388.4      | 1366.5-1428.6 |
| Plutonium required/year                       | kg/year                               | 400.3       | 394.0-411.9   |
|   |                                       |             |               |
| Average discharge burnup                      | GWd/t                                 | 50.3        |               |
| Assembly-averaged peak discharge burnup       | GWd/t                                 | 52.5        | 52.6-52.7     |
| Peak discharge burnup                         | GWd/t                                 | 61.0        | 60.8-61.1     |

<sup>a</sup> Excluding variation in the primary control rods which is 36%

The existing deck, an equilibrium mode problem, should match the homogeneous column of results where the discrete column is the final 6 cycle range from a 60 cycle non-equilibrium calculation with discrete fuel shuffling that provides the real equilibrium state of the reactor. The two columns show that the equilibrium mode approximation in REBUS can quickly provide results consistent with the discrete shuffling non-equilibrium approach. With regard to REBUS verification, the goal of this work is to identify the outputs that appear in REBUS and this table and then demonstrate that the DIF3D restart using the binary files produces the same details. No attempt will be made to take the atom density details included in the regular output and generate an input deck as this problem is very large and the preceding test proved that extracting the atom densities from the regular output is correct. The first excerpt focuses on the DIF3D related outputs which are reproducible while the second excerpt focuses on the REBUS related outputs which are not reproducible with simple DIF3D calculations.

Figure 3-13 shows the DIF3D output taken from the BOC result of REBUS. In Table 3-2, the homogeneous excess reactivity at BOC is reported to be 2186 pcm and the eigenvalue result in Figure 3-13 shows an initial excess reactivity of 2232 pcm (1.0223168).

```
...
DIF3D 11.3072 11/11/19 PAGE 840
...
=VARIANT|OUTER| TIME(s)|Ups| K-effective | Error |pGS| Fis Max , RMS |TCheby Vecs Dom P0 |Src(s) |j+/- (s) |Phi(s) |
=VARIANT| 1| 158.2|001| 1.022317E+00|5.5E-06| T | 6.38E-06, 5.51E-06| T 0 0.00 0.00| 3.4| 82.9| 71.9|
=VARIANT| 2| 171.3|001| 1.022317E+00|2.6E-07| F | 7.86E-07, 4.38E-07| T 0 0.08 0.07| 3.9| 97.1| 70.3|
    OUTER ITERATIONS COMPLETED AT ITERATION 2, ITERATIONS HAVE CONVERGED
    K-EFFECTIVE = 1.02231680

DIF3D 11.3072 11/11/19 PAGE 842
0 REGION AND AREA POWER INTEGRALS FOR K-EFF PROBLEM WITH ENERGY RANGE (EV) = (0.000E+00, 1.419E+07)
  REGION ZONE ZONE VOLUME INTEGRATION(1) POWER POWER DENSITY PEAK DENSITY PEAK TO AVG. POWER
  NO. NAME NO. NAME (CC) WEIGHT FACTOR (WATTS) (WATTS/CC) (WATTS/CC) (2) POWER DENSITY FRACTION
...
  8 I20101 8 I20101 3.85290E+03 1.00000E+00 1.30071E+02 3.37593E-02 6.16827E-02 1.82713E+00 4.33572E-07
  9 I20102 9 I20102 1.03586E+04 1.00000E+00 1.49504E+04 1.44328E+00 3.47992E+00 2.41113E+00 4.98345E-05
 10 I20103 10 I20103 1.01060E+03 1.00000E+00 1.38125E+03 1.36677E+00 1.40504E+00 1.02800E+00 4.60417E-06
 11 I20104 11 I20104 9.60068E+02 1.00000E+00 1.97363E+03 2.05572E+00 2.31788E+00 1.12753E+00 6.57877E-06
 12 I20105 12 I20105 2.12819E+03 1.00000E+00 1.07223E+06 5.03823E+02 5.88321E+02 1.16771E+00 3.57411E-03
 13 I20106 13 I20106 2.12819E+03 1.00000E+00 1.34264E+06 6.30883E+02 6.86926E+02 1.08883E+00 4.47547E-03
 14 I20107 14 I20107 2.12819E+03 1.00000E+00 1.43811E+06 6.75745E+02 6.94189E+02 1.02730E+00 4.79372E-03
 15 I20108 15 I20108 2.12819E+03 1.00000E+00 1.30654E+06 6.13920E+02 6.79177E+02 1.10630E+00 4.35514E-03
 16 I20109 16 I20109 2.12807E+03 1.00000E+00 9.91712E+05 4.66015E+02 5.62376E+02 1.20677E+00 3.30571E-03
 17 I2010A 17 I2010A 3.02586E+03 1.00000E+00 3.06353E+03 1.01245E+00 1.10138E+00 1.08784E+00 1.02118E-05
 18 I2010B 18 I2010B 6.85476E+03 1.00000E+00 3.49574E+03 5.09973E-01 8.92513E-01 1.75012E+00 1.16525E-05
 19 I2010C 19 I2010C 6.63205E+02 1.00000E+00 2.83177E+02 4.26983E-01 4.97982E-01 1.16628E+00 9.43923E-07
 20 I2010D 20 I2010D 7.57948E+03 1.00000E+00 1.38868E+03 1.83239E-01 6.27728E-01 3.42573E+00 4.62952E-06
 21 I2010E 21 I2010E 3.78974E+03 1.00000E+00 1.70729E+01 4.50502E-03 8.56051E-03 1.90022E+00 5.69095E-08
...
DIF3D 11.3072 11/11/19 PAGE 1025
0 REGION AND AREA REAL FLUX INTEGRALS FOR K-EFF PROBLEM WITH ENERGY RANGE (EV) = (0.000E+00, 1.419E+07)
  REGION ZONE ZONE VOLUME TOTAL FLUX PEAK FLUX (1) TOTAL FAST FLUX PEAK FAST FLUX (1)
  NO. NAME NO. NAME (CC) (NEUTRON-CM/SEC) (NEUTRON-CM2-SEC) (NEUTRON-CM/SEC) (NEUTRON-CM2-SEC)
  1 T10101 1 T10101 3.85290E+03 7.88997E+16 4.03813E+13 8.18266E+15 5.13735E+12
  2 T10102 2 T10102 1.13692E+04 9.03520E+18 2.91051E+15 3.33369E+18 1.58994E+15
  3 T10103 3 T10103 4.98983E+03 2.21428E+19 5.73425E+15 1.49382E+19 4.08755E+15
  4 T10104 4 T10104 2.52649E+03 1.47761E+19 5.97832E+15 1.05185E+19 4.30290E+15
  5 T10105 5 T10105 1.46284E+04 2.98270E+19 5.65913E+15 1.79115E+19 4.03747E+15
  6 T10106 6 T10106 7.57948E+03 4.39642E+17 2.21868E+14 8.17603E+16 4.95201E+13
...
  13 I20106 13 I20106 2.12819E+03 1.14552E+19 5.86526E+15 8.31949E+18 4.29851E+15
  14 I20107 14 I20107 2.12819E+03 1.23444E+19 5.95350E+15 9.01067E+18 4.36002E+15
  15 I20108 15 I20108 2.12819E+03 1.11412E+19 5.79245E+15 8.10093E+18 4.24934E+15
...
```

Figure 3-13. REBUS VTR Problem BOC DIF3D Excerpt

In Table 3-2, the peak assembly power at BOC is reported to be 6.45 MWt and the POWER (WATTS) column for regions I20101 to I2010E (the inner most assembly) from Figure 3-13 sums to 6.18 MWt. The test peak fast flux in Table 3-2 is reported to be 4.34E15 n/cm<sup>2</sup>-s while the value from region T10104, the center 20 cm of the test region, in Figure 3-13 is 4.30E15 n/cm<sup>2</sup>-s. Finally, the absolute overall peak fast flux is reported as 4.54E15 n/cm<sup>2</sup>-s while the peak fast flux of region I20107 from Figure 3-13 is 4.36E15 n/cm<sup>2</sup>-s.

As can be seen, these results are not identical, but are within the standard error associated with different cross section processing schemes and material feeds that were being studied for the design work of VTR. With the exception of the absolute peak fast flux result, the errors between the reported numbers and those taken from this REBUS output are negligible. This is especially since no effort was taken in this study to identify the assembly with the peak power or fast flux. This latter aspect is the likely reason why the absolute peak fast flux is not consistent.

Figure 3-14 provides the EOC excerpt of DIF3D results taken from the REBUS output. As seen, the EOC  $k_{eff}$  value is nearly 1.0 which is consistent with the desired operation of the plant. In Table 3-2, the peak assembly power at BOC is reported to be 6.17 MWt and the POWER (WATTS) column for regions I20101 to I2010E (the inner most assembly) from Figure 3-14 sums to 6.06 MWt. The test peak fast flux in Table 3-2 is reported to be 4.23E15 n/cm<sup>2</sup>-s while the value from region T10104, the center 20 cm of the test region, in Figure 3-14 is 4.37E15 n/cm<sup>2</sup>-s. Finally, the absolute overall peak fast flux is reported as 4.43E15 n/cm<sup>2</sup>-s while the peak fast flux of region I20107 from Figure 3-14 is 4.43E15 n/cm<sup>2</sup>-s. As was the case with the BOC results, most of the details are similar, but are not identical which is not entirely important for the current verification work.

```
.....
=VARIANT|OUTER| TIME(s)|Ups| K-effective | Error |pGS| Fis Max , RMS |TCheby Vecs Dom P0 |Src(s) |j+/- (s) |Phi(s) |
=VARIANT| 1| 154.6|001| 9.999514B-01|2.8E-04| T | 3.08E-04, 2.81E-04| T 0 0.00 0.001| 5.3| 80.6| 68.7|
=VARIANT| 2| 158.8|001| 9.999576B-01|6.2E-06| T | 2.04E-05, 1.51E-05| T 0 0.05 0.051| 5.2| 82.9| 70.7|
=VARIANT| 3| 179.4|001| 9.999698E-01|1.2E-05| F | 1.68E-05, 1.34E-05| T 0 0.89 0.991| 5.4| 103.3| 70.8|
=VARIANT| 4| 158.9|001| 9.999703B-01|5.4E-07| T | 3.45E-06, 1.95E-06| T 0 0.15 0.141| 5.4| 83.1| 70.4|
=VARIANT| 5| 186.8|001| 9.999699E-01|4.8E-07| F | 1.08E-06, 5.32E-07| T 1 0.27 0.281| 5.4| 107.6| 73.8|
    OUTER ITERATIONS COMPLETED AT ITERATION 5, ITERATIONS HAVE CONVERGED
    K-EFFECTIVE = 0.99996986
DIF3D 11.3072 11/11/19                                              PAGE 3052
.....
DIF3D 11.3072 11/11/19                                              PAGE 3053
0   REGION AND AREA POWER INTEGRALS FOR K-EFF PROBLEM WITH ENERGY RANGE (EV) = (0.000E+00, 1.419E+07)
    REGION  ZONE  ZONE      VOLUME   INTEGRATION(1)   POWER   POWER DENSITY  PEAK DENSITY  PEAK TO AVG.  POWER
    NO.     NAME   NO.     NAME      (CC)      WEIGHT FACTOR (WATTS) (WATTS) (WATTS/CC) (WATTS/CC) (2) POWER DENSITY FRACTION
.....
8  I20101   8  I20101  3.85290E+03  1.00000E+00  1.33229E+02  3.45789E-02  6.31790E-02  1.82710E+00  4.44097E-07
9  I20102   9  I20102  1.03586E+04  1.00000E+00  1.53584E+04  1.48267E+00  3.58363E+00  2.41702E+00  5.11947E-05
10 I20103  10  I20103  1.01060E+03  1.00000E+00  1.42289E+03  1.40797E+00  1.44685E+00  1.02762E+00  4.74296E-06
11 I20104  11  I20104  9.60068E+02  1.00000E+00  2.03403E+03  2.11863E+00  2.38803E+00  1.12716E+00  6.78011E-06
12 I20105  12  I20105  2.12819E+03  1.00000E+00  1.06195E+06  4.98993E+02  5.81841E+02  1.16603E+00  3.53984E-03
13 I20106  13  I20106  2.12819E+03  1.00000E+00  1.31562E+06  6.18186E+02  6.72302E+02  1.08754E+00  4.38540E-03
14 I20107  14  I20107  2.12819E+03  1.00000E+00  1.40390E+06  6.59666E+02  6.77284E+02  1.02671E+00  4.67965E-03
15 I20108  15  I20108  2.12819E+03  1.00000E+00  1.28310E+06  6.02907E+02  6.65808E+02  1.10433E+00  4.27701E-03
16 I20109  16  I20109  2.12807E+03  1.00000E+00  9.86760E+05  4.63669E+02  5.58528E+02  1.20453E+00  3.28920E-03
17 I2010A  17  I2010A  3.02586E+03  1.00000E+00  3.16275E+03  1.04524E+00  1.13702E+00  1.08781E+00  1.05425E-05
18 I2010B  18  I2010B  6.85476E+03  1.00000E+00  3.60278E+03  5.25588E-01  9.20908E-01  1.75215E+00  1.20093E-05
19 I2010C  19  I2010C  6.63205E+02  1.00000E+00  2.91364E+02  4.39327E-01  5.12493E-01  1.16654E+00  9.71212E-07
20 I2010D  20  I2010D  7.57948E+03  1.00000E+00  1.42731E+03  1.88312E-01  6.45814E-01  3.42949E+00  4.75769E-06
21 I2010E  21  I2010E  3.78974E+03  1.00000E+00  1.75153E+01  4.62176E-03  8.78275E-03  1.90031E+00  5.83842E-08
.....
DIF3D 11.3072 11/11/19                                              PAGE 3236
0   REGION AND AREA REAL FLUX INTEGRALS FOR K-EFF PROBLEM WITH ENERGY RANGE (EV) = (0.000E+00, 1.419E+07)
    REGION  ZONE  ZONE      VOLUME   TOTAL FLUX   PEAK FLUX (1)   TOTAL FAST FLUX PEAK FAST FLUX(1)
    NO.     NAME   NO.     NAME      (CC)      (NEUTRON-CM/SEC) (NEUTRON-CM2/SEC) (NEUTRON-CM/SEC) (NEUTRON-CM2-SEC)
.....
1  T10101   1  T10101  3.85290E+03  8.07699E+16  4.13363E+13  8.36555E+15  5.25146E+12
2  T10102   2  T10102  1.13692E+04  9.25843E+18  2.98174E+15  3.40274E+18  1.62098E+15
3  T10103   3  T10103  4.98983E+03  2.26556E+19  5.85938E+15  1.52057E+19  4.15336E+15
4  T10104   4  T10104  2.52649E+03  1.50991E+19  6.10721E+15  1.06872E+19  4.37055E+15
5  T10105   5  T10105  1.46284E+04  3.05906E+19  5.78620E+15  1.82803E+19  4.10540E+15
6  T10106   6  T10106  7.57948E+03  4.51354E+17  2.27922E+14  8.37881E+16  5.07523E+13
7  T10107   7  T10107  3.78974E+03  1.03528E+16  5.55053E+12  9.61424E+14  6.30931E+11
.....
13 I20106  13  I20106  2.12819E+03  1.17124E+19  5.99105E+15  8.46287E+18  4.36670E+15
14 I20107  14  I20107  2.12819E+03  1.26149E+19  6.08088E+15  9.15804E+18  4.42848E+15
15 I20108  15  I20108  2.12819E+03  1.14039E+19  5.91996E+15  8.25135E+18  4.31959E+15
.....

```

Figure 3-14. REBUS VTR Problem EOC DIF3D Excerpt.

The last aspect to verify are some of the REBUS specific outputs from Table 3-2 where the corresponding REBUS excerpt details are given in Figure 3-15. In Table 3-2 the heavy metal charge per year is reported as 596.2 kg which is consistent with the 596.23 kg computed by summing the CHARGED column of numbers at the top of Figure 3-15. This same column of output data can be used to get the uranium and plutonium loading reported as 462.8 kg and 133.4 kg and computed to be

462.8 kg and 133.43 kg. The average discharge burnup in Table 3-2 is reported as 50.3 GWd/t which is similar to the discharge burnup of 46.6 GWd/t in the middle section of Figure 3-15. Finally, the peak discharge burnup of 61 GWd/t is consistent with the maximum values found in the last section of output in Figure 3-15 of 54.1 GWd/g, 63.7 GWd/t, 66.9 GWd/t, and 65.8 GWd/t for paths ZI1FUE, ZI2FUE, ZO1FUE, and ZO2FUE, respectively. As was the case with the preceding DIF3D excerpts, there are minor differences in these reported results which are negligible for this study and thus the preceding REBUS output excerpts provide the basis for accuracy for the DIF3D calculations that follow.

| EXTERNAL CYCLE SUMMARY IN KILOGRAMS |             |             |               |             |                           |                      | PAGE | 348 |
|-------------------------------------|-------------|-------------|---------------|-------------|---------------------------|----------------------|------|-----|
| ISOTOPE                             | CHARGED     | DISCHARGED  | AFTER COOLING | SOLD        | DELIVERED TO REPROCESSING | LOST IN REPROCESSING |      |     |
| U-234                               | 0.00000E+00 | 4.93635E-03 | 4.93635E-03   | 4.93635E-03 | 0.00000E+00               | 0.00000E+00          |      |     |
| U-235                               | 2.28620E+01 | 1.73913E+01 | 1.73913E+01   | 1.73913E+01 | 0.00000E+00               | 0.00000E+00          |      |     |
| U-236                               | 0.00000E+00 | 1.08765E+00 | 1.08765E+00   | 1.08765E+00 | 0.00000E+00               | 0.00000E+00          |      |     |
| U-238                               | 4.39935E+02 | 4.24725E+02 | 4.24725E+02   | 4.24725E+02 | 0.00000E+00               | 0.00000E+00          |      |     |
| NP237                               | 0.00000E+00 | 1.27900E-01 | 1.27900E-01   | 1.27900E-01 | 0.00000E+00               | 0.00000E+00          |      |     |
| PU236                               | 0.00000E+00 | 1.02045E-06 | 1.02045E-06   | 1.02045E-06 | 0.00000E+00               | 0.00000E+00          |      |     |
| PU238                               | 1.32679E-01 | 1.24841E-01 | 1.24841E-01   | 1.24841E-01 | 0.00000E+00               | 0.00000E+00          |      |     |
| PU239                               | 9.16808E+01 | 8.07121E+01 | 8.07121E+01   | 8.07121E+01 | 0.00000E+00               | 0.00000E+00          |      |     |
| PU240                               | 3.52285E+01 | 3.52506E+01 | 3.52506E+01   | 3.52506E+01 | 0.00000E+00               | 0.00000E+00          |      |     |
| PU241                               | 4.52761E+00 | 4.54806E+00 | 4.54806E+00   | 4.54806E+00 | 0.00000E+00               | 0.00000E+00          |      |     |
| PU242                               | 1.86180E+00 | 1.90346E+00 | 1.90346E+00   | 1.90346E+00 | 0.00000E+00               | 0.00000E+00          |      |     |

| BURNUP SUMMARY BY AREA |                         |  |                          |                                   |  |  | PAGE | 4008 |
|------------------------|-------------------------|--|--------------------------|-----------------------------------|--|--|------|------|
| AREA                   | AVERAGE BURNUP (MWd/MT) | INITIAL LOADING OF FISSIONABLE ISOTOPES (MT) | AVERAGE DAILY POWER (MW) | AVERAGE DISCHARGE BURNUP (MWd/MT) |  |  |      |      |
| ASHIEL                 | 0.0000E+00              | 0.0000E+00                                   | 0.0000E+00               | 0.0000E+00                        |  |  |      |      |
| TCORE                  | 3.0336E+04              | 9.6037E-01                                   | 2.9134E+02               | 4.6576E+04                        |  |  |      |      |

| CUMULATIVE PEAK BURNUP AND FAST FLUENCE AFTER 1 BURNUP SUBSTEPS, FROM 0.000000000E+00 DAYS TO 1.000000000E+02 DAYS. |             |             |             |             |             |             | PAGE        | 4005        |
|---|-------------|-------------|-------------|-------------|-------------|-------------|-------------|-------------|
| PEAK DISCHARGE BURNUP (MWd/MT) OF EACH PATH   |             |             |             |             |             |             |             |             |
| PATH  | ZI1FUE      |
|   | 4.64583E+04 | 5.40677E+04 | 5.45581E+04 | 5.35073E+04 | 4.45239E+04 | 4.64606E+04 | 5.40665E+04 | 5.45575E+04 |
| PATH  | ZI1FUE      |
|   | 4.45310E+04 | 4.64583E+04 | 5.40677E+04 | 5.45581E+04 | 5.35073E+04 | 4.45239E+04 | 4.64606E+04 | 5.40665E+04 |
| PATH  | ZI2FUE      |
|   | 5.93373E+04 | 4.98840E+04 | 5.43804E+04 | 6.32245E+04 | 6.36921E+04 | 6.26021E+04 | 5.21765E+04 | 5.44234E+04 |
| PATH  | ZI2FUE      |
|   | 6.37331E+04 | 6.26497E+04 | 5.22413E+04 | 5.21737E+04 | 6.02376E+04 | 6.10037E+04 | 5.94989E+04 | 5.00914E+04 |
| PATH  | ZO1FUE      |
|   | 6.58012E+04 | 5.48025E+04 | 5.72840E+04 | 6.66412E+04 | 6.69362E+04 | 6.60346E+04 | 5.50170E+04 | 5.72840E+04 |
| PATH  | ZO1FUE      |
|   | 6.69362E+04 | 6.60346E+04 | 5.50170E+04 | 5.71221E+04 | 6.64041E+04 | 6.67468E+04 | 6.58012E+04 | 5.71221E+04 |
| PATH  | ZO1FUE      | ZO1FUE      | ZO1FUE      | ZO2FUE      | ZO2FUE      | ZO2FUE      | ZO2FUE      | ZO2FUE      |
|   | 6.67468E+04 | 6.58012E+04 | 5.48025E+04 | 5.38225E+04 | 6.16887E+04 | 6.20044E+04 | 6.11166E+04 | 5.15401E+04 |
| PATH  | ZO2FUE      |
|   | 6.48608E+04 | 6.58459E+04 | 6.40152E+04 | 5.44601E+04 | 5.70853E+04 | 6.48451E+04 | 6.58379E+04 | 6.40239E+04 |

Figure 3-15. REBUS VTR Problem Excerpt.

As stated, reconstructing the output using the atom densities printed in the REBUS output takes considerable effort. While a script can be used, this action would require verification of the script itself. In fact many users have constructed their own scripts to do just this task and verify them all before using them. In this regard, checking the printed output results was sufficiently covered in the preceding test case which demonstrates that the crux of what the users are doing is a valid path to construct a DIF3D input at each time point.

In the first test, the binary files produced by REBUS at each time point are used to reconstruct the DIF3D input decks at each time point. Figure 3-16 shows the interface files created for the VTR problem where the format `<Name_Index_Days>` is used by REBUS to create the output files. As can be seen, there are three time indexes: 0000, 0001, and 9999. There are only two day specifications of 0.0 days and 100 days which correspond to the fuel cycle being executed. Index 0000 refers to the BOC

configuration while 0001 refers to the EOC result. The index 9999 refers to the unpoisoned  $k_{\text{eff}}$  calculation that REBUS optionally computes at the end of an equilibrium cycle calculation.

```

GEO DST_0000 0.000000
GEO DST_0001 100.000000
GEO DST_0999 0.000000

LABELS_0000 0.000000
LABELS_0001 100.000000
LABELS_0999 0.000000

NDXS RF_0000 0.000000

RFILE S_0000 0.000000
RFILE S_0001 100.000000
RFILE S_0999 0.000000

ZNAT DN_0000 0.000000
ZNAT DN_0001 100.000000
ZNAT DN_0999 0.000000

```

**Figure 3-16. Binary Interface Files Created by REBUS for the VTR Test Problem**

As is typical with REBUS, there is only one NDXSRF file produced by REBUS as all zones are defined for all time points and paths specified in the input at the beginning of the calculation. To define a complete DIF3D input file, only four of the stated files are needed: GEO DST, LABELS, NDXSRF, and ZNAT DN. Using these four files for the BOC and EOC configurations, the DIF3D calculations were executed using identical A.DIF3D input from the original REBUS input. Starting with the BOC case, Figure 3-17 provides the identical set of output as taken from REBUS in Figure 3-13.

```

=VARIANT| 8| 124.1|001| 1.022381E+00|8.6E-05| T | 8.60E-04, 3.95E-04| T | 0 | 0.64 | 0.65| 5.5| 63.8| 54.8|
=VARIANT| 9| 128.1|001| 1.022342E+00|3.8E-05| T | 4.99E-04, 2.15E-04| T | 0 | 0.54 | 0.54| 5.4| 66.1| 56.5|
=VARIANT| 10| 119.4|001| 1.022326E+00|1.6E-05| T | 2.61E-04, 1.09E-04| T | 0 | 0.51 | 0.51| 5.4| 61.3| 52.7|
=VARIANT| 11| 116.2|001| 1.022320E+00|6.3E-06| T | 1.28E-04, 5.45E-05| T | 0 | 0.50 | 0.50| 5.5| 59.7| 51.0|
=VARIANT| 12| 140.6|001| 1.022318E+00|1.8E-06| F | 5.25E-05, 2.52E-05| T | 0 | 0.46 | 0.44| 5.6| 80.8| 54.3|
=VARIANT| 13| 142.2|001| 1.022317E+00|5.0E-07| F | 2.72E-05, 1.48E-05| T | 0 | 0.59 | 0.57| 5.7| 81.2| 55.3|
OUTER ITERATIONS COMPLETED AT ITERATION 13, ITERATIONS HAVE CONVERGED
K-EFFECTIVE = 1.02231718
DIF3D 11.3072 11/11/19 PAGE 9

REGION ZONE ZONE VOLUME INTEGRATION(1) POWER POWER DENSITY PEAK DENSITY PEAK TO AVG. POWER
NO. NAME NO. NAME (CC) WEIGHT FACTOR (WATTS) (WATTS) (WATTS/CC) (WATTS/CC) (2) POWER DENSITY FRACTION
...
8 I20101 8 I20101 3.85290E+03 1.00000E+00 1.30065E+02 3.37577E-02 6.16797E-02 1.82713E+00 4.33551E-07
9 I20102 9 I20102 1.03586E+04 1.00000E+00 1.49498E+04 1.44323E+00 3.47981E+00 2.41113E+00 4.98328E-05
10 I20103 10 I20103 1.01060E+03 1.00000E+00 1.38121E+03 1.36672E+00 1.40499E+00 1.02800E+00 4.60403E-06
11 I20104 11 I20104 9.60068E+02 1.00000E+00 1.97358E+03 2.05567E+00 2.31780E+00 1.12752E+00 6.57860E-06
12 I20105 12 I20105 2.12819E+03 1.00000E+00 1.07220E+06 5.03805E+02 5.88304E+02 1.16772E+00 3.57399E-03
13 I20106 13 I20106 2.12819E+03 1.00000E+00 1.34262E+06 6.30871E+02 6.86922E+02 1.08885E+00 4.47539E-03
14 I20107 14 I20107 2.12819E+03 1.00000E+00 1.43812E+06 6.75746E+02 6.94190E+02 1.02729E+00 4.79373E-03
15 I20108 15 I20108 2.12819E+03 1.00000E+00 1.30657E+06 6.13935E+02 6.79191E+02 1.10629E+00 4.35524E-03
16 I20109 16 I20109 2.12807E+03 1.00000E+00 9.91750E+05 4.66034E+02 5.62395E+02 1.20677E+00 3.30583E-03
17 I2010A 17 I2010A 3.02586E+03 1.00000E+00 3.06362E+03 1.01248E+00 1.10142E+00 1.08784E+00 1.02121E-05
18 I2010B 18 I2010B 6.85476E+03 1.00000E+00 3.49585E+03 5.09989E-01 8.92544E-01 1.75013E+00 1.16528E-05
19 I2010C 19 I2010C 6.63205E+02 1.00000E+00 2.83188E+02 4.26999E-01 4.98000E-01 1.16628E+00 9.43958E-07
20 I2010D 20 I2010D 7.57948E+03 1.00000E+00 1.38891E+03 1.83247E-01 6.27753E-01 3.42573E+00 4.62971E-06
21 I2010E 21 I2010E 3.78974E+03 1.00000E+00 1.70738E+01 4.50528E-03 8.56110E-03 1.90024E+00 5.69128E-08
...
DIF3D 11.3072 11/11/19 PAGE 193
0 REGION AND AREA REAL FLUX INTEGRALS FOR K-EFF PROBLEM WITH ENERGY RANGE (EV) =(0.000E+00,1.419E+07)
REGION ZONE ZONE VOLUME TOTAL FLUX PEAK FLUX (1) TOTAL FAST FLUX PEAK FAST FLUX(1)
NO. NAME NO. NAME (CC) (NEUTRON/CM/SEC) (NEUTRON/CM2-SEC) (NEUTRON-CM/SEC) (NEUTRON/CM2-SEC)
...
1 T10101 1 T10101 3.85290E+03 7.88955E+16 4.03791E+13 8.18206E+15 5.13695E+12
2 T10102 2 T10102 1.13692E+04 9.03487E+18 2.91041E+15 3.33356E+18 1.58987E+15
3 T10103 3 T10103 4.98983E+03 2.21423E+19 5.73419E+15 1.49378E+19 4.08750E+15
4 T10104 4 T10104 2.52649E+03 1.47761E+19 5.97833E+15 1.05185E+19 4.30291E+15
5 T10105 5 T10105 1.46284E+04 2.98279E+19 5.65921E+15 1.79121E+19 4.03753E+15
6 T10106 6 T10106 7.57948E+03 4.39662E+17 2.21878E+14 8.17646E+16 4.95233E+13
7 T10107 7 T10107 3.78974E+03 1.00954E+16 5.41243E+12 9.38474E+14 6.15877E+11
...
13 I20106 13 I20106 2.12819E+03 1.14550E+19 5.86522E+15 8.31933E+18 4.29848E+15
14 I20107 14 I20107 2.12819E+03 1.23444E+19 5.95351E+15 9.01069E+18 4.36002E+15
15 I20108 15 I20108 2.12819E+03 1.11414E+19 5.79255E+15 8.10113E+18 4.24943E+15
...
```

**Figure 3-17. DIF3D BOC Excerpt for the VTR Problem.**

A quick review shows there are numerous differences in almost every number reported, which, upon inspection, are found to be within the convergence tolerances used in DIF3D/REBUS. As an example,

the eigenvalue of 1.02231\_718 from DIF3D 1.02231\_680 are within the stated 1.0E-6 error specified in the input. The various flux and power numbers are all within the 0.0001 error criteria specified for the fission source error criteria. For the EOC case, Figure 3-18 provides the identical outputs to those taken from REBUS in Figure 3-14. Similar to the BOC results, there are numerous differences between the two outputs all of which are within the convergence criteria specified in the input.

```

...=VARIANT| 7| 143.4|001| 1.000117E+00|9.7E-05| T | 1.12E-03, 6.10E-04| T | 0 | 0.57 | 0.58 | 4.7 | 74.4 | 64.3 |
...=VARIANT| 8| 160.6|001| 1.000031E+00|8.5E-05| T | 8.54E-04, 3.91E-04| T | 0 | 0.64 | 0.65 | 5.4 | 82.7 | 72.5 |
...=VARIANT| 9| 142.2|001| 9.999937E-01|3.8E-05| T | 4.95E-04, 2.12E-04| T | 0 | 0.54 | 0.54 | 4.7 | 73.5 | 64.0 |
...=VARIANT| 10| 140.4|001| 9.999784E-01|1.5E-05| T | 2.58E-04, 1.08E-04| T | 0 | 0.51 | 0.51 | 3.3 | 71.8 | 65.3 |
...=VARIANT| 11| 117.5|001| 9.999723E-01|6.1E-06| T | 1.27E-04, 5.43E-05| T | 0 | 0.50 | 0.50 | 3.1 | 59.3 | 55.0 |
...=VARIANT| 12| 132.8|001| 9.999705E-01|1.8E-06| F | 5.22E-05, 2.52E-05| T | 0 | 0.46 | 0.44 | 3.2 | 74.5 | 55.1 |
...=VARIANT| 13| 132.7|001| 9.999700E-01|4.8E-07| F | 2.71E-05, 1.49E-05| T | 0 | 0.59 | 0.57 | 3.2 | 74.4 | 55.2 |
    OUTER ITERATIONS COMPLETED AT ITERATION 13, ITERATIONS HAVE CONVERGED
    K-EFFECTIVE = 0.99997004
DIF3D 11.3072 11/11/19
PAGE 9

... REGION ZONE ZONE VOLUME INTEGRATION(1) POWER POWER DENSITY PEAK DENSITY PEAK TO AVG. POWER
NO. NAME NO. NAME (CC) WEIGHT FACTOR (WATTS) (WATTS) (WATTS/CC) (WATTS/CC) (2) POWER DENSITY FRACTION
...
8 I20101 8 I20101 3.85290E+03 1.00000E+00 1.33223E+02 3.45772E-02 6.31759E-02 1.82710E+00 4.44075E-07
9 I20102 9 I20102 1.03586E+04 1.00000E+00 1.53579E+04 1.48262E+00 3.58351E+00 2.41702E+00 5.11929E-05
10 I20103 10 I20103 1.01060E+03 1.00000E+00 1.42284E+03 1.40792E+00 1.44681E+00 1.02762E+00 4.74281E-06
11 I20104 11 I20104 9.60068E+02 1.00000E+00 2.03398E+03 2.11858E+00 2.38795E+00 1.12715E+00 6.77994E-06
12 I20105 12 I20105 2.12819E+03 1.00000E+00 1.06192E+06 4.98976E+02 5.81825E+02 1.16604E+00 3.53972E-03
13 I20106 13 I20106 2.12819E+03 1.00000E+00 1.31560E+06 6.18175E+02 6.72298E+02 1.08755E+00 4.38532E-03
14 I20107 14 I20107 2.12819E+03 1.00000E+00 1.40390E+06 6.59667E+02 6.77285E+02 1.02671E+00 4.67966E-03
15 I20108 15 I20108 2.12819E+03 1.00000E+00 1.28313E+06 6.02921E+02 6.65821E+02 1.10432E+00 4.27711E-03
16 I20109 16 I20109 2.12807E+03 1.00000E+00 9.86798E+05 4.63707E+02 5.58547E+02 1.20453E+00 3.28933E-03
17 I2010A 17 I2010A 3.02586E+03 1.00000E+00 3.16285E+03 1.04527E+00 1.13706E+00 1.08781E+00 1.05428E-05
18 I2010B 18 I2010B 6.85476E+03 1.00000E+00 3.60289E+03 5.25605E-01 9.20941E-01 1.75216E+00 1.20096E-05
19 I2010C 19 I2010C 6.63205E+02 1.00000E+00 2.91374E+02 4.39343E-01 5.12512E-01 1.16654E+00 9.71248E-07
20 I2010D 20 I2010D 7.57948E+03 1.00000E+00 1.42737E+03 1.88320E-01 6.45840E-01 3.42948E+00 4.75789E-06
21 I2010E 21 I2010E 3.78974E+03 1.00000E+00 1.75163E+01 4.62203E-03 8.78336E-03 1.90033E+00 5.83876E-08
...
DIF3D 11.3072 11/11/19
PAGE 193
0 REGION AND AREA REAL FLUX INTEGRALS FOR K-EFF PROBLEM WITH ENERGY RANGE (EV) = (0.000E+00, 1.419E+07)
  REGION ZONE ZONE VOLUME TOTAL FLUX PEAK FLUX (1) TOTAL FAST FLUX PEAK FAST FLUX(1)
NO. NAME NO. NAME (CC) (NEUTRON-CM/SEC) (NEUTRON-CM2/SEC) (NEUTRON-CM/SEC) (NEUTRON-CM2/SEC)
  1 T10101 1 T10101 3.85290E+03 8.07656E+16 4.13340E+13 8.36495E+15 5.25106E+12
  2 T10102 2 T10102 1.13692E+04 9.25809E+18 2.98164E+15 3.40260E+18 1.62091E+15
  3 T10103 3 T10103 4.98983E+03 2.26551E+19 5.85931E+15 1.52053E+19 4.15330E+15
  4 T10104 4 T10104 2.52649E+03 1.50991E+19 6.10722E+15 1.06872E+19 4.37056E+15
  5 T10105 5 T10105 1.46284E+04 3.05916E+19 5.78629E+15 1.82809E+19 4.10546E+15
  6 T10106 6 T10106 7.57948E+03 4.51374E+17 2.27932E+14 8.37925E+16 5.07556E+13
  7 T10107 7 T10107 3.78974E+03 1.03535E+16 5.55093E+12 9.61526E+14 6.31010E+11
...
  13 I20106 13 I20106 2.12819E+03 1.17122E+19 5.99101E+15 8.46270E+18 4.36667E+15
  14 I20107 14 I20107 2.12819E+03 1.26149E+19 6.08088E+15 9.15806E+18 4.42849E+15
  15 I20108 15 I20108 2.12819E+03 1.14042E+19 5.92006E+15 8.25156E+18 4.31968E+15
...

```

**Figure 3-18. DIF3D EOC Excerpt for the VTR Problem.**

A second pathway to check the above is to reconstruct the A.NIP3 data from the binary files using the Modify.x utility program provided with ARC. Figure 3-19 provides an excerpt of the recreated A.NIP3 result which produces a nearly identical result to the preceding binary detail of Figure 3-17. The slight differences in the convergence history are due to the slight precision differences between the ascii representation of the zone composition details and the binary representation.

With the preceding work complete, tasks A-D of the DIF3D usage in REBUS are verified. REBUS is identically using the same DIF3D application available for steady state analysis.

```
UNFORM=A.NIP3
01 Utility converter of CCCC to ANIP3
02 0 0 30000000 30000000 30000000 0 0 0
03 120
04 4 4 4 4 4 4
PRINT=NO
09 Z 1 15.2500000
09 Z 1 30.5000000
09 Z 1 385.8000000
29 12.0775499 11 1
30 *SB1701* 11 43 43 0.0000000 15.2500000
30 *SB1701* 11 43 43 15.2500000 30.5000000
30 *SB1702* 11 43 43 30.5000000 48.5000000
30 *SB1702* 11 43 43 48.5000000 66.5000000
30 *SB1702* 11 43 43 66.5000000 84.5000000
30 *SB0D02* 11 13 13 341.1845000 355.8000000
30 *SB0D03* 11 13 13 355.8000000 370.8000000
30 *SB0D03* 11 13 13 370.8000000 385.8000000
07 MAXPO I20501 I20502 I20503 I20504 I20505 I20506 I20507 I20508
07 AINNOZ T10101 I20101 I20201 I20301 I20401 I20501 I20601 T30101
07 AINNOZ I30201 T30301 I30401 T30501 I30601 T30701 I30801 T30901
07 TCORE O50I09 O50K05 O50K06 O50K07 O50K08 O50K09 O50M05 O50M06
07 TCORE O50M07 O50M08 O50M09 O50005 O50006 O50007 O50008 O50009
14 T10101 NA23A 1.670440E-02 FE54A 1.040960E-03 FE56A 1.632610E-02
14 T10101 FE57A 3.772350E-04 FE58A 4.982350E-05 NI58A 6.946880E-05
14 T10101 NI60A 2.675470E-05 NI61A 1.163250E-06 NI62A 3.704050E-06
14 T10101 NI64A 9.489700E-07 CR50A 1.188630E-04 CR52A 2.289560E-03
14 T10101 CR53A 2.595870E-04 CR54A 6.476030E-05 MN55A 1.218400E-04
14 T10101 MO92A 1.849260E-05 MO94A 1.164540E-05 MO95A 2.015990E-05
14 T10101 MO96A 2.121620E-05 MO97A 1.221810E-05 MO98A 3.104150E-05
14 T10101 MO00A 1.249810E-05 C_12A 1.957210E-04 P_31A 6.066170E-05
14 T10101 V_51A 6.454370E-05 W182A 7.626280E-06 W183A 4.118200E-06
14 T10101 W184A 8.817700E-06 W186A 8.181700E-06 S_32A 1.469190E-05
14 T10101 N_14A 2.264270E-05
14 SB1N03 N_14H 2.264270E-05
15 *T10101* *T10101*
15 *T10102* *T10102*
15 *T10103* *T10103*
```

**Figure 3-19. Excerpt of the Reconstructed A.NIP3 BOC input for the VTR Problem.**

### 3.3 Control Rod Movement Verification

The preceding verification problems did not include the control rod movement scheme which is the final part needed to verify that the DIF3D result is not adversely impacted by REBUS. In the control rod movement, (card 44 of A.NIP3 and card 38 of A.BURN), the user can identify control rod regions, named banks, and specify their positions at each time point of the burn cycle. Using the same null depletion aspect demonstrated in the preceding verification problem, the control rod movements can be verified in two ways. First, the DIF3D inputs can be manually setup at each time point similar to that done in the previous verification test problem. Second, the binary interface files generated by REBUS at each time point can be used as an alternative to ascii based input. Because REBUS will automatically re-mesh the axial domain to handle the movement of the control rod tip, it is important to demonstrate that at least one control rod movement point tests this feature.

The 3D hexagonal benchmark defined earlier in Figure 3-4 is used here as it already has all of the necessary components. With respect to control rods, it has 5 distinct control regions which are assigned control bank 1 through 5 in this verification test. Table 3-3 shows the axial control rod positions chosen for each control rod where “Position x,y” refers to the input position of the control rod (hexagon ring x and position y along that hexagon). In this input, only time point 4, Bank 1 has an axial coordinate (180 cm) that was not part of the original geometry.

Table 3-4 provides the  $k_{eff}$  control rod results for all time points in the REBUS and DIF3D calculations. The REBUS result is that obtained when REBUS moves the control rods at each time point. The DIF3D A.NIP3 case is that when the steady state DIF3D input is modified to match the

desired control rod position at each time point. Finally, the DIF3D Binaries case provides the results obtained by using the REBUS generated binary files at each time point. All of the eigenvalues are identical at each time point between all three approaches.

**Table 3-3. Axial Rod Positioning at Each Time Point in the Control Rod Test Problem.**

| Time<br>(days) | Bank 1<br>Position 1,1 | Bank 2<br>Position 4,1 | Bank 3<br>Position 4,7 | Bank 4<br>Position 4,13 | Bank 5<br>Position 7,1 |
|----------------|------------------------|------------------------|------------------------|-------------------------|------------------------|
| 0.0            | 200.0                  | 150.0                  | 170.0                  | 190.0                   | 130.0                  |
| 1.0            | 200.0                  | 170.0                  | 190.0                  | 200.0                   | 150.0                  |
| 2.0            | 200.0                  | 190.0                  | 190.0                  | 190.0                   | 170.0                  |
| 3.0            | 190.0                  | 190.0                  | 190.0                  | 190.0                   | 190.0                  |
| 4.0            | 180.0                  | 190.0                  | 190.0                  | 190.0                   | 190.0                  |
| 5.0            | 150.0                  | 190.0                  | 190.0                  | 190.0                   | 190.0                  |

**Table 3-4. Control Rod  $k_{eff}$  at Each Time Point in the Control Rod Test Problem.**

| Time<br>(days) | REBUS       | DIF3D<br>A.NIP3 | DIF3D<br>Binaries |
|----------------|-------------|-----------------|-------------------|
| 0.0            | 1.03566 415 | 1.03566 415     | 1.03566 415       |
| 1.0            | 1.05430 596 | 1.05430 596     | 1.05430 596       |
| 2.0            | 1.06021 500 | 1.06021 500     | 1.06021 500       |
| 3.0            | 1.06037 829 | 1.06037 829     | 1.06037 829       |
| 4.0            | 1.05806 108 | 1.05806 108     | 1.05806 108       |
| 5.0            | 1.03894 691 | 1.03894 691     | 1.03894 691       |

Because the flux solution changes significantly due to the control rod movements, REBUS performs two flux calculations at the end of each time step. At each time point, REBUS will initially assume the beginning and end of the time step flux solution are identical to carry out the depletion calculation and initiate the iteration. Since the control rod position moves, the end of time step flux solution is very different, the depletion results are different and a second iteration is required to converge. Because this is a zero power depletion test, no additional change in the depletion results actually occurs at either time step and REBUS properly exits after completing the second DIF3D calculation. At the beginning of the next step, the flux solution is recalculated based upon the assumption that some decay or fuel shuffling has occurred even though it has not. The isotopes that drive the error are the PU239, DUMP and LFP isotopes which are not present at the beginning of the REBUS calculation and even with a zero power level, they end up with non-zero, although still trivial, total densities at the end of the 5 day depletion.

Based upon the previous work, there is no point in checking the differences in the DIF3D output, however, given the change in axial meshing that occurs in step 4, the same power edit excerpt from the DIF3D output for step 4 for all three calculations are displayed in Figure 3-20. Consistent with the previous verification test problem, the only differences in the three sections of output are the page numbers and the ordering of the data when using the A.NIP3 case. The page numbering is of course expected. The ordering of the region data was altered in the second example by changing the order of the region data provided to DIF3D in the input which was done to make the manual control rod changes easier to setup. The ordering of regions is of course not relevant with regard to the accuracy of a DIF3D or REBUS calculation and a quick review of the displayed results demonstrate that.

| DIF3D Output Taken from REBUS |        |          |                                   |                |               |                          |                              |              |               |             | PAGE 417               |
|-------------------------------|--------|----------|-----------------------------------|----------------|---------------|--------------------------|------------------------------|--------------|---------------|-------------|------------------------|
| 1DIF3D                        | 11.0   | 01/01/12 | ADIF3D: Hexagonal 3D Test Problem |                |               |                          | POWER DENSITY (WATTS/CC) (2) |              |               |             | POWER DENSITY FRACTION |
| REGION                        | ZONE   | ZONE     | VOLUME (CC)                       | INTEGRATION(1) | POWER (WATTS) | POWER DENSITY (WATTS/CC) | PEAK DENSITY (WATTS/CC)      | PEAK TO AVG. | POWER         |             |                        |
| NO.                           | NAME   | NO.      | NAME                              | WEIGHT FACTOR  | (WATTS)       | (WATTS/CC)               | (WATTS/CC)                   | (2)          | POWER DENSITY | FRACTION    |                        |
| 1                             | SHILD  | 1        | SHILD                             | 6.09162E+06    | 1.00000E+00   | 2.62693E-09              | 4.31237E-16                  | 8.03048E-14  | 1.86220E+02   | 2.62693E-03 |                        |
| 2                             | RREFL  | 2        | RREFL                             | 3.06919E+06    | 1.00000E+00   | 1.21831E-09              | 3.96948E-16                  | 3.79228E-15  | 9.55360E+00   | 1.21831E-03 |                        |
| 3                             | EMPTY  | 3        | EMPTY                             | 5.54256E+04    | 1.00000E+00   | 4.20304E-11              | 7.58321E-16                  | 1.46640E-15  | 1.93375E+00   | 4.20304E-05 |                        |
| 4                             | CNTRL1 | 4        | CNTRL1                            | 1.81865E+04    | 1.00000E+00   | 3.38652E-10              | 1.86210E-14                  | 6.53210E-13  | 3.50792E+01   | 3.38652E-04 |                        |
| 5                             | ILSHD  | 5        | ILSHD                             | 1.14315E+05    | 1.00000E+00   | 1.16500E-10              | 1.01911E-15                  | 7.30335E-14  | 7.16640E+01   | 1.16500E-04 |                        |
| 6                             | ILREF  | 6        | ILREF                             | 1.14315E+05    | 1.00000E+00   | 3.44779E-10              | 3.01604E-15                  | 6.86727E-15  | 2.27692E+00   | 3.44779E-04 |                        |
| 7                             | ILBLK  | 7        | ILBLK                             | 2.85788E+04    | 1.00000E+00   | 2.34157E-09              | 8.19336E-14                  | 1.31689E-13  | 1.60726E+00   | 2.34157E-03 |                        |
| 8                             | ICORE  | 8        | ICORE                             | 2.85788E+05    | 1.00000E+00   | 3.50035E-07              | 1.22481E-12                  | 1.73583E-12  | 1.41722E+00   | 3.50035E-01 |                        |
| 9                             | IUBLK  | 9        | IUBLK                             | 2.85788E+04    | 1.00000E+00   | 1.21877E-09              | 4.26460E-14                  | 7.51233E-14  | 1.76156E+00   | 1.21877E-03 |                        |
| 10                            | IPLEN  | 10       | IPLEN                             | 3.14367E+05    | 1.00000E+00   | 1.81925E-11              | 5.78703E-17                  | 3.32170E-16  | 5.73991E+00   | 1.81925E-05 |                        |
| 11                            | IUREF  | 11       | IUREF                             | 1.14315E+05    | 1.00000E+00   | 1.47618E-12              | 1.29132E-17                  | 6.61048E-17  | 5.11916E+00   | 1.47618E-06 |                        |
| 12                            | IUSHD  | 12       | IUSHD                             | 1.14315E+05    | 1.00000E+00   | 3.38246E-13              | 2.95888E-18                  | 3.85196E-16  | 1.30183E+02   | 3.38246E-07 |                        |
| 13                            | CNTRL2 | 13       | CNTRL2                            | 1.73205E+04    | 1.00000E+00   | 2.42618E-10              | 1.40076E-14                  | 1.53638E-12  | 1.09682E+02   | 2.42618E-04 |                        |

| DIF3D Output Based Upon Equivalent A.NIP3 |        |          |                                   |                |               |                          |                              |              |               |             | PAGE 44                |
|---|--------|----------|-----------------------------------|----------------|---------------|--------------------------|------------------------------|--------------|---------------|-------------|------------------------|
| 1DIF3D                                    | 11.0   | 01/01/12 | ADIF3D: Hexagonal 3D Test Problem |                |               |                          | POWER DENSITY (WATTS/CC) (2) |              |               |             | POWER DENSITY FRACTION |
| REGION                                    | ZONE   | ZONE     | VOLUME (CC)                       | INTEGRATION(1) | POWER (WATTS) | POWER DENSITY (WATTS/CC) | PEAK DENSITY (WATTS/CC)      | PEAK TO AVG. | POWER         |             |                        |
| NO.                                       | NAME   | NO.      | NAME                              | WEIGHT FACTOR  | (WATTS)       | (WATTS/CC)               | (WATTS/CC)                   | (2)          | POWER DENSITY | FRACTION    |                        |
| 1   | SHILD  | 11       | ZSHLD                             | 6.09162E+06    | 1.00000E+00   | 2.62693E-09              | 4.31237E-16                  | 8.03048E-14  | 1.86220E+02   | 2.62693E-03 |                        |
| 2   | RREFL  | 10       | ZRREFL                            | 3.06919E+06    | 1.00000E+00   | 1.21831E-09              | 3.96948E-16                  | 3.79228E-15  | 9.55360E+00   | 1.21831E-03 |                        |
| 3   | EMPTY  | 12       | ZSPPOOL                           | 5.54256E+04    | 1.00000E+00   | 4.20304E-11              | 7.58321E-16                  | 1.46640E-15  | 1.93375E+00   | 4.20304E-05 |                        |
| 4   | ILSHD  | 11       | ZSHLD                             | 1.14315E+05    | 1.00000E+00   | 1.16500E-10              | 1.01911E-15                  | 7.30335E-14  | 7.16640E+01   | 1.16500E-04 |                        |
| 5   | ILREF  | 10       | ZRREFL                            | 1.14315E+05    | 1.00000E+00   | 3.44779E-10              | 3.01604E-15                  | 6.86727E-15  | 2.27692E+00   | 3.44779E-04 |                        |
| 6   | ILBLK  | 3        | ZABLKT                            | 2.85788E+04    | 1.00000E+00   | 2.34157E-09              | 8.19336E-14                  | 1.31689E-13  | 1.60726E+00   | 2.34157E-03 |                        |
| 7   | ICORE  | 1        | ZIFBLK                            | 2.85788E+05    | 1.00000E+00   | 3.50035E-07              | 1.22481E-12                  | 1.73583E-12  | 1.41722E+00   | 3.50035E-01 |                        |
| 8   | IUBLK  | 3        | ZABLKT                            | 2.85788E+04    | 1.00000E+00   | 1.21877E-09              | 4.26460E-14                  | 7.51233E-14  | 1.76156E+00   | 1.21877E-03 |                        |
| 9   | IPLEN  | 13       | ZPLEN                             | 3.14367E+05    | 1.00000E+00   | 1.81925E-11              | 5.78703E-17                  | 3.32170E-16  | 5.73991E+00   | 1.81925E-05 |                        |
| 10  | IUREF  | 10       | ZRREFL                            | 1.14315E+05    | 1.00000E+00   | 1.47618E-12              | 1.29132E-17                  | 6.61048E-17  | 5.11916E+00   | 1.47618E-06 |                        |
| 11  | IUSHD  | 11       | ZSHLD                             | 1.14315E+05    | 1.00000E+00   | 3.38246E-13              | 2.95888E-18                  | 3.85196E-16  | 1.30183E+02   | 3.38246E-07 |                        |
| 22  | CNTRL1 | 5        | ZCNTR1                            | 1.81865E+04    | 1.00000E+00   | 3.38652E-10              | 1.86210E-14                  | 6.53210E-13  | 3.50792E+01   | 3.38652E-04 |                        |
| 23  | CNTRL2 | 6        | ZCNTR2                            | 1.73205E+04    | 1.00000E+00   | 2.42618E-10              | 1.40076E-14                  | 1.53638E-12  | 1.09682E+02   | 2.42618E-04 |                        |

| DIF3D Output Based Upon REBUS Binaries |        |          |                                   |                |               |                          |                              |              |               |             | PAGE 16                |
|--|--------|----------|-----------------------------------|----------------|---------------|--------------------------|------------------------------|--------------|---------------|-------------|------------------------|
| 1DIF3D                                 | 11.0   | 01/01/12 | ADIF3D: Hexagonal 3D Test Problem |                |               |                          | POWER DENSITY (WATTS/CC) (2) |              |               |             | POWER DENSITY FRACTION |
| REGION                                 | ZONE   | ZONE     | VOLUME (CC)                       | INTEGRATION(1) | POWER (WATTS) | POWER DENSITY (WATTS/CC) | PEAK DENSITY (WATTS/CC)      | PEAK TO AVG. | POWER         |             |                        |
| NO.                                    | NAME   | NO.      | NAME                              | WEIGHT FACTOR  | (WATTS)       | (WATTS/CC)               | (WATTS/CC)                   | (2)          | POWER DENSITY | FRACTION    |                        |
| 1                                      | SHILD  | 1        | SHILD                             | 6.09162E+06    | 1.00000E+00   | 2.62693E-09              | 4.31237E-16                  | 8.03048E-14  | 1.86220E+02   | 2.62693E-03 |                        |
| 2                                      | RREFL  | 2        | RREFL                             | 3.06919E+06    | 1.00000E+00   | 1.21831E-09              | 3.96948E-16                  | 3.79228E-15  | 9.55360E+00   | 1.21831E-03 |                        |
| 3                                      | EMPTY  | 3        | EMPTY                             | 5.54256E+04    | 1.00000E+00   | 4.20304E-11              | 7.58321E-16                  | 1.46640E-15  | 1.93375E+00   | 4.20304E-05 |                        |
| 4                                      | CNTRL1 | 4        | CNTRL1                            | 1.81865E+04    | 1.00000E+00   | 3.38652E-10              | 1.86210E-14                  | 6.53210E-13  | 3.50792E+01   | 3.38652E-04 |                        |
| 5                                      | ILSHD  | 5        | ILSHD                             | 1.14315E+05    | 1.00000E+00   | 1.16500E-10              | 1.01911E-15                  | 7.30335E-14  | 7.16640E+01   | 1.16500E-04 |                        |
| 6                                      | ILREF  | 6        | ILREF                             | 1.14315E+05    | 1.00000E+00   | 3.44779E-10              | 3.01604E-15                  | 6.86727E-15  | 2.27692E+00   | 3.44779E-04 |                        |
| 7                                      | ILBLK  | 7        | ILBLK                             | 2.85788E+04    | 1.00000E+00   | 2.34157E-09              | 8.19336E-14                  | 1.31689E-13  | 1.60726E+00   | 2.34157E-03 |                        |
| 8                                      | ICORE  | 8        | ICORE                             | 2.85788E+05    | 1.00000E+00   | 3.50035E-07              | 1.22481E-12                  | 1.73583E-12  | 1.41722E+00   | 3.50035E-01 |                        |
| 9                                      | IUBLK  | 9        | IUBLK                             | 2.85788E+04    | 1.00000E+00   | 1.21877E-09              | 4.26460E-14                  | 7.51233E-14  | 1.76156E+00   | 1.21877E-03 |                        |
| 10                                     | IPLEN  | 10       | IPLEN                             | 3.14367E+05    | 1.00000E+00   | 1.81925E-11              | 5.78703E-17                  | 3.32170E-16  | 5.73991E+00   | 1.81925E-05 |                        |
| 11                                     | IUREF  | 11       | IUREF                             | 1.14315E+05    | 1.00000E+00   | 1.47618E-12              | 1.29132E-17                  | 6.61048E-17  | 5.11916E+00   | 1.47618E-06 |                        |
| 12                                     | IUSHD  | 12       | IUSHD                             | 1.14315E+05    | 1.00000E+00   | 3.38246E-13              | 2.95888E-18                  | 3.85196E-16  | 1.30183E+02   | 3.38246E-07 |                        |
| 13                                     | CNTRL2 | 13       | CNTRL2                            | 1.73205E+04    | 1.00000E+00   | 2.42618E-10              | 1.40076E-14                  | 1.53638E-12  | 1.09682E+02   | 2.42618E-04 |                        |

Figure 3-20. DIF3D Output Excerpt for REBUS and Two Different DIF3D Approaches at 4 days

### 3.4 Depletion Chain Verification

The next verification test problem is focused on the accuracy of the depletion chain of REBUS. The REBUS software presently allows the reactions shown in Table 3-5 to be included in the depletion chain. REBUS separates user isotopes into active and inactive. The active isotopes are those that are impacted by the depletion chain while inactive isotopes are those that are not. As an example, for UO<sub>2</sub>, the uranium will be typically be modeled in the depletion chain (active) while oxygen will not (inactive). In this context, the various uranium isotopes will be considered active isotopes while the oxygen isotopes will not be.

In Table 3-5, there are a relatively limited number of reactions that can be modeled with REBUS compared to the actual number of reactions that occur in physics. This limitation is primarily because the ISOTXS data structure used by DIF3D/REBUS only has these reactions presently included as the ARC code system was focused on reactor engineering work as opposed to modeling all possible nuclear reactions and decays. In this regard, the shown reactions are sufficient for the needs of most reactor physics projects and all of them have been used in the past for reactor analysis projects.

**Table 3-5. Depletion Chain Reactions Allowed in REBUS.**

| Reaction Index | Reaction Type   |
|----------------|-----------------|
| 0              | No Reaction     |
| 1              | n, $\gamma$     |
| 2              | n,fission       |
| 3              | n,proton        |
| 4              | n,alpha         |
| 5              | n,2n            |
| 6              | $\beta^-$ decay |
| 7              | $\beta^+$ decay |
| 8              | $\alpha$ decay  |
| 9              | n,deuteron      |
| 10             | n,tritium       |
| 11-19          | arbitrary decay |

For the present work, all of the reaction inputs listed need to be tested to verify that the inputs work properly. It is important to note that none of the reaction operations are actually verified by REBUS to ensure that the mass balance is preserved or that the reactions make sense. As an example, it is a trivial matter to tell REBUS that U-238 decays to Fe-56 in the depletion chain or that a capture in H-1 creates U-235. In that regard, it is imperative that the user defines a proper depletion chain.

The Bateman equation that is used to model isotopic depletion, transmutation, and decay is

$$\frac{\partial N_i}{\partial t} = \sum_{\substack{j=1 \\ j \neq i}}^I \sum_{r=1}^{R_j} \nu_{j,r} \sigma_{j,r} \phi N_j + \sum_{\substack{k=1 \\ j \neq i}}^I \sum_{k=1}^{K_j} \gamma_{k,j} \lambda_{k,j} N_j - \sum_{r=1}^{R_i} \sigma_{i,r} \phi N_i - \sum_{k=1}^{K_i} \lambda_{k,i} N_i. \quad (1)$$

In equation 1, the variable  $N_i$  represents the atom density of nuclide  $i$  where there are a total of  $I$  nuclides in the modeled problem at this point in space. It has neutron reaction contributions from nuclide  $j$  (e.g. neutron capture as an example) defined by the microscopic cross section  $\sigma_{j,r}$  for all reaction types  $r$  that occur for this isotope where the flux multiplier of  $\phi$  in  $\sigma_{j,r} \phi$  is intended to imply an integral over angle and energy at the chosen point in space but written this way for brevity. The factor  $\nu_{j,r}$  accounts for any duplicative amounts of nuclide  $N_i$  that are created by the neutron reaction (e.g. multiple He isotopes being produced from a capture event) and is in general an integer value. For those reactions from isotope  $j$  that do not exist (such as neutron capture followed by alpha emission), the related microscopic cross section is simply zero. The nuclide  $N_i$  has decay related contributions from nuclide  $N_j$ , where  $\lambda_{k,j}$  is the decay constant and  $\gamma_{k,j}$  is the yield fraction (or branching ratio) for this reaction type for all  $k$  decay reactions of this isotope. The removal terms for nuclide  $N_i$  include all  $r$  reactions  $\sigma_{i,r}$  and  $k$  decay reactions  $\lambda_{k,i}$  that exist for the nuclide. It is important to note that for decay processes, the yield fractions must sum to 1.0 as the yield fraction implies in equation 1.

For realistic fuel cycle related problems, Equation 1 does not have an analytic solution. For simplistic depletion chains combined with analytic neutronics solutions, it has analytic solutions which can be used to verify that the various inputs all work. It is important to note that a non-analytic neutron flux will require additional verification of the flux calculations at each time point. The key to making easy, yet valuable, analytic depletion chain problems is to combine a small sized depletion chain which have isotopic density changes that do not impact the actual flux solution. In that regard, the three group cross section problem used for the preceding verification test problems is again used.

The three group data set has isotopes Fe, Na, O-16, B-10, U-235, U-238, Pu-239, Pu-240, and Pu-241 along with the necessary LFP and DUMP. The isotope MAGIC is added to this list which is defined to include all possible reactions present but the total cross section is small to avoid perturbing the flux solution itself. Table 3-6 shows the starting atom densities used for several depletion chains to test the REBUS depletion solver where “NR” refers to no reaction or no depletion. For each depletion chain, the cross section and starting isotopic densities are provided along with the analytic flux solution (infinite homogeneous problem). The analytic solution of the depletion equations are then given, which will assume that the flux solution itself is not perturbed by the depletion process.

**Table 3-6. Depletion Chains Used to Test the REBUS.**

| Active Isotopes | Starting Atom Densities | Depletion Chain #1 | Starting Atom Densities | Depletion Chain #2 | Depletion Chain #3     | Starting Atom Densities | Depletion Chain #4   |
|-----------------|-------------------------|--------------------|-------------------------|--------------------|------------------------|-------------------------|----------------------|
| U-235           | 9.8725E-4               | NR                 | 9.8725E-4               | NR                 | NR                     | 9.8725E-4               | NR                   |
| U-238           | 7.8980E-3               | NR                 | 7.8980E-3               | NR                 | NR                     | 7.8980E-3               | NR                   |
| Pu-239          | -                       | -                  | 10 <sup>-12</sup>       | Fission to LFP     | -                      | 10 <sup>-12</sup>       | Circularly Connected |
| Pu-240          | -                       | -                  | -                       | -                  | -                      | 10 <sup>-12</sup>       |                      |
| Pu-241          | -                       | -                  | -                       | -                  | -                      | 10 <sup>-12</sup>       |                      |
| Pu-242          | -                       | -                  | -                       | -                  | -                      | 10 <sup>-12</sup>       |                      |
| Dump            | 0.0                     | NR                 | 0.0                     | NR                 | NR                     | 10 <sup>-12</sup>       |                      |
| LFP             | 0.0                     | NR                 | 0.0                     | NR                 | NR                     | 10 <sup>-12</sup>       |                      |
| MAGIC           | 10 <sup>-12</sup>       | Decay              | 10 <sup>-12</sup>       | Fission to LFP     | γ,p,α,2n,d,t Reactions | 10 <sup>-12</sup>       |                      |
| B-10            | -                       | -                  | -                       | -                  | Decay product          | 10 <sup>-12</sup>       |                      |

The MAGIC isotope mentioned above is assigned the multi-group cross section data shown in Table 3-7. In this table, the group 1 through group 3 cross sections are set to the same values and there is no scattering ( $n,2n$  principle reaction cross section can be given independent of a scattering matrix). It is also important to point out that the neutron source from fission is effectively forced to zero because of the small value of  $v$ . The atom density threshold for MAGIC, or even Pu-239, that prevents it from impacting the flux solution is  $\sim 10^{-12}$ .

**Table 3-7. MAGIC Cross Section Data.**

| Reaction           | Group 1-3        | Reaction            | Group 1-3 |
|--------------------|------------------|---------------------|-----------|
| $\sigma_{Total}$   | 0.7              | $\sigma_{alpha}$    | 0.1       |
| $\sigma_{\gamma}$  | 0.1              | $\sigma_{tritium}$  | 0.1       |
| $\sigma_{fission}$ | 0.1              | $\sigma_{deuteron}$ | 0.1       |
| $v$                | 10 <sup>-8</sup> | $\sigma_{n,2n}$     | 0.1       |
| $\sigma_{proton}$  | 0.1              | $\sigma_{scatter}$  | 0.0       |

This is primarily because the cross section merging procedure uses real precision math and a macroscopic cross section addition with less than a 10<sup>-8</sup> relative difference will result in a null change to the cross sections that DIF3D uses.

### 3.4.1 Depletion Chain 1

Starting with depletion chain 1, the same 5 day depletion calculation is used for the infinite homogeneous problem. Using the starting atom densities in Table 3-6 and a desired power of 10<sup>6</sup>

watts, the macroscopic cross sections and analytic flux solution shown in Table 3-8 is obtained at each time point.

**Table 3-8. Depletion Chain 1 Macroscopic Cross Sections and Flux Solution.**

| Group | Flux*10 <sup>13</sup> | Total    | Chi      | Nu·Fission | Scattering Matrix |            |            |
|-------|-----------------------|----------|----------|------------|-------------------|------------|------------|
|       |                       |          |          |            | 1.47248E-1        | 0.0        | 0.0        |
| 1     | 1.83423               | 0.130893 | 0.781199 | 1.23191E-2 | 1.47248E-1        | 0.0        | 0.0        |
| 2     | 6.54654               | 0.207445 | 0.209936 | 4.49207E-3 | 2.74053E-2        | 2.23762E-1 | 0.0        |
| 3     | 5.69335               | 0.303421 | 0.008865 | 6.50730E-3 | 5.72039E-4        | 7.20539E-3 | 3.03705E-1 |

In depletion chain 1, there is only a single isotope, MAGIC, which has an actual reaction intended to be decay. From Table 3-5, reactions 6, 7, 8 and 11 to 19 are all decay reactions (12 in total) and should be tested. Because decay of this isotope has no impact on the macroscopic cross sections, the analytic solution from equation 1 is found to simply be:

$$\frac{\partial N_{MAGIC}}{\partial t} = -\lambda N_{MAGIC} \quad \frac{\partial N_{DUMP}}{\partial t} = \lambda N_{MAGIC} \quad T_{1/2} = \frac{\ln(2)}{\lambda}$$

$$N_{MAGIC}(t) = N_{MAGIC}(0) \cdot \exp^{-\lambda \cdot t} \quad N_{DUMP}(t) = N_{MAGIC}(0) [1 - \exp^{-\lambda \cdot t}] + N_{DUMP}(0). \quad (2)$$

Taking the half-life  $T_{1/2}$  as 6 hours, the decay reaction as type 6,  $\beta^-$  decay, the atom density at each time point for MAGIC and DUMP are found to be:

**Table 3-9. Analytical Solution to the First Test of Depletion Chain 1.**

| Time (days) | k-effective | $N_{MAGIC}$              | $N_{DUMP}$               |
|-------------|-------------|--------------------------|--------------------------|
| 0.0         | 1.15228298  | $10^{-12}$               | 0.0                      |
| 1.0         | 1.15228298  | $6.25000 \cdot 10^{-14}$ | $9.37500 \cdot 10^{-13}$ |
| 2.0         | 1.15228298  | $3.90625 \cdot 10^{-15}$ | $9.96094 \cdot 10^{-13}$ |
| 3.0         | 1.15228298  | $2.44141 \cdot 10^{-16}$ | $9.99756 \cdot 10^{-13}$ |
| 4.0         | 1.15228298  | $1.52588 \cdot 10^{-17}$ | $9.99985 \cdot 10^{-13}$ |
| 5.0         | 1.15228298  | $9.53674 \cdot 10^{-19}$ | $9.99999 \cdot 10^{-13}$ |

The REBUS output for this test problem is shown in Figure 3-21. It should be very clear that the REBUS calculated results are slightly different from those computed using the analytic solution. All of these errors are consistent with truncation error that is introduced by REBUS when it uses single precision storage of the atom densities. Therefore, the displayed REBUS results can be considered sufficiently accurate with respect to the reference solution.

```

1FCC004 8.6      03/18/10          PAGE  78
...
    ATOM DENSITIES (IN ATOMS/BARN-CM.) OF ACTIVE ISOTOPES IN EACH REGION
    LFPPS      DUMP      U235      U238      PU239      PU240      PU241      PU242      MAGIC
  ICORE1 0.0000E+00 0.0000E+00 9.8725E-04 7.8980E-03 0.0000E+00 0.0000E+00 0.0000E+00 0.0000E+00 1.0000E-12
  ICORE2 0.0000E+00 0.0000E+00 9.8725E-04 7.8980E-03 0.0000E+00 0.0000E+00 0.0000E+00 0.0000E+00 1.0000E-12
  ICORE3 0.0000E+00 0.0000E+00 9.8725E-04 7.8980E-03 0.0000E+00 0.0000E+00 0.0000E+00 0.0000E+00 1.0000E-12
...
1FCC004 8.6      03/18/10          PAGE 138
...
    BEGINNING OF BURN CYCLE  2
    ATOM DENSITIES (IN ATOMS/BARN-CM.) OF ACTIVE ISOTOPES IN EACH REGION
    LFPPS      DUMP      U235      U238      PU239      PU240      PU241      PU242      MAGIC
  ICORE1 0.0000E+00 9.3750E-13 9.8725E-04 7.8980E-03 0.0000E+00 0.0000E+00 0.0000E+00 0.0000E+00 6.2500E-14
  ICORE2 0.0000E+00 9.3750E-13 9.8725E-04 7.8980E-03 0.0000E+00 0.0000E+00 0.0000E+00 0.0000E+00 6.2500E-14
  ICORE3 0.0000E+00 9.3750E-13 9.8725E-04 7.8980E-03 0.0000E+00 0.0000E+00 0.0000E+00 0.0000E+00 6.2500E-14
...
1FCC004 8.6      03/18/10          PAGE 199
...
    BEGINNING OF BURN CYCLE  3
    ATOM DENSITIES (IN ATOMS/BARN-CM.) OF ACTIVE ISOTOPES IN EACH REGION
    LFPPS      DUMP      U235      U238      PU239      PU240      PU241      PU242      MAGIC
  ICORE1 0.0000E+00 9.9609E-13 9.8725E-04 7.8980E-03 0.0000E+00 0.0000E+00 0.0000E+00 0.0000E+00 3.9062E-15
  ICORE2 0.0000E+00 9.9609E-13 9.8725E-04 7.8980E-03 0.0000E+00 0.0000E+00 0.0000E+00 0.0000E+00 3.9062E-15
  ICORE3 0.0000E+00 9.9609E-13 9.8725E-04 7.8980E-03 0.0000E+00 0.0000E+00 0.0000E+00 0.0000E+00 3.9062E-15
...
1FCC004 8.6      03/18/10          PAGE 260
...
    BEGINNING OF BURN CYCLE  4
    ATOM DENSITIES (IN ATOMS/BARN-CM.) OF ACTIVE ISOTOPES IN EACH REGION
    LFPPS      DUMP      U235      U238      PU239      PU240      PU241      PU242      MAGIC
  ICORE1 0.0000E+00 9.9976E-13 9.8725E-04 7.8980E-03 0.0000E+00 0.0000E+00 0.0000E+00 0.0000E+00 2.4414E-16
  ICORE2 0.0000E+00 9.9976E-13 9.8725E-04 7.8980E-03 0.0000E+00 0.0000E+00 0.0000E+00 0.0000E+00 2.4414E-16
  ICORE3 0.0000E+00 9.9976E-13 9.8725E-04 7.8980E-03 0.0000E+00 0.0000E+00 0.0000E+00 0.0000E+00 2.4414E-16
...
1FCC004 8.6      03/18/10          PAGE 321
...
    BEGINNING OF BURN CYCLE  5
    ATOM DENSITIES (IN ATOMS/BARN-CM.) OF ACTIVE ISOTOPES IN EACH REGION
    LFPPS      DUMP      U235      U238      PU239      PU240      PU241      PU242      MAGIC
  ICORE1 0.0000E+00 9.9998E-13 9.8725E-04 7.8980E-03 0.0000E+00 0.0000E+00 0.0000E+00 0.0000E+00 1.5259E-17
  ICORE2 0.0000E+00 9.9998E-13 9.8725E-04 7.8980E-03 0.0000E+00 0.0000E+00 0.0000E+00 0.0000E+00 1.5259E-17
  ICORE3 0.0000E+00 9.9998E-13 9.8725E-04 7.8980E-03 0.0000E+00 0.0000E+00 0.0000E+00 0.0000E+00 1.5259E-17
...
1FCC004 8.6      03/18/10          PAGE 348
...
    THE AVERAGE ERROR OVER   3 REGIONS IS.....0.000000
    REACTOR CONDITIONS AFTER   1 BURNUP SUBSTEPS AT TIME =      5.0000 DAYS
    ATOM DENSITIES (IN ATOMS/BARN-CM.) OF ACTIVE ISOTOPES IN EACH REGION
    LFPPS      DUMP      U235      U238      PU239      PU240      PU241      PU242      MAGIC
  ICORE1 0.0000E+00 1.0000E-12 9.8725E-04 7.8980E-03 0.0000E+00 0.0000E+00 0.0000E+00 0.0000E+00 9.5367E-19
  ICORE2 0.0000E+00 1.0000E-12 9.8725E-04 7.8980E-03 0.0000E+00 0.0000E+00 0.0000E+00 0.0000E+00 9.5367E-19
  ICORE3 0.0000E+00 1.0000E-12 9.8725E-04 7.8980E-03 0.0000E+00 0.0000E+00 0.0000E+00 0.0000E+00 9.5367E-19

```

Figure 3-21. Atom Density Excerpt for REBUS for the First Test of Depletion Chain 1

The next test to consider is a problem with multiple decays from the same MAGIC isotope. Using equation 1, the coupled matrix system to solve is found to be:

$$\frac{\partial}{\partial t} \begin{bmatrix} N_{MAGIC} \\ N_{DUMP} \\ N_{LFP} \\ N_{PU239} \\ N_{PU240} \\ N_{PU241} \\ N_{PU242} \end{bmatrix} = \bar{D} \cdot \begin{bmatrix} N_{MAGIC} \\ N_{DUMP} \\ N_{LFP} \\ N_{PU239} \\ N_{PU240} \\ N_{PU241} \\ N_{PU242} \end{bmatrix}$$

$$\begin{aligned}
 D_{1,1} &= -\lambda_{DUMP} - \lambda_{LFP} - \lambda_{239} - \lambda_{240} - \lambda_{241} - \lambda_{242} = -\lambda \\
 D_{2,1} &= \lambda_{DUMP} = 1.5281 \cdot 10^{-6} \text{ sec}^{-1} \\
 D_{3,1} &= \lambda_{LFP} = 3.0562 \cdot 10^{-6} \text{ sec}^{-1} \\
 D_{4,1} &= \lambda_{239} = 4.5843 \cdot 10^{-6} \text{ sec}^{-1} \\
 D_{5,1} &= \lambda_{240} = 6.1124 \cdot 10^{-6} \text{ sec}^{-1} \\
 D_{6,1} &= \lambda_{241} = 7.6405 \cdot 10^{-6} \text{ sec}^{-1} \\
 D_{7,1} &= \lambda_{242} = 9.168610^{-6} \text{ sec}^{-1}
 \end{aligned} \quad . \quad (3)$$

As seen, the MAGIC isotope is connected to six other isotopes in the chain with differing magnitudes (input reactions 6, 7, 8, 11, 12, and 19 were chosen). Taking the sum of all of the displayed decay constants corresponds to a half-life of 6.00000883 hours which is slightly larger than the previous test case. The analytic solution to the preceding equation is shown below where x denotes all of the product isotopes of the decaying MAGIC isotope.

$$N_{MAGIC}(t) = N \cdot \exp(-\lambda \cdot t) \quad (4)$$

$$N_x(t) = \frac{\lambda_x}{\lambda} N [1 - \exp(-\lambda \cdot t)]$$

The density solutions obtained using the analytic result in equation 4 are tabulated in Table 3-10. Because the same overall decay half-life from the first test problem was used, the densities for  $N_{MAGIC}$  are effectively identical. Figure 3-22 shows the atom density results taken from REBUS at each time step. As expected, the REBUS calculated results match the analytic solution at all of the time points for all of the isotopes. This is again no surprise and proves that the decay related processes are all setup properly for the REBUS software.

**Table 3-10. Analytical Results for the Second Test of Depletion Chain 1.**

| Time (days) | k-effective | $N_{MAGIC}$ | $N_{DUMP} \cdot 10^{-13}$ | $N_{LFP} \cdot 10^{-13}$ | $N_{239} \cdot 10^{-13}$ | $N_{240} \cdot 10^{-13}$ | $N_{241} \cdot 10^{-13}$ | $N_{242} \cdot 10^{-13}$ |
|-------------|-------------|-------------|---------------------------|--------------------------|--------------------------|--------------------------|--------------------------|--------------------------|
| 0.0         | 1.15228298  | $10^{-12}$  | 0.0                       | 0.0                      | 0.0                      | 0.0                      | 0.0                      | 0.0                      |
| 1.0         | 1.15228298  | 0.06250E-0  | 0.4464                    | 0.8929                   | 1.3393                   | 1.7857                   | 2.2321                   | 2.6786                   |
| 2.0         | 1.15228298  | 3.90628E-3  | 0.4743                    | 0.9487                   | 1.4230                   | 1.8973                   | 2.3717                   | 2.8460                   |
| 3.0         | 1.15228298  | 2.44144E-4  | 0.4761                    | 0.9521                   | 1.4282                   | 1.9043                   | 2.3804                   | 2.8564                   |
| 4.0         | 1.15228298  | 1.52590E-5  | 0.4762                    | 0.9524                   | 1.4285                   | 1.9047                   | 2.3809                   | 2.8571                   |
| 5.0         | 1.15228298  | 9.53694E-7  | 0.4762                    | 0.9524                   | 1.4286                   | 1.9048                   | 2.3810                   | 2.8571                   |

1FCC004 8.6 03/18/10 PAGE 78

LFPPS DUMP U235 U238 PU239 PU240 PU241 PU242 MAGIC  
 ICORE1 0.0000E+00 0.0000E+00 9.8725E-04 7.8980E-03 0.0000E+00 0.0000E+00 0.0000E+00 0.0000E+00 1.0000E-12  
 ICORE2 0.0000E+00 0.0000E+00 9.8725E-04 7.8980E-03 0.0000E+00 0.0000E+00 0.0000E+00 0.0000E+00 1.0000E-12  
 ICORE3 0.0000E+00 0.0000E+00 9.8725E-04 7.8980E-03 0.0000E+00 0.0000E+00 0.0000E+00 0.0000E+00 1.0000E-12

1FCC004 8.6 03/18/10 PAGE 138

LFPPS DUMP U235 U238 PU239 PU240 PU241 PU242 MAGIC  
 ICORE1 8.9286E-14 4.4643E-14 9.8725E-04 7.8980E-03 1.3393E-13 1.7857E-13 2.2321E-13 2.6786E-13 6.2500E-14  
 ICORE2 8.9286E-14 4.4643E-14 9.8725E-04 7.8980E-03 1.3393E-13 1.7857E-13 2.2321E-13 2.6786E-13 6.2500E-14  
 ICORE3 8.9286E-14 4.4643E-14 9.8725E-04 7.8980E-03 1.3393E-13 1.7857E-13 2.2321E-13 2.6786E-13 6.2500E-14

1FCC004 8.6 03/18/10 PAGE 199

LFPPS DUMP U235 U238 PU239 PU240 PU241 PU242 MAGIC  
 ICORE1 9.4866E-14 4.7433E-14 9.8725E-04 7.8980E-03 1.4230E-13 1.8973E-13 2.3717E-13 2.8460E-13 3.9063E-15  
 ICORE2 9.4866E-14 4.7433E-14 9.8725E-04 7.8980E-03 1.4230E-13 1.8973E-13 2.3717E-13 2.8460E-13 3.9063E-15  
 ICORE3 9.4866E-14 4.7433E-14 9.8725E-04 7.8980E-03 1.4230E-13 1.8973E-13 2.3717E-13 2.8460E-13 3.9063E-15

1FCC004 8.6 03/18/10 PAGE 260

LFPPS DUMP U235 U238 PU239 PU240 PU241 PU242 MAGIC  
 ICORE1 9.5215E-14 4.7607E-14 9.8725E-04 7.8980E-03 1.4282E-13 1.9043E-13 2.3804E-13 2.8564E-13 2.4414E-16  
 ICORE2 9.5215E-14 4.7607E-14 9.8725E-04 7.8980E-03 1.4282E-13 1.9043E-13 2.3804E-13 2.8564E-13 2.4414E-16  
 ICORE3 9.5215E-14 4.7607E-14 9.8725E-04 7.8980E-03 1.4282E-13 1.9043E-13 2.3804E-13 2.8564E-13 2.4414E-16

1FCC004 8.6 03/18/10 PAGE 321

LFPPS DUMP U235 U238 PU239 PU240 PU241 PU242 MAGIC  
 ICORE1 9.5237E-14 4.7618E-14 9.8725E-04 7.8980E-03 1.4285E-13 1.9047E-13 2.3809E-13 2.8571E-13 1.5259E-17  
 ICORE2 9.5237E-14 4.7618E-14 9.8725E-04 7.8980E-03 1.4285E-13 1.9047E-13 2.3809E-13 2.8571E-13 1.5259E-17  
 ICORE3 9.5237E-14 4.7618E-14 9.8725E-04 7.8980E-03 1.4285E-13 1.9047E-13 2.3809E-13 2.8571E-13 1.5259E-17

1FCC004 8.6 03/18/10 PAGE 348

REACTOR CONDITIONS AFTER 1 BURNUP SUBSTEPS AT TIME = 5.0000 DAYS  
 LFPPS DUMP U235 U238 PU239 PU240 PU241 PU242 MAGIC  
 ICORE1 9.5238E-14 4.7619E-14 9.8725E-04 7.8980E-03 1.4286E-13 1.9048E-13 2.3810E-13 2.8571E-13 9.5369E-19  
 ICORE2 9.5238E-14 4.7619E-14 9.8725E-04 7.8980E-03 1.4286E-13 1.9048E-13 2.3810E-13 2.8571E-13 9.5369E-19  
 ICORE3 9.5238E-14 4.7619E-14 9.8725E-04 7.8980E-03 1.4286E-13 1.9048E-13 2.3810E-13 2.8571E-13 9.5369E-19

**Figure 3-22. Atom Density Excerpt for REBUS for the Second Test of Depletion Chain 1**

### 3.4.2 Depletion Chain 2

The primary focus of depletion chain 2 is to test out the fission reaction process of the depletion chain. For the first test, the isotope MAGIC is defined to produce 2 LUMP isotopes per fission. The actual

number of product isotopes is not relevant as it depends upon how the LUMP was normalized (typically done such that a yield of 1 per fission). The analytic solution for this decay chain is given as

$$\frac{\partial N_{MAGIC}}{\partial t} = -\sigma\phi \cdot N_{MAGIC} \quad \frac{\partial N_{LUMP}}{\partial t} = 2 \cdot \sigma\phi \cdot N_{MAGIC}$$

$$N_{MAGIC}(t) = N_{MAGIC}(0) \cdot \exp^{-\sigma\phi \cdot t}$$

$$N_{LUMP}(t) = N_{MAGIC}(0) [2 - 2 \exp^{-\sigma\phi \cdot t}] + N_{LUMP}(0). \quad (5)$$

The solution to this equation depends upon the magnitude of the flux which is dependent upon the power level setting used in REBUS. Assuming that DIF3D produces the correct solution for an infinite homogeneous problem, the analytic 3 group flux solution for this problem ( $k_{eff}=1.15228298$ ) is given in Table 3-11 along with the computed densities of the two connected isotopes using REBUS and the analytic solution. A power of  $10^{12}$  W was chosen to produce a relatively large reaction rate,  $\sigma\phi \approx 1.407412 \cdot 10^{-5} \cdot sec^{-1}$ , in the transmutation equations above. From the results displayed, it should be clear that REBUS identically reproduces the analytic solution to the truncation error of the atom density storage in ARC.

**Table 3-11. Results for the First Test of Depletion Chain 2.**

| Time (days) | k-effective | REBUS $N_{MAGIC}$ | Analytic $N_{MAGIC}$ | REBUS $N_{LFP}$ | Analytic $N_{MAGIC}$ | Group | $\phi \cdot 10^{-19}$ |
|-------------|-------------|-------------------|----------------------|-----------------|----------------------|-------|-----------------------|
| 0.0         | 1.15228298  | $10^{-12}$        | $10^{-12}$           | $10^{-12}$      | $10^{-12}$           | 1     | 1.83423               |
| 1.0         | 1.15228298  | 2.9641E-13        | 2.9641E-13           | 2.4072E-12      | 2.4072E-12           | 2     | 6.54654               |
| 2.0         | 1.15228298  | 8.7860E-14        | 8.7860E-14           | 2.8243E-12      | 2.8243E-12           |       |                       |
| 3.0         | 1.15228298  | 2.6043E-14        | 2.6043E-14           | 2.9479E-12      | 2.9479E-12           |       |                       |
| 4.0         | 1.15228298  | 7.7194E-15        | 7.7194E-15           | 2.9846E-12      | 2.9846E-12           |       |                       |
| 5.0         | 1.15228298  | 2.2881E-15        | 2.2881E-15           | 2.9954E-12      | 2.9954E-12           |       |                       |

For the second test, all isotopes of Pu included as fissionable materials in the depletion chain where the same LFP is produced with the yield fractions tabulated in Table 3-12. The analytic solution for each isotope is identical to that of equation 5, except for the fact that the lump contains contributions from each of the fissioning isotopes. The analytic solutions are tabulated in Table 3-12 along with the reaction rates given the flux solution from Table 3-11 still applies although it is reduced by an order of magnitude to correspond to  $10^{11}$  W.

**Table 3-12. Analytical Results for the Second Test of Depletion Chain 2.**

| Yield → Fraction | 2.0         | 1.9        | 1.8        | 1.7        | 1.6        | -           |
|------------------|-------------|------------|------------|------------|------------|-------------|
| Reaction Rate →  | 1.4074E-6   | 2.6809E-5  | 4.9849E-6  | 3.9057E-5  | 5.5427E-7  | -           |
| Time (days)      | $N_{MAGIC}$ | $N_{239}$  | $N_{240}$  | $N_{241}$  | $N_{242}$  | $N_{LFP}$   |
| 0.0              | $10^{-12}$  | $10^{-12}$ | $10^{-12}$ | $10^{-12}$ | $10^{-12}$ | $10^{-12}$  |
| 1.0              | 8.8550E-13  | 9.8641E-14 | 6.5006E-13 | 3.4235E-14 | 9.5324E-13 | 5.28809E-12 |
| 2.0              | 7.8411E-13  | 9.7300E-15 | 4.2257E-13 | 1.1721E-15 | 9.0867E-13 | 6.19679E-12 |
| 3.0              | 6.9433E-13  | 9.5978E-16 | 2.7470E-13 | 4.0126E-17 | 8.6618E-13 | 6.72910E-12 |
| 4.0              | 6.1483E-13  | 9.4673E-17 | 1.7857E-13 | 1.3737E-18 | 8.2567E-13 | 7.12764E-12 |
| 5.0              | 5.4444E-13  | 9.3386E-18 | 1.1608E-13 | 4.7031E-20 | 7.8707E-13 | 7.44286E-12 |

The REBUS calculated results are shown in Figure 3-23 at each time point and one can see that they are identical to the analytic solution for every isotope in Table 3-12. The reason the power had to be reduced in this test problem is that REBUS incorrectly calculated the atom density in the third region

at all time steps for isotope Pu-241. After investigation, there is a yet unidentified operation internal to REBUS that makes the atom density calculations of regions 1, 2, and 3 incorrect as the power level becomes unrealistic. Initially, only region 3 is impacted at  $10^{12}$  W but all three regions are eventually truncated to a solution of 0.0 at  $5 \cdot 10^{13}$  W indicating that there is a real precision operation that is truncating the solution data. Because the flux levels and atom densities are well outside of the typical ones used in REBUS, this limitation is not considered important as real engineering problems would not run into this limitation (a 1000 GW reactor is not realistic).

```

FCC004 11.3072 11/11/19 PAGE 78
...
    LFPPS      DUMP      U235      U238      PU239      PU240      PU241      PU242      MAGIC
  ICORE1 1.0000E-12 0.0000E+00 9.8725E-04 7.8980E-03 1.0000E-12 1.0000E-12 1.0000E-12 1.0000E-12 1.0000E-12
  ICORE2 1.0000E-12 0.0000E+00 9.8725E-04 7.8980E-03 1.0000E-12 1.0000E-12 1.0000E-12 1.0000E-12 1.0000E-12
  ICORE3 1.0000E-12 0.0000E+00 9.8725E-04 7.8980E-03 1.0000E-12 1.0000E-12 1.0000E-12 1.0000E-12 1.0000E-12
...
FCC004 11.3072 11/11/19 PAGE 153
...
    BEGINNING OF BURN CYCLE 2
    LFPPS      DUMP      U235      U238      PU239      PU240      PU241      PU242      MAGIC
  ICORE1 5.2881E-12 0.0000E+00 9.8725E-04 7.8980E-03 9.8641E-14 6.5006E-13 3.4235E-14 9.5324E-13 8.8550E-13
  ICORE2 5.2881E-12 0.0000E+00 9.8725E-04 7.8980E-03 9.8641E-14 6.5006E-13 3.4235E-14 9.5324E-13 8.8550E-13
  ICORE3 5.2881E-12 0.0000E+00 9.8725E-04 7.8980E-03 9.8641E-14 6.5006E-13 3.4235E-14 9.5324E-13 8.8550E-13
  1FCC004 8.6    03/18/10 PAGE 199
...
    BEGINNING OF BURN CYCLE 3
    LFPPS      DUMP      U235      U238      PU239      PU240      PU241      PU242      MAGIC
  ICORE1 6.1968E-12 0.0000E+00 9.8725E-04 7.8980E-03 9.7300E-15 4.2257E-13 1.1721E-15 9.0867E-13 7.8411E-13
  ICORE2 6.1968E-12 0.0000E+00 9.8725E-04 7.8980E-03 9.7300E-15 4.2257E-13 1.1721E-15 9.0867E-13 7.8411E-13
  ICORE3 6.1968E-12 0.0000E+00 9.8725E-04 7.8980E-03 9.7300E-15 4.2257E-13 1.1721E-15 9.0867E-13 7.8411E-13
...
  1FCC004 8.6    03/18/10 PAGE 260
...
    BEGINNING OF BURN CYCLE 4
    LFPPS      DUMP      U235      U238      PU239      PU240      PU241      PU242      MAGIC
  ICORE1 6.7291E-12 0.0000E+00 9.8725E-04 7.8980E-03 9.5977E-16 2.7470E-13 4.0126E-17 8.6618E-13 6.9433E-13
  ICORE2 6.7291E-12 0.0000E+00 9.8725E-04 7.8980E-03 9.5977E-16 2.7470E-13 4.0126E-17 8.6618E-13 6.9433E-13
  ICORE3 6.7291E-12 0.0000E+00 9.8725E-04 7.8980E-03 9.5977E-16 2.7470E-13 4.0126E-17 8.6618E-13 6.9433E-13
...
  1FCC004 8.6    03/18/10 PAGE 321
...
    BEGINNING OF BURN CYCLE 5
    LFPPS      DUMP      U235      U238      PU239      PU240      PU241      PU242      MAGIC
  ICORE1 7.1276E-12 0.0000E+00 9.8725E-04 7.8980E-03 9.4673E-17 1.7857E-13 1.3737E-18 8.2567E-13 6.1483E-13
  ICORE2 7.1276E-12 0.0000E+00 9.8725E-04 7.8980E-03 9.4673E-17 1.7857E-13 1.3737E-18 8.2567E-13 6.1483E-13
  ICORE3 7.1276E-12 0.0000E+00 9.8725E-04 7.8980E-03 9.4673E-17 1.7857E-13 1.3737E-18 8.2567E-13 6.1483E-13
...
  1FCC004 8.6    03/18/10 PAGE 348
...
    REACTOR CONDITIONS AFTER 1 BURNUP SUBSTEPS AT TIME = 5.0000 DAYS
    LFPPS      DUMP      U235      U238      PU239      PU240      PU241      PU242      MAGIC
  ICORE1 7.4429E-12 0.0000E+00 9.8725E-04 7.8980E-03 9.3386E-18 1.1608E-13 4.7031E-20 7.8707E-13 5.4444E-13
  ICORE2 7.4429E-12 0.0000E+00 9.8725E-04 7.8980E-03 9.3386E-18 1.1608E-13 4.7031E-20 7.8707E-13 5.4444E-13
  ICORE3 7.4429E-12 0.0000E+00 9.8725E-04 7.8980E-03 9.3386E-18 1.1608E-13 4.7031E-20 7.8707E-13 5.4444E-13
...

```

**Figure 3-23. Atom Density Excerpt for REBUS for the Second Test of Depletion Chain 2**

### 3.4.3 Depletion Chain 3

The primary focus of depletion chain 3 is to test out the connected component reaction process of the depletion chain. In this case, all reactions of the MAGIC isotope are engaged with the products linked to the other isotopes as outlined in Table 3-13. The analytical solution is similar to that found in equation 5 where each of the product isotopes have an identical form with just the cross section that is producing the reaction being the difference.

In that regard, there are only one reaction rate of interest,  $8.4445E-6$  sec<sup>-1</sup>, for the Bateman equations since the cross sections for each reaction type in MAGIC are identical and the reaction rate fraction is 1/6. The analytic solutions for a  $10^{11}$  MW power level are given in Table 3-14 where the DUMP isotope was given a zero initial atom density.

$$\frac{\partial N_{MAGIC}}{\partial t} = -(\sigma_\gamma + \sigma_p + \sigma_\alpha + \sigma_{2n} + \sigma_{deu} + \sigma_{tri})\phi \cdot N_{MAGIC} = -\sigma_C \phi \cdot N_{MAGIC}$$

$$\begin{aligned}
 \frac{\partial N_x}{\partial t} &= \sigma_x \phi \cdot N_{MAGIC} \\
 N_{MAGIC}(t) &= N_{MAGIC}(0) \cdot \exp^{-\sigma_C \phi \cdot t} \\
 N_x(t) &= \frac{\sigma_x \phi}{\sigma_C \phi} N_{MAGIC}(0) [1 - \exp^{-\sigma_C \phi \cdot t}] + N_x(0)
 \end{aligned} \tag{6}$$

**Table 3-13. Depletion Chain 3 Isotopic Products for the MAGIC isotope.**

| Reaction   | Product Isotope |
|------------|-----------------|
| $\gamma$   | Pu239           |
| Proton     | Pu240           |
| $\alpha$   | Pu241           |
| 2 neutrons | Pu242           |
| Deuteron   | LFP             |
| Tritium    | DUMP            |

**Table 3-14. Analytical Results for the First Test of Depletion Chain 3.**

| Time (days) | $N_{MAGIC}$ | $N_{239,240,241,242,LFP}$ | $N_{DUMP}$ |
|-------------|-------------|---------------------------|------------|
| 0.0         | $10^{-12}$  | $10^{-12}$                | 0.0        |
| 1.0         | 4.8210E-13  | 1.0863E-12                | 8.6317E-14 |
| 2.0         | 2.3242E-13  | 1.1279E-12                | 1.2793E-13 |
| 3.0         | 1.1205E-13  | 1.1480E-12                | 1.4799E-13 |
| 4.0         | 5.4020E-14  | 1.1577E-12                | 1.5766E-13 |
| 5.0         | 2.6043E-14  | 1.1623E-12                | 1.6233E-13 |

Figure 3-24 provides the REBUS atom density edits at three of the five time steps which identically match the values of the analytic solution in Table 3-14. The remaining time step data also match identically and were omitted for brevity.

```

FCC004 11.3072 11/11/19 PAGE 78
...
LFPPS DUMP U235 U238 PU239 PU240 PU241 PU242 MAGIC
ICORE1 1.0000E-12 0.0000E+00 9.8725E-04 7.8980E-03 1.0000E-12 1.0000E-12 1.0000E-12 1.0000E-12 1.0000E-12
ICORE2 1.0000E-12 0.0000E+00 9.8725E-04 7.8980E-03 1.0000E-12 1.0000E-12 1.0000E-12 1.0000E-12 1.0000E-12
ICORE3 1.0000E-12 0.0000E+00 9.8725E-04 7.8980E-03 1.0000E-12 1.0000E-12 1.0000E-12 1.0000E-12 1.0000E-12

FCC004 11.3072 11/11/19 PAGE 138
...
BEGINNING OF BURN CYCLE 2
LFPPS DUMP U235 U238 PU239 PU240 PU241 PU242 MAGIC
ICORE1 1.0863E-12 8.6317E-14 9.8725E-04 7.8980E-03 1.0863E-12 1.0863E-12 1.0863E-12 1.0863E-12 4.8210E-13
ICORE2 1.0863E-12 8.6317E-14 9.8725E-04 7.8980E-03 1.0863E-12 1.0863E-12 1.0863E-12 1.0863E-12 4.8210E-13
ICORE3 1.0863E-12 8.6317E-14 9.8725E-04 7.8980E-03 1.0863E-12 1.0863E-12 1.0863E-12 1.0863E-12 4.8210E-13
FCC004 11.3072 11/11/19 PAGE 348
...
REACTOR CONDITIONS AFTER 1 BURNUP SUBSTEPS AT TIME = 5.0000 DAYS
LFPPS DUMP U235 U238 PU239 PU240 PU241 PU242 MAGIC
ICORE1 1.1623E-12 1.6233E-13 9.8725E-04 7.8980E-03 1.1623E-12 1.1623E-12 1.1623E-12 1.1623E-12 2.6043E-14
ICORE2 1.1623E-12 1.6233E-13 9.8725E-04 7.8980E-03 1.1623E-12 1.1623E-12 1.1623E-12 1.1623E-12 2.6043E-14
ICORE3 1.1623E-12 1.6233E-13 9.8725E-04 7.8980E-03 1.1623E-12 1.1623E-12 1.1623E-12 1.1623E-12 2.6043E-14

```

**Figure 3-24. Atom Density Excerpt for REBUS for the First Test of Depletion Chain 3**

The last aspect that needs to be checked for depletion chain 3 is to introduce a decay reaction for each of the product isotopes that cancels out some of the production via the MAGIC isotope. The DUMP isotope is not decayed in this test as it should reproduce the preceding result and the B-10 isotope is added to the depletion chain to be the product isotope of all of the decaying isotopes. The analytic solution for this test case is shown below which is considerably more complex than the one appearing in equation 6 above.

$$\begin{aligned}
 \frac{\partial N_{MAGIC}}{\partial t} &= -(\sigma_\gamma + \sigma_p + \sigma_\alpha + \sigma_{2n} + \sigma_{deu} + \sigma_{tri})\phi \cdot N_{MAGIC} = -\sigma_C\phi \cdot N_{MAGIC} \\
 \frac{\partial N_x}{\partial t} &= \sigma_x\phi \cdot N_{MAGIC} - \lambda_x \cdot N_x \quad \frac{\partial N_{B10}}{\partial t} = \sum_x \lambda_x \cdot N_x \\
 N_{MAGIC}(t) &= N_{MAGIC}(0) \cdot \exp^{-\sigma_C\phi \cdot t} \\
 N_x(t) &= N_x(0) \exp^{-\lambda_x \cdot t} + \frac{\sigma_x\phi \cdot N_{MAGIC}(0)}{\lambda_x - \sigma_C\phi} (\exp^{-\sigma_C\phi \cdot t} - \exp^{-\lambda_x \cdot t}) \\
 N_{B10}(t) &= N_{B10}(0) + \sum_x \left[ N_x(0) + \frac{\sigma_x\phi \cdot N_{MAGIC}(0)}{\lambda_x - \sigma_C\phi} \left( \frac{\lambda_x}{\sigma_C\phi} - 1 \right) \right. \\
 &\quad \left. - N_x(0) \exp^{-\lambda_x \cdot t} + \frac{\sigma_x\phi \cdot N_{MAGIC}(0)}{\lambda_x - \sigma_C\phi} \left( -\frac{\lambda_x}{\sigma_C\phi} \exp^{-\sigma_C\phi \cdot t} + \exp^{-\lambda_x \cdot t} \right) \right] \quad (7)
 \end{aligned}$$

A close inspection should indicate that for a single isotope with multiple reactions, one cannot select a decay constant that exactly negates the contribution rate from another isotope. Given the reaction rate for MAGIC will remain as 8.4445E-6 sec<sup>-1</sup>, the decay constants for each product isotope were chosen to fall in this range, as seen in Table 3-15, yielding the analytic solutions shown in Table 3-15. The excerpt of the REBUS atom densities is provided in Figure 3-25 for a sub-set of the time steps and a quick comparison shows that REBUS identically reproduces the analytic solution at all of the chosen time steps. Looking at the individual density curves in the analytic solution, one finds that the Pu239 densities are slightly less than those seen with Pu239 in Table 3-14 due to the small decay constant. For Pu240, the larger decay constant leads to an initial increase in the total atom density to a plateau followed by a decrease in the atom density. A similar trend is observed with Pu241 and Pu242 although the larger decay constant causes the peak to occur earlier and the plateau region is not observable with the displayed time step evaluations. For LFP, there is only a slight increase in the concentration and one can clearly infer that as the decay constant is increased further the resulting isotopic decay will decrease at all time points from its initial value. Similar to the MAGIC isotope, the DUMP result is identical to that in Table 3-14. Finally, the B-10 analytic result is seen to constantly increase from its initial value of zero to a number less than 6·10<sup>12</sup> which would be the B-10 atom density at time  $\infty$ .

**Table 3-15. Analytical Results for the Second Test of Depletion Chain 3.**

| Decay $\rightarrow$<br>sec <sup>-1</sup> | 1·10 <sup>-8</sup> | 1·10 <sup>-7</sup> | 3·10 <sup>-7</sup> | 6·10 <sup>-7</sup> | 9·10 <sup>-6</sup> | -          | -          |
|--|--------------------|--------------------|--------------------|--------------------|--------------------|------------|------------|
| Time<br>(days)                           | $N_{239}$          | $N_{240}$          | $N_{241}$          | $N_{242}$          | $N_{LFP}$          | $N_{DUMP}$ | $N_{B10}$  |
| 0.0                                      | 10 <sup>-12</sup>  | 0.0        | 0.0        |
| 1.0                                      | 1.0854E-12         | 1.0773E-12         | 1.0595E-12         | 1.0333E-12         | 1.0078E-12         | 8.6317E-14 | 6.5930E-13 |
| 2.0                                      | 1.1261E-12         | 1.1094E-12         | 1.0734E-12         | 1.0216E-12         | 9.7229E-13         | 1.2793E-13 | 1.0441E-12 |
| 3.0                                      | 1.1451E-12         | 1.1199E-12         | 1.0657E-12         | 9.8944E-13         | 9.1876E-13         | 1.4799E-13 | 1.2847E-12 |
| 4.0                                      | 1.1538E-12         | 1.1199E-12         | 1.0480E-12         | 9.4885E-13         | 8.5929E-13         | 1.5766E-13 | 1.4493E-12 |
| 5.0                                      | 1.1575E-12         | 1.1149E-12         | 1.0257E-12         | 9.0544E-13         | 7.9947E-13         | 1.6233E-13 | 1.5735E-12 |

```

FCC004 11.3072 11/11/19 PAGE 78
...
      B-10      DUMP      U235      U238      MAGIC      PU239      PU240      PU241      PU242
  LFPFS
  ICORE1  0.0000E+00  0.0000E+00  9.8725E-04  7.8980E-03  1.0000E-12  1.0000E-12  1.0000E-12  1.0000E-12
  1.0000E-12
  ICORE2  0.0000E+00  0.0000E+00  9.8725E-04  7.8980E-03  1.0000E-12  1.0000E-12  1.0000E-12  1.0000E-12
  1.0000E-12
  ICORE3  0.0000E+00  0.0000E+00  9.8725E-04  7.8980E-03  1.0000E-12  1.0000E-12  1.0000E-12  1.0000E-12
  1.0000E-12

FCC004 11.3072 11/11/19 PAGE 138
...
      B-10      DUMP      U235      U238      BEGINNING OF BURN CYCLE 2      MAGIC      PU239      PU240      PU241      PU242
  LFPFS
  ICORE1  6.5930E-13  8.6317E-14  9.8725E-04  7.8980E-03  4.8210E-13  1.0854E-12  1.0773E-12  1.0595E-12  1.0333E-12
  5.1675E-13
  ICORE2  6.5930E-13  8.6317E-14  9.8725E-04  7.8980E-03  4.8210E-13  1.0854E-12  1.0773E-12  1.0595E-12  1.0333E-12
  5.1675E-13
  ICORE3  6.5930E-13  8.6317E-14  9.8725E-04  7.8980E-03  4.8210E-13  1.0854E-12  1.0773E-12  1.0595E-12  1.0333E-12
  5.1675E-13

FCC004 11.3072 11/11/19 PAGE 260
...
      B-10      DUMP      U235      U238      BEGINNING OF BURN CYCLE 4      MAGIC      PU239      PU240      PU241      PU242
  LFPFS
  ICORE1  1.2847E-12  1.4799E-13  9.8725E-04  7.8980E-03  1.1205E-13  1.1451E-12  1.1199E-12  1.0657E-12  9.8944E-13
  1.3509E-13
  ICORE2  1.2847E-12  1.4799E-13  9.8725E-04  7.8980E-03  1.1205E-13  1.1451E-12  1.1199E-12  1.0657E-12  9.8944E-13
  1.3509E-13
  ICORE3  1.2847E-12  1.4799E-13  9.8725E-04  7.8980E-03  1.1205E-13  1.1451E-12  1.1199E-12  1.0657E-12  9.8944E-13
  1.3509E-13

FCC004 11.3072 11/11/19 PAGE 348
...
      REACTOR CONDITIONS AFTER      1      BURNUP      SUBSTEPS AT      TIME =      5.0000 DAYS
      B-10      DUMP      U235      U238      MAGIC      PU239      PU240      PU241      PU242
  LFPFS
  ICORE1  1.5735E-12  1.6233E-13  9.8725E-04  7.8980E-03  2.6043E-14  1.1575E-12  1.1149E-12  1.0257E-12  9.0544E-13
  3.4564E-14
  ICORE2  1.5735E-12  1.6233E-13  9.8725E-04  7.8980E-03  2.6043E-14  1.1575E-12  1.1149E-12  1.0257E-12  9.0544E-13
  3.4564E-14
  ICORE3  1.5735E-12  1.6233E-13  9.8725E-04  7.8980E-03  2.6043E-14  1.1575E-12  1.1149E-12  1.0257E-12  9.0544E-13
  3.4564E-14

```

Figure 3-25. Atom Density Excerpt for REBUS for the First Test of Depletion Chain 3

### 3.4.4 Depletion Chain 4

The primary focus of depletion chain 4 is to test out the connected component reaction process of the depletion chain. In this regard, the focus is placed on a coupled absorption and decay process followed by a complex connected depletion system. For the first test, the depletion chain defined by Table 3-16 is used.

Table 3-16. Test #1 of Depletion Chain 4.

| Target Isotope | Reaction | Product Isotopes | Reaction Rate |
|----------------|----------|------------------|---------------|
| MAGIC          | $\alpha$ | Pu239            | 1.40741E-06   |
| Pu239          | $\gamma$ | MAGIC            | 8.72538E-06   |
| Pu240          | Fission  | Pu241            | 4.98490E-06   |
| Pu241          | 2n       | Pu242            | 2.54910E-08   |
| Pu242          | Fission  | Pu240            | 5.54266E-07   |
| LFP            | $\gamma$ | DUMP             | 8.69121E-06   |
| DUMP           | Decay    | LFP              | 1.0E-6        |
| DUMP           | Decay    | B-10             | 1.0E-8        |
| B-10           | Decay    | U238             | 1.0E-7        |

As can be seen, the depletion chain has several circular connections which makes the analytic solution more difficult. Considering two situations with coupled differential equations we can write:

$$\frac{\partial N_1}{\partial t} = -R_1 \cdot N_1 + R_2 \cdot N_2 \quad \frac{\partial N_2}{\partial t} = -R_2 \cdot N_2 + R_1 \cdot N_1 \quad (8)$$

and

$$\frac{\partial N_1}{\partial t} = -R_1 \cdot N_1 + R_3 \cdot N_3 \quad \frac{\partial N_2}{\partial t} = -R_2 \cdot N_2 + R_1 \cdot N_1 \quad \frac{\partial N_3}{\partial t} = -R_3 \cdot N_3 + R_2 \cdot N_2 \quad (9)$$

To solve these systems, the constants that appear in the exponentials must first be identified using

$$\begin{bmatrix} -R_1 & \dots & R_{n-1} \\ \vdots & \ddots & \vdots \\ R_{n-1} & \dots & -R_n \end{bmatrix} \begin{bmatrix} N_1 \\ \vdots \\ N_n \end{bmatrix} = A \cdot \begin{bmatrix} N_1 \\ \vdots \\ N_n \end{bmatrix} \rightarrow |A - \lambda I| = 0. \quad (10)$$

The general solution for the coupled system of equations is found to be

$$N_n(t) = C_n + \sum_i A_{n,i} \cdot \exp(-\lambda_i \cdot t) + \sum_i B_{n,i} \cdot t \cdot \exp(-\lambda_i \cdot t), \quad (11)$$

but, for the set of equations used in the following REBUS calculations, the last term is known to not be present or  $B_{n,i} \equiv 0$ . The analytic solution in the two equation case (MAGIC and Pu239) has only one eigenvalue,  $\lambda_i$ , and an analytic solution of:

$$\begin{aligned} \frac{\partial N_1}{\partial t} &= -R_1 \cdot N_1 + R_2 \cdot N_2 & \frac{\partial N_2}{\partial t} &= -R_2 \cdot N_2 + R_1 \cdot N_1 & \frac{\partial N_1}{\partial t} &= -\frac{\partial N_2}{\partial t} \\ N_1(t) &= \frac{R_2}{R_1 + R_2} \cdot [N_1(0) + N_2(0)] + \left[ \frac{R_1}{R_1 + R_2} N_1(0) - \frac{R_2}{R_1 + R_2} N_2(0) \right] \cdot \exp(-(R_1 + R_2) \cdot t) \\ N_2(t) &= \frac{R_1}{R_1 + R_2} \cdot [N_1(0) + N_2(0)] - \left[ \frac{R_1}{R_1 + R_2} N_1(0) - \frac{R_2}{R_1 + R_2} N_2(0) \right] \cdot \exp(-(R_1 + R_2) \cdot t) \end{aligned} \quad (12)$$

For the three connected equation system in equation 9 (Pu240, Pu241, and Pu242) there are two eigenvalues

$$\begin{aligned} \lambda_1 &= \frac{R1 + R2 + R3}{2} - \frac{1}{2} \sqrt{R1^2 + R2^2 + R3^2 - 2 \cdot R1 \cdot R2 - 2 \cdot R1 \cdot R3 - 2 \cdot R2 \cdot R3} \\ \lambda_2 &= \frac{R1 + R2 + R3}{2} + \frac{1}{2} \sqrt{R1^2 + R2^2 + R3^2 - 2 \cdot R1 \cdot R2 - 2 \cdot R1 \cdot R3 - 2 \cdot R2 \cdot R3} \end{aligned} \quad (13)$$

As one can infer from the large size of these terms, the analytic solution is incredibly more complex than the one in equation 12 and cannot be written compactly in this manuscript. The reference analytic solution, in numerical form, for the three isotope connected system described by Table 3-16 is found to be

$$\begin{aligned} \lambda_1 &= -4.98169032 \cdot 10^{-6} & \lambda_2 &= -5.82966679 \cdot 10^{-7} \\ N_{240}(t) &= 1.45950608 \cdot 10^{-14} + 8.76657883 \cdot 10^{-13} \exp(\lambda_1 \cdot t) + 1.08747056 \cdot 10^{-13} \exp(\lambda_2 \cdot t) \\ N_{241}(t) &= 2.8541414 \cdot 10^{-12} - 8.8173449 \cdot 10^{-13} \exp(\lambda_1 \cdot t) - 9.72406907 \cdot 10^{-13} \exp(\lambda_2 \cdot t) \\ N_{242}(t) &= 1.31263542 \cdot 10^{-13} + 5.07660713 \cdot 10^{-15} \exp(\lambda_1 \cdot t) + 8.63659851 \cdot 10^{-13} \exp(\lambda_2 \cdot t) \end{aligned} \quad (14)$$

A MathCAD [16] document that shows the detailed derivation is included in the repository with the verification test results shown here. The third type of chain that is defined in Table 3-16. (LFP, DUMP, and B-10) is

$$\begin{aligned} \frac{\partial N_1}{\partial t} &= -R_1 \cdot N_1 + R_{2a} \cdot N_2 \\ \frac{\partial N_2}{\partial t} &= -R_{2a} \cdot N_2 - R_{2b} \cdot N_2 + R_1 \cdot N_1 \\ \frac{\partial N_3}{\partial t} &= -R_3 \cdot N_3 + R_{2b} \cdot N_2. \end{aligned} \quad (15)$$

This system has three eigenvalues

$$\begin{aligned} \lambda_1 &= -\frac{R1 + R2a + R2b}{2} + \frac{1}{2} \sqrt{R1^2 + R2a^2 + R2b^2 - 2 \cdot R1 \cdot R2a - 2 \cdot R1 \cdot R2b - 2 \cdot R2a \cdot R2b} \\ \lambda_2 &= -\frac{R1 + R2a + R2b}{2} - \frac{1}{2} \sqrt{R1^2 + R2a^2 + R2b^2 - 2 \cdot R1 \cdot R2a - 2 \cdot R1 \cdot R2b - 2 \cdot R2a \cdot R2b} \end{aligned}$$

$$\lambda_3 = -R3 \quad (16)$$

As was the case in the three coupled isotope set, the detailed analytic solution is too complex to write compactly in this manuscript and thus the analytic solution of

$$\lambda_1 = -8.96718145 \cdot 10^{-9} \quad \lambda_2 = -9.69224282 \cdot 10^{-6} \quad \lambda_3 = -1.0 \cdot 10^{-7}$$

$$N_{LFP}(t) = 2.06648338 \cdot 10^{-13} \exp(\lambda_1 \cdot t) + 7.93351662 \cdot 10^{-13} \exp(\lambda_2 \cdot t)$$

$$N_{DUMP}(t) = 1.79417105 \cdot 10^{-12} \exp(\lambda_1 \cdot t) - 7.9417105 \cdot 10^{-13} \exp(\lambda_2 \cdot t)$$

$$N_{B-10}(t) = 1.97090574 \cdot 10^{-13} \exp(\lambda_1 \cdot t) + 8.02081495 \cdot 10^{-13} \exp(\lambda_3 \cdot t) \quad (17)$$

is again provided in the MathCAD document. The analytic results for five time steps using the preceding analytic solutions in the depletion chain in Table 3-16 are shown in Table 3-17 where the REBUS solution excerpt is given in Figure 3-26. For the first coupled set of isotopes, MAGIC and Pu239, the analytic results are identical to the results shown in the REBUS excerpt. For the second set of coupled isotopes, Pu240, Pu241, and Pu242, the Pu240 and Pu241 isotopes exactly match while the Pu242 isotope shows only a difference in the final time step in the last significant digit.

**Table 3-17. Analytical Results for the First Test of Depletion Chain 4.**

| Time (days) | $N_{MAGIC}$ | $N_{239}$  | $N_{240}$  | $N_{241}$  | $N_{242}$  |
|-------------|-------------|------------|------------|------------|------------|
| 0.0         | $10^{-12}$  | $10^{-12}$ | $10^{-12}$ | $10^{-12}$ | $10^{-12}$ |
| 1.0         | 1.4213E-12  | 5.7871E-13 | 6.8804E-13 | 1.3562E-12 | 9.5580E-13 |
| 2.0         | 1.5968E-12  | 4.0318E-13 | 4.8358E-13 | 1.6021E-12 | 9.1431E-13 |
| 3.0         | 1.6700E-12  | 3.3004E-13 | 3.4911E-13 | 1.7757E-12 | 8.7520E-13 |
| 4.0         | 1.7004E-12  | 2.9956E-13 | 2.6022E-13 | 1.9015E-12 | 8.3823E-13 |
| 5.0         | 1.7131E-12  | 2.8686E-13 | 2.0104E-13 | 1.9957E-12 | 8.0324E-13 |

| Time (days) | $N_{LFP}$  | $N_{DUMP}$ | $N_{B10}$  |
|-------------|------------|------------|------------|
| 0.0         | $10^{-12}$ | $10^{-12}$ | $10^{-12}$ |
| 1.0         | 5.4987E-13 | 1.4490E-12 | 9.9248E-13 |
| 2.0         | 3.5496E-13 | 1.6426E-12 | 9.8528E-13 |
| 3.0         | 2.7050E-13 | 1.7256E-12 | 9.7826E-13 |
| 4.0         | 2.3385E-13 | 1.7607E-12 | 9.7134E-13 |
| 5.0         | 2.1790E-13 | 1.7752E-12 | 9.6451E-13 |

This slight error is assumed to be due to round off truncation between the double precision based calculations of MathCAD and the single precision limited calculations of REBUS. The final set of coupled isotopes, LFP, DUMP, B-10, and U-238, the analytic and REBUS solutions are again identical. Note that the output precision of the U-238 isotope density in REBUS cannot display the change in the U-238 atom density and thus it was omitted from the above analytic solutions and the tabulated results. In summary, REBUS has been successfully shown to reproduce the analytic solution to the Bateman equations.

The second depletion chain would ideally consider a larger circularly connected system. However, an attempt to construct an analytic solution with 8 circularly connected isotopes could not be completed due to the limitations of double precision math and a general inability to compute the system eigenvalues. Thus, the second test of depletion chain 4 considers a double connected circular depletion chain shown in Table 3-18. As was the case in the first test, the analytic solution is too complex to compactly write in this manuscript.

```

FCC004 11.3072 11/11/19                                PAGE      137
...                                                 BEGINNING OF BURN CYCLE  2
...          U235      U238      MAGIC      PU239      PU240      PU241      PU242      LFPPS      DUMP
...          B-10
ICORE1  9.8725E-04  7.8980E-03  1.4213E-12  5.7871E-13  6.8804E-13  1.3562E-12  9.5580E-13  5.4987E-13  1.4490E-12
9.9248E-13
ICORE2  9.8725E-04  7.8980E-03  1.4213E-12  5.7871E-13  6.8804E-13  1.3562E-12  9.5580E-13  5.4987E-13  1.4490E-12
9.9248E-13
ICORE3  9.8725E-04  7.8980E-03  1.4213E-12  5.7871E-13  6.8804E-13  1.3562E-12  9.5580E-13  5.4987E-13  1.4490E-12
9.9248E-13

FCC004 11.3072 11/11/19                                PAGE      198
...                                                 BEGINNING OF BURN CYCLE  3
...          U235      U238      MAGIC      PU239      PU240      PU241      PU242      LFPPS      DUMP
...          B-10
ICORE1  9.8725E-04  7.8980E-03  1.5968E-12  4.0318E-13  4.8358E-13  1.6021E-12  9.1431E-13  3.5496E-13  1.6426E-12
9.8528E-13
ICORE2  9.8725E-04  7.8980E-03  1.5968E-12  4.0318E-13  4.8358E-13  1.6021E-12  9.1431E-13  3.5496E-13  1.6426E-12
9.8528E-13
ICORE3  9.8725E-04  7.8980E-03  1.5968E-12  4.0318E-13  4.8358E-13  1.6021E-12  9.1431E-13  3.5496E-13  1.6426E-12
9.8528E-13

FCC004 11.3072 11/11/19                                PAGE      259
...                                                 BEGINNING OF BURN CYCLE  4
...          U235      U238      MAGIC      PU239      PU240      PU241      PU242      LFPPS      DUMP
...          B-10
ICORE1  9.8725E-04  7.8980E-03  1.6700E-12  3.3004E-13  3.4911E-13  1.7757E-12  8.7520E-13  2.7050E-13  1.7256E-12
9.7826E-13
ICORE2  9.8725E-04  7.8980E-03  1.6700E-12  3.3004E-13  3.4911E-13  1.7757E-12  8.7520E-13  2.7050E-13  1.7256E-12
9.7826E-13
ICORE3  9.8725E-04  7.8980E-03  1.6700E-12  3.3004E-13  3.4911E-13  1.7757E-12  8.7520E-13  2.7050E-13  1.7256E-12
9.7826E-13

FCC004 11.3072 11/11/19                                PAGE      347
...                                                 REACTOR CONDITIONS AFTER 1 BURNUP SUBSTEPS AT TIME = 5.000000000E+00 DAYS
...          U235      U238      MAGIC      PU239      PU240      PU241      PU242      LFPPS      DUMP
...          B-10
ICORE1  9.8725E-04  7.8980E-03  1.7131E-12  2.8686E-13  2.0104E-13  1.9957E-12  8.0323E-13  2.1790E-13  1.7752E-12
9.6451E-13
ICORE2  9.8725E-04  7.8980E-03  1.7131E-12  2.8686E-13  2.0104E-13  1.9957E-12  8.0323E-13  2.1790E-13  1.7752E-12
9.6451E-13
ICORE3  9.8725E-04  7.8980E-03  1.7131E-12  2.8686E-13  2.0104E-13  1.9957E-12  8.0323E-13  2.1790E-13  1.7752E-12
9.6451E-13

```

**Figure 3-26. Atom Density Excerpt for REBUS for the First Test of Depletion Chain 4**

**Table 3-18. Test #2 of Depletion Chain 4.**

| Target Isotope | Reaction | Product Isotopes | Reaction Rate |
|----------------|----------|------------------|---------------|
| MAGIC          | decay    | Pu239            | 1.407412E-06  |
| MAGIC          | decay    | Pu240            | 1.407412E-06  |
| Pu239          | decay    | Pu240            | 8.725380E-06  |
| Pu239          | decay    | Pu241            | 2.680868E-05  |
| Pu240          | decay    | Pu241            | 9.625767E-06  |
| Pu240          | decay    | MAGIC            | 4.984896E-06  |
| Pu241          | decay    | MAGIC            | 7.779904E-06  |
| Pu241          | decay    | Pu239            | 3.905662E-05  |

The coupled equations can be written as:

$$\frac{\partial N_{MAGIC}(t)}{\partial t} = -(R_{MAGIC,1} + R_{MAGIC,2}) \cdot N_{MAGIC}(t) + R_{241,1} \cdot N_{241}(t) + R_{240,2} \cdot N_{240}(t)$$

$$\frac{\partial N_{239}(t)}{\partial t} = -(R_{239,1} + R_{239,2}) \cdot N_{239}(t) + R_{MAGIC,1} \cdot N_{MAGIC}(t) + R_{241,2} \cdot N_{241}(t)$$

$$\frac{\partial N_{240}(t)}{\partial t} = -(R_{240,1} + R_{240,2}) \cdot N_{240}(t) + R_{239,1} \cdot N_{239}(t) + R_{MAGIC,2} \cdot N_{MAGIC}(t)$$

$$\frac{\partial N_{241}(t)}{\partial t} = -(R_{241,1} + R_{241,2}) \cdot N_{241}(t) + R_{240,1} \cdot N_{240}(t) + R_{239,2} \cdot N_{239}(t). \quad (18)$$

The analytic solution is again obtained in the MathCAD document and has three eigenvalues of  $\lambda_1 = -6.72620753998521 \cdot 10^{-6}$

$$\lambda_2 = -1.99866076635878 \cdot 10^{-5}$$

$$\lambda_3 = -7.308325931442701 \cdot 10^{-5}. \quad (19)$$

The analytic solution, its first derivative, and initial condition take the form

$$N_i(t) = C_i + A_{i,1} \cdot \exp(-\lambda_1 \cdot t) + A_{i,2} \cdot \exp(-\lambda_2 \cdot t) + A_{i,3} \cdot \exp(-\lambda_3 \cdot t)$$

$$\frac{\partial N_i(t)}{\partial t} = -\lambda_1 \cdot A_{i,1} \cdot \exp(-\lambda_1 \cdot t) - \lambda_2 \cdot A_{i,2} \cdot \exp(-\lambda_2 \cdot t) - \lambda_3 \cdot A_{i,3} \cdot \exp(-\lambda_3 \cdot t)$$

$$N_i(0) = C_i + A_{i,1} + A_{i,2} + A_{i,3}. \quad (20)$$

This system of equations has 16 unknowns with 4 initial condition equations and 4 constraint equations derived from each equation in equation 18. The constraint equations have the general form of

$$\frac{\partial N_1(t)}{\partial t} = -(R_{1,1} + R_{1,2}) \cdot N_1(t) + R_{2,1} \cdot N_2(t) + R_{3,2} \cdot N_3(t)$$

$$0 = -(R_{1,1} + R_{1,2}) \cdot C_1 + R_{2,1} \cdot C_2 + R_{3,2} \cdot C_3$$

$$-\lambda_1 \cdot A_{1,1} = -(R_{1,1} + R_{1,2}) \cdot A_{1,1} + R_{2,1} \cdot A_{2,1} + R_{3,2} \cdot A_{3,1}$$

$$-\lambda_2 \cdot A_{1,2} = -(R_{1,1} + R_{1,2}) \cdot A_{1,2} + R_{2,1} \cdot A_{2,2} + R_{3,2} \cdot A_{3,2}$$

$$-\lambda_3 \cdot A_{1,3} = -(R_{1,1} + R_{1,2}) \cdot A_{1,3} + R_{2,1} \cdot A_{2,3} + R_{3,2} \cdot A_{3,3}. \quad (21)$$

Where the indices 1, 2, and 3 dereference to the necessary isotope connections seen in equation 18. As was the case with the previous depletion case, the last set of the constraint equations are dropped leading to 16 equations for 16 unknowns. The analytic solution obtained for these four isotopes is found to be

$$N_{MAGIC}(t) = 2.33607E-12 - 1.31466E-12 \cdot \exp(-\lambda_1 \cdot t) \\ - 8.61770E-15 \cdot \exp(-\lambda_2 \cdot t) - 1.27942E-14 \cdot \exp(-\lambda_3 \cdot t)$$

$$N_{Pu239}(t) = 6.07530E-13 + 5.28070E-13 \cdot \exp(-\lambda_1 \cdot t) \\ - 2.68976E-14 \cdot \exp(-\lambda_2 \cdot t) - 1.08702E-13 \cdot \exp(-\lambda_3 \cdot t)$$

$$N_{Pu240}(t) = 5.87841E-13 + 3.49718E-13 \cdot \exp(-\lambda_1 \cdot t) \\ + 4.59120E-14 \cdot \exp(-\lambda_2 \cdot t) + 1.65286E-14 \cdot \exp(-\lambda_3 \cdot t) \quad . \quad (22)$$

$$N_{Pu241}(t) = 4.68555E-13 + 4.36874E-13 \cdot \exp(-\lambda_1 \cdot t) \\ - 1.03967E-14 \cdot \exp(-\lambda_2 \cdot t) + 1.04968E-13 \cdot \exp(-\lambda_3 \cdot t)$$

The numerical solution at 5 time steps using the above analytic solution is provided in Table 3-19 for all four isotopes. The same depletion problem was setup in REBUS and the excerpt of the atom density output at several of the time steps is provided in Figure 3-27. A quick comparison of the results shows that they are identical at all displayed time points such that REBUS is verified to reproduce the analytic solution. During this verification test problem, it was observed that the depletion chain could not use more than one fission operation to connect the isotopes. As an example, the Pu239 isotope fissions to Pu240 which fissions to Pu241 which fissions to Pu239. This is of course a non-physical occurrence for any depletion code. While such an approach effectively worked in the first depletion chain 4 test when the isotope is doubly coupled, in this example the burn matrix is not constructed properly by REBUS. Given this setup error is not plausible for any user problem, no additional documentation of the limitation is required.

**Table 3-19. Analytical Results for the Second Test of Depletion Chain 4.**

| Time<br>(days) | $N_{MAGIC}$ | $N_{239}$  | $N_{240}$  | $N_{241}$  |
|----------------|-------------|------------|------------|------------|
| 0.0            | $10^{-12}$  | $10^{-12}$ | $10^{-12}$ | $10^{-12}$ |
| 1.0            | 1.5993E-12  | 8.9788E-13 | 7.9162E-13 | 7.1122E-13 |
| 2.0            | 1.9246E-12  | 7.7184E-13 | 6.9867E-13 | 6.0487E-13 |
| 3.0            | 2.1061E-12  | 6.9975E-13 | 6.4927E-13 | 5.4491E-13 |
| 4.0            | 2.2075E-12  | 6.5916E-13 | 6.2210E-13 | 5.1128E-13 |
| 5.0            | 2.2641E-12  | 6.3642E-13 | 6.0698E-13 | 4.9245E-13 |

```

FCC004 11.3072 11/11/19                                PAGE    138
                                                BEGINNING OF BURN CYCLE  2
...
U235      U238      MAGIC      PU239      PU240      PU241      PU242      LFPPS      DUMP
B-10
ICORE1  9.8725E-04  7.8980E-03  1.5993E-12  8.9788E-13  7.9162E-13  7.1122E-13  1.0000E-12  1.0000E-12  1.0000E-12
1.0000E-12
ICORE2  9.8725E-04  7.8980E-03  1.5993E-12  8.9788E-13  7.9162E-13  7.1122E-13  1.0000E-12  1.0000E-12  1.0000E-12
1.0000E-12
ICORE3  9.8725E-04  7.8980E-03  1.5993E-12  8.9788E-13  7.9162E-13  7.1122E-13  1.0000E-12  1.0000E-12  1.0000E-12
1.0000E-12...
FCC004 11.3072 11/11/19                                PAGE    199
...
U235      U238      MAGIC      PU239      PU240      PU241      PU242      LFPPS      DUMP
B-10
ICORE1  9.8725E-04  7.8980E-03  1.9246E-12  7.7184E-13  6.9867E-13  6.0487E-13  1.0000E-12  1.0000E-12  1.0000E-12
1.0000E-12
ICORE2  9.8725E-04  7.8980E-03  1.9246E-12  7.7184E-13  6.9867E-13  6.0487E-13  1.0000E-12  1.0000E-12  1.0000E-12
1.0000E-12
ICORE3  9.8725E-04  7.8980E-03  1.9246E-12  7.7184E-13  6.9867E-13  6.0487E-13  1.0000E-12  1.0000E-12  1.0000E-12
1.0000E-12...
FCC004 11.3072 11/11/19                                PAGE    260
...
U235      U238      MAGIC      PU239      PU240      PU241      PU242      LFPPS      DUMP
B-10
ICORE1  9.8725E-04  7.8980E-03  2.1061E-12  6.9975E-13  6.4927E-13  5.4491E-13  1.0000E-12  1.0000E-12  1.0000E-12
1.0000E-12
ICORE2  9.8725E-04  7.8980E-03  2.1061E-12  6.9975E-13  6.4927E-13  5.4491E-13  1.0000E-12  1.0000E-12  1.0000E-12
1.0000E-12
ICORE3  9.8725E-04  7.8980E-03  2.1061E-12  6.9975E-13  6.4927E-13  5.4491E-13  1.0000E-12  1.0000E-12  1.0000E-12
1.0000E-12...
FCC004 11.3072 11/11/19                                PAGE    347
...
U235      U238      MAGIC      PU239      PU240      PU241      PU242      LFPPS      DUMP
B-10
REACTOR CONDITIONS AFTER 1 BURNUP SUBSTEPS AT TIME = 5.000000000E+00 DAYS
ICORE1  9.8725E-04  7.8980E-03  2.2641E-12  6.3642E-13  6.0698E-13  4.9245E-13  1.0000E-12  1.0000E-12  1.0000E-12
1.0000E-12
ICORE2  9.8725E-04  7.8980E-03  2.2641E-12  6.3642E-13  6.0698E-13  4.9245E-13  1.0000E-12  1.0000E-12  1.0000E-12
1.0000E-12
ICORE3  9.8725E-04  7.8980E-03  2.2641E-12  6.3642E-13  6.0698E-13  4.9245E-13  1.0000E-12  1.0000E-12  1.0000E-12
1.0000E-12...

```

**Figure 3-27. Atom Density Excerpt for REBUS for the Second Test of Depletion Chain 4**

### 3.4.5 Flux Impacted Depletion Verification

The preceding four depletion chain verifications are proof that REBUS can properly setup the depletion chain. This infers that the reaction rates computed for the depletion matrix are properly constructed and the depletion matrix itself, for simple and complex problems, is setup properly. For real depletion problems where the eigenvalue and flux magnitudes are impacted by the depletion process, the analytic solutions are more difficult to generate. This is primarily because the problem specified must have an analytic solution for the flux equation (diffusion or transport) and for the proposed depletion chain. From the DIF3D verification report [14], analytic solutions of the diffusion

and transport equation are hard to come by unless the geometry is simplified in some way (such as slab geometry). In addition, the analytic solutions to the flux equation itself might require substantial mesh refinement in DIF3D such that the flux solver invokes a huge computational burden. As a consequence of this, this work focuses on an infinite homogeneous problem noting that this is still a valid test of the REBUS depletion capability itself.

The analytic flux solution of a multi-group system has the form:

$$\begin{aligned}\bar{\phi}(t) &= \frac{1}{k(t)} \bar{A}^{-1}(t) \bar{F}(t) \bar{\phi}(t) \\ \bar{F}_{g,g'}(t) &= \sum_{isotope} N_i(t) \cdot \chi_{i,g} v_{i,g'} \sigma_{f,i,g'} \\ \bar{A}_{g,g'}(t) &= \sum_{isotope} N_i(t) \cdot (\sigma_{t,i,g} \delta_{g,g'} - \sigma_{s,i,g,g'}) \\ k(t) &= 1 / \min |\lambda \bar{I} - \bar{A}^{-1}(t) \bar{F}(t)| \\ P(t) &= \sum_{isotope} \sum_g V \cdot \kappa_{i,g} N_i(t) \sigma_{f,i,g} \phi_g(t).\end{aligned}\quad (23)$$

With an infinite homogeneous system, there is only one non-zero eigenvalue and eigenvector for a given multi-group system. If the three-group system used in the previous depletion chain tests is used, the roots of a third order system for  $\lambda$  must be found for all time points. The most difficult aspect of this equation to deal with is the power normalization. In almost all depletion codes today, the power is assumed to be constant over a given time step. This effectively turns the last equation into a boundary condition for the flux at all time points:

$$P_0 = \bar{\phi}^T(t) \cdot \bar{Q} \cdot \bar{N}(t) \quad Q_{g,i} = V \cdot \sum_{isotope} \sum_g \kappa_{f,i,g} \sigma_{f,i,g} + \kappa_{c,i,g} \sigma_{c,i,g} \quad (24)$$

While the flux spectrum and spatial distribution can change, the power level itself does not change. This can be particularly difficult to manage as it effectively links the flux back to the atom densities. Ignoring decay reactions, the differential equation for each atom density can be written generically as:

$$\frac{\partial N_i(t)}{\partial t} = -\bar{\sigma}_i^T \bar{\phi}(t) \cdot N_i(t) + \sum_{i' \neq i} \bar{\sigma}_{i' \rightarrow i}^T \bar{\phi}(t) \cdot N_{i'}(t). \quad (25)$$

If equation 24 is not simplistic, then a compact analytic solution is not possible. As an example, consider the one-group system with three depleting isotopes written as

$$\begin{aligned}\frac{\partial N_1(t)}{\partial t} &= -\sigma_1 \phi(t) N_1(t) \\ \frac{\partial N_2(t)}{\partial t} &= -\sigma_2 \phi(t) N_2(t) + \sigma_{1 \rightarrow 2} \phi(t) N_1(t) \\ \frac{\partial N_3(t)}{\partial t} &= -\sigma_3 \phi(t) N_3(t) + \sigma_{1 \rightarrow 3} \phi(t) N_1(t) + \sigma_{2 \rightarrow 3} \phi(t) N_2(t).\end{aligned}\quad (26)$$

With this equation the power is assumed to come from two of the isotopes to define:

$$\phi(t) = \frac{P_0}{V \kappa_{f,1} N_1(t) + V \kappa_{f,2} N_2(t)}. \quad (27)$$

The differential equations for the density equation of the three isotopes takes the form:

$$\begin{aligned}\frac{\partial N_1(t)}{\partial t} &= \frac{-\sigma_1 N_1(t)}{\kappa_1 \sigma_{f,1} N_1(t) + \kappa_2 \sigma_{f,2} N_2(t)} \frac{P_0}{V} \\ \frac{\partial N_2(t)}{\partial t} &= \frac{-\sigma_2 N_2(t) + \sigma_{1 \rightarrow 2} N_1(t)}{\kappa_1 \sigma_{f,1} N_1(t) + \kappa_2 \sigma_{f,2} N_2(t)} \frac{P_0}{V} \\ \frac{\partial N_3(t)}{\partial t} &= \frac{-\sigma_3 N_3(t) + \sigma_{1 \rightarrow 3} N_1(t) + \sigma_{2 \rightarrow 3} N_2(t)}{\kappa_1 \sigma_{f,1} N_1(t) + \kappa_2 \sigma_{f,2} N_2(t)} \frac{P_0}{V}.\end{aligned}\quad (28)$$

This set of differential equations is non-trivial to solve and one can understand that more complicated systems will be even more difficult to derive analytic solutions.

Based upon the above simplistic system, it should come as no surprise that easy analytic solutions for the coupled flux and Bateman equations are only obtained by implementing considerable simplifications. One approach is to introduce a fixed source driven system where no fission is present but decay and absorption reactions impact the flux levels. This approach cannot be taken with REBUS as fission is required to exist in the system. Another approach would be to make the depletion chain only consist of decay reactions which make the density equations independent of the flux equation. Other alternatives deploy simplifications of the multi-group cross sections such that the steady state flux solution is trivial to obtain at all time points. This can involve using a one-group data set or modifying the cross section data to accomplish the simplification. Because a multi-group approach with scattering will lead to incredibly complex expressions similar to those seen in equation 28, this section will only consider the one group cross section library shown in Table 3-20 where all of the cross sections are entirely made up and given regular isotope labels only for convenience.

**Table 3-20. Microscopic cross sections for the Flux Impacted Depletion Test.**

|                 | U-235      | U-238 | Pu239      | Pu240 | Pu241  | LFP        | Na-23 | O-16   | MAGIC  |
|-----------------|------------|-------|------------|-------|--------|------------|-------|--------|--------|
| Test #1 Density | 0.0025     | 0.02  | $10^{-20}$ | -     | -      | $10^{-20}$ | 0.01  | 0.02   | -      |
| Test #2 Density | 0.0025     | 0.02  | 0.001      | 0.001 | 0.0005 | $10^{-20}$ | 0.01  | 0.02   | 0.0005 |
| $\kappa_f$      | $10^{-11}$ | —     | —          | —     | —      | —          | —     | —      | —      |
| $\kappa_c$      | $10^{-12}$ | —     | —          | —     | —      | —          | —     | —      | —      |
| $\sigma_t$      | 0.29       | 0.30  | 0.32       | 0.31  | 0.31   | 0.20       | 0.10  | 0.1000 | 1.0    |
| $\sigma_\gamma$ | 0.08       | 0.12  | 0.08       | 0.11  | 0.07   | 0.05       | 0.01  | 0.0001 | 0.5    |
| $\sigma_f$      | 0.09       | 0.02  | 0.10       | 0.09  | 0.10   | —          | —     | —      | —      |
| $v$             | 2.3        | 2.2   | 2.4        | 2.2   | 2.4    | —          | —     | —      | —      |
| $\sigma_s$      | 0.12       | 0.16  | 0.14       | 0.11  | 0.14   | 0.15       | 0.09  | 0.0999 | 0.5    |

As seen, only U-235 is allowed to produce power from either capture or fission reactions. This is done to ensure that the system of density equations is tractable. The power normalization for this set of equations can be written as

$$\begin{aligned}
 P(t) &= P_0 = V \cdot (\kappa_c \sigma_{c,U2} + \kappa_f \sigma_{f,U235}) N_{U235}(t) \phi(t) \\
 N_0 &= \frac{P_0}{V \cdot (\kappa_c \sigma_{c,U235} + \kappa_f \sigma_{f,U235})} \\
 \phi(t) &= \frac{N_0}{N_{U235}(t)}. \tag{29}
 \end{aligned}$$

### 3.4.5.1 Flux Impacted Depletion Chain Test #1

Table 3-21 shows the first depletion chain test where only two of the isotopes are allowed to deplete.

**Table 3-21. Flux Impacted Depletion Chain Test #1.**

| Target Isotope | Reaction | Product Isotopes |
|----------------|----------|------------------|
| U-235          | fission  | LFP              |
| U-238          | $\gamma$ | Pu239            |

The time dependent eigenvalue and macroscopic cross sections that results from this depletion chain can be written as:

$$\begin{aligned}
 k(t) &= \frac{\Sigma_{vf}(t)}{\Sigma_t(t) - \Sigma_s(t)} \\
 \Sigma_t(t) &= N_{U235}(t)\sigma_{t,U235} + N_{U238}(t)\sigma_{t,U238} + N_{Pu239}(t)\sigma_{t,Pu239} \\
 &\quad + N_{LFP}(t)\sigma_{t,LFP} + N_{NA}\sigma_{t,NA} + N_{O16}\sigma_{t,O16} \\
 \Sigma_s(t) &= N_{U235}(t)\sigma_{s,U235} + N_{U238}(t)\sigma_{s,U238} + N_{Pu239}(t)\sigma_{s,Pu239} \\
 &\quad + N_{LFP}(t)\sigma_{s,LFP} + N_{NA}\sigma_{s,NA} + N_{O16}\sigma_{s,O16} \\
 \Sigma_f(t) &= N_{U235}(t)\sigma_{f,U235} + N_{U238}(t)\sigma_{f,U238} + N_{Pu239}(t)\sigma_{f,Pu239} \\
 &\quad + N_{LFP}(t)\sigma_{f,LFP} + N_{NA}\sigma_{f,NA} + N_{O16}\sigma_{f,O16} \\
 \Sigma_{vf}(t) &= N_{U235}(t)\sigma_{vf,U235} + N_{U238}(t)\sigma_{vf,U238} + N_{Pu239}(t)\sigma_{vf,Pu239} \\
 &\quad + N_{LFP}(t)\sigma_{vf,LFP} + N_{NA}\sigma_{vf,NA} + N_{O16}\sigma_{vf,O16}
 \end{aligned} \tag{30}$$

The coupled density equations are written as

$$\begin{aligned}
 \frac{\partial N_{U235}(t)}{\partial t} &= -\sigma_{f,U235} \cdot \phi(t) \cdot N_{U235}(t) = -\sigma_{f,U235} N_0 \\
 \frac{\partial N_{U238}(t)}{\partial t} &= -\sigma_{c,U238} \cdot \phi(t) \cdot N_{U238}(t) = -N_0 \frac{\sigma_{c,U238} N_{U238}(t)}{N_{U235}(t)} \\
 \frac{\partial N_{LFP}(t)}{\partial t} &= \sigma_{f,U235} \cdot \phi(t) \cdot N_{U235}(t) = \sigma_{f,U235} N_0 \\
 \frac{\partial N_{Pu239}(t)}{\partial t} &= \sigma_{c,U238} \cdot \phi(t) \cdot N_{U238}(t) = N_0 \frac{\sigma_{c,U238} N_{U238}(t)}{N_{U235}(t)}.
 \end{aligned} \tag{31}$$

The U-235 and LFP isotopes and the flux have the trivial solution of:

$$\begin{aligned}
 N_{U235}(t) &= N_{U235}(0) - \sigma_{f,U235} \cdot N_0 \cdot t \\
 N_{LFP}(t) &= N_{LFP}(0) + \sigma_{f,U235} \cdot N_0 \cdot t \\
 \phi(t) &= \frac{N_0}{N_{U235}(0) - \sigma_{f,U235} \cdot N_0 \cdot t}.
 \end{aligned} \tag{32}$$

The U-238 and Pu-239 isotope densities are also relatively trivial to solve and have the following analytic solutions

$$\begin{aligned}
 \frac{\partial N_{U238}(t)}{\partial t} &= -\frac{N_0 \sigma_{c,U238}}{N_{U235}(0) - \sigma_{f,U235} N_0 \cdot t} N_{U238}(t) \\
 N_{U238}(t) &= N_{U238}(0) \cdot \left[ N_{U235}(0) \right]^{\frac{\sigma_{c,U238}}{\sigma_{f,U235}}} \cdot \left( N_{U235}(0) - \sigma_{f,U235} N_0 \cdot t \right)^{\frac{\sigma_{c,U238}}{\sigma_{f,U235}}} \\
 \frac{\partial N_{Pu239}(t)}{\partial t} &= N_0 \sigma_{c,U238} N_{U238}(0) \cdot \left[ N_{U235}(0) \right]^{\frac{\sigma_{c,U238}}{\sigma_{f,U235}}} \cdot \left( N_{U235}(0) - \sigma_{f,U235} N_0 \cdot t \right)^{\frac{\sigma_{c,U238}}{\sigma_{f,U235}} - 1} \\
 N_{Pu239}(t) &= N_{Pu239}(0) + N_{U238}(0) \\
 &\quad - N_{U238}(0) \cdot \left[ N_{U235}(0) \right]^{\frac{\sigma_{c,U238}}{\sigma_{f,U235}}} \left( N_{U235}(0) - \sigma_{f,U235} N_0 \cdot t \right)^{\frac{\sigma_{c,U238}}{\sigma_{f,U235}}}
 \end{aligned} \tag{33}$$

With a Power of  $10^9$  watts, a volume of  $98726.896 \cdot \text{cm}^3$  and the stated cross sections, the analytic solution can be written numerically as

$$\begin{aligned}
 \phi(t) &= \frac{1.03356654 \cdot 10^{16}}{0.0025 - 9.30209886 \cdot 10^{-10} \cdot t} \\
 k(t) &= \frac{\{0.0053175 - 1.92553446 \cdot 10^{-10} \cdot t}{\{-11.55312278 \cdot (0.0025 - 9.30209886 \cdot 10^{-10} \cdot t)^{1.333333333}\}} \\
 N_{U23}(t) &= 0.0025 - 9.30209886 \cdot 10^{-1} \cdot t \\
 N_{LFP}(t) &= 10^{-20} + 9.30209886 \cdot 10^{-10} \cdot t \\
 N_{U23}(t) &= 58.944504 \cdot (0.0025 - 9.30209886 \cdot 10^{-1} \cdot t)^{1.333333333} \\
 N_{PU239}(t) &= 0.02 - 58.944504 \cdot (0.0025 - 9.30209886 \cdot 10^{-10} \cdot t). \tag{34}
 \end{aligned}$$

The excerpt of the REBUS atom densities are provided in Figure 3-28 while the REBUS computed  $k_{\text{eff}}$  and analytic solutions to the atom densities are given in Table 3-22. Starting with the eigenvalue results of Table 3-22, it should be rather clear that a non-negligible amount of error is present between REBUS and the analytic solution for the eigenvalue. The atom density results, however, are very similar except for the very last time step. A perturbation analysis with the analytic solution indicates that a 5<sup>th</sup> significant digit error is being made internal to REBUS. Close inspection of the output of REBUS indicates that the flux magnitude computed at each time step is the point at which the error begins and given this is a time dependent calculation, it should come as no surprise that the small errors grow to larger ones as the errors are propagated. Using more time steps in REBUS eliminates these discrepancies and thus the REBUS depletion methodology and the power normalization are contributing factors to the errors displayed here.

| BEGINNING OF BURN CYCLE 1   |            |            |            |            |
|---|------------|------------|------------|------------|
| REGION  | U235       | U238       | LFPPS      | PU239      |
| ICORE1  | 2.5000E-03 | 2.0000E-02 | 0.0000E+00 | 0.0000E+00 |
| ICORE2  | 2.5000E-03 | 2.0000E-02 | 0.0000E+00 | 0.0000E+00 |
| ICORE3  | 2.5000E-03 | 2.0000E-02 | 0.0000E+00 | 0.0000E+00 |
| ...   | ...        | ...        | ...        | ...        |
| BEGINNING OF BURN CYCLE 2   |            |            |            |            |
| REGION  | U235       | U238       | LFPPS      | PU239      |
| ICORE1  | 2.4196E-03 | 1.9147E-02 | 8.0384E-05 | 8.5281E-04 |
| ICORE2  | 2.4196E-03 | 1.9147E-02 | 8.0384E-05 | 8.5281E-04 |
| ICORE3  | 2.4196E-03 | 1.9147E-02 | 8.0384E-05 | 8.5281E-04 |
| ...   | ...        | ...        | ...        | ...        |
| BEGINNING OF BURN CYCLE 3   |            |            |            |            |
| REGION  | U235       | U238       | LFPPS      | PU239      |
| ICORE1  | 2.3392E-03 | 1.8304E-02 | 1.6077E-04 | 1.6962E-03 |
| ICORE2  | 2.3392E-03 | 1.8304E-02 | 1.6077E-04 | 1.6962E-03 |
| ICORE3  | 2.3392E-03 | 1.8304E-02 | 1.6077E-04 | 1.6962E-03 |
| ...   | ...        | ...        | ...        | ...        |
| BEGINNING OF BURN CYCLE 4   |            |            |            |            |
| REGION  | U235       | U238       | LFPPS      | PU239      |
| ICORE1  | 2.2588E-03 | 1.7470E-02 | 2.4116E-04 | 2.5301E-03 |
| ICORE2  | 2.2588E-03 | 1.7470E-02 | 2.4116E-04 | 2.5301E-03 |
| ICORE3  | 2.2588E-03 | 1.7470E-02 | 2.4116E-04 | 2.5301E-03 |
| ...   | ...        | ...        | ...        | ...        |
| BEGINNING OF BURN CYCLE 5   |            |            |            |            |
| REGION  | U235       | U238       | LFPPS      | PU239      |
| ICORE1  | 2.1785E-03 | 1.6646E-02 | 3.2154E-04 | 3.3541E-03 |
| ICORE2  | 2.1785E-03 | 1.6646E-02 | 3.2154E-04 | 3.3541E-03 |
| ICORE3  | 2.1785E-03 | 1.6646E-02 | 3.2154E-04 | 3.3541E-03 |
| ...   | ...        | ...        | ...        | ...        |
| REACTOR CONDITIONS AFTER 1 BURNUP SUBSTEPS AT TIME = 5.000000000E+00 DAYS |            |            |            |            |
| REGION  | U235       | U238       | LFPPS      | PU239      |
| ICORE1  | 2.0981E-03 | 1.5832E-02 | 4.0193E-04 | 4.1680E-03 |
| ICORE2  | 2.0981E-03 | 1.5832E-02 | 4.0193E-04 | 4.1680E-03 |
| ICORE3  | 2.0981E-03 | 1.5832E-02 | 4.0193E-04 | 4.1680E-03 |
| ...   | ...        | ...        | ...        | ...        |

Figure 3-28. Atom Density Excerpt for REBUS for the Flux Impacted Depletion Chain #1

**Table 3-22. Chain #1  $k_{\text{eff}}$  and Atom Density Results From the Analytic Solution.**

| Time<br>(days) | Atom Density |            |            |            | $k_{\text{eff}}$ | REBUS<br>$k_{\text{eff}}$ |
|----------------|--------------|------------|------------|------------|------------------|---------------------------|
|                | U-235        | U-238      | Pu-239     | LFP        |                  |                           |
| 0.0            | 2.5000E-03   | 2.0000E-02 | 0.0000E+00 | 0.0000E+00 | 0.42004 809      | 0.42004 810               |
| 1.0            | 2.4196E-03   | 1.9147E-02 | 8.5265E-04 | 8.0370E-05 | 0.46188 315      | 0.46189 052               |
| 2.0            | 2.3393E-03   | 1.8304E-02 | 1.6959E-03 | 1.6074E-04 | 0.50262 270      | 0.50263 753               |
| 3.0            | 2.2589E-03   | 1.7470E-02 | 2.5296E-03 | 2.4111E-04 | 0.54229 256      | 0.54231 498               |
| 4.0            | 2.1785E-03   | 1.6647E-02 | 3.3534E-03 | 3.2148E-04 | 0.58091 688      | 0.58094 705               |
| 5.0            | 2.0982E-03   | 1.5833E-02 | 4.1672E-03 | 4.0185E-04 | 0.61851 815      | 0.61855 627               |

While the isotope names would seem reasonable, a quick inspection of the actual density changes shows a 16% reduction in the U-235 content and a 21% reduction in the U-238 content which are a consequence of the made up cross section data and not consistent with reality. Unlike the previous burnup test problems, this verification problem appears to be extremely sensitive to the power normalization errors which comes as no surprise since this is the first test where the flux magnitude changes over each time step. Because the REBUS density errors are small and the eigenvalue errors only become concerning at the last two time points, the REBUS calculated result is sufficient to demonstrate that it can accurately model the verification test problem within the bounds of the underlying real precision math calculations.

### 3.4.5.2 Flux Impacted Depletion Chain Test #2

Table 3-23 shows the second depletion chain test where many more isotopes are allowed to deplete. It should be clear from earlier analytic solutions that an analytic solution with more than two connected isotopes is not practical here. Hence the reason for this simplistic depletion chain which considers the types of connections that can be tested rather than the number of connected isotopes. In this regard, the inclusion of the MAGIC isotope imposes an exponential behavior of the solution system. Note that the MAGIC isotope cannot be used to create U-235 as an analytic solution for all of the other isotopes in the depletion chain is no longer possible due to the flux being dependent upon the U-235 content.

**Table 3-23. Flux Impacted Depletion Chain Test #1.**

| Target<br>Isotope | Reaction | Product<br>Isotopes |
|-------------------|----------|---------------------|
| MAGIC             | decay    | Pu241               |
| U-235             | fission  | LFP                 |
| U-235             | $\gamma$ | Pu240               |
| U-238             | $\gamma$ | Pu239               |
| U-238             | fission  | LFP                 |
| Pu239             | $\gamma$ | DUMP                |
| Pu239             | fission  | LFP                 |
| Pu240             | $\gamma$ | DUMP                |
| Pu240             | fission  | LFP                 |

The time dependent eigenvalue and cross sections are found to be

$$\begin{aligned}
 k(t) &= \frac{\Sigma_{vf}(t)}{\Sigma_t(t) - \Sigma_s(t)} \\
 \sigma_a &= \sigma_f + \sigma_c \\
 \Sigma_x(t) &= N_{U235}(t)\sigma_{x,U235} + N_{U238}(t)\sigma_{x,U238} + N_{Pu239}(t)\sigma_{x,Pu239} + N_{Pu240}(t)\sigma_{x,Pu240} \\
 &\quad + N_{Pu241}(t)\sigma_{x,Pu241} + N_{MAGIC}(t)\sigma_{x,MAGIC} + N_{LFP}(t)\sigma_{x,LFP} + N_{DUMP}(t)\sigma_{x,DUMP} \\
 &\quad + N_{NA}\sigma_{x,NA} + N_{O16}\sigma_{x,O16}
 \end{aligned} \quad . \quad (35)$$

The macroscopic cross section data was written generically for all cross sections for brevity. The density equations begin with the MAGIC and Pu241 isotopes which are independent of the power level with analytic solutions of

$$\begin{aligned}
 \frac{\partial N_{MAGIC}(t)}{\partial t} &= -\lambda_{MAGIC} \cdot N_{MAGIC}(t) \\
 N_{MAGIC}(t) &= N_{MAGIC}(0) \cdot \exp(-\lambda_{MAGIC} \cdot t) \\
 \frac{\partial N_{Pu241}(t)}{\partial t} &= \lambda_{MAGIC} \cdot N_{MAGIC}(t) \\
 N_{Pu241}(t) &= N_{Pu241}(0) + N_{MAGIC}(0) - N_{MAGIC}(0) \cdot \exp(-\lambda_{MAGIC} \cdot t)
 \end{aligned} \quad . \quad (36)$$

Any attempt to include the absorptive losses on the Pu241 into the differential equation restricts the ratio of the U235 absorption and Pu241 absorption cross section which was deemed to be undesirable for this work. Because the power normalization from equation 29 still applies, the U-235 density equation and its analytic solution along with the analytic flux solution are found to be very similar to the previous one

$$\begin{aligned}
 \frac{\partial N_{U235}(t)}{\partial t} &= -\sigma_{a,U235} \cdot \phi(t) \cdot N_{U235}(t) = -\sigma_{a,U235} N_0 \\
 N_{U235}(t) &= N_{U235}(0) - \sigma_{a,U235} \cdot N_0 \cdot t \\
 \phi(t) &= \frac{N_0}{N_{U235}(0) - \sigma_{a,U235} \cdot N_0 \cdot t}
 \end{aligned} \quad . \quad (37)$$

The U-238 density equation has an analytic solution of

$$\begin{aligned}
 \frac{\partial N_{U238}(t)}{\partial t} &= -\sigma_{a,U238} \cdot \phi(t) \cdot N_{U238}(t) = \frac{-\sigma_{a,U238} \cdot N_0 \cdot N_{U238}(t)}{N_{U235}(0) - \sigma_{a,U235} \cdot N_0 \cdot t} \\
 N_{U238}(t) &= C_{U238} \cdot (N_{U235}(0) - \sigma_{a,U235} N_0 \cdot t)^{\frac{\sigma_{a,U238}}{\sigma_{a,U235}}} \\
 C_{U238} &= N_{U238}(0) \cdot [N_{U235}(0)]^{-\frac{\sigma_{a,U238}}{\sigma_{a,U235}}}
 \end{aligned} \quad . \quad (38)$$

The Pu-239 density equation is the most difficult to solve which has the analytic solution of

$$\begin{aligned}
 \frac{\partial N_{Pu239}(t)}{\partial t} &= -\sigma_{a,Pu239} \cdot \phi(t) \cdot N_{Pu239}(t) + \sigma_{c,U238} \cdot \phi(t) \cdot N_{U238}(t) \\
 &= -\frac{\sigma_{a,Pu239} \cdot N_0}{N_{U235}(0) - \sigma_{a,U235} \cdot N_0 \cdot t} N_{Pu239}(t) \\
 &\quad + \sigma_{c,U238} \cdot N_0 \cdot C_{U238} \cdot (N_{U235}(0) - \sigma_{a,U235} N_0 \cdot t)^{\frac{\sigma_{a,U238}-1}{\sigma_{a,U235}}-1} \\
 N_{Pu239}(t) &= -\frac{\sigma_{c,U238}}{\sigma_{a,U238} - \sigma_{a,Pu239}} \cdot C_{U238} \cdot (N_{U235}(0) - \sigma_{a,U235} N_0 \cdot t)^{\frac{\sigma_{a,U238}}{\sigma_{a,U235}}} \\
 &\quad + C_{Pu239} \cdot (N_{U235}(0) - \sigma_{a,U235} N_0 \cdot t)^{\frac{\sigma_{a,Pu239}}{\sigma_{a,U235}}} \\
 C_{Pu239} &= \left\{ N_{Pu239}(0) + \frac{\sigma_{c,U238}}{\sigma_{a,U238} - \sigma_{a,Pu239}} N_{U238}(0) \right\} \left[ N_{U235}(0) \right]^{\frac{\sigma_{a,Pu239}}{\sigma_{a,U235}}}
 \end{aligned} \quad . \quad (39)$$

The Pu240 density equation has an analytic solution of

$$\begin{aligned}
 \frac{\partial N_{Pu240}(t)}{\partial t} &= -\sigma_{a,Pu240} \cdot \phi(t) \cdot N_{Pu240}(t) + \sigma_{c,U235} \cdot \phi(t) \cdot N_{U235}(t) \\
 &\quad - \frac{\sigma_{a,Pu240} \cdot N_0}{N_{U235}(0) - \sigma_{a,U235} \cdot N_0 \cdot t} N_{Pu240}(t) + \sigma_{c,U235} \cdot N_0 \\
 N_{Pu240}(t) &= \frac{\sigma_{c,U235}}{\sigma_{a,Pu240} - \sigma_{a,U235}} (N_{U235}(0) - \sigma_{a,U235} N_0 \cdot t) \\
 &\quad + C_{Pu240} \cdot (N_{U235}(0) - \sigma_{a,U235} N_0 \cdot t)^{\frac{\sigma_{a,Pu240}}{\sigma_{a,U235}}} \\
 C_{Pu240} &= N_{Pu240}(0) \left[ N_{U235}(0) \right]^{\frac{\sigma_{a,Pu240}}{\sigma_{a,U235}}} - \frac{\sigma_{c,U235}}{\sigma_{a,Pu240} - \sigma_{a,U235}} \left[ N_{U235}(0) \right]^{\frac{\sigma_{a,Pu240}}{\sigma_{a,U235}}+1}
 \end{aligned} \quad . \quad (40)$$

From Table 3-23, the LFP isotope is connected to U235, U238, Pu239, and Pu240 through the fission reactions and has the simple form of

$$\begin{aligned}
 \frac{\partial N_{LFP}(t)}{\partial t} &= \sigma_{f,U235} \cdot \phi(t) \cdot N_{U235}(t) + \sigma_{f,U238} \cdot \phi(t) \cdot N_{U238}(t) \\
 &\quad + \sigma_{f,Pu239} \cdot \phi(t) \cdot N_{Pu239}(t) + \sigma_{f,Pu240} \cdot \phi(t) \cdot N_{Pu240}(t)
 \end{aligned} \quad . \quad (41)$$

The expanded relationship for the LFP isotope is written as

$$\begin{aligned}
 \frac{\partial N_{LFP}(t)}{\partial t} = & \sigma_{f,U235} \cdot N_0 \\
 & + \sigma_{f,U238} \cdot N_0 \cdot C_{U238} \cdot \left( N_{U235}(0) - \sigma_{a,U235} N_0 \cdot t \right)^{\frac{\sigma_{a,U238}-1}{\sigma_{a,U235}}} \\
 & - \frac{\sigma_{f,Pu239} \cdot N_0 \sigma_{c,U238}}{\sigma_{a,U238} - \sigma_{a,Pu239}} \cdot C_{U238} \cdot \left( N_{U235}(0) - \sigma_{a,U235} N_0 \cdot t \right)^{\frac{\sigma_{a,U238}-1}{\sigma_{a,U235}}} \\
 & + \sigma_{f,Pu239} \cdot N_0 C_{Pu239} \cdot \left( N_{U235}(0) - \sigma_{a,U235} N_0 \cdot t \right)^{\frac{\sigma_{a,Pu239}-1}{\sigma_{a,U235}}} \\
 & + \frac{\sigma_{f,Pu240} \cdot N_0 \cdot \sigma_{c,U235}}{\sigma_{a,Pu240} - \sigma_{a,U235}} + \sigma_{f,Pu240} \cdot N_0 \cdot C_{Pu240} \cdot \left( N_{U235}(0) - \sigma_{a,U235} N_0 \cdot t \right)^{\frac{\sigma_{a,Pu240}-1}{\sigma_{a,U235}}}
 \end{aligned} \tag{42}$$

which has no dependence upon the LFP isotope itself. In this case, the analytic solution is trivial although quite complex.

$$\begin{aligned}
 N_{LFP}(t) = & C_{LFP} + \sigma_{f,U235} \cdot N_0 \cdot t - \frac{\sigma_{f,U238}}{\sigma_{a,U238}} C_{U238} \cdot \left( N_{U235}(0) - \sigma_{a,U235} N_0 \cdot t \right)^{\frac{\sigma_{a,U238}}{\sigma_{a,U235}}} \\
 & + \frac{\sigma_{f,Pu239} \cdot \sigma_{c,U238}}{\sigma_{a,U238} - \sigma_{a,Pu239}} \cdot \frac{C_{U238}}{\sigma_{a,U238}} \cdot \left( N_{U235}(0) - \sigma_{a,U235} N_0 \cdot t \right)^{\frac{\sigma_{a,U238}}{\sigma_{a,U235}}} \\
 & - \frac{\sigma_{f,Pu239}}{\sigma_{a,Pu239}} C_{Pu239} \cdot \left( N_{U235}(0) - \sigma_{a,U235} N_0 \cdot t \right)^{\frac{\sigma_{a,Pu239}}{\sigma_{a,U235}}} \\
 & + \frac{\sigma_{f,Pu240} \cdot N_0 \sigma_{c,U235}}{\sigma_{a,Pu240} - \sigma_{a,U235}} t - \frac{\sigma_{f,Pu240}}{\sigma_{a,Pu240}} \cdot C_{Pu240} \cdot \left( N_{U235}(0) - \sigma_{a,U235} N_0 \cdot t \right)^{\frac{\sigma_{a,Pu240}}{\sigma_{a,U235}}} \\
 C_{LFP} = & N_{LFP}(0) + \frac{\sigma_{f,U238}}{\sigma_{a,U238}} N_{U238}(0) + \frac{\sigma_{f,Pu239}}{\sigma_{a,Pu239}} \left( N_{Pu239}(0) + \frac{\sigma_{c,U238} \cdot N_{U238}(0)}{\sigma_{a,U238} - \sigma_{a,Pu239}} \right) \\
 & - \frac{\sigma_{f,Pu239} \cdot \sigma_{c,U238}}{\sigma_{a,U238} - \sigma_{a,Pu239}} \cdot \frac{N_{U238}(0)}{\sigma_{a,U238}} + \frac{\sigma_{f,Pu240}}{\sigma_{a,Pu240}} \left( N_{Pu240}(0) - \frac{\sigma_{c,U235} \cdot N_{U235}(0)}{\sigma_{a,Pu240} - \sigma_{a,U235}} \right)
 \end{aligned} \tag{43}$$

The last isotope to consider is the DUMP isotope which is connected to Pu239 and Pu240 and has the following differential form

$$\begin{aligned}
 \frac{\partial N_{DUMP}(t)}{\partial t} &= \sigma_{c,Pu239} \cdot \phi(t) \cdot N_{Pu239}(t) + \sigma_{c,Pu240} \cdot \phi(t) \cdot N_{Pu240}(t) \\
 &= -\frac{\sigma_{c,Pu239} \cdot N_0 \cdot \sigma_{c,U238}}{\sigma_{a,U238} - \sigma_{a,Pu239}} \cdot C_{U238} \cdot (N_{U235}(0) - \sigma_{a,U235} N_0 \cdot t)^{\frac{\sigma_{a,U238}-1}{\sigma_{a,U235}}} \\
 &\quad + \sigma_{c,Pu239} \cdot N_0 \cdot C_{Pu239} \cdot (N_{U235}(0) - \sigma_{a,U235} N_0 \cdot t)^{\frac{\sigma_{a,Pu239}-1}{\sigma_{a,U235}}} \\
 &\quad + \frac{\sigma_{c,Pu240} \cdot N_0 \sigma_{c,U235}}{\sigma_{a,Pu240} - \sigma_{a,U235}} + \sigma_{c,Pu240} \cdot N_0 \cdot C_{Pu240} \cdot (N_{U235}(0) - \sigma_{a,U235} N_0 \cdot t)^{\frac{\sigma_{a,Pu240}-1}{\sigma_{a,U235}}}
 \end{aligned} \quad . \quad (44)$$

The analytic solution for the DUMP isotope is found to be

$$\begin{aligned}
 N_{DUMP}(t) &= C_{DUMP} + \frac{\sigma_{c,Pu239} \cdot \sigma_{c,U238}}{\sigma_{a,U238} - \sigma_{a,Pu239}} \cdot \frac{C_{U238}}{\sigma_{a,U238}} \cdot (N_{U235}(0) - \sigma_{a,U235} N_0 \cdot t)^{\frac{\sigma_{a,U238}-1}{\sigma_{a,U235}}} \\
 &\quad - \frac{\sigma_{c,Pu239}}{\sigma_{a,Pu239}} C_{Pu239} \cdot (N_{U235}(0) - \sigma_{a,U235} N_0 \cdot t)^{\frac{\sigma_{a,Pu239}-1}{\sigma_{a,U235}}} \\
 &\quad + \frac{\sigma_{c,Pu240} \cdot N_0 \sigma_{c,U235}}{\sigma_{a,Pu240} - \sigma_{a,U235}} t - \frac{\sigma_{c,Pu240}}{\sigma_{a,Pu240}} \cdot C_{Pu240} \cdot (N_{U235}(0) - \sigma_{a,U235} N_0 \cdot t)^{\frac{\sigma_{a,Pu240}-1}{\sigma_{a,U235}}} \\
 C_{DUMP} &= N_{DUMP}(0) + \frac{\sigma_{c,Pu239}}{\sigma_{a,Pu239}} \left( N_{Pu239}(0) + \frac{\sigma_{c,U238} \cdot N_{U238}(0)}{\sigma_{a,U238} - \sigma_{a,Pu239}} \right) \\
 &\quad - \frac{\sigma_{c,Pu239} \cdot \sigma_{c,U238}}{\sigma_{a,U238} - \sigma_{a,Pu239}} \cdot \frac{N_{U238}(0)}{\sigma_{a,U238}} \\
 &\quad + \frac{\sigma_{c,Pu240}}{\sigma_{a,Pu240} - \sigma_{a,U235}} \left( N_{Pu240}(0) - \frac{\sigma_{c,U235} \cdot N_{U235}(0)}{\sigma_{a,Pu240} - \sigma_{a,U235}} \right)
 \end{aligned} \quad . \quad (45)$$

For REBUS, the power level was decreased to  $10^8$  watts to demonstrate that the importance of the normalization error is reduced as the error propagates as a function of used energy rather than just time. The decay half-life of the MAGIC isotope was set to 12 hours to ensure that the isotope was mostly decayed after a 5 day depletion period. The atom density excerpt from REBUS is presented in Figure 3-29 while the analytic density results are provided in Table 3-24. Also included are the analytic eigenvalue results and the REBUS computed eigenvalue details.

Starting with the atom density results, the atom density computed by REBUS for every depleting isotope is nearly identical to the analytic result. There is a slight amount of error visible in the LFP and DUMP isotopes, the last significant digit, which is mostly visible because of the zero starting atom density and the impact that the power normalization error has on the overall solution. The final point of comparison is the eigenvalue which shows a near trivial amount of error present between the REBUS and analytic solution in Table 3-24. The total burnup is on the order 3% for U-235 and U-238 which are considerably less than that found in the previous test case. The 5 day results of this test

case are thus comparable to the 1 day time results of Table 3-22 which were of comparable accuracy to the analytic solution.

```

...
                BEGINNING OF BURN CYCLE  1
REGION
    MAGIC      U235      U238      PU239      PU240      LFPPS      DUMP      PU241
ICORE1  5.0000E-04  2.5000E-03  2.0000E-02  1.0000E-03  1.0000E-03  1.0000E-03  0.0000E+00  5.0000E-04
ICORE2  5.0000E-04  2.5000E-03  2.0000E-02  1.0000E-03  1.0000E-03  1.0000E-03  0.0000E+00  5.0000E-04
ICORE3  5.0000E-04  2.5000E-03  2.0000E-02  1.0000E-03  1.0000E-03  1.0000E-03  0.0000E+00  5.0000E-04
...
                BEGINNING OF BURN CYCLE  2
REGION
    MAGIC      U235      U238      PU239      PU240      LFPPS      DUMP      PU241
ICORE1  1.2495E-04  2.4848E-03  1.9900E-02  1.0791E-03  9.9998E-04  1.0293E-03  6.9211E-06  8.7505E-04
ICORE2  1.2495E-04  2.4848E-03  1.9900E-02  1.0791E-03  9.9998E-04  1.0293E-03  6.9211E-06  8.7505E-04
ICORE3  1.2495E-04  2.4848E-03  1.9900E-02  1.0791E-03  9.9998E-04  1.0293E-03  6.9211E-06  8.7505E-04
...
                BEGINNING OF BURN CYCLE  3
REGION
    MAGIC      U235      U238      PU239      PU240      LFPPS      DUMP      PU241
ICORE1  3.1223E-05  2.4696E-03  1.9800E-02  1.1577E-03  9.9991E-04  1.0589E-03  1.4112E-05  9.6878E-04
ICORE2  3.1223E-05  2.4696E-03  1.9800E-02  1.1577E-03  9.9991E-04  1.0589E-03  1.4112E-05  9.6878E-04
ICORE3  3.1223E-05  2.4696E-03  1.9800E-02  1.1577E-03  9.9991E-04  1.0589E-03  1.4112E-05  9.6878E-04
...
                BEGINNING OF BURN CYCLE  4
REGION
    MAGIC      U235      U238      PU239      PU240      LFPPS      DUMP      PU241
ICORE1  7.8025E-06  2.4545E-03  1.9699E-02  1.2358E-03  9.9980E-04  1.0889E-03  2.1574E-05  9.9220E-04
ICORE2  7.8025E-06  2.4545E-03  1.9699E-02  1.2358E-03  9.9980E-04  1.0889E-03  2.1574E-05  9.9220E-04
ICORE3  7.8025E-06  2.4545E-03  1.9699E-02  1.2358E-03  9.9980E-04  1.0889E-03  2.1574E-05  9.9220E-04
...
                BEGINNING OF BURN CYCLE  5
REGION
    MAGIC      U235      U238      PU239      PU240      LFPPS      DUMP      PU241
ICORE1  1.9498E-06  2.4393E-03  1.9599E-02  1.3135E-03  9.9965E-04  1.1192E-03  2.9309E-05  9.9805E-04
ICORE2  1.9498E-06  2.4393E-03  1.9599E-02  1.3135E-03  9.9965E-04  1.1192E-03  2.9309E-05  9.9805E-04
ICORE3  1.9498E-06  2.4393E-03  1.9599E-02  1.3135E-03  9.9965E-04  1.1192E-03  2.9309E-05  9.9805E-04
...
                REACTOR CONDITIONS AFTER  1 BURNUP SUBSTEPS AT TIME =  5.000000000E+00 DAYS
REGION
    MAGIC      U235      U238      PU239      PU240      LFPPS      DUMP      PU241
ICORE1  4.8724E-07  2.4241E-03  1.9499E-02  1.3907E-03  9.9945E-04  1.1499E-03  3.7320E-05  9.9951E-04
ICORE2  4.8724E-07  2.4241E-03  1.9499E-02  1.3907E-03  9.9945E-04  1.1499E-03  3.7320E-05  9.9951E-04
ICORE3  4.8724E-07  2.4241E-03  1.9499E-02  1.3907E-03  9.9945E-04  1.1499E-03  3.7320E-05  9.9951E-04
...

```

Figure 3-29. Atom Density Excerpt for REBUS for the Flux Impacted Depletion Chain #2

Table 3-24. Chain #2  $k_{eff}$  and Atom Density Results From the Analytic Solution.

| Time<br>(days) | U-235       | U-238       | Pu-239      | Pu-240      | Pu-241             |
|----------------|-------------|-------------|-------------|-------------|--------------------|
| 0              | 2.50000E-03 | 2.00000E-02 | 1.00000E-03 | 1.00000E-03 | 5.00000E-04        |
| 1              | 2.48482E-03 | 1.98999E-02 | 1.07907E-03 | 9.99978E-04 | 8.75053E-04        |
| 2              | 2.46964E-03 | 1.97998E-02 | 1.15768E-03 | 9.99913E-04 | 9.68777E-04        |
| 3              | 2.45446E-03 | 1.96995E-02 | 1.23582E-03 | 9.99804E-04 | 9.92197E-04        |
| 4              | 2.43928E-03 | 1.95991E-02 | 1.31350E-03 | 9.99651E-04 | 9.98050E-04        |
| 5              | 2.42409E-03 | 1.94986E-02 | 1.39071E-03 | 9.99453E-04 | 9.99513E-04        |
| Time<br>(days) | LFP         | DUMP        | MAGIC       | $k_{eff}$   | REBUS<br>$k_{eff}$ |
| 0              | 1.00000E-03 | 0.00000E+00 | 5.00000E-04 | 0.47788 368 | 0.47788 370        |
| 1              | 1.02928E-03 | 6.92102E-06 | 1.24947E-04 | 0.51846 896 | 0.51846 900        |
| 2              | 1.05891E-03 | 1.41116E-05 | 3.12234E-05 | 0.53126 160 | 0.53126 166        |
| 3              | 1.08887E-03 | 2.15737E-05 | 7.80253E-06 | 0.53673 149 | 0.53673 158        |
| 4              | 1.11919E-03 | 2.93090E-05 | 1.94980E-06 | 0.54033 069 | 0.54033 078        |
| 5              | 1.14985E-03 | 3.73194E-05 | 4.87243E-07 | 0.54344 644 | 0.54344 656        |

### 3.4.6 REBUS Depletion Chain Summary

In the first analytic benchmark test of this section, the decay processes of REBUS were verified to be working properly. In the second analytic benchmark test, the fission process was verified to be working properly in REBUS for multiple isotopes. In the third analytic benchmark test, the full set of absorptive neutron interactions combined with decay processes was tested and verified that these input options are working as expected. In the fourth analytic benchmark test, a couple of circularly connected depletion chains were tested and verified that the typical complicated isotopic connections present in real reactors was working properly in REBUS. In the fifth analytic benchmark test, the flux impacted aspects of the REBUS depletion were verified for coupled absorptive and decay processes. Combined, the preceding five analytic benchmark cases are sufficient to demonstrate that the REBUS depletion methodology has been implemented correctly as it reproduces the analytic solution within the limits of real precision calculations.

Although not shown, the REBUS depletion chain setup does not allow certain reactions to be modeled. An example is when a nuclear reaction causes two product isotopes that are identical. In this case the yield fraction of that isotope should be 2.0 but REBUS does not allow this for generic reactions, only fission. As a consequence, REBUS cannot at present model these types of reactions which is fortunately not relevant for VTR as those types of reactions are common in light water reactor modeling for which REBUS was not intended.

To improve upon the depletion chain verification work above, one can consider a two region slab geometry problem consisting of a fuel and reflector region. The fueled region atom densities would only be dependent upon the average flux in that region. The steady state flux solution for this problem has a rather compact analytic solution for multi-group problems. For a coupled depletion/flux solution, an analytic solution of the coupled equations is possible if the total and scattering cross sections in the fueled region are not modified by the atom density change. This restricts the flux impact to simple rebalancing of the capture and fission rates and leads to a near trivial alteration from the fifth analytic benchmark case shown in this section. Another approach that will yield an analytic solution forces the removal cross section to remain constant but allow changes in all of the remaining cross sections. The complexity of this problem is again no greater than that shown in the fifth benchmark test shown in this section.

Finally, the power normalization can be isolated from the atom density changes by making it only a function of an isotope with a constant density. While the spatial flux solution can immediately be as complex as desired, the flux level does not change over the time step and all that would occur is a simple test of the DIF3D code to produce the analytic flux solution with different cross sections. Any errors that result in DIF3D would propagate in time through the Bateman equations. In this manner, the comparison at each time point is dependent on how well DIF3D does modeling the problem and it provides no additional real test over that shown in the preceding tests. Consequently, any further testing of the depletion capability of REBUS using analytic solutions is deemed unnecessary.

In the requirements document, the possibility of using an external depletion code to check REBUS was discussed. The motivation behind this work was the general lack of analytic solutions in the literature that were competent at testing out the REBUS capabilities. In the preceding work, several analytic test problems were created that demonstrate the fuel depletion (atom density) calculations with REBUS are accurate so long as the DIF3D flux calculation is accurate. Given the DIF3D calculation has been verified for a given atom density input in both diffusion theory and transport, and the preceding verification demonstrates that REBUS properly uses the DIF3D solver, the DIF3D flux

solution accuracy can be considered accurate for a given space-angle approximation. In this regard, for a more complex depletion problem, any external depletion code would invariably require a DIF3D type solver to produce a flux solution for a given problem. Or in summary, the comparison depletion code must not only do what DIF3D does, but also what REBUS does to prove the depletion process is accurate which itself is nothing but a duplicated REBUS code with equivalent requirements to REBUS with respect to software verification. As a consequence, because of the success in creating the preceding analytic benchmarks, the creation of an independent depletion capability is not included in this verification process.

## 3.5 REBUS Model Building Verification

With the DIF3D usage in REBUS verified and the REBUS depletion chain verified to be accurate, the remaining functionalities of REBUS can be tested. This section thus focuses on satisfying the REBUS verification task list given earlier in Table 2-1. The preceding sections have verified tasks a-e of category 1 and tasks a-g of category 2, however, in all of the preceding analytic depletion calculations, the input used that was verified was not discussed. Thus in this section, the first task is to display some of the inputs for the analytic benchmarks and state how they satisfy the category 2 verification tasks in Table 3-25. In several cases, modifications to those inputs are provided to demonstrate the correct interpretation by the REBUS software. Any parts of the input that are not covered by the analytic benchmark problems, and the associated verification of it, are discussed later in this section.

### 3.5.1 Category 2 Input Verification

Depletion chain #3 covers almost all of the ISOTXS reactions that need to be tested and thus it demonstrates most of task a) of category 2. The input for the benchmark problem is provided in Figure 3-30. Starting with the A.NIP3 input, the input has three spatial regions ICORE1, ICORE2, and ICORE3 for hexagon rings 1, 2, and 3, respectively. Three separate sub-zones (IFUEL1, IFUEL2, and IFUEL3) which are assigned to three zones (ZIFUE1, ZIFUE2, and ZIFUE3) and then the three spatial regions. This geometry setup requires REBUS to treat the three regions separately as will be shown shortly. The card type 04 and 05 set the boundary conditions to be reflected on all surfaces such that this is effectively an infinite homogeneous domain although it is broken into three regions with different volumes.

Continuing with A.BURN, the input provided uses card types 01, 02, 03, 09, 10, 24, 25, 28, 31, and 35. Card type 01 is the title declaration for REBUS. The important parts of card type 2 are the specification of “region density convergence criteria” (the atom density error is set to 0.0001) and the maximum number of region density iterations (set to 5). The important parts of card type 03 are the specification of the starting time (0.0 days), the shutdown time between cycles (0.0 days), the fuel cycle burn time (1.0 days), the number of sub-intervals per fuel cycle (1) and the number of fuel cycles to execute (4). As can be inferred, all of these input cards are required just to define the basic setup and purpose of the depletion calculation. Because the A.NIP3 input has three different zones assigned to unique regions, the path specification (assignment path of the zone as it traverses the time domain) requires three paths (PATH1, PATH2, and PATH3) as found in the card types 35. In this input, the sub-zone and zone are used to define the depletion chain and this input just as easily could have used the zone and region.

```

UNFORM=A.NIP3
01 ANIP3: Hexagonal 3D Test Problem
02 0 1 5000 0 5000 0 0 0 0
03 120
04 4 4 4 4 4 4
05 XL 0.0 1 3
05 XU 0.0 1 3
05 YL 0.0 1 3
05 YU 0.0 1 3
05 ZL 0.0 1 3
05 ZU 0.0 1 3
07 CORE ICORE1 ICORE2 ICORE3
09 Z 3 60.0
13 FUEL1 U235 0.0025
13 FUEL1 U238 0.02
13 FUEL2 U235 0.0025
13 FUEL2 U238 0.02
13 FUEL3 U235 0.0025
13 FUEL3 U238 0.02
13 SODIUM NA .0219
13 STEEL FE .085
13 OXY O-16 .03789
14 IFUEL1 FUEL1 .3949 OXY .3949 SODIUM .406
14 IFUEL1 STEEL .2067 MAGIC 1.0E-12 LFP 1.0E-12
14 IFUEL1 PU239 1.0E-12 PU240 1.0E-12 DUMP 1.0E-20
14 IFUEL1 PU241 1.0E-12 PU242 1.0E-12
14 ZIFUE1 IFUEL1 1.0
14 ZIFUE1 IFUEL2 .3949 OXY .3949 SODIUM .406
14 ZIFUE1 IFUEL3 .3949 OXY .3949 SODIUM .406
14 ZIFUE2 IFUEL2 .2067 MAGIC 1.0E-12 LFP 1.0E-12
14 ZIFUE2 IFUEL3 .2067 MAGIC 1.0E-12 LFP 1.0E-12
14 ZIFUE3 IFUEL1 1.0
14 ZIFUE3 IFUEL2 1.0
14 ZIFUE3 IFUEL3 1.0
15 ZIFUE1 ICORE1
15 ZIFUE2 ICORE2
15 ZIFUE3 ICORE3
29 10.0 0 1
30 ICORE1 1 0 0 0.0 60.0
30 ICORE2 2 0 0 0.0 60.0
30 ICORE3 3 0 0 0.0 60.0
UNFORM=A.BURN
01 ABURN: Hexagonal 3D Test Problem
02 0 10000000 10000000 0.0001 1.0000 1.00000 5 5
03 0 0.00000 0.0 1.0000 1.0 1 4
09 LFPSS 0
09 DUMP 0
09 U235 0
09 U238 0
09 PU239 0
09 PU240 0
09 PU241 0
09 PU242 0
09 MAGIC 1 PU239 1.0
09 MAGIC 3 PU240 1.0
09 MAGIC 4 PU241 1.0
09 MAGIC 5 PU242 1.0
09 MAGIC 9 LFPSS 1.0
25 MAGIC 9 LFPSS 1.00E-31
09 MAGIC 10 DUMP 1.0
10 MAGIC MAGIC
10 U235 U235
10 U238 U238
10 PU239 PU239
10 PU240 PU240
10 PU241 PU241
10 PU242 PU242
10 DUMP DUMP
10 LFPSS LFP
24 U235 0 235.117
24 U238 1 238.125
24 PU239 0 239.127
24 PU240 1 240.129
24 PU241 0 241.132
24 PU242 1 242.134
24 LFPSS 0 237.000
24 DUMP 0 236.000
24 MAGIC 0 100.000
28 0.602472E+24
31 1 U238 PU242
31 2 U235 PU239 PU241
31 3 DUMP
31 4 LFPSS
35 PATH1 IFUEL1 ZIFUE1 1 1
35 PATH1 IFUEL1 ZIFUE1 2 2
35 PATH1 IFUEL1 ZIFUE1 3 3
35 PATH1 IFUEL1 ZIFUE1 4 4
35 PATH1 IFUEL1 ZIFUE1 5 5
35 PATH2 IFUEL2 ZIFUE2 1 1
35 PATH2 IFUEL2 ZIFUE2 2 2
35 PATH2 IFUEL2 ZIFUE2 3 3
35 PATH2 IFUEL2 ZIFUE2 4 4
35 PATH2 IFUEL2 ZIFUE2 5 5
35 PATH3 IFUEL3 ZIFUE3 1 1
35 PATH3 IFUEL3 ZIFUE3 2 2
35 PATH3 IFUEL3 ZIFUE3 3 3
35 PATH3 IFUEL3 ZIFUE3 4 4
35 PATH3 IFUEL3 ZIFUE3 5 5

```

Figure 3-30. Depletion Chain #3 A.NIP3 and A.BURN Inputs

Continuing with task a) of category 2 in Table 3-25, the card type 09 data is used to specify the neutron reactions in a REBUS input. In the input of Figure 3-30, reactions 0, 1, 3, 4, 5, 9, and 10 are all used by the card type 09 input which correspond to no reaction (0), gamma (1), proton (3), alpha (4), 2n (5), deuteron (9), and tritium (10) reactions. The fission reaction is the only capture related reaction which is not tested in this problem but it is tested in both depletion chain 2 and the flux impacted depletion chain work (combined with other capture reactions). It is important to note that a card type 25 is included for the deuteron reaction (9) which is invalid from the depletion chain setup perspective of REBUS. REBUS correctly ignores this input and it has no impact on the solution. Because the input shown in Figure 3-30 is known to produce the analytic solution as shown earlier, it can be confirmed that REBUS properly interprets the card type 09 input data for the cited reactions used in this problem. For brevity, the input for depletion chain #2 is not shown here and it is simply concluded that the fission reaction combined with other capture and decay reactions is also verified. This outcome should come as no surprise as this software feature is instrumental to the operation of the software and has been rigorously tested for over 40 years.

Task b) of category 2 implies detailed testing of decay reactions 6, 7, 8, and 11-19. As was the case with the preceding capture reactions, the analytic solutions, the preceding analytic solutions all tested out these decay reactions where the excerpted card 09 and 25 inputs are provided in Figure 3-31. These inputs use decay operations 6, 7, 8, 11, 12, 16-19 leaving only inputs 13-15 as untested. Given

all of the preceding testing with REBUS using these inputs proved to yield the analytic solution, one can conclude that REBUS is accurately handling the input for decay processes. To fully test all of the input options, the second test of decay chain #1 was modified to replace reactions 6, 7, 8 with reactions 13, 14, 15, respectively. This test yielded an output file identical to the case using 6, 7, 8 (excluding the input difference), and is included as test 3 of depletion chain #1 in the verification test suite. No additional output detail is given as the results of Figure 3-22 are unchanged. With this stated, task b) of category 2 is verified.

|  |  |
|--|--|
| <pre> ... 09  LFPPS  0 09  DUMP   0 09  U235   0 09  U238   0 09  PU239   0 09  PU240   0 09  PU241   0 09  PU242   0 09  MAGIC   6  DUMP 09  MAGIC   7  LFPPS 09  MAGIC   8  PU239 09  MAGIC   11 PU240 09  MAGIC   12 PU241 09  MAGIC   19 PU242 25  MAGIC   6  DUMP   1.5281E-6 25  MAGIC   7  LFPPS   3.0562E-6 25  MAGIC   8  PU239   4.5843E-6 25  MAGIC   11 PU240   6.1124E-6 25  MAGIC   12 PU241   7.6405E-6 25  MAGIC   19 PU242   9.1686E-6 ... </pre> | <pre> ... 09  B-10   0 09  DUMP   0 09  U235   0 09  U238   0 09  MAGIC   1  PU239   1.0 09  MAGIC   3  PU240   1.0 09  MAGIC   4  PU241   1.0 09  MAGIC   5  PU242   1.0 09  MAGIC   9  LFPPS   1.0 25  MAGIC   9  LFPPS   1.00E-31 09  MAGIC   10 DUMP   1.0 09  PU239   6  B-10 09  PU240   7  B-10 09  PU241   8  B-10 09  PU242   11 B-10 09  LFPPS   19 B-10 25  PU239   6  B-10   1.E-8 25  PU240   7  B-10   1.E-7 25  PU241   8  B-10   3.E-7 25  PU242   11 B-10   6.E-7 25  LFPPS   19 B-10   9.E-6 ... </pre>  |
| <p>Input for Second Test of Decay Chain #1</p>   | <p>Input for Second Test of Decay Chain #3</p>   |
| <pre> ... 09  U235   0 09  U238   0 09  MAGIC   4  PU239   1.0 09  PU239   1  MAGIC   1.0 09  PU240   2  PU241   1.0 09  PU241   5  PU242   1.0 09  PU242   2  PU240   1.0 09  LFPSS   1  DUMP   1.0 09  DUMP   18 LFPPS   1.0 25  DUMP   18 LFPPS   1.00E-6 09  DUMP   17 B-10   1.0 25  DUMP   17 B-10   1.00E-8 09  B-10   16 U238   1.0 25  B-10   16 U238   1.0E-7 ... </pre>   | <pre> ... 09  U235   0 09  U238   0 09  MAGIC   11 PU239   1.0 09  MAGIC   12 PU240   1.0 09  PU239   11 PU240   1.0 09  PU239   12 PU241   1.0 09  PU240   11 PU241   1.0 09  PU240   12 MAGIC   1.0 09  PU241   11 MAGIC   1.0 09  PU241   12 PU239   1.0 25  MAGIC   11 PU239   1.407412E-06 25  MAGIC   12 PU240   1.407412E-06 25  PU239   11 PU240   8.725380E-06 25  PU239   12 PU241   2.680868E-05 25  PU240   11 PU241   9.625767E-06 25  PU240   12 MAGIC   4.984896E-06 25  PU241   11 MAGIC   7.779904E-06 25  PU241   12 PU239   3.905662E-05 09  PU242   0 09  LFPSS   0 09  DUMP   0 09  B-10   0 ... </pre> |
| <p>Input for First Test of Decay Chain #4</p>  | <p>Input for Second Test of Decay Chain #4</p>   |

Figure 3-31. Depletion Excerpts from the Analytic Test Problems

Task c) and d) of category 2 are connected and deal with Avogadro's number and the atom mass of each isotope. The Avogadro number can be defined using card type 28 while the atom mass is handled using card type 24 data both of which are used in Figure 3-30. In Figure 3-30, Avogadro's constant is set to 0.602472E+24. Because the REBUS input is done in atom density, this number is only used when computing the mass details of the output. To verify that the calculation is being done properly, only a simple hand calculation is needed to verify that the mass and atom density details are properly computed.

The second test of depletion chain #3 is first verified to produce the correct U235 and U238 masses. Then, the constant is reduced by an order of magnitude to ensure that the expected behavior occurs; this is added as test 3 of depletion chain #3. Finally, to ensure that the base isotope masses that are

included with the cross section data are used, the card type 24 input for U235 is removed and becomes test 4 of depletion chain #3.

Because this is a handmade cross section input, the key inputs to compute the mass are taken from the input of Figure 3-30 and the atom masses from the cross section data input provided in Figure 3-32. From Figure 3-30, the atom density of U235 can be computed as  $0.0025 \cdot 0.3949 = 0.00098725$  while for U238 it is  $0.02 \cdot 0.3949 = 0.007898$ . The mass and atom density output excerpts are given in Figure 3-33 and the relevant atom densities and masses of U235 and U238 are highlighted. As can be seen, the computed U235 and U238 densities identically match those present in the REBUS output as generated by the initial input processing (GNIP4C) and then later REBUS time step details (FCC004).

```

NOSORT=A.ISO
 0V ISOTXS *XS.ISOISOTXS*      1
 1D   3   15   0   3   0   1   4   1
 2D *THREE-GROUP ISOTXS
 *   * NA   FE   O-16   B-10   C   PU239  U238   MAGIC   FEH
 U235   PU242   LFP   DUMP   PU240   PU241
 ...
 4D U-238S ENDF/B U-238S
 2.38051E+02 3.09930E-11 9.09490E-13 1.20000E+03 0.00000E+00 0.00000E+00
 0   1   1   1   1   1   0   0   2   1   0   100
 200  300   0   1   1   1   0   1   2   2   1   2
 3   1   2   3   0   0   0   1   1   1   1   1
 1   1   1   1   0   0   0
 5D 4.84190E+00 8.16624E+00 1.35578E+01 7.33086E+00 1.00316E+01
 1.39560E+01 7.33086E+00 1.00316E+01 1.39560E+01 6.85670E-02 1.39283E-01
 ...
 4D U235   ENDF/B PU239S
 2.39053E+02 3.17282E-11 1.04375E-12 2.40000E+03 0.00000E+00 0.00000E+00
 0   1   1   1   1   1   0   0   2   1   0   100
 200  300   0   1   1   1   0   1   2   2   1   2
 3   1   2   3   0   0   0   1   1   1   1   1
 1   1   1   1   0   0   0
 5D 4.89761E+00 7.91685E+00 1.41909E+01 7.30386E+00 9.62705E+00
 1.44894E+01 7.30386E+00 9.62705E+00 1.44894E+01 1.50223E-02 1.78799E-01
 1.28808E+00 1.83896E+00 1.55634E+00 2.28678E+00 3.17907E+00 2.91926E+00
 ...

```

**Figure 3-32. Cross Section Data Input Excerpt for Depletion Chain 3**

To determine the masses, the volume of each region must be computed. From Figure 3-30, the hexagonal area of each assembly can be computed as  $0.5 \cdot \sqrt{3} \cdot 10^2 \text{ cm}^2 = 86.60254038 \cdot \text{cm}^2$ . The height of each assembly is 60 cm and with 1, 6, and 12 assemblies in the three rings, the volumes of region ICORE1, ICORE2, and ICORE3 are  $5196.15242271 \cdot \text{cm}^3$ ,  $31176.91453624 \cdot \text{cm}^3$ , and  $62353.82907248 \cdot \text{cm}^3$ , respectively. Using the cross section based atom mass of U235, the mass of U235 for ICORE1 is  $9.8725E-4 \cdot 239.053 / 0.602472 \cdot 5196.15242271 = 2.03548 \text{ kg}$ . The reported output for ICORE is 2.0020 kg which indicates a considerable error is present. Because Figure 3-30 includes a card type 24 for U235, the U235 atom mass should be 235.117 instead of 239.053 and thus the mass is  $9.8725E-4 \cdot 235.117 / 0.602472 \cdot 5196.15242271 = 2.00196 \text{ kg}$  which is consistent with the REBUS output of 2.0020 kg in Figure 3-33.

Using the card type 24 input for U238, 238.125, the U238 mass in ICORE1 can be computed as  $7.898E-3 \cdot 238.125 / 0.602472 \cdot 5196.15242271 = 16.2206 \text{ kg}$  which is consistent with the 16.621 kg reported in Figure 3-33. The total mass of U235 in the domain can be computed as  $2.00196 \text{ kg} \cdot (1 + 6 + 12) = 38.03731 \cdot \text{kg}$  which also matches the total U235 loading in the domain at the end of Figure 3-33. A similar hand calculation can be shown to yield the reported U238 mass in the domain.

To prove that the Avogadro number impacts the result as expected, its value on card type 28 is reduced by an order of magnitude. The atom density and mass output excerpts of interest are shown in Figure 3-34.

```
GNIP4C 11.3072 11/11/19      ANIP3: Hexagonal 3D Test Problem          PAGE      53
*** ATOM DENSITIES OF ZONES (INCLUDING CONTRIBUTIONS FROM SUBZONES) ***
THE ISOTOPE NUMBERS SHOWN ARE THE ISOTXS NUCLIDE NUMBERS

ZONE   NUCLIDE      ISOTOPE  ATOM DENSITY      ISOTOPE  ATOM DENSITY      ISOTOPE  ATOM DENSITY      ISOTOPE  ATOM DENSITY
NO.  NAME       SET      NO.  NAME (ATOMS/B-CM)  NO.  NAME (ATOMS/B-CM)  NO.  NAME (ATOMS/B-CM)  NO.  NAME (ATOMS/B-CM)
1  ZIFUE1      1  NA      8.8914E-03      2  FE      1.7570E-02      3  O-16     1.4963E-02      4  B-10     1.0000E-20
      6  PU239     1.0000E-12      7  U238     7.8980E-03      8  MAGIC    1.0000E-12      10 U235     9.8725E-04

FCC004 11.3072 11/11/19          PAGE      78

BEGINNING OF BURN CYCLE 1
ATOM DENSITIES (IN ATOMS/BARN-CM.) OF ACTIVE ISOTOPES IN EACH REGION
REGION      B-10      DUMP      U235      U238      MAGIC      PU239      PU240      PU241      PU242
ICORE1      0.0000E+00  0.0000E+00  9.8725E-04  7.8980E-03  1.0000E-12  1.0000E-12  1.0000E-12  1.0000E-12  1.0000E-12
      1.0000E-12

ABURN: Hexagonal 3D Test Problem          PAGE      81

MASSES (IN KG) OF ACTIVE ISOTOPES IN EACH REGION
REGION      INITIAL TOTAL MASS OF FISSIONABLE ISOTOPES IN THIS REGION = 0.00000E+00
B-10      DUMP      U235      U238      MAGIC      PU239      PU240      PU241      PU242
ICORE1      0.0000E+00  0.0000E+00  2.0020E+00  1.6221E+01  8.6247E-10  2.0624E-09  2.0710E-09  2.0797E-09  2.0883E-09
      2.0441E-09
      B-10      DUMP      U235      U238      MAGIC      PU239      PU240      PU241      PU242
ICORE2      0.0000E+00  0.0000E+00  1.2012E+01  9.7324E+01  5.1748E-09  1.2374E-08  1.2426E-08  1.2478E-08  1.2530E-08
      1.2264E-08
      B-10      DUMP      U235      U238      MAGIC      PU239      PU240      PU241      PU242
ICORE3      0.0000E+00  0.0000E+00  2.4024E+01  1.9465E+02  1.0350E-08  2.4749E-08  2.4853E-08  2.4956E-08  2.5060E-08
      2.4529E-08

TOTAL REACTOR LOADING (IN KG) OF ACTIVE ISOTOPES AT TIME NODE 0 AT 0.00000000E+00 DAYS.
ISOTOPE  REACTOR LOADING
B-10      0.00000E+00
DUMP      0.00000E+00
U235     3.80373E+01
U238     3.08192E+02
MAGIC    1.63870E-08
PU239    3.91857E-08
PU240    3.93499E-08
PU241    3.95142E-08
PU242    3.96784E-08
LFPPS    3.88371E-08
Total    3.46229E+02
Total Actinide 1.57728E-07
```

Figure 3-33. Atom Density and Mass Output Excerpts for Test 2 of Depletion Chain 3

```
FCC004 11.3072 11/11/19          PAGE      78

BEGINNING OF BURN CYCLE 1
ATOM DENSITIES (IN ATOMS/BARN-CM.) OF ACTIVE ISOTOPES IN EACH REGION
REGION      B-10      DUMP      U235      U238      MAGIC      PU239      PU240      PU241      PU242
ICORE1      0.0000E+00  0.0000E+00  9.8725E-04  7.8980E-03  1.0000E-12  1.0000E-12  1.0000E-12  1.0000E-12  1.0000E-12
      1.0000E-12

MASSES (IN KG) OF ACTIVE ISOTOPES IN EACH REGION
REGION      INITIAL TOTAL MASS OF FISSIONABLE ISOTOPES IN THIS REGION = 0.00000E+00
B-10      DUMP      U235      U238      MAGIC      PU239      PU240      PU241      PU242
ICORE1      0.0000E+00  0.0000E+00  2.0020E+01  1.6221E+02  8.6247E-09  2.0624E-08  2.0710E-08  2.0797E-08  2.0883E-08
      2.0441E-08

TOTAL REACTOR LOADING (IN KG) OF ACTIVE ISOTOPES AT TIME NODE 0 AT 0.00000000E+00 DAYS.
ISOTOPE  REACTOR LOADING
B-10      0.00000E+00
DUMP      0.00000E+00
U235     3.80373E+02
U238     3.08192E+03
MAGIC    1.63870E-07
PU239    3.91857E-07
PU240    3.93499E-07
PU241    3.95142E-07
PU242    3.96784E-07
LFPPS    3.88371E-07
Total    3.46229E+03
Total Actinide 1.57728E-06
```

Figure 3-34. Select Atom Density and Mass Output Excerpts for Test 3 of Depletion Chain 3

A comparison of Figure 3-33 and Figure 3-34 shows that the atom density details are identical and that the mass is consistently increased by an order of magnitude for each region and the total reactor loading of every isotope. To prove that the atom mass detail is impacted properly by the card type 24 inputs, the card type 24 input for U235 is removed which should result in the U235 mass being 239.038. The atom density and mass output excerpts of interest are provided in Figure 3-35. Comparing Figure 3-35 with Figure 3-33 shows that the atom densities of each isotope are identical and that only the atom mass of U235, and all connected outputs, are impacted. The reported output of 2.0355 kg matches the hand calculation discussed earlier based upon the 239.038 atom mass. Because the atom mass of U235 is clearly not 239.038, one can be confident that REBUS is properly taking whatever value is present in the cross section data for that isotope as the atom mass instead of using some internal constant.

```

FCC004 11.3072 11/11/19          PAGE      78
...
          BEGINNING OF BURN CYCLE 1
          ATOM DENSITIES (IN ATOMS/BARN-CM.) OF ACTIVE ISOTOPES IN EACH REGION
          REGION      B-10      DUMP      U235      U238      MAGIC      PU239      PU240      PU241      PU242
          ICORE1  0.0000E+00  0.0000E+00  9.8725E-04  7.8980E-03  1.0000E-12  1.0000E-12  1.0000E-12  1.0000E-12  1.0000E-12
          1.0000E-12
...
          MASSES (IN KG) OF ACTIVE ISOTOPES IN EACH REGION
          REGION      INITIAL TOTAL MASS OF FISSIONABLE ISOTOPES IN THIS REGION = 0.00000E+00
          B-10      DUMP      U235      U238      MAGIC      PU239      PU240      PU241      PU242
          ICORE1  0.0000E+00  0.0000E+00  2.0355E+00  1.6221E+01  8.6247E-10  2.0624E-09  2.0710E-09  2.0797E-09  2.0883E-09
          2.0441E-09
...
          TOTAL REACTOR LOADING (IN KG) OF ACTIVE ISOTOPES AT TIME NODE 0 AT 0.00000000E+00 DAYS.
          ISOTOPE      REACTOR LOADING
          B-10      0.00000E+00
          DUMP      0.00000E+00
          U235      3.86741E+01
          U238      3.08192E+02
          MAGIC      1.63870E-08
          PU239      3.91857E-08
          PU240      3.93499E-08
          PU241      3.95142E-08
          PU242      3.96784E-08
          LFPPS      3.88371E-08
          Total      3.46866E+02
          Total Actinide  1.57728E-07
...

```

**Figure 3-35. Select Atom Density and Mass Output Excerpts for Test 3 of Depletion Chain 3**

The preceding work with card type 24 and 28 of A.BURN demonstrates that the two inputs are being properly used by REBUS and thus task c) and d) of category 2 are verified. It is also important to note that none of the atom density edits were perturbed by the modification of Avogadro's number or the isotopic atom masses. Only masses and mass related quantities (burnup), were altered by these input cards such that additional features not of interest to the VTR project will be similarly impacted.

Tasks e) and f) in category 2 are the next two to verify. Task e) deals with the mapping of isotopes in ISOTXS to the depletion chain which is handled with card type 10 in A.BURN as seen in Figure 3-30. Task f) similarly deals with the active isotope selections that REBUS uses when performing depletion chains. Because the built in depletion chains are not used by VTR, and are not to be tested, the card type 10 and 24 detail are required for all other input specifications. In that regard, all of the preceding depletion tests demonstrate that the active isotope list is being defined based upon the card type 10 detail provided by the user. As an example, Figure 3-30 provides the input to depletion chain #3 and Figure 3-33 shows that the only isotopes reported in the depletion chain are those included on card type 10.

To fully demonstrate this aspect, the first test of depletion chain #3 is modified to alter the mapping of isotopes Pu239, Pu240, Pu241, and Pu242, all of which have starting atom densities of  $10^{-12}$  in this test problem. Figure 3-36 shows the input excerpt with the modified lines of input highlighted. It is important to note that the depletion chain isotope names were modified from "PU239" to "APU239" as a bug was identified in an atom density output from REBUS (the erroneous output from the perturbed isotope card type 10 mappings yielded clearly invalid atom density edits). Changing the isotope names used in the depletion chain obviates the error by forcing REBUS to rely upon the ISOTXS isotope names instead of the depletion chain isotope names. In this regard, the only way this can happen in a user problem is if they defined the depletion chain names identical to those in the ISOTXS data and then miss-mapped two of the isotopes. Given this is inherently an invalid setup, no further work was done to resolve the issue or notify users.

```
...
14      IFUEL1  FUEL1  .3949    OXY   .3949    SODIUM .406
14      IFUEL1  STEEL   .2067   MAGIC 1.0E-12   LFP 1.0E-12
14      IFUEL1  PU239 1.0E-12  PU240 1.0E-12   DUMP 1.0E-20    09  aLFPPS   0
14      IFUEL1  PU241 1.0E-12  PU242 1.0E-12    09  aDUMP   0
14      ZIFUE1 IFUEL1 1.0    09  aU235   0
14      IFUEL2  FUEL2  .3949    OXY   .3949    SODIUM .406
14      IFUEL2  STEEL   .2067   MAGIC 1.0E-12   LFP 1.0E-12
14      IFUEL2  PU239 1.0E-12  PU240 1.0E-12   DUMP 1.0E-20    09  aPU239   0
14      IFUEL2  PU241 1.0E-12  PU242 1.0E-12    09  aPU240   0
14      ZIFUE2 IFUEL2 1.0    09  aPU241   0
14      IFUEL3  FUEL3  .3949    OXY   .3949    SODIUM .406
14      IFUEL3  STEEL   .2067   MAGIC 1.0E-12   LFP 1.0E-12
14      IFUEL3  PU239 1.0E-12  PU240 1.0E-12   DUMP 1.0E-20    09  aMAGIC   1  aPU239  1.0
14      IFUEL3  PU241 1.0E-12  PU242 1.0E-12    09  aMAGIC   3  aPU240  1.0
14      ZIFUE3 IFUEL3 1.0    09  aMAGIC   4  aPU241  1.0
14      ZIFUE3 IFUEL3 1.0    09  aMAGIC   5  aPU242  1.0
14      ZIFUE3 IFUEL3 1.0    09  aMAGIC   9  aLFPPS  1.0
14      ZIFUE3 IFUEL3 1.0    25  aMAGIC   9  aLFPPS 1.00E-31
14      ZIFUE3 IFUEL3 1.0    09  aMAGIC  10  aDUMP   1.0
...
4D  PU239S ENDF/B PU239S
2.39053E+02 3.17282E-11 1.04375E-12 1.20000E+03 0.00000E+00 0.00000E+00 10  aMAGIC  MAGIC
...
4D  PU242  ENDF/B U-238S
2.38051E+02 3.09930E-11 9.09490E-13 2.40000E+03 0.00000E+00 0.00000E+00 10  aU235  U235
...
4D  PU242  ENDF/B U-238S
2.38051E+02 3.09930E-11 9.09490E-13 2.40000E+03 0.00000E+00 0.00000E+00 10  aU238  U238
...
4D  PU242  ENDF/B U-238S
2.38051E+02 3.09930E-11 9.09490E-13 2.40000E+03 0.00000E+00 0.00000E+00 10  aPU239  PU240
...
4D  PU240  ENDF/B U-238S
2.38051E+02 3.09930E-11 9.09490E-13 2.40000E+03 0.00000E+00 0.00000E+00 10  aPU240  PU241
...
4D  PU241  ENDF/B U-238S
2.38051E+02 3.09930E-11 9.09490E-13 2.40000E+03 0.00000E+00 0.00000E+00 10  aPU241  PU242
...
4D  PU242  ENDF/B U-238S
2.38051E+02 3.09930E-11 9.09490E-13 2.40000E+03 0.00000E+00 0.00000E+00 10  aPU242  PU239
...
4D  PU240S ENDF/B PU240S
2.40054E+02 3.11528E-11 8.37562E-13 1.20000E+03 0.00000E+00 0.00000E+00 10  aDUMP  DUMP
...
4D  PU241S ENDF/B PU241S
2.41049E+02 3.20159E-11 1.00859E-12 1.20000E+03 0.00000E+00 0.00000E+00 10  aLFPPS  LFP
...

```

**Figure 3-36. Input Excerpt of Modified Test 1 of Depletion Chain 3**

In Table 3-14 one can see that the various product isotopes atom densities are all identical because the MAGIC reaction cross sections are all identical. Thus, to make this a clearer test, the principle cross sections are modified (from 0.1) to have a gamma, fission, alpha, proton, n2n, deuteron, and tritium cross section values of 0.15, 0.05, 0.09, 0.11, 0.08, 0.09, and 0.13, respectively. It is a trivial matter to evaluate the analytic solution shown earlier in Eq. (6) with the updated MAGIC isotope cross sections and thus it is not displayed here. As expected, REBUS produces the analytic solution with similar accuracy to that observed when comparing Figure 3-24 and Table 3-14. The time step results for the final time step are provided for the base mapping case in Figure 3-37 while those of the perturbed state are given in Figure 3-38.

```
ATOM DENSITIES USED IN THE NEUTRONICS SOLUTION AT TIME NODE 1 AT 5.000000000E+00 DAYS.
(EXCEPT FOR POISON SEARCH ATOM DENSITIES)
REGION ICORE1 ZONE 1
ISOTOPE / DENSITY IN ATOMS/BARN-CM
NA / 8.89140E-03 FE / 1.75695E-02 O-16 / 1.49628E-02 PU239 / 1.22633E-12 U238 / 7.89800E-03
MAGIC / 1.92160E-14 U235 / 9.87250E-04 PU242 / 1.12071E-12 LFP / 1.13580E-12 DUMP / 1.96157E-13
PU240 / 1.16598E-12 PU241 / 1.13580E-12

REGION ICORE2 ZONE 2
ISOTOPE / DENSITY IN ATOMS/BARN-CM
NA / 8.89140E-03 FE / 1.75695E-02 O-16 / 1.49628E-02 PU239 / 1.22633E-12 U238 / 7.89800E-03
MAGIC / 1.92160E-14 U235 / 9.87250E-04 PU242 / 1.12071E-12 LFP / 1.13580E-12 DUMP / 1.96157E-13
PU240 / 1.16598E-12 PU241 / 1.13580E-12

REGION ICORE3 ZONE 3
ISOTOPE / DENSITY IN ATOMS/BARN-CM
NA / 8.89140E-03 FE / 1.75695E-02 O-16 / 1.49628E-02 PU239 / 1.22633E-12 U238 / 7.89800E-03
MAGIC / 1.92160E-14 U235 / 9.87250E-04 PU242 / 1.12071E-12 LFP / 1.13580E-12 DUMP / 1.96157E-13
PU240 / 1.16598E-12 PU241 / 1.13580E-12

REACTOR CONDITIONS AFTER 1 BURNUP SUBSTEPS AT TIME = 5.000000000E+00 DAYS
ATOM DENSITIES (IN ATOMS/BARN-CM.) OF ACTIVE ISOTOPES IN EACH REGION
REGION
aLFPSS aDUMP aU235 aU238 aPU239 aPU240 aPU241 aPU242 aMAGIC
ICORE1 1.1358E-12 1.9616E-13 9.8725E-04 7.8980E-03 1.22633E-12 1.1660E-12 1.1358E-12 1.1207E-12 1.9216E-14
aLFPSS aDUMP aU235 aU238 aPU239 aPU240 aPU241 aPU242 aMAGIC
ICORE2 1.1358E-12 1.9616E-13 9.8725E-04 7.8980E-03 1.22633E-12 1.1660E-12 1.1358E-12 1.1207E-12 1.9216E-14
aLFPSS aDUMP aU235 aU238 aPU239 aPU240 aPU241 aPU242 aMAGIC
ICORE3 1.1358E-12 1.9616E-13 9.8725E-04 7.8980E-03 1.22633E-12 1.1660E-12 1.1358E-12 1.1207E-12 1.9216E-14
```

Figure 3-37. Base Output Excerpt for REBUS for the Modified Setup of Depletion Chain 3

```
ATOM DENSITIES USED IN THE NEUTRONICS SOLUTION AT TIME NODE 1 AT 5.000000000E+00 DAYS.
(EXCEPT FOR POISON SEARCH ATOM DENSITIES)
REGION ICORE1 ZONE 1
ISOTOPE / DENSITY IN ATOMS/BARN-CM
NA / 8.89140E-03 FE / 1.75695E-02 O-16 / 1.49628E-02 PU239 / 1.12071E-12 U238 / 7.89800E-03
MAGIC / 1.92160E-14 U235 / 9.87250E-04 PU242 / 1.13580E-12 LFP / 1.13580E-12 DUMP / 1.96157E-13
PU240 / 1.22633E-12 PU241 / 1.16598E-12

REGION ICORE2 ZONE 2
ISOTOPE / DENSITY IN ATOMS/BARN-CM
NA / 8.89140E-03 FE / 1.75695E-02 O-16 / 1.49628E-02 PU239 / 1.12071E-12 U238 / 7.89800E-03
MAGIC / 1.92160E-14 U235 / 9.87250E-04 PU242 / 1.13580E-12 LFP / 1.13580E-12 DUMP / 1.96157E-13
PU240 / 1.22633E-12 PU241 / 1.16598E-12

REGION ICORE3 ZONE 3
ISOTOPE / DENSITY IN ATOMS/BARN-CM
NA / 8.89140E-03 FE / 1.75695E-02 O-16 / 1.49628E-02 PU239 / 1.12071E-12 U238 / 7.89800E-03
MAGIC / 1.92160E-14 U235 / 9.87250E-04 PU242 / 1.13580E-12 LFP / 1.13580E-12 DUMP / 1.96157E-13
PU240 / 1.22633E-12 PU241 / 1.16598E-12

ATOM DENSITIES (IN ATOMS/BARN-CM.) OF ACTIVE ISOTOPES IN EACH REGION
REGION
aLFPSS aDUMP aU235 aU238 aPU239 aPU240 aPU241 aPU242 aMAGIC
ICORE1 1.1358E-12 1.9616E-13 9.8725E-04 7.8980E-03 1.22633E-12 1.1660E-12 1.1358E-12 1.1207E-12 1.9216E-14
aLFPSS aDUMP aU235 aU238 aPU239 aPU240 aPU241 aPU242 aMAGIC
ICORE2 1.1358E-12 1.9616E-13 9.8725E-04 7.8980E-03 1.22633E-12 1.1660E-12 1.1358E-12 1.1207E-12 1.9216E-14
aLFPSS aDUMP aU235 aU238 aPU239 aPU240 aPU241 aPU242 aMAGIC
ICORE3 1.1358E-12 1.9616E-13 9.8725E-04 7.8980E-03 1.22633E-12 1.1660E-12 1.1358E-12 1.1207E-12 1.9216E-14
```

Figure 3-38. Perturbed Output Excerpt for REBUS for the Modified Setup of Depletion Chain 3

As shown in Figure 3-36, the perturbed output should show the rotation of the isotope densities such that Pu239 maps to the Pu242 atom density as indicated in Figure 3-38. Because no modification to the card type 24 input was made, this is the only REBUS output that actually changes. Both the atom density and atom mass detail are provided in terms of the depletion chain isotopes which are not impacted by the isotope mapping modification itself in this test. This is the expected result and thus the task e) and f) are verified to be working properly with the noted bug in the output edit described.

Task g) is the last to confirm in category 2, but this task has already been fully verified by the various analytic solutions displayed in the previous section. As shown in this section, the analytic test problems can be manipulated to demonstrate that all of the tasks of category 2 are working as expected. Thus combined, all of the tasks for category 2 are verified. While a minor bug was identified in one output of REBUS, it was for a clearly invalid input specification which is of little interest to the VTR project.

### 3.5.2 Category 3 Input Verification

The category 3 section of Table 2-1, reproduced here as Table 3-25, has three tasks which are focused on verifying the region path input specification. Each of these tasks consider independent aspects of the input and thus are covered individually. In all three cases, new inputs are required as the preceding inputs focused on analytic solutions that are too simplistic to be effective test problems. For convenience, the same 3-group cross section set used in the previous section is used to define all of the problems in this section noting that the existing isotope data is duplicated to create multiple region-wise cross section sets. The region-wise isotope labels of aU235, bU235, cU235, and dU235 were chosen where the remaining isotopes are manipulated similarly to this example.

**Table 3-25. REBUS Identified Verification Tasks for Category 3**

| Category | Verification Tasks  |
|----------|---|
| 3        | Verify the region path specification <ul style="list-style-type: none"> <li>a) The fuel paths are composed on input regions (cards 11, 35)</li> <li>b) The burnup limits specified by path are imposed (cards 5, 6, 7, 8)</li> <li>c) The equilibrium calculation is consistent with the equilibrium state of a given core</li> </ul> |

Task a) of category 3 is intended to verify that the region path specification using card types 11 and 35 are handled properly. To understand the purpose of these cards, the details are summarized in Table 3-26. Conceptually, REBUS tracks zones (material compositions) and these two card types are used to detail how each zone is assigned to each region in the domain in each time step of the problem which it terms “path.” From Table 3-26, it should be clear that there are many different ways to orchestrate the assignment of zones to regions and this section will verify the status of all valid approaches for constructing input.

**Table 3-26. REBUS A.BURN Card Type 11 and 35 Descriptions**

| Input             | Description   |
|-------------------|---|
| 11.2              | The name of the path                                      |
| 11.3              | Number of previous burn cycle                             |
| 11.4, 11.7        | Stage number  |
| 11.5, 11.8        | Sub-zone name or discharge name                           |
| 11.6, 11.9        | Zone name, region name, or fuel management group name     |
| 35.2              | The name of the path                                      |
| 35.3              | Zone name or sub-zone name                                |
| 35.4, 35.7, 35.10 | Region label or fuel management group label or zone label |
| 35.5, 35.8, 35.11 | Beginning stage number for assignment                     |
| 35.6, 35.9, 35.12 | Ending stage number for assignment                        |

Because the hexagonal geometry is used for all VTR related work, this section only focuses on demonstrating the hexagonal geometry capability. It should be obvious that using Cartesian or hexagonal geometry with REBUS is not a relevant issue. Figure 3-39 shows the assembly layout of the test geometry which has 4 zones and 4 different regions. The outer zone (dark blue) is a reflector region while the inner three regions are fueled using three region-wise cross section definitions (zone 1 uses aU235, zone 2 uses bU235, and zone 3 uses cU235). The inner three regions are designed to have equal volumes. Figure 3-40 provides the A.NIP3 input excerpt to further clarify the geometry and composition setup. It is important to note that the energy recovery factors in ISOTXS are zeroed for all isotopes except fission of U235 (e.g. aU235, bU235, etc...) and that U235 is only destroyed by

the fission reaction. This will allow a simple hand calculation to guarantee a minimal measure of confidence that the depletion results of REBUS are accurate.

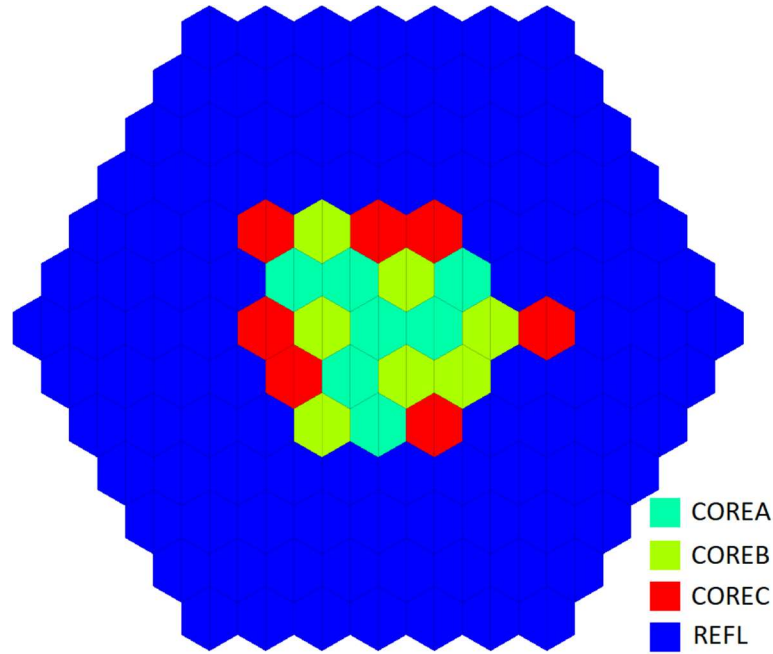


Figure 3-39. Geometry Setup for Path Specification Verification

```

...
03      120
04      4      4      4      4      4      4
09      Z      1      30.0
09      Z      3      90.0
09      Z      1      120.0
14      FUELA  aNA    0.010
14      FUELA  aO16   0.016
14      FUELA  aFE    0.02
14      FUELA  aU235  0.001
14      FUELA  aU238  0.02
14      FUELA  aPU239 0.0005
14      FUELA  aPU240 0.0004
14      FUELA  aPU241 0.0003
14      FUELA  aPU242 0.0001
14      FUELA  aLFP   1.0E-12
14      FUELA  aDUMP  1.0E-12
14      ZFUELA FUELA 1.0
...
14      FUELB  bNA    0.010
14      FUELB  bO16   0.016
14      FUELB  bFE    0.02
14      FUELB  bU235  0.0001
14      FUELB  bU238  0.02
14      FUELB  bPU239 0.001
14      FUELB  bPU240 0.00001
14      FUELB  bPU241 0.00001
14      FUELB  bPU242 0.00001
14      FUELB  bLFP   1.0E-12
14      FUELB  bDUMP  1.0E-12
14      ZFUELB FUELB 1.0
...
14      FUELCL cLFP   1.0E-12
14      FUELCL cDUMP  1.0E-12
14      ZFUELCL FUELCL 1.0
14      REFL   aFEH   0.03
15      REFL   REFL
15      ZFUELA COREA
15      ZFUELB COREB
15      ZFUELCL COREC
29      10.0      0      1
30      REFL   1      0      0      0.0      120.0
30      REFL   2      0      0      0.0      120.0
30      REFL   3      0      0      0.0      120.0
30      REFL   4      0      0      0.0      120.0
30      REFL   5      0      0      0.0      120.0
30      REFL   6      0      0      0.0      120.0
30      REFL   7      0      0      0.0      120.0
30      COREA  1      0      0      30.0      90.0
30      COREA  2      1      1      30.0      90.0
30      COREB  2      2      2      30.0      90.0
30      COREA  2      3      3      30.0      90.0
30      COREB  2      4      4      30.0      90.0
30      COREA  2      5      5      30.0      90.0
30      COREB  2      6      6      30.0      90.0
30      COREB  3      1      1      30.0      90.0
30      COREA  3      2      2      30.0      90.0
30      COREC  3      3      3      30.0      90.0
30      COREC  3      4      4      30.0      90.0
30      COREB  3      5      5      30.0      90.0
30      COREA  3      6      6      30.0      90.0
30      COREC  3      7      7      30.0      90.0
30      COREC  3      8      8      30.0      90.0
30      COREB  3      9      9      30.0      90.0
30      COREA  3      10     10     30.0      90.0
30      COREC  3      11     11     30.0      90.0
30      COREB  3      12     12     30.0      90.0
30      COREC  4      1      1      30.0      90.0
30      COREC  4      8      8      30.0      90.0
...
14      FUELCL cNA    0.010
14      FUELCL cO16   0.016
14      FUELCL cFE    0.02
14      FUELCL cU235  0.0001
14      FUELCL cU238  0.02
14      FUELCL cPU239 0.0015
14      FUELCL cPU240 0.0008
14      FUELCL cPU241 0.0004
14      FUELCL cPU242 0.0001

```

Figure 3-40. A.NIP3 Input Excerpt for Card Type 11 Testing

### 3.5.2.1 Non-equilibrium Testing of Card Type 11

For the first set of path tests, a non-equilibrium problem is defined and each assignment option of card type 11 is tested. Because there are three different mapping options, the REBUS input, A.BURN, excerpts for the tested cases are provided in Figure 3-41. From these inputs, one can see that the path names PATH1, PATH2, and PATH3 are used for the three different sub-zones (card input 11.2). The number of previous burn cycles is set to zero for all three test cases (card input 11.3) where later testing will demonstrate this input. Finally, the non-equilibrium problem is defined to have 3 time steps and thus there are three stages to define for each sub-zone in each path.

|   |  |   |  |   |   |   |
|---|--|---|--|---|---|---|
| <pre>... 11  PATH1 0  1  FUELA ZFUELA 11  PATH1 0  2  FUELA ZFUELA 11  PATH1 0  3  FUELA ZFUELA</pre> | <pre>... 11  PATH1 0  1  FUELA COREA 11  PATH1 0  2  FUELA COREB 11  PATH1 0  3  FUELA COREC</pre> | <pre>... 11  PATH2 0  1  FUELB ZFUELB 11  PATH2 0  2  FUELB ZFUELB 11  PATH2 0  3  FUELB ZFUELB</pre> | <pre>... 11  PATH2 0  1  FUELB COREB 11  PATH2 0  2  FUELB COREC 11  PATH2 0  3  FUELB COREA</pre> | <pre>... 11  PATH3 0  1  FUELCL ZFUELCL 11  PATH3 0  2  FUELCL ZFUELCL 11  PATH3 0  3  FUELCL ZFUELCL</pre> | <pre>... 11  PATH3 0  1  FUELCL COREC 11  PATH3 0  2  FUELCL COREA 11  PATH3 0  3  FUELCL COREB</pre> | <pre>... 45  FMG1 45  FMG2 45  FMG3</pre> |
| Primary Zone  | Region   | Fuel Management Group   |  |   |   |   |

Figure 3-41. A.BURN Input Excerpt for Card Type 11 Verification

The card input 11.5 is used to select a sub-zone (secondary composition) which are FUELA, FUELB, and FUELCL from Figure 3-41 and consistent with the sub-zone setup in Figure 3-40. That sub-zone can be assigned to a zone, a region, or a fuel management path. The input rules for card type 11 requires that the sub-zone be assigned to the same path for all stages. Also, it is forbidden to allow the sub-zone and primary zone mapping to change between stages and thus the input is very simple for the “primary zone” input example in Figure 3-41. This input option of card type 11 is primarily used for an equilibrium cycle mode calculation where the user wants the zone to be a mixture of multiple burned compositions as will be shown later.

In the second input example for card type 11, the sub-zone is assigned to a region (COREA, COREB, or COREC). **This simultaneously reassigns the zone to the same region.** The primary purpose of this example is to allow the user to simulate spatial movements of the fuel in either equilibrium or non-equilibrium options. It is important to note that the volume of the various regions must be consistent to avoid issues where only a fraction of the zone is actively burned during a given stage. REBUS will error out if the volumes are not accurate to 0.1% noting that if a volume mismatch is present, REBUS will effectively change the density of the material to impose mass conservation during the depletion step.

In the final example of Figure 3-41, fuel management groups FMG1, FMG2, and FMG3 are defined using card type 45 of A.BURN. Each fuel management group can be composed of regions or areas and the intention is to simplify the user input by allowing the PATH specification to point to multiple regions with a single input. The only negative of this input option is that fuel shuffling cannot be modeled as the volumes of the fuel management groups are assumed to be different. As a consequence, a given sub-zone can only be assigned to one fuel management group for all stages of a path and thus this input is just a simpler version of the primary zone mapping which, given the zone is mapped to the same regions in the fuel management group, would accomplish the same result.

It is important to note that in all card type 11 inputs, the user cannot arbitrarily reassign the sub-zone assignment in stage 1 from that setup in the A.NIP3 input. Thus, the stage 1 definition must exactly agree with the A.NIP3 input otherwise REBUS will error out. In that regard, the three examples cover the totality of user options with regard to card type inputs 11.2 and 11.4 to 11.9.

The power was set to 100 MW, the U-235 fission conversion factor was defined as  $10^{-11}$  watt-sec/fission (62.415 MeV/fission), and a 1.5 day cycle length was used in all three test cases. All other isotope fission and capture power conversion factors were set to  $10^{-18}$  watt-sec. The collected eigenvalue results from all three calculations are provided in Table 3-27. The three respective REBUS output excerpts for the three test cases are given in Figure 3-42, Figure 3-43, and Figure 3-44. Starting with the eigenvalue results, it should be very apparent that Test#1 and Test #3 have identical results. This is because the fuel management setup for each PATH is identical. Comparing the Test #1 output from Figure 3-42 with the output from Test #3 in Figure 3-44, one can see that they are identical such that no additional study of the Figure 3-44 result is necessary.

Continuing with the eigenvalue results for Test #1 and Test #2, one can see that the first two points are identical but after that, considerable differences exist. This is expected of course as the PATH specifications for Test #2 move materials in each stage. Given the higher eigenvalue at 3.0 days in Test #2, it should be clear that a higher worth material was moved to the center of the core. These results should also impact the atom density details of Figure 3-43.

**Table 3-27.  $k_{eff}$  Results for the Three Non-Equilibrium Test Problems of Card Type 11**

|                      | Test #1         | Test #2   | Test #3                     |
|----------------------|-----------------|-----------|-----------------------------|
| Time Point<br>(days) | Primary<br>Zone | Region    | Fuel<br>Management<br>Group |
| 0.0                  | 0.64369 5       | 0.64369 5 | 0.64369 5                   |
| 1.5                  | 0.64738 8       | 0.64738 8 | 0.64738 8                   |
| 3.0                  | 0.65093 6       | 0.70630 1 | 0.65093 6                   |
| 4.5                  | 0.65433 5       | 0.64825 2 | 0.65433 5                   |

Each REBUS output excerpt provides the atom density and atom mass results for the beginning of the first cycle along with the initial total reactor loading output. This is followed by the atom density results at the end of the first cycle (1.5 days) and those used at the beginning of the second cycle (burn cycle 2). The atom density output for the end of cycle 2 and cycle 3 is given along with the total reactor loading at the end of the calculation.

Because of its simplicity, the verification work will begin with Test #1 in Figure 3-42. The first part of the output to verify is the atom density of U235 in each region which is reported as 0.001, 0.0001, and 0.0001 in COREA, COREB, and COREC in Figure 3-42. Looking at the input specification in Figure 3-40, one can easily identify the atom densities of U235 in FUELA, FUELB, and FUELc are 0.001, 0.0001, and 0.0001, respectively. Noting that the output in Figure 3-42 only includes the active isotopes, the remaining isotopic atom densities can also be easily matched. This verifies that REBUS is correctly transferring the user input from DIF3D through to REBUS with regard to setting up depleting isotope atom densities.

```
*****
*     START OF A COMPLETE BURN CYCLE  *
*****
THE BURN CYCLE TIME IS 1.500000000E+00 DAYS.
THE ENRICHMENT MODIFICATION FACTOR IS 0.00000E+00.
* TIME NODE 0 DIFFUSION THEORY NEUTRONICS SOLUTION AT 0.000000000E+00 DAYS FOLLOWS *
...
ATOM DENSITIES (IN ATOMS/BARN-CM.) OF ACTIVE ISOTOPES IN EACH REGION
U235   U238   PU239   PU240   PU241   PU242   LFPPS   DUMP
COREA 1.0000E-03 2.0000E-02 5.0000E-04 4.0000E-04 3.0000E-04 1.0000E-04 1.0000E-12 1.0000E-12
U235   U238   PU239   PU240   PU241   PU242   LFPPS   DUMP
COREB 1.0000E-04 2.0000E-02 1.0000E-03 1.0000E-05 1.0000E-05 1.0000E-05 1.0000E-12 1.0000E-12
U235   U238   PU239   PU240   PU241   PU242   LFPPS   DUMP
COREC 1.0000E-04 2.0000E-02 1.5000E-03 8.0000E-04 4.0000E-04 1.0000E-04 1.0000E-12 1.0000E-12
...
INITIAL TOTAL MASS OF FISSIONABLE ISOTOPES IN THIS REGION = 3.20705E+02
U235   U238   PU239   PU240   PU241   PU242   LFPPS   DUMP
COREA 1.4201E+01 2.8765E+02 7.2215E+00 5.8014E+00 4.3692E+00 1.4625E+00 1.4315E-08 1.4254E-08
INITIAL TOTAL MASS OF FISSIONABLE ISOTOPES IN THIS REGION = 3.03950E+02
U235   U238   PU239   PU240   PU241   PU242   LFPPS   DUMP
COREB 1.4201E+00 2.8765E+02 1.4443E+01 1.4504E-01 1.4564E-01 1.4625E-01 1.4315E-08 1.4254E-08
INITIAL TOTAL MASS OF FISSIONABLE ISOTOPES IN THIS REGION = 3.29625E+02
U235   U238   PU239   PU240   PU241   PU242   LFPPS   DUMP
COREC 1.4201E+00 2.8765E+02 2.1665E+01 1.1603E+01 5.8256E+00 1.4625E+00 1.4315E-08 1.4254E-08
...
TOTAL REACTOR LOADING (IN KG) OF ACTIVE ISOTOPES AT TIME NODE 0 AT 0.000000000E+00 DAYS.
ISOTOPE REACTOR LOADING
U235 1.70410E+01
U238 8.62949E+02
PU239 4.33290E+01
PU240 1.75493E+01
PU241 1.03405E+01
PU242 3.07117E+00
LFPPS 4.29436E-08
DUMP 4.27624E-08
...
REACTOR CONDITIONS AFTER 1 BURNUP SUBSTEPS AT TIME = 1.500000000E+00 DAYS
ATOM DENSITIES (IN ATOMS/BARN-CM.) OF ACTIVE ISOTOPES IN EACH REGION
U235   U238   PU239   PU240   PU241   PU242   LFPPS   DUMP
COREA 9.6878E-04 1.9894E-02 5.6270E-04 3.9711E-04 2.8899E-04 1.0157E-04 8.6777E-05 4.3112E-07
U235   U238   PU239   PU240   PU241   PU242   LFPPS   DUMP
COREB 9.7403E-05 1.9911E-02 1.0377E-03 1.6375E-05 9.6913E-06 1.0015E-05 4.7687E-05 3.6443E-08
U235   U238   PU239   PU240   PU241   PU242   LFPPS   DUMP
COREC 9.8180E-05 1.9938E-02 1.5147E-03 7.9868E-04 3.9272E-04 1.0136E-04 5.6377E-05 2.5348E-07
...
BEGINNING OF BURN CYCLE 2
ATOM DENSITIES (IN ATOMS/BARN-CM.) OF ACTIVE ISOTOPES IN EACH REGION
U235   U238   PU239   PU240   PU241   PU242   LFPPS   DUMP
COREA 9.6878E-04 1.9894E-02 5.6270E-04 3.9711E-04 2.8899E-04 1.0157E-04 8.6777E-05 4.3112E-07
U235   U238   PU239   PU240   PU241   PU242   LFPPS   DUMP
COREB 9.7403E-05 1.9911E-02 1.0377E-03 1.6375E-05 9.6913E-06 1.0015E-05 4.7687E-05 3.6443E-08
U235   U238   PU239   PU240   PU241   PU242   LFPPS   DUMP
COREC 9.8180E-05 1.9938E-02 1.5147E-03 7.9868E-04 3.9272E-04 1.0136E-04 5.6377E-05 2.5348E-07
...
REACTOR CONDITIONS AFTER 1 BURNUP SUBSTEPS AT TIME = 3.000000000E+00 DAYS
ATOM DENSITIES (IN ATOMS/BARN-CM.) OF ACTIVE ISOTOPES IN EACH REGION
U235   U238   PU239   PU240   PU241   PU242   LFPPS   DUMP
COREA 9.3759E-04 1.9785E-02 6.2426E-04 3.9466E-04 2.7817E-04 1.0309E-04 1.7676E-04 8.8197E-07
U235   U238   PU239   PU240   PU241   PU242   LFPPS   DUMP
COREB 9.4792E-05 1.9820E-02 1.0748E-03 2.3090E-05 9.4344E-06 1.0028E-05 9.7898E-05 7.4041E-08
U235   U238   PU239   PU240   PU241   PU242   LFPPS   DUMP
COREC 9.6340E-05 1.9874E-02 1.5294E-03 7.9740E-04 3.8542E-04 1.0272E-04 1.1446E-04 5.1788E-07
...
REACTOR CONDITIONS AFTER 1 BURNUP SUBSTEPS AT TIME = 4.500000000E+00 DAYS
ATOM DENSITIES (IN ATOMS/BARN-CM.) OF ACTIVE ISOTOPES IN EACH REGION
REGION
U235   U238   PU239   PU240   PU241   PU242   LFPPS   DUMP
COREA 9.0644E-04 1.9673E-02 6.8466E-04 3.9263E-04 2.6754E-04 1.0457E-04 2.7012E-04 1.3536E-06
U235   U238   PU239   PU240   PU241   PU242   LFPPS   DUMP
COREB 9.2168E-05 1.9726E-02 1.1114E-03 3.0156E-05 9.2326E-06 1.0041E-05 1.5078E-04 1.1287E-07
U235   U238   PU239   PU240   PU241   PU242   LFPPS   DUMP
COREC 9.4480E-05 1.9808E-02 1.5439E-03 7.9615E-04 3.7812E-04 1.0408E-04 1.7435E-04 7.9392E-07
...
TOTAL REACTOR LOADING (IN KG) OF ACTIVE ISOTOPES AT TIME NODE 1 AT 4.500000000E+00 DAYS.
ISOTOPE REACTOR LOADING
U235 1.55228E+01
U238 8.51542E+02
PU239 4.82395E+01
PU240 1.76789E+01
PU241 9.53794E+00
PU242 3.19836E+00
LFPPS 8.52077E+00
DUMP 3.22201E-02
...
```

Figure 3-42. REBUS Output Excerpt for the Primary Zone Assignment Option of Card Type 11

```
*****
* START OF A COMPLETE BURN CYCLE *
*****
THE BURN CYCLE TIME IS 1.500000000E+00 DAYS.
THE ENRICHMENT MODIFICATION FACTOR IS 0.00000E+00.
* TIME NODE 0 DIFFUSION THEORY NEUTRONICS SOLUTION AT 0.000000000E+00 DAYS FOLLOWS *
...
ATOM DENSITIES (IN ATOMS/BARN-CM.) OF ACTIVE ISOTOPES IN EACH REGION
U235 U238 PU239 PU240 PU241 PU242 LFPPS DUMP
COREA 1.0000E-03 2.0000E-02 5.0000E-04 4.0000E-04 3.0000E-04 1.0000E-04 1.0000E-12 1.0000E-12
U235 U238 PU239 PU240 PU241 PU242 LFPPS DUMP
COREB 1.0000E-04 2.0000E-02 1.0000E-03 1.0000E-05 1.0000E-05 1.0000E-05 1.0000E-12 1.0000E-12
U235 U238 PU239 PU240 PU241 PU242 LFPPS DUMP
COREC 1.0000E-04 2.0000E-02 1.5000E-03 8.0000E-04 4.0000E-04 1.0000E-04 1.0000E-12 1.0000E-12
...
INITIAL TOTAL MASS OF FISSIONABLE ISOTOPES IN THIS REGION = 3.20705E+02
U235 U238 PU239 PU240 PU241 PU242 LFPPS DUMP
COREA 1.4201E+01 2.8765E+02 7.2215E+00 5.8014E+00 4.3692E+00 1.4625E+00 1.4315E-08 1.4254E-08
INITIAL TOTAL MASS OF FISSIONABLE ISOTOPES IN THIS REGION = 3.03950E+02
U235 U238 PU239 PU240 PU241 PU242 LFPPS DUMP
COREB 1.4201E+00 2.8765E+02 1.4443E+01 1.4504E-01 1.4564E-01 1.4625E-01 1.4315E-08 1.4254E-08
INITIAL TOTAL MASS OF FISSIONABLE ISOTOPES IN THIS REGION = 3.29625E+02
U235 U238 PU239 PU240 PU241 PU242 LFPPS DUMP
COREC 1.4201E+00 2.8765E+02 2.1665E+01 1.1603E+01 5.8256E+00 1.4625E+00 1.4315E-08 1.4254E-08
...
TOTAL REACTOR LOADING (IN KG) OF ACTIVE ISOTOPES AT TIME NODE 0 AT 0.000000000E+00 DAYS.
ISOTOPE REACTOR LOADING
U235 1.70410E+01
U238 8.62949E+02
PU239 4.33290E+01
PU240 1.75493E+01
PU241 1.03405E+01
PU242 3.07117E+00
LFPPS 4.29436E-08
DUMP 4.27624E-08
...
REACTOR CONDITIONS AFTER 1 BURNUP SUBSTEPS AT TIME = 1.500000000E+00 DAYS
ATOM DENSITIES (IN ATOMS/BARN-CM.) OF ACTIVE ISOTOPES IN EACH REGION
U235 U238 PU239 PU240 PU241 PU242 LFPPS DUMP
COREA 9.6878E-04 1.9894E-02 5.6270E-04 3.9711E-04 2.8899E-04 1.0157E-04 8.6777E-05 4.3112E-07
U235 U238 PU239 PU240 PU241 PU242 LFPPS DUMP
COREB 9.7403E-05 1.9911E-02 1.0377E-03 1.6375E-05 9.6913E-06 1.0015E-05 4.7687E-05 3.6443E-08
U235 U238 PU239 PU240 PU241 PU242 LFPPS DUMP
COREC 9.8180E-05 1.9938E-02 1.5147E-03 7.9868E-04 3.9272E-04 1.0136E-04 5.6377E-05 2.5348E-07
...
BEGINNING OF BURN CYCLE 2
ATOM DENSITIES (IN ATOMS/BARN-CM.) OF ACTIVE ISOTOPES IN EACH REGION
U235 U238 PU239 PU240 PU241 PU242 LFPPS DUMP
COREB 9.6878E-04 1.9894E-02 5.6270E-04 3.9711E-04 2.8899E-04 1.0157E-04 8.6777E-05 4.3112E-07
U235 U238 PU239 PU240 PU241 PU242 LFPPS DUMP
COREC 9.7403E-05 1.9911E-02 1.0377E-03 1.6375E-05 9.6913E-06 1.0015E-05 4.7687E-05 3.6443E-08
U235 U238 PU239 PU240 PU241 PU242 LFPPS DUMP
COREA 9.8180E-05 1.9938E-02 1.5147E-03 7.9868E-04 3.9272E-04 1.0136E-04 5.6377E-05 2.5348E-07
...
REACTOR CONDITIONS AFTER 1 BURNUP SUBSTEPS AT TIME = 3.000000000E+00 DAYS
ATOM DENSITIES (IN ATOMS/BARN-CM.) OF ACTIVE ISOTOPES IN EACH REGION
U235 U238 PU239 PU240 PU241 PU242 LFPPS DUMP
COREB 9.3866E-04 1.9789E-02 6.2208E-04 3.9474E-04 2.7854E-04 1.0304E-04 1.7349E-04 8.6559E-07
U235 U238 PU239 PU240 PU241 PU242 LFPPS DUMP
COREC 9.5535E-05 1.9845E-02 1.0659E-03 2.1401E-05 9.5015E-06 1.0026E-05 8.2335E-05 6.4214E-08
U235 U238 PU239 PU240 PU241 PU242 LFPPS DUMP
COREA 9.4530E-05 1.9812E-02 1.5407E-03 7.9552E-04 3.7836E-04 1.0393E-04 1.7397E-04 7.6664E-07
...
REACTOR CONDITIONS AFTER 1 BURNUP SUBSTEPS AT TIME = 4.500000000E+00 DAYS
ATOM DENSITIES (IN ATOMS/BARN-CM.) OF ACTIVE ISOTOPES IN EACH REGION
U235 U238 PU239 PU240 PU241 PU242 LFPPS DUMP
COREC 9.1167E-04 1.9691E-02 6.7584E-04 3.9305E-04 2.6927E-04 1.0436E-04 2.5369E-04 1.2806E-06
U235 U238 PU239 PU240 PU241 PU242 LFPPS DUMP
COREA 9.0935E-05 1.9681E-02 1.1296E-03 3.3797E-05 9.1607E-06 1.0047E-05 1.7559E-04 1.3226E-07
U235 U238 PU239 PU240 PU241 PU242 LFPPS DUMP
COREB 9.0480E-05 1.9667E-02 1.5699E-03 7.9254E-04 3.6272E-04 1.0679E-04 3.0929E-04 1.3853E-06
...
TOTAL REACTOR LOADING (IN KG) OF ACTIVE ISOTOPES AT TIME NODE 1 AT 4.500000000E+00 DAYS.
ISOTOPE REACTOR LOADING
U235 1.55228E+01
U238 8.49120E+02
PU239 4.87495E+01
PU240 1.76854E+01
PU241 9.33785E+00
PU242 3.23491E+00
LFPPS 1.05724E+01
DUMP 3.98855E-02
...
```

Figure 3-43. REBUS Output Excerpt for the Region Assignment Option of Card Type 11

```
*****
* START OF A COMPLETE BURN CYCLE *
*****
THE BURN CYCLE TIME IS 1.500000000E+00 DAYS.
THE ENRICHMENT MODIFICATION FACTOR IS 0.00000E+00.
* TIME NODE 0 DIFFUSION THEORY NEUTRONICS SOLUTION AT 0.000000000E+00 DAYS FOLLOWS *
...
ATOM DENSITIES (IN ATOMS/BARN-CM.) OF ACTIVE ISOTOPES IN EACH REGION
U235 U238 PU239 PU240 PU241 PU242 LFPSS DUMP
COREA 1.0000E-03 2.0000E-02 5.0000E-04 4.0000E-04 3.0000E-04 1.0000E-04 1.0000E-12 1.0000E-12
U235 U238 PU239 PU240 PU241 PU242 LFPSS DUMP
COREB 1.0000E-04 2.0000E-02 1.0000E-03 1.0000E-05 1.0000E-05 1.0000E-05 1.0000E-12 1.0000E-12
U235 U238 PU239 PU240 PU241 PU242 LFPSS DUMP
COREC 1.0000E-04 2.0000E-02 1.5000E-03 8.0000E-04 4.0000E-04 1.0000E-04 1.0000E-12 1.0000E-12
...
INITIAL TOTAL MASS OF FISSIONABLE ISOTOPES IN THIS REGION = 3.20705E+02
U235 U238 PU239 PU240 PU241 PU242 LFPSS DUMP
COREA 1.4201E+01 2.8765E+02 7.2215E+00 5.8014E+00 4.3692E+00 1.4625E+00 1.4315E-08 1.4254E-08
INITIAL TOTAL MASS OF FISSIONABLE ISOTOPES IN THIS REGION = 3.03950E+02
U235 U238 PU239 PU240 PU241 PU242 LFPSS DUMP
COREB 1.4201E+00 2.8765E+02 1.4443E+01 1.4504E-01 1.4564E-01 1.4625E-01 1.4315E-08 1.4254E-08
INITIAL TOTAL MASS OF FISSIONABLE ISOTOPES IN THIS REGION = 3.29625E+02
U235 U238 PU239 PU240 PU241 PU242 LFPSS DUMP
COREC 1.4201E+00 2.8765E+02 2.1665E+01 1.1603E+01 5.8256E+00 1.4625E+00 1.4315E-08 1.4254E-08
...
TOTAL REACTOR LOADING (IN KG) OF ACTIVE ISOTOPES AT TIME NODE 0 AT 0.000000000E+00 DAYS.
ISOTOPE REACTOR LOADING
U235 1.70410E+01
U238 8.62949E+02
PU239 4.33290E+01
PU240 1.75493E+01
PU241 1.03405E+01
PU242 3.07117E+00
LFPSS 4.29436E-08
DUMP 4.27624E-08
...
REACTOR CONDITIONS AFTER 1 BURNUP SUBSTEPS AT TIME = 1.500000000E+00 DAYS
ATOM DENSITIES (IN ATOMS/BARN-CM.) OF ACTIVE ISOTOPES IN EACH REGION
U235 U238 PU239 PU240 PU241 PU242 LFPSS DUMP
COREA 9.6878E-04 1.9894E-02 5.6270E-04 3.9711E-04 2.8899E-04 1.0157E-04 8.6777E-05 4.3112E-07
U235 U238 PU239 PU240 PU241 PU242 LFPSS DUMP
COREB 9.7403E-05 1.9911E-02 1.0377E-03 1.6375E-05 9.6913E-06 1.0015E-05 4.7687E-05 3.6443E-08
U235 U238 PU239 PU240 PU241 PU242 LFPSS DUMP
COREC 9.8180E-05 1.9938E-02 1.5147E-03 7.9868E-04 3.9272E-04 1.0136E-04 5.6377E-05 2.5348E-07
...
BEGINNING OF BURN CYCLE 2
ATOM DENSITIES (IN ATOMS/BARN-CM.) OF ACTIVE ISOTOPES IN EACH REGION
U235 U238 PU239 PU240 PU241 PU242 LFPSS DUMP
COREA 9.6878E-04 1.9894E-02 5.6270E-04 3.9711E-04 2.8899E-04 1.0157E-04 8.6777E-05 4.3112E-07
U235 U238 PU239 PU240 PU241 PU242 LFPSS DUMP
COREB 9.7403E-05 1.9911E-02 1.0377E-03 1.6375E-05 9.6913E-06 1.0015E-05 4.7687E-05 3.6443E-08
U235 U238 PU239 PU240 PU241 PU242 LFPSS DUMP
COREC 9.8180E-05 1.9938E-02 1.5147E-03 7.9868E-04 3.9272E-04 1.0136E-04 5.6377E-05 2.5348E-07
...
REACTOR CONDITIONS AFTER 1 BURNUP SUBSTEPS AT TIME = 3.000000000E+00 DAYS
ATOM DENSITIES (IN ATOMS/BARN-CM.) OF ACTIVE ISOTOPES IN EACH REGION
U235 U238 PU239 PU240 PU241 PU242 LFPSS DUMP
COREA 9.3759E-04 1.9785E-02 6.2426E-04 3.9466E-04 2.7817E-04 1.0309E-04 1.7676E-04 8.8197E-07
U235 U238 PU239 PU240 PU241 PU242 LFPSS DUMP
COREB 9.4792E-05 1.9820E-02 1.0748E-03 2.3090E-05 9.4344E-06 1.0028E-05 9.7898E-05 7.4041E-08
U235 U238 PU239 PU240 PU241 PU242 LFPSS DUMP
COREC 9.6340E-05 1.9874E-02 1.5294E-03 7.9740E-04 3.8542E-04 1.0272E-04 1.1446E-04 5.1788E-07
...
REACTOR CONDITIONS AFTER 1 BURNUP SUBSTEPS AT TIME = 4.500000000E+00 DAYS
ATOM DENSITIES (IN ATOMS/BARN-CM.) OF ACTIVE ISOTOPES IN EACH REGION
U235 U238 PU239 PU240 PU241 PU242 LFPSS DUMP
COREA 9.0644E-04 1.9673E-02 6.8466E-04 3.9263E-04 2.6754E-04 1.0457E-04 2.7012E-04 1.3536E-06
U235 U238 PU239 PU240 PU241 PU242 LFPSS DUMP
COREB 9.2168E-05 1.9726E-02 1.1114E-03 3.0156E-05 9.2326E-06 1.0041E-05 1.5078E-04 1.1287E-07
U235 U238 PU239 PU240 PU241 PU242 LFPSS DUMP
COREC 9.4480E-05 1.9808E-02 1.5439E-03 7.9615E-04 3.7812E-04 1.0408E-04 1.7435E-04 7.9392E-07
...
TOTAL REACTOR LOADING (IN KG) OF ACTIVE ISOTOPES AT TIME NODE 1 AT 4.500000000E+00 DAYS.
ISOTOPE REACTOR LOADING
U235 1.55228E+01
U238 8.51542E+02
PU239 4.82395E+01
PU240 1.76789E+01
PU241 9.53794E+00
PU242 3.19836E+00
LFPSS 8.52077E+00
DUMP 3.22201E-02
...
```

Figure 3-44. REBUS Output Excerpt for the Fuel Management Group Option of Card Type 11

The volume of each region is identical as seen in Figure 3-39 earlier. Using the assembly pitch of 10.0 cm and height of 60 cm from Figure 3-40, the volume of each assembly is  $5196.15 \text{ cm}^3$  and volume of each region is  $36373.06 \text{ cm}^3$  which matches the output from DIF3D in all three cases (not shown for brevity). Card type 24 input was provided for all active isotopes setting the U235 atom mass to 235.117 and additional card type 28 input set Avogadro's number to  $6.022141 \cdot 10^{23}$ . Combining the atom density of 0.001 with these values, the mass of U235 in COREA can be calculated as 14200.8 g which matches the result in REBUS of  $1.4201\text{E+01}$  kg. Note that the other regions have an order of magnitude lower atom density and thus masses of 1420.08 g. The remaining isotope masses in this section of REBUS output are also found to identically match those from hand calculations. The total reactor loading is obtained by simply summing the three regions together such that the U235 mass is 17041.0 g ( $14200.8 + 1420.08 \cdot 2$ ) which matches the REBUS output of  $1.70410\text{E+01}$  kg. It is a trivial matter in this problem to sum the mass of the remaining active isotopes and obtain the REBUS output in the total reactor loading. This verifies that REBUS is correctly computing the mass of each active isotope in the region and total reactor loading edits as displayed.

As stated, the depletion itself is not being verified here, but the problem setup allows a simple hand calculation to verify the U235 mass removal. From Figure 3-42, the U235 density of each region has changed from 0.001, 0.0001, and 0.0001 to  $9.6878\text{E-04}$ ,  $9.7403\text{E-05}$ , and  $9.8180\text{E-05}$  in the first time step. Using the same hand calculation, these can be converted to region masses of 13.757 kg, 1.3832 kg, and 1.3942 kg for COREA, COREB, and COREC. These values match those reported in the REBUS output (not shown for brevity) and indicate that the spatial burnup in each region is slightly different. The total mass change in U235 can be calculated using the region masses as .50607 kg. Using the power conversion factor defined earlier, the total energy released by fission of this isotope is  $12.96 \cdot 10^{12}$  Joules which when combined with the cycle time is 100.017 MW of power. The slight amount of error with respect to the input value of 100 MW is attributable to the round off error derived from reading the atom density information from the REBUS output file. One can conversely take the stated power level and cycle length and compute the expected mass change in U235 as 0.50599 kg. This should be the exact number, but again, the reported masses from REBUS are single precision and when the sum over all regions is applied for mass, the observed error occurs. Given the earlier verification of the Bateman equation solution capability of REBUS, this hand calculation verifies that the same capability is working properly for a generic problem. The same calculation can be used on each time step yielding a matching power production. It is important to note that the reduction in atom mass can also be obtained from the simple one isotope reaction equation by using the average U235 reaction rate over the time interval.

With the preceding work, we can verify that all of the displayed outputs in Figure 3-42 are confirmed to be correct. The remaining work to complete is an understanding of how Test #2 differs from Test #1 and whether it is physically correct. The first check is to verify that, regardless of what REBUS computes as the end of the time step densities, that the isotopic content is correctly remapped to the correct region as defined by the input. For this check, only FUELB will be displayed although all three were checked to be accurate.

From the middle input section of Figure 3-41, one can see that FUELB is initially assigned to COREB, then COREC, and finally COREA. In Figure 3-43, the atom density detail at the end of burn substep 1.5 days (EOTS-1) is provided followed by the atom density edit at the beginning of burn cycle 2 (BOTS-2). Starting with the U235 isotope at EOTS-1 one should find that all three values for each region are different with  $9.7403\text{E-05}$  being the value in COREB. In BOTS-1, the same  $9.7403\text{E-05}$  is assigned to

COREC. A close inspection shows that the output data is arranged by fuel path and is effectively identical for points EOTS-1 and BOTS-2. The only thing that changes is the region assignment and one finds that at the end of burnup substep 3.0 days (EOTS-2), the region ordering is consistent with BOTS-2. The atom density detail at the end of burnup substep 4.5 days indicates that fuel path 2 was reassigned to region COREA. This verifies that the stated COREB-COREC-COREA pattern specified by the input is followed by REBUS. Similarly, the other fuel paths are found to follow their specified input assignment.

The last aspect to verify is whether the actual changes correspond to the correct power applied to each region in the problem. With the given output, the U235 total reactor loading starts at 17.0410 kg and ends at 15.5228 kg consistent with the other two output cases and thus a loss of 1.5182 kg of U235 occurs for all three time steps. Using the U235 atom mass, the power conversion factor, and Avogadro's number defined earlier the total energy released is  $1518.2/235.117*0.6022141E24*1.E-11=3.8886E13$  Joule. Dividing by the total burn time of 4.5 days, the average power rating is 100.016 MW which is consistent with the input power of 100 MW noting that the error is a result of the output truncation.

For the region-wise power calculation, the power details from DIF3D must be extracted which are provided in Figure 3-45 for the beginning and end of each time step. Unlike the REBUS output which is ordered by path, the DIF3D output is ordered by region which is decided based upon the ordering of the card type 15 input in A.NIP3. The U235 atom density detail from Figure 3-43 is combined with the region power output from DIF3D in Figure 3-45 to get the region-wise comparison results in Table 3-28. Note that the DIF3D region power data was ordered to be consistent with the atom density detail from REBUS. The first calculated result is the change in U235 mass for each region, which, when summed over all rows, equals the loss of 1.5182 kg of U235 over all three time steps computed earlier from the total reactor loading detail. Given the change in U235 mass, the power derived from its fission can be computed as shown above. To get the comparative DIF3D result, the power results from the beginning and end of each time step must be averaged as provided in Table 3-28. As can be seen, the power computation based upon the U235 mass change in each region is accurate to 4 significant digits with the average value of the DIF3D reported powers. This outcome is consistent with the previous mass and power calculations and is primarily limited by the truncation of the numbers in the REBUS and DIF3D output edits.

Given the preceding hand calculations consistently reproduced the REBUS results, one can be confident that REBUS is properly interpreting the user input for card type 11 with non-equilibrium problems.

## Verification of the REBUS Software

July 2025

```

DIF3D 11.3072 11/11/19      ADIF3D: Hexagonal 3D Test Problem      PAGE      96
0      REGION AND AREA POWER INTEGRALS FOR K-EFF PROBLEM WITH ENERGY RANGE (EV)      =(4.140E-01,1.000E+07)
      REGION  ZONE  ZONE  VOLUME  INTEGRATION(1)  POWER  POWER DENSITY  PEAK DENSITY  PEAK TO AVG.  POWER
      NO.  NAME  NO.  NAME  (CC)  WEIGHT FACTOR  (WATTS)  (WATTS/CC)  (WATTS/CC) (2)  POWER DENSITY  FRACTION
      1  REFL   1  REFL   1.21070E+06  1.00000E+00  5.44771E+00  4.49962E-06  2.56102E-05  5.69165E+00  5.44771E-08
      2  COREA  2  COREA  3.63731E+04  1.00000E+00  8.76506E+07  2.40977E+03  4.49089E+03  1.86362E+00  8.76506E-01
      3  COREB  3  COREB  3.63731E+04  1.00000E+00  7.26953E+06  1.99860E+02  4.42526E+02  2.21418E+00  7.26953E-02
      4  COREC  4  COREC  3.63731E+04  1.00000E+00  5.07984E+06  1.39659E+02  3.44966E+02  2.47005E+00  5.07984E-02
      TOTALS   1.31982E+06  0.00000E+00  1.00000E+08  7.57678E+01  4.49089E+03  5.92717E+01  1.00000E+00

DIF3D 11.3072 11/11/19      ADIF3D: Hexagonal 3D Test Problem      PAGE      152
0      REGION AND AREA POWER INTEGRALS FOR K-EFF PROBLEM WITH ENERGY RANGE (EV)      =(4.140E-01,1.000E+07)
      REGION  ZONE  ZONE  VOLUME  INTEGRATION(1)  POWER  POWER DENSITY  PEAK DENSITY  PEAK TO AVG.  POWER
      NO.  NAME  NO.  NAME  (CC)  WEIGHT FACTOR  (WATTS)  (WATTS/CC)  (WATTS/CC) (2)  POWER DENSITY  FRACTION
      1  REFL   1  REFL   1.21070E+06  1.00000E+00  5.61026E+00  4.63388E-06  2.63116E-05  5.67809E+00  5.61026E-08
      2  COREA  2  COREA  3.63731E+04  1.00000E+00  8.75593E+07  2.40726E+03  4.48613E+03  1.86359E+00  8.75593E-01
      3  COREB  3  COREB  3.63731E+04  1.00000E+00  7.30667E+06  2.00881E+02  4.45472E+02  2.21311E+00  7.30667E-02
      4  COREC  4  COREC  3.63731E+04  1.00000E+00  5.13399E+06  1.41148E+02  3.48759E+02  2.47087E+00  5.13399E-02
      TOTALS   1.31982E+06  0.00000E+00  1.00000E+08  7.57678E+01  4.48613E+03  5.92090E+01  1.00000E+00

DIF3D 11.3072 11/11/19      ADIF3D: Hexagonal 3D Test Problem      PAGE      186
0      REGION AND AREA POWER INTEGRALS FOR K-EFF PROBLEM WITH ENERGY RANGE (EV)      =(4.140E-01,1.000E+07)
      REGION  ZONE  ZONE  VOLUME  INTEGRATION(1)  POWER  POWER DENSITY  PEAK DENSITY  PEAK TO AVG.  POWER
      NO.  NAME  NO.  NAME  (CC)  WEIGHT FACTOR  (WATTS)  (WATTS/CC)  (WATTS/CC) (2)  POWER DENSITY  FRACTION
      1  REFL   1  REFL   1.21070E+06  1.00000E+00  5.98222E+00  4.94111E-06  2.57600E-05  5.21340E+00  5.98222E-08
      2  COREA  2  COREA  3.63731E+04  1.00000E+00  1.02781E+07  2.82575E+02  5.48697E+02  1.94178E+00  1.02781E-01
      3  COREB  3  COREB  3.63731E+04  1.00000E+00  8.45148E+07  3.23256E+03  5.25053E+03  2.25970E+00  8.45148E-01
      4  COREC  4  COREC  3.63731E+04  1.00000E+00  5.20705E+06  1.43157E+02  3.65163E+02  2.55079E+00  5.20705E-02
      TOTALS   1.31982E+06  0.00000E+00  1.00000E+08  7.57678E+01  5.25053E+03  6.92976E+01  1.00000E+00

DIF3D 11.3072 11/11/19      ADIF3D: Hexagonal 3D Test Problem      PAGE      243
0      REGION AND AREA POWER INTEGRALS FOR K-EFF PROBLEM WITH ENERGY RANGE (EV)      =(4.140E-01,1.000E+07)
      REGION  ZONE  ZONE  VOLUME  INTEGRATION(1)  POWER  POWER DENSITY  PEAK DENSITY  PEAK TO AVG.  POWER
      NO.  NAME  NO.  NAME  (CC)  WEIGHT FACTOR  (WATTS)  (WATTS/CC)  (WATTS/CC) (2)  POWER DENSITY  FRACTION
      1  REFL   1  REFL   1.21070E+06  1.00000E+00  6.17810E+00  5.10290E-06  2.66044E-05  5.21358E+00  6.17810E-08
      2  COREA  2  COREA  3.63731E+04  1.00000E+00  1.02074E+07  2.80630E+02  5.44642E+02  1.94078E+00  1.02074E-01
      3  COREB  3  COREB  3.63731E+04  1.00000E+00  8.45142E+07  3.23254E+03  5.24483E+03  2.25726E+00  8.45142E-01
      4  COREC  4  COREC  3.63731E+04  1.00000E+00  5.27843E+06  1.45119E+02  3.69856E+02  2.54864E+00  5.27843E-02
      TOTALS   1.31982E+06  0.00000E+00  1.00000E+08  7.57678E+01  5.24483E+03  6.92225E+01  1.00000E+00

DIF3D 11.3072 11/11/19      ADIF3D: Hexagonal 3D Test Problem      PAGE      277
0      REGION AND AREA POWER INTEGRALS FOR K-EFF PROBLEM WITH ENERGY RANGE (EV)      =(4.140E-01,1.000E+07)
      REGION  ZONE  ZONE  VOLUME  INTEGRATION(1)  POWER  POWER DENSITY  PEAK DENSITY  PEAK TO AVG.  POWER
      NO.  NAME  NO.  NAME  (CC)  WEIGHT FACTOR  (WATTS)  (WATTS/CC)  (WATTS/CC) (2)  POWER DENSITY  FRACTION
      1  REFL   1  REFL   1.21070E+06  1.00000E+00  8.81650E+00  7.28213E-06  3.79785E-05  5.21530E+00  8.81650E-08
      2  COREA  2  COREA  3.63731E+04  1.00000E+00  1.29852E+07  3.57000E+02  6.52828E+02  1.82865E+00  1.29852E-01
      3  COREB  3  COREB  3.63731E+04  1.00000E+00  1.14185E+07  3.13928E+02  6.40797E+02  2.04122E+00  1.14185E-01
      4  COREC  4  COREC  3.63731E+04  1.00000E+00  7.55963E+07  2.07836E+03  4.95677E+03  2.38495E+00  7.55963E-01
      TOTALS   1.31982E+06  0.00000E+00  1.00000E+08  7.57678E+01  4.95677E+03  6.54206E+01  1.00000E+00

DIF3D 11.3072 11/11/19      ADIF3D: Hexagonal 3D Test Problem      PAGE      334
      REGION  ZONE  ZONE  VOLUME  INTEGRATION(1)  POWER  POWER DENSITY  PEAK DENSITY  PEAK TO AVG.  POWER
      NO.  NAME  NO.  NAME  (CC)  WEIGHT FACTOR  (WATTS)  (WATTS/CC)  (WATTS/CC) (2)  POWER DENSITY  FRACTION
      1  REFL   1  REFL   1.21070E+06  1.00000E+00  9.10599E+00  7.52124E-06  3.93009E-05  5.22533E+00  9.10599E-08
      2  COREA  2  COREA  3.63731E+04  1.00000E+00  1.28281E+07  3.52680E+02  6.46265E+02  1.83244E+00  1.28281E-01
      3  COREB  3  COREB  3.63731E+04  1.00000E+00  1.13085E+07  3.10903E+02  6.37274E+02  2.04975E+00  1.13085E-01
      4  COREC  4  COREC  3.63731E+04  1.00000E+00  7.58634E+07  2.08570E+03  4.98206E+03  2.38867E+00  7.58634E-01
      TOTALS   1.31982E+06  0.00000E+00  1.00000E+08  7.57678E+01  4.98206E+03  6.57544E+01  1.00000E+00
  
```

Figure 3-45. DIF3D Power Detail for the Region Assignment Option of Card Type 11

Table 3-28. Region Power Comparison for the Region Assignment Option of Card Type 11

| Time Step | Region | Starting Atom Density | Ending Atom Density | Change in mass (kg) | Power (MW) | DIF3D Reported Region Power (MW) | Average Power (MW) |
|-----------|--------|-----------------------|---------------------|---------------------|------------|----------------------------------|--------------------|
| 1         | COREA  | 1.0000E-03            | 9.6878E-04          | 0.44335             | 87.621     | 87.65                            | 87.56              |
|           | COREB  | 1.0000E-04            | 9.7403E-05          | 0.03688             | 7.289      | 7.27                             | 7.31               |
|           | COREC  | 1.0000E-04            | 9.8180E-05          | 0.02585             | 5.108      | 5.08                             | 5.13               |
| 2         | COREB  | 9.6878E-04            | 9.3866E-04          | 0.42773             | 84.534     | 84.51                            | 84.515             |
|           | COREC  | 9.7403E-05            | 9.5535E-05          | 0.02653             | 5.243      | 5.21                             | 5.28               |
|           | COREA  | 9.8180E-05            | 9.4530E-05          | 0.05183             | 10.244     | 10.28                            | 10.21              |
| 3         | COREC  | 9.3866E-04            | 9.1167E-04          | 0.38328             | 75.749     | 75.60                            | 75.86              |
|           | COREA  | 9.5535E-05            | 9.0935E-05          | 0.06532             | 12.910     | 12.99                            | 12.83              |
|           | COREB  | 9.4530E-05            | 9.0480E-05          | 0.05751             | 11.367     | 11.42                            | 11.31              |

### 3.5.2.2 Non-equilibrium Testing of Card Type 35

The path specification for non-equilibrium problems in REBUS is done using card type 35. From Table 3-26 one can see that card type 11 and 35 are similar in concept, but inherently different in the implementation. The first difference to notice is that input 35.3 can use the zone name whereas input 11.5 is restricted to the sub-zone name. Both allow assignments to zone, region, or fuel management group. The other difference is that card type 35 requires both the beginning and ending stage for each assignment while card type 11 only requires the stage number. An additional concept that comes with card type 35 is external storage of compositions which allows a given composition to not be loaded into the reactor for several stages. As part of this work, all viable input options are explored where again the same problem setup used to test card type 11 is used here.

For the first set of tests is intended to replicate the card type 11 results obtained in the previous section. In this regard, the A.BURN input shown earlier in Figure 3-41 is simply replaced with the input shown in Figure 3-46. It is important to note that with card type 35, one cannot assign sub-zones to anything other than a zone (“Primary Zone” example in Figure 3-46). Assigning sub-zones to regions for fuel management groups, like that done in Figure 3-41 for card type 11, is not allowed with card type 35. The basic design of REBUS is to align each path with a given composition and assign that zone to a given region (or fuel management group) at each stage. This emulates the concept of moving an assembly from one position to another. The volumes of the regions that the zone is assigned to must be the same for all stages.

|   |  |   |
|---|--|---|
| <pre>...<br/>35 PATH1 FUEL A ZFUELA 1 1<br/>35 PATH1 FUEL A ZFUELA 2 2<br/>35 PATH1 FUEL A ZFUELA 3 3</pre> | <pre>...<br/>35 PATH1 ZFUELA COREA 1 1<br/>35 PATH1 ZFUELA COREB 2 2<br/>35 PATH1 ZFUELA COREC 3 3</pre> | <pre>...<br/>35 PATH1 ZFUELA FMG1 1 1<br/>35 PATH1 ZFUELA FMG1 2 2<br/>35 PATH1 ZFUELA FMG1 3 3</pre> |
| <pre>35 PATH2 FUEL B ZFUELB 1 1<br/>35 PATH2 FUEL B ZFUELB 2 2<br/>35 PATH2 FUEL B ZFUELB 3 3</pre>         | <pre>35 PATH2 ZFUELB COREB 1 1<br/>35 PATH2 ZFUELB COREC 2 2<br/>35 PATH2 ZFUELB COREA 3 3</pre>         | <pre>35 PATH2 ZFUELB FMG2 1 1<br/>35 PATH2 ZFUELB FMG2 2 2<br/>35 PATH2 ZFUELB FMG2 3 3</pre>         |
| <pre>35 PATH3 FUEL C ZFUELC 1 1<br/>35 PATH3 FUEL C ZFUELC 2 2<br/>35 PATH3 FUEL C ZFUELC 3 3</pre>         | <pre>35 PATH3 ZFUELC COREC 1 1<br/>35 PATH3 ZFUELC COREA 2 2<br/>35 PATH3 ZFUELC COREB 3 3</pre>         | <pre>35 PATH3 ZFUELC FMG3 1 1<br/>35 PATH3 ZFUELC FMG3 2 2<br/>35 PATH3 ZFUELC FMG3 3 3</pre>         |
| <pre>...<br/>35 PATH4 FUEL D ZFUELD 1 1<br/>35 PATH4 FUEL D ZFUELD 2 2<br/>35 PATH4 FUEL D ZFUELD 3 3</pre> | <pre>35 PATH4 ZFUELD COREA 1 1<br/>35 PATH4 ZFUELD COREB 2 2<br/>35 PATH4 ZFUELD AREAC 3 3</pre>         | <pre>45 FMG1 COREA<br/>45 FMG2 COREB<br/>45 FMG3 AREAC<br/>...</pre>                                  |

Primary Zone

Region

Fuel Management Group

**Figure 3-46. A.BURN Input Excerpt for Card Type 35 Verification**

Because the output files are virtually identical (input card differences cause pagination differences), there is no point in redoing the preceding analysis as all aspects of the calculations are identical between the card type 11 input of Figure 3-41 and card type 35 of Figure 3-46. In this manner, the basic functionality of card type 35 is verified noting that the input is fundamentally different from card type 11.

To fully test out all features of card type 35, the external storage feature must be checked as it is a commonly used component of REBUS. Figure 3-47 provides the test input for this feature.

```

UNIFORM=A.NIP3
...
14    FUEL0D  bNA    0.010
14    FUEL0D  b016   0.016
14    FUEL0D  bFE    0.02
14    FUEL0D  bU235  1.0E-11
14    FUEL0D  bU238  0.02
14    FUEL0D  bPU239 0.001
14    FUEL0D  bPU240 0.00001
14    FUEL0D  bPU241 0.00001
14    FUEL0D  bPU242 0.00001
14    FUEL0D  bLFP   1.0E-12
14    FUEL0D  bDUMP  1.0E-12
14    ZFUEL0D FUEL0D 1.0
...
14    FUEL0E  cNA    0.010
14    FUEL0E  c016   0.016
14    FUEL0E  cFE    0.02
14    FUEL0E  cU235  1.0E-11
14    FUEL0E  cU238  0.02
14    FUEL0E  cPU239 0.0015
14    FUEL0E  cPU240 0.0008
14    FUEL0E  cPU241 0.0004
14    FUEL0E  cPU242 0.0001
14    FUEL0E  cLFP   1.0E-12
14    FUEL0E  cDUMP  1.0E-12
14    ZFUEL0E FUEL0E 1.0
...

```

```

UNIFORM=A.BURN
...
35    PATH1  ZFUELA COREA  1    1
35    PATH1  ZFUELA ''     2    2
35    PATH1  ZFUELA COREB  3    3
35    PATH1  ZFUELA COREC  4    4
35    PATH1  ZFUELA COREB  5    5
35    PATH1  ZFUELA ''     6    6
35    PATH2  ZFUEL0B COREB  1    1
35    PATH2  ZFUEL0B COREC  2    2
35    PATH2  ZFUEL0B ''     3    3
35    PATH2  ZFUEL0B COREA  4    4
35    PATH2  ZFUEL0B COREC  5    5
35    PATH3  ZFUEL0C COREC  1    1
35    PATH3  ZFUEL0C COREA  2    2
35    PATH3  ZFUEL0C COREC  3    3
35    PATH3  ZFUEL0C ''     4    5
35    PATH3  ZFUEL0C COREA  6    6
35    PATH4  ZFUEL0D COREB  2    2
35    PATH4  ZFUEL0D COREA  3    3
35    PATH4  ZFUEL0D COREB  4    4
35    PATH4  ZFUEL0D ''     5    5
35    PATH4  ZFUEL0D COREB  6    6
35    PATH5  ZFUEL0E COREA  5    5
35    PATH5  ZFUEL0E COREC  6    6
...

```

**Figure 3-47. Modified Input Excerpt for Testing the External Storage with Card Type 35**

To begin, two additional zones (and sub-zones) are added to the A.NIP3 section called ZFUEL0D and ZFUEL0E. These zones are not assigned to any regions in the A.NIP3 input (i.e. no card type 15 assignments). In the A.BURN input, card type 35 is modified to introduce blanks or '' to indicate where in each path the fuel is held in internal storage. Starting with Path1 (ZFUELA), one can see it is initially (stage 1) loaded in COREA, then external storage (stage 2), then COREB (stage 3), COREC (stage 4), COREB (stage 5), and finally external storage (stage 6). The new zones ZFUEL0D and ZFUEL0E are assigned to path5 and path6, respectively. For path 5 (ZFUEL0D), the first stage is 2 (instead of 1) indicating that it is not used until the second stage. It starts in COREB (stage 2), and is moved to COREA (stage 3), COREC (stage 4), external storage (stage 5), and finally it is reloaded in COREB (stage 6). As one can see, this is a very convoluted fuel loading pattern and it is easiest to just look at it from the region assignment as done in Table 3-29. Note that only the unique letter of the zone and region name are used in this table.

In Table 3-29, one can see that a single zone is assigned to a given region of the domain for each stage (time step). Further, there are exactly 2 zones sitting in external storage at any given time point. The only exception to this is stage 6 of path2 which was not specified in Figure 3-47 which REBUS will assume is permanently discharged from the reactor. If additional cycles were specified, this zone could not be introduced back into the loading scheme unless all intermediate locations are specified (typically done by putting it in external storage).

**Table 3-29. Zone to Region Assignment for Testing the External Storage with Card Type 35**

| Stage | COREA | COREB | COREC | External Storage |
|-------|-------|-------|-------|------------------|
| 1     | A     | B     | C     | D, E             |
| 2     | C     | D     | B     | A, E             |
| 3     | D     | A     | C     | B, E             |
| 4     | B     | D     | A     | C, E             |
| 5     | E     | A     | B     | C, D             |
| 6     | C     | D     | E     | A, <b>B</b>      |

The eigenvalue and region power summary are provided in Table 3-30. What should be apparent is that in multiple time steps the power of certain regions is zero. This is caused by the near zero concentration of U235 in ZFUEL and ZFUELE which was done to help identify where those materials were loaded. A quick comparison with Table 3-29 shows that the zero power states of each region are caused by the loading of either ZFUEL or ZFUELE into the region. This is of course artificial because of the problem setup, but this outcome is expected in those problems where test assemblies are loaded in at certain stages which have significantly reduced power production, and thus not entirely unrealistic.

**Table 3-30. Eigenvalue and Power Results for Testing the External Storage with Card Type 35**

| Stage | k <sub>eff</sub> |           | COREA |       | COREB |       | COREC |       |
|-------|------------------|-----------|-------|-------|-------|-------|-------|-------|
|       | Start            | End       | Start | End   | Start | End   | Start | End   |
| 1     | 0.64369 5        | 0.64738 8 | 87.65 | 87.56 | 7.27  | 7.31  | 5.08  | 5.13  |
| 2     | 0.63327 9        | 0.65372 1 | 66.49 | 63.06 | 0.00  | 0.00  | 33.51 | 36.94 |
| 3     | 0.63828 1        | 0.64283 0 | 0.00  | 0.00  | 94.94 | 94.90 | 5.06  | 5.10  |
| 4     | 0.57656 1        | 0.58598 4 | 13.07 | 12.88 | 0.00  | 0.00  | 86.93 | 87.12 |
| 5     | 0.70296 8        | 0.70438 9 | 0.00  | 0.00  | 94.77 | 94.70 | 5.23  | 5.30  |
| 6     | 0.66488 9        | 0.66767 0 | 93.02 | 92.97 | 6.98  | 7.03  | 0.00  | 0.00  |

The depletion aspects of this second test problem are not analytically verifiable because of the complex spatial flux distribution. However, since only one isotope (U-235) is producing power, the total depletion of that isotope can be computed at each time point and verified. From the output, the change in mass of this isotope can be taken from several different outputs given the reactor loading information. Figure 3-48 displays some of the output edits that can be used which include region-wise atom density, total fissionable isotope masses, and the total reactor loading. The region-wise power edit is also displayed as it is needed to compute the average power of the region over the time step.

```

ATOM DENSITIES (IN ATOMS/BARN-CM.) OF ACTIVE ISOTOPES IN EACH REGION
U235      U238      PU239      PU240      PU241      PU242      LFPPS      DUMP
COREA  1.0000E-03  2.0000E-02  5.0000E-04  4.0000E-04  3.0000E-04  1.0000E-04  1.0000E-12  1.0000E-12
COREB  1.0000E-04  2.0000E-02  1.0000E-03  1.0000E-05  1.0000E-05  1.0000E-05  1.0000E-12  1.0000E-12
COREC  1.0000E-04  2.0000E-02  1.5000E-03  8.0000E-04  4.0000E-04  1.0000E-04  1.0000E-12  1.0000E-12
...
MASSES (IN KG) OF ACTIVE ISOTOPES IN EACH REGION
INITIAL TOTAL MASS OF FISSIONABLE ISOTOPES IN THIS REGION = 3.20705E+02
U235      U238      PU239      PU240      PU241      PU242      LFPPS      DUMP
COREA  1.4201E+01  2.8765E+02  7.2215E+00  5.8014E+00  4.3692E+00  1.4625E+00  1.4315E-08  1.4254E-08
COREB  1.4201E+00  2.8765E+02  1.4443E+01  1.4504E+01  1.4564E+01  1.4625E+01  1.4315E-08  1.4254E-08
COREC  1.4201E+00  2.8765E+02  2.1665E+01  1.1603E+01  5.8256E+00  1.4625E+00  1.4315E-08  1.4254E-08
...
TOTAL REACTOR LOADING (IN KG) OF ACTIVE ISOTOPES AT TIME NODE 0 AT 0.00000000E+00 DAYS.
ISOTOPE      REACTOR LOADING
U235      1.70410E+01
U238      8.62949E+02
PU239      4.33290E+01
PU240      1.75493E+01
PU241      1.03405E+01
PU242      3.07117E+00
LFPPS      4.29436E-08
DUMP      4.27624E-08
...
REGION      ZONE      ZONE      VOLUME      INTEGRATION(1)      POWER      POWER DENSITY      PEAK DENSITY      PEAK TO AVG.      POWER
NO.      NAME      NO.      NAME      (CC)      WEIGHT FACTOR      (WATTS)      (WATTS/CC)      (WATTS/CC) (2)      POWER DENSITY      FRACTION
1      REFL      1      REFL      1.21070E+06  1.00000E+00  5.60771E+00  4.63178E-06  2.63005E-05  5.67827E+00  5.60771E-08
2      COREA      2      COREA      3.63731E+04  1.00000E+00  8.75608E+07  2.40730E+03  4.48621E+03  1.86359E+00  8.75608E-01
3      COREB      3      COREB      3.63731E+04  1.00000E+00  7.30617E+06  2.00868E+02  4.44546E+02  2.21313E+00  7.30617E-02
4      COREC      4      COREC      3.63731E+04  1.00000E+00  5.13304E+06  1.41122E+02  3.48694E+02  2.47086E+00  5.13304E-02
...

```

**Figure 3-48. Atom Output Excerpt for the External Storage Test of Card Type 35**

The atom density outputs from REBUS are collected in Table 3-31 and used to compute the time point U-235 masses and total reactor loading masses.

**Table 3-31. U-235 Mass Loading in the External Storage Test of Card Type 35**

| Time<br>(days) | REBUS Outputted<br>U-235 Atom Density |          |          | Calculated<br>U-235 Mass (kg) |       |       | Total<br>U-235 Loading (kg) |         |
|----------------|---------------------------------------|----------|----------|-------------------------------|-------|-------|-----------------------------|---------|
|                | COREA                                 | COREB    | COREC    | COREA                         | COREB | COREC | Calc.                       | REBUS   |
| 0              | 1.00E-03                              | 1.00E-04 | 1.00E-04 | 14.20                         | 1.42  | 1.42  | 17.0410                     | 17.0410 |
| 1.5            | 9.69E-04                              | 9.74E-05 | 9.82E-05 | 13.76                         | 1.38  | 1.39  | 16.5349                     | 16.5349 |
| 1.5            | 9.82E-05                              | 1.00E-11 | 9.74E-05 | 1.39                          | 0.00  | 1.38  | 2.7774                      | 2.7774  |
| 3              | 7.49E-05                              | 8.03E-12 | 8.48E-05 | 1.06                          | 0.00  | 1.20  | 2.2674                      | 2.2675  |
| 3              | 8.03E-12                              | 9.69E-04 | 7.49E-05 | 0.00                          | 13.76 | 1.06  | 14.8211                     | 14.8211 |
| 4.5            | 7.71E-12                              | 9.35E-04 | 7.31E-05 | 0.00                          | 13.28 | 1.04  | 14.3150                     | 14.3150 |
| 4.5            | 8.48E-05                              | 7.71E-12 | 9.35E-04 | 1.20                          | 0.00  | 13.28 | 14.4808                     | 14.4809 |
| 6              | 8.01E-05                              | 7.35E-12 | 9.04E-04 | 1.14                          | 0.00  | 12.84 | 13.9748                     | 13.9748 |
| 6              | 1.00E-11                              | 9.04E-04 | 8.01E-05 | 0.00                          | 12.84 | 1.14  | 13.9748                     | 13.9748 |
| 7.5            | 9.56E-12                              | 8.70E-04 | 7.83E-05 | 0.00                          | 12.36 | 1.11  | 13.4687                     | 13.4687 |
| 7.5            | 8.70E-04                              | 7.83E-05 | 9.56E-12 | 12.36                         | 1.11  | 0.00  | 13.4687                     | 13.4687 |
| 9              | 8.37E-04                              | 7.58E-05 | 9.35E-12 | 11.89                         | 1.08  | 0.00  | 12.9625                     | 12.9626 |

The REBUS reported total loading of U-235 is provided for comparison and one can observe only two differences which are attributable to the round off error associated with converting the REBUS output. The total U-235 mass and the power derived from it along with the power of each region produced by REBUS are given in Table 3-32. As can be seen, the power derived from the total mass change has significant differences from the reported power from REBUS. The error in the region and total power computation is attributable to round off mistakes when extracting the REBUS output values and to some degree the single precision math internal to REBUS itself. It is important to note that at each time point, DIF3D exactly produces a solution which has the stated power level and that the real precision factors in for the computation of the atom density results at the end of each time step. This error can be observed in the analytic verification test results shown earlier that involve large mass changes.

**Table 3-32. Power Calculation Comparison for the External Storage Test of Card Type 35**

| Time<br>Step | COREA                  |               |                        | COREB                  |               |                        | COREC                  |               |                        |
|--------------|------------------------|---------------|------------------------|------------------------|---------------|------------------------|------------------------|---------------|------------------------|
|              | Mass<br>Change<br>(kg) | Power<br>(MW) | REBUS<br>Power<br>(MW) | Mass<br>Change<br>(kg) | Power<br>(MW) | REBUS<br>Power<br>(MW) | Mass<br>Change<br>(kg) | Power<br>(MW) | REBUS<br>Power<br>(MW) |
| 1            | 0.44335                | 87.62         | 87.60                  | 0.03688                | 7.29          | 7.29                   | 0.025845               | 5.11          | 5.11                   |
| 2            | 0.330581               | 65.33         | 64.78                  | 2.8E-08                | 0.00          | 0.00                   | 0.179413               | 35.46         | 35.22                  |
| 3            | 4.52E-09               | 0.00          | 0.00                   | 0.480414               | 94.95         | 94.92                  | 0.025718               | 5.08          | 5.08                   |
| 4            | 0.065679               | 12.98         | 12.98                  | 5.14E-09               | 0.00          | 0.00                   | 0.440367               | 87.03         | 87.02                  |
| 5            | 6.31E-09               | 0.00          | 0.00                   | 0.47942                | 94.75         | 94.73                  | 0.026641               | 5.27          | 5.27                   |
| 6            | 0.470757               | 93.04         | 93.00                  | 0.035445               | 7.01          | 7.00                   | 2.97E-09               | 0.00          | 0.00                   |

Given the consistent results, the card type 35 input options for non-equilibrium analysis are verified. Any additional testing of this card type and solution mode would be supplemental to the shown results and thus detailed inspection of the results should not be necessary.

### 3.5.2.3 Equilibrium Testing of Card Type 11

The non-equilibrium testing is generally straightforward as it is focused on discrete movements of fuel. For equilibrium cycle testing, only card type 11 is appropriate and from the non-equilibrium case, there are only two real modeling options. As shown earlier in Table 3-26, card type 11 only allows the user to reassign a sub-zone to either a zone or a region. In the first option, the intention is to allow the zone to be filled with a mixture of different depletion states of that material. It can also simulate movement of that material into another zone. In the second option (region assignment), one can model a repeating shuffling pattern. Both options are intended to rapidly produce the converged state of a repetitive reactor system.

The standard equilibrium calculation requires fuel fabrication where reprocessing is optional. The reprocessing option is of no interest to VTR and thus will not be verified. The fuel fabrication option is required as equilibrium problems involve an enrichment search but it can trivially be disabled with input. The purpose of the enrichment search is to have REBUS adjust the fuel content to meet user specified criticality and burnup constraints. There is a considerable amount of input options to check and several calculations to be verified. Given the coupled flux solution is not going to be analytic, the way this is managed is by including a trace isotope that only undergoes decay. In this manner, its inclusion throughout the problem should be analytically definable for all regions at all time points and thus traceable with regard to whether REBUS is setting up the problem consistent with expectations.

#### 3.5.2.3.1 Equilibrium Cycle Reproduction of Non-equilibrium Primary Zone Assignment

For the first test, the goal is to identically reproduce the results displayed in Figure 3-42. This figure is for the primary zone assignment option for a non-equilibrium solve using card type 11. Figure 3-49 gives an excerpt of the input changes that are required to make this happen. As discussed, the first aspect to deal with is the setup of fuel fabrication to give the identical result to the non-equilibrium problem. Fuel fabrication involves specifying A.BURN inputs 4, 12, 13, 18, 19, 20, 21, and 22 all of which are found in Figure 3-49.

The first requirement of fuel fabrication is to modify the A.NIP3 input to set the atom density of all isotopes in the depletion chain (active isotopes) to 1.0. The non-active isotope atom densities should remain as they were originally where Figure 3-40 can be referred to for differences in this input section. Although not displayed, all three compositions are different and will require different fuel fabrication setups to produce the correct atom densities. Table 3-33 provides the desired atom densities and the corresponding mass densities of those isotopes. The fabrication density for each composition is obtained by summing the mass densities to get the fabrication density. For FUELA, the fabrication density is 8.817 g/cc. The U-235 fabrication density is then defined as  $8.817/235.117*0.6022=0.02258$  and corresponds to the card type 13 input for FAB1 of 0.0225836 in Figure 3-49. The other isotope fabrication densities are computed similarly and not shown for brevity.

For the enrichment process, the U238 isotope is defined as class 2 and all other isotopes are CLASS1 as outlined by the card type 18 input in Figure 3-49 (only U238 has a zero assignment while all other isotopes have 1.0). The feed atom fraction numbers shown in Table 3-33 are calculated directly from the targeted atom densities and imposition of the class separation.

```

...
14      FUEL A aNA      0.010
14      FUEL A aO16     0.016
14      FUEL A aF8      0.02
14      FUEL A aU235    1.0
14      FUEL A aU238    1.0
...
14      ZFUEL A FUEL A 1.0
...
UNFORM=A, BURN
02 0 10000000 10000000 0.0001 1.0 1.0 5 5
03 0 0.00000 0.0 4.5 1.0 3 0
04 1.0 1.0 0.0 0.103071214 0.103071214
...
11      PATH1 0      1      FUEL A ZFUEL A
11      PATH2 0      1      FUEL B ZFUEL B
11      PATH3 0      1      FUEL C ZFUEL C
12      PATH1      FAB1 0.0 0 1.00      1.00
12      PATH2      FAB2 0.0 0 0.520297495 1.00
12      PATH3      FAB3 0.0 0 1.235491658 1.00
13 FAB1 U235 2.258359072E-02
13 FAB1 U238 2.229831433E-02
13 FAB1 PU239 2.220487900E-02
...
13 FAB2 U235 2.140370390E-02
13 FAB2 U238 2.113333187E-02
13 FAB2 PU239 2.104477809E-02
...
18 CLASS1 U235 1.0
18 CLASS1 U238 0.0
18 CLASS1 PU239 1.0
...
19 PATH1      FEED1 1
19 PATH2      FEED2 1
19 PATH3      FEED3 1
20 PATH1      FEEDB 1
20 PATH2      FEEDB 1
20 PATH3      FEEDB 1
21 FEED1 CLASS1 1.0E30
21 FEED2 CLASS1 1.0E30
21 FEED3 CLASS1 1.0E30
...
21 FEEDB CLASS1 1.0E30
22 FEED1A U235 4.347807180E-01
22 FEED1A PU239 2.173903590E-01
...
22 FEED2A U235 8.849400880E-02
22 FEED2A PU239 8.849400880E-01
...
22 FEEDB U238 1.00000E+00

```

**Figure 3-49. REBUS Input Excerpt for the First Equilibrium Test of Card Type 11**

**Table 3-33. Key Input Setup Data For Fuel Fabrication For the First Equilibrium Test**

| Isotope      | Desired Atom Densities |         |         | Density (g/cc) |        |        | Feed Atom Fractions |        |        |
|--------------|------------------------|---------|---------|----------------|--------|--------|---------------------|--------|--------|
|              | FUEL A                 | FUEL B  | FUEL C  | FUEL A         | FUEL B | FUEL C | FUEL A              | FUEL B | FUEL C |
| U235         | 0.001                  | 0.0001  | 0.0001  | 0.390          | 0.039  | 0.039  | 0.435               | 0.088  | 0.034  |
| PU239        | 0.0005                 | 0.001   | 0.0015  | 0.199          | 0.397  | 0.596  | 0.217               | 0.885  | 0.517  |
| PU240        | 0.0004                 | 0.00001 | 0.0008  | 0.159          | 0.004  | 0.319  | 0.174               | 0.009  | 0.276  |
| PU241        | 0.0003                 | 0.00001 | 0.0004  | 0.120          | 0.004  | 0.160  | 0.130               | 0.009  | 0.138  |
| PU242        | 0.0001                 | 0.00001 | 0.0001  | 0.040          | 0.004  | 0.040  | 0.043               | 0.009  | 0.034  |
| DUMP         | 1E-12                  | 1E-12   | 1E-12   | 0.000          | 0.000  | 0.000  | 0.000               | 0.000  | 0.000  |
| LFPPS        | 1E-12                  | 1E-12   | 1E-12   | 0.000          | 0.000  | 0.000  | 0.000               | 0.000  | 0.000  |
| TRACE        | 1E-08                  | 2E-08   | 3E-08   | 0.000          | 0.000  | 0.000  | 0.000               | 0.000  | 0.000  |
| U238         | 0.02                   | 0.02    | 0.02    | 7.908          | 7.908  | 7.908  | 1                   | 1      | 1      |
| Fab. Density |                        |         |         | 8.817          | 8.356  | 9.062  |                     |        |        |
| Enrich.      | 0.10307                | 0.05363 | 0.12734 |                |        |        |                     |        |        |

The feed atom fractions (actually interpreted by REBUS as atom densities) are given on card type 22 for each feed. There are 4 feeds because U238 is treated as a separate feed in the input approach above. One could have included U238 in card type 22 with an atom density of 1.0 in FEED1, FEED2, and FEED3 and gotten the same result because of the class separation rules. The displayed approach is more consistent with the intended usage and is preferred.

The targeted enrichment is specified using card type 04 and 12. For FUELA, the goal is to make the enrichment modification factor (EMF) equal that needed to fabricate the desired atom densities. The (atom) enrichment of the compositions in Table 3-33 calculated the conventional way leads to values of 0.10314, 0.05348, and 0.12664 for FUELA, FUELB, and FUELc. Because REBUS does not use the conventional enrichment methodology, one must provide (mass) enrichment values of 0.10307, 0.05363, and 0.12734. The calculation of these values from FEED1 through FEED3 is a non-trivial exercise and beyond the scope of this manuscript, however, it is included in a companion excel document. The density (g/cc) values in Table 3-33 can be used to calculate the (mass) enrichment values cited ( $1-7.908/8.817=0.10309 \sim 0.10307$ ).

In the REBUS card type 04 input, only a single EMF value is possible and thus card type 12 must be used to impose the three values cited. To impose the input value is used, the search input bounds for card type 04 are set to the desired 0.10307 and the error on the criticality criteria is set to 1.0 or 100% error. It is important to ensure that the  $k_{eff}$  of the target problem,  $\sim 0.64315$ , is close to the input target for  $k_{eff}$  and at the correct time point (a  $k_{eff}$  of 1.0 and 0.0 fraction of the burn cycle time are selected in card type 04).

Card type 12 is likely the most difficult to understand from an input perspective. For the FUELA composition (PATH1), the initial enrichment is set to 1.0 while the other two fuel paths have initial enrichments of  $\sim 0.52030$  and  $\sim 1.2355$ . The delta factor for all three paths is set to 1.0. These last two initial enrichment numbers are obtained by taking the ratio of the desired enrichment 0.05363 and the desired enrichment of FUELA 0.10307 ( $0.05363/0.10307=0.52030$ ). Given REBUS is going to obtain an EMF of 0.10307, this initial enrichment will lead to an enrichment for PATH2 of 0.05363 and thus we obtain the desired initial composition.

The last parts of the input that must change compared to the non-equilibrium case is on card type 02 of A.BURN. Because the original problem ran three time steps of length 1.5 days, the cycle length must be set to 4.5 days and the number of subintervals set to 3. Since the fuel stays at the same location over the cycle, only a single card type 11 is needed for each fuel path as seen in Figure 3-49. Including more card type 11 instructions to place the material in more stages will cause the material to be a mixture of those stages instead of the discrete result that occurred in the non-equilibrium problem and thus is not desired here.

Figure 3-50 displays the atom density excerpt from REBUS for the first time point. It is important to note that for equilibrium problems, one must skip to the section of output labeled as "Start of Final Pass." All previous output to this part is not converged and should not be used. The header and nearest pagination excerpt are included to make it clear that all data extracted from the output is taken after this point. Note that the number of calculations required for an equilibrium problem, even without a real search on the enrichment itself, is considerably larger than that needed for the non-equilibrium problem shown earlier.

```

FCC004 11.3114 04/10/20 PAGE 339
+++++
+ START OF FINAL PASS WITH FULL EDITS +
+++++
FCC004 11.3114 04/10/20 ABURN: Hexagonal 3D Test Problem PAGE 343
ATOM DENSITIES USED IN THE NEUTRONICS SOLUTION AT TIME NODE 0 AT 0.000000000E+00 DAYS.

REGION COREA ZONE 2
ISOTOPE / DENSITY IN ATOMS/BARN-CM
aNA / 1.00000E-02 aFE / 2.00000E-02 a016 / 1.60000E-02 aPU239/ 5.00000E-04 aU238 / 2.00000E-02
aMAGIC/ 1.00000E-08 aU235 / 1.00000E-03 aPU242/ 1.00000E-04 alFP / 1.00000E-12 aDUMP / 1.00000E-12
aPU240/ 4.00000E-04 aPU241/ 3.00000E-04

REGION COREB ZONE 3
ISOTOPE / DENSITY IN ATOMS/BARN-CM
bNA / 1.00000E-02 bFE / 2.00000E-02 b016 / 1.60000E-02 bPU239/ 1.00000E-03 bU238 / 2.00000E-02
bMAGIC/ 2.00000E-08 bU235 / 1.00000E-04 bPU242/ 1.00000E-05 blFP / 1.00000E-12 bDUMP / 1.00000E-12
bPU240/ 1.00000E-05 bPU241/ 1.00000E-05

REGION COREC ZONE 4
ISOTOPE / DENSITY IN ATOMS/BARN-CM
cNA / 1.00000E-02 cFE / 2.00000E-02 c016 / 1.60000E-02 cPU239/ 1.50000E-03 cU238 / 2.00000E-02
cMAGIC/ 3.00000E-08 cU235 / 1.00000E-04 cPU242/ 1.00000E-04 clFP / 1.00000E-12 cDUMP / 1.00000E-12
cPU240/ 8.00000E-04 cPU241/ 4.00000E-04

```

**Figure 3-50. Atom Density Output Excerpt for the First Equilibrium Test of Card Type 11**

Looking at the atom densities in Figure 3-50 for the active isotopes one finds these values exactly match those defined in Table 3-33. Figure 3-51 provides the first and last time point region-wise power detail for the equilibrium and non-equilibrium problems. The power for regions COREA, COREB, and COREC are identical to five significant digits. The  $k_{eff}$  results for this test case are provided in Table 3-34 along with the earlier non-equilibrium results for comparison. They are also nearly identical for all time points.

Figure 3-52 provides the atom density and total reactor mass loading detail consistent with that done for the non-equilibrium calculation in Figure 3-42. Looking only at the end, one finds that the U235 mass is 15.5228 kg in the non-equilibrium case and 15.5228 kg in the equilibrium cycle calculation. The total mass change in U235 for the equilibrium problem is 1.5182 kg which is identical to the mass change in U235 for the non-equilibrium case. Because all of the other quantities were checked and this input is intended to be consistent with a previously verified output, the only remaining aspect to consider is the MAGIC isotope which was included as active isotope TRACE. This isotope only undergoes decay. A half-life of 1 day was selected for the isotope and thus its concentration should decrease as  $\exp(-8.0225E-6 \cdot t \cdot \text{sec}^{-1})$ . At 4.5 days only 4.419% of the TRACE isotope should remain in any region. For region COREA, the ratio of end of cycle TRACE atom density of 4.4194E-10 to the beginning of cycle concentration of 1.0000E-8 is exactly 4.419%. This confirms that the input is setup properly and combined with the previous checks, the sub-zone to primary zone assignment of the equilibrium option of card type 11 is confirmed.

EQUILIBRIUM

```

DIF3D 11.3114 04/10/20 ADIF3D: Hexagonal 3D Test Problem PAGE 354
0 REGION AND AREA POWER INTEGRALS FOR K-EFF PROBLEM WITH ENERGY RANGE (EV) = (4.140E-01, 1.000E+07)
  REGION ZONE ZONE VOLUME INTEGRATION(1) POWER POWER DENSITY PEAK DENSITY PEAK TO AVG. POWER
  NO. NAME NO. NAME (CC) WEIGHT FACTOR (WATTS) (WATTS/CC) (WATTS/CC) (2) POWER DENSITY FRACTION
  1 REFL 1 REFL 1.21070E+06 1.00000E+00 5.44770E+00 4.49962E-06 2.56102E-05 5.69165E+00 5.44770E-08
  2 COREA 2 COREA 3.63731E+04 1.00000E+00 8.76506E+07 2.40977E+03 4.49089E+03 1.86362E+00 8.76506E-01
  3 COREB 3 COREB 3.63731E+04 1.00000E+00 7.26953E+06 1.99860E+02 4.42527E+02 2.21418E+00 7.26953E-02
  4 COREC 4 COREC 3.63731E+04 1.00000E+00 5.07984E+06 1.39659E+02 3.44966E+02 2.47005E+00 5.07984E-02
  TOTALS 1.31982E+06 0.00000E+00 1.00000E+08 7.57678E+01 4.49089E+03 5.92718E+01 1.00000E+00
  ...
  DIF3D 11.3114 04/10/20 ADIF3D: Hexagonal 3D Test Problem PAGE 496
0 REGION AND AREA POWER INTEGRALS FOR K-EFF PROBLEM WITH ENERGY RANGE (EV) = (4.140E-01, 1.000E+07)
  REGION ZONE ZONE VOLUME INTEGRATION(1) POWER POWER DENSITY PEAK DENSITY PEAK TO AVG. POWER
  NO. NAME NO. NAME (CC) WEIGHT FACTOR (WATTS) (WATTS/CC) (WATTS/CC) (2) POWER DENSITY FRACTION
  1 REFL 1 REFL 1.21070E+06 1.00000E+00 5.96855E+00 4.92982E-06 2.78639E+05 5.65212E+00 5.96855E-08
  2 COREA 2 COREA 3.63731E+04 1.00000E+00 8.73641E+07 2.40189E+03 4.47673E+03 1.86384E+00 8.73641E-01
  3 COREB 3 COREB 3.63731E+04 1.00000E+00 7.38382E+06 2.03003E+02 4.48824E+02 2.21093E+00 7.38382E-02
  4 COREC 4 COREC 3.63731E+04 1.00000E+00 5.25206E+06 1.44394E+02 3.56988E+02 2.47231E+00 5.25206E-02
  TOTALS 1.31982E+06 0.00000E+00 1.00000E+08 7.57678E+01 4.47673E+03 5.90849E+01 1.00000E+00
  ...
  NON-EQUILIBRIUM
  ...
  DIF3D 11.3072 11/11/19 ADIF3D: Hexagonal 3D Test Problem PAGE 96
0 REGION AND AREA POWER INTEGRALS FOR K-EFF PROBLEM WITH ENERGY RANGE (EV) = (4.140E-01, 1.000E+07)
  REGION ZONE ZONE VOLUME INTEGRATION(1) POWER POWER DENSITY PEAK DENSITY PEAK TO AVG. POWER
  NO. NAME NO. NAME (CC) WEIGHT FACTOR (WATTS) (WATTS/CC) (WATTS/CC) (2) POWER DENSITY FRACTION
  1 REFL 1 REFL 1.21070E+06 1.00000E+00 5.44771E+00 4.49962E-06 2.56102E-05 5.69165E+00 5.44771E-08
  2 COREA 2 COREA 3.63731E+04 1.00000E+00 8.76506E+07 2.40977E+03 4.49089E+03 1.86362E+00 8.76506E-01
  3 COREB 3 COREB 3.63731E+04 1.00000E+00 7.26953E+06 1.99860E+02 4.42526E+02 2.21418E+00 7.26953E-02
  4 COREC 4 COREC 3.63731E+04 1.00000E+00 5.07984E+06 1.39659E+02 3.44966E+02 2.47005E+00 5.07984E-02
  TOTALS 1.31982E+06 0.00000E+00 1.00000E+08 7.57678E+01 4.49089E+03 5.92717E+01 1.00000E+00
  ...
  DIF3D 11.3072 11/11/19 ADIF3D: Hexagonal 3D Test Problem PAGE 319
0 REGION AND AREA POWER INTEGRALS FOR K-EFF PROBLEM WITH ENERGY RANGE (EV) = (4.140E-01, 1.000E+07)
  REGION ZONE ZONE VOLUME INTEGRATION(1) POWER POWER DENSITY PEAK DENSITY PEAK TO AVG. POWER
  NO. NAME NO. NAME (CC) WEIGHT FACTOR (WATTS) (WATTS/CC) (WATTS/CC) (2) POWER DENSITY FRACTION
  1 REFL 1 REFL 1.21070E+06 1.00000E+00 5.96851E+00 4.92978E-06 2.78637E+05 5.65212E+00 5.96851E-08
  2 COREA 2 COREA 3.63731E+04 1.00000E+00 8.73641E+07 2.40189E+03 4.47673E+03 1.86384E+00 8.73641E-01
  3 COREB 3 COREB 3.63731E+04 1.00000E+00 7.38381E+06 2.03002E+02 4.48824E+02 2.21093E+00 7.38381E-02
  4 COREC 4 COREC 3.63731E+04 1.00000E+00 5.25204E+06 1.44394E+02 3.56986E+02 2.47231E+00 5.25204E-02
  TOTALS 1.31982E+06 0.00000E+00 1.00000E+08 7.57678E+01 4.47673E+03 5.90849E+01 1.00000E+00
  ...

```

Figure 3-51. REBUS Region Power Differences for the First Equilibrium Test of Card Type 11

Table 3-34.  $k_{eff}$  Results for the First Equilibrium Test of Card Type 11

| Time Point (days) | Non-Equilibrium | Equilibrium |
|-------------------|-----------------|-------------|
| 0.0               | 0.64369 5       | 0.64369 5   |
| 1.5               | 0.64738 8       | 0.64738 8   |
| 3.0               | 0.65093 6       | 0.65093 6   |
| 4.5               | 0.65433 5       | 0.65433 6   |

It is important to note that the region assignment option of card type 11, cannot be directly compared to the non-equilibrium case as the introduction of more than 1 stage in the input stream implies that the material exists fractionally. In this case, using the non-equilibrium card type 11 input for region-wise assignment would imply that COREA contains ZFUELA, ZFUELB, and ZFUELCA at the beginning of cycle noting that the depletion state of those materials would be different (i.e. not all fresh). This aspect of card type 11 input will be tested out later in this section.

```

FCC004 11.3114 04/10/20 PAGE 361
...
BEGINNING OF BURN CYCLE 1
ATOM DENSITIES (IN ATOMS/BARN-CM.) OF ACTIVE ISOTOPES IN EACH REGION
U235 U238 PU239 PU240 PU241 PU242 LFPPS DUMP TRACE
1 COREA 1.0000E-03 2.0000E-02 5.0000E-04 4.0000E-04 3.0000E-04 1.0000E-04 1.0000E-12 1.0000E-12 1.0000E-08
U235 U238 PU239 PU240 PU241 PU242 LFPPS DUMP TRACE
1 COREB 1.0000E-04 2.0000E-02 1.0000E-03 1.0000E-05 1.0000E-05 1.0000E-05 1.0000E-12 1.0000E-12 2.0000E-08
U235 U238 PU239 PU240 PU241 PU242 LFPPS DUMP TRACE
1 COREC 1.0000E-04 2.0000E-02 1.5000E-03 8.0000E-04 4.0000E-04 1.0000E-04 1.0000E-12 1.0000E-12 3.0000E-08
...
TOTAL REACTOR LOADING (IN KG) OF ACTIVE ISOTOPES AT TIME NODE 0 AT 0.000000000E+00 DAYS.
U235 1.70410E+01
U238 8.62949E+02
PU239 4.33290E+01
PU240 1.75493E+01
PU241 1.03405E+01
PU242 3.07117E+00
LFPPS 4.29436E-08
DUMP 4.27624E-08
TRACE 3.62393E-04

FCC004 11.3114 04/10/20 PAGE 419
REACTOR CONDITIONS AFTER 1 BURNUP SUBSTEPS AT TIME = 1.500000000E+00 DAYS
ATOM DENSITIES (IN ATOMS/BARN-CM.) OF ACTIVE ISOTOPES IN EACH REGION
U235 U238 PU239 PU240 PU241 PU242 LFPPS DUMP TRACE
1 COREA 9.6878E-04 1.9894E-02 5.6270E-04 3.9711E-04 2.8899E-04 1.0157E-04 8.6777E-05 4.3758E-07 3.5355E-09
1 COREB 9.7403E-05 1.9911E-02 1.0377E-03 1.6375E-05 9.6913E-06 1.0015E-05 4.7687E-05 4.9372E-08 7.0711E-09
1 COREC 9.8180E-05 1.9938E-02 1.5147E-03 7.9868E-04 3.9272E-04 1.0136E-04 5.6377E-05 2.7287E-07 1.0607E-08
...
FCC004 11.3114 04/10/20 PAGE 461
REACTOR CONDITIONS AFTER 2 BURNUP SUBSTEPS AT TIME = 3.000000000E+00 DAYS
U235 U238 PU239 PU240 PU241 PU242 LFPPS DUMP TRACE
1 COREA 9.3759E-04 1.9785E-02 6.2426E-04 3.9466E-04 2.7817E-04 1.0309E-04 1.7676E-04 8.9072E-07 1.2500E-09
1 COREB 9.4792E-05 1.9820E-02 1.0748E-03 2.3090E-05 9.4344E-06 1.0028E-05 9.7898E-05 9.1541E-08 2.5000E-09
1 COREC 9.6340E-05 1.9874E-02 1.5294E-03 7.9740E-04 3.8542E-04 1.0272E-04 1.1446E-04 5.4413E-07 3.7500E-09
...
FCC004 11.3114 04/10/20 PAGE 503
REACTOR CONDITIONS AFTER 3 BURNUP SUBSTEPS AT TIME = 4.500000000E+00 DAYS
U235 U238 PU239 PU240 PU241 PU242 LFPPS DUMP TRACE
1 COREA 9.0644E-04 1.9673E-02 6.8466E-04 3.9263E-04 2.6754E-04 1.0457E-04 2.7012E-04 1.3632E-06 4.4194E-10
1 COREB 9.2168E-05 1.9726E-02 1.1114E-03 3.0156E-05 9.2326E-06 1.0041E-05 1.5078E-04 1.3198E-07 8.8388E-10
1 COREC 9.4480E-05 1.9808E-02 1.5439E-03 7.9615E-04 3.7812E-04 1.0408E-04 1.7435E-04 8.2259E-07 1.3258E-09
...
FCC004 11.3114 04/10/20 ABURN: Hexagonal 3D Test Problem PAGE 507
TOTAL REACTOR LOADING (IN KG) OF ACTIVE ISOTOPES AT TIME NODE 3 AT 4.500000000E+00 DAYS.
U235 1.55228E+01
U238 8.51542E+02
PU239 4.82396E+01
PU240 1.76789E+01
PU241 9.53794E+00
PU242 3.19836E+00
LFPPS 8.52078E+00
DUMP 3.30376E-02
TRACE 1.60157E-05

```

**Figure 3-52. REBUS Output Excerpt for the First Equilibrium Test of Card Type 11**

### 3.5.2.3.2 Zero Power Test of the Multi-Stage Equilibrium Problem

The multi-stage aspect of the equilibrium problem is the next task which is first verified using a zero power test. By using a zero power, the active isotope atom density loaded at all stages should remain constant except for any isotopes that undergo decay. The first equilibrium test case of card type 11 is modified slightly for use here where Figure 3-53 shows the major input changes.

In Figure 3-53, the A.DIF3D input section is modified to set the power from 1.0E8 watts to 1.0E-8 watts. Because the half-life for the TRACE isotope is 1 day, the cycle length is reduced from 4.5 days to 1.5 days. In the previous calculation, 3 time points were used to correspond to the 3 steps taken in the non-equilibrium case. That aspect does not apply in a multi-stage scheme and thus while only 1 is required, 2 steps are taken to give more output detail on the TRACE isotope. The final modification is the card type 11 path specification. In Figure 3-53, PATH1 has 2 stages, PATH2 has 3 stages, and PATH3 has 4 stages. Thus for PATH1, the region will assume the fuel at BOC contains 50% fresh fuel and 50% once-burned (1.5 days) fuel. PATH2 is comprised of fresh, once burned, and twice burned. PATH3 is comprised of fresh, once burned, twice burned, and thrice burned fuel. This is the typical

usage of this input option where the number of stages is typically selected to give a desired burnup. In this example without real burnup, it is only done to verify that the TRACE isotope decays properly and that REBUS handles the input properly.

```
...
UNIFORM=A.DIF3D
...
06           1.0      .001      .005      1.0E-8
...
UNIFORM=A.BURN
03           0      0.00000      0.0      1.5000      1.0      2      0
...
11  PATH1 0      1      FUELA ZFUELA
11  PATH1 0      2      FUELA ZFUELA
11  PATH2 0      1      FUELB ZFUELB
11  PATH2 0      2      FUELB ZFUELB
11  PATH2 0      3      FUELB ZFUELB
11  PATH3 0      1      FUEL C ZFUEL C
11  PATH3 0      2      FUEL C ZFUEL C
11  PATH3 0      3      FUEL C ZFUEL C
11  PATH3 0      4      FUEL C ZFUEL C
...
```

**Figure 3-53. REBUS Input Excerpt for the Zero Power Multi-stage Equilibrium Test**

Because only two sub-steps were chosen for the cycle, the atom density detail only contains three points (0.0 days, 0.75 days, and 1.5 days). The atom density excerpt from the REBUS output is provided at each time point in Figure 3-54. A quick inspection and one should find that the active isotope atom densities are identical at all time points except for the TRACE or aMAGIC, bMAGIC, and cMAGIC isotopes. Excluding the TRACE isotope, all of the other isotope densities exactly match those from Figure 3-52 for the first time point. Because the initial time point is identical to the preceding test case, the originating atom density of the TRACE isotope in each fuel form can be identified from Figure 3-52. For COREA, COREB, and COREC, the TRACE isotope density of the fresh fuel is 1.0000E-08, 2.0E-08, and 3.0E-08. The same atom density information can be identified from the current REBUS output file as the first stage atom density output which is also provided in Figure 3-54.

Because there is no power and no fuel burnup, the only verification task that needs to be performed is to verify that the TRACE atom density makes sense with regards to the way the input is to be interpreted. In this regard, the TRACE isotope in each region should be decayed exactly by the number of stages (cycles) that it resides at that position. The formula  $\exp(-8.0225E-6 \cdot t \cdot \text{sec}^{-1})$  still applies and the REBUS output and comparison (assuming the fabricated values from REBUS) are tabulated in Table 3-35. In the first part of the table, the stage density output from Figure 3-54 for each region is verified by using the analytic formula. As can be seen, the errors are very small and attributable to round off errors. In the second part of the table, the total atom density of the TRACE isotope (simple average of the stage densities) is checked where the REBUS output is taken from the atom density edits citing the inclusion of the MAGIC isotopes. The errors are again very small. This work proves that the stage density detail is handled properly by REBUS and that the interpretation of the input is done correctly by REBUS. The results at later time points were also compared with the analytic solution and yielded similar errors to those shown above. This is not shown here for brevity.

```

FCC004 11.3114 04/10/20          ABURN: Hexagonal 3D Test Problem          PAGE    265
...
ATOM DENSITIES USED IN THE NEUTRONICS SOLUTION AT TIME NODE 0 AT 0.000000000E+00 DAYS.
...
      REGION COREA   ZONE 2
aNA / 1.00000E-02  aFE / 2.00000E-02  a016 / 1.60000E-02  aPU239/ 5.00000E-04  aU238 / 2.00000E-02
aMAGIC/ 6.76777E-09  aU235 / 1.00000E-03  aPU242/ 1.00000E-04  alFP / 1.00000E-12  aDUMP / 3.23323E-09
aPU240/ 4.00000E-04  aPU241/ 3.00000E-04
      REGION COREB   ZONE 3
bNA / 1.00000E-02  bFE / 2.00000E-02  bo16 / 1.60000E-02  bPU239/ 1.00000E-03  bU238 / 2.00000E-02
bMAGIC/ 9.85702E-09  bU235 / 1.00000E-04  bPU242/ 1.00000E-05  blFP / 1.00000E-12  bDUMP / 1.01440E-08
bPU240/ 1.00000E-05  bPU241/ 1.00000E-05
      REGION COREC   ZONE 4
cNA / 1.00000E-02  cFE / 2.00000E-02  co16 / 1.60000E-02  cPU239/ 1.50000E-03  cU238 / 2.00000E-02
cMAGIC/ 1.14206E-08  cU235 / 1.00000E-04  cPU242/ 1.00000E-04  clFP / 1.00000E-12  cDUMP / 1.85804E-08
cPU240/ 8.00000E-04  cPU241/ 4.00000E-04
...
FCC004 11.3114 04/10/20          ABURN: Hexagonal 3D Test Problem          PAGE    283
...
BEGINNING OF BURN CYCLE 1
...
ATOM DENSITIES (IN ATOMS/BARN-CM.) OF ACTIVE ISOTOPES IN EACH STAGE OF EACH PATH
+          U235      U238      PU239      PU240      PU241      PU242      LFPPS      DUMP      TRACE
1  COREA  1.0000E-03  2.0000E-02  5.0000E-04  4.0000E-04  3.0000E-04  1.0000E-04  1.0000E-12  1.0000E-12  1.0000E-08
2  COREA  1.0000E-03  2.0000E-02  5.0000E-04  4.0000E-04  3.0000E-04  1.0000E-04  1.0000E-12  6.4655E-09  3.5355E-09
+          U235      U238      PU239      PU240      PU241      PU242      LFPPS      DUMP      TRACE
1  COREB  1.0000E-04  2.0000E-02  1.0000E-03  1.0000E-05  1.0000E-05  1.0000E-05  1.0000E-12  1.0000E-12  2.0000E-08
2  COREB  1.0000E-04  2.0000E-02  1.0000E-03  1.0000E-05  1.0000E-05  1.0000E-05  1.0000E-12  1.2930E-08  7.0711E-09
3  COREB  1.0000E-04  2.0000E-02  1.0000E-03  1.0000E-05  1.0000E-05  1.0000E-05  1.0000E-12  1.7501E-08  2.5000E-09
+          U235      U238      PU239      PU240      PU241      PU242      LFPPS      DUMP      TRACE
1  COREC  1.0000E-04  2.0000E-02  1.5000E-03  8.0000E-04  4.0000E-04  1.0000E-04  1.0000E-12  1.0000E-12  3.0000E-08
2  COREC  1.0000E-04  2.0000E-02  1.5000E-03  8.0000E-04  4.0000E-04  1.0000E-04  1.0000E-12  1.9394E-08  1.0607E-08
3  COREC  1.0000E-04  2.0000E-02  1.5000E-03  8.0000E-04  4.0000E-04  1.0000E-04  1.0000E-12  2.6251E-08  3.7500E-09
4  COREC  1.0000E-04  2.0000E-02  1.5000E-03  8.0000E-04  4.0000E-04  1.0000E-04  1.0000E-12  2.8675E-08  1.3258E-09
...
FCC004 11.3114 04/10/20          ABURN: Hexagonal 3D Test Problem          PAGE    294
...
ATOM DENSITIES USED IN THE NEUTRONICS SOLUTION AT TIME NODE 1 AT 7.500000000E-01 DAYS.
...
      REGION COREA   ZONE 2
aNA / 1.00000E-02  aFE / 2.00000E-02  a016 / 1.60000E-02  aPU239/ 5.00000E-04  aU238 / 2.00000E-02
aMAGIC/ 4.02414E-09  aU235 / 1.00000E-03  aPU242/ 1.00000E-04  alFP / 1.00000E-12  aDUMP / 5.97686E-09
aPU240/ 4.00000E-04  aPU241/ 3.00000E-04
      REGION COREB   ZONE 3
bNA / 1.00000E-02  bFE / 2.00000E-02  bo16 / 1.60000E-02  bPU239/ 1.00000E-03  bU238 / 2.00000E-02
bMAGIC/ 5.86102E-09  bU235 / 1.00000E-04  bPU242/ 1.00000E-05  blFP / 1.00000E-12  bDUMP / 1.41400E-08
bPU240/ 1.00000E-05  bPU241/ 1.00000E-05
      REGION COREC   ZONE 4
cNA / 1.00000E-02  cFE / 2.00000E-02  co16 / 1.60000E-02  cPU239/ 1.50000E-03  cU238 / 2.00000E-02
cMAGIC/ 6.79073E-09  cU235 / 1.00000E-04  cPU242/ 1.00000E-04  clFP / 1.00000E-12  cDUMP / 2.32103E-08
cPU240/ 8.00000E-04  cPU241/ 4.00000E-04
...
FCC004 11.3114 04/10/20          ABURN: Hexagonal 3D Test Problem          PAGE    320
...
ATOM DENSITIES USED IN THE NEUTRONICS SOLUTION AT TIME NODE 2 AT 1.500000000E+00 DAYS.
...
      REGION COREA   ZONE 2
aNA / 1.00000E-02  aFE / 2.00000E-02  a016 / 1.60000E-02  aPU239/ 5.00000E-04  aU238 / 2.00000E-02
aMAGIC/ 2.39277E-09  aU235 / 1.00000E-03  aPU242/ 1.00000E-04  alFP / 1.00000E-12  aDUMP / 7.60823E-09
aPU240/ 4.00000E-04  aPU241/ 3.00000E-04
      REGION COREB   ZONE 3
bNA / 1.00000E-02  bFE / 2.00000E-02  bo16 / 1.60000E-02  bPU239/ 1.00000E-03  bU238 / 2.00000E-02
bMAGIC/ 3.48498E-09  bU235 / 1.00000E-04  bPU242/ 1.00000E-05  blFP / 1.00000E-12  bDUMP / 1.65160E-08
bPU240/ 1.00000E-05  bPU241/ 1.00000E-05
      REGION COREC   ZONE 4
cNA / 1.00000E-02  cFE / 2.00000E-02  co16 / 1.60000E-02  cPU239/ 1.50000E-03  cU238 / 2.00000E-02
cMAGIC/ 4.03779E-09  cU235 / 1.00000E-04  cPU242/ 1.00000E-04  clFP / 1.00000E-12  cDUMP / 2.59632E-08
cPU240/ 8.00000E-04  cPU241/ 4.00000E-04
...

```

Figure 3-54. Atom Density Excerpt for the Zero Power Multi-stage Equilibrium Test

**Table 3-35. TRACE Isotope Results for the First Equilibrium Test of Card Type 11**

|       | REBUS       | Formula     | Error    |
|-------|-------------|-------------|----------|
| COREA | 1.00000E-08 | 1.00000E-08 | 0.0000%  |
|       | 3.53550E-09 | 3.53555E-09 | 0.0014%  |
| COREB | 2.00000E-08 | 2.00000E-08 | 0.0000%  |
|       | 7.07110E-09 | 7.07110E-09 | 0.0000%  |
|       | 2.50000E-09 | 2.50002E-09 | 0.0010%  |
| COREC | 3.00000E-08 | 3.00000E-08 | 0.0000%  |
|       | 1.06070E-08 | 1.06067E-08 | -0.0033% |
|       | 3.75000E-09 | 3.75004E-09 | 0.0010%  |
|       | 1.32580E-09 | 1.32584E-09 | 0.0033%  |
| Total | REBUS       | Formula     |          |
| COREA | 6.76777E-09 | 6.76778E-09 | 0.0001%  |
| COREB | 9.85702E-09 | 9.85704E-09 | 0.0002%  |
| COREC | 1.14206E-08 | 1.14206E-08 | 0.0003%  |

### 3.5.2.3.3 Full Power Test of the Multi-Stage Equilibrium Problem

A full power, multi-stage equilibrium problem is not something that can be checked with a comparable, non-trivial non-equilibrium problem. However, in the preceding setup, the TRACE isotope usage combined with a single power producing isotope (U235) allows for a rather easy verification the logic of the equilibrium problem. This is all that is required as the multi-region depletion work was already verified earlier.

The identical problem to the non-zero test above is used here where the power is set to 1.0E8 watts. The stage densities and region densities output excerpts are given in Figure 3-55 and Figure 3-56, respectively, for all time points. Because the region density output is nothing but the sum of the stage densities, it will be checked first. For U235 in COREA, the loaded density of 1.0000E-03 is combined with the once burned value of 9.6824E-04 to give 9.8412E-04 which is consistent with the 9.84119E-04 from Figure 3-56. The error comes from the different round off values given in the stage density table (5 significant digits instead of 6). Similarly, the U235 stage densities for COREC from time point 1.5 days of 9.8151E-05, 9.6336E-05, 9.4554E-05, and 9.2806E-05 can be averaged to obtain the region-wise density value of 9.5462E-05 which is consistent with the REBUS reported value of 9.54617E-05 atom density for this region reported in Figure 3-56. The error again comes from the different round off values provided for the stage densities.

Two isotopes with significant differences between the stage and region-wise atom densities are the LFPPS and DUMP isotopes. As an example, the LFPPS stage densities for COREB from time point 0.75 days of 2.4006E-05, 7.3099E-05, and 1.2307E-04 can be averaged to obtain 7.3392E-5 which is not consistent with the reported bLFP atom density of 7.3188E-05 in Figure 3-56. The reason for this difference is that the region-wise atom densities are not reported consistently by REBUS. In the excerpt below, they are the intermediate results after 1 region density iteration where the stage density results are for 2 region density iterations. Thus the mistake is the attempted use of the region-wise densities by the user rather than the stage densities. The LFPPS isotope is the most impacted because its concentration is strictly defined as the small loss of content in the other isotopes. In reality, all of the isotopes will display some amount of difference with the stage densities because of this output limitation in REBUS.

FCC004 11.3114 04/10/20 PAGE 296

BEGINNING OF BURN CYCLE 1

| STAGE | REGION | ATOM DENSITIES (IN ATOMS/BARN-CM.) | OF ACTIVE ISOTOPES | IN EACH STAGE | OF EACH PATH |            |            |            |            |            |
|-------|--------|------------------------------------|--------------------|---------------|--------------|------------|------------|------------|------------|------------|
|       |        | U235                               | U238               | PU239         | PU240        | PU241      | PU242      | LFPPS      | DUMP       | TRACE      |
| 1     | COREA  | 1.0000E-03                         | 2.0000E-02         | 5.0000E-04    | 4.0000E-04   | 3.0000E-04 | 1.0000E-04 | 1.0000E-12 | 1.0000E-12 | 1.0000E-08 |
| 2     | COREA  | 9.6824E-04                         | 1.9892E-02         | 5.6369E-04    | 3.9706E-04   | 2.8881E-04 | 1.0159E-04 | 8.8347E-05 | 4.4476E-07 | 3.5355E-09 |
| 1     | COREB  | 1.0000E-04                         | 2.0000E-02         | 1.0000E-03    | 1.0000E-05   | 1.0000E-05 | 1.0000E-05 | 1.0000E-12 | 1.0000E-12 | 2.0000E-08 |
| 2     | COREB  | 9.7355E-05                         | 1.9910E-02         | 1.0382E-03    | 1.6478E-05   | 9.6863E-06 | 1.0015E-05 | 4.8646E-05 | 4.9980E-08 | 7.0711E-09 |
| 3     | COREB  | 9.4781E-05                         | 1.9819E-02         | 1.0749E-03    | 2.3105E-05   | 9.4333E-06 | 1.0028E-05 | 9.8185E-05 | 9.1653E-08 | 2.5000E-09 |
| 1     | COREC  | 1.0000E-04                         | 2.0000E-02         | 1.5000E-03    | 8.0000E-04   | 4.0000E-04 | 1.0000E-04 | 1.0000E-12 | 1.0000E-12 | 3.0000E-08 |
| 2     | COREC  | 9.8151E-05                         | 1.9937E-02         | 1.5149E-03    | 7.9865E-04   | 3.9260E-04 | 1.0138E-04 | 5.7303E-05 | 2.7684E-07 | 1.0607E-08 |
| 3     | COREC  | 9.6336E-05                         | 1.9874E-02         | 1.5294E-03    | 7.9739E-04   | 3.8540E-04 | 1.0272E-04 | 1.1462E-04 | 5.4462E-07 | 3.7500E-09 |
| 4     | COREC  | 9.4554E-05                         | 1.9811E-02         | 1.5433E-03    | 7.9620E-04   | 3.7841E-04 | 1.0403E-04 | 1.7195E-04 | 8.1135E-07 | 1.3258E-09 |

FCC004 11.3114 04/10/20 PAGE 338

REACTOR CONDITIONS AFTER 1 BURNUP SUBSTEPS AT TIME = 7.500000000E-01 DAYS

| STAGE | REGION |            | U235       | U238       | PU239      | PU240      | PU241      | PU242      | LFPPS      | DUMP       | TRACE |
|-------|--------|------------|------------|------------|------------|------------|------------|------------|------------|------------|-------|
| 1     | COREA  | 9.8411E-04 | 1.9946E-02 | 5.3199E-04 | 3.9848E-04 | 2.9438E-04 | 1.0080E-04 | 4.3770E-05 | 2.2072E-07 | 5.9460E-09 |       |
| 2     | COREA  | 9.5286E-04 | 1.9838E-02 | 5.9420E-04 | 3.9580E-04 | 2.8345E-04 | 1.0235E-04 | 1.3232E-04 | 6.6625E-07 | 2.1022E-09 |       |
| 1     | COREB  | 9.8679E-05 | 1.9955E-02 | 1.0192E-03 | 1.3196E-05 | 9.8367E-06 | 1.0008E-05 | 2.4006E-05 | 2.6488E-08 | 1.1892E-08 |       |
| 2     | COREB  | 9.6070E-05 | 1.9865E-02 | 1.0566E-03 | 1.9750E-05 | 9.5533E-06 | 1.0022E-05 | 7.3099E-05 | 7.1253E-08 | 4.2045E-09 |       |
| 3     | COREB  | 9.3529E-05 | 1.9775E-02 | 1.0925E-03 | 2.6447E-05 | 9.3300E-06 | 1.0034E-05 | 1.2307E-04 | 1.1110E-07 | 1.4865E-09 |       |
| 1     | COREC  | 9.9078E-05 | 1.9969E-02 | 1.5075E-03 | 7.9932E-04 | 3.9630E-04 | 1.0069E-04 | 2.8438E-05 | 1.3952E-07 | 1.7838E-08 |       |
| 2     | COREC  | 9.7246E-05 | 1.9905E-02 | 1.5222E-03 | 7.9802E-04 | 3.8900E-04 | 1.0205E-04 | 8.5748E-05 | 4.1023E-07 | 6.3067E-09 |       |
| 3     | COREC  | 9.5447E-05 | 1.9842E-02 | 1.5363E-03 | 7.9679E-04 | 3.8191E-04 | 1.0337E-04 | 1.4307E-04 | 6.7692E-07 | 2.2298E-09 |       |
| 4     | COREC  | 9.3682E-05 | 1.9780E-02 | 1.5501E-03 | 7.9563E-04 | 3.7501E-04 | 1.0466E-04 | 2.0040E-04 | 9.4432E-07 | 7.8834E-10 |       |

FCC004 11.3114 04/10/20 PAGE 364

REACTOR CONDITIONS AFTER 2 BURNUP SUBSTEPS AT TIME = 1.500000000E+00 DAYS

| STAGE | REGION |            | U235       | U238       | PU239      | PU240      | PU241      | PU242      | LFPPS      | DUMP       | TRACE |
|-------|--------|------------|------------|------------|------------|------------|------------|------------|------------|------------|-------|
| 1     | COREA  | 9.6824E-04 | 1.9892E-02 | 5.6369E-04 | 3.9706E-04 | 2.8881E-04 | 1.0159E-04 | 8.8347E-05 | 4.4476E-07 | 3.5355E-09 |       |
| 2     | COREA  | 9.3748E-04 | 1.9784E-02 | 6.2443E-04 | 3.9465E-04 | 2.7814E-04 | 1.0310E-04 | 1.7709E-04 | 8.9208E-07 | 1.2500E-09 |       |
| 1     | COREB  | 9.7355E-05 | 1.9910E-02 | 1.0382E-03 | 1.6478E-05 | 9.6863E-06 | 1.0015E-05 | 4.8646E-05 | 4.9980E-08 | 7.0711E-09 |       |
| 2     | COREB  | 9.4781E-05 | 1.9819E-02 | 1.0749E-03 | 2.3105E-05 | 9.4333E-06 | 1.0028E-05 | 9.8185E-05 | 9.1653E-08 | 2.5000E-09 |       |
| 3     | COREB  | 9.2274E-05 | 1.9730E-02 | 1.1100E-03 | 2.9871E-05 | 9.2397E-06 | 1.0040E-05 | 1.4858E-04 | 1.3042E-07 | 8.8388E-10 |       |
| 1     | COREC  | 9.8151E-05 | 1.9937E-02 | 1.5149E-03 | 7.9865E-04 | 3.9260E-04 | 1.0138E-04 | 5.7303E-05 | 2.7684E-07 | 1.0607E-08 |       |
| 2     | COREC  | 9.6336E-05 | 1.9874E-02 | 1.5294E-03 | 7.9739E-04 | 3.8540E-04 | 1.0272E-04 | 1.1462E-04 | 5.4462E-07 | 3.7500E-09 |       |
| 3     | COREC  | 9.4554E-05 | 1.9811E-02 | 1.5433E-03 | 7.9620E-04 | 3.7841E-04 | 1.0403E-04 | 1.7195E-04 | 8.1135E-07 | 1.3258E-09 |       |
| 4     | COREC  | 9.2806E-05 | 1.9748E-02 | 1.5568E-03 | 7.9508E-04 | 3.7161E-04 | 1.0530E-04 | 2.2928E-04 | 1.0798E-06 | 4.6875E-10 |       |

Figure 3-55. Stage Density Output Excerpt for the Multi-stage Equilibrium Test

The correct region-wise atom density detail can be obtained by manually summing the stage densities or obtaining the region-wise density data from the SUMMARY files that are produced by REBUS. For most problems, these errors are generally negligible and they are only large in this case because of the nature of the test problem. A quick inspection of the time point 0 stage densities and region-wise atom densities shows a near perfect match with the stage density at the end of the problem with that used for the next stage at the beginning of the problem.

In light of this aspect, only the stage density results will be verified in this section where the region-wise density results will be re-calculated from the stage densities. Using the stage density output in Figure 3-55, the total mass of U235 and the power derived from it can be calculated as shown in Table 3-36. The REBUS output excerpt of the regional power is provided in Figure 3-57. The average power over each time interval is calculated from the REBUS output and also provided in Table 3-36. As can be seen, the region-wise power is consistent with the U235 mass destroyed in each region and any inaccuracies are due to round off error in the reported values from the REBUS output.

The last aspect to compare is the TRACE isotope content. Using the stage density information from Figure 3-55, it is very easy to compute the TRACE isotope in COREC after four 1.5 day time points using  $3.0E-08 \cdot \exp(-8.0225E-6 \cdot t \cdot \text{sec}^{-1})$  as 1.06067E-08, 3.75004E-09, 1.32584E-09, and 4.68759E-10. The first three of these match the TRACE stage densities in COREC at time point 0.0 in Figure 3-55 within the round off error of the reported results. At time point 1.5 days in Figure 3-55, all four numbers match the reported results within round off error.

```

FCC004 11.3114 04/10/20 ABURN: Hexagonal 3D Test Problem PAGE 278
ATOM DENSITIES USED IN THE NEUTRONICS SOLUTION AT TIME NODE 0 AT 0.000000000E+00 DAYS.

...
      REGION COREA   ZONE 2
aNA / 1.00000E-02 aFE / 2.00000E-02 a016 / 1.60000E-02 aPU239/ 5.31846E-04 aU238 / 1.99459E-02
aMAGIC/ 6.76777E-09 aU235 / 9.84119E-04 aPU242/ 1.00796E-04 aLFP / 4.41733E-05 aDUMP / 2.22382E-07
aPU240/ 3.98531E-04 aPU241/ 2.94404E-04

      REGION COREB   ZONE 3
bNA / 1.00000E-02 bFE / 2.00000E-02 b016 / 1.60000E-02 bPU239/ 1.03771E-03 bU238 / 1.99097E-02
bMAGIC/ 9.85702E-09 bU235 / 9.73786E-05 bPU242/ 1.00145E-05 bLFP / 4.89436E-05 bDUMP / 4.72111E-08
bPU240/ 1.65277E-05 bPU241/ 9.70654E-06

      REGION COREC   ZONE 4
cNA / 1.00000E-02 cFE / 2.00000E-02 c016 / 1.60000E-02 cPU239/ 1.52190E-03 cU238 / 1.99053E-02
cMAGIC/ 1.14206E-08 cU235 / 9.72601E-05 cPU242/ 1.02031E-04 cLFP / 8.59675E-05 cDUMP / 4.08201E-07
cPU240/ 7.98059E-04 cPU241/ 3.89103E-04

FCC004 11.3114 04/10/20 ABURN: Hexagonal 3D Test Problem PAGE 307
ATOM DENSITIES USED IN THE NEUTRONICS SOLUTION AT TIME NODE 1 AT 7.500000000E-01 DAYS.

...
      REGION COREA   ZONE 2
aNA / 1.00000E-02 aFE / 2.00000E-02 a016 / 1.60000E-02 aPU239/ 5.62873E-04 aU238 / 1.98927E-02
aMAGIC/ 4.02414E-09 aU235 / 9.68606E-04 aPU242/ 1.01570E-04 aLFP / 8.76978E-05 aDUMP / 4.41872E-07
aPU240/ 3.97150E-04 aPU241/ 2.88957E-04

      REGION COREB   ZONE 3
bNA / 1.00000E-02 bFE / 2.00000E-02 b016 / 1.60000E-02 bPU239/ 1.05598E-03 bU238 / 1.98653E-02
bMAGIC/ 5.86102E-09 bU235 / 9.61027E-05 bPU242/ 1.00213E-05 bLFP / 7.31880E-05 bDUMP / 6.94759E-08
bPU240/ 1.97740E-05 bPU241/ 9.57431E-06

      REGION COREC   ZONE 4
cNA / 1.00000E-02 cFE / 2.00000E-02 c016 / 1.60000E-02 cPU239/ 1.52896E-03 cU238 / 1.98742E-02
cMAGIC/ 6.79073E-09 cU235 / 9.63698E-05 cPU242/ 1.02689E-04 cLFP / 1.14206E-04 cDUMP / 5.41815E-07
cPU240/ 7.97445E-04 cPU241/ 3.85581E-04

FCC004 11.3114 04/10/20 ABURN: Hexagonal 3D Test Problem PAGE 349
ATOM DENSITIES USED IN THE NEUTRONICS SOLUTION AT TIME NODE 2 AT 1.500000000E+00 DAYS.

...
      REGION COREA   ZONE 2
aNA / 1.00000E-02 aFE / 2.00000E-02 a016 / 1.60000E-02 aPU239/ 5.94056E-04 aU238 / 1.98380E-02
aMAGIC/ 2.39277E-09 aU235 / 9.52864E-04 aPU242/ 1.02344E-04 aLFP / 1.32708E-04 aDUMP / 6.68369E-07
aPU240/ 3.95854E-04 aPU241/ 2.83474E-04

      REGION COREB   ZONE 3
bNA / 1.00000E-02 bFE / 2.00000E-02 b016 / 1.60000E-02 bPU239/ 1.07438E-03 bU238 / 1.98196E-02
bMAGIC/ 3.48498E-09 bU235 / 9.48036E-05 bPU242/ 1.00279E-05 bLFP / 9.84645E-05 bDUMP / 9.06790E-08
bPU240/ 2.31507E-05 bPU241/ 9.45313E-06

      REGION COREC   ZONE 4
cNA / 1.00000E-02 cFE / 2.00000E-02 c016 / 1.60000E-02 cPU239/ 1.53609E-03 cU238 / 1.98423E-02
cMAGIC/ 4.03779E-09 cU235 / 9.54617E-05 cPU242/ 1.03357E-04 cLFP / 1.43281E-04 cDUMP / 6.78123E-07
cPU240/ 7.96830E-04 cPU241/ 3.82006E-04

```

**Figure 3-56. Region Atom Density Output Excerpt for the Multi-stage Equilibrium Test**

**Table 3-36. Regional Power for Multi-stage Equilibrium Test**

|       | 0 day to 0.75 day  |            |                  | 0.75 day to 1.5 day |            |                  |
|-------|--------------------|------------|------------------|---------------------|------------|------------------|
|       | Change in mass (g) | Power (MW) | REBUS Power (MW) | Change in mass (g)  | Power (MW) | REBUS Power (MW) |
| COREA | 222.03             | 87.761     | 87.747           | 221.89              | 87.705     | 87.701           |
| COREB | 18.31              | 7.218      | 7.218            | 18.31               | 7.237      | 7.237            |
| COREC | 12.80              | 5.035      | 5.034            | 12.80               | 5.060      | 5.062            |
| Total | 253.14             | 100.015    | 100.000          | 253.00              | 100.003    | 100.000          |

Based upon the accuracy of the U235 destruction and the TRACE isotope content, it should be clear that the multi-stage equilibrium problem aspect of REBUS is working as intended. It is important to note that the stage densities computed at the end of 1.5 days for all isotopes identically match the stage density results appearing at the beginning of the problem for the next stage (i.e. stage 1 result

at 1.5 days matches stage 2 result at 0.0 days). This is the expected behavior of this input approach and thus the primary zone assignment approach to card type 11 is verified.

```
...
DIF3D 11.3114 04/10/20      ADIF3D: Hexagonal 3D Test Problem      PAGE  289
0      REGION AND AREA POWER INTEGRALS FOR K-EFF PROBLEM WITH ENERGY RANGE (EV)      =(4.140E-01,1.000E+07)
      REGION  ZONE  ZONE  VOLUME  INTEGRATION(1)  POWER  POWER DENSITY  PEAK DENSITY  PEAK TO AVG.  POWER
      NO.  NAME  NO.  NAME  (CC)  WEIGHT FACTOR  (WATTS)  (WATTS/CC)  (WATTS/CC) (2)  POWER DENSITY  FRACTION
      1  REFL   1  REFL  1.21070E+06  1.00000E+00  5.53788E+00  4.57410E-06  2.59762E-05  5.67897E+00  5.53788E-08
      2  COREA  2  COREA  3.63731E+04  1.00000E+00  8.77702E+07  2.41306E+03  4.49630E+03  1.86332E+00  8.77702E-01
      3  COREB  3  COREB  3.63731E+04  1.00000E+00  7.20927E+06  1.98203E+02  4.38537E+02  2.21256E+00  7.20927E-02
      4  COREC  4  COREC  3.63731E+04  1.00000E+00  5.02051E+06  1.38028E+02  3.41004E+02  2.47054E+00  5.02051E-02
      TOTALS          1.31982E+06  0.00000E+00  1.00000E+08  7.57678E+01  4.49630E+03  5.93431E+01  1.00000E+00
...
DIF3D 11.3114 04/10/20      ADIF3D: Hexagonal 3D Test Problem      PAGE  331
0      REGION AND AREA POWER INTEGRALS FOR K-EFF PROBLEM WITH ENERGY RANGE (EV)      =(4.140E-01,1.000E+07)
      REGION  ZONE  ZONE  VOLUME  INTEGRATION(1)  POWER  POWER DENSITY  PEAK DENSITY  PEAK TO AVG.  POWER
      NO.  NAME  NO.  NAME  (CC)  WEIGHT FACTOR  (WATTS)  (WATTS/CC)  (WATTS/CC) (2)  POWER DENSITY  FRACTION
      1  REFL   1  REFL  1.21070E+06  1.00000E+00  5.62078E+00  4.64258E-06  2.63345E-05  5.67239E+00  5.62078E-08
      2  COREA  2  COREA  3.63731E+04  1.00000E+00  8.77247E+07  2.41180E+03  4.49395E+03  1.86332E+00  8.77247E-01
      3  COREB  3  COREB  3.63731E+04  1.00000E+00  7.22768E+06  1.98710E+02  4.39558E+02  2.21206E+00  7.22768E-02
      4  COREC  4  COREC  3.63731E+04  1.00000E+00  5.04764E+06  1.38774E+02  3.42904E+02  2.47096E+00  5.04764E-02
      TOTALS          1.31982E+06  0.00000E+00  1.00000E+08  7.57678E+01  4.49395E+03  5.93122E+01  1.00000E+00
...
DIF3D 11.3114 04/10/20      ADIF3D: Hexagonal 3D Test Problem      PAGE  357
0      REGION AND AREA POWER INTEGRALS FOR K-EFF PROBLEM WITH ENERGY RANGE (EV)      =(4.140E-01,1.000E+07)
      REGION  ZONE  ZONE  VOLUME  INTEGRATION(1)  POWER  POWER DENSITY  PEAK DENSITY  PEAK TO AVG.  POWER
      NO.  NAME  NO.  NAME  (CC)  WEIGHT FACTOR  (WATTS)  (WATTS/CC)  (WATTS/CC) (2)  POWER DENSITY  FRACTION
      1  REFL   1  REFL  1.21070E+06  1.00000E+00  5.70637E+00  4.71327E-06  2.67050E-05  5.66591E+00  5.70637E-08
      2  COREA  2  COREA  3.63731E+04  1.00000E+00  8.76781E+07  2.41052E+03  4.49155E+03  1.86331E+00  8.76781E-01
      3  COREB  3  COREB  3.63731E+04  1.00000E+00  7.24633E+06  1.99222E+02  4.40593E+02  2.21156E+00  7.24633E-02
      4  COREC  4  COREC  3.63731E+04  1.00000E+00  5.07555E+06  1.39542E+02  3.44857E+02  2.47136E+00  5.07555E-02
      TOTALS          1.31982E+06  0.00000E+00  1.00000E+08  7.57678E+01  4.49155E+03  5.92805E+01  1.00000E+00
...
```

Figure 3-57. Region Power Output Excerpt for the Multi-stage Equilibrium Test

### 3.5.2.3.4 Region Assignments in Equilibrium Cycle

The region assignment is the next option of card type 11 to verify in equilibrium mode. Conceptually they are identical tests as a fuel management group is simply a collection of regions. The region assignment option is more difficult to verify than the primary zone assignment as the intention is for the fuel in a given region to consist of multiple states of different materials. The TRACE isotope inclusion will again prove instrumental in the verification process.

Because fuel fabrication is involved, this verification test problem takes the first equilibrium test problem as the starting point which has the base input shown earlier in Figure 3-49. The modifications to that input are only in A.BURN and shown in Figure 3-58. As can be seen, the cycle length is reduced to 1.5 days with 1 sub-step at 0.75 days and the card type 11 data is replaced with a fuel shuffling scenario.

```
...
UNIFORM=A.BURN
03      0      0.00000      0.0      1.5000      1.0      2      0
...
11      PATH1 0      1      FUEL A COREA
11      PATH1 0      2      FUEL A COREB
11      PATH1 0      3      FUEL A COREC

11      PATH2 0      1      FUEL B COREB
11      PATH2 0      2      FUEL B COREC
11      PATH2 0      3      FUEL B COREA

11      PATH3 0      1      FUEL C COREC
11      PATH3 0      2      FUEL C COREA
11      PATH3 0      3      FUEL C COREB
...
```

Figure 3-58. REBUS Input Excerpt for the Equilibrium Fuel Shuffling Test

The excerpt of the REBUS stage density results for the three time points (0.0, 0.75, and 1.5 days) is given in Figure 3-59. Because the TRACE atom density results are known for this problem, it will be checked first as it is the most easy way to understand what is happening. For FUEL A, the fabricated atom density of TRACE is 1.0E-8 (1.0000E-08 in the stage density output). From Figure 3-58 one can

see that FUELA, FUELB, and FUELc all exist in the three stages and thus we can compute the three TRACE atom density results using  $1.0E-08 \cdot \exp(-8.0225E-6 \cdot t \cdot \text{sec}^{-1})$  as  $3.53555E-09$ ,  $1.25001E-09$ , and  $4.41948E-10$  for FUELA. These values are highlighted in Figure 3-58 noting that because the fuel fabrication imposes different starting densities of TRACE, the results are unique by composition. In the stage density results, it should be apparent that only PATH1 deals with the FUELA but that the composition is assigned to different regions as prescribed by the card type 11 data in Figure 3-58. Thus in this regard, the stage density output is simply a direct representation of the user input and provides the most reliable means of determining the atom density details in an equilibrium cycle calculation.

```

FCC004 11.3114 04/10/20 PAGE 296
...
          BEGINNING OF BURN CYCLE 1
          ATOM DENSITIES (IN ATOMS/BARN-CM.) OF ACTIVE ISOTOPES IN EACH STAGE OF EACH PATH
+          U235      U238      PU239      PU240      PU241      PU242      LFPPS      DUMP      TRACE
STAGE REGION
          PATH PATH1
1  COREA  1.0000E-03  2.0000E-02  5.0000E-04  4.0000E-04  3.0000E-04  1.0000E-04  1.0000E-12  1.0000E-12  1.0000E-08
2  COREB  9.8659E-04  1.9955E-02  5.2528E-04  3.9874E-04  2.9531E-04  1.0064E-04  3.5578E-05  1.7890E-07  3.5355E-09
3  COREC  9.7600E-04  1.9924E-02  5.4520E-04  3.9779E-04  2.9162E-04  1.0114E-04  6.4025E-05  3.2015E-07  1.2500E-09
          PATH PATH2
1  COREB  1.0000E-04  2.0000E-02  1.0000E-03  1.0000E-05  1.0000E-05  1.0000E-05  1.0000E-12  1.0000E-12  2.0000E-08
2  COREC  9.8927E-05  1.9966E-02  1.0138E-03  1.2297E-05  9.8688E-06  1.0006E-05  1.8985E-05  2.6707E-08  7.0711E-09
3  COREA  9.8350E-05  1.9948E-02  1.0213E-03  1.3575E-05  9.8010E-06  1.0009E-05  2.9260E-05  3.8845E-08  2.5000E-09
          PATH PATH3
1  COREC  1.0000E-04  2.0000E-02  1.5000E-03  8.0000E-04  4.0000E-04  1.0000E-04  1.0000E-12  1.0000E-12  3.0000E-08
2  COREA  9.9417E-05  1.9982E-02  1.5041E-03  7.9955E-04  3.9766E-04  1.0041E-04  1.7283E-05  9.5163E-08  1.0607E-08
3  COREB  9.8084E-05  1.9939E-02  1.5129E-03  7.9843E-04  3.9235E-04  1.0133E-04  5.7387E-05  2.7540E-07  3.7500E-09
...
FCC004 11.3114 04/10/20 PAGE 338
...
          REACTOR CONDITIONS AFTER 1 BURNUP SUBSTEPS AT TIME = 7.500000000E-01 DAYS
+          U235      U238      PU239      PU240      PU241      PU242      LFPPS      DUMP      TRACE
STAGE REGION
          PATH PATH1
1  COREA  9.9329E-04  1.9979E-02  5.1267E-04  3.9936E-04  2.9765E-04  1.0032E-04  1.7730E-05  8.9911E-08  5.9460E-09
2  COREB  9.8129E-04  1.9941E-02  5.3525E-04  3.9826E-04  2.9346E-04  1.0089E-04  4.9757E-05  2.4955E-07  2.1022E-09
3  COREC  9.7315E-04  1.9915E-02  5.5062E-04  3.9755E-04  2.9063E-04  1.0128E-04  7.1684E-05  3.5882E-07  7.4325E-10
          PATH PATH2
1  COREB  9.9463E-05  1.9983E-02  1.0069E-03  1.1143E-05  9.9335E-06  1.0003E-05  9.4494E-06  1.4979E-08  1.1892E-08
2  COREC  9.8639E-05  1.9957E-02  1.0175E-03  1.2933E-05  9.8347E-06  1.0007E-05  2.4105E-05  3.3347E-08  4.2045E-09
3  COREA  9.7690E-05  1.9927E-02  1.0296E-03  1.5018E-05  9.7263E-06  1.0012E-05  4.1231E-05  4.8439E-08  1.4865E-09
          PATH PATH3
1  COREC  9.9709E-05  1.9991E-02  1.5020E-03  7.9977E-04  3.9883E-04  1.0021E-04  8.6188E-06  4.9913E-08  1.7838E-08
2  COREA  9.8750E-05  1.9960E-02  1.5085E-03  7.9899E-04  3.9500E-04  1.0087E-04  3.7279E-05  1.8573E-07  6.3067E-09
3  COREB  9.7557E-05  1.9922E-02  1.5164E-03  7.9801E-04  3.9025E-04  1.0169E-04  7.3349E-05  3.4665E-07  2.2298E-09
...
FCC004 11.3114 04/10/20 PAGE 364
...
          REACTOR CONDITIONS AFTER 2 BURNUP SUBSTEPS AT TIME = 1.500000000E+00 DAYS
+          U235      U238      PU239      PU240      PU241      PU242      LFPPS      DUMP      TRACE
STAGE REGION
          PATH PATH1
1  COREA  9.8659E-04  1.9958E-02  5.2528E-04  3.9874E-04  2.9531E-04  1.0064E-04  3.5578E-05  1.7890E-07  3.5355E-09
2  COREB  9.7600E-04  1.9924E-02  5.4520E-04  3.9779E-04  2.9162E-04  1.0114E-04  6.4025E-05  3.2015E-07  1.2500E-09
3  COREC  9.7031E-04  1.9906E-02  5.5604E-04  3.9732E-04  2.8964E-04  1.0141E-04  7.9387E-05  3.9754E-07  4.4194E-10
          PATH PATH2
1  COREB  9.8927E-05  1.9966E-02  1.0138E-03  1.2297E-05  9.8688E-06  1.0006E-05  1.8986E-05  2.6707E-08  7.0711E-09
2  COREC  9.8350E-05  1.9948E-02  1.0213E-03  1.3575E-05  9.8010E-06  1.0009E-05  2.9260E-05  3.8845E-08  2.5000E-09
3  COREA  9.7031E-05  1.9906E-02  1.0380E-03  1.6476E-05  9.6543E-06  1.0015E-05  5.3322E-05  5.7670E-08  8.8388E-10
          PATH PATH3
1  COREC  9.9417E-05  1.9982E-02  1.5041E-03  7.9955E-04  3.9766E-04  1.0041E-04  1.7283E-05  9.5163E-08  1.0607E-08
2  COREA  9.8084E-05  1.9939E-02  1.5129E-03  7.9843E-04  3.9235E-04  1.0133E-04  5.7387E-05  2.7540E-07  3.7500E-09
3  COREB  9.7031E-05  1.9906E-02  1.5199E-03  7.9758E-04  3.8817E-04  1.0205E-04  8.9400E-05  4.1789E-07  1.3258E-09
...

```

Figure 3-59. Stage Density Output Excerpt for the Equilibrium Fuel Shuffling Test

The atom density output excerpt for the beginning of the problem is given in Figure 3-60. What should be clear is that in each region COREA, COREB, and COREC, the region specific isotope set is present such that 3 times the number of isotopes is present compared with the previous examples (e.g. aU235, bU235, and cU235 are all present in all regions). Looking at the atom densities assigned to each region, one can directly find them in the stage density output excerpt as the loaded stage of each fuel zone FUELA, FUELB, and FUELc for the given time point. In this regard, one can rearrange the card type 11 data by the assigned region and find that stage 1 of FUELA, stage 3 of FUELb, and stage 2 of

FUELC are assigned to COREA. The atom densities in Figure 3-60 identically match the stage density results from Figure 3-59. In this manner, the shuffling approach is verified without having to perform any real calculations.

```
FCC004 11.3114 04/10/20          ABURN: Hexagonal 3D Test Problem          PAGE  278
                                  ATOM DENSITIES USED IN THE NEUTRONICS SOLUTION AT TIME NODE 0 AT  0.000000000E+00 DAYS.

...
      REGION COREA   ZONE  2
aNA   / 1.00000E-02  aFE   / 2.00000E-02  a016 / 1.60000E-02  aPU239/ 5.00000E-04  aU238 / 2.00000E-02
aMAGIC/ 1.00000E-08  aU235 / 1.00000E-03  aPU242/ 1.00000E-04  aLFP  / 1.00000E-12  aDUMP / 1.00000E-12
aPU240 / 4.00000E-04  aPU241/ 3.00000E-04  bPU239/ 1.02128E-03  bU238 / 1.99477E-02  bMAGIC/ 2.50000E-09
bU235 / 9.83501E-05  bPU242/ 1.00087E-05  bLFP  / 2.92602E-05  bDUMP / 3.88449E-08  bPU240/ 1.35745E-05
bPU241/ 9.80102E-06  cPU239/ 1.50408E-03  cU238 / 1.99815E-02  cMAGIC/ 1.06066E-08  cU235 / 9.94172E-05
cPU242/ 1.00411E-04  cLFP  / 1.72830E-05  cDUMP / 9.51628E-08  cPU240/ 7.99548E-04  cPU241/ 3.97662E-04
      REGION COREB   ZONE  3
aPU239/ 5.25280E-04  aU238 / 1.99577E-02  aMAGIC/ 3.53553E-09  aU235 / 9.86586E-04  aPU242/ 1.00639E-04
aLFP  / 3.55779E-05  aDUMP / 1.78904E-07  aPU240/ 3.98739E-04  aPU241/ 2.95307E-04  bNA  / 1.00000E-02
bFE   / 2.00000E-02  b016 / 1.60000E-02  bPU239/ 1.00000E-03  bU238 / 2.00000E-02  bMAGIC/ 2.00000E-08
bU235 / 1.00000E-04  bPU242/ 1.00000E-05  bLFP  / 1.00000E-12  bDUMP / 1.00000E-12  bPU240/ 1.00000E-05
bPU241/ 1.00000E-05  cPU239/ 1.51291E-03  cU238 / 1.99393E-02  cMAGIC/ 3.75000E-09  cU235 / 9.80836E-05
cPU242/ 1.01328E-04  cLFP  / 5.73872E-05  cDUMP / 2.75404E-07  cPU240/ 7.98433E-04  cPU241/ 3.92345E-04
      REGION COREC   ZONE  4
aPU239/ 5.45198E-04  aU238 / 1.99239E-02  aMAGIC/ 1.25000E-09  aU235 / 9.75995E-04  aPU242/ 1.01142E-04
aLFP  / 6.40251E-05  aDUMP / 3.20149E-07  aPU240/ 3.97794E-04  aPU241/ 2.91619E-04  bPU239/ 1.01376E-03
bU238 / 1.99661E-02  bMAGIC/ 7.07107E-09  bU235 / 9.89266E-05  bPU242/ 1.00057E-05  bLFP  / 1.89861E-05
bDUMP / 2.67070E-08  bPU240/ 1.22967E-05  bPU241/ 9.86882E-06  cNA  / 1.00000E-02  cFE  / 2.00000E-02
c016 / 1.60000E-02  cPU239/ 1.50000E-03  cU238 / 2.00000E-02  cMAGIC/ 3.00000E-08  cU235 / 1.00000E-04
cPU242/ 1.00000E-04  cLFP  / 1.00000E-12  cDUMP / 1.00000E-12  cPU240/ 8.00000E-04  cPU241/ 4.00000E-04
...
```

**Figure 3-60. Atom Density Output Excerpt for the Equilibrium Fuel Shuffling Test**

Unlike the Primary Zone assignment input approach, the shuffling approach does not average the zones assigned to a given region. It just merges them. Thus if one wanted to emulate the problem consistently with the Primary Zone assignment approach, the card type 14 input of each zone here would have to be modified to include a factor of one-third. For a region that has a two assembly shuffling pattern, a factor of one-half would have to be applied and one with a seven assembly shuffling pattern would have to have a factor of one-seventh. To see this clearly, the active isotope loading results were extracted from REBUS and are given in Figure 3-61.

```
FCC004 11.3114 04/10/20          ABURN: Hexagonal 3D Test Problem          PAGE  299
                                  TOTAL REACTOR LOADING (IN KG) OF ACTIVE ISOTOPES AT TIME NODE 0 AT  0.000000000E+00 DAYS.

U235   5.05174E+01
U238   2.58477E+03
PU239  1.31756E+02
PU240  5.26534E+01
PU241  3.06808E+01
PU242  9.26520E+00
LFPSS  3.18526E+00
DUMP   1.33301E-02
TRACE  5.35818E-04

...
FCC004 11.3114 04/10/20          ABURN: Hexagonal 3D Test Problem          PAGE  341
                                  TOTAL REACTOR LOADING (IN KG) OF ACTIVE ISOTOPES AT TIME NODE 1 AT  7.500000000E-01 DAYS.

U235   5.02644E+01
U238   2.58273E+03
PU239  1.32580E+02
PU240  5.26628E+01
PU241  3.05164E+01
PU242  9.29070E+00
LFPSS  4.76964E+00
DUMP   1.96328E-02
TRACE  3.18599E-04

...
FCC004 11.3114 04/10/20          ABURN: Hexagonal 3D Test Problem          PAGE  367
                                  TOTAL REACTOR LOADING (IN KG) OF ACTIVE ISOTOPES AT TIME NODE 2 AT  1.500000000E+00 DAYS.

U235   5.00114E+01
U238   2.58069E+03
PU239  1.33401E+02
PU240  5.26733E+01
PU241  3.03525E+01
PU242  9.31612E+00
LFPSS  6.36465E+00
DUMP   2.57753E-02
TRACE  1.89440E-04
...
```

**Figure 3-61. Total Reactor Loading Output Excerpt for the Equilibrium Fuel Shuffling Test**

Comparing the U235 mass loading with the previous equilibrium test cases such as Figure 3-52 one finds that the total mass is at least three times larger (compare 1.70410E+01 with 5.05174E+01). Using the output in Figure 3-61, the change in U235 mass over the 1.5 day cycle is found to be 506 g which is consistent with that of Table 3-36.

It should come as no surprise that the  $k_{eff}$  results are considerably higher than those of the other equilibrium test cases as this shuffling approach has 3 times the fuel loading. For comparison purposes, two additional test cases were created. In the first modification, all zones use the “a” set of isotopes noting that there was no difference between any of the actual cross sections (i.e. aU235, bU235, and cU235 have all identical cross sections). In the second modification, the factor of one-third is applied to each zone to mimic the Primary Zone approach. The  $k_{eff}$  results for the 1.5 day primary zone assignment test problem, and the three shuffling tests described in this section are tabulated in Table 3-37. As seen, the shuffling result without the factor of one-third is considerably higher than the primary zone (1.09 versus 0.64). Switching all of the zone wise isotope assignments to the “a” set makes no difference in the solution as expected. Including the factor of one-third reduces the criticality results back to something similar to the primary zone input. The reason it is not identical is because the three zones are not identical and the shuffling scheme effectively mixes them together which is not consistent with the Primary Zone approach.

**Table 3-37. Criticality Results for the Equilibrium Fuel Shuffling Test**

| Time | Primary Zone | Fuel Assembly Shuffling |         |           |
|------|--------------|-------------------------|---------|-----------|
|      |              | Base                    | “a” Set | One-Third |
| 0.00 | 0.64679      | 1.09313                 | 1.09313 | 0.63292   |
| 0.75 | 0.64859      | 1.09388                 | 1.09388 | 0.63360   |
| 1.50 | 0.65035      | 1.09462                 | 1.09462 | 0.63424   |

Based upon the preceding analysis work, the region assignment input of card type 11 is verified. Both the TRACE and U235 content were both consistent with the intended behavior of the REBUS software.

### **3.5.2.3.5 Fuel Management Group Assignments in Equilibrium Cycle**

The fuel management group (FMG) assignment is the last option of card type 11 to verify in equilibrium mode. Conceptually it is identical to the region assignment as a fuel management group is simply a collection of regions. However, the FMG input does not allow shuffling and thus is really just another way of specifying the Primary Zone input approach. As a consequence of this fact, the easiest way to verify that it is working is to define the previous regions as FMG as was done in the non-equilibrium testing. To demonstrate another feature of the REBUS software, the existing number of regions is changed which will lead to a slightly different result from the previous primary zone multi-stage equilibrium problem.

The modifications to the input are given in Figure 3-62. The most important modifications to note are the inclusion of more regions in A.NIP3 by simply appending a 1 or 2 indicator to the previous name (i.e. COREA -> COREA1 & COREA2). A new area, AREAC, is added (type 07 of A.NIP3) as it will be used as a FMG. Finally, the zone to region assignment (type 15 of A.NIP3) has to be modified consistent with the new region names. For the A.BURN input, the fuel management groups (FMG1, FMG2, and FMG3) have to be defined using card type 45. Given those, the card type 11 fuel management cards are defined by just replacing the primary zone name with the equivalent FMG name.

The output from this input test is effectively identical to that of the full power primary zone equilibrium test displayed in Figure 3-55, Figure 3-56, and Figure 3-57. However, the inclusion of more regions forces REBUS to treat the depletion in those regions differently. For comparison, the stage density output for the first time point is displayed in Figure 3-63. This output can be directly compared to Figure 3-55. One should note that PATH1 is split into two sections for COREA1 and COREA2. REBUS is built to take a given region and follow the material assigned to that region and this input not only forces it to proliferate the zone to match the number of regions that zone is assigned to the region, but also the PATH specification. Thus in this output, there are twice the number of fissionable zones and the path specification is duplicated as seen.

```

...
UNFORM=A.NIP3
...
07 CORE COREA1 COREB1 COREC1 COREA2 COREB2 COREC2
07 AREAC COREC1 COREC2
15 ZFUELA COREA1 COREA2
15 ZFUELB COREB1 COREB2
15 ZFUELC COREC1 COREC2
30 COREA1 1 0 0 30.0 90.0
30 COREA2 2 1 1 30.0 90.0
30 COREB1 2 2 2 30.0 90.0
30 COREA2 2 3 3 30.0 90.0
30 COREB1 2 4 4 30.0 90.0
30 COREA2 2 5 5 30.0 90.0
30 COREB1 2 6 6 30.0 90.0
30 COREB2 3 1 1 30.0 90.0
30 COREA1 3 2 2 30.0 90.0
30 COREC1 3 3 3 30.0 90.0
30 COREC2 3 4 4 30.0 90.0
30 COREB2 3 5 5 30.0 90.0
30 COREA1 3 6 6 30.0 90.0
30 COREC2 3 7 7 30.0 90.0
30 COREC2 3 8 8 30.0 90.0
30 COREB1 3 9 9 30.0 90.0
30 COREA2 3 10 10 30.0 90.0
30 COREC1 3 11 11 30.0 90.0
30 COREB2 3 12 12 30.0 90.0
30 COREC2 4 1 1 30.0 90.0
30 COREC1 4 8 8 30.0 90.0
... UNFORM=A.BURN
11 PATH1 0 1 FUEL A FMG1
11 PATH1 0 2 FUEL A FMG1
11 PATH2 0 1 FUEL B FMG2
11 PATH2 0 2 FUEL B FMG2
11 PATH2 0 3 FUEL B FMG2
11 PATH3 0 1 FUEL C FMG3
11 PATH3 0 2 FUEL C FMG3
11 PATH3 0 3 FUEL C FMG3
11 PATH3 0 4 FUEL C FMG3
... FMG1 COREA1 COREA2
45 FMG2 COREB1 COREB2
45 FMG3 AREAC

```

**Figure 3-62. REBUS Input Excerpt for the FMG Equilibrium Test**

| BEGINNING OF BURN CYCLE 1  |        |            |            |            |            |            |            |            |            | PAGE       | 308 |
|--|--------|------------|------------|------------|------------|------------|------------|------------|------------|------------|-----|
| ATOM DENSITIES (IN ATOMS/BARN-CM.) OF ACTIVE ISOTOPES IN EACH STAGE OF EACH PATH |        |            |            |            |            |            |            |            |            |            |     |
| STAGE  | REGION | PATH PATH1 |            |            |            |            |            |            |            |            |     |
| +  |        | U235       | U238       | PU239      | PU240      | PU241      | PU242      | LFPSS      | DUMP       | TRACE      |     |
| 1  | COREA1 | 1.0000E-03 | 2.0000E-02 | 5.0000E-04 | 4.0000E-04 | 3.0000E-04 | 1.0000E-04 | 1.0000E-12 | 1.0000E-12 | 1.0000E-08 |     |
| 2  | COREA1 | 9.6915E-04 | 1.9895E-02 | 5.6187E-04 | 3.9714E-04 | 2.8913E-04 | 1.0155E-04 | 8.5801E-05 | 4.3186E-07 | 3.5355E-09 |     |
|  |        | PATH PATH1 |            |            |            |            |            |            |            |            |     |
| 1  | COREA2 | 1.0000E-03 | 2.0000E-02 | 5.0000E-04 | 4.0000E-04 | 3.0000E-04 | 1.0000E-04 | 1.0000E-12 | 1.0000E-12 | 1.0000E-08 |     |
| 2  | COREA2 | 9.6754E-04 | 1.9889E-02 | 5.6506E-04 | 3.9700E-04 | 2.8857E-04 | 1.0163E-04 | 9.0288E-05 | 4.5452E-07 | 3.5355E-09 |     |
|  |        | PATH PATH2 |            |            |            |            |            |            |            |            |     |
| 1  | COREB1 | 1.0000E-04 | 2.0000E-02 | 1.0000E-03 | 1.0000E-05 | 1.0000E-05 | 1.0000E-05 | 1.0000E-12 | 1.0000E-12 | 2.0000E-08 |     |
| 2  | COREB1 | 9.6688E-05 | 1.9894E-02 | 1.0443E-03 | 1.7554E-05 | 9.6370E-06 | 1.0017E-05 | 5.7812E-05 | 5.6232E-08 | 7.0711E-09 |     |
| 3  | COREB1 | 9.3873E-05 | 1.9788E-02 | 1.0864E-03 | 2.5305E-05 | 9.3563E-06 | 1.0032E-05 | 1.1684E-04 | 1.0417E-07 | 2.5000E-09 |     |
|  |        | PATH PATH2 |            |            |            |            |            |            |            |            |     |
| 1  | COREB2 | 1.0000E-04 | 2.0000E-02 | 1.0000E-03 | 1.0000E-05 | 1.0000E-05 | 1.0000E-05 | 1.0000E-12 | 1.0000E-12 | 2.0000E-08 |     |
| 2  | COREB2 | 9.7981E-05 | 1.9931E-02 | 1.0301E-03 | 1.5048E-05 | 9.7547E-06 | 1.0012E-05 | 3.6467E-05 | 4.1643E-08 | 7.0711E-09 |     |
| 3  | COREB2 | 9.6004E-05 | 1.9861E-02 | 1.0593E-03 | 2.0192E-05 | 9.5463E-06 | 1.0023E-05 | 7.3475E-05 | 7.4960E-08 | 2.5000E-09 |     |
|  |        | PATH PATH3 |            |            |            |            |            |            |            |            |     |
| 1  | COREC1 | 1.0000E-04 | 2.0000E-02 | 1.5000E-03 | 8.0000E-04 | 4.0000E-04 | 1.0000E-04 | 1.0000E-12 | 1.0000E-12 | 3.0000E-08 |     |
| 2  | COREC1 | 9.8302E-05 | 1.9942E-02 | 1.5140E-03 | 7.9883E-04 | 3.9319E-04 | 1.0128E-04 | 5.2412E-05 | 2.5745E-07 | 1.0607E-08 |     |
| 3  | COREC1 | 9.6632E-05 | 1.9884E-02 | 1.5276E-03 | 7.9773E-04 | 3.8656E-04 | 1.0253E-04 | 1.0484E-04 | 5.0536E-07 | 3.7500E-09 |     |
| 4  | COREC1 | 9.4991E-05 | 1.9826E-02 | 1.5407E-03 | 7.9670E-04 | 3.8010E-04 | 1.0374E-04 | 1.5728E-04 | 7.5175E-07 | 1.3258E-09 |     |
|  |        | PATH PATH3 |            |            |            |            |            |            |            |            |     |
| 1  | COREC2 | 1.0000E-04 | 2.0000E-02 | 1.5000E-03 | 8.0000E-04 | 4.0000E-04 | 1.0000E-04 | 1.0000E-12 | 1.0000E-12 | 3.0000E-08 |     |
| 2  | COREC2 | 9.8038E-05 | 1.9933E-02 | 1.5156E-03 | 7.9852E-04 | 3.9216E-04 | 1.0145E-04 | 6.0959E-05 | 2.9135E-07 | 1.0607E-08 |     |
| 3  | COREC2 | 9.6115E-05 | 1.9866E-02 | 1.5307E-03 | 7.9713E-04 | 3.8454E-04 | 1.0286E-04 | 1.2193E-04 | 5.7402E-07 | 3.7500E-09 |     |
| 4  | COREC2 | 9.4229E-05 | 1.9800E-02 | 1.5452E-03 | 7.9582E-04 | 3.7715E-04 | 1.0424E-04 | 1.8290E-04 | 8.5602E-07 | 1.3258E-09 |     |

Figure 3-63. First Stage Density Output Excerpt for the FMG Equilibrium Test

From Figure 3-63, one can see that the TRACE atom density is identical for a given stage of all regions in each PATH. All of the other isotopes are only identical for the first stage corresponding to the fabricated fuel. All other stages have slight differences in the atom density of each isotope due to the slightly different region flux levels and thus different burnups. As an example, from Figure 3-55, U235 has an atom density of 0.96824E-04 in stage 2, while in Figure 3-63, COREA1 is 9.6915E-04 and COREA2 is 9.6754E-04. Noting that there are four COREA2 assemblies in Figure 3-62 and three COREA1 assemblies, the volume weighted average of the two U235 atom densities from stage 2 is 9.6823E-04 which is within round off error of the primary zone result and indicates that the average burnup is still equivalent between the two models.

The total reactor loading details, extracted for all three time points is given in Figure 3-64, and the  $k_{eff}$  results are nearly identical between this problem and the multi-stage primary zone assignment result shown earlier. This is the expected behavior noting that severe burnup has to occur in the domain in order for the equilibrium cycle calculation to really have a different outcome. Or if you will, the flux shape has to be severely perturbed regionally to lead to dramatic changes in the region-wise depletion. This problem is clearly too simple to cause that issue. Because the TRACE isotope densities exactly match the previous results in Figure 3-55 and the total U235 mass change in Figure 3-64 is again 506 g, we can state that the FMG input option of card type 11 is confirmed.

```

FCC004 11.3114 04/10/20      ABURN: Hexagonal 3D Test Problem      PAGE      314
                               TOTAL REACTOR LOADING (IN KG) OF ACTIVE ISOTOPES AT TIME NODE 0 AT 0.000000000E+00 DAYS.
                               U235      1.67393E+01
                               U238      8.59510E+02
                               PU239      4.46492E+01
                               PU240      1.75946E+01
                               PU241      1.00961E+01
                               PU242      3.11273E+00
                               LFPPS      2.56388E+00
                               DUMP      9.66151E-03
                               TRACE      1.69391E-04

FCC004 11.3114 04/10/20      ABURN: Hexagonal 3D Test Problem      PAGE      358
                               TOTAL REACTOR LOADING (IN KG) OF ACTIVE ISOTOPES AT TIME NODE 1 AT 7.500000000E-01 DAYS.
                               U235      1.64863E+01
                               U238      8.57646E+02
                               PU239      4.54684E+01
                               PU240      1.76128E+01
                               PU241      9.96257E+00
                               PU242      3.13392E+00
                               LFPPS      3.94938E+00
                               DUMP      1.50505E-02
                               TRACE      1.00721E-04

FCC004 11.3114 04/10/20      ABURN: Hexagonal 3D Test Problem      PAGE      386
                               TOTAL REACTOR LOADING (IN KG) OF ACTIVE ISOTOPES AT TIME NODE 2 AT 1.500000000E+00 DAYS.
                               U235      1.62333E+01
                               U238      8.55758E+02
                               PU239      4.62812E+01
                               PU240      1.76340E+01
                               PU241      9.82989E+00
                               PU242      3.15495E+00
                               LFPPS      5.36168E+00
                               DUMP      2.04877E-02
                               TRACE      5.98888E-05

```

**Figure 3-64. Total Reactor Loading Output Excerpt for the FMG Equilibrium Test**

### 3.5.2.3.6 Multi-Stage Equilibrium Cycle Fuel Shuffling Test

From the previous verified region assignment input option of card type 11, only three zones and three paths were considered all of which had a three region shuffling pattern. For a fuel shuffling methodology, one inherently has to select a number of stages that is a multiple of the patterns desired. Thus, if a 2 and 3 stage shuffling pattern are desired, then one must use 6 stages such that the fuel shuffling of the connected regions can be setup properly. For completeness, this aspect is tested here. The primary modifications to the input are given in Figure 3-65. As can be seen, the A.NIP3 input is modified to introduce more regions similarly to the FMG testing. In this case, the base geometry was

altered to ensure that COREA1, COREA2, and COREA3 consist of exactly 3 assembly positions each. Similarly, COREB1 and COREB2 each have 5 assembly positions each and COREC1, COREC2, and COREC3 have 6 assembly positions each. The zone to region assignment (type 15) and area definitions (type 7) cards are modified appropriately with the geometry change.

Moving to the PATH specification, one can see that COREA grouping (COREA1, COREA2, and COREA3) have shuffling changes occurring only on stages 1, 3 and 5. The COREB grouping have shuffling changes on stages 1 and 4 while the COREC grouping has shuffling changes on stages 1, 3, and 5 similar to COREA. Given the cycle length is kept at 1.5 days, assemblies in COREA and COREC are only shuffled every 2 cycles or 3.0 days. For COREB, the assemblies are shuffled every 4.5 days. Note that the enrichment and feed specifications had to be modified consistently with the changes in the PATH specifications.

```
UNIFORM=A.NIP3
...
07 CORE COREA1 COREB1 COREC1 COREA2 COREB2 COREC2
07 CORE COREA3 COREC3
15 ZFUELA COREA1 COREA2 COREA3
15 ZFUELB COREB1 COREB2
15 ZFUELc COREC1 COREC2 COREC3
30 COREA1 1 0 0 30.0 90.0
30 COREA2 2 1 1 30.0 90.0
30 COREA3 2 2 2 30.0 90.0
30 COREA1 2 3 3 30.0 90.0
30 COREA2 2 4 4 30.0 90.0
30 COREA3 2 5 5 30.0 90.0
30 COREA1 2 6 6 30.0 90.0
30 COREA2 3 1 1 30.0 90.0
30 COREA3 3 2 2 30.0 90.0
11 PATHA2 0 4 FUELA COREA3
11 PATHA2 0 5 FUELA COREA1
11 PATHA2 0 6 FUELA COREA1
11 PATHA3 0 1 FUELA COREA3
11 PATHA3 0 2 FUELA COREA3
11 PATHA3 0 3 FUELA COREA1
11 PATHA3 0 4 FUELA COREA1
11 PATHA3 0 5 FUELA COREA2
11 PATHA3 0 6 FUELA COREA2
11 PATHB1 0 1 FUELb COREB1
11 PATHB1 0 2 FUELb COREB1
11 PATHB1 0 3 FUELb COREB1
11 PATHB1 0 4 FUELb COREB2
11 PATHB1 0 5 FUELb COREB2
11 PATHB1 0 6 FUELb COREB2
11 PATHB2 0 1 FUELb COREB2
11 PATHB2 0 2 FUELb COREB2
11 PATHB2 0 3 FUELb COREB2
11 PATHB2 0 4 FUELb COREB1
11 PATHB2 0 5 FUELb COREB1
11 PATHB2 0 6 FUELb COREB1
11 PATHC1 0 1 FUELc COREC1
11 PATHC1 0 2 FUELc COREC1
11 PATHC1 0 3 FUELc COREC2
11 PATHC1 0 4 FUELc COREC2
11 PATHC1 0 5 FUELc COREC3
11 PATHC1 0 6 FUELc COREC3
11 PATHC2 0 1 FUELc COREC2
11 PATHC2 0 2 FUELc COREC2
11 PATHC2 0 3 FUELc COREC3
11 PATHC2 0 4 FUELc COREC3
11 PATHC2 0 5 FUELc COREC1
11 PATHC2 0 6 FUELc COREC1
11 PATHC3 0 1 FUELc COREC3
11 PATHC3 0 2 FUELc COREC3
11 PATHC3 0 3 FUELc COREC1
11 PATHC3 0 4 FUELc COREC1
11 PATHC3 0 5 FUELc COREC2
11 PATHC3 0 6 FUELc COREC2
11 PATHA1 FAB1 0.0 0 1.00 1.00
11 PATHA1 FAB1 0.0 0 1.00 1.00
11 PATHA3 FAB1 0.0 0 1.00 1.00
11 PATHB1 FAB2 0.0 0 0.520297495 1.00
11 PATHB2 FAB2 0.0 0 0.520297495 1.00
11 PATHC1 FAB3 0.0 0 1.235491658 1.00
11 PATHC2 FAB3 0.0 0 1.235491658 1.00
11 PATHC3 FAB3 0.0 0 1.235491658 1.00
...
11 PATHA1 0 1 FUELA COREA1
11 PATHA1 0 2 FUELA COREA1
11 PATHA1 0 3 FUELA COREA2
11 PATHA1 0 4 FUELA COREA2
11 PATHA1 0 5 FUELA COREA3
11 PATHA1 0 6 FUELA COREA3
11 PATHA2 0 1 FUELA COREA2
11 PATHA2 0 2 FUELA COREA2
11 PATHA2 0 3 FUELA COREA3
19 PATHA1 FEED1 1
19 PATHC3 FEED3 1
20 PATHA1 FEEDB 1
20 PATHC3 FEEDB 1
...
```

**Figure 3-65. REBUS Input Excerpt for the Three Region Equilibrium Shuffling Test**

Given the input is considerably larger, the output is also considerably larger. Figure 3-66 shows the stage density excerpt at the first time point for all stages of all paths. Because it was shown previously that many of these outputs are consistent with the results at the end of the cycle length, only this

output will be checked. To begin, the fabricated TRACE density at stage 1 is consistent with the previous results. Using the same decay formula from earlier, the TRACE concentration in each stage can be computed analytically and it is tabulated in Table 3-38 with the REBUS collected results above. It is important to note that the TRACE concentrations for a given fuel form are independent of the actual placement in the domain and thus there are only three unique results in Figure 3-66. As can be seen, the REBUS calculated results are effectively identical to the formula results where the differences are due to the formula using the initial density for all of the calculations while the REBUS result involves single precision round off error applied at each time step.

| FCC004 11.3114 04/10/20 |        |            |            |            |            |            |            |            |            | PAGE       | 314 |
|-------------------------|--------|------------|------------|------------|------------|------------|------------|------------|------------|------------|-----|
| ...                     |        |            |            |            |            |            |            |            |            |            |     |
| PATH PATHA1             |        |            |            |            |            |            |            |            |            |            |     |
| +                       |        | U235       | U238       | PU239      | PU240      | PU241      | PU242      | LFPPS      | DUMP       | TRACE      |     |
| 1                       | COREA1 | 1.0000E-03 | 2.0000E-02 | 5.0000E-04 | 4.0000E-04 | 3.0000E-04 | 1.0000E-04 | 1.0000E-12 | 1.0000E-12 | 1.0000E-08 |     |
| 2                       | COREA1 | 9.9128E-04 | 1.9973E-02 | 5.1644E-04 | 3.9917E-04 | 2.9695E-04 | 1.0042E-04 | 2.3059E-05 | 1.1814E-07 | 3.5355E-09 |     |
| 3                       | COREA2 | 9.8264E-04 | 1.9945E-02 | 5.3268E-04 | 3.9838E-04 | 2.9393E-04 | 1.0083E-04 | 4.6143E-05 | 2.3255E-07 | 1.2500E-09 |     |
| 4                       | COREA2 | 9.7436E-04 | 1.9919E-02 | 5.4811E-04 | 3.9764E-04 | 2.9106E-04 | 1.0121E-04 | 6.8492E-05 | 3.4171E-07 | 4.4194E-10 |     |
| 5                       | COREA3 | 9.6615E-04 | 1.9892E-02 | 5.6335E-04 | 3.9693E-04 | 2.8822E-04 | 1.0160E-04 | 9.0862E-05 | 4.5076E-07 | 1.5625E-10 |     |
| 6                       | COREA3 | 9.5800E-04 | 1.9866E-02 | 5.7849E-04 | 3.9626E-04 | 2.8541E-04 | 1.0198E-04 | 1.1328E-04 | 5.6054E-07 | 5.5243E-11 |     |
| PATH PATHA2             |        |            |            |            |            |            |            |            |            |            |     |
| 1                       | COREA2 | 1.0000E-03 | 2.0000E-02 | 5.0000E-04 | 4.0000E-04 | 3.0000E-04 | 1.0000E-04 | 1.0000E-12 | 1.0000E-12 | 1.0000E-08 |     |
| 2                       | COREA2 | 9.9158E-04 | 1.9974E-02 | 5.1582E-04 | 3.9920E-04 | 2.9705E-04 | 1.0040E-04 | 2.2303E-05 | 1.1394E-07 | 3.5355E-09 |     |
| 3                       | COREA3 | 9.8323E-04 | 1.9947E-02 | 5.3145E-04 | 3.9842E-04 | 2.9414E-04 | 1.0079E-04 | 4.4629E-05 | 2.2412E-07 | 1.2500E-09 |     |
| 4                       | COREA3 | 9.7493E-04 | 1.9921E-02 | 5.4697E-04 | 3.9768E-04 | 2.9126E-04 | 1.0119E-04 | 6.7002E-05 | 3.3375E-07 | 4.4194E-10 |     |
| 5                       | COREA1 | 9.6670E-04 | 1.9894E-02 | 5.6230E-04 | 3.9698E-04 | 2.8841E-04 | 1.0157E-04 | 8.9397E-05 | 4.4327E-07 | 1.5625E-10 |     |
| 6                       | COREA1 | 9.5827E-04 | 1.9867E-02 | 5.7797E-04 | 3.9628E-04 | 2.8550E-04 | 1.0196E-04 | 1.1254E-04 | 5.5678E-07 | 5.5243E-11 |     |
| PATH PATHA3             |        |            |            |            |            |            |            |            |            |            |     |
| 1                       | COREA3 | 1.0000E-03 | 2.0000E-02 | 5.0000E-04 | 4.0000E-04 | 3.0000E-04 | 1.0000E-04 | 1.0000E-12 | 1.0000E-12 | 1.0000E-08 |     |
| 2                       | COREA3 | 9.9156E-04 | 1.9973E-02 | 5.1590E-04 | 3.9920E-04 | 2.9704E-04 | 1.0040E-04 | 2.2303E-05 | 1.1444E-07 | 3.5355E-09 |     |
| 3                       | COREA1 | 9.8319E-04 | 1.9947E-02 | 5.3161E-04 | 3.9843E-04 | 2.9412E-04 | 1.0080E-04 | 4.4682E-05 | 2.2512E-07 | 1.2500E-09 |     |
| 4                       | COREA1 | 9.7462E-04 | 1.9921E-02 | 5.4766E-04 | 3.9767E-04 | 2.9114E-04 | 1.0120E-04 | 6.7787E-05 | 3.3849E-07 | 4.4194E-10 |     |
| 5                       | COREA2 | 9.6612E-04 | 1.9892E-02 | 5.6351E-04 | 3.9694E-04 | 2.8820E-04 | 1.0160E-04 | 9.0916E-05 | 4.5178E-07 | 1.5625E-10 |     |
| 6                       | COREA2 | 9.5798E-04 | 1.9866E-02 | 5.7856E-04 | 3.9626E-04 | 2.8540E-04 | 1.0198E-04 | 1.1331E-04 | 5.6105E-07 | 5.5243E-11 |     |
| PATH PATHB1             |        |            |            |            |            |            |            |            |            |            |     |
| 1                       | COREB1 | 1.0000E-04 | 2.0000E-02 | 1.0000E-03 | 1.0000E-05 | 1.0000E-05 | 1.0000E-05 | 1.0000E-12 | 1.0000E-12 | 2.0000E-08 |     |
| 2                       | COREB1 | 9.9556E-05 | 1.9986E-02 | 1.0064E-03 | 1.1050E-05 | 9.9436E-06 | 1.0003E-05 | 7.3431E-06 | 1.9032E-08 | 7.0711E-09 |     |
| 3                       | COREB1 | 9.9115E-05 | 1.9971E-02 | 1.0128E-03 | 1.2104E-05 | 9.8888E-06 | 1.0006E-05 | 1.4712E-05 | 2.9706E-08 | 2.5000E-09 |     |
| 4                       | COREB2 | 9.8675E-05 | 1.9957E-02 | 1.0191E-03 | 1.3162E-05 | 9.8358E-06 | 1.0009E-05 | 2.2106E-05 | 3.7427E-08 | 8.8388E-10 |     |
| 5                       | COREB2 | 9.8165E-05 | 1.9940E-02 | 1.0264E-03 | 1.4397E-05 | 9.7760E-06 | 1.0012E-05 | 3.0771E-05 | 4.5102E-08 | 3.1250E-10 |     |
| 6                       | COREB2 | 9.7658E-05 | 1.9924E-02 | 1.0336E-03 | 1.5638E-05 | 9.7185E-06 | 1.0015E-05 | 3.9469E-05 | 5.2409E-08 | 1.1049E-10 |     |
| PATH PATHB2             |        |            |            |            |            |            |            |            |            |            |     |
| 1                       | COREB2 | 1.0000E-04 | 2.0000E-02 | 1.0000E-03 | 1.0000E-05 | 1.0000E-05 | 1.0000E-05 | 1.0000E-12 | 1.0000E-12 | 2.0000E-08 |     |
| 2                       | COREB2 | 9.9483E-05 | 1.9983E-02 | 1.0074E-03 | 1.1220E-05 | 9.9344E-06 | 1.0003E-05 | 8.5756E-06 | 2.0027E-08 | 7.0711E-09 |     |
| 3                       | COREB2 | 9.8969E-05 | 1.9967E-02 | 1.0148E-03 | 1.2446E-05 | 9.8711E-06 | 1.0007E-05 | 1.7186E-05 | 3.1698E-08 | 2.5000E-09 |     |
| 4                       | COREB1 | 9.8457E-05 | 1.9950E-02 | 1.0221E-03 | 1.3678E-05 | 9.8101E-06 | 1.0010E-05 | 2.5831E-05 | 4.0416E-08 | 8.8388E-10 |     |
| 5                       | COREB1 | 9.8021E-05 | 1.9936E-02 | 1.0284E-03 | 1.4742E-05 | 9.7595E-06 | 1.0013E-05 | 3.3262E-05 | 4.7095E-08 | 3.1250E-10 |     |
| 6                       | COREB1 | 9.7586E-05 | 1.9922E-02 | 1.0346E-03 | 1.5811E-05 | 9.7105E-06 | 1.0015E-05 | 4.0719E-05 | 5.3406E-08 | 1.1049E-10 |     |
| PATH PATHC1             |        |            |            |            |            |            |            |            |            |            |     |
| 1                       | COREC1 | 1.0000E-04 | 2.0000E-02 | 1.5000E-03 | 8.0000E-04 | 4.0000E-04 | 1.0000E-04 | 1.0000E-12 | 1.0000E-12 | 3.0000E-08 |     |
| 2                       | COREC1 | 9.9785E-05 | 1.9993E-02 | 1.5014E-03 | 7.9980E-04 | 3.9914E-04 | 1.0015E-04 | 6.4440E-06 | 4.6548E-08 | 1.0607E-08 |     |
| 3                       | COREC2 | 9.9571E-05 | 1.9986E-02 | 1.5028E-03 | 7.9961E-04 | 3.9829E-04 | 1.0029E-04 | 1.2888E-05 | 8.0598E-08 | 3.7500E-09 |     |
| 4                       | COREC2 | 9.9273E-05 | 1.9977E-02 | 1.5048E-03 | 7.9934E-04 | 3.9709E-04 | 1.0050E-04 | 2.1883E-05 | 1.2120E-07 | 1.3258E-09 |     |
| 5                       | COREC3 | 9.8975E-05 | 1.9968E-02 | 1.5067E-03 | 7.9908E-04 | 3.9590E-04 | 1.0070E-04 | 3.0878E-05 | 1.6032E-07 | 4.6875E-10 |     |
| 6                       | COREC3 | 9.8680E-05 | 1.9958E-02 | 1.5086E-03 | 7.9882E-04 | 3.9473E-04 | 1.0090E-04 | 3.9821E-05 | 1.9876E-07 | 1.6573E-10 |     |
| PATH PATHC2             |        |            |            |            |            |            |            |            |            |            |     |
| 1                       | COREC2 | 1.0000E-04 | 2.0000E-02 | 1.5000E-03 | 8.0000E-04 | 4.0000E-04 | 1.0000E-04 | 1.0000E-12 | 1.0000E-12 | 3.0000E-08 |     |
| 2                       | COREC2 | 9.9700E-05 | 1.9991E-02 | 1.5020E-03 | 7.9973E-04 | 3.9880E-04 | 1.0021E-04 | 8.9968E-06 | 5.7465E-08 | 1.0607E-08 |     |
| 3                       | COREC3 | 9.9401E-05 | 1.9981E-02 | 1.5039E-03 | 7.9946E-04 | 3.9760E-04 | 1.0041E-04 | 1.7993E-05 | 1.0247E-07 | 3.7500E-09 |     |
| 4                       | COREC3 | 9.9104E-05 | 1.9972E-02 | 1.5059E-03 | 7.9920E-04 | 3.9642E-04 | 1.0061E-04 | 2.6937E-05 | 1.4292E-07 | 1.3258E-09 |     |
| 5                       | COREC1 | 9.8809E-05 | 1.9962E-02 | 1.5078E-03 | 7.9894E-04 | 3.9524E-04 | 1.0082E-04 | 3.5880E-05 | 1.8188E-07 | 4.6875E-10 |     |
| 6                       | COREC1 | 9.8597E-05 | 1.9956E-02 | 1.5092E-03 | 7.9875E-04 | 3.9440E-04 | 1.0096E-04 | 4.2322E-05 | 2.0956E-07 | 1.6573E-10 |     |
| PATH PATHC3             |        |            |            |            |            |            |            |            |            |            |     |
| 1                       | COREC3 | 1.0000E-04 | 2.0000E-02 | 1.5000E-03 | 8.0000E-04 | 4.0000E-04 | 1.0000E-04 | 1.0000E-12 | 1.0000E-12 | 3.0000E-08 |     |
| 2                       | COREC3 | 9.9702E-05 | 1.9991E-02 | 1.5020E-03 | 7.9973E-04 | 3.9881E-04 | 1.0020E-04 | 8.9453E-06 | 5.7265E-08 | 1.0607E-08 |     |
| 3                       | COREC1 | 9.9404E-05 | 1.9981E-02 | 1.5039E-03 | 7.9947E-04 | 3.9762E-04 | 1.0041E-04 | 1.7890E-05 | 1.0207E-07 | 3.7500E-09 |     |
| 4                       | COREC1 | 9.9191E-05 | 1.9974E-02 | 1.5053E-03 | 7.9927E-04 | 3.9577E-04 | 1.0055E-04 | 2.4333E-05 | 1.3176E-07 | 1.3258E-09 |     |
| 5                       | COREC2 | 9.8978E-05 | 1.9968E-02 | 1.5067E-03 | 7.9908E-04 | 3.9592E-04 | 1.0070E-04 | 3.0776E-05 | 1.5992E-07 | 4.6875E-10 |     |
| 6                       | COREC2 | 9.8681E-05 | 1.9958E-02 | 1.5086E-03 | 7.9882E-04 | 3.9474E-04 | 1.0090E-04 | 3.9770E-05 | 1.9856E-07 | 1.6573E-10 |     |

**Figure 3-66. Stage Density Excerpt for the Three Region Equilibrium Shuffling Test**

Given the TRACE concentrations behave as expected, the next aspect to check is to verify that the region assigned within the path is correct according to the input. Comparing Figure 3-66 to Figure 3-65, one can verify that for each specified path, the stage output corresponds to the inputted region for that stage. To check that each region has the correct atom density, one can again inspect the REBUS

output for the atom densities used in the neutronics calculations of each problem. As stated previously, for each region, the composition is a direct combination of all materials that are assigned to that position for a given stage. Figure 3-67 displays the first atom density excerpt for the nine regions in the problem.

**Table 3-38. TRACE Atom Density Results for the Equilibrium Fuel Shuffling Test**

| Time<br>(days) | FUELA      |            | FUELB      |            | FUELc      |            |
|----------------|------------|------------|------------|------------|------------|------------|
|                | REBUS      | Formula    | REBUS      | Formula    | REBUS      | Formula    |
| 0.0            | 1.0000E-08 | 1.0000E-08 | 2.0000E-08 | 2.0000E-08 | 3.0000E-08 | 3.0000E-08 |
| 1.5            | 3.5355E-09 | 3.5356E-09 | 7.0711E-09 | 7.0711E-09 | 1.0607E-08 | 1.0607E-08 |
| 3.0            | 1.2500E-09 | 1.2500E-09 | 2.5000E-09 | 2.5000E-09 | 3.7500E-09 | 3.7500E-09 |
| 4.5            | 4.4194E-10 | 4.4195E-10 | 8.8388E-10 | 8.8390E-10 | 1.3258E-09 | 1.3258E-09 |
| 6.0            | 1.5625E-10 | 1.5625E-10 | 3.1250E-10 | 3.1251E-10 | 4.6875E-10 | 4.6876E-10 |
| 7.5            | 5.5243E-11 | 5.5244E-11 | 1.1049E-10 | 1.1049E-10 | 1.6573E-10 | 1.6573E-10 |

```

FCC004 11.3114 04/10/20          ABURN: Hexagonal 3D Test Problem          PAGE    295
          ATOM DENSITIES USED IN THE NEUTRONICS SOLUTION AT TIME NODE 0 AT 0.000000000E+00 DAYS.
          REGION COREA1 ZONE 2
aNA / 1.00000E-02  aFE / 2.00000E-02  a016 / 1.60000E-02  aPU239/ 1.61799E-03  aU238 / 5.98001E-02
aMAGIC/ 7.71948E-09  aU235 / 2.93703E-03  aPU242/ 3.02977E-04  aLFP / 1.68735E-04  aDUMP / 8.40902E-07
aPU240/ 1.19426E-03  aPU241/ 8.78061E-04

          REGION COREA2 ZONE 3
aNA / 1.00000E-02  aFE / 2.00000E-02  a016 / 1.60000E-02  aPU239/ 1.61934E-03  aU238 / 5.97979E-02
aMAGIC/ 7.71948E-09  aU235 / 2.93634E-03  aPU242/ 3.03011E-04  aLFP / 1.70580E-04  aDUMP / 8.50514E-07
aPU240/ 1.19421E-03  aPU241/ 8.77819E-04

          REGION COREA3 ZONE 4
aNA / 1.00000E-02  aFE / 2.00000E-02  a016 / 1.60000E-02  aPU239/ 1.61808E-03  aU238 / 5.97999E-02
aMAGIC/ 7.71948E-09  aU235 / 2.93693E-03  aPU242/ 3.02979E-04  aLFP / 1.69051E-04  aDUMP / 8.41802E-07
aPU240/ 1.19425E-03  aPU241/ 8.78034E-04

          REGION COREB1 ZONE 5
bNA / 1.00000E-02  bFE / 2.00000E-02  b016 / 1.60000E-02  bPU239/ 2.03476E-03  bU238 / 3.99215E-02
bMAGIC/ 1.02926E-08  bU235 / 1.97578E-04  bPU242/ 2.00156E-05  bLFP / 4.06224E-05  bDUMP / 6.32185E-08
bPU240/ 2.57948E-05  bPU241/ 1.97042E-05

          REGION COREB2 ZONE 6
bNA / 1.00000E-02  bFE / 2.00000E-02  b016 / 1.60000E-02  bPU239/ 2.03377E-03  bU238 / 3.99238E-02
bMAGIC/ 1.02926E-08  bU235 / 1.97650E-04  bPU242/ 2.00152E-05  bLFP / 3.93693E-05  bDUMP / 6.22215E-08
bPU240/ 2.56210E-05  bPU241/ 1.97120E-05

          REGION COREC1 ZONE 7
cNA / 1.00000E-02  cFE / 2.00000E-02  c016 / 1.60000E-02  cPU239/ 4.51380E-03  cU238 / 5.99335E-02
cMAGIC/ 2.31584E-08  cU235 / 2.97893E-04  cPU242/ 3.01443E-04  cLFP / 6.34342E-05  cDUMP / 3.35908E-07
cPU240/ 2.39811E-03  cPU241/ 1.19158E-03

          REGION COREC2 ZONE 8
cNA / 1.00000E-02  cFE / 2.00000E-02  c016 / 1.60000E-02  cPU239/ 4.51242E-03  cU238 / 5.99401E-02
cMAGIC/ 2.31584E-08  cU235 / 2.98102E-04  cPU242/ 3.01299E-04  cLFP / 5.71565E-05  cDUMP / 3.08873E-07
cPU240/ 2.39829E-03  cPU241/ 1.19242E-03

          REGION COREC3 ZONE 9
cNA / 1.00000E-02  cFE / 2.00000E-02  c016 / 1.60000E-02  cPU239/ 4.51355E-03  cU238 / 5.99347E-02
cMAGIC/ 2.31584E-08  cU235 / 2.97931E-04  cPU242/ 3.01417E-04  cLFP / 6.22870E-05  cDUMP / 3.30869E-07
cPU240/ 2.39814E-03  cPU241/ 1.19173E-03

```

**Figure 3-67. Atom Density Excerpt for the Three Region Equilibrium Shuffling Test**

Focusing on the U235 content in COREC2, the REBUS value is 2.98102E-04. From Figure 3-66 one can identify the U235 stage atom densities assigned to COREC2 that sum to 5.96203E-04, highlighted in green, which is exactly twice that of the REBUS atom density. For COREB1, one finds the sum is 5.92735E-04 which is exactly 3 times that of the REBUS value of 1.97578E-04. All of the atom densities for the remaining isotopes follow the same pattern. The factor of 2 and 3 comes from the fact that for a given path, the material is assigned to the same region for 2 and 3 stages. Thus one can understand that REBUS is, within a path, computing the average composition assigned to a given region but between paths it is simply summing them. This is consistent with the manual and the expected behavior. As an example, for a primary zone assignment, the composition is assigned to multiple stages within a given path and the composition is the simple average. For shuffling, those paths that intersect are assumed to be a simple sum and thus one should adjust the atom density of

the various zones by the fraction of the region that the composition will be assigned which turns out to be 1/3 for the COREA and COREC groupings and 1/2 for the COREB grouping. In this manner, the total loading would be consistent. This approach was not taken for this particular input as the existing input is sufficient to check the logic of the software.

The other time points were also checked and the atom density output excerpt was consistent with the stage densities reported for those time points. The total U235 loading can also be checked where the total loading from the output at 0.0 days is 6.85099E+01 kg and at 1.5 days is 6.80040E+01 kg. This yields a total U235 mass change of 506 g which is consistent with the previous calculations. The larger core and higher loading causes the  $k_{eff}$  results to be higher than those observed in previous problems. There are no additional checks to perform on card type 11 or card type 35 as the preceding verification work demonstrates that all possible options and usages of the input cards are working properly. This completes verification of task a) of category 3 as described in Table 3-25.

### 3.5.2.4 Verification that Burnup Limits Are Applied Correctly

Task b) is the next task to verify from Table 3-25 which deals with the burnup limits and how they can be used to impact the cycle length and enrichment. By design, this input requires the use of card types 5, 6, 7, and 8. Burnup limits are typically applied to equilibrium problems and not applied to non-equilibrium problems (use of card type 35). It can, however, be applied to non-equilibrium calculations with repetitive fuel management schemes (card type 11 non-equilibrium calculations), but this is rather expensive as REBUS is effectively rerunning the entire calculation multiple times to achieve convergence on the cycle length. The only use of burnup limits of interest for this verification work are those applied to equilibrium cycle analysis.

In order for this input specification to be verified, the table of burnup data must also be verified. Card type 05 defines a Burnup Test Group as a selection of PATH inputs provided by the user. Card type 06 defines the burnup limits applied to each Burnup Test Group defined in card type 05. Card type 07 allows the user to define the isotopes to include in the numerator of burnup and card type 08 the denominator. Burnup is defined as the total number of atoms destroyed divided by the total number of atoms initially present. By rule, only those isotopes included in the depletion chain can be considered as part of the burnup calculation. The default setup is to define both the numerator and denominator in terms of any isotopes from the depletion chain that are fissionable.

To test out the input specification, the default burnup definition will be tested followed by a user defined specification of burnup. The easiest problem to choose for testing is the Primary Zone test problems studied in Section 3.5.2.3.1 or Section 3.5.2.3.3. Because the enrichment can be altered by a modification to the cycle length, the test cases must also consider a true enrichment search problem. Due to the difficulty of investigating a multi-stage approach, the verification of this work will primarily focus on modifications to the input from Section 3.5.2.3.1.

The burnup that REBUS reports is not the typical definition of burnup and was chosen by the software developers for convenience. To understand this, the atom fraction burnup  $b_{m,t}$  is typically for a given material (fuel assembly)  $m$ , and time point  $t$ , as

$$b_{m,t} = 1 - \frac{\sum_{i=1}^I N_{t,i,m} \cdot V_m}{\sum_{i=1}^I N_{0,i,m} \cdot V_m}. \quad (46)$$

In this equation, the volume associated with the material is introduced but it cancels out as it is in the numerator and denominator. The  $N_{t,i,r}$  represents the atom density of a depleting isotope  $i$  at a given time point in a given material. The isotopes typically of interest in this burnup calculation are

actinides such as U-235, Pu-239, etc... It is important to note that REBUS is arbitrary and one could just as easily include B-10 in the burnup definition via input. By default REBUS will only consider fissionable isotopes. As stated, REBUS calculates the burnup in a different manner than the simple equation above which is detailed elsewhere [1-3]. Verifying the REBUS approach is non-trivial and is not done here for brevity.

The alternative way to represent burnup is in MWD/MT. Conceptually this is calculated using the formula

$$B_{m,t} = \frac{\frac{1}{t} \int_0^t P_m(t) dt}{\sum_{i=1}^I \frac{N_{0,i,m}}{C_{Av}} \cdot A_i \cdot V_m} \quad (47)$$

In this equation, the power applied to the material over the time period of interest is integrated for the numerator where REBUS only allows an average power to be applied for a given time step. The denominator consists of the initial total mass of the isotopes of interest (typically all actinides) in the material. The constant  $C_{Av}$  is Avogadro's number while  $A_i$  is the atom mass. Note that the burnup definition of  $B_{m,t}$  *is not* equivalent to that of  $b_{m,t}$ . They are in fact two different ways to assess the depletion of the material.

To demonstrate how broken the REBUS output can be, given poor user input, the stated verification test problem was executed with several different cycle lengths. Using the converged atom density results from REBUS, known to be correct from the previous verification work, the formula results above are compared with the REBUS reported values for each region in Table 3-39.

Table 3-39. REBUS Burnup Output Comparisons Against Simple Formula

| Cycle Length (days) | Region | Atom Burnup (%) |         | Error  | Burnup MWD/MT |        |
|---------------------|--------|-----------------|---------|--------|---------------|--------|
|                     |        | Formula         | REBUS   |        | Formula       | REBUS  |
| 0.25                | COREA  | 0.0649          | 0.0637  | 1.80%  | 68.3          | 602    |
|                     | COREB  | 0.0371          | 0.0367  | 1.14%  | 6.0           | 346    |
|                     | COREC  | 0.0400          | 0.0405  | -1.20% | 3.9           | 382    |
| 1.0                 | COREA  | 0.2549          | 0.2552  | -0.12% | 273.2         | 2410   |
|                     | COREB  | 0.1486          | 0.1472  | 0.92%  | 24.0          | 1390   |
|                     | COREC  | 0.1642          | 0.1627  | 0.91%  | 15.5          | 1535   |
| 10                  | COREA  | 2.6204          | 2.6190  | 0.05%  | 2720.1        | 24731  |
|                     | COREB  | 1.5506          | 1.5506  | 0.00%  | 243.4         | 14639  |
|                     | COREC  | 1.7448          | 1.7445  | 0.02%  | 162.8         | 16458  |
| 30                  | COREA  | 11.5723         | 11.5708 | 0.01%  | 7947.4        | 109262 |
|                     | COREB  | 7.7590          | 7.7573  | 0.02%  | 790.3         | 73234  |
|                     | COREC  | 9.3368          | 9.3362  | 0.01%  | 640.2         | 88082  |

Before starting the analysis of these results, it is important to note that the user input has broken REBUS and that the actual formulas internal to REBUS are not incorrect. Starting with the atom percent burnup, the result shows very small errors at each time point. In this particular example, the error becomes smaller as the cycle length is increased. That behavior is not guaranteed for all problems and is just a circumstance of this one. Overall the atom fraction burnup results are acceptable. One should understand that the simple formula for  $b_{m,t}$  is the typical quantity that the user wants and is relatively easy to hand calculate given the stage density output from REBUS. The

actual formula used internal to REBUS constitutes a slight approximation to the formula shown above for  $b_{m,t}$  and thus the errors occur.

For the  $B_{m,t}$  results in Table 3-39, one finds that all of the REBUS and formula results are in strong disagreement. The most important aspect is that COREB and COREA are separated by a factor of  $\sim 2$  in the REBUS output while the formula above indicates that COREA should have an order of magnitude more burnup. Looking at the power production in the three regions ( $\sim 87$  MW,  $\sim 7$  MW, and  $\sim 5$  MW, respectively), one finds that the formula based results are more consistent with the actual burnup expression. Internal to REBUS, the atom percent burnup is simply converted into the other units assuming the power emission from all actinides is similar. This can be seen in the table of provided data as the ratio between the REBUS atom % and MWD/MT results have almost identically the same value for all points in the table ( $\sim 9440$ ).

The broken aspect of the user input is that only the U235 isotope produced power but all of the other actinides were fissionable. This input is thus not consistent with the assumptions of proper input by REBUS and the erroneous output occurs for  $B_{m,t}$ . However, because REBUS is using a simple conversion, one should understand that  $B_{m,t}$  will never be exact relative to the equation shown above for  $B_{m,t}$ . Similarly, the atom fraction burnup in REBUS is also broken as it considers all of the isotopes in the depletion chain but the imposition that a single isotope produces power also alters the conventional interpretation of the atom fraction burnup. In this context, the burnup  $b_{m,t}$  and  $B_{m,t}$  should only consider the U235 isotope which would lead to a result that is similar to that in REBUS.

For regular reactor input, all of the actinides would produce power and the atom fraction calculations would be very accurate (typically less than 0.01% error). The REBUS output for the  $B_{m,t}$  burnup is still not consistent with the equation shown above, but it is reasonably close enough for users to make decisions on the reactor fuel cycle. Overall, the  $B_{m,t}$  representation of burnup in the REBUS output should be used with caution. This aspect will be detailed later in this report when the tables of output from REBUS are verified more thoroughly.

Returning to the input from Figure 3-49, the REBUS output that is needed to verify this aspect is collected in Figure 3-68. Note that the volumes of each region are  $3.63731E+04$  cm<sup>3</sup> as discussed in the earlier section. From Figure 3-68, one can see that isotopes U235, U238, PU239, PU240, PU241, and PU242 are the only fissionable isotopes in the depletion chain. Using the formula for  $b_{m,t}$ , the burnup was calculated for all time points (not shown for brevity) and tabulated in Table 3-40. As can be seen, the burnup has errors consistent with those displayed in the previous results of Table 3-39. Take note that the reported burnup for each time step is different and thus a non-linear relationship is present which is the typical outcome for reactor problems with higher actinides.

Given that the REBUS atom burnup output is used to restrict the cycle length, the first test will focus on specifying a limit on just the COREB region where the card type 05 and 06 data is provided on the left in Figure 3-69. As can be seen, limits are given for all paths even though it is not actually necessary. The output excerpt of interest from this calculation is displayed in Figure 3-70. As stated in the output, the cycle length was adjusted from 4.5 days to  $\sim 3.83$  days. The atom percent burnup for all three regions is consistently reduced from the values in Table 3-40. No effort was made to verify that the stage density outputs for the three regions yield the reported burnup. Instead, the base input (without a burnup constraint) was modified to have the reported cycle length and the burnup output edit is shown in Figure 3-71. As can be seen, the two results for atom burnup are identical. This will only occur if the conditions for the two problems are identical.

```
FCI002 11.3114 04/10/20 PAGE 83
...
ACTIVE ISOTOPE SPECIFICATIONS
  INCLUDED IN          BURNUP
ISOTOPE    MASS    USER SPECIFIED BREEDING RATIO FISSIONABLE DEPENDENT
U235      235.1170E+00 YES           NO           YES           NO
U238      238.1250E+00 YES           YES          YES          NO
PU239     239.1270E+00 YES           NO           YES          NO
PU240     240.1290E+00 YES           YES          YES          NO
PU241     241.1320E+00 YES           NO           YES          NO
PU242     242.1340E+00 YES           YES          YES          NO
LFPSS     237.0000E+00 YES           NO           NO           NO
DUMP      236.0000E+00 YES           NO           NO           NO
TRACE     100.0000E+00 NO            NO           NO           NO
...
FCC004 11.3114 04/10/20 PAGE 361
...
BEGINNING OF BURN CYCLE 1
  PATH PATH1
+      U235      U238      PU239      PU240      PU241      PU242      LFPSS      DUMP      TRACE
1  COREA  1.0000E-03  2.0000E-02  5.0000E-04  4.0000E-04  3.0000E-04  1.0000E-04  1.0000E-12  1.0000E-12  1.0000E-08
  PATH PATH2
1  COREB  1.0000E-04  2.0000E-02  1.0000E-03  1.0000E-05  1.0000E-05  1.0000E-05  1.0000E-12  1.0000E-12  2.0000E-08
  PATH PATH3
1  COREC  1.0000E-04  2.0000E-02  1.5000E-03  8.0000E-04  4.0000E-04  1.0000E-04  1.0000E-12  1.0000E-12  3.0000E-08
...
FCC004 11.3114 04/10/20 PAGE 503
...
REACTOR CONDITIONS AFTER 3 BURNUP SUBSTEPS AT TIME = 4.500000000E+00 DAYS
  PATH PATH1
+      U235      U238      PU239      PU240      PU241      PU242      LFPSS      DUMP      TRACE
1  COREA  9.0644E-04  1.9673E-02  6.8466E-04  3.9263E-04  2.6754E-04  1.0457E-04  2.7012E-04  1.3632E-06  4.4194E-10
  PATH PATH2
1  COREB  9.2168E-05  1.9726E-02  1.1114E-03  3.0156E-05  9.2326E-06  1.0041E-05  1.5078E-04  1.3198E-07  8.8388E-10
  PATH PATH3
1  COREC  9.4480E-05  1.9808E-02  1.5439E-03  7.9615E-04  3.7812E-04  1.0408E-04  1.7435E-04  8.2259E-07  1.3258E-09
...
FCC004 11.3114 04/10/20 ABURN: Hexagonal 3D Test Problem PAGE 517
  CUMULATIVE BURNUP AFTER 3 BURNUP SUBSTEPS, FROM 0.000000000E+00 DAYS TO 4.500000000E+00 DAYS.
  AVERAGE BURNUP (ATOM %) OF EACH STAGE OF EACH PATH
STAGE/REGION 1/COREA
  1.21129E+00
STAGE/REGION 1/COREB
  7.13605E-01
STAGE/REGION 1/COREC
  7.61361E-01
...

```

Figure 3-68. REBUS Output Excerpt for Burnup in Equilibrium Problems

Table 3-40. Atom % Burnup Output Verification of Default Setup in Equilibrium Problems

| Region | 1.5 days |        | 3.0 days |        | 4.5 days |        |
|--------|----------|--------|----------|--------|----------|--------|
|        | Formula  | REBUS  | Formula  | REBUS  | Formula  | REBUS  |
| COREA  | 0.3895   | 0.3891 | 0.7948   | 0.7926 | 1.2160   | 1.2113 |
| COREB  | 0.2263   | 0.2257 | 0.4631   | 0.4633 | 0.7146   | 0.7136 |
| COREC  | 0.2461   | 0.2462 | 0.5010   | 0.4998 | 0.7654   | 0.7614 |

|                       |                    |
|-----------------------|--------------------|
| UNFORM=A.BURN         | UNFORM=A.BURN      |
| ...                   | ...                |
| 05 BLIMIT PATH2       | 05 LIMIT1 PATH1    |
| 05 NLIMIT PATH1 PATH3 | 05 LIMIT2 PATH2    |
| 06 BLIMIT 0.006       | 05 LIMIT3 PATH3    |
| 06 NLIMIT 0.90        | 06 LIMIT1 0.013324 |
| ...                   | 06 LIMIT2 0.007850 |
|                       | 06 LIMIT3 0.008375 |
|                       | ...                |

Figure 3-69. REBUS Inputs for Applying Burnup Limits to the Equilibrium Problems

```

FCC004 11.3114 04/10/20      ABURN: Hexagonal 3D Test Problem      PAGE  565
                                CUMULATIVE BURNUP AFTER 3 BURNUP SUBSTEPS, FROM 0.000000000E+00 DAYS TO 3.830006451E+00 DAYS.
                                AVERAGE BURNUP (ATOM %) OF EACH STAGE OF EACH PATH

STAGE/REGION 1/COREA
              1.02232E+00
STAGE/REGION 1/COREB
              6.00165E-01
STAGE/REGION 1/COREC
              6.43491E-01
...
FCC004 11.3114 04/10/20      ABURN: Hexagonal 3D Test Problem      PAGE  566
                                BURNUP CALCULATION TO OBTAIN CONVERGENCE TO THE SPECIFIED BURNUP CONSTRAINTS

                                FOR BURN CYCLE TIME OF 3.830006451E+00 DAYS
PATH OR      SPECIFIED      ACTUAL      ALLOWABLE      ACTUAL
TEST GROUP   BURNUP LIMIT   DISCHARGE BURNUP  ERROR (EPSG)  ERROR
BLIMIT       6.00000E-03   6.00165E-03   1.00000E-05   -1.65370E-06
NLIMIT       9.00000E-01   8.30389E-03   1.00000E-05   8.91696E-01
...

```

**Figure 3-70. REBUS Output Excerpt for PATH2 Burnup Limited Equilibrium Problem**

```

FCC004 11.3114 04/10/20      ABURN: Hexagonal 3D Test Problem      PAGE  517
                                CUMULATIVE BURNUP AFTER 3 BURNUP SUBSTEPS, FROM 0.000000000E+00 DAYS TO 3.837083372E+00 DAYS.
                                AVERAGE BURNUP (ATOM %) OF EACH STAGE OF EACH PATH

STAGE/REGION 1/COREA
              1.02232E+00
STAGE/REGION 1/COREB
              6.00165E-01
STAGE/REGION 1/COREC
              6.43491E-01
...

```

**Figure 3-71. REBUS Output Excerpt for Adjusted 3.3837 Day Cycle Length Problem**

The next test is to verify that REBUS will increase the cycle length based upon the burnup limits. In this approach, the burnup limit input on the right of Figure 3-69 is used with a guess of 4.5 days. The limits were obtained by multiplying the REBUS reported atom percent burnup outputs in Table 3-40 by 1.1. As a consequence, one can expect the cycle length to increase slightly. Based upon the trend in Table 3-40, one would expect PATH2 to limit the burnup (step 2 to step 3 burnup ratios are 1.53, 1.54, and 1.52 for the three core regions, respectively). The REBUS output excerpt for this case is provided in Figure 3-72 and one can see that PATH2 does in fact become the limiting case. The same modification of the cycle length without a burnup constraint was used to verify that the searched cycle length was identically what was expected and is not included here for brevity.

```

FCC004 11.3114 04/10/20      ABURN: Hexagonal 3D Test Problem      PAGE  565
                                CUMULATIVE BURNUP AFTER 3 BURNUP SUBSTEPS, FROM 0.000000000E+00 DAYS TO 4.914482440E+00 DAYS.
                                AVERAGE BURNUP (ATOM %) OF EACH STAGE OF EACH PATH

STAGE/REGION 1/COREA
              1.32981E+00
STAGE/REGION 1/COREB
              7.85132E-01
STAGE/REGION 1/COREC
              8.35132E-01
...
FCC004 11.3114 04/10/20      ABURN: Hexagonal 3D Test Problem      PAGE  566
                                BURNUP CALCULATION TO OBTAIN CONVERGENCE TO THE SPECIFIED BURNUP CONSTRAINTS

                                FOR BURN CYCLE TIME OF 4.914482440E+00 DAYS
PATH OR      SPECIFIED      ACTUAL      ALLOWABLE      ACTUAL
TEST GROUP   BURNUP LIMIT   DISCHARGE BURNUP  ERROR (EPSG)  ERROR
LIMIT1       1.33240E-02   1.32981E-02   1.00000E-05   2.59394E-05
LIMIT2       7.85000E-03   7.85132E-03   1.00000E-05   -1.31504E-06
LIMIT3       8.37500E-03   8.35132E-03   1.00000E-05   2.36818E-05
...

```

**Figure 3-72. REBUS Output Excerpt for Multiple Limit Burnup Equilibrium Problem**

The next check of the burnup limit has all three paths included on a single card type 05 and a single burnup limit of 0.08 applied to it on card type 06. The REBUS output excerpt of interest is included in Figure 3-73. As seen, REBUS reduces the cycle length to meet the burnup constraint. One problem is where REBUS comes up with the discharge burnup of 0.800197%. The simple (volume) average of

the three region discharge burnups results in a 0.798% average burnup which is relatively close to the REBUS outputted result. The actual approach used in REBUS sums the numerator and denominator over all paths (materials) in the equation for  $b_{m,t}$  shown earlier. This is not exactly the volume averaged burnup and makes the user's use of the burnup constraint somewhat more difficult. However, as seen in this example, the simple average result is still close to the REBUS computed value and within the typical uncertainty for depletion calculations and thus acceptable for most users. Using the stage density output in Figure 3-73 and the 0.0 day stage density from Figure 3-68, one can compute the average burnup of the three paths similar to REBUS as 0.8024% which is also close to the 0.8002% result reported in Figure 3-73 but not exact. Note that the actual number reported in REBUS cannot be calculated directly from the REBUS output as was the case with the atom percent burnup itself. Consequently, these two hand calculations are deemed sufficient for the verification purposes of this manuscript.

```

FCC004 11.3114 04/10/20 PAGE 551
...
REACTOR CONDITIONS AFTER 3 BURNUP SUBSTEPS AT TIME = 4.037238142E+00 DAYS
ATOM DENSITIES (IN ATOMS/BARN-CM.) OF ACTIVE ISOTOPES IN EACH STAGE OF EACH PATH
+ PATH PATH1
+ 1 COREA U235 U238 PU239 PU240 PU241 PU242 LFPSS DUMP TRACE
  9.1605E-04 1.9708E-02 6.6615E-04 3.9321E-04 2.7080E-04 1.0412E-04 2.4093E-04 1.2152E-06 6.0907E-10
  1 COREB 9.2979E-05 1.9755E-02 1.1002E-03 2.7937E-05 9.2888E-06 1.0037E-05 1.3417E-04 1.1953E-07 1.2181E-09
  1 COREC 9.5056E-05 1.9829E-02 1.5394E-03 7.9653E-04 3.8037E-04 1.0366E-04 1.5567E-04 7.3562E-07 1.8272E-09
...
FCC004 11.3114 04/10/20 ABURN: Hexagonal 3D Test Problem PAGE 565
CUMULATIVE BURNUP AFTER 3 BURNUP SUBSTEPS, FROM 0.000000000E+00 DAYS TO 4.037238142E+00 DAYS.
AVERAGE BURNUP (ATOM %) OF EACH STAGE OF EACH PATH
STAGE/REGION 1/COREA 1.08043E+00
STAGE/REGION 1/COREB 6.34969E-01
STAGE/REGION 1/COREC 6.79769E-01
...
FCC004 11.3114 04/10/20 ABURN: Hexagonal 3D Test Problem PAGE 566
BURNUP CALCULATION TO OBTAIN CONVERGENCE TO THE SPECIFIED BURNUP CONSTRAINTS
...
FOR BURN CYCLE TIME OF 4.037238142E+00 DAYS
PATH OR SPECIFIED ACTUAL ALLOWABLE ACTUAL
TEST GROUP BURNUP LIMIT DISCHARGE BURNUP ERROR (EPSG) ERROR
LIMIT 8.00000E-03 8.00197E-03 1.00000E-05 -1.97412E-06
...

```

**Figure 3-73. REBUS Output Excerpt for Single Limit Burnup Equilibrium Problem**

Because equilibrium cycle problems do not allow assemblies to be placed into "storage," the only remaining test to consider is a multi-stage case where a burnup limit is placed on the residence time of a given material. As is typical, all fuel assemblies should have burnup limits applied to them, typically done individually as opposed to the average result as shown in the last test case. To demonstrate the use of Primary Zone and Fuel shuffling in the same input, this example modifies the previous geometry description to that shown in Figure 3-74.

Compared with the previous problem geometries, the COREA region in this example was split into two equal sized pieces (COREA1 and COREA2) and an additional assembly position was given to COREB. The important parts of the input changes are given in Figure 3-75. As seen, the FUELA composition was also duplicated into FUELA1 and FUELA2 and the primary zone ZFUELA was replaced with ZFUEL1 and ZFUEL2. In the card type 11 specification, the ZFUEL1 composition is assigned PATHA1 while ZFUEL2 is assigned PATHA2 and the secondary zone to region mapping is used to shuffle the compositions between the two regions with each stage. The FUELB composition was assigned to PATH2 and assumed to be composed of 7 stages while FUELc was assigned to PATH3 and assigned 8 stages. All of these actions have significant consequences on the power distribution.

From the provided input, the initial guess for the cycle length is 200 days. The burnup limits for each path shown were determined as slightly lower values than the computed values using a 200 day time period.

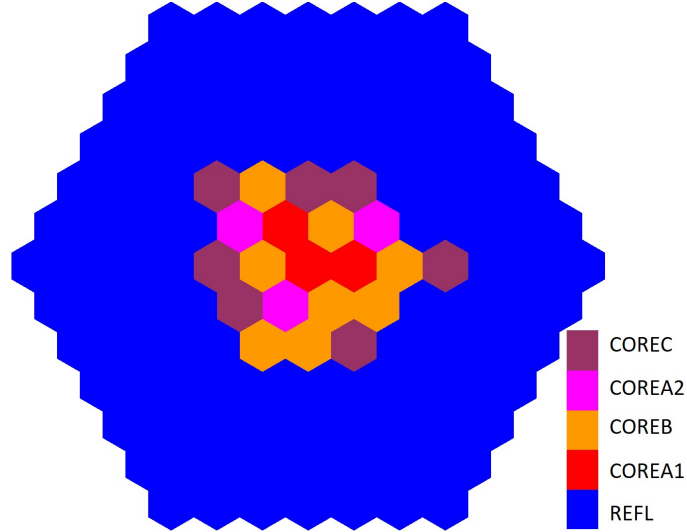


Figure 3-74. Geometry for Multi-stage Burnup Limited Equilibrium Problem

| UNIFORM=A.NIP3 |        |        |       |   |      |       |  |  |  | UNIFORM=A.BURN |        |         |       |        |        |   |   |  |  |
|----------------|--------|--------|-------|---|------|-------|--|--|--|----------------|--------|---------|-------|--------|--------|---|---|--|--|
| ...            |        |        |       |   |      |       |  |  |  | 03             | 0      | 0.00000 | 0.0   | 200.   | 1.0E-5 | 1 | 0 |  |  |
| 14             | FUELA1 | aNA    | 0.010 |   |      |       |  |  |  | ...            |        |         |       |        |        |   |   |  |  |
| 14             | FUELA1 | aO16   | 0.016 |   |      |       |  |  |  | 05             | LIMIT1 | PATHA1  |       |        |        |   |   |  |  |
| 14             | FUELA1 | aFE    | 0.02  |   |      |       |  |  |  | 05             | LIMIT2 | PATHA2  |       |        |        |   |   |  |  |
| 14             | FUELA1 | aU235  | 1.0   |   |      |       |  |  |  | 05             | LIMIT3 | PATH2   |       |        |        |   |   |  |  |
| 14             | FUELA1 | aU238  | 1.0   |   |      |       |  |  |  | 05             | LIMIT4 | PATH3   |       |        |        |   |   |  |  |
| 14             | FUELA1 | aPU239 | 1.0   |   |      |       |  |  |  | 06             | LIMIT1 |         | 0.02  |        |        |   |   |  |  |
| 14             | FUELA1 | aPU240 | 1.0   |   |      |       |  |  |  | 06             | LIMIT2 |         | 0.02  |        |        |   |   |  |  |
| 14             | FUELA1 | aPU241 | 1.0   |   |      |       |  |  |  | 06             | LIMIT3 |         | 0.011 |        |        |   |   |  |  |
| 14             | FUELA1 | aPU242 | 1.0   |   |      |       |  |  |  | 06             | LIMIT4 |         | 0.012 |        |        |   |   |  |  |
| 14             | FUELA1 | aLFP   | 1.0   |   |      |       |  |  |  | 11             | PATHA1 | 0       | 1     | FUELA1 | COREA1 |   |   |  |  |
| 14             | FUELA1 | aDUMP  | 1.0   |   |      |       |  |  |  | 11             | PATHA1 | 0       | 2     | FUELA1 | COREA2 |   |   |  |  |
| 14             | FUELA1 | aMAGIC | 1.0   |   |      |       |  |  |  | 11             | PATHA1 | 0       | 3     | FUELA1 | COREA1 |   |   |  |  |
| 14             | ZFUEL1 | FUELA1 | 1.0   |   |      |       |  |  |  | 11             | PATHA1 | 0       | 4     | FUELA1 | COREA2 |   |   |  |  |
| ...            |        |        |       |   |      |       |  |  |  | 11             | PATHA1 | 0       | 5     | FUELA1 | COREA1 |   |   |  |  |
| 14             | ZFUEL2 | FUELA2 | 1.0   |   |      |       |  |  |  | 11             | PATHA1 | 0       | 6     | FUELA1 | COREA2 |   |   |  |  |
| ...            |        |        |       |   |      |       |  |  |  | 11             | PATHA2 | 0       | 1     | FUELA2 | COREA2 |   |   |  |  |
| 15             | REFL   | REFL   |       |   |      |       |  |  |  | 11             | PATHA2 | 0       | 2     | FUELA2 | COREA1 |   |   |  |  |
| 15             | ZFUEL1 | COREA1 |       |   |      |       |  |  |  | 11             | PATHA2 | 0       | 3     | FUELA2 | COREA2 |   |   |  |  |
| 15             | ZFUEL2 | COREA2 |       |   |      |       |  |  |  | 11             | PATHA2 | 0       | 4     | FUELA2 | COREA1 |   |   |  |  |
| 15             | ZFUELB | COREB  |       |   |      |       |  |  |  | 11             | PATHA2 | 0       | 5     | FUELA2 | COREA2 |   |   |  |  |
| 15             | ZFUELc | COREC  |       |   |      |       |  |  |  | 11             | PATHA2 | 0       | 6     | FUELA2 | COREA1 |   |   |  |  |
| ...            |        |        |       |   |      |       |  |  |  | ...            |        |         |       |        |        |   |   |  |  |
| 30             | REFL   | 5      | 0     | 0 | 0.0  | 120.0 |  |  |  | 11             | PATH2  | 0       | 1     | FUELb  | ZFUELb |   |   |  |  |
| 30             | REFL   | 6      | 0     | 0 | 0.0  | 120.0 |  |  |  | 11             | PATH2  | 0       | 2     | FUELb  | ZFUELb |   |   |  |  |
| 30             | REFL   | 7      | 0     | 0 | 0.0  | 120.0 |  |  |  | 11             | PATH2  | 0       | 3     | FUELb  | ZFUELb |   |   |  |  |
| 30             | COREA1 | 1      | 0     | 0 | 30.0 | 90.0  |  |  |  | 11             | PATH2  | 0       | 4     | FUELb  | ZFUELb |   |   |  |  |
| 30             | COREA1 | 2      | 1     | 1 | 30.0 | 90.0  |  |  |  | 11             | PATH2  | 0       | 5     | FUELb  | ZFUELb |   |   |  |  |
| 30             | COREB  | 2      | 2     | 2 | 30.0 | 90.0  |  |  |  | 11             | PATH2  | 0       | 6     | FUELb  | ZFUELb |   |   |  |  |
| 30             | COREA1 | 2      | 3     | 3 | 30.0 | 90.0  |  |  |  | 11             | PATH2  | 0       | 7     | FUELb  | ZFUELb |   |   |  |  |
| 30             | COREB  | 2      | 4     | 4 | 30.0 | 90.0  |  |  |  | ...            |        |         |       |        |        |   |   |  |  |
| 30             | COREA2 | 2      | 5     | 5 | 30.0 | 90.0  |  |  |  | 11             | PATH3  | 0       | 1     | FUELc  | ZFUELc |   |   |  |  |
| 30             | COREB  | 2      | 6     | 6 | 30.0 | 90.0  |  |  |  | 11             | PATH3  | 0       | 2     | FUELc  | ZFUELc |   |   |  |  |
| 30             | COREB  | 3      | 1     | 1 | 30.0 | 90.0  |  |  |  | 11             | PATH3  | 0       | 3     | FUELc  | ZFUELc |   |   |  |  |
| 30             | COREA2 | 3      | 2     | 2 | 30.0 | 90.0  |  |  |  | 11             | PATH3  | 0       | 4     | FUELc  | ZFUELc |   |   |  |  |
| 30             | COREA2 | 3      | 3     | 3 | 30.0 | 90.0  |  |  |  | 11             | PATH3  | 0       | 5     | FUELc  | ZFUELc |   |   |  |  |
| 30             | COREC  | 3      | 4     | 4 | 30.0 | 90.0  |  |  |  | 11             | PATH3  | 0       | 6     | FUELc  | ZFUELc |   |   |  |  |
| 30             | COREC  | 3      | 5     | 5 | 30.0 | 90.0  |  |  |  | 11             | PATH3  | 0       | 7     | FUELc  | ZFUELc |   |   |  |  |
| 30             | COREC  | 3      | 6     | 6 | 30.0 | 90.0  |  |  |  | 11             | PATH3  | 0       | 8     | FUELc  | ZFUELc |   |   |  |  |
| ...            |        |        |       |   |      |       |  |  |  | ...            |        |         |       |        |        |   |   |  |  |

Figure 3-75. REBUS Input for the Multi-Stage Burnup Limited Equilibrium Problem

To simplify the comparison process, a single time step was used from 0.0 to ~200 days, the total power was reduced to 1 MW and the TRACE isotope decay constant was reduced by two orders of

magnitude. The stage density output for both time points is collected in Figure 3-76. It is noted that the expected behavior is that the atom density details of PATHA1 and PATHA2 should “match up” (as seen) at every other time point when both zones are subjected to the “same” conditions. The atom density of the actinides can be added together for the first stage of each path in the first time point and the last stage of each path in the last time point to compute the burnup. The calculated results resulting from the REBUS output are provided in Table 3-41. The REBUS results were extracted from the output, the excerpt of which is shown in Figure 3-77.

FCC004 11.3114 04/10/20

PAGE 296

| BEGINNING OF BURN CYCLE 1 |        |            |            |            |            |            |            |            |            |            |
|---------------------------|--------|------------|------------|------------|------------|------------|------------|------------|------------|------------|
| PATH PATHA1               |        |            |            |            |            |            |            |            |            |            |
| +                         |        | U235       | U238       | PU239      | PU240      | PU241      | PU242      | LFPPS      | DUMP       | TRACE      |
| 1                         | COREA1 | 1.0000E-03 | 2.0000E-02 | 5.0000E-04 | 4.0000E-04 | 3.0000E-04 | 1.0000E-04 | 1.0000E-12 | 1.0000E-12 | 1.0000E-08 |
| 2                         | COREA2 | 9.6939E-04 | 1.9900E-02 | 5.5741E-04 | 3.9699E-04 | 2.8936E-04 | 1.0144E-04 | 8.5053E-05 | 4.0577E-07 | 2.7728E-09 |
| 3                         | COREA1 | 9.4970E-04 | 1.9834E-02 | 5.9463E-04 | 3.9529E-04 | 2.8257E-04 | 1.0236E-04 | 1.4111E-04 | 6.7815E-07 | 7.6882E-10 |
| 4                         | COREA2 | 9.2063E-04 | 1.9734E-02 | 6.4788E-04 | 3.9298E-04 | 2.7269E-04 | 1.0367E-04 | 2.2661E-04 | 1.0863E-06 | 2.1318E-10 |
| 5                         | COREA1 | 9.0193E-04 | 1.9669E-02 | 6.8244E-04 | 3.9173E-04 | 2.6638E-04 | 1.0452E-04 | 2.8293E-04 | 1.3627E-06 | 5.9109E-11 |
| 6                         | COREA2 | 8.7433E-04 | 1.9570E-02 | 7.3179E-04 | 3.9005E-04 | 2.5722E-04 | 1.0571E-04 | 3.6880E-04 | 1.7787E-06 | 1.6389E-11 |
| PATH PATHA2               |        |            |            |            |            |            |            |            |            |            |
| 1                         | COREA2 | 1.0000E-03 | 2.0000E-02 | 5.0000E-04 | 4.0000E-04 | 3.0000E-04 | 1.0000E-04 | 1.0000E-12 | 1.0000E-12 | 1.0000E-08 |
| 2                         | COREA1 | 9.7969E-04 | 1.9933E-02 | 5.3891E-04 | 3.9801E-04 | 2.9289E-04 | 1.0098E-04 | 5.5878E-05 | 2.7386E-07 | 2.7728E-09 |
| 3                         | COREA2 | 9.4970E-04 | 1.9834E-02 | 5.9463E-04 | 3.9529E-04 | 2.8257E-04 | 1.0236E-04 | 1.4111E-04 | 6.7815E-07 | 7.6882E-10 |
| 4                         | COREA1 | 9.3041E-04 | 1.9768E-02 | 6.3075E-04 | 3.9378E-04 | 2.7597E-04 | 1.0325E-04 | 1.9731E-04 | 9.5151E-07 | 2.1318E-10 |
| 5                         | COREA2 | 9.0193E-04 | 1.9669E-02 | 6.8240E-04 | 3.9172E-04 | 2.6638E-04 | 1.0452E-04 | 2.8297E-04 | 1.3627E-06 | 5.9109E-11 |
| 6                         | COREA1 | 8.8361E-04 | 1.9603E-02 | 7.1592E-04 | 3.9064E-04 | 2.6026E-04 | 1.0533E-04 | 3.3940E-04 | 1.6412E-06 | 1.6389E-11 |
| PATH PATH2                |        |            |            |            |            |            |            |            |            |            |
| 1                         | COREB  | 1.0000E-04 | 2.0000E-02 | 1.0000E-03 | 1.0000E-05 | 1.0000E-05 | 1.0000E-05 | 1.0000E-12 | 1.0000E-12 | 2.0000E-08 |
| 2                         | COREB  | 9.8265E-05 | 1.9942E-02 | 1.0251E-03 | 1.4198E-05 | 9.7879E-06 | 1.0011E-05 | 3.0777E-05 | 3.8607E-08 | 5.5455E-09 |
| 3                         | COREB  | 9.6560E-05 | 1.9884E-02 | 1.0495E-03 | 1.8462E-05 | 9.6018E-06 | 1.0020E-05 | 6.1942E-05 | 6.6791E-08 | 1.5376E-09 |
| 4                         | COREB  | 9.4884E-05 | 1.9826E-02 | 1.0733E-03 | 2.2788E-05 | 9.4413E-06 | 1.0029E-05 | 9.3486E-05 | 9.2100E-08 | 4.2635E-10 |
| 5                         | COREB  | 9.3237E-05 | 1.9768E-02 | 1.0964E-03 | 2.7174E-05 | 9.3060E-06 | 1.0037E-05 | 1.2540E-04 | 1.1663E-07 | 1.1822E-10 |
| 6                         | COREB  | 9.1619E-05 | 1.9711E-02 | 1.1189E-03 | 3.1617E-05 | 9.1956E-06 | 1.0045E-05 | 1.5767E-04 | 1.4095E-07 | 3.2779E-11 |
| 7                         | COREB  | 9.0030E-05 | 1.9653E-02 | 1.1408E-03 | 3.6112E-05 | 9.1095E-06 | 1.0053E-05 | 1.9028E-04 | 1.6523E-07 | 9.0888E-12 |
| PATH PATH3                |        |            |            |            |            |            |            |            |            |            |
| 1                         | COREC  | 1.0000E-04 | 2.0000E-02 | 1.5000E-03 | 8.0000E-04 | 4.0000E-04 | 1.0000E-04 | 1.0000E-12 | 1.0000E-12 | 3.0000E-08 |
| 2                         | COREC  | 9.8857E-05 | 1.9961E-02 | 1.5097E-03 | 7.9937E-04 | 3.9540E-04 | 1.0088E-04 | 3.4319E-05 | 1.8293E-07 | 8.3183E-09 |
| 3                         | COREC  | 9.7726E-05 | 1.9923E-02 | 1.5193E-03 | 7.9877E-04 | 3.9087E-04 | 1.0174E-04 | 6.8650E-05 | 3.5158E-07 | 2.3065E-09 |
| 4                         | COREC  | 9.6609E-05 | 1.9884E-02 | 1.5286E-03 | 7.9820E-04 | 3.8643E-04 | 1.0259E-04 | 1.0299E-04 | 5.1726E-07 | 6.3953E-10 |
| 5                         | COREC  | 9.5504E-05 | 1.9846E-02 | 1.5373E-03 | 7.9766E-04 | 3.8206E-04 | 1.0342E-04 | 1.3735E-04 | 6.8308E-07 | 1.7733E-10 |
| 6                         | COREC  | 9.4413E-05 | 1.9807E-02 | 1.5467E-03 | 7.9715E-04 | 3.7777E-04 | 1.0424E-04 | 1.7171E-04 | 8.4990E-07 | 4.9168E-11 |
| 7                         | COREC  | 9.3333E-05 | 1.9769E-02 | 1.5555E-03 | 7.9667E-04 | 3.7356E-04 | 1.0505E-04 | 2.0609E-04 | 1.0179E-06 | 1.3633E-11 |
| 8                         | COREC  | 9.2266E-05 | 1.9731E-02 | 1.5641E-03 | 7.9621E-04 | 3.6942E-04 | 1.0584E-04 | 2.4047E-04 | 1.1872E-06 | 3.7802E-12 |

FCC004 11.3114 04/10/20

PAGE 340

| REACTOR CONDITIONS AFTER 1 BURNUP SUBSTEPS AT TIME = 1.850602618E+02 DAYS |        |            |            |            |            |            |            |            |            |            |
|---|--------|------------|------------|------------|------------|------------|------------|------------|------------|------------|
| PATH PATHA1   |        |            |            |            |            |            |            |            |            |            |
| +   |        | U235       | U238       | PU239      | PU240      | PU241      | PU242      | LFPPS      | DUMP       | TRACE      |
| 1   | COREA1 | 9.6939E-04 | 1.9900E-02 | 5.5741E-04 | 3.9699E-04 | 2.8936E-04 | 1.0144E-04 | 8.5055E-05 | 4.0578E-07 | 2.7728E-09 |
| 2   | COREA2 | 9.4970E-04 | 1.9834E-02 | 5.9463E-04 | 3.9529E-04 | 2.8257E-04 | 1.0236E-04 | 1.4111E-04 | 6.7815E-07 | 7.6882E-10 |
| 3   | COREA1 | 9.2063E-04 | 1.9734E-02 | 6.4788E-04 | 3.9298E-04 | 2.7269E-04 | 1.0367E-04 | 2.2661E-04 | 1.0863E-06 | 2.1318E-10 |
| 4   | COREA2 | 9.0193E-04 | 1.9669E-02 | 6.8240E-04 | 3.9173E-04 | 2.6638E-04 | 1.0452E-04 | 2.8293E-04 | 1.3627E-06 | 5.9109E-11 |
| 5   | COREA1 | 8.7433E-04 | 1.9570E-02 | 7.3179E-04 | 3.9005E-04 | 2.5722E-04 | 1.0571E-04 | 3.6880E-04 | 1.7787E-06 | 1.6389E-11 |
| 6   | COREA2 | 8.5657E-04 | 1.9505E-02 | 7.6383E-04 | 3.8920E-04 | 2.5137E-04 | 1.0648E-04 | 4.2536E-04 | 2.0602E-06 | 4.5444E-12 |
| PATH PATHA2   |        |            |            |            |            |            |            |            |            |            |
| 1   | COREA2 | 9.7969E-04 | 1.9933E-02 | 5.3891E-04 | 3.9801E-04 | 2.9289E-04 | 1.0098E-04 | 5.5880E-05 | 2.7387E-07 | 2.7728E-09 |
| 2   | COREA1 | 9.4970E-04 | 1.9834E-02 | 5.9462E-04 | 3.9529E-04 | 2.8257E-04 | 1.0236E-04 | 1.4113E-04 | 6.7818E-07 | 7.6882E-10 |
| 3   | COREA2 | 9.3041E-04 | 1.9768E-02 | 6.3075E-04 | 3.9378E-04 | 2.7597E-04 | 1.0325E-04 | 1.9731E-04 | 9.5152E-07 | 2.1318E-10 |
| 4   | COREA1 | 9.0193E-04 | 1.9669E-02 | 6.8240E-04 | 3.9172E-04 | 2.6638E-04 | 1.0452E-04 | 2.8293E-04 | 1.3627E-06 | 5.9109E-11 |
| 5   | COREA2 | 8.8361E-04 | 1.9603E-02 | 7.1593E-04 | 3.9064E-04 | 2.6026E-04 | 1.0533E-04 | 3.3940E-04 | 1.6412E-06 | 1.6389E-11 |
| 6   | COREA1 | 8.5657E-04 | 1.9505E-02 | 7.6378E-04 | 3.8920E-04 | 2.5137E-04 | 1.0648E-04 | 4.2541E-04 | 2.0603E-06 | 4.5444E-12 |
| PATH PATH2  |        |            |            |            |            |            |            |            |            |            |
| 1   | COREB  | 9.8265E-05 | 1.9942E-02 | 1.0251E-03 | 1.4198E-05 | 9.7879E-06 | 1.0011E-05 | 3.0778E-05 | 3.8608E-08 | 5.5455E-09 |
| 2   | COREB  | 9.6559E-05 | 1.9884E-02 | 1.0495E-03 | 1.8462E-05 | 9.6018E-06 | 1.0020E-05 | 6.1943E-05 | 6.6791E-08 | 1.5376E-09 |
| 3   | COREB  | 9.4884E-05 | 1.9826E-02 | 1.0733E-03 | 2.2788E-05 | 9.4413E-06 | 1.0029E-05 | 9.3486E-05 | 9.2101E-08 | 4.2635E-10 |
| 4   | COREB  | 9.3237E-05 | 1.9768E-02 | 1.0964E-03 | 2.7175E-05 | 9.3060E-06 | 1.0037E-05 | 1.2540E-04 | 1.1663E-07 | 1.1822E-10 |
| 5   | COREB  | 9.1619E-05 | 1.9711E-02 | 1.1189E-03 | 3.1617E-05 | 9.1956E-06 | 1.0045E-05 | 1.5767E-04 | 1.4095E-07 | 3.2779E-11 |
| 6   | COREB  | 9.0030E-05 | 1.9653E-02 | 1.1408E-03 | 3.6112E-05 | 9.1095E-06 | 1.0053E-05 | 1.9028E-04 | 1.6523E-07 | 9.0888E-12 |
| 7   | COREB  | 8.8467E-05 | 1.9596E-02 | 1.1621E-03 | 4.0657E-05 | 9.0474E-06 | 1.0060E-05 | 2.2324E-04 | 1.8951E-07 | 2.5201E-12 |
| PATH PATH3  |        |            |            |            |            |            |            |            |            |            |
| 1   | COREC  | 9.8857E-05 | 1.9961E-02 | 1.5097E-03 | 7.9937E-04 | 3.9540E-04 | 1.0088E-04 | 3.4320E-05 | 1.8293E-07 | 8.3183E-09 |
| 2   | COREC  | 9.7726E-05 | 1.9923E-02 | 1.5193E-03 | 7.9877E-04 | 3.9087E-04 | 1.0174E-04 | 6.8651E-05 | 3.5158E-07 | 2.3065E-09 |
| 3   | COREC  | 9.6609E-05 | 1.9884E-02 | 1.5286E-03 | 7.9820E-04 | 3.8643E-04 | 1.0259E-04 | 1.0299E-04 | 5.1726E-07 | 6.3953E-10 |
| 4   | COREC  | 9.5504E-05 | 1.9846E-02 | 1.5373E-03 | 7.9766E-04 | 3.8206E-04 | 1.0342E-04 | 1.3735E-04 | 6.8308E-07 | 1.7733E-10 |
| 5   | COREC  | 9.4412E-05 | 1.9807E-02 | 1.5467E-03 | 7.9715E-04 | 3.7777E-04 | 1.0424E-04 | 1.7171E-04 | 8.4990E-07 | 4.9168E-11 |
| 6   | COREC  | 9.3333E-05 | 1.9769E-02 | 1.5555E-03 | 7.9667E-04 | 3.7356E-04 | 1.0505E-04 | 2.0609E-04 | 1.0179E-06 | 1.3633E-11 |
| 7   | COREC  | 9.2266E-05 | 1.9731E-02 | 1.5641E-03 | 7.9621E-04 | 3.6942E-04 | 1.0585E-04 | 2.4047E-04 | 1.1872E-06 | 3.7802E-12 |
| 8   | COREC  | 9.1211E-05 | 1.9692E-02 | 1.5725E-03 | 7.9579E-04 | 3.6535E-04 | 1.0663E-04 | 2.7486E-04 | 1.3578E-06 | 1.0482E-12 |

Figure 3-76. REBUS Stage Density Output Excerpt for Multi-Stage Burnup Limited Problem

As was the case with the previous tests of the burnup limit, the hand calculated burnup results are very similar to the reported REBUS values. The errors are again attributable to the slight difference in the way that REBUS calculates the atom percent burnup. It is important to note that the burnup summary in Figure 3-77 lists the burnup at each stage which can also be calculated using the stage densities. This is not done here for brevity.

**Table 3-41. Atom % Burnup Verification of Multi-Stage Burnup Limited Equilibrium Problem**

|        | 0.0 days    | ~186 days   | Formula | REBUS  |
|--------|-------------|-------------|---------|--------|
| PATHA1 | 2.23000E-02 | 2.18725E-02 | 1.917%  | 1.907% |
| PATHA2 | 2.23000E-02 | 2.18724E-02 | 1.917%  | 1.908% |
| PATH2  | 2.11300E-02 | 2.09063E-02 | 1.059%  | 1.057% |
| PATH3  | 2.29000E-02 | 2.26235E-02 | 1.208%  | 1.200% |

```

FCC004 11.3114 04/10/20      ABURN: Hexagonal 3D Test Problem      PAGE      354
                                CUMULATIVE BURNUP AFTER 1 BURNUP SUBSTEPS, FROM 0.00000000E+00 DAYS TO 1.850602618E+02 DAYS.

AVERAGE BURNUP (ATOM %) OF EACH STAGE OF EACH PATH

STAGE/REGION 1/COREA1 2/COREA2 3/COREA1 4/COREA2 5/COREA1 6/COREA2
              3.81414E-01 6.32792E-01 1.01620E+00 1.26879E+00 1.65387E+00 1.90747E+00
STAGE/REGION 1/COREA2 2/COREA1 3/COREA2 4/COREA1 5/COREA2 6/COREA1
              2.50582E-01 6.32885E-01 8.84805E-01 1.26897E+00 1.52201E+00 1.90773E+00
STAGE/REGION 1/COREB 2/COREB 3/COREB 4/COREB 5/COREB 6/COREB 7/COREB
              1.45660E-01 2.93157E-01 4.42443E-01 5.93469E-01 7.46190E-01 9.00558E-01 1.05653E+00
STAGE/REGION 1/COREC 2/COREC 3/COREC 4/COREC 5/COREC 6/COREC 7/COREC 8/COREC
              1.49868E-01 2.99792E-01 4.49766E-01 5.99789E-01 7.49856E-01 8.99964E-01 1.05011E+00 1.20029E+00

BURNUP CALCULATION TO OBTAIN CONVERGENCE TO THE SPECIFIED BURNUP CONSTRAINTS
FOR BURN CYCLE TIME OF 1.850602618E+02 DAYS

PATH OR      SPECIFIED      ACTUAL      ALLOWABLE      ACTUAL
TEST GROUP    BURNUP LIMIT    DISCHARGE BURNUP    ERROR (EPSG)    ERROR
LIMIT1        2.00000E-02    1.90747E-02    1.00000E-05    9.25338E-04
LIMIT2        2.00000E-02    1.90773E-02    1.00000E-05    9.22713E-04
LIMIT3        1.10000E-02    1.05653E-02    1.00000E-05    4.34683E-04
LIMIT4        1.20000E-02    1.20029E-02    1.00000E-05    -2.89800E-06

```

**Figure 3-77. REBUS Burnup Output Excerpt for Multi-Stage Burnup Limited Problem**

The last two aspects to check are the total U235 consumption and the TRACE isotope content. The TRACE isotope content can be calculated at any time point as it varies according to  $\exp(-8.0225E-8 t \cdot \text{sec}^{-1})$  from its initial concentration. The initial concentrations of TRACE for each composition are taken directly from the stage densities in Figure 3-76 and the calculated versus REBUS reported values of TRACE for COREA1, COREB, and COREC are given in Table 3-42. As seen, the REBUS calculated results are effectively identical to the formula. The COREA2 result was not computed as it is identical to the COREA1 given the fuel composition is identical.

For the U235 verification, only the total core consumption is considered as the region wise details are sufficiently covered in previous test problems. The total change in the U235 content can be determined from the stage densities and the total reactor loading. The region-wise atom density information can also produce an approximate answer noting that REBUS does not report the final converged result. The REBUS output excerpt for the total reactor loading is given in Figure 3-78. These values were verified using the sum of stage densities in Figure 3-76 noting that COREA1 and COREA2 both have to be multiplied by a factor of 1/3 while COREB requires a 1/7 and COREC requires a 1/8. These factors come from the fact that a given region has the zone loaded into that position at multiple stages. In this manner, one should understand that COREA1 and COREA2 not only consider shuffling, but multi-stage behavior of the assembly.

**Table 3-42. TRACE Isotope Verification in Multi-Stage Burnup Limited Equilibrium Problem**

| Time<br>(days) | COREA1     |            | COREB      |            | COREC      |            |
|----------------|------------|------------|------------|------------|------------|------------|
|                | REBUS      | Formula    | REBUS      | Formula    | REBUS      | Formula    |
| 0              | 1.0000E-08 | 1.0000E-08 | 2.0000E-08 | 2.0000E-08 | 3.0000E-08 | 3.0000E-08 |
| 186            | 2.7728E-09 | 2.7728E-09 | 5.5455E-09 | 5.5455E-09 | 8.3183E-09 | 8.3183E-09 |
| 372            | 7.6882E-10 | 7.6882E-10 | 1.5376E-09 | 1.5376E-09 | 2.3065E-09 | 2.3065E-09 |
| 558            | 2.1318E-10 | 2.1318E-10 | 4.2635E-10 | 4.2635E-10 | 6.3953E-10 | 6.3953E-10 |
| 744            | 5.9109E-11 | 5.9109E-11 | 1.1822E-10 | 1.1822E-10 | 1.7733E-10 | 1.7733E-10 |
| 930            | 1.6389E-11 | 1.6389E-11 | 3.2779E-11 | 3.2779E-11 | 4.9168E-11 | 4.9168E-11 |
| 1116           |            |            | 9.0888E-12 | 9.0888E-12 | 1.3633E-11 | 1.3633E-11 |
| 1302           |            |            |            |            | 3.7802E-12 | 3.7802E-12 |

```

FCC004 11.3114 04/10/20      ABURN: Hexagonal 3D Test Problem      PAGE      302
TOTAL REACTOR LOADING (IN KG) OF ACTIVE ISOTOPES AT TIME NODE 0 AT 0.000000000E+00 DAYS.
ISOTOPE      REACTOR LOADING
U235        2.57511E+01
U238        1.09960E+03
PU239        5.50523E+01
PU240        2.17672E+01
PU241        1.27192E+01
PU242        4.25190E+00
LFPPS        7.59968E+00
DUMP        3.07873E-02
TRACE        8.24899E-05

FCC004 11.3114 04/10/20      ABURN: Hexagonal 3D Test Problem      PAGE      346
TOTAL REACTOR LOADING (IN KG) OF ACTIVE ISOTOPES AT TIME NODE 1 AT 1.850602618E+02 DAYS.
ISOTOPE      REACTOR LOADING
U235        2.51268E+01
U238        1.09607E+03
PU239        5.66540E+01
PU240        2.17874E+01
PU241        1.24516E+01
PU242        4.29125E+00
LFPPS        1.03530E+01
DUMP        4.20384E-02
TRACE        2.28725E-05

```

**Figure 3-78. REBUS Total Loading Output Excerpt for Multi-Stage Burnup Limited Problem**

The total change in the U235 mass from the output is 0.6243 kg. Using the energy conversion factor, U235 atom mass, and Avogadro's number, this amounts to an average power of 1.00008 MW over the 185 day period. This is consistent with the inputted 1.0 MW and thus the preceding calculation can be confirmed to produce the correct solution. As for the burnup constraints, the results of Table 3-41 and Figure 3-77 are sufficient to demonstrate that the inputted guess, and computed burnup are properly used and obeyed.

### 3.5.2.5 Verification that an Equilibrium Problem is an Equilibrium State

By design the equilibrium analysis capability of REBUS is an approximation of the real state of the reactor when operating in equilibrium. In several of the preceding tests, the equilibrium of the reactor is tested, but not qualitatively verified. Verification that the equilibrium calculation capability represents the equilibrium state of a given reactor for all possible reactor and fuel shuffling scenarios is not possible. Conversely, demonstrating that a repetitive fuel shuffling pattern is well represented by the equilibrium calculation capability does not prove that it will do so for another case. As a consequence, the applicability of the equilibrium problem requires a judgement call by the reactor design team which should be backed up by a detailed analysis of the system when a shuffling pattern

is decided upon. In this section, a repeating fuel shuffling pattern is implemented that is consistent with the VTR project concept as it is today.

A single enrichment fuel form is presently being considered in VTR and the shuffling pattern considers the fuel to be resident in the reactor for  $\sim 6$  cycles and 100 days per cycle. Given the steep flux gradient across the reactor, this implies significant fuel shuffling. The easiest way to construct a problem similar to this is to pick a number of hexagons that has symmetry and a repeatable loading pattern consistent with the six batch concept. Figure 3-79 displays the chosen reactor geometry and shuffling pattern. The central assembly position is filled with sodium and the core is surrounded radially and axially by reflector. As seen, the core has a 60 degree periodic setup and there are exactly 6 unique assembly positions.

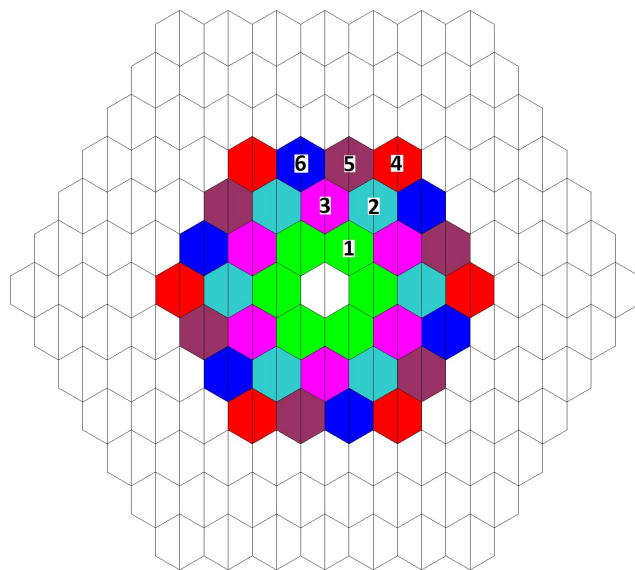


**Figure 3-79. REBUS Geometry and Shuffling Setup for Equilibrium State Verification**

In the non-equilibrium approach, fresh fuel is always loaded into position 1 and discharged fuel is taken from position 6. For each consecutive cycle, the fuel loaded into position 1 transitions to position 2, 3, 4, 5, and 6. This loading pattern is not ideal for VTR but only illustrative as it will cause the power shape to be even more steep. As will be shown, this loading pattern cannot be exactly matched using the equilibrium cycle modeling capability of REBUS.

The same three group cross section problem used previously in this section are again used here. The power is reduced to 10 MW and the cycle length increased to 100 days for this test. The input for the non-equilibrium shuffling problem is extensive and a 6 cycle example is used in its place here. The 6 cycle example input for the non-equilibrium problem is given in Figure 3-80. As can be seen, the A.NIP3 input is used to define a single material which is used to define all of the fuel compositions (Z0001 to Z0011). In the zone to region mapping, only the first six are used (Z0001 to Z0006). The A.BURN input data begins by stating that there are 5 fuel cycle operations and thus 6 stages to model. In the card type 35 data, each zone is assigned to a unique path name (e.g. Z0001 to P0001). For the fuel initially loaded into position 1 one can see that it is progressively transitioned to core positions 2 to 6. The remaining first six zones follow a similar pattern but are discharged from the system after they are loaded into CORE6. This creates increasingly shorter path specifications for each of these fuel zones. Starting at stage 2, the fresh fuel zones Z0007 to Z0011 are introduced to CORE1. Note

that each of these zones have truncated shuffling patterns because the problem only contains 6 cycles. In a larger cycle case, each new fuel zone introduced would cycle through all 6 core positions once.

|                          |                          |
|--------------------------|--------------------------|
| UNFORM=A.NIP3            | ...                      |
| ...                      | 35 P0001 Z0001 CORE1 1 1 |
| 13 FUEL aNA 0.010        | 35 P0001 Z0001 CORE2 2 2 |
| 13 FUEL aO16 0.016       | 35 P0001 Z0001 CORE3 3 3 |
| 13 FUEL aFE 0.02         | 35 P0001 Z0001 CORE4 4 4 |
| 13 FUEL aU235 0.001      | 35 P0001 Z0001 CORE5 5 5 |
| 13 FUEL aU238 0.02       | 35 P0001 Z0001 CORE6 6 6 |
| 13 FUEL aPU239 0.0005    | 35 P0002 Z0002 CORE2 1 1 |
| 13 FUEL aPU240 0.0004    | 35 P0002 Z0002 CORE3 2 2 |
| 13 FUEL aPU241 0.0003    | 35 P0002 Z0002 CORE4 3 3 |
| 13 FUEL aPU242 0.0001    | 35 P0002 Z0002 CORE5 4 4 |
| 13 FUEL aLFP 1.0E-12     | 35 P0002 Z0002 CORE6 5 5 |
| 13 FUEL aDUMP 1.0E-12    | 35 P0002 Z0002 '' 6 6    |
| 14 F0001 FUEL 1.0        | 35 P0003 Z0003 CORE3 1 1 |
| 14 F0002 FUEL 1.0        | 35 P0003 Z0003 CORE4 2 2 |
| 14 F0003 FUEL 1.0        | 35 P0003 Z0003 CORE5 3 3 |
| ...                      | 35 P0003 Z0003 CORE6 4 4 |
| 14 F0011 FUEL 1.0        | 35 P0003 Z0003 ''        |
| ...                      | 35 P0004 Z0004 CORE4 1 1 |
| 14 Z0001 F0001 1.0       | 35 P0004 Z0004 CORE5 2 2 |
| 14 Z0002 F0002 1.0       | 35 P0004 Z0004 CORE6 3 3 |
| 14 Z0003 F0003 1.0       | 35 P0004 Z0004 ''        |
| ...                      | 35 P0005 Z0005 CORE5 1 1 |
| 14 Z0011 F0011 1.0       | 35 P0005 Z0005 CORE6 2 2 |
| ...                      | 35 P0005 Z0005 ''        |
| 14 CENT aNA 0.02         | 35 P0006 Z0006 CORE6 1 1 |
| 14 REFL aFEH 0.03        | 35 P0006 Z0006 ''        |
| ...                      | 35 P0007 Z0007 CORE1 2 2 |
| 15 REFL REFL             | 35 P0007 Z0007 CORE2 3 3 |
| 15 CENT CENT             | 35 P0007 Z0007 CORE3 4 4 |
| 15 Z0001 CORE1           | 35 P0007 Z0007 CORE4 5 5 |
| 15 Z0002 CORE2           | 35 P0007 Z0007 CORE5 6 6 |
| 15 Z0003 CORE3           | 35 P0008 Z0008 CORE1 3 3 |
| 15 Z0004 CORE4           | 35 P0008 Z0008 CORE2 4 4 |
| 15 Z0005 CORE5           | 35 P0008 Z0008 CORE3 5 5 |
| 15 Z0006 CORE6           | 35 P0008 Z0008 CORE4 6 6 |
| ...                      | 35 P0009 Z0009 CORE1 4 4 |
| UNFORM=A.BURN            | 35 P0009 Z0009 CORE2 5 5 |
| ...                      | 35 P0009 Z0009 CORE3 6 6 |
| 03 0 0.0 0.0 100. 1. 1 5 | 35 P0010 Z0010 CORE1 5 5 |
| ...                      | 35 P0010 Z0010 CORE2 6 6 |
| ...                      | 35 P0011 Z0011 CORE1 6 6 |
| ...                      | ...                      |

**Figure 3-80. REBUS 6 Cycle Shuffling Input Excerpt for the Equilibrium State Verification**

This approach to finding the non-equilibrium state is not unusual and is known to eventually stabilize. The quickest way to assess the convergence is to simply look at the  $k_{eff}$  curve which is detailed in Figure 3-81. In total, 102 cycles were executed where the  $k_{eff}$  result is plotted along with the error reported in pcm. As can be seen, convergence is reached in this example after 20 cycles. Because this is a rather simple fuel shuffling case, it should come as no surprise that convergence is achieved so quickly. For larger and more complex fuel shuffling scenarios, convergence can take considerably more than 100 cycles.

The Primary Zone assignment approach can take two approaches: 1) the entire 6 assembly region is treated homogeneously with 6 batches and 2) each assembly position is treated uniquely but with 6 batches. As stated, neither of these will exactly match the non-equilibrium problem. The input excerpt of interest for the two Primary Zone input options is shown in Figure 3-82. The example on the left is the first approach while the one on the right is the second approach. The differences between the inputs are small where the 6 assembly case simply requires the single zone case to be duplicated for each assembly.

The fuel shuffling approach to equilibrium problems can only model fresh fuel transitioning through all spatial positions in all 6 batches. The input excerpt of interest for this problem is given in Figure 3-83. This approach is also not the same as the non-equilibrium case. The first major difference is that all assembly positions are filled with fresh fuel at stage 1. At stage 2, the zones simply swap

positions. This input is conceptually most similar to the first Primary Zone approach noting that the zone definition requires a factor of one-sixth to ensure the proper fuel loading.

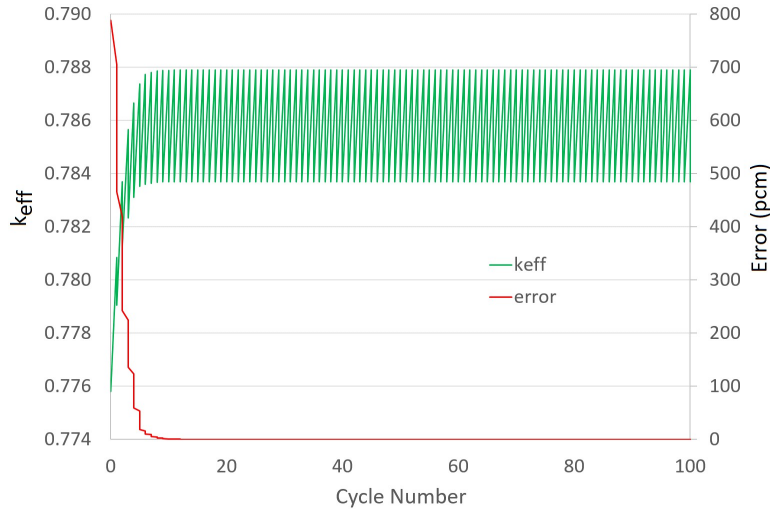


**Figure 3-81. Non-equilibrium  $k_{eff}$  Curve for the Equilibrium State Verification**

```

UNIFORM=A.NIP3
...
13      FUEL  aNA    0.010
13      FUEL  aO16   0.016
13      FUEL  aFE    0.02
13      FUEL  aU235  1.0
13      FUEL  aU238  1.0
13      FUEL  aPU239 1.0
13      FUEL  aPU240 1.0
13      FUEL  aPU241 1.0
13      FUEL  aPU242 1.0
13      FUEL  aLFP   1.0
13      FUEL  aDUMP  1.0
14      F0001 FUEL 1.0
14      Z0001 F0001 1.0
14      CENT   aNA   0.02
14      REFL   aFEH  0.03
15      REFL   REFL
15      CENT   CENT
15      Z0001 CORE1
15      Z0001 CORE2
15      Z0001 CORE3
15      Z0001 CORE4
15      Z0001 CORE5
15      Z0001 CORE6
...
UNIFORM=A.BURN
...
11      PATH1 0    1    F0001 Z0001
11      PATH1 0    2    F0001 Z0001
11      PATH1 0    3    F0001 Z0001
11      PATH1 0    4    F0001 Z0001
11      PATH1 0    5    F0001 Z0001
11      PATH1 0    6    F0001 Z0001
...
14      F0001 FUEL 1.0
14      F0002 FUEL 1.0
14      F0003 FUEL 1.0
14      F0004 FUEL 1.0
14      F0005 FUEL 1.0
14      F0006 FUEL 1.0
14      Z0001 F0001 1.0
14      Z0002 F0002 1.0
14      Z0003 F0003 1.0
14      Z0004 F0004 1.0
14      Z0005 F0005 1.0
14      Z0006 F0006 1.0
15      Z0001 CORE1
15      Z0002 CORE2
15      Z0003 CORE3
15      Z0004 CORE4
15      Z0005 CORE5
15      Z0006 CORE6
...
11      PATH1 0    1    F0001 Z0001
11      PATH1 0    2    F0001 Z0001
11      PATH1 0    3    F0001 Z0001
11      PATH1 0    4    F0001 Z0001
11      PATH1 0    5    F0001 Z0001
11      PATH1 0    6    F0001 Z0001
...
11      PATH2 0    6    F0002 Z0002
11      PATH3 0    1    F0003 Z0003
11      PATH3 0    6    F0003 Z0003
11      PATH6 0    1    F0006 Z0006
11      PATH6 0    6    F0006 Z0006
...

```

**Figure 3-82. REBUS Primary Zone Input Excerpts for the Equilibrium State Verification**

The  $k_{eff}$  results for the equilibrium state for the three equilibrium calculations and the non-equilibrium (converged result) are collected in Table 3-43. The error in the equilibrium results relative to the non-equilibrium one is provided at the bottom of the table. As can be seen, the two Primary Zone input approaches have identical results while the shuffling case produces a result

slightly closer to the non-equilibrium one. In general, these errors are acceptable given that the equilibrium approaches cannot really model the true fuel shuffling behavior. Nevertheless, one should be able to identify that the  $k_{eff}$  error changes between the beginning and end of cycle and thus there is some amount of error being introduced in the actual depletion results of the compositions.

| UNIFORM=A.NIP3 |  |       |        |              |       | UNIFORM=A.BURN |    |       |       |   |       |       |
|----------------|--|-------|--------|--------------|-------|----------------|----|-------|-------|---|-------|-------|
| 13             |  | NFUEL | aNA    | 0.010        |       | 11             |    | PATH1 | 0     | 1 | F0001 |       |
| 13             |  | NFUEL | aO16   | 0.016        |       | 11             |    | PATH1 | 0     | 2 | F0001 |       |
| 13             |  | NFUEL | aFE    | 0.02         |       | 11             |    | PATH1 | 0     | 3 | F0001 |       |
| 13             |  | FUEL  | aU235  | 1.0          |       | 11             |    | PATH1 | 0     | 4 | F0001 |       |
| 13             |  | FUEL  | aU238  | 1.0          |       | 11             |    | PATH1 | 0     | 5 | F0001 |       |
| 13             |  | FUEL  | aPU239 | 1.0          |       | 11             |    | PATH1 | 0     | 6 | F0001 |       |
| 13             |  | FUEL  | aPU240 | 1.0          |       | 11             |    | PATH2 | 0     | 1 | F0002 |       |
| 13             |  | FUEL  | aPU241 | 1.0          |       | 11             |    | PATH2 | 0     | 2 | F0002 |       |
| 13             |  | FUEL  | aPU242 | 1.0          |       | 11             |    | PATH2 | 0     | 3 | F0002 |       |
| 13             |  | FUEL  | aLFP   | 1.0          |       | 11             |    | PATH2 | 0     | 4 | F0002 |       |
| 13             |  | FUEL  | aDUMP  | 1.0          |       | 11             |    | PATH2 | 0     | 5 | F0002 |       |
| 14             |  | F0001 | FUEL   | 0.1666666667 | NFUEL | 1.0            | 11 |       | PATH2 | 0 | 6     | F0002 |
| 14             |  | F0002 | FUEL   | 0.1666666667 | NFUEL | 1.0            | 11 |       | PATH3 | 0 | 1     | F0003 |
| 14             |  | F0003 | FUEL   | 0.1666666667 | NFUEL | 1.0            | 11 |       | PATH3 | 0 | 2     | F0003 |
| 14             |  | F0004 | FUEL   | 0.1666666667 | NFUEL | 1.0            | 11 |       | PATH3 | 0 | 3     | F0003 |
| 14             |  | F0005 | FUEL   | 0.1666666667 | NFUEL | 1.0            | 11 |       | PATH3 | 0 | 4     | F0003 |
| 14             |  | F0006 | FUEL   | 0.1666666667 | NFUEL | 1.0            | 11 |       | PATH3 | 0 | 5     | F0003 |
| 14             |  | Z0001 | F0001  | 1.0          |       | 11             |    | PATH3 | 0     | 6 | F0003 |       |
| 14             |  | Z0002 | F0002  | 1.0          |       | 11             |    | PATH3 | 0     | 1 | F0004 |       |
| 14             |  | Z0003 | F0003  | 1.0          |       | 11             |    | PATH4 | 0     | 6 | F0004 |       |
| 14             |  | Z0004 | F0004  | 1.0          |       | 11             |    | PATH5 | 0     | 1 | F0005 |       |
| 14             |  | Z0005 | F0005  | 1.0          |       | 11             |    | PATH5 | 0     | 6 | F0005 |       |
| 14             |  | Z0006 | F0006  | 1.0          |       | 11             |    | PATH6 | 0     | 1 | F0006 |       |
| 15             |  | Z0001 | CORE1  |              |       |                | 11 |       | PATH6 | 0 | 6     | F0006 |
| 15             |  | Z0002 | CORE2  |              |       |                | 11 |       |       |   |       |       |
| 15             |  | Z0003 | CORE3  |              |       |                | 11 |       |       |   |       |       |
| 15             |  | Z0004 | CORE4  |              |       |                | 11 |       |       |   |       |       |
| 15             |  | Z0005 | CORE5  |              |       |                | 11 |       |       |   |       |       |
| 15             |  | Z0006 | CORE6  |              |       |                | 11 |       |       |   |       |       |
|                |  |       |        |              |       |                |    |       |       |   |       |       |

Figure 3-83. REBUS Shuffling Input Excerpt for the Equilibrium State Verification

Table 3-43. REBUS  $k_{eff}$  Results for the Equilibrium State Verification

| Time<br>(days) | Primary<br>Zone #1 | Primary<br>Zone #2 | Shuffling | Non-<br>Equilibrium |
|----------------|--------------------|--------------------|-----------|---------------------|
| 0              | 0.78602            | 0.78602            | 0.78514   | 0.78370             |
| 100            | 0.78898            | 0.78898            | 0.78865   | 0.78790             |
| Error (pcm)    |                    |                    |           |                     |
| 0              | -232               | -232               | -144      |                     |
| 100            | -108               | -108               | -75       |                     |

In all three cases, an identical amount of fresh fuel is introduced into the system. The first check is to look at the total reactor loading details at the beginning and end of the cycle for each case which are collected in Table 3-44. A quick review of the 0 day result shows that the equilibrium cases all have higher U235 and U238 content and lower Plutonium concentrations. This difference in results is indicative of the aspect that the fuel shuffling scheme of the non-equilibrium depletion has a different impact upon the depletion process itself. Given there is no direct comparable stage composition from the equilibrium to the non-equilibrium case, there is no real point in comparing the detailed stage densities with the non-equilibrium problem results.

One way to impose that the comparison is similar is to modify the shuffling pattern in the non-equilibrium problem to more closely match the first Primary Zone approach. This would involve breaking the existing cycle into shorter cycles with more fuel shuffling. Eventually, with short enough time steps and a cyclic shuffling pattern, the non-equilibrium problem can become similar to the

equilibrium one. Another potential way to impose the similarity is to define a infinite homogeneous reactor with a shuffling pattern. In this situation, symmetry could be imposed such that the non-equilibrium problem would more easily match the equilibrium one given shorter cycles. Neither of these approaches, or others, are deemed necessary as there simply is no practical way that the equilibrium feature of REBUS is meant to exactly match the non-equilibrium one. In that regard, the preceding set of calculations is sufficient to demonstrate that the equilibrium capability is representative of the non-equilibrium one thereby satisfying the verification task.

**Table 3-44. REBUS Total Reactor Loading Results for the Equilibrium State Verification**

| Time<br>(days) |       | Primary<br>Zone #1 | Primary<br>Zone #2 | Shuffling | Non-<br>Equilibrium |
|----------------|-------|--------------------|--------------------|-----------|---------------------|
| 0              | U235  | 64.00              | 64.00              | 64.08     | 62.41               |
|                | U238  | 1445.68            | 1445.68            | 1446.26   | 1439.80             |
|                | PU239 | 55.17              | 55.17              | 55.10     | 58.33               |
|                | PU240 | 29.41              | 29.41              | 29.38     | 29.33               |
|                | PU241 | 19.33              | 19.33              | 19.35     | 18.78               |
|                | PU242 | 7.97               | 7.97               | 7.97      | 8.05                |
|                | LFPPS | 27.66              | 27.66              | 27.08     | 32.50               |
|                | DUMP  | 0.15               | 0.15               | 0.14      | 0.17                |
| 100            | U235  | 60.62              | 60.62              | 60.71     | 59.03               |
|                | U238  | 1432.37            | 1432.37            | 1433.17   | 1426.70             |
|                | PU239 | 61.69              | 61.69              | 61.68     | 64.92               |
|                | PU240 | 29.34              | 29.34              | 29.29     | 29.25               |
|                | PU241 | 18.20              | 18.20              | 18.20     | 17.64               |
|                | PU242 | 8.13               | 8.13               | 8.13      | 8.21                |
|                | LFPPS | 38.80              | 38.80              | 37.99     | 43.41               |
|                | DUMP  | 0.21               | 0.21               | 0.20      | 0.23                |

### 3.6 Category 4 Verification

The category 4 section of Table 2-1, reproduced here as Table 3-45, has three tasks which are focused on verifying the fuel fabrication and enrichment search capabilities of REBUS. In the preceding tests of equilibrium cycle, the fuel fabrication and enrichment capabilities were used and verified to be accurate. However, those were simple tests and a more thorough evaluation consistent with the VTR usage is appropriate. Unlike the previous category verification work, all of these cards are connected and thus must be verified simultaneously. Because the input is independent of the number of energy groups, the same 3-group cross section will be used in this section.

**Table 3-45. REBUS Identified Verification Tasks for Category 4**

| Category | Verification Tasks   |
|----------|--|
| 4        | Verify the fuel fabrication specification<br>a) The external feed details (cards 19, 20, 21, 22)<br>b) The enrichment modification factor usage (cards 4, 12, 18)<br>c) The fuel fabrication density (card 13) |

There are three aspects to consider with regard to verifying task 4: 1) the external feed must consider multiple feed options for multiple parts of the core, 2) the enrichment modification factor should reach the correct result given the stated goal, 3) the fuel should be fabricated correctly with the correct region specific isotopes in all parts of the geometry based upon the single enrichment modification factor. To satisfy the first part, the external feeds shown in Table 3-46 are defined for use in the domain. All of these feeds are made up and not necessarily consistent with real world feed materials. The volumes shown are those provided on card type 21 when the particular input (atom fraction or atom density) is provided on card type 22. These volumes were chosen to be on the order of the actual volumes needed given a 0.15 enrichment modification factor.

**Table 3-46. REBUS External Feeds for Category 4 Verification Work**

|  | DU               | NATU   | EU               | WPU  | RLWR | RFR    | RDW    |
|--|------------------|--------|------------------|------|------|--------|--------|
| U235                                       | 0.0001           | 0.0072 | 0.17             |      |      | 0.0085 | 0.0005 |
| U238                                       | 0.9999           | 0.9928 | 0.83             |      |      | 0.0415 | 0.9995 |
| PU239                                      |                  |        |                  | 0.99 | 0.6  | 0.9405 |        |
| PU240                                      |                  |        |                  | 0.01 | 0.22 | 0.0095 |        |
| PU241                                      |                  |        |                  |      | 0.11 |        |        |
| PU242                                      |                  |        |                  |      | 0.07 |        |        |
| Volume (cm <sup>3</sup> )<br>Atom Density  | 10 <sup>30</sup> | 9732   | 10 <sup>30</sup> | 6842 | 1470 | 977    | 53533  |
| Volume (cm <sup>3</sup> )<br>Atom Fraction | 10 <sup>30</sup> | 200    | 10 <sup>30</sup> | 140  | 30   | 20     | 1100   |

To maximize the combination of feeds, the geometry in Figure 3-79 is assigned to 5 paths and the fuel fabrication specification shown in Table 3-47. The volumes of the five paths are given to better understand the requirements of the external feeds in Table 3-46. As an example, applying the enrichment modification factor of 0.15 to the PATH1 volume of 31176.9 cm<sup>3</sup> yields an enriched material volume of 4676 cm<sup>3</sup>. This volume is on the order of the selected volume limit for the highest priority WPU feed. The intention of the testing will demonstrate how REBUS selects which PATH to fill first and how those feed materials are distributed in REBUS.

**Table 3-47. REBUS External Feed Usage for Category 4 Verification Work**

| Class                     | PATH1   | PATH2   | PATH3   | PATH4   | PATH5   |
|---------------------------|---------|---------|---------|---------|---------|
| Volume (cm <sup>3</sup> ) | 31176.9 | 31176.9 | 31176.9 | 31176.9 | 62353.8 |
| Stages                    | 1       | 2       | 3       | 4       | 6       |
| 1                         | WPU     | WPU     | RLWR    | RFR     | EU      |
|                           | RLWR    | RFR     | RFR     | RLWR    |         |
|                           | EU      | EU      | EU      | EU      |         |
| 2                         | RDU     | RDU     | RDU     | RDU     | NATU    |
|                           | NATU    | NATU    | DU      | DU      | DU      |
|                           | DU      | DU      |         |         | RDU     |

With regard to the fuel fabrication in REBUS, the critical piece of information is the mass density of the fabricated fuel. Given the atom fractions of each feed, the atom mass of the mixture for each external feed can be defined using

$$M_{feed} = \sum_i a_i M_i, \quad (49)$$

Where  $a_i$  is the atom fractions from Table 3-46 and  $M_i$  is the atom mass of each isotope. Using this mixture atom mass, the fabrication density can be converted to an atom density. As an example, assume a 0.15 enrichment modification factor and a fuel composed of EU as the CLASS 1 feed and DU as the CLASS 2 feed (both have infinite volumes). The mixture atom mass of the EU feed is 237.6136 while that of the DU feed is 238.1247. The atom density of each feed is calculated using

$$N_{feed} = \frac{\rho_{fuel}}{M_{feed}} \cdot Avogadro = \frac{\rho_{fuel}}{M_{feed}} \cdot 0.6022141 \cdot barn. \quad (50)$$

The variable  $\rho_{fuel}$  is the desired fabricated fuel mass density and  $N_{feed}$  is the atom density of the feed that will give the fabricated fuel mass density. With a 8.125 g/cc fabrication density, the EU feed atom density is 2.05922E-02 atom-barn/cm while for the DU feed the atom density is 2.05480E-02 atom-barn/cm. The isotopic components of each feed are then obtained by multiplying the feed atom density by the atom fraction of each isotope in each feed.

$$N_{feed,i} = a_i \cdot N_{feed}. \quad (51)$$

These feed atom densities will exactly produce the desired fabricated density of the fuel regardless of the enrichment modification factor. In the REBUS input, only a single fabrication density (card type 13) can be assigned to a given path. In this sense, REBUS applies that fabrication density to all external feeds that are used by the PATH. For the EU and DU example, the entire calculation is presented in Table 3-48 noting that this material is not present in the follow-on REBUS examples.

**Table 3-48. REBUS Fuel Fabrication Example Calculation**

|                      | EU Feed     | DU Feed     | Fabricated Fuel |
|----------------------|-------------|-------------|-----------------|
| Atom Fractions       |             |             |                 |
| U235                 | 0.17        | 0.0001      |                 |
| U238                 | 0.83        | 0.9999      |                 |
| Mixture Atom Mass    | 237.6136    | 238.1247    |                 |
| Mixture Atom Density | 2.05922E-02 | 2.05480E-02 |                 |
| Atom Density         |             |             |                 |
| U235                 | 3.50068E-03 | 2.05480E-06 | 5.26848E-04     |
| U238                 | 1.70915E-02 | 2.05460E-02 | 2.00278E-02     |
| Mass Density         |             |             |                 |
| U235                 |             |             | 0.205692        |
| U238                 |             |             | 7.919308        |
|                      |             |             | 8.125           |

The important part to understand is that the atom density of the feed material is based upon the desired fabricated mass density. For problems with real fuel feed limits, one must not only provide the fictitious card type 13 input (fabrication atom density of a pure isotope), but also the fabrication atom densities on card type 22 along with the appropriate volume limit on card type 21. If any changes occur in the fabrication density due to the enrichment, the input setup becomes quite painful and most users resort to using atom fraction inputs on card type 22 for a given feed as those do not change. In that regard, the card type 13 input can be quickly updated with the correct fabrication density and the calculation reran. The pseudo volume constraint for atom fractions is calculated using

$$\tilde{V} = \frac{V_{limit} \cdot \rho_{fuel} \cdot Avogadro}{M_{feed}} = \frac{mass_{limit} \cdot Avogadro}{M_{feed}}, \quad (52)$$

which is independent of the fabrication density and thus constant for all of the calculations. If the user provides an atom density detail in card type 22 that is not consistent with the fabrication density or the volume constraint, then REBUS will of course not execute the problem consistent with the

manner desired by the user. One should easily identify that the REBUS input for card type 13 provides somewhat useless information as a simple mixture based fabrication density would have been sufficient and easier to use.

In REBUS, each feed is assigned a volume limit  $V_{feed}$ . In the manual, this volume is stated to be applied such that the total number of atoms in each zone are defined to achieve the desired fabrication density. In this sense, REBUS takes the atom densities from card type 22 for each feed and multiplies by the volume constraint on card type 21 for each feed to get the total atoms  $A_{feed}$  available for use in each feed

$$A_{feed} = V_{feed} \cdot N_{feed}. \quad (53)$$

From Table 3-46, the selection of the volumes was done to cause REBUS to run out of several feeds during the fabrication process and thereby attempt to use priority 2 and 3 feed materials. The priority scheme was arbitrarily chosen in this case and during fabrication, the total number of atoms for each feed is reduced by the number used in previous fabrication priority levels. There is no order of treatment for fabrication of the PATH data in REBUS. REBUS assumes each path is of equal importance at a given priority level and thus equally distributes the available atoms. The intention is that each PATH get the identical atom density of the feed and thus the amount of feed placed in each PATH is dependent upon the volume of the PATH.

In the example shown, PATH1 and PATH2 will split the available WPU feed. One aspect to consider for all of this is the number of stages. If the number of stages is 1, then entire PATH volume is fabricated at BOC. If the number of stages is 2 or more, only a fraction of the material is fabricated at BOC and thus the total volume constraint is reduced. As stated, the displayed volume constraints were chosen to cause a specific behavior in the fabrication process.

### 3.6.1.1 Verification of Fuel Fabrication

The easiest way to check the REBUS approach is to use a manufactured solution. In this situation, REBUS conveniently provides such an ability by allowing the user to select the enrichment modification factor instead of search on it (the error criteria on the target of the search is set to 1.0 or larger). The search capability can be easily tested by running the fixed enrichment calculation and using the  $k_{eff}$  results as the targets in a searched input. Each search calculation should identically yield the fixed enrichment result.

In this section, the fixed enrichment test problem is verified by direct calculation of the composition in each region. This is a tedious process and requires an inherent understanding of the fuel fabrication process internal to REBUS. An excerpt of the important REBUS input parts is given in Figure 3-84. Unlike many of the previous excerpts, this one is very extensive to more clearly show how the fabrication input is implemented. To begin, one can see that the A.NIP3 input has only 5 compositions for the 6 regions and that Z0005 is assigned to both CORE5 and CORE6. This choice is consistent with the PATH56 usage indicating that both of these regions will be assigned the same PATH. Internal to REBUS, the two regions will be assigned their own compositions and deplete separately. A single fabrication card input is provided and assigned to all paths and thus the fabrication mass density of all paths is the same. The external feed and the priority of use in each path is defined consistent with that shown earlier in Table 3-46 and Table 3-47.

```

UNIFORM=A.NIP3
...
14      F0001 FUEL 1.0
14      F0002 FUEL 1.0
14      F0003 FUEL 1.0
14      F0004 FUEL 1.0
14      F0005 FUEL 1.0
14      Z0001 F0001 1.0
14      Z0002 F0002 1.0
14      Z0003 F0003 1.0
14      Z0004 F0004 1.0
14      Z0005 F0005 1.0
15      Z0001 CORE1
15      Z0002 CORE2
15      Z0003 CORE3
15      Z0004 CORE4
15      Z0005 CORE5
15      Z0006 CORE6
...
UNIFORM=A.BURN
...
04  1.0  1.0  0.0  0.15  0.1500000001
06  CORE          0.99
...
11  PATH1 0    1    F0001 Z0001
11  PATH2 0    1    F0002 Z0002
11  PATH2 0    2    F0002 Z0002
11  PATH3 0    1    F0003 Z0003
11  PATH3 0    2    F0003 Z0003
11  PATH3 0    3    F0003 Z0003
11  PATH4 0    1    F0004 Z0004
11  PATH4 0    2    F0004 Z0004
11  PATH4 0    3    F0004 Z0004
11  PATH4 0    4    F0004 Z0004
11  PATH56 0   1    F0005 Z0005
11  PATH56 0   2    F0005 Z0005
11  PATH56 0   3    F0005 Z0005
11  PATH56 0   4    F0005 Z0005
11  PATH56 0   5    F0005 Z0005
11  PATH56 0   6    F0005 Z0005
...
12  PATH1    FAB1  0.0  0  1.00  1.00
12  PATH2    FAB1  0.0  0  1.00  1.00
12  PATH3    FAB1  0.0  0  1.00  1.00
12  PATH4    FAB1  0.0  0  1.00  1.00
12  PATH56   FAB1  0.0  0  1.00  1.00
13  FAB1 U235  2.08109E-02
13  FAB1 U238  2.05480E-02
13  FAB1 PU239  2.04619E-02
13  FAB1 PU240  2.03765E-02
13  FAB1 PU241  2.02917E-02
13  FAB1 PU242  2.02078E-02
13  FAB1 DUMP   2.06455E-02
13  FAB1 LFPPS  2.07330E-02
18  CLASS1 U235  1.0
18  CLASS1 U238  1.0
18  CLASS1 PU239  1.0
18  CLASS1 PU240  1.0
18  CLASS1 PU241  1.0
18  CLASS1 PU242  1.0
18  CLASS1 DUMP   1.0
18  CLASS1 LFPPS  1.0
18  CLASS1 TRACE  1.0
18  CLASS2 U235  0.0
18  CLASS2 U238  0.0
19  PATH1    WPU      1
19  PATH1    RLWR     2
19  PATH1    EU       3
19  PATH2    WPU      1
19  PATH2    RFR      2
19  PATH2    EU       3
19  PATH3    RLWR     1
19  PATH3    RFR      2
19  PATH3    EU       3
19  PATH4    RFR      1
19  PATH4    RLWR     2
19  PATH4    EU       3
19  PATH56   EU       1
20  PATH1    RDU      1
20  PATH1    NATU     2
20  PATH1    DU       3
20  PATH2    RDU      1
20  PATH2    NATU     2
20  PATH2    DU       3
20  PATH3    RDU      1
20  PATH3    DU       2
20  PATH4    RDU      1
20  PATH4    DU       2
20  PATH56   NATU     1
20  PATH56   DU       2
20  PATH56   RDU      3
21  EU      CLASS1  1.0E30
21  WPU     CLASS1  140.
21  RLWR    CLASS1  30.
21  RFR     CLASS1  20.
21  DU      CLASS2  1.0E30
21  NATU    CLASS2  200.
21  RDU     CLASS2  1100.
22  EU      U235   0.17
22  EU      U238   0.83
22  WPU    PU239  0.99
22  WPU    PU240  0.01
22  RLWR   PU239  0.6
22  RLWR   PU240  0.22
22  RLWR   PU241  0.11
22  RLWR   PU242  0.07
22  RFR    U235   0.0085
22  RFR    U238   0.0415
22  RFR    PU239  0.9405
22  RFR    PU240  0.0095
22  DU     U235   0.0001
22  DU     U238   0.9999
22  NATU   U235   0.0072
22  NATU   U238   0.9928
22  RDU    U235   0.0005
22  RDU    U238   0.9995

```

Figure 3-84. REBUS Input Excerpt for the Fixed Enrichment Test Case

The first part of the verification is to check the REBUS fabrication. Because the details of the depletion are not of interest for this test case, the only output of interest is the first stage of any given path which is summarized in Figure 3-85. As discussed in earlier sections, the first stage in REBUS at the first time point is the fabricated content for that fuel PATH. In this regard the atom densities that must be verified for each path are collected into Table 3-49 and the volume by class that was filled in each path is also provided. As part of the verification, the fabricated atom densities for each feed are provided in Table 3-50 using the formulas above along with the volume limits provided for each feed.

Because the feeds are tied to multiple PATHS, the verification will follow each feed and how it is used at each priority level. In the problem the CLASS 1 feeds are EU, WPU, RLWR, and RFR while the CLASS 2 feeds are DU, NATU, and RDU. Because EU and DU are infinite, they will not be inspected closely.

FCC004 11.3114 04/10/20

PAGE 266

BEGINNING OF BURN CYCLE 1  
ATOM DENSITIES (IN ATOMS/BARN-CM.) OF ACTIVE ISOTOPES IN EACH STAGE OF EACH PATH  
PATH PATH1

| STAGE | REGION  | U235       | U238       | PU239      | PU240       | PU241      | PU242      | LFPPS      | DUMP       |
|-------|---------|------------|------------|------------|-------------|------------|------------|------------|------------|
| +     | 1 CORE1 | 2.4241E-05 | 1.7518E-02 | 2.9637E-03 | 2.9937E-05  | 0.0000E+00 | 0.0000E+00 | 0.0000E+00 | 0.0000E+00 |
|       |         |            |            |            | PATH PATH2  |            |            |            |            |
| +     | U235    | U238       | PU239      | PU240      | PU241       | PU242      | LFPPS      | DUMP       |            |
| 1     | CORE2   | 2.4241E-05 | 1.7518E-02 | 2.9637E-03 | 2.9937E-05  | 0.0000E+00 | 0.0000E+00 | 0.0000E+00 |            |
| 2     | CORE2   | 2.3596E-05 | 1.7446E-02 | 2.9192E-03 | 4.1578E-05  | 1.7811E-07 | 3.7971E-10 | 1.0489E-04 | 3.3715E-13 |
|       |         |            |            |            | PATH PATH3  |            |            |            |            |
| +     | U235    | U238       | PU239      | PU240      | PU241       | PU242      | LFPPS      | DUMP       |            |
| 1     | CORE3   | 3.8403E-05 | 1.7603E-02 | 1.7321E-03 | 6.3509E-04  | 3.1754E-04 | 2.0207E-04 | 0.0000E+00 | 0.0000E+00 |
| 2     | CORE3   | 3.7288E-05 | 1.7525E-02 | 1.7248E-03 | 6.3264E-04  | 3.0863E-04 | 2.0269E-04 | 9.6983E-05 | 6.0248E-07 |
| 3     | CORE3   | 3.6205E-05 | 1.7447E-02 | 1.7176E-03 | 6.3019E-04  | 3.0005E-04 | 2.0326E-04 | 1.9327E-04 | 1.2067E-06 |
|       |         |            |            |            | PATH PATH4  |            |            |            |            |
| +     | U235    | U238       | PU239      | PU240      | PU241       | PU242      | LFPPS      | DUMP       |            |
| 1     | CORE4   | 1.1656E-04 | 1.7985E-02 | 2.4133E-03 | 2.4377E-05  | 0.0000E+00 | 0.0000E+00 | 0.0000E+00 |            |
| 2     | CORE4   | 1.1472E-04 | 1.7941E-02 | 2.3992E-03 | 3.0832E-05  | 9.0924E-08 | 1.2696E-10 | 5.3560E-05 | 7.2812E-14 |
| 3     | CORE4   | 1.1290E-04 | 1.7897E-02 | 2.3853E-03 | 3.7192E-05  | 2.0094E-07 | 5.4460E-10 | 1.0687E-04 | 6.1492E-13 |
| 4     | CORE4   | 1.1112E-04 | 1.7853E-02 | 2.3715E-03 | 4.3460E-05  | 3.2931E-07 | 1.3064E-09 | 1.5994E-04 | 2.1830E-12 |
|       |         |            |            |            | PATH PATH56 |            |            |            |            |
| +     | U235    | U238       | PU239      | PU240      | PU241       | PU242      | LFPPS      | DUMP       |            |
| 1     | CORE5   | 6.5087E-04 | 1.9905E-02 | 0.0000E+00 | 0.0000E+00  | 0.0000E+00 | 0.0000E+00 | 0.0000E+00 |            |
| 2     | CORE5   | 6.3863E-04 | 1.9848E-02 | 4.0140E-05 | 6.5705E-08  | 8.5647E-11 | 7.3521E-14 | 2.9823E-05 | 3.0556E-17 |
| 3     | CORE5   | 6.2662E-04 | 1.9790E-02 | 7.9277E-05 | 2.5975E-07  | 6.7468E-10 | 1.1612E-12 | 6.0122E-05 | 9.6702E-16 |
| 4     | CORE5   | 6.1484E-04 | 1.9732E-02 | 1.1743E-04 | 5.7760E-07  | 2.2422E-09 | 5.8033E-12 | 9.0882E-05 | 7.2646E-15 |
| 5     | CORE5   | 6.0328E-04 | 1.9675E-02 | 1.5463E-04 | 1.0149E-06  | 5.2336E-09 | 1.8106E-11 | 1.2209E-04 | 3.0286E-14 |
| 6     | CORE5   | 5.9193E-04 | 1.9618E-02 | 1.9090E-04 | 1.5672E-06  | 1.0066E-08 | 4.3638E-11 | 1.5374E-04 | 9.1437E-14 |
|       |         |            |            |            | PATH PATH56 |            |            |            |            |
| +     | U235    | U238       | PU239      | PU240      | PU241       | PU242      | LFPPS      | DUMP       |            |
| 1     | CORE6   | 6.5087E-04 | 1.9905E-02 | 0.0000E+00 | 0.0000E+00  | 0.0000E+00 | 0.0000E+00 | 0.0000E+00 |            |
| 2     | CORE6   | 6.3863E-04 | 1.9848E-02 | 4.0140E-05 | 6.5705E-08  | 8.5647E-11 | 7.3521E-14 | 2.9823E-05 | 3.0556E-17 |
| 3     | CORE6   | 6.2662E-04 | 1.9790E-02 | 7.9277E-05 | 2.5975E-07  | 6.7468E-10 | 1.1612E-12 | 6.0122E-05 | 9.6702E-16 |
| 4     | CORE6   | 6.1484E-04 | 1.9732E-02 | 1.1743E-04 | 5.7760E-07  | 2.2422E-09 | 5.8033E-12 | 9.0882E-05 | 7.2646E-15 |
| 5     | CORE6   | 6.0328E-04 | 1.9675E-02 | 1.5463E-04 | 1.0149E-06  | 5.2336E-09 | 1.8106E-11 | 1.2209E-04 | 3.0286E-14 |
| 6     | CORE6   | 5.9193E-04 | 1.9618E-02 | 1.9090E-04 | 1.5672E-06  | 1.0066E-08 | 4.3638E-11 | 1.5374E-04 | 9.1437E-14 |

FCC004 11.3114 04/10/20

ABURN: Hexagonal 3D Test Problem

PAGE 358

REACTOR CHARACTERISTICS SUMMARY

=====

BOEC EEOC

-----

KEFF 0.79557 0.79017

PEAKING FACTOR 0.00000 0.00000

**Figure 3-85. REBUS Fabricated Atom Density Excerpt for the Fixed Enrichment Test**

**Table 3-49. Fabricated Atom Densities Produced by REBUS for the Fixed Enrichment Test**

|                | PATH1      | PATH2      | PATH3      | PATH4      | PATH56     |
|----------------|------------|------------|------------|------------|------------|
| U235           | 2.4241E-05 | 2.4241E-05 | 3.8403E-05 | 1.1656E-04 | 6.5087E-04 |
| U238           | 1.7518E-02 | 1.7518E-02 | 1.7603E-02 | 1.7985E-02 | 1.9905E-02 |
| PU239          | 2.9637E-03 | 2.9637E-03 | 1.7321E-03 | 2.4133E-03 |            |
| PU240          | 2.9937E-05 | 2.9937E-05 | 6.3509E-04 | 2.4377E-05 |            |
| PU241          |            |            | 3.1754E-04 |            |            |
| PU242          |            |            | 2.0207E-04 |            |            |
| CLASS 1 Volume | 4676.54    | 2338.27    | 1558.85    | 1169.13    | 1558.85    |
| CLASS 2 Volume | 26500.37   | 13250.18   | 8833.46    | 6625.09    | 8833.46    |

Starting with the WPU feed, the fabrication process begins by summing the volume over all PATHs in priority 1 which is 7014.80 cm<sup>3</sup> (PATH1 plus PATH2). This can be multiplied by the fabrication atom densities in Table 3-50 to determine the atoms required to fill each volume. Given the available atoms is defined by the volume limit of 6842 cm<sup>3</sup> from Table 3-50 it should be clear that all of WPU will be used to fabricate the fuel at BOC and additional feed from lower priorities will be required. The actual atom densities used from this feed for PATH1 and PATH2 is simply the WPU fabrication atom densities in Table 3-50 multiplied by the fraction 0.15\*6842.28/7014.80=0.1463. Because none of

the lower priority feeds in PATH1 or PATH2 use PU239, it is a trivial matter to verify that  $0.020256*0.1463 \sim 0.0029637$ . Note that the PU239 and PU240 atom density for PATH1 and PATH2 are identical indicating an equal distribution. WPU is not used for any lower priority feed and thus this concludes the verification done with it. Because PATH1 and PATH2 have additional feed required which are not identical, the remaining atoms required to fill it needs to be calculated. This is most easily expressed using volume where PATH1 has  $4676.54/7014.80 * (7014.80 - 6842.28) \sim 115.02 \text{ cm}^3$  and PATH2 has  $57.51 \text{ cm}^3$  left to fill.

**Table 3-50. Fabrication Atom Densities for Each Feed**

|                             | DU         | NATU       | EU         | WPU        | RLWR       | RFR        | RDU        |
|-----------------------------|------------|------------|------------|------------|------------|------------|------------|
| U235                        | 2.0548E-06 | 1.4796E-04 | 3.5007E-03 |            |            | 1.7397E-04 | 1.0274E-05 |
| U238                        | 2.0546E-02 | 2.0402E-02 | 1.7092E-02 |            |            | 8.4940E-04 | 2.0538E-02 |
| PU239                       |            |            |            | 2.0256E-02 | 1.2244E-02 | 1.9250E-02 |            |
| PU240                       |            |            |            | 2.0461E-04 | 4.4894E-03 | 1.9444E-04 |            |
| PU241                       |            |            |            |            | 2.2447E-03 |            |            |
| PU242                       |            |            |            |            | 1.4284E-03 |            |            |
| Volume<br>( $\text{cm}^3$ ) | $10^{30}$  | 9732.43    | $10^{30}$  | 6842.28    | 1470.13    | 977.16     | 53532.88   |

The RLWR is the next feed to consider which is only used in the PATH3 fabrication at priority 1. The CLASS 1 volume of  $1558.85 \text{ cm}^3$  is larger than the available feed volume of  $1470 \text{ cm}^3$  and thus the entire feed will be consumed to fabricate PATH3. Because RLWR is the only non-zero feed for Pu in PATH3, the Pu atom densities can be directly compared at this point. For PU242 the density of  $0.0014284*0.15*1470.13/1558.85=0.00020207$  which is identical to the REBUS computed atom density for PU242. Since the feed was fully used there is no additional verification work to be done with this feed. PATH3 has  $88.71 \text{ cm}^3$  left to fill at lower priorities.

The RFR feed is the next feed to work with which is used in the PATH4 fabrication at priority 1. As was the case with the preceding two feeds, the RFR feed is fully consumed by the PATH4 fabrication process because the feed volume of  $977.16 \text{ cm}^3$  is lower than the PATH volume of  $1169.13 \text{ cm}^3$ . Because the RLWR feed was completely used at priority 1, the Pu isotopes are again only derived from the RFR feed in PATH4. The Pu240 atom density can be computed using  $1.9444E-04*0.15*977.16/1169.13=2.4377E-05$  which is identical to the REBUS reported result. Since the U235 and U238 isotopes will include contributions from CLASS1 and CLASS2 sources, the U235 atom density from this section is also provided here as  $1.7397E-04*0.15*977.16/1169.13=2.1811E-05$ . This density only makes up a small amount of the total U235 density of  $1.1656E-04$  from Table 3-49. Because the RFR feed was fully used in the fabrication of PATH4, there is no additional verification work to do with it. The volume remaining in PATH4 to fill is  $191.98 \text{ cm}^3$ .

The EU feed is used as priority 1 for PATH56 and since there is a very large amount of it relevant to the CLASS 1 volume of PATH56, the fabrication atom densities will simply be those in Table 3-50 multiplied by the 0.15 factor. Since PATH56 only has uranium isotopes in its feeds, it is important to track how the different isotopes from different feeds are added together. The U238 isotope density from the EU feed in PATH56 is  $0.15*1.7092E-02=2.5638E-03$ . Since this feed has a volume much larger than all other feeds, there is no point in tracking how much of the volume was removed because of its use in PATH56.

For priority 2 of PATH1, PATH2, PATH3, and PATH4, the feeds RLWR and RFR were selected which were exhausted in the priority 1 feed work. As a consequence, there is no work to be done in priority 2. For priority 3 the EU feed is used for all of the PATHs in the problem. For PATH1, the U235 atom density contribution from the EU feed is calculated as  $0.15*115.02/4676.54*3.5007E-03=1.2915E-05$  which is less than the REBUS calculated U235 density of  $2.4241E-05$ . The remaining uranium component comes from the CLASS 2 feed which is discussed later in this section and this same outcome occurs for other PATHs in this problem. For PATH2, the U235 atom density contribution from the EU feed is calculated similarly as  $0.15*57.51/2338.27*3.5007E-03=1.2915E-05$ . The PATH1 and PATH2 results are identical because the same fraction of both PATHs was filled by the WPU feed earlier. The PATH3 U235 atom density concentration from the EU feed is calculated using  $0.15*88.71/1558.85*3.5007E-03=2.9882E-05$ . The PATH4 U235 atom density concentration is calculated using  $0.15*191.98/1169.13*3.5007E-03=8.6226E-05$ . As can be seen, the atom density fraction is calculated using the enrichment modification factor and the volume fraction of a given PATH to be filled with the given feed. The numerator is of course constrained by the available feed which is the likely reason why the developers of REBUS felt it was necessary to make the user provide this information in the input.

This concludes the CLASS 1 fabrication verification work although at this point the results for PATH3, PATH4, and PATH56 have not been fully verified due to their dependence on U235 and U238 from the CLASS 2 fabrication. For CLASS 2, RDU is used as priority 1 for PATH1, PATH2, PATH3, and PATH4 while NATU is used for PATH56. The sum of all CLASS 2 volumes for PATH1, PATH2, PATH3, and PATH4 is  $55209.09 \text{ cm}^3$  which is larger than the available volume of RDU. The volume of PATH56 is smaller than that of NATU and thus it is wiser to start the verification with the RDU feed.

The RDU feed has a total volume of  $53533 \text{ cm}^3$  and the four PATHs in priority 1 are only partially filled. For PATH1, PATH2, PATH3, and PATH4, the U235 atom density was computed in the preceding paragraphs while U238 was computed for PATH56. For PATH1 the U235 contribution from the RDU feed is calculated using  $0.85*53532.88/55209.09*1.0274E-05=8.4678E-06$ . In this equation, the  $0.85=1-0.15$  or the volume fraction associated with the CLASS 2 fuel. The ratio  $53533.88/55209.09$  is the fraction of the total volume that can be filled by the available feed in RDU. Because RDU is equally distributed amongst FEED1, FEED2, FEED3, and FEED4, they all have this same U235 atom density. The remaining CLASS 2 volumes ( $\text{cm}^3$ ) to fill for PATH1, PATH2, PATH3, and PATH4 are 804.58, 402.29, 268.19, and 201.15, respectively. These are all calculated similarly where PATH1 was obtained using  $26500.37*(1-53532.88/55209.09)$ . Since the RDU feed was completely used up in priority 1, there is no additional work to be done with it.

The NATU fabrication feed has a total volume of  $9732.43 \text{ cm}^3$  and PATH56 only requires  $8833.46 \text{ cm}^3$ . Much like the EU feed for PATH56, the NATU feed is calculated by multiplying the fabrication atom densities by the enrichment modification factor. The U238 atom density from the NATU feed is  $0.85*2.0402E-02=1.7342E-02$  which, when combined with  $2.5638E-03$  from the EU feed, produces  $1.9906E-02$  which is consistent with the REBUS reported result in Table 3-49 for PATH56. The remaining feed volume of NATU usable in the next priority is computed as  $9732.43-8833.46=898.97 \text{ cm}^3$ . NATU is used as priority 2 feed for PATH1 and PATH2. The remaining volume for these two paths is  $804.58+402.29=1206.87 \text{ cm}^3$  and thus we know that the remainder of feed NATU will be completely used to fabricate fuel for PATH1 and PATH2. The U235 contribution for PATH1 is calculated as  $0.85*898.97/1206.87*804.58/26500.37*1.4796E-04=2.8442E-06$  which is identical to the REBUS reported value. The ratio  $898.97/1206.87$  is the amount of the remaining volume in PATH1 and PATH2 that can be filled with this feed. The ratio  $804.58/26500.37$  is the fraction of the total CLASS 2 volume that is being filled by this feed and 0.85 is the enrichment modification factor. The U235

contribution for PATH2 is also 2.8442E-06 calculated using  $0.85*898.97/1206.87*402.29/13250.18*1.4796E-04$ . Given the NATU feed was completely exhausted in priority 1, there is no additional work to be done with it. The remaining volumes of PATH1 and PATH2 to be filled are 205.27 and 102.63 cm<sup>3</sup>.

The DU feed is the last CLASS 2 feed used and is used as priority 3 in PATH1 and PATH2, priority 2 in PATH3 and PATH4, and priority 2 in PATH56. Given that PATH56 was completely filled with NATU, there is no work to be done with the DU feed. Because there is an infinite amount of DU feed available, the calculation of the remaining PATH details is quite easy. For PATH1, the U235 contribution from DU is calculated as  $0.85*205.27/26500.37*2.0548E-06=1.3529E-08$  where the ratio 205.27/26500.37 is the fraction of the volume being filled by this feed. Combining this with the 1.2915E-05 from CLASS 1 EU feed, 8.4678E-06 from the CLASS 2 RDU feed, and 2.8442E-05 from the NATU feed produces 2.4240E-05 which is consistent with the 2.4241E-05 from REBUS in Table 3-49. The PATH2 U235 contribution from  $0.85*102.63/13250.18*2.0548E-06=1.3529E-08$ . For PATH2, the preceding values for U235 of 1.2915E-05 from CLASS 1 EU feed, 8.4678E-06 from the CLASS 2 RDU feed, and 2.8442E-05 from the NATU feed produces 2.4240E-05, the same as PATH1.

For PATH3, the U235 contribution is  $0.85*268.19/8833.46*2.0548E-06=5.3027E-08$  while PATH4 is  $0.85*201.15/6625.09*2.0548E-06=5.3029E-08$ . These two values should be identical but the round off error in the hand calculation is quite evident. For PATH3, the previous result of 2.9882E-05 from the CLASS 1 EU feed and the 8.4678E-06 result from CLASS 2 RDU can be combined with 5.3029E-08 to obtain 3.8403E-05 which is identical with the REBUS reported result. For PATH4, the 2.1811E-05 from the CLASS 1 RFR feed, the 8.6224E-05 from the CLASS 1 EU feed, the 8.4678E-06 from the CLASS 2 RDU feed can be combined with the 5.3029E-08 from the CLASS 2 DU feed to obtain 1.1656E-04 which is identical to the REBUS reported result.

All of the atom densities produced by REBUS for this fuel fabrication were reproduced in an EXCEL document included with the verification problem. The preceding displayed hand calculation is sufficient to demonstrate how the fabrication process works in REBUS and that it is working as expected. While more complicated fabrication schemes can be tested, they would provide no additional testing over the example shown here because of the use of different combinations of feeds, exhaustion of feeds, and use of multiple stages. Given the REBUS fabrication process has been rigorously tested for over 40 years, it should come as no surprise that it is working properly.

Given the atom densities have been verified, the other aspect that needs to be verified are the reprocessing plant and external feed mass summary along with the external cycle feed. Figure 3-86 provides the reprocessing plant and external feed mass summary while Figure 3-87 provides the external cycle mass summary. As discussed above, Table 3-50 cites the available volume of each feed and the preceding hand calculations can be used to identify how much volume is filled by each feed at each priority level. The mass calculations shown in Figure 3-86 are simply the fabrication atom densities converted to mass density and multiplied by the volume filled in the domain by that feed. The hand calculated results for the class 1 feeds are in Table 3-51 while the class 2 results are in Table 3-52. Comparison with the results in Figure 3-86 shows an identical match in the result. For a quick verification, the RFR feed has a stated volume of 977.16 cm<sup>3</sup> which is completely used in the fabrication process above. For U235, the mass for this feed can be calculated with the fabrication atom density of 1.7397E-04 as  $1.7397E-04/0.6022141*235.117*977.16=66.3702$  g which is effectively identical to the reported value of 0.0663716 kg given the round off error.

The external cycle details are also easy to calculate as this is an equilibrium cycle calculation. As there are no reprocessing plants, the charged material is simply the sum of the feed used which is a trivial sum of the values, by isotope, in Table 3-51 and Table 3-52 which is omitted here for brevity. Similarly, the external feed, fabrication, and after storage columns are nothing but the sum of the external feed as no time delays were given for any of these stages. The discharged and sold columns for this problem is the total remaining fuel mass at the EOEC which for this un-powered check are also identical to the loaded materials. No additional effort is required to verify these outputs as they are easy to calculate given a basic understanding of the volume available from and volume filled with each feed along with the fabrication atom densities.

| REPROCESSING PLANT AND EXTERNAL FEED SUMMARY IN KILOGRAMS |             | MATERIAL SUPPLIED BY EXTERNAL FEED DU   |             |
|---|-------------|---|-------------|
| MATERIAL SUPPLIED BY EXTERNAL FEED EU                     |             |   |             |
| ISOTOPE   | MATERIAL    | U235                                    | 6.23582E-04 |
| U235  | 2.74997E+00 | U238                                    | 6.31497E+00 |
| U238  | 1.35981E+01 | PU239                                   | 0.00000E+00 |
| PU239   | 0.00000E+00 | PU240                                   | 0.00000E+00 |
| PU240   | 0.00000E+00 | PU241                                   | 0.00000E+00 |
| PU241   | 0.00000E+00 | PU242                                   | 0.00000E+00 |
| PU242   | 0.00000E+00 | LFPPS                                   | 0.00000E+00 |
| LFPPS   | 0.00000E+00 | DUMP                                    | 0.00000E+00 |
| DUMP  | 0.00000E+00 | MATERIAL SUPPLIED BY EXTERNAL FEED NATU |             |
| U235  | 0.00000E+00 | U235                                    | 5.62206E-01 |
| U238  | 0.00000E+00 | U238                                    | 7.85138E+01 |
| PU239   | 5.50352E+01 | PU239                                   | 0.00000E+00 |
| PU240   | 5.58241E-01 | PU240                                   | 0.00000E+00 |
| PU241   | 0.00000E+00 | PU241                                   | 0.00000E+00 |
| PU242   | 0.00000E+00 | PU242                                   | 0.00000E+00 |
| LFPPS   | 0.00000E+00 | LFPPS                                   | 0.00000E+00 |
| DUMP  | 0.00000E+00 | DUMP                                    | 0.00000E+00 |
| MATERIAL SUPPLIED BY EXTERNAL FEED WPU                    |             | MATERIAL SUPPLIED BY EXTERNAL FEED RDU  |             |
| U235  | 0.00000E+00 | U235                                    | 2.14732E-01 |
| U238  | 0.00000E+00 | U238                                    | 4.34740E+02 |
| PU239   | 5.50352E+01 | PU239                                   | 0.00000E+00 |
| PU240   | 5.58241E-01 | PU240                                   | 0.00000E+00 |
| PU241   | 0.00000E+00 | PU241                                   | 0.00000E+00 |
| PU242   | 0.00000E+00 | PU242                                   | 0.00000E+00 |
| LFPPS   | 0.00000E+00 | LFPPS                                   | 0.00000E+00 |
| DUMP  | 0.00000E+00 | DUMP                                    | 0.00000E+00 |
| MATERIAL SUPPLIED BY EXTERNAL FEED RLWR                   |             | MATERIAL SUPPLIED BY EXTERNAL FEED RFR  |             |
| U235  | 0.00000E+00 | U235                                    | 6.63716E-02 |
| U238  | 0.00000E+00 | U238                                    | 3.28195E-01 |
| PU239   | 7.14743E+00 | PU239                                   | 7.46907E+00 |
| PU240   | 2.63171E+00 | PU240                                   | 7.57613E-02 |
| PU241   | 1.32135E+00 | PU241                                   | 0.00000E+00 |
| PU242   | 8.44353E-01 | PU242                                   | 0.00000E+00 |
| LFPPS   | 0.00000E+00 | LFPPS                                   | 0.00000E+00 |
| DUMP  | 0.00000E+00 | DUMP                                    | 0.00000E+00 |
| MATERIAL SUPPLIED BY EXTERNAL FEED RFR                    |             | ...                                     |             |
| U235  | 6.63716E-02 | U235                                    | 0.00000E+00 |
| U238  | 3.28195E-01 | U238                                    | 0.00000E+00 |
| PU239   | 7.46907E+00 | PU239                                   | 0.00000E+00 |
| PU240   | 7.57613E-02 | PU240                                   | 0.00000E+00 |
| PU241   | 0.00000E+00 | PU241                                   | 0.00000E+00 |
| PU242   | 0.00000E+00 | PU242                                   | 0.00000E+00 |
| LFPPS   | 0.00000E+00 | LFPPS                                   | 0.00000E+00 |
| DUMP  | 0.00000E+00 | DUMP                                    | 0.00000E+00 |

Figure 3-86. Reprocessing Plant and External Feed Output for the Fixed Enrichment Test

| EXTERNAL CYCLE SUMMARY IN KILOGRAMS |                           |                                |                      |                              |                           |                            |
|-------------------------------------|---------------------------|--------------------------------|----------------------|------------------------------|---------------------------|----------------------------|
| ISOTOPE                             | CHARGED                   | DISCHARGED                     | AFTER COOLING        | SOLD                         | DELIVERED TO REPROCESSING | LOST IN REPROCESSING       |
| U235                                | 3.59390E+00               | 3.25657E+00                    | 3.25657E+00          | 3.25657E+00                  | 0.00000E+00               | 0.00000E+00                |
| U238                                | 5.33495E+02               | 5.28539E+02                    | 5.28539E+02          | 5.28539E+02                  | 0.00000E+00               | 0.00000E+00                |
| PU239                               | 6.96518E+01               | 6.90514E+01                    | 6.90514E+01          | 6.90514E+01                  | 0.00000E+00               | 0.00000E+00                |
| PU240                               | 3.26571E+00               | 3.64723E+00                    | 3.64723E+00          | 3.64723E+00                  | 0.00000E+00               | 0.00000E+00                |
| PU241                               | 1.32135E+00               | 1.22120E+00                    | 1.22120E+00          | 1.22120E+00                  | 0.00000E+00               | 0.00000E+00                |
| PU242                               | 8.44353E-01               | 8.51562E-01                    | 8.51562E-01          | 8.51562E-01                  | 0.00000E+00               | 0.00000E+00                |
| LFPPS                               | 0.00000E+00               | 5.57457E+00                    | 5.57457E+00          | 5.57457E+00                  | 0.00000E+00               | 0.00000E+00                |
| DUMP                                | 0.00000E+00               | 7.38218E-03                    | 7.38218E-03          | 7.38218E-03                  | 0.00000E+00               | 0.00000E+00                |
| ISOTOPE                             | RECOVERED IN REPROCESSING | REPROCESSED AND USED IN MAKEUP | REPROCESSED AND SOLD | EXTERNAL FEED USED IN MAKEUP | AFTER FABRICATION         | AFTER STORAGE (NEW CHARGE) |
| U235                                | 0.00000E+00               | 0.00000E+00                    | 0.00000E+00          | 3.59390E+00                  | 3.59390E+00               | 3.59390E+00                |
| U238                                | 0.00000E+00               | 0.00000E+00                    | 0.00000E+00          | 5.33495E+02                  | 5.33495E+02               | 5.33495E+02                |
| PU239                               | 0.00000E+00               | 0.00000E+00                    | 0.00000E+00          | 6.96518E+01                  | 6.96518E+01               | 6.96518E+01                |
| PU240                               | 0.00000E+00               | 0.00000E+00                    | 0.00000E+00          | 3.26571E+00                  | 3.26571E+00               | 3.26571E+00                |
| PU241                               | 0.00000E+00               | 0.00000E+00                    | 0.00000E+00          | 1.32135E+00                  | 1.32135E+00               | 1.32135E+00                |
| PU242                               | 0.00000E+00               | 0.00000E+00                    | 0.00000E+00          | 8.44353E-01                  | 8.44353E-01               | 8.44353E-01                |
| LFPPS                               | 0.00000E+00               | 0.00000E+00                    | 0.00000E+00          | 0.00000E+00                  | 0.00000E+00               | 0.00000E+00                |
| DUMP                                | 0.00000E+00               | 0.00000E+00                    | 0.00000E+00          | 0.00000E+00                  | 0.00000E+00               | 0.00000E+00                |

Figure 3-87. External Cycle Excerpt for the Fixed Enrichment Test

The last aspect to verify in this task is that REBUS will properly search the enrichment. In this regard it is very important to point out the presence of A.BURN card type 06 in Figure 3-84. There is a known bug in REBUS where the enrichment search procedure is not initialized or executed properly unless a card type 06 input is provided. The displayed input card serves no purpose as no card type 05 inputs were provided, but it is required in order to allow REBUS to search the enrichment properly in equilibrium problems.

**Table 3-51. Mass (kg) Used in the Class 1 Feed**

|                                | EU          | WPU         | RLWR        | RFR         |
|--------------------------------|-------------|-------------|-------------|-------------|
| Volume Used (cm <sup>3</sup> ) | 2012.06     | 6842.28     | 1470.13     | 977.157     |
| U235                           | 2.74996E+00 | 0.00000E+00 | 0.00000E+00 | 6.63716E-02 |
| U238                           | 1.35980E+01 | 0.00000E+00 | 0.00000E+00 | 3.28195E-01 |
| PU239                          | 0.00000E+00 | 5.50352E+01 | 7.14743E+00 | 7.46907E+00 |
| PU240                          | 0.00000E+00 | 5.58241E-01 | 2.63171E+00 | 7.57613E-02 |
| PU241                          | 0.00000E+00 | 0.00000E+00 | 1.32135E+00 | 0.00000E+00 |
| PU242                          | 0.00000E+00 | 0.00000E+00 | 8.44353E-01 | 0.00000E+00 |

**Table 3-52. Mass (kg) Used in the Class 2 Feed**

|             | DU          | NATU        | RDU         |
|-------------|-------------|-------------|-------------|
| Volume Used | 777.236     | 9732.43     | 53532.88    |
| U235        | 6.23528E-04 | 5.62206E-01 | 2.14732E-01 |
| U238        | 6.31442E+00 | 7.85138E+01 | 4.34740E+02 |
| PU239       | 0.00000E+00 | 0.00000E+00 | 0.00000E+00 |
| PU240       | 0.00000E+00 | 0.00000E+00 | 0.00000E+00 |
| PU241       | 0.00000E+00 | 0.00000E+00 | 0.00000E+00 |
| PU242       | 0.00000E+00 | 0.00000E+00 | 0.00000E+00 |

In the manufactured test case, the BOC  $k_{eff}$  was 0.79557 while the EOC  $k_{eff}$  was 0.79017 as shown in the REBUS output excerpt of Figure 3-85. These values, with more precision, were used to construct the BOC  $k_{eff}$  search and EOC  $k_{eff}$  input modifications displayed in Figure 3-88. As can be seen, only one line of the input needs to be changed although all of the inputs on that line change. The first change on card type 04, compared with Figure 3-84, is to set the  $k_{eff}$  value to the desired target and set the  $k_{eff}$  convergence on the enrichment search to  $10^{-6}$ . For the BOC case, the fraction of the burn time is set to 0.0 while for EOC it is set to 1.0. The initial enrichment guesses are set to 0.1 and 0.9 for both search cases where the fixed one they were both set to 0.15.

|                                    |                                   |
|------------------------------------|-----------------------------------|
| 04 0.79556809 1.0E-6 0.0 0.10 0.90 | 04 0.79017265 1.0E-6 1.0 0.1 0.90 |
| BOC                                | EOC                               |

**Figure 3-88. REBUS Input Modifications for the Search Cases**

The calculated  $k_{eff}$  values obtained by REBUS during the search are plotted in Figure 3-89. As can be seen, the BOC search case required nearly 90 flux solves to obtain the final solution while the EOC case required 84. The fixed enrichment case used 16 flux solves. In each case at least 3 flux solves were completed to converged the EOC atom densities due to the depletion. This last aspect accounts for a significant portion of the  $k_{eff}$  solve requirement as convergence of the EOC system is required

when the enrichment search parameter is updated. Note that the performance of the enrichment search is quite poor as the guesses are so widely spread. Using enrichment guesses closer to the known result can reduce the computational effort substantially.

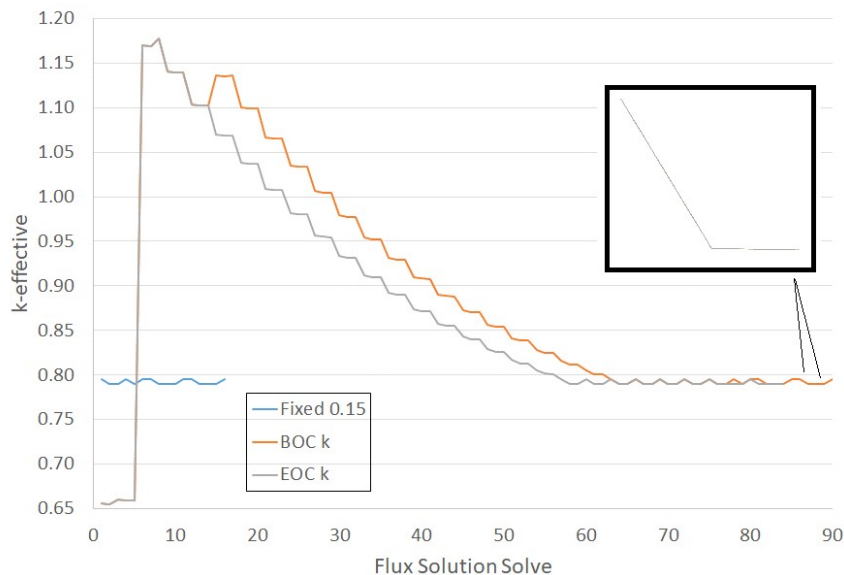


Figure 3-89.  $k_{\text{eff}}$  Convergence Behavior for the Search Cases

The final computed eigenvalues for all three cases match with less than 1 pcm error for both BOC and EOC. For completeness of the verification process, the same section of output is taken from each test case and collected in Figure 3-90. The enrichment search parameters were identical to 5 significant digits which is not shown for brevity.

| FIXED ENRICHMENT CASE   |  |           |
|-------------------------|--|-----------|
| FCC004 11.3114 04/10/20 | ABURN: Hexagonal 3D Test Problem<br>REACTOR CHARACTERISTICS SUMMARY<br>===== | PAGE 358  |
|                         | BOEC EOC   |           |
|                         | KEFF 0.79557 0.79017   |           |
|                         | PEAKING FACTOR 0.00000 0.00000   |           |
| BOC SEARCH CASE         |  |           |
| FCC004 11.3114 04/10/20 | ABURN: Hexagonal 3D Test Problem<br>REACTOR CHARACTERISTICS SUMMARY<br>===== | PAGE 1395 |
|                         | BOEC EOC   |           |
|                         | KEFF 0.79557 0.79017   |           |
|                         | PEAKING FACTOR 0.00000 0.00000   |           |
| EOC SEARCH CASE         |  |           |
| FCC004 11.3114 04/10/20 | ABURN: Hexagonal 3D Test Problem<br>REACTOR CHARACTERISTICS SUMMARY<br>===== | PAGE 1311 |
|                         | BOEC EOC   |           |
|                         | KEFF 0.79557 0.79017   |           |

Figure 3-90. REBUS Output Excerpt for all Three Enrichment Search Cases

As a final note, for equilibrium problems, REBUS performs a “un-poisoned  $k_{\text{eff}}$ ” calculation after the equilibrium fuel cycle calculations are completed. Thus the last eigenvalue for the fixed 0.15 case and BOC search cases returns to 0.79557 as the fraction of the cycle length target was set to 0.0 in both

cases. For the EOC search case, it repeats the 0.79017 point as the cycle length target was set to 1.0. Thus this aspect of the output is normal and expected.

### 3.6.1.2 Detailed Verification of Card Type 12 and 13 Input

With the preceding fabrication process displayed, tasks a and c of category 4 are completely verified. This leaves task b which deals specifically with card type 12. Since this task targets A.BURN card type 12 input, there is no need to specify a complicated fuel fabrication scheme. In that regard, the preceding input is modified to just use the EU feed in CLASS 1 and the DU feed in CLASS 2 both of which are given infinite volumes. The excerpt of the REBUS input is provided in Figure 3-91.

|   |   |
|---|---|
| <pre> UNIFORM=A.BURN 04      1.0      1.0      0.0  0.15  0.15 06      CORE      0.99 09      TRACE      6 DUMP 25      TRACE      6 DUMP      8.02254E-8 ... 11      PATH1      0      1      F0001 Z0001 11      PATH2      0      1      F0002 Z0002 11      PATH2      0      2      F0002 Z0002 11      PATH3      0      1      F0003 Z0003 11      PATH3      0      2      F0003 Z0003 11      PATH3      0      3      F0003 Z0003 11      PATH4      0      1      F0004 Z0004 11      PATH4      0      2      F0004 Z0004 11      PATH4      0      3      F0004 Z0004 11      PATH4      0      4      F0004 Z0004 11      PATH56     0      1      F0005 Z0005 11      PATH56     0      2      F0005 Z0005 11      PATH56     0      3      F0005 Z0005 11      PATH56     0      4      F0005 Z0005 11      PATH56     0      5      F0005 Z0005 11      PATH56     0      6      F0005 Z0005 12      PATH1      FAB1      0.0  0.0  1.00      1.00 12      PATH2      FAB2      50.0 30.0  1.05      0.95 12      PATH3      FAB3      100.0 10.0  1.10      1.05 12      PATH4      FAB4      150.0 10.0  0.95      0.90 12      PATH56     FAB56     200.0 10.0  0.90      0.80 13      FAB1 U235  1.92100E-02 13      FAB1 U238  1.89674E-02 13      FAB1 PU239  1.88879E-02 13      FAB1 PU240  1.88091E-02 13      FAB1 PU241  1.87308E-02 13      FAB1 PU242  1.86533E-02 13      FAB1 DUMP   1.90574E-02 13      FAB1 LFPPS  1.91382E-02 13      FAB1 TRACE   4.51661E-02 13      FAB2 U235  1.98504E-02 13      FAB2 U238  1.95996E-02 13      FAB2 PU239  1.95175E-02 13      FAB2 PU240  1.94361E-02 13      FAB2 PU241  1.93552E-02 13      FAB2 PU242  1.92751E-02 13      FAB2 DUMP   1.96927E-02 13      FAB2 LFPPS  1.97761E-02 13      FAB2 TRACE   4.66716E-02 13      FAB3 U235  2.04907E-02 13      FAB3 U238  2.02319E-02 13      FAB3 PU239  2.01471E-02 13      FAB3 PU240  2.00630E-02 </pre> | <pre> 13      FAB3 PU241  1.99796E-02 13      FAB3 PU242  1.98969E-02 13      FAB3 DUMP   2.03279E-02 13      FAB3 LFPPS  2.04140E-02 13      FAB3 TRACE   4.81771E-02 13      FAB4 U235  2.11310E-02 13      FAB4 U238  2.08641E-02 13      FAB4 PU239  2.07767E-02 13      FAB4 PU240  2.06900E-02 13      FAB4 PU241  2.06039E-02 13      FAB4 PU242  2.05187E-02 13      FAB4 DUMP   2.09631E-02 13      FAB4 LFPPS  2.10520E-02 13      FAB4 TRACE   4.96827E-02 13      FAB56 U235  2.17714E-02 13      FAB56 U238  2.14964E-02 13      FAB56 PU239  2.14063E-02 13      FAB56 PU240  2.13170E-02 13      FAB56 PU241  2.12283E-02 13      FAB56 PU242  2.11404E-02 13      FAB56 DUMP   2.15984E-02 13      FAB56 LFPPS  2.16899E-02 13      FAB56 TRACE   5.11882E-02 18      CLASS1 U235  1.0 18      CLASS1 U238  1.0 18      CLASS1 PU239  1.0 18      CLASS1 PU240  1.0 18      CLASS1 PU241  1.0 18      CLASS1 PU242  1.0 18      CLASS2 U235  0.0 18      CLASS2 U238  0.0 18      CLASS2 TRACE   0.0 19      PATH1      EU      1 19      PATH2      EU      1 19      PATH3      EU      1 19      PATH4      EU      1 19      PATH56     EU      1 20      PATH1      DU      1 20      PATH2      DU      1 20      PATH3      DU      1 20      PATH4      DU      1 20      PATH56     DU      1 21      EU      CLASS1      1.0E30 21      DU      CLASS2      1.0E30 22      EU      U235      0.17 22      EU      U238      0.83 22      DU      U235      0.0001 22      DU      U238      0.9998999 22      DU      TRACE      0.0000001 </pre> |
|---|---|

Figure 3-91. REBUS Input Excerpt for the Multiple Fabrication Density Test Case

As seen, the card type 12 and 13 data was expanded to have 5 different fabrication densities and considerable differences in the fabrication time, storage time, initial enrichment, and the enrichment modification factor between the PATHs. The fabrication itself will only consist of U235, U238, and TRACE because of the feed definition. Because the TRACE isotope is not impacted by the flux level, it will serve as the means to verify that the fabrication and storage times are being applied correctly. The TRACE isotope was added to the CLASS 2 feed in this example.

To assist in the hand calculation work, the card type 12 data is translated from the user input to the final enrichment of each PATH and the fabrication density (g/cc) is converted to the fabrication atom density (conventional units) for each feed consistent with the approach shown earlier. All of this is

compiled in Table 3-53 where the equations for the enrichment given the card type 12 input can be found in the manual or the REBUS input description.

**Table 3-53. Fabrication Details of the Multiple Fabrication Density Test Case**

|                                  | PATH1      | PATH2      | PATH3      | PATH4      | PATH56     |
|----------------------------------|------------|------------|------------|------------|------------|
| Volume (cm <sup>3</sup> )        | 31176.9    | 31176.9    | 31176.9    | 31176.9    | 62353.8    |
| Stages                           | 1          | 2          | 3          | 4          | 6          |
| Density (g/cc)                   | 7.50       | 7.75       | 8.00       | 8.25       | 8.50       |
| EU Feed Fabrication Atom Density | 1.9008E-02 | 1.9642E-02 | 2.0275E-02 | 2.0909E-02 | 2.1543E-02 |
| DU Feed Fabrication Atom Density | 1.8967E-02 | 1.9600E-02 | 2.0232E-02 | 2.0864E-02 | 2.1496E-02 |
| Initial Enrichment               | 1.00       | 1.05       | 1.10       | 0.95       | 0.90       |
| EMF                              | 1.00       | 0.95       | 1.05       | 0.90       | 0.80       |
| Enrichment                       | 0.150000   | 0.202125   | 0.118250   | 0.223250   | 0.288000   |
| Fabrication Time (days)          | 0.0        | 50.0       | 100.0      | 150.0      | 200.0      |
| Preloading Storage Time (days)   | 0.0        | 30.0       | 10.0       | 10.0       | 10.0       |

Because of the simple fabrication feed setup, the fabrication densities are trivial to compute. As an example, the U235 content of PATH1 is  $1.9008E-02 * 0.17 * 0.15 + 1.8967E-02 * 0.0001 * 0.85 = 4.8632E-04$ . The 0.17 is the EU feed atom fraction of U235 where 1.9008E-02 is the EU fabrication atom density from Table 3-53 and 0.15 is the final enrichment for PATH1 in Table 3-53. The remaining values are the equivalent numbers for the DU feed instead of the EU feed. The excerpt of the stage densities from REBUS are provided in Figure 3-92 and one can readily see that the U235 hand calculation for PATH1 is correct.

FCC004 11.3114 04/10/20

PAGE 280

```

BEGINNING OF BURN CYCLE 1
ATOM DENSITIES (IN ATOMS/BARN-CM.) OF ACTIVE ISOTOPES IN EACH STAGE OF EACH PATH
PATH PATH1
STAGE REGION
+ 1 CORE1 4.8632E-04 1.8487E-02 0.0000E+00 0.0000E+00 0.0000E+00 0.0000E+00 0.0000E+00 0.0000E+00 0.0000E+00 1.6122E-09
1 CORE2 6.7648E-04 1.8932E-02 0.0000E+00 0.0000E+00 0.0000E+00 0.0000E+00 0.0000E+00 0.0000E+00 6.6564E-10 8.9817E-10
2 CORE2 6.7157E-04 1.8910E-02 1.4971E-05 9.6141E-09 4.9111E-12 1.6406E-15 1.1194E-05 1.1147E-09 4.4908E-10
PATH PATH3
1 CORE3 4.0937E-04 1.9828E-02 0.0000E+00 0.0000E+00 0.0000E+00 0.0000E+00 0.0000E+00 0.0000E+00 9.5171E-10 8.3224E-10
2 CORE3 4.0622E-04 1.9804E-02 1.6692E-05 1.1440E-08 6.2301E-12 2.2172E-15 1.0005E-05 1.3678E-09 4.1612E-10
3 CORE3 4.0310E-04 1.9781E-02 3.3212E-05 4.5541E-08 4.9527E-11 3.5287E-14 2.0107E-05 1.5759E-09 2.0806E-10
PATH PATH4
1 CORE4 7.9517E-04 2.0079E-02 0.0000E+00 0.0000E+00 0.0000E+00 0.0000E+00 0.0000E+00 0.0000E+00 1.0860E-09 5.3461E-10
2 CORE4 7.9138E-04 2.0064E-02 1.0777E-05 4.7817E-09 1.6742E-12 3.8020E-16 8.0693E-06 1.3533E-09 2.6730E-10
3 CORE4 7.8760E-04 2.0049E-02 2.1485E-05 1.9069E-08 1.3341E-11 6.0631E-15 1.6169E-05 1.4870E-09 1.3365E-10
4 CORE4 7.8385E-04 2.0034E-02 3.2124E-05 4.2777E-08 4.4847E-11 3.0593E-14 2.4299E-05 1.5538E-09 6.6826E-11
PATH PATH56
1 CORE5 1.0563E-03 2.0453E-02 0.0000E+00 0.0000E+00 0.0000E+00 0.0000E+00 0.0000E+00 0.0000E+00 1.1735E-09 3.5701E-10
2 CORE5 1.0503E-03 2.0435E-02 1.2800E-05 6.5492E-09 2.6573E-12 7.0263E-16 1.1340E-05 1.3520E-09 1.7851E-10
3 CORE5 1.0443E-03 2.0417E-02 2.5503E-05 2.6103E-08 2.1159E-11 1.1198E-14 2.2715E-05 1.4413E-09 8.9253E-11
4 CORE5 1.0384E-03 2.0399E-02 3.8109E-05 5.8524E-08 7.1079E-11 5.6468E-14 3.4123E-05 1.4859E-09 4.4626E-11
5 CORE5 1.0325E-03 2.0381E-02 5.0619E-05 1.0367E-07 1.6770E-10 1.7777E-13 4.5564E-05 1.5082E-09 2.2313E-11
6 CORE5 1.0266E-03 2.0363E-02 6.3034E-05 1.6141E-07 3.2601E-10 4.3230E-13 5.7039E-05 1.5194E-09 1.1157E-11
PATH PATH56
1 CORE6 1.0563E-03 2.0453E-02 0.0000E+00 0.0000E+00 0.0000E+00 0.0000E+00 0.0000E+00 0.0000E+00 1.1735E-09 3.5701E-10
2 CORE6 1.0503E-03 2.0435E-02 1.2800E-05 6.5492E-09 2.6573E-12 7.0263E-16 1.1340E-05 1.3520E-09 1.7851E-10
3 CORE6 1.0443E-03 2.0417E-02 2.5503E-05 2.6103E-08 2.1159E-11 1.1198E-14 2.2715E-05 1.4413E-09 8.9253E-11
4 CORE6 1.0384E-03 2.0399E-02 3.8109E-05 5.8524E-08 7.1079E-11 5.6468E-14 3.4123E-05 1.4859E-09 4.4626E-11
5 CORE6 1.0325E-03 2.0381E-02 5.0619E-05 1.0367E-07 1.6770E-10 1.7777E-13 4.5564E-05 1.5082E-09 2.2313E-11
6 CORE6 1.0266E-03 2.0363E-02 6.3034E-05 1.6141E-07 3.2601E-10 4.3230E-13 5.7039E-05 1.5194E-09 1.1157E-11

```

**Figure 3-92. REBUS Output Excerpt for the Multiple Fabrication Density Test Case**

Because of the simplicity, the hand calculation of these atom densities is easiest to display in table form as done in Table 3-54. A quick comparison of the U235 and U238 atom densities with the REBUS results in Figure 3-92 shows a near perfect match for all feeds with slight errors caused by round off error in the fabrication atom density data displayed in Table 3-53. The TRACE atom density results are only accurate for PATH1 which is because the fabrication or storage time in Table 3-53 was not accounted for in Table 3-54. Using the decay constant for TRACE from Figure 3-91, the TRACE atom densities can easily be calculated to produce the fabrication TRACE atom densities in Table 3-55. These results are again identical to the REBUS produced results in Figure 3-92.

**Table 3-54. Hand Calculation of the Multiple Fabrication Density Test Case**

|        | U235   | U238  | TRACE (no decay)                        |
|--------|--|---|---|
| PATH1  | 4.8632E-04<br>=1.9008E-02*0.17*0.15<br>+1.8967E-02*0.0001*0.85         | 1.8487E-02<br>=1.9008E-02*0.83*0.15<br>+1.8967E-02*0.9998999*0.85         | 1.6122E-09<br>=1.8967E-02*1E-7*0.85     |
| PATH2  | 6.7649E-04<br>=1.9642E-02*0.17*0.202125<br>+1.9600E-02*0.0001*0.797875 | 1.8932E-02<br>=1.9642E-02*0.83*0.202125<br>+1.9600E-02*0.9998999*0.797875 | 1.5638E-09<br>=1.9600E-02*1E-7*0.797875 |
| PATH3  | 4.0936E-04<br>=2.0275E-02*0.17*0.11825<br>+2.0232E-02*0.0001*0.88175   | 1.9828E-02<br>=2.0275E-02*0.83*0.11825<br>+2.0232E-02*0.9998999*0.88175   | 1.7840E-09<br>=2.0232E-02*1E-7*0.88175  |
| PATH4  | 7.9517E-04<br>=2.0909E-02*0.17*0.22325<br>+2.0864E-02*0.0001*0.77675   | 2.0079E-02<br>=2.0909E-02*0.83*0.22325<br>+2.0864E-02*0.9998999*0.77675   | 1.6206E-09<br>=2.0864E-02*1E-7*0.77675  |
| PATH56 | 1.0563E-03<br>=2.1543E-02*0.17*0.288<br>+2.1496E-02*0.0001*0.712       | 2.0453E-02<br>=2.1543E-02*0.83*0.288<br>+2.1496E-02*0.9998999*0.712       | 1.5305E-09<br>=2.1496E-02*1E-7*0.712    |

**Table 3-55. TRACE Isotope Density in the Multiple Fabrication Density Test Case**

|        | TRACE<br>No Decay | Decay Time<br>(days) | TRACE<br>With Decay |
|--------|-------------------|----------------------|---------------------|
| PATH1  | 1.6122E-09        | 0.0                  | 1.6122E-09          |
| PATH2  | 1.5638E-09        | 80.0                 | 8.9817E-10          |
| PATH3  | 1.7840E-09        | 110.                 | 8.3224E-10          |
| PATH4  | 1.6206E-09        | 160.0                | 5.3461E-10          |
| PATH56 | 1.5305E-09        | 210.0                | 3.5701E-10          |

Given the verification work in this section, task b of category 4 is verified. No additional testing of card types 4, 12, 13, 18-22 are necessary as the preceding work verified all of the fabrication details with hand calculations. The enrichment search functionality was verified by defining a manufactured test and then using the enrichment search routine to reproduce that manufactured solution. No additional tests are required noting that all of these features have been extensively tested over the past 40 years and are continuously tested today.

### 3.7 Category 5 Verification

The category 5 section of Table 2-1, reproduced here as Table 3-56, has one task which is focused on verifying the various output edits used by users. Several of these were addressed in previous sections such as the burnup and power edits. In this section, the specific output edits for a given test case will be displayed from REBUS and a hand calculation will be displayed that explains how REBUS is

computing the stated output. Because the peaking calculations in REBUS depend upon the SFEDIT file produced by DIF3D, this section will also cover the verification of the SFEDIT file.

**Table 3-56. REBUS Identified Verification Tasks for Category 5**

|   |  |
|---|--|
| 5 | Verify the mass, burnup, power, and fluence edits<br>a) Controlled by default REBUS names or user input (cards 29, 30) |
|---|--|

### 3.7.1 Verification of the SFEDIT Data File

The origination of the SFEDIT file (Surface Flux EDIT) is a result of the cell centered quantities in the finite difference methodology not providing the true peak flux in the domain. This information is important for fuel cycle analysis and thus the SFEDIT file was added to DIF2D for the use by the REBUS software. As inferred from its name, the purpose of the SFEDIT file was to provide the surface fluxes where the cell centered and surface flux data is stored with respect to the GEODST mesh ordering. The numbering of the surface data from DIF3D-FD is displayed in Figure 3-93 which is notably different from that of DIF3D-Nodal and DIF3D-VARIANT. For DIF3D-FD, the surface centered quantities are the only ones that exist from the formulation and thus the number of data points is fixed for all data files. Because the data is stored by mesh, there is duplication of the surface data in DIF3D-FD where as DIF3D-Nodal and DIF3D-VARIANT have spatially discontinuous flux approximations at mesh interfaces and the storage approach does not constitute duplication. Although not indicated, the lower and upper plane surface data is also given in DIF3D-FD for the triangular (surfaces 4 and 5) and Cartesian (5 and 6) geometry options. For DIF3D-Nodal and DIF3D-VARIANT, the lower and upper surface information is complicated as it is primarily used to construct the axial profile of the radial sample data as will be shown.

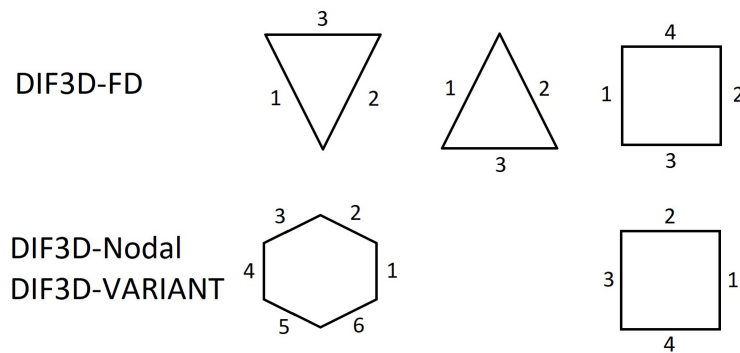


**Figure 3-93. Surface Numbering in the SFEDIT**

Later in the development of DIF3D, the surface flux file was too large and was replaced with power density and fast flux as these were the only two quantities being used by REBUS and with DIF3D providing them it avoids REBUS having to recalculate what DIF3D was already calculating for its output editing. A final modification made was to store the data on a region basis instead of a mesh basis. The mesh based result was very large and required REBUS to cycle through all meshes to collect the information by region. Again, DIF3D was already built to compute the region-wise quantities and thus it was more convenient for REBUS to simply use the DIF3D computed details. These two options are referred to as SFEDIT option 1 (mesh-wise) and SFEDIT option 2 (region-wise). Internal to REBUS it forces DIF3D to export both sets of data to a single SFEDIT file (mesh-wise data first followed by region-wise data). REBUS only uses the region-wise data when computing the peak data and thus only the region-wise data needs to be verified. For the user, the DIF3D calculation must be executed

twice with different card type 04 input options as it only writes the data to the SFEDIT file for either option (it will overwrite the SFEDIT file in a block based restart). In this manner, the SFEDIT file used by REBUS is not consistent with the SFEDIT file format itself. While it is stored on the STACK file and can be extracted and verified, it is not clear which SFEDIT data is being used as REBUS only appears to store the first time point SFEDIT on STACK. Given the same parts of DIF3D are used by REBUS for SFEDIT in the same manner, the SFEDIT data can be verified with DIF3D first. Given that process is verified, the task of verifying how REBUS uses this data can be investigated and verified in REBUS.

For the SFEDIT data, the DIF3D-FD approach is rather easy to verify given one has the cell centered flux solution values from DIF3D and the macroscopic cross section data for each mesh. The inclusion of DIF3D-Nodal, a transverse integrated methodology, introduced a serious problem with the peaking calculation as the formulation did not define a three-dimensional basis. For DIF3D-VARIANT this is not an issue as there is a three-dimensional basis as demonstrated in the DIF3D verification document when evaluating the peak flux output [14]. For DIF3D-Nodal, the developers devised an axial interpolation methodology for the center and 6 radial surfaces. A fixed 11 axial planes per Nodal mesh are used to sample the peaking data. This approach produces a single value for each surface on each plane and thus  $66=11*6$  total surface values per mesh along with 11 values at the center of the mesh. The methodology is of course not accurate, but it is all the developers of DIF3D-Nodal could do given the limitations of the formulation. It is unfortunate that the developers of DIF3D-VARIANT implemented the same approach as it is knowingly inaccurate and a more accurate approach was readily available for DIF3D-VARIANT.

### 3.7.1.1 DIF3D-FD Procedure for Calculating the SFEDIT Sample Points

As discussed, the surface flux information in the finite difference formulation is evaluated using the finite difference equations. From equation 2.18 in the DIF3D manual the interface flux between two adjacent meshes  $p$  and  $q$  can be evaluated using

$$F_{g,p} = \frac{D_{g,p} \cdot A_{p \leftrightarrow q}}{V_p} \quad F_{g,q} = \frac{D_{g,q} \cdot A_{p \leftrightarrow q}}{V_q}$$

$$\phi_{g,surf} = \frac{F_{g,p}}{F_{g,p} + F_{g,q}} \phi_{g,p} + \frac{F_{g,q}}{F_{g,p} + F_{g,q}} \phi_{g,q}. \quad (54)$$

In this equation,  $D_{g,p}$  and  $D_{g,q}$  are the diffusion coefficients for the two meshes for group  $g$ ,  $V_p$  and  $V_q$  are the volumes of the two meshes,  $\phi_{g,p}$  and  $\phi_{g,q}$  are the cell averaged group flux values for the two meshes. The variable  $A_{p \leftrightarrow q}$  is the area of the surface that connects the two meshes. For boundary flux values, equation 2.22 from the DIF3D-FD manual applies to give

$$F_{g,\Gamma} = \frac{\beta_g}{2\alpha_g} \quad \phi_{g,surf} = \frac{F_{g,p}}{F_{g,p} + F_{g,\Gamma}} \phi_{g,p}. \quad (55)$$

The common boundary conditions used by DIF3D are taken as

$$\begin{array}{ll} \text{reflective} & \alpha = 1; \beta = 0 \\ \text{zero flux} & \alpha = 0; \beta = 1 \end{array} \quad . \quad (56)$$

*extrapolated*  $\alpha = 1/0.46920; \beta = 1$

The DIF3D-FD implementation is setup to prevent singularities from occurring in the formulation because of the boundary condition constants. It is important to note that the existing methodology simply sets the boundary flux to the cell centered flux for reflected boundary conditions. This is a result of the fact that the derivative for the current is composed of the difference between the mesh centered and surface flux. Given that the derivative must equal zero for reflected b.c.s, the surface flux must equal the cell centered flux. Higher order finite difference discretizations simply push this equivalence closer to the edge of the mesh.

As mentioned, the DIF3D-FD approach only allows for a single sample point per surface which are calculated with the preceding equations. Combined with the volume term, simply the solution vector itself, this translates to 6 points per triangular-z mesh for the power density and another 6 points for the fast flux. As noted, there is a substantial amount of duplication of information as the surface fluxes are identical between adjacent meshes.

### 3.7.1.2 Special Nodal Procedure for Calculating the SFEDIT Sample Points

The peaking calculation methodology used by DIF3D-VARIANT is a little more difficult to extract from the DIFED-Nodal manual. Focusing only on the diffusion theory approach, when DIF3D-VARIANT is executed, it computes the flux moments  $\phi_{g,m,i}$  for energy group  $g$  internal to each mesh  $m$  based upon a polynomial expansion  $f_i(x, y, z)$  which can be written as:

$$\phi_{g,m}(x, y, z) = \sum_i f_i(x, y, z) \cdot \phi_{g,m,i} \quad (57)$$

It also computes the flux  $\varphi_{g,\gamma,j}$  and current  $J_{g,\gamma,j}$  moments on each interface in the domain  $\gamma$  for the polynomial approximation  $g_j(x, y, z)$  which can be written as

$$\begin{aligned} \varphi_{g,\gamma}(x, y, z) &= \sum_j g_j(x, y, z) \cdot \varphi_{g,\gamma,j} \\ J_{g,\gamma}(x, y, z) &= \sum_j g_j(x, y, z) \cdot J_{g,\gamma,j}. \end{aligned} \quad (58)$$

Note that on some surfaces the spatial dependence of the flux and current on the interface do not span all three coordinate directions (i.e. neither are real functions of x for Cartesian surface 1 in Figure 3-93). DIF3D-VARIANT actually works with the partial currents which are written in terms of the surface flux and current and the surface expansion as:

$$j_{g,\gamma}^{\pm}(x, y, z) = \frac{1}{4} \varphi_{g,\gamma}(x, y, z) \pm \frac{1}{2} J_{g,\gamma}(x, y, z) = \sum_j g_j(x, y, z) j_{g,\gamma,j}^{\pm}. \quad (59)$$

The mesh wise flux solution  $\phi_{g,m,i}$  and the partial currents  $j_{g,\gamma,j}^{\pm}$  are stored in the NHFLUX binary interface file. The partial currents are actually partitioned by x-y and z orientated surfaces and stored by global interface (i.e.  $j_{g,\Gamma,j}$ ) rather than  $j_{g,\gamma,j}^+$  and  $j_{g,\gamma,j}^-$  where one can consider the range of  $\Gamma$  to be twice the range of  $\gamma$ . The mapping between each mesh surface and each global surface by orientation (+ or -) is also provided on the NHFLUX file.

For the SFEDIT file, the flux peaking calculation is only concerned with peaks in  $\phi_{g,m}(x, y, z)$  and  $\varphi_{g,\gamma}(x, y, z)$ . As mentioned, DIF3D-Nodal does not contain enough information to accurately predict the peak flux internal to each mesh. The developers created a “special nodal procedure” in which a 5<sup>th</sup> order 1-D axial basis is applied of the form

$$\bar{\varphi}(\zeta) = \begin{bmatrix} 1 \\ \zeta \\ 3\zeta^2 - 0.25 \\ \zeta^3 - 0.25\zeta \\ (\zeta^2 - 0.05)(\zeta^2 - 0.25) \end{bmatrix}. \quad (60)$$

The coordinate  $\zeta$  is relative to the reference space of each mesh (-0.5 to 0.5) rather than the global domain coordinate system. The axial shaping function is multiplied by the cell averaged flux to give the center line axial shape in each mesh. The axial shaping function is further multiplied by each surface flux to define an axial surface flux shape. Eleven axial sample points are defined (including both upper and lower surfaces) and all seven functions are evaluated to produce 77 samples of the power density and 77 samples of the fast flux. These 144 values are stored in SFEDIT for every mesh in the domain and used by REBUS when computing the power peaking of a region. For DIF3D-VARIANT, the axial basis is somewhat truncated as it does not apply the DIF3D-Nodal approximation

and thus the basis is truncated to 2<sup>nd</sup> order. In DIF3D-Nodal, the basis is also truncated for hexagonal geometries to just the first three or four polynomials depending upon the input specification [7].

The first step in translating the DIF3D-VARIANT NHFLUX quantities is to recast the flux and current data into the flux shape information. This is discussed extensively in the manual for DIF3D-Nodal [7] and only the final results are displayed here. For each energy group the cell averaged flux  $\bar{\phi}_{g,m}$  used in the interpolation procedure is obtained with

$$\bar{\phi}_{g,m} = \phi_{g,m,1}. \quad (61)$$

Because DIF3D-VARIANT uses an orthonormal set of polynomials for the spatial approximation, the first moment is by definition the average flux in the mesh and thus it is simply copied from the NHFLUX data file as indicated. The x-y surface average flux values  $\bar{\phi}_{g,m,l}$  for hexagonal geometry are computed using

$$\begin{aligned} \bar{\phi}_{g,m,l} &= \frac{2\sqrt{3}}{P \cdot \Delta_m} (j_{g,\Xi(m,l),1} + j_{g,\Pi(m,l),1}) \quad l \in 1,6 \\ \bar{\phi}_{g,m,l} &= \frac{4}{\sqrt{3}P^2} (j_{g,\Xi(m,l),1} + j_{g,\Pi(m,l),1}) \quad l \in 7,8 \end{aligned} \quad (62)$$

As was the case with the volumetric flux shape, the partial currents in VARIANT also use orthonormal functions and thus the first moment is the average partial current on the surface. The variable  $P$  is the assembly pitch, the variable  $\Delta_m$  is the axial height of the mesh being worked on, and the variable  $l$  is the index for the surface on each mesh. Figure 3-93 displays the x-y surface numbering in DIF3D-VARIANT while surface 7 is the lower surface of each mesh and surface 8 is the upper surface. The two functions  $\Xi(m, l)$  and  $\Pi(m, l)$  are the global mapping arrays which return global index values of  $\gamma$  consistent with equation 59 earlier given the mesh index  $m$  and local surface numbering  $l$ . In the NHFLUX file, one will find the radial and axial partial currents are stored in separate containers and while the equation above is still valid, the axial surfaces require mapping into a different container than the radial surfaces.

With these 9 flux values in the domain, the axial profile for the Nodal formulation is constructed. The set of coefficients associated with equation 60 earlier are

$$\begin{aligned} H_{g,m,1} &= 1 \\ H_{g,m,2} &= \frac{\bar{\phi}_{g,m,8} - \bar{\phi}_{g,m,7}}{\bar{\phi}_{g,m}} \quad H_{g,m,3} = \frac{\bar{\phi}_{g,m,8} + \bar{\phi}_{g,m,7}}{\bar{\phi}_{g,m}} - 2 \\ H_{g,m,4} &= -120 \cdot \frac{\bar{\phi}_{g,m,2}}{\bar{\phi}_{g,m}} + 10 \cdot H_{g,m,2} \rightarrow 0 \quad H_{g,m,5} = -700 \cdot \frac{\bar{\phi}_{g,m,3}}{\bar{\phi}_{g,m}} + 35 \cdot H_{g,m,3} \rightarrow 0 \end{aligned} \quad (63)$$

The two new terms  $\bar{\phi}_{g,m,2}$  and  $\bar{\phi}_{g,m,3}$  are the expansion coefficients from the Nodal axial expansion that are obtained as part of the Nodal solution scheme. These terms are not consistent with the DIF3D-VARIANT formulation and thus the  $H_{g,m,4}$  and  $H_{g,m,5}$  coefficients are set to zero as seen. It is important to note that this will restrict the peaking calculation in VARIANT to a simple quadratic and it can very easily mis-interpret the peak flux when the node size is large. The general form of the axial profile at the center of the mesh is given as

$$\Phi_{CL}(\zeta) = \bar{\phi}_{g,m} \cdot \sum_i \bar{\phi}_i(\zeta) H_{g,m,i}. \quad (64)$$

The axial profile along each surface of each mesh is defined as

$$\Phi_{g,m,l}(\zeta) = \bar{\phi}_{g,m,l} \cdot \sum_i \bar{\phi}_i(\zeta) H_{g,m,i} \quad l \in 1,6. \quad (65)$$

From here, seven power profiles are constructed by multiplying the above with the group-wise power conversion factors for the material assigned to each mesh [7] and the group flux magnitudes obtained earlier. The fast flux is a simple sum over those energy groups that are in the fast range and thus similar to the power calculation [6, 7].

### 3.7.1.3 Simple Problem Used to Verify the SFEDIT Data

Given the peak values reported by DIF3D-FD and DIF3D-VARIANT were already verified as part of the DIF3D verification [14], the only goal of this work is to verify that the SFEDIT file contains reasonable data for the power density and fast flux. The specific problem that is used to verify the REBUS details is not important and thus a simple seven assembly test problem was created as shown in Figure 3-94. This problem has 4 DIF3D regions (COREA, COREB, COREC, REFL) which are readily identifiable by the coloring scheme.

Reflected boundary conditions are applied on all X and Y directed surfaces with extrapolated vacuum boundary conditions on the upper and lower surfaces. The center assembly is filled with the same material as the upper and lower reflector regions. All of the hexagons in ring 2 are filled with core material consistent with other problems in this section. The only power producing isotopes in this test are fission in the U-235 isotope in the fuel regions and capture in the Fe isotope only present in the reflector region. The energy range of the cross section set was modified, consistent with the manner described in the DIF3D manual [6], and displayed in the DIF3D verification document [14], such that the fast flux will include all of group 1 and group 2.

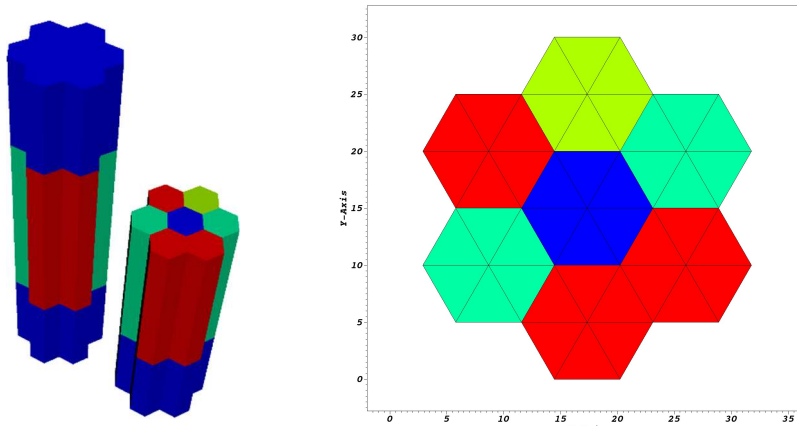


Figure 3-94. Test Problem Geometry Used for SFEDIT Verification

For DIF3D-FD, six triangles per hexagon is combined with 30 axial meshes to produce a total of 1260 cell centered quantities and 6300 surface quantities. Verifying all of these surface points is a non-trivial exercise and only a subset of the surface data will be checked given the location of the peak power density and fast flux can be identified in each region. For DIF3D-VARIANT, there are 7 radial meshes combined with 5 axial meshes to give 35 total meshes. Using 11 interpolating planes per mesh results in  $7 \times 11 \times 35 = 2695$  samples to be verified. As was the case with the DIF3D-FD result, verifying all of the planer results is a non-trivial exercise and only a subset of the surface data will be checked near the identified peaks.

Because the SFEDIT file is a binary interface file that is not displayed by either DIF3D or REBUS, we use the utility program PrintTables.x provided with the ARC package to display the data in the GEODST (geometry), COMPXS (macroscopic cross sections), RTFLUX (DIF3D-FD cell centered flux data), NHFLUX (DIF3D-VARIANT mesh wise flux and currents), PWDINT (mesh wise power density), and the SFEDIT files. The cross section data of interest for the verification is provided in Table 3-57.

**Table 3-57. COMPXS Cross Section Data of Importance**

| Group | COREA   |                  | COREB   |                  |
|-------|---------|------------------|---------|------------------|
|       | D       | Power Conversion | D       | Power Conversion |
| 1     | 1.62159 | 1.8390E-14       | 1.66756 | 1.8390E-15       |
| 2     | 1.00633 | 1.5563E-14       | 1.03563 | 1.5563E-15       |
| 3     | 0.65662 | 2.2868E-14       | 0.67957 | 2.2868E-15       |
| COREC |         | REFL             |         |                  |
| 1     | 1.59894 | 1.8390E-15       | 5.1090  | 2.0033E-16       |
| 2     | 0.99213 | 1.5564E-15       | 3.9526  | 2.3977E-16       |
| 3     | 0.64520 | 2.2868E-15       | 2.3421  | 4.8430E-16       |

### 3.7.1.4 Verification of the SFEDIT Data File for Triangular-Z Based DIF3D-FD

The power density and fast flux profile for the test problem is shown in Figure 3-95. For verification purposes, the goal will be to identify the peaks in all four regions of the power density and fast flux. Figure 3-95 shows that the power is peaked differently in each region and thus this is an acceptable test of the SFEDIT output.

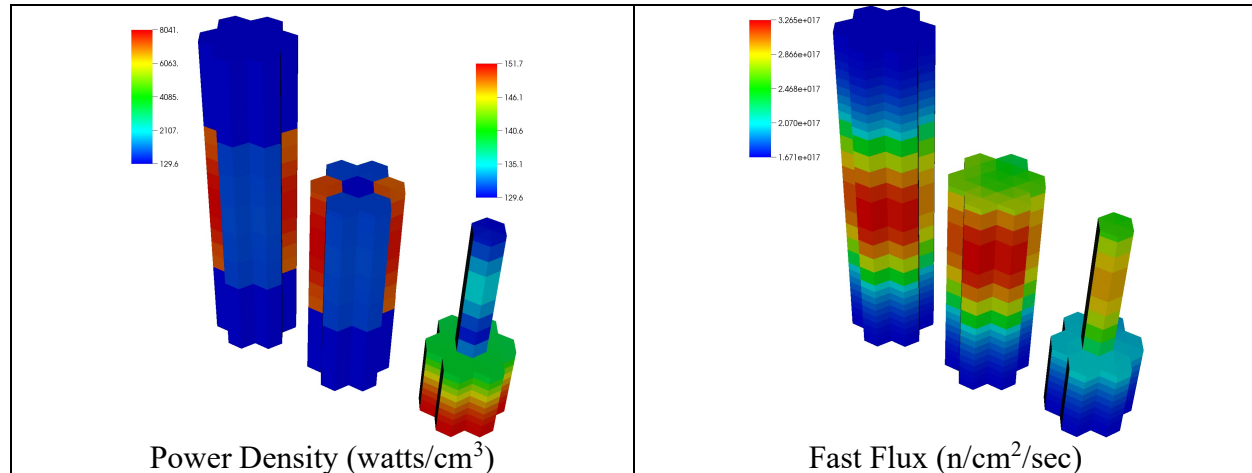


**Figure 3-95. Power Density and Fast Flux Profiles for the SFEDIT Verification**

To follow the hand calculation of the surface fluxes, the layout of the binary data must first be understood. Figure 3-96 shows excerpts of the GEODST, PWDINT, and RTFLUX binary files where the six triangles of the central assembly are highlighted. A quick comparison between the layout of this data with the triangle meshing in Figure 3-94 shows that DIF3D is allocating storage for triangles that are not used in the domain. As an example, for the J=1 row in GEODST, there are 4 zeros followed by three 4's and then 4 zeros. From Figure 3-94 the three 4's correspond to the triangles at the bottom of the picture which have different orientations. The approach taken by DIF3D for each geometry type is well defined in the DIF3D manual [6, 7] and this example is only meant to display the connection between the PrintTables.x utility program output and the DIF3D output.

The power density and flux edits from the DIF3D regular output are shown at the bottom of Figure 3-96 for the same axial plane as those chosen in the PWDINT and RTFLUX files. A quick comparison of the highlighted data from Figure 3-96 shows an identical layout and numerical match. This should

come as no surprise as these files are directly written by DIF3D with the same data that is used in the regular output edits.

Using a notation of (I,J,K), COREA occupies ring 2, positions 1 and 4 which translate to mesh positions (8:10,4:5,11:20) and (2:4, 2:3,11:20), respectively. The PWDINT file can be scanned to locate the peak value in this region which is 8041.04 W/cm<sup>3</sup> and occurs in meshes (3,2,15) and (3,2,16) corresponding to the assembly at ring 2 position 4. Because this problem is axially symmetric, the peak is identical between the two meshes that surround the center of the active core and it should be closest to the radial reflected boundary because the center assembly is not powered. To construct the surface fluxes, the surrounding flux moments are necessary which are extracted from the RTFLUX output and provided in Figure 3-97 along with the power density information from PWDINT.

```

GEO DST
[GEO DST]...REGION NUMBERS ASSIGNED TO COARSE MESH ON Z PLANE          2
[GEO DST]...J= 6 -> 0 0 0 0 3 3 0 0 0
[GEO DST]...J= 5 -> 0 4 4 4 3 3 2 2 2 0
[GEO DST]...J= 4 -> 0 4 4 4 1 1 1 2 2 2 0
[GEO DST]...J= 3 -> 0 2 2 2 1 1 1 4 4 4 0
[GEO DST]...J= 2 -> 0 2 2 2 4 4 4 4 4 4 0
[GEO DST]...J= 1 -> 0 0 0 0 4 4 4 0 0 0 0

PWD INT
[PWD INT].....POWER DENSITY FOR AXIAL PLANE..... 1
[PWD INT]...I -> 1 2 3 4 5 6 7 ...
[PWD INT]...J= 6 0.00000E+00 0.00000E+00 0.00000E+00 0.00000E+00 1.51590E+02 1.51588E+02 1.51590E+02...
[PWD INT]...J= 5 0.00000E+00 1.51608E+02 1.51605E+02 1.51605E+02 1.51598E+02 1.51602E+02 1.51598E+02...
[PWD INT]...J= 4 0.00000E+00 1.51613E+02 1.51620E+02 1.51614E+02 1.51619E+02 1.51613E+02 1.51620E+02...
[PWD INT]...J= 3 0.00000E+00 1.51640E+02 1.51633E+02 1.51638E+02 1.51639E+02 1.51632E+02 1.51639E+02...
[PWD INT]...J= 2 0.00000E+00 1.51645E+02 1.51647E+02 1.51647E+02 1.51654E+02 1.51650E+02 1.51654E+02...
[PWD INT]...J= 1 0.00000E+00 0.00000E+00 0.00000E+00 0.00000E+00 1.51661E+02 1.51663E+02 1.51661E+02...

RTFLUX
[RTFLUX].....REGULAR FLUX FOR AXIAL PLANE 1 GROUP ..... 1
[RTFLUX]...I -> 1 2 3 4 5 6 7 ...
[RTFLUX]...J= 6 0.00000E+00 0.00000E+00 0.00000E+00 0.00000E+00 1.55975E+16 1.55891E+16 1.55963E+16...
[RTFLUX]...J= 5 0.00000E+00 1.56551E+16 1.56462E+16 1.56423E+16 1.56200E+16 1.56303E+16 1.56180E+16...
[RTFLUX]...J= 4 0.00000E+00 1.56676E+16 1.56820E+16 1.56670E+16 1.56795E+16 1.56615E+16 1.56789E+16...
[RTFLUX]...J= 3 0.00000E+00 1.57276E+16 1.57122E+16 1.57244E+16 1.57112E+16 1.57272E+16 1.57121E+16...
[RTFLUX]...J= 2 0.00000E+00 1.57391E+16 1.57454E+16 1.57460E+16 1.57618E+16 1.57535E+16 1.57641E+16...
[RTFLUX]...J= 1 0.00000E+00 0.00000E+00 0.00000E+00 0.00000E+00 1.57778E+16 1.57838E+16 1.57791E+16...

DIF3D Power Density Output
0 POWER DENSITY BY MESH CELL FOR K-EFF PROBLEM FOR PLANE 1 WITH ENERGY RANGE (EV) =(4.140E-01,1.000E+07)
Y-AXIS X-AXIS X-AXIS X-AXIS X-AXIS X-AXIS X-AXIS X-AXIS X-AXIS X-AXIS
1 2 3 4 5 6 7 8 9
6 0.00000E+00 0.00000E+00 0.00000E+00 0.00000E+00 1.51590E+02 1.51588E+02 1.51590E+02 0.00000E+00 0.00000E+00
5 0.00000E+00 1.51608E+02 1.51605E+02 1.51605E+02 1.51598E+02 1.51602E+02 1.51598E+02 1.51605E+02 1.51605E+02
4 0.00000E+00 1.51613E+02 1.51620E+02 1.51614E+02 1.51619E+02 1.51613E+02 1.51620E+02 1.51614E+02 1.51620E+02
3 0.00000E+00 1.51640E+02 1.51633E+02 1.51638E+02 1.51639E+02 1.51632E+02 1.51639E+02 1.51633E+02 1.51633E+02
2 0.00000E+00 1.51645E+02 1.51647E+02 1.51647E+02 1.51654E+02 1.51650E+02 1.51649E+02 1.51649E+02 1.51649E+02
1 0.00000E+00 0.00000E+00 0.00000E+00 0.00000E+00 1.51661E+02 1.51663E+02 1.51661E+02 0.00000E+00 0.00000E+00

DIF3D Flux Output
REAL FLUX FOR K-EFF PROBLEM FOR PLANE 1 FOR GROUP 1 WITH ENERGY RANGE (EV) =(8.006E+05,1.000E+07)
Y-AXIS X-AXIS X-AXIS X-AXIS X-AXIS X-AXIS X-AXIS X-AXIS X-AXIS
1 2 3 4 5 6 7 8 9
6 0.00000E+00 0.00000E+00 0.00000E+00 0.00000E+00 1.55975E+16 1.55891E+16 1.55963E+16 0.00000E+00 0.00000E+00
5 0.00000E+00 1.56551E+16 1.56462E+16 1.56423E+16 1.56200E+16 1.56303E+16 1.56180E+16 1.56383E+16 1.56397E+16
4 0.00000E+00 1.56676E+16 1.56820E+16 1.56670E+16 1.56795E+16 1.56615E+16 1.56789E+16 1.56646E+16 1.56802E+16
3 0.00000E+00 1.57276E+16 1.57122E+16 1.57244E+16 1.57112E+16 1.57272E+16 1.57121E+16 1.57276E+16 1.57150E+16
2 0.00000E+00 1.57391E+16 1.57454E+16 1.57460E+16 1.57618E+16 1.57535E+16 1.57641E+16 1.57507E+16 1.57529E+16
1 0.00000E+00 0.00000E+00 0.00000E+00 0.00000E+00 1.57778E+16 1.57838E+16 1.57791E+16 0.00000E+00 0.00000E+00

```

Figure 3-96. Output Excerpts from DIF3D-FD, the GEO DST, PWD INT, and RTFLUX Binary Files

```

[RTFLUX].....REGULAR FLUX FOR AXIAL PLANE 15 GROUP .....1
[RTFLUX]...I -> 1 2 3 4 5 6 7
[RTFLUX]...J= 6 0.00000E+00 0.00000E+00 0.00000E+00 5.15936E+16 5.00083E+16 5.10463E+16
[RTFLUX]...J= 5 0.00000E+00 7.09500E+16 6.88727E+16 6.44218E+16 5.60860E+16 5.61460E+16 5.48883E+16
[RTFLUX]...J= 4 0.00000E+00 7.10073E+16 6.89967E+16 6.52285E+16 6.11393E+16 5.94573E+16 6.08482E+16
[RTFLUX]...J= 3 0.00000E+00 6.89934E+16 6.82270E+16 6.62566E+16 6.23538E+16 6.31995E+16 6.26774E+16
[RTFLUX]...J= 2 0.00000E+00 6.94103E+16 6.95184E+16 6.93227E+16 7.18779E+16 6.92826E+16 7.32032E+16
[RTFLUX]...J= 1 0.00000E+00 0.00000E+00 0.00000E+00 0.00000E+00 7.47758E+16 7.58873E+16 7.53871E+16
[RTFLUX].....REGULAR FLUX FOR AXIAL PLANE 15 GROUP .....2
[RTFLUX]...I -> 1 2 3 4 5 6 7
[RTFLUX]...J= 6 0.00000E+00 0.00000E+00 0.00000E+00 2.17830E+17 2.15479E+17 2.17088E+17
[RTFLUX]...J= 5 0.00000E+00 2.38585E+17 2.35670E+17 2.30976E+17 2.23792E+17 2.25269E+17 2.22435E+17
[RTFLUX]...J= 4 0.00000E+00 2.39220E+17 2.37624E+17 2.33092E+17 2.31184E+17 2.29680E+17 2.31001E+17
[RTFLUX]...J= 3 0.00000E+00 2.41115E+17 2.38941E+17 2.37122E+17 2.32894E+17 2.33854E+17 2.33119E+17
[RTFLUX]...J= 2 0.00000E+00 2.42306E+17 2.42491E+17 2.41646E+17 2.44276E+17 2.40470E+17 2.45828E+17
[RTFLUX]...J= 1 0.00000E+00 0.00000E+00 0.00000E+00 0.00000E+00 2.48744E+17 2.50592E+17 2.49594E+17
[RTFLUX].....REGULAR FLUX FOR AXIAL PLANE 15 GROUP .....3
[RTFLUX]...I -> 1 2 3 4 5 6 7
[RTFLUX]...J= 6 0.00000E+00 0.00000E+00 0.00000E+00 1.34974E+17 1.35196E+17 1.35219E+17
[RTFLUX]...J= 5 0.00000E+00 1.25764E+17 1.26606E+17 1.29601E+17 1.34184E+17 1.36286E+17 1.34822E+17
[RTFLUX]...J= 4 0.00000E+00 1.26431E+17 1.28694E+17 1.31537E+17 1.37004E+17 1.37671E+17 1.37191E+17
[RTFLUX]...J= 3 0.00000E+00 1.30335E+17 1.30525E+17 1.33107E+17 1.36918E+17 1.36710E+17 1.36751E+17
[RTFLUX]...J= 2 0.00000E+00 1.30431E+17 1.30692E+17 1.31143E+17 1.29990E+17 1.31973E+17 1.29398E+17
[RTFLUX]...J= 1 0.00000E+00 0.00000E+00 0.00000E+00 0.00000E+00 1.28705E+17 1.28327E+17 1.28499E+17
[PWDINT].....POWER DENSITY FOR AXIAL PLANE.....15
[PWDINT]...I -> 1 2 3 4 5 6 7
[PWDINT]...J= 6 0.00000E+00 0.00000E+00 0.00000E+00 0.00000E+00 7.42555E+02 7.36488E+02 7.40955E+02
[PWDINT]...J= 5 0.00000E+00 7.89392E+02 7.82962E+02 7.74320E+02 7.58289E+02 7.65505E+02 7.55435E+02
[PWDINT]...J= 4 0.00000E+00 7.92011E+02 7.91005E+02 7.83524E+02 1.34030E+02 1.33655E+02 1.34018E+02
[PWDINT]...J= 3 0.00000E+00 8.00182E+03 7.95821E+03 7.95273E+03 1.34641E+02 1.34940E+02 1.34679E+02
[PWDINT]...J= 2 0.00000E+00 8.03021E+03 8.04104E+03 8.03461E+03 8.09622E+02 8.03460E+02 8.13119E+02
[PWDINT]...J= 1 0.00000E+00 0.00000E+00 0.00000E+00 0.00000E+00 8.18966E+02 8.23021E+02 8.20942E+02

```

Figure 3-97. DIF3D-FD RTFLUX and PWDINT Excerpt for COREA Surface Calculation

As seen, only the data for plane 15 is displayed as plane 16 was identical. The data for plane 15 and 16 is put into the surface flux calculation in Table 3-58. In this table, the flux magnitude for all six triangles of the assembly are duplicated for the two planes adjacent to the identified PWDINT peak power density. Because all six triangles are assigned the same composition, there is no reason to compute anything but the surfaces that connect to a triangle (3,2,15) with the observed peak in the power density (highlighted for convenience). For this mesh, only 4 of the 5 surfaces need to be calculated as the other surface (connection to plane 14) has a lower flux level. One of the surfaces on this triangle is on the reflected boundary condition and from the earlier discussion it will have the same value as the peak or 8041.14 W/cm<sup>3</sup>. From Figure 3-94, that leaves the connection with the triangle to the left (2,2,15), the triangle to the right (4,2,15), and the triangle above this mesh (3,2,16). Because the three adjacent triangles of interest all have the same radial and axial dimensions, the factors  $F_{g,p}$  are equal to  $\frac{1}{2}$  and no cross section data is needed. The power conversion factors for group 1, 2 and 3 are 1.83896E-14, 1.55634E-14, and 2.28678E-14, respectively. This is the natural result for the radial-plane as it implies the surface flux between two meshes interior to a homogeneous region will simply be the average of the two positions in hexagonal geometry. Axially, the relative thickness of the two meshes would still play a role but it does not here because these meshes have identical sizes.

Because the adjoining mesh fluxes are lower than the one with the peak, the surface flux results are always less than the values that occur in the identified peak power density mesh. Since the problem is axially symmetric, the solution at the surface between planes 15 and 16 is the same as the solution at planes 15 and 16 which is consistent with applying a reflected boundary condition at that point. This is of course consistent with the way the radial reflected boundary condition is handled. As a consequence, the peak power densities will be 8041.14 on surfaces 3 and 5 of the triangular-z mesh. In Table 3-58, the power density on the left surface (numbered surface 1 earlier) and right surface (surface 2) are 8035.62 and 8037.82 W/cm<sup>3</sup> both of which are below the original peak value. The result for surface 5 is as discussed.

Because of the modified energy spectrum of the cross section set, the peak fast flux is simply the sum of the first two energy groups. Applying this approach for the RTFLUX data in the whole domain, the peak of the fast flux is also found to be in the same triangle (3,2,15). This is no surprise as the fission rate and power density are peaked in this mesh. The peak value is 3.1201E+17 which is identical to the axial surface result in Table 3-58.

For verification of the SFEDIT data, the plane 15 data was extracted and is provided in Figure 3-98. For DIF3D-FD, the 6<sup>th</sup> “surface” data is actually the cell centered average power density and it should identically match the PWDINT data. Comparison against that provided in Figure 3-97 indicates a perfect match. The remaining surface data are consistently ordered with the surface numbering shown earlier. For surface 4, the PWDINT value of power density at this mesh point on plane 14 is 7906.93 which when averaged with 8041.04 is 7973.99 which is consistent with the 7973.98 result in Figure 3-98.

The region-wise output excerpt for COREA is shown in Figure 3-99. Unlike the mesh-wise ordering above, the cell (or mesh) number of interest is a bit complicated to figure out as it is a derivative ordering from the regular GEODST ordering of the meshes. For COREA, the first three cells will be the lower triangles shown in Figure 3-94 of the assembly in ring 2, position 4. The next three cells will be the upper triangles of the same assembly. The next three cells will be the lower triangles of the assembly in ring 2, position 1 followed by the upper triangles of that same assembly. Per plane there are 12 triangles and thus a total of 120 cells in the region output (10 planes). The cells of interest for comparison can be calculated as  $(15-11)*12+1=49$  to  $(15-11)*12+6=54$  for the plane 15 triangles and 61:66 for plane 16.

**Table 3-58. COREA Peak Surface Power Density and Fast Flux Calculation**

|   |               | Extracted RTFLUX Data |                   |            |
|---|---------------|-----------------------|-------------------|------------|
|   |               | Group                 | 1                 | 2          |
| Plane 15                                  | 1             | 6.8993E+16            | 6.8227E+16        | 6.6257E+16 |
|   |               | 6.9410E+16            | <b>6.9518E+16</b> | 6.9323E+16 |
|   | 2             | 2.4112E+17            | 2.3894E+17        | 2.3712E+17 |
|   |               | 2.4231E+17            | <b>2.4249E+17</b> | 2.4165E+17 |
|   | 3             | 1.3034E+17            | 1.3053E+17        | 1.3311E+17 |
|   |               | 1.3043E+17            | <b>1.3069E+17</b> | 1.3114E+17 |
| Plane 16                                  | 1             | 6.8993E+16            | 6.8227E+16        | 6.6257E+16 |
|   |               | 6.9410E+16            | <b>6.9518E+16</b> | 6.9323E+16 |
|   | 2             | 2.4112E+17            | 2.3894E+17        | 2.3712E+17 |
|   |               | 2.4231E+17            | <b>2.4249E+17</b> | 2.4165E+17 |
|   | 3             | 1.3034E+17            | 1.3053E+17        | 1.3311E+17 |
|   |               | 1.3043E+17            | <b>1.3069E+17</b> | 1.3114E+17 |
| Triangle with Peak Power Density (3,2,15) | Group         |                       | Surface Fluxes    |            |
|   |               |                       | 1                 | 2          |
|   | 1             | 6.9464E+16            | 6.9421E+16        | 6.9518E+16 |
|   | 2             | 2.4240E+17            | 2.4207E+17        | 2.4249E+17 |
|   | 3             | 1.3056E+17            | 1.3092E+17        | 1.3069E+17 |
|   | Power Density | 8035.62               | 8037.82           | 8041.04    |
|   | Fast Flux     | 3.1186E+17            | 3.1149E+17        | 3.1201E+17 |

```

[SFEDIT] (2D) Sample 1 of 1 of surface 1 of 6 center power density (w/cc) for axial mesh 15 of 30
[SFEDIT]...I -> 1 2 3 4 5 6 7
[SFEDIT]...J= 6 0.00000E+00 0.00000E+00 0.00000E+00 0.00000E+00 7.42555E+02 7.39522E+02 7.38721E+02
[SFEDIT]...J= 5 0.00000E+00 7.89392E+02 7.86177E+02 7.78641E+02 7.66159E+02 7.61898E+02 7.60471E+02
[SFEDIT]...J= 4 0.00000E+00 7.92011E+02 7.91508E+02 7.87265E+02 1.33745E+02 1.33842E+02 1.33837E+02
[SFEDIT]...J= 3 0.00000E+00 8.00182E+03 7.98002E+03 7.95547E+03 1.34631E+02 1.34791E+02 1.34810E+02
[SFEDIT]...J= 2 0.00000E+00 8.03020E+03 8.03562E+03 8.03783E+03 8.06525E+02 8.06541E+02 8.08290E+02
[SFEDIT]...J= 1 0.00000E+00 0.00000E+00 0.00000E+00 0.00000E+00 8.18966E+02 8.20993E+02 8.21981E+02
...
[SFEDIT] (2D) Sample 1 of 1 of surface 2 of 6 center power density (w/cc) for axial mesh 15 of 30
[SFEDIT]...I -> 1 2 3 4 5 6 7
[SFEDIT]...J= 6 0.00000E+00 0.00000E+00 0.00000E+00 0.00000E+00 7.39522E+02 7.38721E+02 7.40955E+02
[SFEDIT]...J= 5 0.00000E+00 7.86177E+02 7.78641E+02 7.66160E+02 7.61898E+02 7.60471E+02 7.61635E+02
[SFEDIT]...J= 4 0.00000E+00 7.91508E+02 7.87265E+02 7.85225E+02 1.33842E+02 1.33837E+02 1.33703E+02
[SFEDIT]...J= 3 0.00000E+00 7.98002E+03 7.95547E+03 7.91387E+03 1.34791E+02 1.34810E+02 1.34712E+02
[SFEDIT]...J= 2 0.00000E+00 8.03020E+03 8.03562E+03 8.06520E+03 8.06541E+02 8.08290E+02 8.12023E+02
[SFEDIT]...J= 1 0.00000E+00 0.00000E+00 0.00000E+00 0.00000E+00 8.20993E+02 8.21981E+02 8.20942E+02
...
[SFEDIT] (2D) Sample 1 of 1 of surface 3 of 6 center power density (w/cc) for axial mesh 15 of 30
[SFEDIT]...I -> 1 2 3 4 5 6 7
[SFEDIT]...J= 6 0.00000E+00 0.00000E+00 0.00000E+00 0.00000E+00 7.50422E+02 7.36488E+02 7.48195E+02
[SFEDIT]...J= 5 0.00000E+00 7.90701E+02 7.82962E+02 7.78922E+02 7.50422E+02 7.77991E+02 7.48195E+02
[SFEDIT]...J= 4 0.00000E+00 7.90701E+02 7.93436E+02 7.78922E+02 1.34336E+02 1.33121E+02 1.34349E+02
[SFEDIT]...J= 3 0.00000E+00 8.01601E+03 7.93432E+03 7.99336E+03 1.34336E+02 1.35054E+02 1.34349E+02
[SFEDIT]...J= 2 0.00000E+00 8.01601E+03 8.04104E+03 7.99336E+03 8.14294E+02 7.95202E+02 8.17031E+02
[SFEDIT]...J= 1 0.00000E+00 0.00000E+00 0.00000E+00 0.00000E+00 8.14294E+02 8.23021E+02 8.17031E+02
...
[SFEDIT] (2D) Sample 1 of 1 of surface 4 of 6 center power density (w/cc) for axial mesh 15 of 30
[SFEDIT]...I -> 1 2 3 4 5 6 7
[SFEDIT]...J= 6 0.00000E+00 0.00000E+00 0.00000E+00 0.00000E+00 7.37060E+02 7.31029E+02 7.35490E+02
[SFEDIT]...J= 5 0.00000E+00 7.82967E+02 7.76722E+02 7.68459E+02 7.52741E+02 7.60269E+02 7.49943E+02
[SFEDIT]...J= 4 0.00000E+00 7.85601E+02 7.84825E+02 7.77926E+02 1.33361E+02 1.32997E+02 1.33350E+02
[SFEDIT]...J= 3 0.00000E+00 7.93568E+03 7.89537E+03 7.89436E+03 1.33956E+02 1.34247E+02 1.33992E+02
[SFEDIT]...J= 2 0.00000E+00 7.96268E+03 7.97398E+03 7.97002E+03 8.03022E+02 7.97435E+02 8.06450E+02
[SFEDIT]...J= 1 0.00000E+00 0.00000E+00 0.00000E+00 0.00000E+00 8.11936E+02 8.15836E+02 8.13875E+02
...
[SFEDIT] (2D) Sample 1 of 1 of surface 5 of 6 center power density (w/cc) for axial mesh 15 of 30
[SFEDIT]...I -> 1 2 3 4 5 6 7
[SFEDIT]...J= 6 0.00000E+00 0.00000E+00 0.00000E+00 0.00000E+00 7.42555E+02 7.36488E+02 7.40955E+02
[SFEDIT]...J= 5 0.00000E+00 7.89392E+02 7.82962E+02 7.74320E+02 7.58289E+02 7.65506E+02 7.55435E+02
[SFEDIT]...J= 4 0.00000E+00 7.92011E+02 7.91005E+02 7.83524E+02 1.34030E+02 1.33655E+02 1.34018E+02
[SFEDIT]...J= 3 0.00000E+00 8.00182E+03 7.95821E+03 7.95273E+03 1.34641E+02 1.34940E+02 1.34679E+02
[SFEDIT]...J= 2 0.00000E+00 8.03021E+03 8.04104E+03 8.03461E+03 8.09622E+02 8.03460E+02 8.13119E+02
[SFEDIT]...J= 1 0.00000E+00 0.00000E+00 0.00000E+00 0.00000E+00 8.18966E+02 8.23021E+02 8.20942E+02
...
[SFEDIT] (2D) Sample 1 of 1 of surface 6 of 6 center power density (w/cc) for axial mesh 15 of 30
[SFEDIT]...I -> 1 2 3 4 5 6 7
[SFEDIT]...J= 6 0.00000E+00 0.00000E+00 0.00000E+00 0.00000E+00 7.42555E+02 7.36488E+02 7.40955E+02
[SFEDIT]...J= 5 0.00000E+00 7.89392E+02 7.82962E+02 7.74320E+02 7.58289E+02 7.65506E+02 7.55435E+02
[SFEDIT]...J= 4 0.00000E+00 7.92011E+02 7.91005E+02 7.83524E+02 1.34030E+02 1.33655E+02 1.34018E+02
[SFEDIT]...J= 3 0.00000E+00 8.00182E+03 7.95821E+03 7.95273E+03 1.34641E+02 1.34940E+02 1.34679E+02
[SFEDIT]...J= 2 0.00000E+00 8.03020E+03 8.04104E+03 8.03461E+03 8.09622E+02 8.03460E+02 8.13119E+02
[SFEDIT]...J= 1 0.00000E+00 0.00000E+00 0.00000E+00 0.00000E+00 8.18966E+02 8.23021E+02 8.20942E+02

```

Figure 3-98. SFEDIT Mesh-wise Power Output Excerpt for COREA Verification in DIF3D-FD

```

[SFEDIT]...| Region | Cell | Sample | Surface data ->
...
[SFEDIT]...| 2| 49| 1| 8.030205E+03 8.035623E+03 8.016013E+03 7.962684E+03 8.030205E+03 8.030205E+03
[SFEDIT]...| 2| 50| 1| 8.035623E+03 8.037827E+03 8.041040E+03 7.973985E+03 8.041040E+03 8.041040E+03
[SFEDIT]...| 2| 51| 1| 8.037827E+03 8.065199E+03 7.993670E+03 7.970017E+03 8.034614E+03 8.034614E+03
[SFEDIT]...| 2| 52| 1| 8.001822E+03 7.980018E+03 8.016013E+03 7.935682E+03 8.001822E+03 8.001822E+03
[SFEDIT]...| 2| 53| 1| 7.980018E+03 7.955471E+03 7.934318E+03 7.895369E+03 7.958215E+03 7.958214E+03
[SFEDIT]...| 2| 54| 1| 7.955471E+03 7.913869E+03 7.993670E+03 7.894360E+03 7.952728E+03 7.952727E+03
...
[SFEDIT]...| 2| 61| 1| 8.030206E+03 8.035623E+03 8.016014E+03 8.030205E+03 7.962685E+03 8.030205E+03
[SFEDIT]...| 2| 62| 1| 8.035623E+03 8.037827E+03 8.041041E+03 8.041040E+03 7.973986E+03 8.041041E+03
[SFEDIT]...| 2| 63| 1| 8.037827E+03 8.065200E+03 7.993671E+03 8.034614E+03 7.970018E+03 8.034614E+03
[SFEDIT]...| 2| 64| 1| 8.001823E+03 7.980019E+03 8.016014E+03 8.001822E+03 7.935683E+03 8.001823E+03
[SFEDIT]...| 2| 65| 1| 7.980019E+03 7.955471E+03 7.934318E+03 7.958215E+03 7.895370E+03 7.958215E+03
[SFEDIT]...| 2| 66| 1| 7.955471E+03 7.913869E+03 7.993671E+03 7.952728E+03 7.894361E+03 7.952728E+03

```

Figure 3-99. SFEDIT Region-wise Power Output Excerpt for COREA Verification in DIF3D-FD

The mesh with the identified peak power of 8041.04 is highlighted for convenience. A quick comparison of the surface power densities in this output with those of Figure 3-98 shows the two outputs are an identical match. This should not be a surprise as the calculation itself is identical and it is just the ordering of the data that is changed.

The excerpt of the fast flux for both SFEDIT options are collected in Figure 3-100. For brevity, the SFEDIT Option 1 table of data was restricted to only display the mesh of interest. A quick comparison shows that the two sets of data have identical results for the mesh of interest. These results are consistent with the hand calculated values shown earlier in Table 3-58. Given this result, the COREA peak power density and fast flux output for DIF3D-FD is confirmed.

```

SFEDIT Option 1
...
[SFEDIT]...I ->      1      2      3      4      5      6      7
[SFEDIT]...J= 2  0.00000E+00  3.11716E+17  3.11863E+17  3.11489E+17  3.13543E+17  3.12953E+17  3.14392E+17
[SFEDIT]...J= 2  0.00000E+00  3.11863E+17  3.11489E+17  3.13543E+17  3.12953E+17  3.14392E+17  3.18508E+17
[SFEDIT]...J= 2  0.00000E+00  3.10912E+17  3.12010E+17  3.07174E+17  3.19837E+17  2.99831E+17  3.22006E+17
[SFEDIT]...J= 2  0.00000E+00  3.08368E+17  3.08650E+17  3.07611E+17  3.12732E+17  3.06378E+17  3.15577E+17
[SFEDIT]...J= 2  0.00000E+00  3.11716E+17  3.12010E+17  3.10969E+17  3.16154E+17  3.09753E+17  3.19031E+17
[SFEDIT]...J= 2  0.00000E+00  3.11716E+17  3.12010E+17  3.10969E+17  3.16154E+17  3.09753E+17  3.19031E+17
...
SFEDIT Option 2
...
[SFEDIT]...| 2| 49| 1| 3.117159E+17  3.118627E+17  3.109122E+17  3.083680E+17  3.117159E+17  3.117159E+17
[SFEDIT]...| 2| 50| 1| 3.118627E+17  3.114893E+17  3.120096E+17  3.086500E+17  3.120096E+17  3.120096E+17
[SFEDIT]...| 2| 51| 1| 3.114893E+17  3.135432E+17  3.071740E+17  3.076106E+17  3.109690E+17  3.109690E+17
[SFEDIT]...| 2| 52| 1| 3.101086E+17  3.086380E+17  3.109122E+17  3.067880E+17  3.101086E+17  3.101086E+17
[SFEDIT]...| 2| 53| 1| 3.086380E+17  3.052732E+17  3.068962E+17  3.038843E+17  3.071675E+17  3.071675E+17
[SFEDIT]...| 2| 54| 1| 3.052732E+17  2.970462E+17  3.071740E+17  3.000881E+17  3.033790E+17  3.033789E+17
...

```

**Figure 3-100. SFEDIT Fast Flux Output Excerpt for COREA Verification in DIF3D-FD**

Continuing with COREB, the scan of the PWDINT file shows a power density peak at mesh (6,5,15) and (6,5,16). The three planes of PWDINT data are displayed in Figure 3-101 with the six triangles of COREB highlighted. For the region-wise edits of SFEDIT, this cell corresponds to  $(15-11)*6+2=26$ . The peak is found to be 765.506 and, based upon the experience with the COREA results, a quick look at the adjacent triangles would indicate that this will be the peak in the entire region as the surface fluxes will all be lower. Because it is again on plane 15, the RTFLUX parts of interest were provided earlier in Figure 3-97.

The hand calculation of the surface power densities is provided in Table 3-59. The mesh averaged power density details are available in Figure 3-101 where the calculation of that value and the peak fast flux are provided in Table 3-59. The SFEDIT output excerpt for the 26<sup>th</sup> mesh of COREB is provided in Figure 3-102 where the targeted mesh is highlighted for convenience. A quick comparison of the power density for surfaces 1 to 3 in Table 3-59 with that of surfaces 1 to 3 in Figure 3-102 shows an identical match. The power density for surface 4 can be easily calculated as the average of plane 14 and 15 in Figure 3-101. The power density on the upper axial surface can also be calculated as the average value of plane 15 and 16 which simply results in the same values as the volume averaged quantities. The hand calculation of the average power density and peak fast flux also matches. For this region, the peak power density and fast flux occurs on surface 3 of the targeted triangle which is the boundary between the COREB and REFL regions at this axial height. With the displayed and hand calculated results in agreement, the verification of COREB peaking data is confirmed.

```
[PWDINT].....POWER DENSITY FOR AXIAL PLANE.....14
[PWDINT]...I -> 1 2 3 4 5 6 7
[PWDINT]...J= 6 0.00000E+00 0.00000E+00 0.00000E+00 7.31565E+02 7.25571E+02 7.30025E+02
[PWDINT]...J= 5 0.00000E+00 7.76543E+02 7.70482E+02 7.62597E+02 7.47193E+02 7.55032E+02 7.44451E+02
[PWDINT]...J= 4 0.00000E+00 7.79190E+02 7.78644E+02 7.72327E+02 1.32691E+02 1.32340E+02 1.32682E+02
[PWDINT]...J= 3 0.00000E+00 7.86954E+03 7.83252E+03 7.83599E+03 1.33271E+02 1.33553E+02 1.33306E+02
[PWDINT]...J= 2 0.00000E+00 7.89516E+03 7.90693E+03 7.90542E+03 7.96421E+02 7.91410E+02 7.99781E+02
[PWDINT]...J= 1 0.00000E+00 0.00000E+00 0.00000E+00 0.00000E+00 8.04906E+02 8.08651E+02 8.06808E+02
[PWDINT].....POWER DENSITY FOR AXIAL PLANE.....15
[PWDINT]...I -> 1 2 3 4 5 6 7
[PWDINT]...J= 6 0.00000E+00 0.00000E+00 0.00000E+00 7.42555E+02 7.36488E+02 7.40955E+02
[PWDINT]...J= 5 0.00000E+00 7.89392E+02 7.82962E+02 7.74320E+02 7.58289E+02 7.65506E+02 7.55435E+02
[PWDINT]...J= 4 0.00000E+00 7.92011E+02 7.91005E+02 7.83524E+02 1.34030E+02 1.33655E+02 1.34018E+02
[PWDINT]...J= 3 0.00000E+00 8.00182E+03 7.95821E+03 7.95273E+03 1.34641E+02 1.34940E+02 1.34679E+02
[PWDINT]...J= 2 0.00000E+00 8.03021E+03 8.04104E+03 8.03461E+03 8.09622E+02 8.03460E+02 8.13119E+02
[PWDINT]...J= 1 0.00000E+00 0.00000E+00 0.00000E+00 0.00000E+00 8.18966E+02 8.23021E+02 8.20942E+02
[PWDINT].....POWER DENSITY FOR AXIAL PLANE.....16
[PWDINT]...I -> 1 2 3 4 5 6 7
[PWDINT]...J= 6 0.00000E+00 0.00000E+00 0.00000E+00 7.42555E+02 7.36488E+02 7.40955E+02
[PWDINT]...J= 5 0.00000E+00 7.89392E+02 7.82962E+02 7.74320E+02 7.58289E+02 7.65506E+02 7.55435E+02
[PWDINT]...J= 4 0.00000E+00 7.92011E+02 7.91005E+02 7.83524E+02 1.34030E+02 1.33655E+02 1.34018E+02
[PWDINT]...J= 3 0.00000E+00 8.00182E+03 7.95821E+03 7.95273E+03 1.34641E+02 1.34940E+02 1.34679E+02
[PWDINT]...J= 2 0.00000E+00 8.03021E+03 8.04104E+03 8.03461E+03 8.09622E+02 8.03460E+02 8.13119E+02
[PWDINT]...J= 1 0.00000E+00 0.00000E+00 0.00000E+00 0.00000E+00 8.18966E+02 8.23021E+02 8.20942E+02
```

Figure 3-101. PWDINT Output Excerpt for COREB Verification in DIF3D-FD

Table 3-59. COREB Peak Surface Power Density and Fast Flux Calculation

| Group         |            | Extracted RTFLUX Data |            |            |
|---------------|------------|-----------------------|------------|------------|
| 1             | 5.1594E+16 | 5.0008E+16            | 5.1046E+16 |            |
|               | 5.6086E+16 | <b>5.6146E+16</b>     | 5.4888E+16 |            |
|               | 6.1139E+16 | 5.9457E+16            | 6.0848E+16 |            |
| 2             | 2.1783E+17 | 2.1548E+17            | 2.1709E+17 |            |
|               | 2.2379E+17 | <b>2.2527E+17</b>     | 2.2244E+17 |            |
|               | 2.3118E+17 | 2.2968E+17            | 2.3100E+17 |            |
| 3             | 1.3497E+17 | 1.3520E+17            | 1.3522E+17 |            |
|               | 1.3418E+17 | <b>1.3629E+17</b>     | 1.3482E+17 |            |
|               | 1.3700E+17 | 1.3767E+17            | 1.3719E+17 |            |
| Group         |            | Surface Fluxes        |            |            |
|               |            | 1                     | 2          | 3          |
| 1             |            | 5.6116E+16            | 5.5517E+16 | 5.8642E+16 |
| 2             |            | 2.2453E+17            | 2.2385E+17 | 2.2876E+17 |
| 3             |            | 1.3524E+17            | 1.3555E+17 | 1.3736E+17 |
| Power Density |            | 761.90                | 760.47     | 777.99     |
| Fast Flux     |            | 2.8065E+17            | 2.7937E+17 | 2.8741E+17 |
|               |            |                       |            | Volume     |
|               |            |                       |            | 5.6146E+16 |
|               |            |                       |            | 2.2527E+17 |
|               |            |                       |            | 1.3629E+17 |
|               |            |                       |            | 2.8142E+17 |

```

SFEDIT Option 1
...
[SFEDIT]...I ->      1      2      3      4      5      6      7
[SFEDIT]...J= 5 0.00000E+00 7.89392E+02 7.86177E+02 7.78641E+02 7.66159E+02 7.6198E+02 7.60471E+02
[SFEDIT]...J= 5 0.00000E+00 7.86177E+02 7.78641E+02 7.66160E+02 7.61898E+02 7.60471E+02 7.61635E+02
[SFEDIT]...J= 5 0.00000E+00 7.90701E+02 7.82962E+02 7.78922E+02 7.50422E+02 7.77991E+02 7.48195E+02
[SFEDIT]...J= 5 0.00000E+00 7.82967E+02 7.76722E+02 7.68459E+02 7.52741E+02 7.60269E+02 7.49943E+02
[SFEDIT]...J= 5 0.00000E+00 7.89392E+02 7.82962E+02 7.74320E+02 7.58289E+02 7.65506E+02 7.55435E+02
[SFEDIT]...J= 5 0.00000E+00 7.89392E+02 7.82962E+02 7.74320E+02 7.58289E+02 7.65506E+02 7.55435E+02
...
[SFEDIT]...J= 5 0.00000E+00 3.09535E+17 3.07039E+17 2.99970E+17 2.87473E+17 2.80647E+17 2.79369E+17
[SFEDIT]...J= 5 0.00000E+00 3.07039E+17 2.99970E+17 2.87473E+17 2.80647E+17 2.79369E+17 2.83047E+17
[SFEDIT]...J= 5 0.00000E+00 3.09881E+17 3.04543E+17 2.96859E+17 2.74651E+17 2.87407E+17 2.72729E+17
[SFEDIT]...J= 5 0.00000E+00 3.06317E+17 3.01376E+17 2.92297E+17 2.76920E+17 2.78388E+17 2.74390E+17
[SFEDIT]...J= 5 0.00000E+00 3.09535E+17 3.04543E+17 2.95397E+17 2.79878E+17 2.81415E+17 2.77323E+17
[SFEDIT]...J= 5 0.00000E+00 3.09535E+17 3.04543E+17 2.95397E+17 2.79878E+17 2.81415E+17 2.77323E+17
...
SFEDIT Option 2
...
[SFEDIT] (5D) Cell and surface averaged power density (w/cc)
[SFEDIT]...| Region | Cell | Sample | Surface data ->
...
[SFEDIT]...|      3| 25|      1| 7.661588E+02 7.618977E+02 7.504221E+02 7.527412E+02 7.582890E+02 7.582890E+02
[SFEDIT]...|      3| 26|      1| 7.618977E+02 7.604706E+02 7.779907E+02 7.602693E+02 7.655065E+02 7.655064E+02
[SFEDIT]...|      3| 27|      1| 7.604706E+02 7.616345E+02 7.481947E+02 7.499430E+02 7.554349E+02 7.554348E+02
...
[SFEDIT] (6D) Cell and surface averaged fast flux (n/cm^2/sec)
[SFEDIT]...| Region | Cell | Sample | Surface data ->
...
[SFEDIT]...|      3| 25|      1| 2.874730E+17 2.806467E+17 2.746506E+17 2.769199E+17 2.798780E+17 2.798780E+17
[SFEDIT]...|      3| 26|      1| 2.806467E+17 2.793694E+17 2.874070E+17 2.783875E+17 2.814154E+17 2.814154E+17
[SFEDIT]...|      3| 27|      1| 2.793694E+17 2.830466E+17 2.727287E+17 2.743905E+17 2.773234E+17 2.773234E+17
...

```

**Figure 3-102. SFEDIT Output Excerpt for COREB Verification in DIF3D-FD**

The next region is COREC which fills the remaining three assemblies and the peak power of 823.021 Watts/cm<sup>3</sup> is on plane 15 and was also provided earlier in Figure 3-96. The triangle position is (6,1,15). The associated assembly is at position 5 of ring 2. Looking at the surrounding power and flux data, it should be rather clear that the peak will occur on the reflected surface of this assembly in this mesh. The hand calculation is provided in Table 3-60 where the plane 14 data used to compute the surface 4 results is not shown for brevity. As can be seen, surface 3 and 5 have identical values to the volume peak which is associated with reflected boundary conditions that would be applied at those points.

**Table 3-60. COREC Peak Surface Power Density and Fast Flux Calculation**

| Group         | Extracted RTFLUX Data |                   |                   |                   | Volume            |                   |
|---------------|-----------------------|-------------------|-------------------|-------------------|-------------------|-------------------|
| 1             | 7.1878E+16            | 6.9283E+16        | 7.3203E+16        |                   |                   |                   |
|               | 7.4776E+16            | <b>7.5887E+16</b> | 7.5387E+16        |                   |                   |                   |
| 2             | 2.4428E+17            | 2.4047E+17        | 2.4583E+17        |                   |                   |                   |
|               | 2.4874E+17            | <b>2.5059E+17</b> | 2.4959E+17        |                   |                   |                   |
| 3             | 1.2999E+17            | 1.3197E+17        | 1.2940E+17        |                   |                   |                   |
|               | 1.2871E+17            | <b>1.2833E+17</b> | 1.2850E+17        |                   |                   |                   |
| Group         | Surface Fluxes        |                   |                   |                   |                   |                   |
|               | 1                     | 2                 | 3                 | 4                 | 5                 |                   |
| 1             | 7.5332E+16            | <b>7.5637E+16</b> | <b>7.5887E+16</b> | <b>7.5102E+16</b> | <b>7.5887E+16</b> | <b>7.5887E+16</b> |
| 2             | 2.4967E+17            | 2.5009E+17        | 2.5059E+17        | 2.4783E+17        | 2.5059E+17        | 2.5059E+17        |
| 3             | 1.2852E+17            | 1.2841E+17        | 1.2833E+17        | 1.2769E+17        | 1.2833E+17        | 1.2833E+17        |
| Power Density | 820.99                | 821.98            | 823.02            | 815.84            | 823.02            | 823.02            |
| Fast Flux     | 3.2500E+17            | 3.2573E+17        | 3.2648E+17        | 3.2293E+17        | 3.2648E+17        | 3.2648E+17        |

For the region-wise edits of SFEDIT, this cell corresponds to  $(15-11)*18+2=74$ . The SFEDIT output data for option 1 and 2 are provided in Figure 3-103. As can be seen, the two sets of data again match (within round off error) indicating that the two calculations are equivalent but the ordering of the data is simply different. Comparing the hand calculation with the SFEDIT data shows that the two are also a match within round-off error. Given this outcome, the peak and surface calculation of COREC is complete.

```

SFEDIT Option 1
...
[SFEDIT]...I ->      1      2      3      4      5      6      7
[SFEDIT]...J= 1 0.00000E+00 0.00000E+00 0.00000E+00 0.00000E+00 8.18966E+02 8.20993E+02 8.21981E+02
[SFEDIT]...J= 1 0.00000E+00 0.00000E+00 0.00000E+00 0.00000E+00 8.20993E+02 8.21981E+02 8.20942E+02
[SFEDIT]...J= 1 0.00000E+00 0.00000E+00 0.00000E+00 0.00000E+00 8.14294E+02 8.23021E+02 8.17031E+02
[SFEDIT]...J= 1 0.00000E+00 0.00000E+00 0.00000E+00 0.00000E+00 8.11936E+02 8.15836E+02 8.13875E+02
[SFEDIT]...J= 1 0.00000E+00 0.00000E+00 0.00000E+00 0.00000E+00 8.18966E+02 8.23021E+02 8.20942E+02
[SFEDIT]...J= 1 0.00000E+00 0.00000E+00 0.00000E+00 0.00000E+00 8.18966E+02 8.23021E+02 8.20942E+02
...
[SFEDIT]...J= 1 0.00000E+00 0.00000E+00 0.00000E+00 0.00000E+00 3.23520E+17 3.25000E+17 3.25730E+17
[SFEDIT]...J= 1 0.00000E+00 0.00000E+00 0.00000E+00 0.00000E+00 3.25000E+17 3.25730E+17 3.24981E+17
[SFEDIT]...J= 1 0.00000E+00 0.00000E+00 0.00000E+00 0.00000E+00 3.19837E+17 3.26480E+17 3.22006E+17
[SFEDIT]...J= 1 0.00000E+00 0.00000E+00 0.00000E+00 0.00000E+00 3.20012E+17 3.22935E+17 3.21456E+17
[SFEDIT]...J= 1 0.00000E+00 0.00000E+00 0.00000E+00 0.00000E+00 3.23520E+17 3.26480E+17 3.24981E+17
[SFEDIT]...J= 1 0.00000E+00 0.00000E+00 0.00000E+00 0.00000E+00 3.23520E+17 3.26480E+17 3.24981E+17
...
SFEDIT Option 2
...
[SFEDIT] (5D) Cell and surface averaged power density (w/cc)
[SFEDIT]...| Region | Cell | Sample | Surface data ->
[SFEDIT]...| 4| 73| 1| 8.189656E+02 8.209931E+02 8.142939E+02 8.119361E+02 8.189656E+02 8.189656E+02
[SFEDIT]...| 4| 74| 1| 8.209931E+02 8.21981E+02 8.230205E+02 8.158360E+02 8.230205E+02 8.230205E+02
[SFEDIT]...| 4| 75| 1| 8.219814E+02 8.209423E+02 8.170309E+02 8.138752E+02 8.209423E+02 8.209423E+02
...
[SFEDIT] (6D) Cell and surface averaged fast flux (n/cm^2/sec)
[SFEDIT]...| Region | Cell | Sample | Surface data ->
[SFEDIT]...| 4| 73| 1| 3.235199E+17 3.249997E+17 3.198370E+17 3.200120E+17 3.235199E+17 3.235199E+17
[SFEDIT]...| 4| 74| 1| 3.249997E+17 3.257304E+17 3.264796E+17 3.229347E+17 3.264796E+17 3.264796E+17
[SFEDIT]...| 4| 75| 1| 3.257304E+17 3.249813E+17 3.220062E+17 3.214561E+17 3.249813E+17 3.249813E+17
...

```

**Figure 3-103. SFEDIT Output Excerpt for COREC Verification in DIF3D-FD**

The last region to test is the REFL region. A close inspection of Figure 3-95 indicates that the peak power and peak of the fast flux occur at different points in this region. For the power density, the peak occurs in plane 1 and plane 30 (due to axial symmetry) and has a magnitude of  $151.663 \text{ W/cm}^3$ . The RTFLUX and PWDINT output for plane 1 are provided in Figure 3-104. For the fast flux, the peak occurs at axial plane 15 and the data of importance is already provided in Figure 3-96. Because this region requires the calculation of two different meshes, the power density is done first followed by the fast flux.

The hand calculation of the surface power densities is provided in Table 3-61 for all five surfaces and the volume of the mesh which is triangle (6,1,1). The assembly is ring 2 position 5. The plane 2 RTFLUX data was used to calculate the surface 5 in Table 3-61 and is not shown here for brevity. The SFEDIT data for the power density is provided in Figure 3-105. For the region-wise data, the triangle is the second triangle in the data set. A quick comparison between the SFEDIT data shows that the region-wise and mesh-wise data is identical. Comparing either with the hand calculation also shows an identical match in the computed results.

The hand calculation of the surface fast fluxes is provided in Table 3-62 where the plane 14 data is not shown for brevity. For the SFEDIT, this triangle corresponds to  $420+(15-11)*6+2=446$  in this region and position (6,3,15). The SFEDIT fast flux data for the triangle is provided in Figure 3-105. A comparison between the SFEDIT region-wise and mesh-wise result match within the round off error. Similarly, the hand calculation matches the SFEDIT data within round off data.

From the preceding calculation of four locations of the peak power density and four locations of the peak fast flux, one can conclude that the procedure used by DIF3D-FD to compute the surface fluxes is accurate. Further, the SFEDIT output data is correct given a triangular-Z mesh and is thus fully verified for DIF3D-FD. Because this effort will be repeated for another problem later in this section, no additional verification of the DIF3D-FD capability is needed.

```
[RTFLUX].....REGULAR FLUX FOR AXIAL PLANE 1 GROUP ..... 1
[RTFLUX]...I -> 1 2 3 4 5 6 7
[RTFLUX]...J= 6 0.00000E+00 0.00000E+00 0.00000E+00 0.00000E+00 1.55975E+16 1.55891E+16 1.55963E+16
[RTFLUX]...J= 5 0.00000E+00 1.56551E+16 1.56462E+16 1.56423E+16 1.56200E+16 1.56303E+16 1.56180E+16
[RTFLUX]...J= 4 0.00000E+00 1.56676E+16 1.56820E+16 1.56670E+16 1.56795E+16 1.56615E+16 1.56789E+16
[RTFLUX]...J= 3 0.00000E+00 1.57276E+16 1.57122E+16 1.57244E+16 1.57112E+16 1.57272E+16 1.57121E+16
[RTFLUX]...J= 2 0.00000E+00 1.57391E+16 1.57454E+16 1.57460E+16 1.57618E+16 1.57535E+16 1.57641E+16
[RTFLUX]...J= 1 0.00000E+00 0.00000E+00 0.00000E+00 0.00000E+00 1.57778E+16 1.57838E+16 1.57791E+16

[RTFLUX].....REGULAR FLUX FOR AXIAL PLANE 1 GROUP ..... 2
[RTFLUX]...I -> 1 2 3 4 5 6 7
[RTFLUX]...J= 6 0.00000E+00 0.00000E+00 0.00000E+00 0.00000E+00 1.51558E+17 1.51545E+17 1.51556E+17
[RTFLUX]...J= 5 0.00000E+00 1.51639E+17 1.51626E+17 1.51623E+17 1.51591E+17 1.51609E+17 1.51589E+17
[RTFLUX]...J= 4 0.00000E+00 1.51659E+17 1.51685E+17 1.51663E+17 1.51685E+17 1.51658E+17 1.51685E+17
[RTFLUX]...J= 3 0.00000E+00 1.51761E+17 1.51736E+17 1.51757E+17 1.51736E+17 1.51762E+17 1.51738E+17
[RTFLUX]...J= 2 0.00000E+00 1.51780E+17 1.51791E+17 1.51792E+17 1.51818E+17 1.51804E+17 1.51820E+17
[RTFLUX]...J= 1 0.00000E+00 0.00000E+00 0.00000E+00 0.00000E+00 1.51843E+17 1.51852E+17 1.51844E+17

[RTFLUX].....REGULAR FLUX FOR AXIAL PLANE 1 GROUP ..... 3
[RTFLUX]...I -> 1 2 3 4 5 6 7
[RTFLUX]...J= 6 0.00000E+00 0.00000E+00 0.00000E+00 0.00000E+00 2.31523E+17 2.31528E+17 2.31524E+17
[RTFLUX]...J= 5 0.00000E+00 2.31496E+17 2.31499E+17 2.31502E+17 2.31512E+17 2.31508E+17 2.31514E+17
[RTFLUX]...J= 4 0.00000E+00 2.31491E+17 2.31486E+17 2.31491E+17 2.31486E+17 2.31494E+17 2.31487E+17
[RTFLUX]...J= 3 0.00000E+00 2.31471E+17 2.31475E+17 2.31470E+17 2.31474E+17 2.31468E+17 2.31474E+17
[RTFLUX]...J= 2 0.00000E+00 2.31467E+17 2.31464E+17 2.31463E+17 2.31457E+17 2.31459E+17 2.31456E+17
[RTFLUX]...J= 1 0.00000E+00 0.00000E+00 0.00000E+00 0.00000E+00 2.31452E+17 2.31450E+17 2.31452E+17

[PWDINT].....POWER DENSITY FOR AXIAL PLANE..... 1
[PWDINT]...I -> 1 2 3 4 5 6 7
[PWDINT]...J= 6 0.00000E+00 0.00000E+00 0.00000E+00 0.00000E+00 1.51590E+02 1.51588E+02 1.51590E+02
[PWDINT]...J= 5 0.00000E+00 1.51608E+02 1.51605E+02 1.51605E+02 1.51598E+02 1.51602E+02 1.51598E+02
[PWDINT]...J= 4 0.00000E+00 1.51613E+02 1.51620E+02 1.51614E+02 1.51619E+02 1.51613E+02 1.51620E+02
[PWDINT]...J= 3 0.00000E+00 1.51640E+02 1.51633E+02 1.51638E+02 1.51632E+02 1.51639E+02 1.51632E+02
[PWDINT]...J= 2 0.00000E+00 1.51645E+02 1.51647E+02 1.51647E+02 1.51654E+02 1.51650E+02 1.51654E+02
[PWDINT]...J= 1 0.00000E+00 0.00000E+00 0.00000E+00 0.00000E+00 1.51661E+02 1.51663E+02 1.51661E+02
```

Figure 3-104. PWDINT and RTFLUX Output Excerpt for REFL Verification in DIF3D-FD

Table 3-61. REFL Peak Surface Power Density Calculation

| Group          | Extracted RTFLUX Data |            |            |            |            | Volume      |
|----------------|-----------------------|------------|------------|------------|------------|-------------|
| 1              | 1.5762E+16            | 1.5754E+16 | 1.5764E+16 | 1.5784E+16 | 1.5779E+16 |             |
|                | 1.5778E+16            | 1.5784E+16 | 1.5779E+16 |            |            |             |
| 2              | 1.5182E+17            | 1.5180E+17 | 1.5182E+17 | 1.5185E+17 | 1.5184E+17 | 2.31450E+17 |
|                | 1.5184E+17            | 1.5185E+17 | 1.5184E+17 |            |            |             |
| 3              | 2.3146E+17            | 2.3146E+17 | 2.3146E+17 | 2.3145E+17 | 2.3145E+17 | 2.3145E+17  |
|                | 2.3145E+17            | 2.3145E+17 | 2.3145E+17 |            |            |             |
| Surface Fluxes |                       |            |            |            |            | Volume      |
| Group          | 1                     | 2          | 3          | 4          | 5          |             |
| 1              | 1.5781E+16            | 1.5781E+16 | 1.5784E+16 | 1.5784E+16 | 1.5949E+16 | 1.5784E+16  |
| 2              | 1.5185E+17            | 1.5185E+17 | 1.5185E+17 | 1.5185E+17 | 1.5210E+17 | 1.5185E+17  |
| 3              | 2.3145E+17            | 2.3145E+17 | 2.3145E+17 | 2.3145E+17 | 2.3100E+17 | 2.3145E+17  |
| Power density  | 151.662               | 151.662    | 151.663    | 151.663    | 151.535    | 151.663     |

```

SFEDIT Option 1
...
[SFEDIT]...I ->          1          2          3          4          5          6          7
[SFEDIT]...J= 1  0.00000E+00  0.00000E+00  0.00000E+00  0.00000E+00  1.51661E+02  1.51662E+02  1.51662E+02
[SFEDIT]...J= 1  0.00000E+00  0.00000E+00  0.00000E+00  0.00000E+00  1.51662E+02  1.51662E+02  1.51661E+02
[SFEDIT]...J= 1  0.00000E+00  0.00000E+00  0.00000E+00  0.00000E+00  1.51657E+02  1.51663E+02  1.51657E+02
[SFEDIT]...J= 1  0.00000E+00  0.00000E+00  0.00000E+00  0.00000E+00  1.51661E+02  1.51663E+02  1.51661E+02
[SFEDIT]...J= 1  0.00000E+00  0.00000E+00  0.00000E+00  0.00000E+00  1.51532E+02  1.51535E+02  1.51532E+02
[SFEDIT]...J= 1  0.00000E+00  0.00000E+00  0.00000E+00  0.00000E+00  1.51661E+02  1.51663E+02  1.51661E+02
...
[SFEDIT]...J= 3  0.00000E+00  3.10109E+17  3.08638E+17  3.05273E+17  2.97046E+17  2.96151E+17  2.96151E+17
[SFEDIT]...J= 3  0.00000E+00  3.08638E+17  3.05273E+17  2.97046E+17  2.96151E+17  2.96425E+17  2.98382E+17
[SFEDIT]...J= 3  0.00000E+00  3.10912E+17  3.06896E+17  3.07174E+17  2.93786E+17  2.99831E+17  2.99831E+17
[SFEDIT]...J= 3  0.00000E+00  3.06788E+17  3.03884E+17  3.00088E+17  2.91980E+17  2.93760E+17  2.92523E+17
[SFEDIT]...J= 3  0.00000E+00  3.10109E+17  3.07168E+17  3.03379E+17  2.95248E+17  2.97054E+17  2.95797E+17
[SFEDIT]...J= 3  0.00000E+00  3.10109E+17  3.07168E+17  3.03379E+17  2.95248E+17  2.97054E+17  2.95797E+17
...
SFEDIT Option 2
...
[SFEDIT] (5D) Cell and surface averaged power density (w/cc)
[SFEDIT]...| Region | Cell | Sample | Surface data ->
[SFEDIT]...| 1| 1| 1| 1.516606E+02 1.516618E+02 1.516571E+02 1.516606E+02 1.515322E+02 1.516606E+02
[SFEDIT]...| 1| 2| 1| 1.516618E+02 1.516619E+02 1.516630E+02 1.516630E+02 1.515348E+02 1.516630E+02
[SFEDIT]...| 1| 3| 1| 1.516619E+02 1.516608E+02 1.516574E+02 1.516608E+02 1.515324E+02 1.516608E+02
...
[SFEDIT] (6D) Cell and surface averaged fast flux (n/cm^2/sec)
[SFEDIT]...| Region | Cell | Sample | Surface data ->
[SFEDIT]...| 1| 445| 1| 2.970462E+17 2.961508E+17 2.937857E+17 2.919799E+17 2.952479E+17 2.952479E+17
[SFEDIT]...| 1| 446| 1| 2.961508E+17 2.964251E+17 2.998311E+17 2.937601E+17 2.970537E+17 2.970537E+17
[SFEDIT]...| 1| 447| 1| 2.964251E+17 2.983822E+17 2.938227E+17 2.925226E+17 2.957965E+17 2.957965E+17
...

```

Figure 3-105. SFEDIT Output Excerpt for REFL Verification in DIF3D-FD

Table 3-62. REFL Peak Surface Fast Flux Calculation

| Group     | Extracted RTFLUX Data |                   |            | Volume     |            |
|-----------|-----------------------|-------------------|------------|------------|------------|
|           | 1                     | 2                 | 3          |            |            |
| 1         | 6.2354E+16            | <b>6.3200E+16</b> | 6.2677E+16 | 6.3200E+16 |            |
|           | 7.1878E+16            | 6.9283E+16        | 7.3203E+16 |            |            |
| 2         | 2.3289E+17            | <b>2.3385E+17</b> | 2.3312E+17 | 2.3385E+17 |            |
|           | 2.4428E+17            | 2.4047E+17        | 2.4583E+17 |            |            |
| 3         | 1.3692E+17            | <b>1.3671E+17</b> | 1.3675E+17 | 1.3671E+17 |            |
|           | 1.2999E+17            | 1.3197E+17        | 1.2940E+17 |            |            |
| Group     | Surface Fluxes        |                   |            |            |            |
|           | 1                     | 2                 | 3          | 4          |            |
| 1         | 6.2777E+16            | 6.2938E+16        | 6.4649E+16 | 6.2441E+16 | 6.3200E+16 |
| 2         | 2.3337E+17            | 2.3349E+17        | 2.3518E+17 | 2.3132E+17 | 2.3385E+17 |
| 3         | 1.3681E+17            | 1.3673E+17        | 1.3569E+17 | 1.3685E+17 | 1.3671E+17 |
| Fast Flux | 2.9615E+17            | 2.9642E+17        | 2.9983E+17 | 2.9376E+17 | 2.9705E+17 |

### 3.7.1.5 Verification of the SFEDIT Data File for Hexagonal-Z Based DIF3D-VARIANT

Compared to the preceding DIF3D-FD verification work, the verification of DIF3D-VARIANT is far more complex. To keep matters simple, the exact same test problem is used for the verification work to DIF3D-FD. There is a single mesh used for the lower reflector region, 3 meshes used for the active core, and a single mesh used in the upper reflector to help cut down on the amount of data to be processed. For verification purposes, the same goal of identifying the peaks in all four regions of will be done.

Because the surface partial currents are not exported in any fashion from DIF3D other than the NHFLUX file, a breakdown of that dataset printed using PrintTables.x is required for a complete understanding of the data being displayed. Figure 3-106 provides the major parts of the NHFLUX

output edit. The first segment is the partial current index offset (-1) into the partial current array for a given surface of a given mesh. Because there are 7 assemblies, there are 7 lines of output. In this output, a radial partial current index is provided for each surface of each mesh which factors in the number of space-angle moments on the surface (3 in this case). The lowest number seen is 0 and the highest is 177. These translate to partial current surface 1 and 60 respectively or  $k/3+1$ . The next segment of output gives the index for the outgoing partial currents on the boundary of the domain. In ring 2 there are three surfaces on the outer boundary for each assembly and thus 18 lines in this part of the NHFLUX file output (not shown for brevity). This data is ordered by NODAL mesh ordering followed by mesh surface ordering. The transformation map is the next segment of output which, given the GEODST order [6] gives the NODAL mesh index number [7]. Because there are seven meshes, there will be seven numbers. Note that GEODST stores the zero positions in its grid and thus it has a total of 9 GEODST positions while NODAL will only have 7. These three pieces of information are all that is required to complete the mapping of data between GEODST and NODAL along with identify the partial current moments on each surface.

Following the geometry mapping details in NHFLUX are the mesh-wise flux and partial current arrays. The mesh-wise flux details provide the space-angle expansion for each NODAL mesh. If there are 10 spatial polynomials in the flux approximation, the first 10 moments will be the scalar flux moments ( $P_0$ ) followed by the higher order angular moments (i.e.  $P_2$ ,  $P_4$ , etc...). This data is provided per plane per group in the output.

Following the mesh-wise flux are the x-y directed currents. The total number of partial currents present is dependent upon the number of NODAL meshes in the domain. For NODAL, there are two surfaces per unique mesh surface and the maximum number of partial currents of  $7*6*2=84$ . Counting the number of unique surfaces in the domain, there are 12 interior surfaces and 18 boundary surfaces. Multiplying the sum together gives 60 partial currents needed to fully define the currents for this problem. The ordering of the outgoing partial currents for each NODAL mesh is  $(i-1)*6+j$  where  $i$  is the nodal hex number and  $j$  is the local x-y surface on each mesh. Thus another way to calculate the total number of partial currents needed is to take the total number of NODAL meshes multiplied by the number of surfaces ( $7*6=42$ ) and add the number of boundary surfaces (18). For each line of x-y partial current output, there are 3 moments corresponding to a linear expansion (1, y, z as an example). As was the case with the mesh-wise flux, the x-y partial currents are given per plane per group.

The last piece of data in the output is the axially directed outward partial current. This data is ordered by surface by group where there is one more surface than there are planes. The orientation of the partial currents for each surface are described as -z and +z. Thus for the first surface  $k$ , the mesh in plane  $k$  has the outgoing moment as -z and incoming as +z. For the upper surface ( $k+1$ ) on the mesh in plane  $k$ , the outgoing partial currents is +z while the incoming is -z which is switched from the orientation of the first surface. There are seven NODAL meshes per plane and thus 7 lines for the +z and -z partial currents. Each line has 3 moments corresponding to the space-angle approximation on the interface (3 spatial and 1 angular in this case).

From the description of the NHFLUX file, it should be very clear that the output excerpts will become extremely large as the partial current mapping will require the collection of at least twelve x-y partial current data lines and two z partial current lines per group per mesh. As a consequence, only a few of the fitting calculations will be displayed in the following hand calculations as the entire process is considerably difficult to display.

```

...[NHFLUX]...POINTERS TO INCOMING XY PLANE PARTIAL CURRENTS...[1, 27] [2, 48] [3, 69] [4, 72] [5, 93] [6, 114]
[NHFLUX]...POINTERS TO INCOMING XY PLANE PARTIAL CURRENTS...[1, 126] [2, 129] [3, 51] [4, 0] [5, 111] [6, 132]
[NHFLUX]...POINTERS TO INCOMING XY PLANE PARTIAL CURRENTS...[1, 135] [2, 138] [3, 141] [4, 54] [5, 3] [6, 24]
[NHFLUX]...POINTERS TO INCOMING XY PLANE PARTIAL CURRENTS...[1, 45] [2, 144] [3, 147] [4, 150] [5, 75] [6, 6]
[NHFLUX]...POINTERS TO INCOMING XY PLANE PARTIAL CURRENTS...[1, 9] [2, 66] [3, 153] [4, 156] [5, 159] [6, 96]
[NHFLUX]...POINTERS TO INCOMING XY PLANE PARTIAL CURRENTS...[1, 117] [2, 12] [3, 87] [4, 162] [5, 165] [6, 168]
[NHFLUX]...POINTERS TO INCOMING XY PLANE PARTIAL CURRENTS...[1, 171] [2, 30] [3, 15] [4, 90] [5, 174] [6, 177]

...[NHFLUX]...POINTERS TO OUTGOING PARTIAL CURRENTS..... 1..... 7
[NHFLUX]...POINTERS TO OUTGOING PARTIAL CURRENTS..... 2..... 8
[NHFLUX]...POINTERS TO OUTGOING PARTIAL CURRENTS..... 3..... 12
[NHFLUX]...POINTERS TO OUTGOING PARTIAL CURRENTS..... 4..... 13
[NHFLUX]...POINTERS TO OUTGOING PARTIAL CURRENTS..... 5..... 14
[NHFLUX]...POINTERS TO OUTGOING PARTIAL CURRENTS..... 6..... 15

...[NHFLUX]...TRANSFORMATION MAP BETWEEN NODAL AND GEODST..... 1..... 5
[NHFLUX]...TRANSFORMATION MAP BETWEEN NODAL AND GEODST..... 2..... 6
[NHFLUX]...TRANSFORMATION MAP BETWEEN NODAL AND GEODST..... 3..... 9
[NHFLUX]...TRANSFORMATION MAP BETWEEN NODAL AND GEODST..... 4..... 8
[NHFLUX]...TRANSFORMATION MAP BETWEEN NODAL AND GEODST..... 5..... 4

...[NHFLUX]...REGULAR FLUX MOMENTS FOR AXIAL PLANE. 1 Group 1
[NHFLUX]...XY Node; Nodal moments ->
 1 2.261906232E+16 -1.490684288E+13 -5.5587802662E+15 -1.569721566E+13 -1.836977220E+13
 2 2.230406232E+16 -2.494257757E+13 -1.421740704E+14 -5.265656046E+15 1.957531212E+13 3.261191743E+13
 3 2.182270043E+16 -1.095708209E+14 -1.465683568E+14 -4.758594544E+15 2.530104136E+13 -1.337427713E+12
 4 2.242460589E+16 -3.176892535E+14 -3.616694693E+13 -5.409682316E+15 -3.315810664E+13 -9.350166413E+12
 5 2.273938370E+16 -1.499778541E+13 -5.692574640E+13 -5.625381536E+15 1.021010795E+12 -1.898262065E+13
 6 2.298821345E+16 -1.684096232E+13 -7.377389453E+13 -5.856001863E+15 -4.752501507E+12 6.615342465E+12
 7 2.286459807E+16 -3.394062932E+13 -9.858734833E+13 -5.773668259E+15 7.296349942E+12 -1.883835862E+13

...[NHFLUX]...RADially DIRECTED PARTIAL CURRENTS FOR AXIAL PLANE. 1 Group 1
[NHFLUX]...XY Surface Index; Current moments ->
 1 9.953406036E+17 -5.623320395E+15 -2.613431100E+17
 2 1.010201121E+18 2.835288781E+14 -2.724024428E+17
 3 9.898212682E+17 -5.874123766E+15 -2.558352883E+17
 4 9.887298623E+17 -6.645009419E+15 -2.552526128E+17
 5 9.845564533E+17 -2.577375278E+14 -2.549052992E+17
 6 9.831232707E+17 -6.352687404E+15 -2.496836780E+17
 7 9.651675463E+17 -1.993773366E+15 -2.284756046E+17

...[NHFLUX]...j PARTIAL CURRENT IN -Z FOR AXIAL SURFACE 1 Group 1
 1 3.644260636E+17 3.379912593E+14 5.879852330E+14
 2 3.536162747E+17 3.847599912E+14 8.534518219E+14
 3 3.470752574E+17 1.171118151E+15 1.616664287E+15
 4 3.557013697E+17 6.814000504E+14 1.125796139E+14
 5 3.546942489E+17 -6.714737608E+14 4.370101810E+13
 6 3.571792283E+17 -3.187190458E+14 -1.363472723E+14
 7 3.568073387E+17 2.362905080E+14 9.002304403E+13

...[NHFLUX]...j PARTIAL CURRENT IN +Z FOR AXIAL SURFACE 1 Group 1
 1 3.644260636E+17 3.379912593E+14 5.879852330E+14
 2 3.536162747E+17 3.847599912E+14 8.534518219E+14
 3 3.470752574E+17 1.171118151E+15 1.616664287E+15
 4 3.557013697E+17 6.814000504E+14 1.125796139E+14
 5 3.546942489E+17 -6.714737608E+14 4.370101810E+13
 6 3.571792283E+17 -3.187190458E+14 -1.363472723E+14
 7 3.568073387E+17 2.362905080E+14 9.002304403E+13
...

```

**Figure 3-106. NHFLUX Output Example for DIF3D-VARIANT**

The first region to determine the peak flux is COREA. This region consists of two hexagons (ring 2 positions 1 and 4) and three axial meshes. Using the (I,J,K) indexing described previously, the location in hexagon geometry for ring 2 position 1 is (3,2,\*) while for position 4 it is (1,2,\*). The PWDINT data of interest have been extracted and is provided in Figure 3-107. With the knowledge of the DIF3D-FD verification work carried out in the previous section the peak powers should occur on plane 3 and for position 1 it is 7747.8 W/cm<sup>3</sup> and position 4 it is 7954.48 W/cm<sup>3</sup> which are considerably larger than plane 1 and plane 2. Compared with the DIF3D-FD result, it should be clear that the peak power, and peak flux, is again in ring 2 position 4 for this region. With respect to the NODAL ordering, this position corresponds to the 5<sup>th</sup> mesh. From the previous DIF3D-FD analysis, only the plane 3 flux data is of interest for COREA, COREB, COREC, and REFL while plane 1 is needed for the peak power calculation in region REFL.

Focusing on the 5<sup>th</sup> mesh, the NHFLUX details have been collected in Figure 3-108. The outgoing partial current indexes for this meshes six surfaces are 25, 26, 27, 28, 29, and 30. Using the pointer details from Figure 3-106, the incoming partial current surfaces are computed to be 4, 23, 52, 53, 54,

and 33. Together the partial current data is extracted as 4,23,25-30,33,52-54 as seen in Figure 3-108 for all three groups

```
[PWDINT].....POWER DENSITY FOR AXIAL PLANE.....1
[PWDINT]...I -> 1 2 3
[PWDINT]...J= 3 0.00000E+00 1.44586E+02 1.44565E+02
[PWDINT]...J= 2 1.44693E+02 1.44657E+02 1.44601E+02
[PWDINT]...J= 1 1.44728E+02 1.44685E+02 0.00000E+00
[PWDINT].....POWER DENSITY FOR AXIAL PLANE.....2
[PWDINT]...I -> 1 2 3
[PWDINT]...J= 3 0.00000E+00 7.35500E+02 7.15797E+02
[PWDINT]...J= 2 7.45657E+03 1.30489E+02 7.31772E+03
[PWDINT]...J= 1 7.53691E+02 7.50054E+02 0.00000E+00
[PWDINT].....POWER DENSITY FOR AXIAL PLANE.....3
[PWDINT]...I -> 1 2 3
[PWDINT]...J= 3 0.00000E+00 7.80684E+02 7.51359E+02
[PWDINT]...J= 2 7.95448E+03 1.33299E+02 7.74780E+03
[PWDINT]...J= 1 8.07845E+02 8.02369E+02 0.00000E+00
```

Figure 3-107. PWDINT Output Excerpt for DIF3D-VARIANT

|                           |                           |                           |
|---------------------------|---------------------------|---------------------------|
| 5 6.830356481E+16 ... vol | 5 2.389436901E+17 ... vol | 5 1.302977413E+17 ... vol |
| 4 1.683033469E+18 x-y pc  | 4 6.616081346E+18 x-y pc  | 4 3.934404702E+18 x-y pc  |
| 23 1.972507477E+18        | 23 6.787490542E+18        | 23 3.724120471E+18        |
| 25 2.015250389E+18        | 25 6.841461726E+18        | 25 3.803649263E+18        |
| 26 1.925224739E+18        | 26 6.838202245E+18        | 26 3.767852777E+18        |
| 27 1.990736399E+18        | 27 6.916271813E+18        | 27 3.729696082E+18        |
| 28 1.998583116E+18        | 28 6.957984961E+18        | 28 3.740848264E+18        |
| 29 2.013729836E+18        | 29 6.974997297E+18        | 29 3.743829162E+18        |
| 30 1.926248011E+18        | 30 6.886673779E+18        | 30 3.781683993E+18        |
| 33 2.076219549E+18        | 33 6.970716621E+18        | 33 3.750464526E+18        |
| 52 1.990736399E+18        | 52 6.916271813E+18        | 52 3.729696082E+18        |
| 53 1.998583116E+18        | 53 6.957984961E+18        | 53 3.740848264E+18        |
| 54 2.013729836E+18        | 54 6.974997297E+18        | 54 3.743829162E+18        |
| 5 1.418062611E+18 z- pc   | 5 4.998527060E+18 z- pc   | 5 2.802329724E+18 z- pc   |
| 5 1.479106231E+18 z+      | 5 5.130372034E+18 z+      | 5 2.808366406E+18 z-      |
| 5 1.479106231E+18 z-      | 5 5.130372034E+18 z-      | 5 2.808366406E+18 z-      |
| 5 1.418062611E+18 z+      | 5 4.998527060E+18 z+      | 5 2.802329724E+18 z+      |

Group 1

Group 2

Group 3

Figure 3-108. NHFLUX Output Excerpt for COREA SFEDIT Verification with DIF3D-VARIANT

In Figure 3-108, all but the first moment in each line is removed as that is the only one needed in the actual calculation. Additional comments (vol for volumetric flux) were added to help indicate the purpose of each line. The first step is to compute the surface fluxes on all eight surfaces of the hexagon. The results are shown in Table 3-63. Because the calculation is only unique for two of the surfaces, the surface 1 and surface 7 calculation will be displayed only for group 1. From Figure 3-108, the average flux value is simply the first line in each set of column data. The surface 1 data requires partial current 25 (j+) and 4 (j-) which are 2.01525E+18 and 1.68303E+18 from Figure 3-108. The pitch is 10 cm and the axial mesh size is 20 cm and thus the surface fluxes is calculated using

$$\bar{\varphi}_1 = \frac{2\sqrt{3}}{10 \cdot 20} (2.01525 + 1.68303) \cdot 10^{18} = 6.4056 \cdot 10^{16}. \quad (66)$$

The axial surfaces are more simple as the set of data is already adjacent in Figure 3-108 leading to

$$\bar{\varphi}_7 = \frac{4}{100\sqrt{3}} (1.41806 + 1.47910) \cdot 10^{18} = 6.6907 \cdot 10^{16}. \quad (67)$$

Note that these values match those for the corresponding surfaces in Table 3-63 for group 1. The remaining calculations of the surface fluxes follow the same methodology and are not shown for brevity.

Given the average volumetric flux and the surface fluxes, the next step is to compute the axial shaping function. As discussed, the first expansion coefficient is 1.0 and the fourth and fifth expansion coefficients are zero and thus only the second and third need to be calculated. Table 3-64 provides the calculated coefficients and the resulting axial shaping function evaluated at the fixed 11 points in

the mesh. Note that this basis is independent of the actual size of the mesh and thus the 11 points are always at these coordinates for all meshes.

**Table 3-63. COREA Node Volume and Surface Flux Moments**

|                  | Group 1    | Group 2    | Group 3    |
|------------------|------------|------------|------------|
| Average Flux     | 6.8304E+16 | 2.3894E+17 | 1.3030E+17 |
| Surface Fluxes   |            |            |            |
| 1                | 6.4056E+16 | 2.3309E+17 | 1.3403E+17 |
| 2                | 6.7511E+16 | 2.3600E+17 | 1.2976E+17 |
| 3                | 6.8961E+16 | 2.3959E+17 | 1.2920E+17 |
| 4                | 6.9233E+16 | 2.4103E+17 | 1.2959E+17 |
| 5                | 6.9758E+16 | 2.4162E+17 | 1.2969E+17 |
| 6                | 6.9325E+16 | 2.4002E+17 | 1.3046E+17 |
| 7                | 6.6907E+16 | 2.3392E+17 | 1.2957E+17 |
| 8                | 6.6907E+16 | 2.3392E+17 | 1.2957E+17 |
| Power Conversion | 1.8390E-14 | 1.5563E-14 | 2.2868E-14 |

**Table 3-64. COREA Hand Calculation of the Axial Fitting Function and its Evaluation**

| H coefficients          |                   |             |             |             |
|-------------------------|-------------------|-------------|-------------|-------------|
|                         |                   | Group 1     | Group 2     | Group 3     |
| 1                       |                   | 1.0000E+00  | 1.0000E+00  | 1.0000E+00  |
| 2                       |                   | 0.0000E+00  | 0.0000E+00  | 0.0000E+00  |
| 3                       |                   | -4.0886E-02 | -4.2075E-02 | -1.1117E-02 |
| Axial Sample Evaluation |                   |             |             |             |
| Sample Index            | Sample Coordinate | Group 1     | Group 2     | Group 3     |
| · 101                   | -0.5              | 0.9796      | 0.9790      | 0.9944      |
| 2                       | -0.4              | 0.9906      | 0.9903      | 0.9974      |
| 3                       | -0.3              | 0.9992      | 0.9992      | 0.9998      |
| 4                       | -0.2              | 1.0053      | 1.0055      | 1.0014      |
| 5                       | -0.1              | 1.0090      | 1.0093      | 1.0024      |
| 6                       | 0                 | 1.0102      | 1.0105      | 1.0028      |
| 7                       | 0.1               | 1.0090      | 1.0093      | 1.0024      |
| 8                       | 0.2               | 1.0053      | 1.0055      | 1.0014      |
| 9                       | 0.3               | 0.9992      | 0.9992      | 0.9998      |
| 10                      | 0.4               | 0.9906      | 0.9903      | 0.9974      |
| 11                      | 0.5               | 0.9796      | 0.9790      | 0.9944      |

Using the group 1, 7<sup>th</sup> and 8<sup>th</sup> surface flux data from Table 3-63 and the equations shown earlier, the coefficients are found to be

$$H_2 = \frac{\bar{\phi}_8 - \bar{\phi}_7}{\bar{\phi}} = \frac{6.6907 - 6.6907}{6.8304} = 0.0$$

$$H_3 = \frac{\bar{\phi}_8 + \bar{\phi}_7}{\bar{\phi}} - 2 = \frac{6.6907 + 6.6907}{6.8304} - 2 = -0.040905. \quad (68)$$

These match those provided in Table 3-64. The first two polynomials evaluated at -0.5 are calculated as

$$\bar{\Phi}(\zeta) = \begin{bmatrix} 1 \\ -0.3 \\ 0.020 \\ 0.048 \\ -0.006 \end{bmatrix} \rightarrow \sum_i \bar{\Phi}_i(\zeta) H_{g,m,i} = 1 \cdot 1 + (-0.3 \cdot 0.0) + (0.020 \cdot -0.040905) = 0.99918. \quad (69)$$

This result matches the value in Table 3-64 for sample coordinate -0.3. The remaining evaluation points are computed similarly and not shown for brevity.

For the mesh centered axial power shape, the last step is to multiply the axial sample point data in Table 3-64 by the average flux from Table 3-63 and the power conversion factor provided in Table 3-63 and sum over all three groups. This same process is used for each surface flux in Table 3-63 and the results for all are provided in Table 3-65 where the peak of the power in this mesh is highlighted.

**Table 3-65. COREA Power Evaluation at the Axial Sample Points**

| Axial Sample | Mesh Centered  | x-y Surface |         |         |         |                |         |
|--------------|----------------|-------------|---------|---------|---------|----------------|---------|
|              |                | 1           | 2       | 3       | 4       | 5              | 6       |
| 1            | 7834.00        | 7753.13     | 7762.81 | 7830.69 | 7866.39 | 7887.17        | 7872.45 |
| 2            | 7899.06        | 7816.55     | 7827.15 | 7895.92 | 7931.95 | 7952.95        | 7937.92 |
| 3            | <b>7949.66</b> | 7865.87     | 7877.19 | 7946.65 | 7982.95 | 8004.11        | 7988.83 |
| 4            | 7985.80        | 7901.10     | 7912.93 | 7982.89 | 8019.37 | 8040.66        | 8025.20 |
| 5            | 8007.48        | 7922.24     | 7934.38 | 8004.63 | 8041.23 | 8062.59        | 8047.03 |
| 6            | 8014.71        | 7929.28     | 7941.53 | 8011.88 | 8048.51 | <b>8069.90</b> | 8054.30 |
| 7            | 8007.48        | 7922.24     | 7934.38 | 8004.63 | 8041.23 | 8062.59        | 8047.03 |
| 8            | 7985.80        | 7901.10     | 7912.93 | 7982.89 | 8019.37 | 8040.66        | 8025.20 |
| 9            | 7949.66        | 7865.87     | 7877.19 | 7946.65 | 7982.95 | 8004.11        | 7988.83 |
| 10           | 7899.06        | 7816.55     | 7827.15 | 7895.92 | 7931.95 | 7952.95        | 7937.92 |
| 11           | 7834.00        | 7753.13     | 7762.81 | 7830.69 | 7866.39 | 7887.17        | 7872.45 |

Using the third mesh centered point value as an example, also highlighted in the table, it is calculated as

$$\begin{aligned} \Phi &= 6.8304 \cdot 1.8390 \cdot 100 \cdot 0.9992 + 2.3894 \cdot 1.5563 \cdot 1000 \cdot 0.9992 \\ &+ 1.3030 \cdot 2.2868 \cdot 1000 \cdot 0.9998 = 7950. \end{aligned} \quad (70)$$

This result is within the round off error of the value provided in Table 3-65. The fast flux data is a bit more simple to calculate as it only considers the first two energy groups in this problem. Similar to the power evaluation, the fast flux evaluation at the sample points is given in Table 3-66 where the example calculation and the overall peak are highlighted. Using the third axial sample point on surface 5 as an example, it is calculated as

$$\Phi_5 = 6.9758 \cdot 10^{16} \cdot 0.9992 + 2.4162 \cdot 10^{17} \cdot 0.9992 = 3.1113 \cdot 10^{17}. \quad (71)$$

This value is within the round off error of that provided in Table 3-66.

**Table 3-66. COREA Fast Flux Evaluation at the Axial Sample Points**

| Axial Sample | Mesh Centered | x-y Surface |            |            |            |                   |            |
|--------------|---------------|-------------|------------|------------|------------|-------------------|------------|
|              |               | 1           | 2          | 3          | 4          | 5                 | 6          |
| 1            | 3.0082E+17    | 2.9093E+17  | 2.9717E+17 | 3.0210E+17 | 3.0378E+17 | 3.0487E+17        | 3.0288E+17 |
| 2            | 3.0429E+17    | 2.9429E+17  | 3.0060E+17 | 3.0558E+17 | 3.0728E+17 | 3.0838E+17        | 3.0637E+17 |
| 3            | 3.0699E+17    | 2.9690E+17  | 3.0326E+17 | 3.0829E+17 | 3.1001E+17 | <b>3.1112E+17</b> | 3.0908E+17 |
| 4            | 3.0892E+17    | 2.9876E+17  | 3.0516E+17 | 3.1022E+17 | 3.1195E+17 | 3.1307E+17        | 3.1102E+17 |
| 5            | 3.1007E+17    | 2.9988E+17  | 3.0631E+17 | 3.1139E+17 | 3.1312E+17 | 3.1424E+17        | 3.1219E+17 |
| 6            | 3.1046E+17    | 3.0025E+17  | 3.0669E+17 | 3.1177E+17 | 3.1351E+17 | <b>3.1463E+17</b> | 3.1258E+17 |
| 7            | 3.1007E+17    | 2.9988E+17  | 3.0631E+17 | 3.1139E+17 | 3.1312E+17 | 3.1424E+17        | 3.1219E+17 |
| 8            | 3.0892E+17    | 2.9876E+17  | 3.0516E+17 | 3.1022E+17 | 3.1195E+17 | 3.1307E+17        | 3.1102E+17 |
| 9            | 3.0699E+17    | 2.9690E+17  | 3.0326E+17 | 3.0829E+17 | 3.1001E+17 | 3.1112E+17        | 3.0908E+17 |
| 10           | 3.0429E+17    | 2.9429E+17  | 3.0060E+17 | 3.0558E+17 | 3.0728E+17 | 3.0838E+17        | 3.0637E+17 |
| 11           | 3.0082E+17    | 2.9093E+17  | 2.9717E+17 | 3.0210E+17 | 3.0378E+17 | 3.0487E+17        | 3.0288E+17 |

With the calculation of all of the sample points displayed, the last step is to compare the hand calculated results to the SFEDIT results. As shown previously for the DIF3D-FD case, the mesh-wise data is displayed in a grid format. Thus to display all 77 values in both tables above would constitute a large amount of information. To simplify the work, the 2nd surface is selected for detailed inspection in the power computation and the 3<sup>rd</sup> surface is selected for detailed inspection for the fast flux output.

The mesh-wise and region-wise SFEDIT output excerpt is collected in Figure 3-109. Because there are two meshes per plane and only three total planes in COREA, the mesh is the 4<sup>th</sup> one for this region in the region-wise data. The surface 2 result is highlighted in both sets of SFEDIT data for convenience and one can easily see that the mesh-wise and region-wise results are identical. The entire set of axial sample results is within the round off error from the power data displayed in Table 3-65 indicating that the preceding methodology for calculating the points is consistent with DIF3D-VARIANT. Because the region-wise data is organized by mesh, it can be used to verify that the volume (surface 1 value) and all surface data (surface 2 through 7) also match the results provided in Table 3-65 for all sample points within round-off error.

The fast flux result is similarly collected for surface 3 (numbered 4 in the SFEDIT file) and provided in Figure 3-110. The selected surface data is again highlighted and the mesh-wise and region-wise results are consistent. As was the case with the power edit, the region-wise result provides the sample data for all surfaces. A comparison of the results in Figure 3-110 with the hand calculated results in Table 3-66 shows that the two sets of data are within round-off error of each other. Because this mesh straddles the center of the domain, it should come as no surprise that the peak occurs at the center sample point (#6). The peak power is found to occur on surface 5 (surface 6 in the output data). This peak is consistent with the DIF3D-FD result. The peak fast flux is also found to occur on this surface.

With the results for COREA verified, the COREB, COREC, and REFL results will not be displayed in similar detail. A companion EXCEL document [17] provided with the verification test problems that are discussed in this section can be used to calculate all of the axial sample results from all meshes in the domain. Because the intermediate quantities like the axial fitting coefficients are not reproducible from the DIF3D output, they are omitted from this point on. Also, since the mesh-wise data is not used by REBUS in the peaking calculation, only the region-wise data will be displayed from SFEDIT and for

the hand calculation as it provides a direct comparison of all of the hand calculated data. Both sets of data were checked for accuracy.

```

MESH
...
[SFEDIT] (2D) Sample 1 of 11 of surface 3 of 7 center power density (w/cc) for axial mesh      3 of      5
[SFEDIT]...I ->      1          2          3
[SFEDIT]...J= 2      7.76281E+03  1.30881E+02  7.55080E+03
[SFEDIT]...J= 2      7.82715E+03  1.31599E+02  7.61015E+03
[SFEDIT]...J= 2      7.87719E+03  1.32157E+02  7.65630E+03
[SFEDIT]...J= 2      7.91294E+03  1.32555E+02  7.68927E+03
[SFEDIT]...J= 2      7.93438E+03  1.32794E+02  7.70905E+03
[SFEDIT]...J= 2      7.94153E+03  1.32874E+02  7.71564E+03
[SFEDIT]...J= 2      7.93438E+03  1.32794E+02  7.70905E+03
[SFEDIT]...J= 2      7.91294E+03  1.32555E+02  7.68927E+03
[SFEDIT]...J= 2      7.87719E+03  1.32157E+02  7.65630E+03
[SFEDIT]...J= 2      7.82715E+03  1.31599E+02  7.61015E+03
[SFEDIT]...J= 2      7.76281E+03  1.30881E+02  7.55080E+03
...
REGION
...
[SFEDIT] (5D) Cell and surface averaged power density (w/cc)
[SFEDIT]...|Region|Cell|Sample| Surface data ->
[SFEDIT]...| 2| 4| 1| 7.834005E+03  7.753136E+03  7.762812E+03  7.830694E+03  7.866391E+03  7.887170E+03  7.872459E+03
[SFEDIT]...| 2| 4| 2| 7.899061E+03  7.816551E+03  7.827151E+03  7.895922E+03  7.931956E+03  7.952953E+03  7.937923E+03
[SFEDIT]...| 2| 4| 3| 7.949660E+03  7.865874E+03  7.877192E+03  7.946654E+03  7.982951E+03  8.004117E+03  7.988839E+03
[SFEDIT]...| 2| 4| 4| 7.985802E+03  7.901104E+03  7.912936E+03  7.982892E+03  8.019376E+03  8.040663E+03  8.025208E+03
[SFEDIT]...| 2| 4| 5| 8.007487E+03  7.922242E+03  7.934382E+03  8.004635E+03  8.041231E+03  8.062591E+03  8.047030E+03
[SFEDIT]...| 2| 4| 6| 8.014716E+03  7.929288E+03  7.941531E+03  8.011882E+03  8.048516E+03  8.069900E+03  8.054304E+03
[SFEDIT]...| 2| 4| 7| 8.007487E+03  7.922242E+03  7.934382E+03  8.004635E+03  8.041231E+03  8.062591E+03  8.047030E+03
[SFEDIT]...| 2| 4| 8| 7.985802E+03  7.901104E+03  7.912936E+03  7.982892E+03  8.019376E+03  8.040663E+03  8.025208E+03
[SFEDIT]...| 2| 4| 9| 7.949660E+03  7.865874E+03  7.877192E+03  7.946654E+03  7.982951E+03  8.004117E+03  7.988839E+03
[SFEDIT]...| 2| 4| 10| 7.899061E+03  7.816551E+03  7.827151E+03  7.895922E+03  7.931956E+03  7.952953E+03  7.937923E+03
[SFEDIT]...| 2| 4| 11| 7.834005E+03  7.753136E+03  7.762812E+03  7.830694E+03  7.866391E+03  7.887170E+03  7.872459E+03
...

```

**Figure 3-109. SFEDIT Power Output Excerpt for COREA Verification in DIF3D-VARIANT**

```

MESH
...
[SFEDIT] (3D) Sample 1 of 11 of surface 4 of 7 center fast flux (n/cm^2/sec) for axial mesh      3 of      5
[SFEDIT]...I ->      1          2          3
[SFEDIT]...J= 2      3.02098E+17  2.87026E+17  2.77484E+17
[SFEDIT]...J= 2      3.05581E+17  2.90073E+17  2.80621E+17
[SFEDIT]...J= 2      3.08290E+17  2.92443E+17  2.83061E+17
[SFEDIT]...J= 2      3.10225E+17  2.94135E+17  2.84804E+17
[SFEDIT]...J= 2      3.11386E+17  2.95151E+17  2.85849E+17
[SFEDIT]...J= 2      3.11773E+17  2.95489E+17  2.86198E+17
[SFEDIT]...J= 2      3.11386E+17  2.95151E+17  2.85849E+17
[SFEDIT]...J= 2      3.10225E+17  2.94135E+17  2.84804E+17
[SFEDIT]...J= 2      3.08290E+17  2.92443E+17  2.83061E+17
[SFEDIT]...J= 2      3.05581E+17  2.90073E+17  2.80621E+17
[SFEDIT]...J= 2      3.02098E+17  2.87026E+17  2.77484E+17
...
REGION
...
[SFEDIT] (6D) Cell and surface averaged fast flux (n/cm^2/sec)
[SFEDIT]...|Region|Cell|Sample| Surface data ->
[SFEDIT]...| 2| 4| 1| 3.008242E+17  2.909345E+17  2.971696E+17  3.020977E+17  3.037786E+17  3.048695E+17  3.028753E+17
[SFEDIT]...| 2| 4| 2| 3.042926E+17  2.942896E+17  3.005959E+17  3.055808E+17  3.072810E+17  3.083844E+17  3.063672E+17
[SFEDIT]...| 2| 4| 3| 3.069903E+17  2.968991E+17  3.032608E+17  3.082898E+17  3.100052E+17  3.111183E+17  3.090832E+17
[SFEDIT]...| 2| 4| 4| 3.0389173E+17  2.987631E+17  3.051643E+17  3.102248E+17  3.119510E+17  3.130710E+17  3.110231E+17
[SFEDIT]...| 2| 4| 5| 3.100734E+17  2.998814E+17  3.063064E+17  3.113858E+17  3.131185E+17  3.142427E+17  3.121871E+17
[SFEDIT]...| 2| 4| 6| 3.104588E+17  3.002542E+17  3.066871E+17  3.117729E+17  3.135076E+17  3.146332E+17  3.125751E+17
[SFEDIT]...| 2| 4| 7| 3.100734E+17  2.998814E+17  3.063064E+17  3.113858E+17  3.131185E+17  3.142427E+17  3.121871E+17
[SFEDIT]...| 2| 4| 8| 3.089173E+17  2.987631E+17  3.051643E+17  3.102248E+17  3.119510E+17  3.130710E+17  3.110231E+17
[SFEDIT]...| 2| 4| 9| 3.069903E+17  2.968991E+17  3.032608E+17  3.082898E+17  3.100052E+17  3.111183E+17  3.090832E+17
[SFEDIT]...| 2| 4| 10| 3.042926E+17  2.942896E+17  3.005959E+17  3.055808E+17  3.072810E+17  3.083844E+17  3.063672E+17
[SFEDIT]...| 2| 4| 11| 3.008242E+17  2.909345E+17  2.971696E+17  3.020977E+17  3.037786E+17  3.048695E+17  3.028753E+17
...
```

**Figure 3-110. SFEDIT Fast Flux Output Excerpt for COREA Verification in DIF3D-VARIANT**

The next region to verify is COREB which occupies position 2 of ring 4. This hex is identified as (3,3,\*) and in the region-wise ordering it is 2 noting that there are only three meshes in region 2. The COREB flux data was extracted from the NHFLUX file and is assembled in Table 3-67. As was done for COREA, the calculation of these flux moments requires a complicated lookup process which was omitted here for brevity.

Using the flux moments in Table 3-67, the axial curve was constructed and the results for the volume and surface axial sample points of the power density are provided in Table 3-68. The fast flux volume and surface axial sample points were calculated and are provided in Table 3-69. Both peak values are highlighted in these tables for convenience. Comparison of the power and fast flux with those in COREA shows that this data is consistently lower which was also the case for the DIF3D-FD verification work.

**Table 3-67. COREB Node Volume and Surface Flux Moments**

|                  | Group 1    | Group 2    | Group 3    |
|------------------|------------|------------|------------|
| Average Flux     | 5.4269E+16 | 2.2108E+17 | 1.3446E+17 |
| Surface Fluxes   |            |            |            |
| 1                | 5.2477E+16 | 2.1849E+17 | 1.3435E+17 |
| 2                | 5.0422E+16 | 2.1601E+17 | 1.3485E+17 |
| 3                | 5.3435E+16 | 2.1958E+17 | 1.3382E+17 |
| 4                | 6.0094E+16 | 2.2689E+17 | 1.3205E+17 |
| 5                | 5.9318E+16 | 2.2815E+17 | 1.3550E+17 |
| 6                | 5.8157E+16 | 2.2514E+17 | 1.3327E+17 |
| 7                | 5.3246E+16 | 2.1670E+17 | 1.3392E+17 |
| 8                | 5.3246E+16 | 2.1670E+17 | 1.3392E+17 |
| Power Conversion | 1.8390E-15 | 1.5564E-15 | 2.2868E-15 |

**Table 3-68. COREB Power Evaluation at the Axial Sample Points**

| Axial Sample | Mesh Centered | x-y Surface |         |         |         |                |         |
|--------------|---------------|-------------|---------|---------|---------|----------------|---------|
|              |               | 1           | 2       | 3       | 4       | 5              | 6       |
| 1            | 741.435       | 733.988     | 727.658 | 736.180 | 755.321 | 763.703        | 751.917 |
| 2            | 746.793       | 739.269     | 732.862 | 741.495 | 760.874 | 769.279        | 757.410 |
| 3            | 750.961       | 743.377     | 736.910 | 745.629 | 765.192 | 773.616        | 761.682 |
| 4            | 753.938       | 746.311     | 739.801 | 748.582 | 768.277 | 776.713        | 764.734 |
| 5            | 755.725       | 748.071     | 741.536 | 750.353 | 770.128 | 778.572        | 766.565 |
| 6            | 756.320       | 748.658     | 742.114 | 750.944 | 770.745 | <b>779.192</b> | 767.176 |
| 7            | 755.725       | 748.071     | 741.536 | 750.353 | 770.128 | 778.572        | 766.565 |
| 8            | 753.938       | 746.311     | 739.801 | 748.582 | 768.277 | 776.713        | 764.734 |
| 9            | 750.961       | 743.377     | 736.910 | 745.629 | 765.192 | 773.616        | 761.682 |
| 10           | 746.793       | 739.269     | 732.862 | 741.495 | 760.874 | 769.279        | 757.410 |
| 11           | 741.435       | 733.988     | 727.658 | 736.180 | 755.321 | 763.703        | 751.917 |

The region-wise SFEDIT data excerpt for this axial mesh is provided in Figure 3-111 where the peaks within the mesh are highlighted. A close comparison of the SFEDIT results with the hand calculated results in Table 3-68 and Table 3-69 shows that every number matches within round-off error. All values peak at the center most axial sample (#6), similar to the COREA and COREB results, and surface 5 (ordered 6 in the SFEDIT data) has the overall peak of power and fast flux. For this hexagon, surface 5 is adjacent to the RREFL region which was also the case for the DIF3D-FD verification work

displayed earlier. Given the two sets of data match, there is nothing further to verify for the SFEDIT COREB results.

**Table 3-69. COREB Fast Flux Evaluation at the Axial Sample Points**

| Axial Sample | Mesh Centered | x-y Surface |            |            |            |                   |            |
|--------------|---------------|-------------|------------|------------|------------|-------------------|------------|
|              |               | 1           | 2          | 3          | 4          | 5                 | 6          |
| 1            | 2.6995E+17    | 2.6565E+17  | 2.6121E+17 | 2.6766E+17 | 2.8136E+17 | 2.8183E+17        | 2.7774E+17 |
| 2            | 2.7287E+17    | 2.6852E+17  | 2.6403E+17 | 2.7055E+17 | 2.8440E+17 | 2.8488E+17        | 2.8074E+17 |
| 3            | 2.7514E+17    | 2.7075E+17  | 2.6623E+17 | 2.7280E+17 | 2.8676E+17 | 2.8724E+17        | 2.8307E+17 |
| 4            | 2.7676E+17    | 2.7235E+17  | 2.6780E+17 | 2.7441E+17 | 2.8845E+17 | 2.8893E+17        | 2.8474E+17 |
| 5            | 2.7773E+17    | 2.7330E+17  | 2.6874E+17 | 2.7537E+17 | 2.8946E+17 | 2.8995E+17        | 2.8574E+17 |
| 6            | 2.7805E+17    | 2.7362E+17  | 2.6905E+17 | 2.7569E+17 | 2.8980E+17 | <b>2.9029E+17</b> | 2.8607E+17 |
| 7            | 2.7773E+17    | 2.7330E+17  | 2.6874E+17 | 2.7537E+17 | 2.8946E+17 | 2.8995E+17        | 2.8574E+17 |
| 8            | 2.7676E+17    | 2.7235E+17  | 2.6780E+17 | 2.7441E+17 | 2.8845E+17 | 2.8893E+17        | 2.8474E+17 |
| 9            | 2.7514E+17    | 2.7075E+17  | 2.6623E+17 | 2.7280E+17 | 2.8676E+17 | 2.8724E+17        | 2.8307E+17 |
| 10           | 2.7287E+17    | 2.6852E+17  | 2.6403E+17 | 2.7055E+17 | 2.8440E+17 | 2.8488E+17        | 2.8074E+17 |
| 11           | 3.0082E+17    | 2.9093E+17  | 2.9717E+17 | 3.0210E+17 | 3.0378E+17 | 3.0487E+17        | 3.0288E+17 |

```
[SFEDIT] (5D) Cell and surface averaged power density (w/cc)
[SFEDIT]...|Region|Cell|Sample| Surface data ->
[SFEDIT]...| 3| 2| 1| 7.414350E+02 7.339880E+02 7.276582E+02 7.361807E+02 7.553218E+02 7.637031E+02 7.519174E+02
[SFEDIT]...| 3| 2| 2| 7.467938E+02 7.392695E+02 7.328625E+02 7.414957E+02 7.608744E+02 7.692791E+02 7.574105E+02
[SFEDIT]...| 3| 2| 3| 7.509617E+02 7.433773E+02 7.369103E+02 7.456296E+02 7.651930E+02 7.736161E+02 7.616829E+02
[SFEDIT]...| 3| 2| 4| 7.539388E+02 7.463114E+02 7.398016E+02 7.485823E+02 7.682778E+02 7.767139E+02 7.647347E+02
[SFEDIT]...| 3| 2| 5| 7.557250E+02 7.480719E+02 7.415363E+02 7.503540E+02 7.701287E+02 7.785725E+02 7.665657E+02
[SFEDIT]...| 3| 2| 6| 7.563205E+02 7.486587E+02 7.421146E+02 7.509445E+02 7.707456E+02 7.791921E+02 7.671761E+02
[SFEDIT]...| 3| 2| 7| 7.557250E+02 7.480719E+02 7.415363E+02 7.503540E+02 7.701287E+02 7.785725E+02 7.665657E+02
[SFEDIT]...| 3| 2| 8| 7.539388E+02 7.463114E+02 7.398016E+02 7.485823E+02 7.682778E+02 7.767139E+02 7.647347E+02
[SFEDIT]...| 3| 2| 9| 7.509617E+02 7.433773E+02 7.369103E+02 7.456296E+02 7.651930E+02 7.736161E+02 7.616829E+02
[SFEDIT]...| 3| 2| 10| 7.467938E+02 7.392695E+02 7.328625E+02 7.414957E+02 7.608744E+02 7.692791E+02 7.574105E+02
[SFEDIT]...| 3| 2| 11| 7.414350E+02 7.339880E+02 7.276582E+02 7.361807E+02 7.553218E+02 7.637031E+02 7.519174E+02
...
[SFEDIT] (6D) Cell and surface averaged fast flux (n/cm^2/sec)
[SFEDIT]...|Region|Cell|Sample| Surface data ->
[SFEDIT]...| 3| 2| 1| 2.699506E+17 2.656478E+17 2.612065E+17 2.676586E+17 2.813566E+17 2.818316E+17 2.777374E+17
[SFEDIT]...| 3| 2| 2| 2.728679E+17 2.685190E+17 2.640304E+17 2.705513E+17 2.843952E+17 2.848758E+17 2.807376E+17
[SFEDIT]...| 3| 2| 3| 2.751368E+17 2.707522E+17 2.662267E+17 2.728011E+17 2.867586E+17 2.872435E+17 2.830710E+17
[SFEDIT]...| 3| 2| 4| 2.767575E+17 2.723473E+17 2.677955E+17 2.744081E+17 2.884467E+17 2.889347E+17 2.847377E+17
[SFEDIT]...| 3| 2| 5| 2.777299E+17 2.733044E+17 2.687368E+17 2.753723E+17 2.894596E+17 2.899494E+17 2.857378E+17
[SFEDIT]...| 3| 2| 6| 2.780540E+17 2.736234E+17 2.690505E+17 2.756938E+17 2.897972E+17 2.902877E+17 2.860711E+17
[SFEDIT]...| 3| 2| 7| 2.777299E+17 2.733044E+17 2.687368E+17 2.753723E+17 2.894596E+17 2.899494E+17 2.857378E+17
[SFEDIT]...| 3| 2| 8| 2.767575E+17 2.723473E+17 2.677955E+17 2.744081E+17 2.884467E+17 2.889347E+17 2.847377E+17
[SFEDIT]...| 3| 2| 9| 2.751368E+17 2.707522E+17 2.662267E+17 2.728011E+17 2.867586E+17 2.872435E+17 2.830710E+17
[SFEDIT]...| 3| 2| 10| 2.728679E+17 2.685190E+17 2.640304E+17 2.705513E+17 2.843952E+17 2.848758E+17 2.807376E+17
[SFEDIT]...| 3| 2| 11| 2.699506E+17 2.656478E+17 2.612065E+17 2.676586E+17 2.813566E+17 2.818316E+17 2.777374E+17
```

**Figure 3-111. SFEDIT Output Excerpt for COREB Verification in DIF3D-VARIANT**

The next region to verify is COREC which occupies positions 3, 5, and 6 of ring 2. From the PWDINT results shown previously the peak occurs in position 5 at axial plane 3. This hex is identified as (1,1,\*) and for the region-wise ordering it is mesh 5 noting that there are 9 total meshes in region 3. The COREC flux data was extracted from the NHFLUX file and is assembled in Table 3-70. As was done for COREA and COREB, the calculation of these flux moments requires a complicated lookup process which was omitted here for brevity.

Using the flux moments in Table 3-70, the axial curve was constructed and the volume and surface axial sample points for the power density are provided in Table 3-71. The fast flux volume and surface axial sample points were calculated and are provided in Table 3-72. The overall peak values are highlighted for convenience in both tables which occur on surface 5 near the reflected boundary condition. Comparison to those in COREA and COREB shows that these are consistently higher which

was also the case for the DIF3D-FD verification work noting that this is the assembly with the peak power in the entire domain.

**Table 3-70. COREC Node Volume and Surface Flux Moments**

|                  | Group 1    | Group 2    | Group 3    |
|------------------|------------|------------|------------|
| Average Flux     | 7.2521E+16 | 2.4407E+17 | 1.2884E+17 |
| Surface Fluxes   |            |            |            |
| 1                | 7.1444E+16 | 2.4202E+17 | 1.2929E+17 |
| 2                | 6.5292E+16 | 2.3447E+17 | 1.3369E+17 |
| 3                | 6.9325E+16 | 2.4002E+17 | 1.3046E+17 |
| 4                | 7.3807E+16 | 2.4620E+17 | 1.2802E+17 |
| 5                | 7.5398E+16 | 2.4858E+17 | 1.2736E+17 |
| 6                | 7.4862E+16 | 2.4745E+17 | 1.2754E+17 |
| 7                | 7.0987E+16 | 2.3883E+17 | 1.2806E+17 |
| 8                | 7.0987E+16 | 2.3883E+17 | 1.2806E+17 |
| Power Conversion | 1.8390E-15 | 1.5564E-15 | 2.2868E-15 |

**Table 3-71. COREC Power Evaluation at the Axial Sample Points**

| Axial Sample | Mesh Centered | x-y Surface |         |         |         |                |         |
|--------------|---------------|-------------|---------|---------|---------|----------------|---------|
|              |               | 1           | 2       | 3       | 4       | 5              | 6       |
| 1            | 795.086       | 791.058     | 778.475 | 786.852 | 798.779 | 803.792        | 801.491 |
| 2            | 801.976       | 797.892     | 785.075 | 793.614 | 805.729 | 810.813        | 808.482 |
| 3            | 807.335       | 803.207     | 790.209 | 798.873 | 811.134 | 816.273        | 813.919 |
| 4            | 811.163       | 807.004     | 793.877 | 802.630 | 814.994 | 820.174        | 817.802 |
| 5            | 813.460       | 809.281     | 796.077 | 804.884 | 817.311 | 822.514        | 820.133 |
| 6            | 814.225       | 810.041     | 796.810 | 805.635 | 818.083 | <b>823.294</b> | 820.909 |
| 7            | 813.460       | 809.281     | 796.077 | 804.884 | 817.311 | 822.514        | 820.133 |
| 8            | 811.163       | 807.004     | 793.877 | 802.630 | 814.994 | 820.174        | 817.802 |
| 9            | 807.335       | 803.207     | 790.209 | 798.873 | 811.134 | 816.273        | 813.919 |
| 10           | 801.976       | 797.892     | 785.075 | 793.614 | 805.729 | 810.813        | 808.482 |
| 11           | 795.086       | 791.058     | 778.475 | 786.852 | 798.779 | 803.792        | 801.491 |

The region-wise SFEDIT data for this axial mesh is provided in Figure 3-112 where the peaks on surface 5 are highlighted for convenience. A comparison of the SFEDIT results with the hand calculated results of Table 3-71 and Table 3-72 shows they match within round-off error. The peak is again at the center most axial sample (#6) and is on surface 5 (ordered 6 in the SFEDIT data). Given the two sets of data match, this concludes the work to be done on verifying the SFEDIT COREC results.

**Table 3-72. COREC Fast Flux Evaluation at the Axial Sample Points**

| Axial Sample | Mesh Centered | x-y Surface |            |            |            |                   |            |
|--------------|---------------|-------------|------------|------------|------------|-------------------|------------|
|              |               | 1           | 2          | 3          | 4          | 5                 | 6          |
| 1            | 3.0981E+17    | 3.0675E+17  | 2.9334E+17 | 3.0272E+17 | 3.1316E+17 | 3.1705E+17        | 3.1541E+17 |
| 2            | 3.1347E+17    | 3.1037E+17  | 2.9681E+17 | 3.0629E+17 | 3.1686E+17 | 3.2079E+17        | 3.1913E+17 |
| 3            | 3.1632E+17    | 3.1319E+17  | 2.9950E+17 | 3.0908E+17 | 3.1973E+17 | 3.2371E+17        | 3.2203E+17 |
| 4            | 3.1836E+17    | 3.1521E+17  | 3.0143E+17 | 3.1106E+17 | 3.2179E+17 | 3.2579E+17        | 3.2410E+17 |
| 5            | 3.1958E+17    | 3.1641E+17  | 3.0258E+17 | 3.1226E+17 | 3.2302E+17 | 3.2703E+17        | 3.2534E+17 |
| 6            | 3.1998E+17    | 3.1682E+17  | 3.0297E+17 | 3.1265E+17 | 3.2343E+17 | <b>3.2745E+17</b> | 3.2576E+17 |
| 7            | 3.1958E+17    | 3.1641E+17  | 3.0258E+17 | 3.1226E+17 | 3.2302E+17 | 3.2703E+17        | 3.2534E+17 |
| 8            | 3.1836E+17    | 3.1521E+17  | 3.0143E+17 | 3.1106E+17 | 3.2179E+17 | 3.2579E+17        | 3.2410E+17 |
| 9            | 3.1632E+17    | 3.1319E+17  | 2.9950E+17 | 3.0908E+17 | 3.1973E+17 | 3.2371E+17        | 3.2203E+17 |
| 10           | 3.1347E+17    | 3.1037E+17  | 2.9681E+17 | 3.0629E+17 | 3.1686E+17 | 3.2079E+17        | 3.1913E+17 |
| 11           | 3.0981E+17    | 3.0675E+17  | 2.9334E+17 | 3.0272E+17 | 3.1316E+17 | 3.1705E+17        | 3.1541E+17 |

```
[SFEDIT] (5D) Cell and surface averaged power density (w/cc)
[SFEDIT] ... |Region|Cell|Sample| Surface data ->
[SFEDIT] ... | 4| 5| 1| 7.950859E+02 7.910579E+02 7.784743E+02 7.868520E+02 7.987788E+02 8.037912E+02 8.014910E+02
[SFEDIT] ... | 4| 5| 2| 8.019759E+02 7.978915E+02 7.850751E+02 7.936137E+02 8.057281E+02 8.108122E+02 8.084815E+02
[SFEDIT] ... | 4| 5| 3| 8.073347E+02 8.032066E+02 7.902090E+02 7.988728E+02 8.111332E+02 8.162729E+02 8.139185E+02
[SFEDIT] ... | 4| 5| 4| 8.111625E+02 8.070031E+02 7.938761E+02 8.026293E+02 8.149939E+02 8.201734E+02 8.178020E+02
[SFEDIT] ... | 4| 5| 5| 8.134591E+02 8.092810E+02 7.960764E+02 8.048832E+02 8.173103E+02 8.225137E+02 8.201322E+02
[SFEDIT] ... | 4| 5| 6| 8.142247E+02 8.100403E+02 7.968098E+02 8.056345E+02 8.180825E+02 8.232938E+02 8.209089E+02
[SFEDIT] ... | 4| 5| 7| 8.134591E+02 8.092810E+02 7.960764E+02 8.048832E+02 8.173103E+02 8.225137E+02 8.201322E+02
[SFEDIT] ... | 4| 5| 8| 8.111625E+02 8.070031E+02 7.938761E+02 8.026293E+02 8.149939E+02 8.201734E+02 8.178020E+02
[SFEDIT] ... | 4| 5| 9| 8.073347E+02 8.032066E+02 7.902090E+02 7.988728E+02 8.111332E+02 8.162729E+02 8.139185E+02
[SFEDIT] ... | 4| 5| 10| 8.019759E+02 7.978915E+02 7.850751E+02 7.936137E+02 8.057281E+02 8.108122E+02 8.084815E+02
[SFEDIT] ... | 4| 5| 11| 7.950859E+02 7.910579E+02 7.784743E+02 7.868520E+02 7.987788E+02 8.037912E+02 8.014910E+02
...
[SFEDIT] (6D) Cell and surface averaged fast flux (n/cm^2/sec)
[SFEDIT] ... |Region|Cell|Sample| Surface data ->
[SFEDIT] ... | 4| 5| 1| 3.098145E+17 3.067502E+17 2.933395E+17 3.027182E+17 3.131556E+17 3.170467E+17 3.154073E+17
[SFEDIT] ... | 4| 5| 2| 3.134748E+17 3.103744E+17 2.968058E+17 3.062950E+17 3.168552E+17 3.207922E+17 3.191335E+17
[SFEDIT] ... | 4| 5| 3| 3.163217E+17 3.131932E+17 2.995018E+17 3.090769E+17 3.197328E+17 3.237054E+17 3.220317E+17
[SFEDIT] ... | 4| 5| 4| 3.183552E+17 3.152066E+17 3.014275E+17 3.110640E+17 3.217882E+17 3.257863E+17 3.241018E+17
[SFEDIT] ... | 4| 5| 5| 3.195753E+17 3.164146E+17 3.025829E+17 3.122562E+17 3.230214E+17 3.270348E+17 3.253438E+17
[SFEDIT] ... | 4| 5| 6| 3.199820E+17 3.168173E+17 3.029681E+17 3.126536E+17 3.234325E+17 3.274509E+17 3.257579E+17
[SFEDIT] ... | 4| 5| 7| 3.195753E+17 3.164146E+17 3.025829E+17 3.122562E+17 3.230214E+17 3.270348E+17 3.253438E+17
[SFEDIT] ... | 4| 5| 8| 3.183552E+17 3.152066E+17 3.014275E+17 3.110640E+17 3.217882E+17 3.257863E+17 3.241018E+17
[SFEDIT] ... | 4| 5| 9| 3.163217E+17 3.131932E+17 2.995018E+17 3.090769E+17 3.197328E+17 3.237054E+17 3.220317E+17
[SFEDIT] ... | 4| 5| 10| 3.134748E+17 3.103744E+17 2.968058E+17 3.062950E+17 3.168552E+17 3.207922E+17 3.191335E+17
[SFEDIT] ... | 4| 5| 11| 3.098145E+17 3.067502E+17 2.933395E+17 3.027182E+17 3.131556E+17 3.170467E+17 3.154073E+17
```

**Figure 3-112. SFEDIT Output Excerpt for COREC Verification in DIF3D-VARIANT**

The last region to verify is REFL which has a different location for the peak power and peak fast flux as identified in the DIF3D-FD analysis. The peak power occurs in the first plane in position 5 of ring 2, indexed as (1,1,1) in the PWDINT data, while the peak fast flux occurs in the third plane in the center assembly, indexed as (2,2,3). For the region-wise ordering (1,1,1) corresponds to mesh 6 while (2,2,3) corresponds to mesh 9 where there are 17 total meshes in this region (7+1+1+1+7). The REFL flux data was extracted from the NHFLUX file and is assembled in Table 3-73. As was done for the other regions, the calculation of these flux moments requires a complicated lookup process which was omitted here for brevity.

Using the flux moments in Table 3-73, the axial curve was constructed and the volume and surface axial sample points for the power density for (1,1,1) were calculated and are provided in Table 3-74. The fast flux volume and surface axial sample points for (2,2,3) were calculated and are provided in Table 3-75. The overall peak values are highlighted for convenience in both tables. The peak power occurs on the lower axial sample point on surface 3 while the peak fast flux occurs on axial sample 6

on surface 5 which is closest to the mesh with the peak fast flux in the domain. It is notable that the power peak occurs on a different surface than that observed for DIF3D-FD (was on surface 5).

**Table 3-73. REFL Node Volume and Surface Flux Moments**

|                  | Peak Fast Flux Mesh (2,2,3) |            |            | Peak Power Mesh (1,1,1) |            |            |
|------------------|-----------------------------|------------|------------|-------------------------|------------|------------|
|                  | Group 1                     | Group 2    | Group 3    | Group 1                 | Group 2    | Group 3    |
| Average Flux     | 6.2239E+16                  | 2.3127E+17 | 1.3500E+17 | 2.2988E+16              | 1.6058E+17 | 2.0983E+17 |
| Surface Fluxes   |                             |            |            |                         |            |            |
| 1                | 6.1603E+16                  | 2.3017E+17 | 1.3462E+17 | 2.2941E+16              | 1.6057E+17 | 2.0985E+17 |
| 2                | 5.9318E+16                  | 2.2815E+17 | 1.3550E+17 | 2.2866E+16              | 1.6066E+17 | 2.0982E+17 |
| 3                | 6.2167E+16                  | 2.3050E+17 | 1.3424E+17 | 2.2855E+16              | 1.6052E+17 | 2.0993E+17 |
| 4                | 6.4056E+16                  | 2.3309E+17 | 1.3403E+17 | 2.3012E+16              | 1.6056E+17 | 2.0982E+17 |
| 5                | 6.5292E+16                  | 2.3447E+17 | 1.3369E+17 | 2.3103E+16              | 1.6060E+17 | 2.0974E+17 |
| 6                | 6.4668E+16                  | 2.3348E+17 | 1.3368E+17 | 2.3066E+16              | 1.6059E+17 | 2.0978E+17 |
| 7                | 6.1018E+16                  | 2.2683E+17 | 1.3491E+17 | 1.6497E+16              | 1.5294E+17 | 2.2609E+17 |
| 8                | 6.1018E+16                  | 2.2683E+17 | 1.3491E+17 | 3.7575E+16              | 1.7426E+17 | 1.7676E+17 |
| Power Conversion | 2.0033E-16                  | 2.3977E-16 | 4.8430E-16 | 2.0033E-16              | 2.3977E-16 | 4.8430E-16 |

**Table 3-74. REFL Power Evaluation at the Axial Sample Points**

| Axial Sample | Mesh Centered | x-y Surface |         |                |         |         |         |
|--------------|---------------|-------------|---------|----------------|---------|---------|---------|
|              |               | 1           | 2       | 3              | 4       | 5       | 6       |
| 1            | 149.470       | 149.472     | 149.465 | <b>149.486</b> | 149.465 | 149.444 | 149.456 |
| 2            | 149.384       | 149.386     | 149.379 | 149.400        | 149.379 | 149.358 | 149.370 |
| 3            | 148.994       | 148.995     | 148.988 | 149.009        | 148.989 | 148.969 | 148.980 |
| 4            | 148.299       | 148.300     | 148.293 | 148.313        | 148.294 | 148.276 | 148.287 |
| 5            | 147.300       | 147.300     | 147.293 | 147.311        | 147.295 | 147.279 | 147.289 |
| 6            | 145.997       | 145.996     | 145.988 | 146.004        | 145.992 | 145.978 | 145.987 |
| 7            | 144.389       | 144.387     | 144.378 | 144.392        | 144.385 | 144.374 | 144.382 |
| 8            | 142.477       | 142.473     | 142.463 | 142.475        | 142.473 | 142.466 | 142.473 |
| 9            | 140.260       | 140.254     | 140.244 | 140.253        | 140.257 | 140.254 | 140.259 |
| 10           | 137.739       | 137.731     | 137.719 | 137.725        | 137.737 | 137.739 | 137.742 |
| 11           | 134.914       | 134.904     | 134.890 | 134.892        | 134.913 | 134.920 | 134.921 |

The region-wise SFEDIT data for this axial mesh is provided in Figure 3-113 where the peaks are highlighted for convenience. A comparison of the SFEDIT results with the hand calculated results of Table 3-74 and Table 3-75 shows they match within round-off error. The peaks are matched exactly and occur in the expected places. Given the two sets of data match, this concludes the work to be done on verifying the SFEDIT results for the REFL region.

With all power and fast flux peaks verified and displayed in each region, the SFEDIT output details are fully verified. As stated, these outputs from DIF3D are used by REBUS to compute the peak fast fluence and the peak burnup of a given path. The peak power and peak fast flux edits also appear in the regular DIF3D output which is displayed for the DIF3D-VARIANT calculation in Figure 3-114 and

highlighted for convenience. As can be seen, the peak powers of COREA, COREB, COREC, and REFL reported by DIF3D are 8069.9, 779.192, 823.294, and 149.495 W/cm<sup>3</sup>, respectively.

**Table 3-75. REFL Fast Flux Evaluation at the Axial Sample Points**

| Axial Sample | Mesh Centered | x-y Surface |            |            |            |            |            |
|--------------|---------------|-------------|------------|------------|------------|------------|------------|
|              |               | 1           | 2          | 3          | 4          | 5          | 6          |
| 1            | 2.8785E+17    | 2.8615E+17  | 2.8193E+17 | 2.8703E+17 | 2.9142E+17 | 2.9398E+17 | 2.9240E+17 |
| 2            | 2.9090E+17    | 2.8919E+17  | 2.8492E+17 | 2.9007E+17 | 2.9451E+17 | 2.9710E+17 | 2.9551E+17 |
| 3            | 2.9328E+17    | 2.9155E+17  | 2.8725E+17 | 2.9244E+17 | 2.9692E+17 | 2.9953E+17 | 2.9792E+17 |
| 4            | 2.9498E+17    | 2.9324E+17  | 2.8891E+17 | 2.9414E+17 | 2.9864E+17 | 3.0126E+17 | 2.9965E+17 |
| 5            | 2.9599E+17    | 2.9425E+17  | 2.8991E+17 | 2.9515E+17 | 2.9967E+17 | 3.0230E+17 | 3.0068E+17 |
| 6            | 2.9633E+17    | 2.9458E+17  | 2.9024E+17 | 2.9549E+17 | 3.0001E+17 | 3.0265E+17 | 3.0103E+17 |
| 7            | 2.9599E+17    | 2.9425E+17  | 2.8991E+17 | 2.9515E+17 | 2.9967E+17 | 3.0230E+17 | 3.0068E+17 |
| 8            | 2.9498E+17    | 2.9324E+17  | 2.8891E+17 | 2.9414E+17 | 2.9864E+17 | 3.0126E+17 | 2.9965E+17 |
| 9            | 2.9328E+17    | 2.9155E+17  | 2.8725E+17 | 2.9244E+17 | 2.9692E+17 | 2.9953E+17 | 2.9792E+17 |
| 10           | 2.9090E+17    | 2.8919E+17  | 2.8492E+17 | 2.9007E+17 | 2.9451E+17 | 2.9710E+17 | 2.9551E+17 |
| 11           | 2.8785E+17    | 2.8615E+17  | 2.8193E+17 | 2.8703E+17 | 2.9142E+17 | 2.9398E+17 | 2.9240E+17 |

```
[SFEDIT] (5D) Cell and surface averaged power density (w/cc)
[SFEDIT] ...|Region|Cell|Sample| Surface data ->
[SFEDIT] ...| 1| 5| 1| 1.494670E+02 1.494625E+02 1.494429E+02 1.494423E+02 1.494463E+02 1.494728E+02 1.494952E+02
[SFEDIT] ...| 1| 5| 2| 1.493741E+02 1.493699E+02 1.493499E+02 1.493493E+02 1.493534E+02 1.493800E+02 1.494026E+02
...
[SFEDIT] ...| 1| 6| 1| 1.494698E+02 1.494716E+02 1.494647E+02 1.494858E+02 1.494646E+02 1.494442E+02 1.494561E+02
[SFEDIT] ...| 1| 6| 2| 1.493840E+02 1.493857E+02 1.493790E+02 1.493999E+02 1.493787E+02 1.493584E+02 1.493702E+02
[SFEDIT] ...| 1| 6| 3| 1.489937E+02 1.489952E+02 1.489884E+02 1.490088E+02 1.489885E+02 1.489689E+02 1.489804E+02
[SFEDIT] ...| 1| 6| 4| 1.482991E+02 1.483000E+02 1.482930E+02 1.483125E+02 1.482940E+02 1.482757E+02 1.482867E+02
[SFEDIT] ...| 1| 6| 5| 1.473001E+02 1.473002E+02 1.472928E+02 1.473109E+02 1.472953E+02 1.472788E+02 1.472891E+02
[SFEDIT] ...| 1| 6| 6| 1.459967E+02 1.459958E+02 1.459878E+02 1.460042E+02 1.459922E+02 1.459782E+02 1.459875E+02
[SFEDIT] ...| 1| 6| 7| 1.443889E+02 1.443867E+02 1.443779E+02 1.443922E+02 1.443849E+02 1.443740E+02 1.443820E+02
[SFEDIT] ...| 1| 6| 8| 1.424768E+02 1.424729E+02 1.424731E+02 1.424750E+02 1.424733E+02 1.424660E+02 1.424725E+02
[SFEDIT] ...| 1| 6| 9| 1.402602E+02 1.402545E+02 1.402436E+02 1.402527E+02 1.402573E+02 1.402544E+02 1.402591E+02
[SFEDIT] ...| 1| 6| 10| 1.377393E+02 1.377314E+02 1.377191E+02 1.377251E+02 1.377371E+02 1.377391E+02 1.377418E+02
[SFEDIT] ...| 1| 6| 11| 1.349140E+02 1.349037E+02 1.348899E+02 1.348922E+02 1.349126E+02 1.349202E+02 1.349206E+02
...
[SFEDIT] (6D) Cell and surface averaged fast flux (n/cm2/sec)
[SFEDIT] ...|Region|Cell|Sample| Surface data ->
[SFEDIT] ...| 1| 9| 1| 2.878469E+17 2.861481E+17 2.819280E+17 2.870264E+17 2.914189E+17 2.939793E+17 2.924040E+17
[SFEDIT] ...| 1| 9| 2| 2.909022E+17 2.891853E+17 2.849201E+17 2.900730E+17 2.945124E+17 2.971001E+17 2.955081E+17
[SFEDIT] ...| 1| 9| 3| 2.932786E+17 2.915476E+17 2.872473E+17 2.924426E+17 2.969185E+17 2.995274E+17 2.979223E+17
[SFEDIT] ...| 1| 9| 4| 2.949760E+17 2.932350E+17 2.889096E+17 2.941352E+17 2.986373E+17 3.012612E+17 2.996468E+17
[SFEDIT] ...| 1| 9| 5| 2.959945E+17 2.942474E+17 2.899070E+17 2.951508E+17 2.996683E+17 3.023015E+17 3.006815E+17
[SFEDIT] ...| 1| 9| 6| 2.963340E+17 2.945849E+17 2.902395E+17 2.954893E+17 3.000120E+17 3.026482E+17 3.010264E+17
[SFEDIT] ...| 1| 9| 7| 2.959945E+17 2.942474E+17 2.899070E+17 2.951508E+17 2.996683E+17 3.023015E+17 3.006815E+17
[SFEDIT] ...| 1| 9| 8| 2.949760E+17 2.932350E+17 2.889096E+17 2.941352E+17 2.986373E+17 3.012612E+17 2.996468E+17
[SFEDIT] ...| 1| 9| 9| 2.932786E+17 2.915476E+17 2.872473E+17 2.924426E+17 2.969185E+17 2.995274E+17 2.979223E+17
[SFEDIT] ...| 1| 9| 10| 2.909022E+17 2.891853E+17 2.849201E+17 2.900730E+17 2.945124E+17 2.971001E+17 2.955081E+17
[SFEDIT] ...| 1| 9| 11| 2.878469E+17 2.861481E+17 2.819280E+17 2.870264E+17 2.914189E+17 2.939793E+17 2.924040E+17
```

**Figure 3-113. SFEDIT Output Excerpt for REFL Verification in DIF3D-VARIANT**

For the peak power, COREA was 8069.90 W/cm<sup>3</sup> in Table 3-65, COREB was 779.192 W/cm<sup>3</sup> in Table 3-68, COREC was 823.294 W/cm<sup>3</sup> in Table 3-71, and REFL was 149.486 in Table 3-74. Only the REFL result has a significant amount of error and it is due to the fact that the actual peak occurs in the adjacent assembly on its surface 6. The relevant lines from SFEDIT for this mesh were included in Figure 3-113 and the true peak highlighted. The EXCEL document was used to confirm that this peak power value was correct. This demonstrates that relying upon the peak value from the PWDINT data is not sufficient in determining the location of the peak in the domain noting that the algorithm in DIF3D properly selects the peak value for each region. From Figure 3-114, the peak fast flux values for COREA, COREB, COREC, and REFL are 3.14633E+17, 2.90288E+17, 3.27451E+17, and 3.02648E+17, respectively. For the fast flux, COREA was 3.1463E+17 in Table 3-66, COREB was

2.029E+17 in Table 3-69, COREC was 3.2745E+17 in Table 3-72, and REFL was 3.0265E+17 in Table 3-75. All of these values match the DIF3D reported results within round-off error.

```

DIF3D 11.3114 04/10/20      ADIF3D: Hexagonal 3D Test Problem      PAGE 42
0      REGION AND AREA POWER INTEGRALS FOR K-EFF PROBLEM WITH ENERGY RANGE (EV)      = (4.140E-01,1.000E+07)

REGION      ZONE      ZONE      VOLUME      INTEGRATION(1)      POWER      POWER DENSITY      PEAK DENSITY      PEAK TO AVG.      POWER
NO.      NAME      NO.      NAME      (CC)      WEIGHT FACTOR      (WATTS)      (WATTS/CC)      (WATTS/CC) (2)      POWER DENSITY      FRACTION
1      REFL      4      REFL      4.15692E+04      1.00000E+00      5.94409E+06      1.42993E+02      1.49495E+02      1.04548E+00      5.94409E-02
2      COREA      1      ZFUELA      1.03923E+04      1.00000E+00      7.83768E+07      7.54181E+03      8.06990E+03      1.07002E+00      7.83768E-01
3      COREB      2      ZFUELB      5.19615E+03      1.00000E+00      3.78099E+06      7.27651E+02      7.79192E+02      1.07083E+00      3.78099E-02
4      COREC      3      ZFUELC      1.55885E+04      1.00000E+00      1.18981E+07      7.63265E+02      8.23294E+02      1.07865E+00      1.18981E-01
TOTALS          7.27461E+04      0.00000E+00      1.00000E+08      1.37464E+03      8.06990E+03      5.87054E+00      1.00000E+00

AREA      AREA      VOLUME      INTEGRATION(1)      POWER      POWER DENSITY      PEAK DENSITY      PEAK TO AVG.      POWER
NO.      NAME      (CC)      WEIGHT FACTOR      (WATTS)      (WATTS/CC)      (WATTS/CC) (2)      POWER DENSITY      FRACTION
1      CORE      3.11769E+04      0.00000E+00      9.40559E+07      3.01684E+03      8.06990E+03      2.67495E+00      9.40559E-01

(1) INTEGRATION WEIGHT FACTOR = (2/B)*SIN(B*H)      H=UNEXTRAPOLATED HALF HEIGHT, B=BUCKLING COEFFICIENT
(2) THE PEAK POWER DENSITY IS CALCULATED BY THE SPECIAL NODAL PROCEDURE DOCUMENTED IN ANL 83-1

DIF3D 11.3114 04/10/20      ADIF3D: Hexagonal 3D Test Problem      PAGE 59
0      REGION AND AREA REAL FLUX INTEGRALS FOR K-EFF PROBLEM WITH ENERGY RANGE (EV)      = (4.140E-01,1.000E+07)

REGION      ZONE      ZONE      VOLUME      TOTAL FLUX      PEAK FLUX (1)      TOTAL FAST FLUX      PEAK FAST FLUX (1)
NO.      NAME      NO.      NAME      (CC)      (NEUTRON-CM/SEC)      (NEUTRON-CM2-SEC)      (NEUTRON-CM/SEC)      (NEUTRON-CM2-SEC)
1      REFL      4      REFL      4.15692E+04      1.64239E+22      4.36382E+17      8.04132E+21      3.02648E+17
2      COREA      1      ZFUELA      1.03923E+04      4.26443E+21      4.44684E+17      2.85907E+21      3.14633E+17
3      COREB      2      ZFUELB      5.19615E+03      2.04196E+21      4.26059E+17      1.31459E+21      2.90288E+17
4      COREC      3      ZFUELC      1.55885E+04      6.49110E+21      4.55198E+17      4.41361E+21      3.27451E+17
TOTALS          7.27461E+04      2.92214E+22      4.55198E+17      1.66286E+22      3.27451E+17

AREA      AREA      VOLUME      TOTAL FLUX      PEAK FLUX (1)      TOTAL FAST FLUX      PEAK FAST FLUX (1)
NO.      NAME      (CC)      (NEUTRON-CM/SEC)      (NEUTRON-CM2-SEC)      (NEUTRON-CM/SEC)      (NEUTRON-CM2-SEC)
1      CORE      3.11769E+04      1.27975E+22      4.55198E+17      8.58728E+21      3.27451E+17

```

**Figure 3-114. DIF3D Output Excerpt for SFEDIT Verification in DIF3D-VARIANT**

For completeness, an inspection of the real peak flux on this problem for DIF3D-VARIANT will be performed using the EvaluateFlux utility program. Because the peak should occur near the points where DIF3D is computing them to be, the potential sample points are significantly reduced. Figure 3-115 shows the sample point selections in each hexagon. Because most of the peaks occur at the reactor midpoint, results for all seven hexes at the core midplane are obtained which eliminates the consideration of the peak power in the REFL region. The same axial sample points that DIF3D-VARIANT uses are used in the EvaluateFlux calculations.

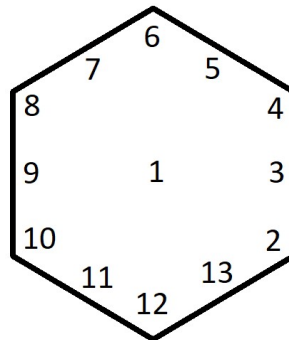


**Figure 3-115. EvaluateFlux.x X-Y Sample Points in Each Hexagon for DIF3D-VARIANT**

Starting with COREA, Figure 3-116 provides the power plot of all 13 EvaluateFlux.x curves for the assembly at position 4 of ring 2 along with the curves produced by the SFEDIT methodology. What should be clear is that the quadratic axial approximation is not bad as all of the curves have the same basic shape. In the figure, the two peak curves of either approach are given unique colors while all others of a given type are given a single color (i.e. all of the EF curves are black except for point 12 or EF(12) which is red). What should be apparent is that EF(12) is the largest magnitude for EvaluateFlux and SF(5) is the largest magnitude curve for the SFEDIT field and they have a significant

discrepancy. SF(5) is of course equivalent to EF(11), or the face centered quantity and EF(12) is on the corner point which should be the true peak location for this problem. This error in the peaking calculation is consistent with that found in the DIF3D verification report [14] and should come as no surprise.

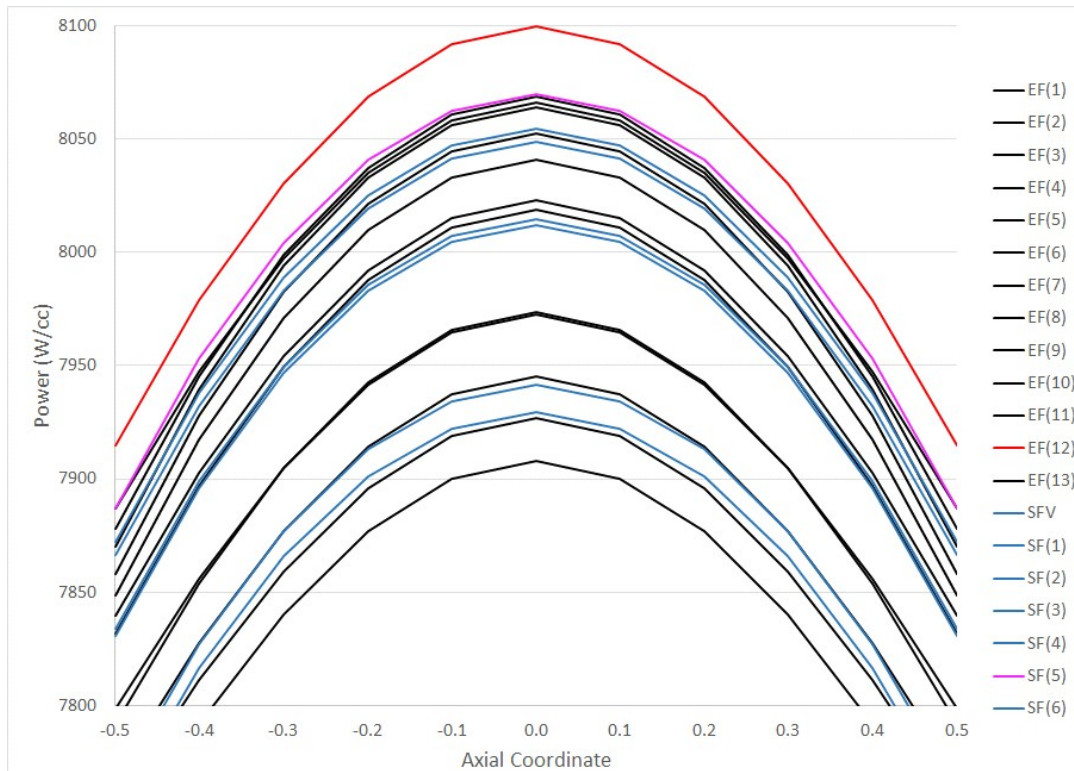


**Figure 3-116. EvaluateFlux.x Versus SFEDIT Methodology for COREA DIF3D-VARIANT**

Skipping COREB, the same data for COREC is plotted in Figure 3-117 using the same color scheme. Unlike the COREA result above, the COREC result from EvaluateFlux and SFEDIT are much closer where SFEDIT is only slightly lower than the EvaluateFlux result. It is also important to note that VARIANT can have a spatial discontinuity near the interface where the high order flux distribution is truncated to the low order boundary conditions and thus these 13 points will not always produce the maximum. This aspect cannot be captured when using the SFEDIT methodology as the currents on the interface will always preserve the average flux on the surface.

Plotting the RREFL and COREB results does not provide any additional information beyond that shown with COREA and COREC. It is important to note that for both the COREA and COREC result, the SFEDIT methodology does produce a result similar to the EvaluateFlux result near the center of the surface. While this is not guaranteed given a high order flux shape on the surface, it is good to see that the SFEDIT methodology does not produce inaccurate results.

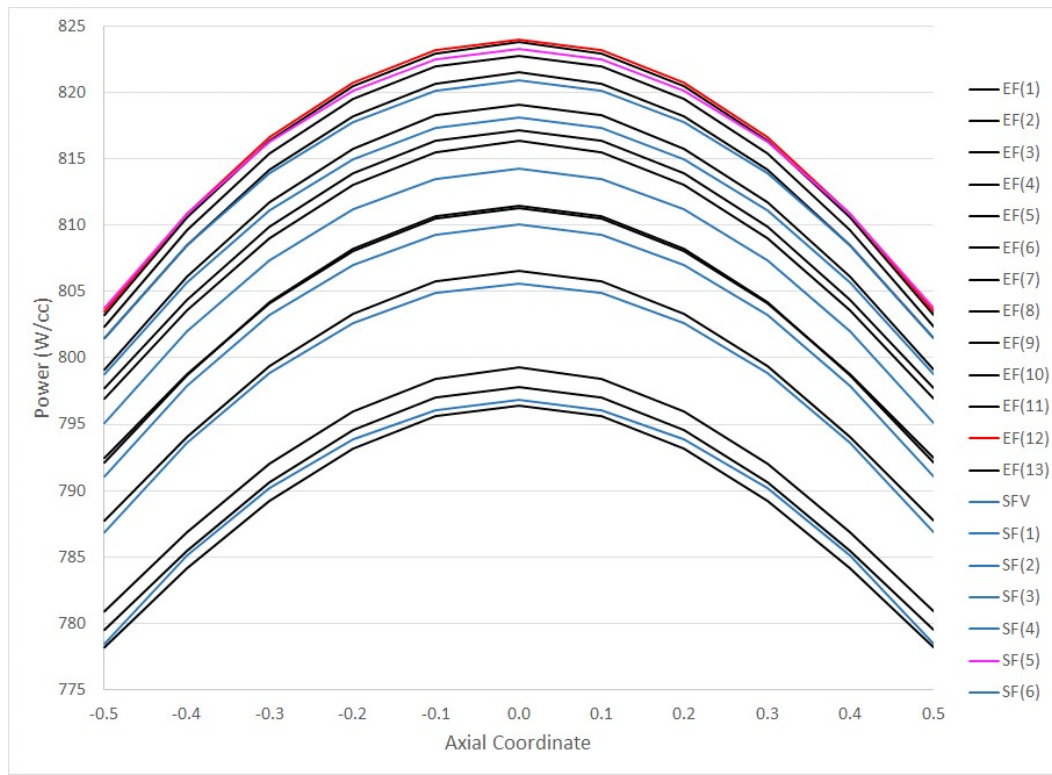


Figure 3-117. EvaluateFlux.x Versus SFEDIT Methodology for COREC DIF3D-VARIANT

### 3.7.1.6 REBUS Equilibrium Problem Used to Verify the SFEDIT Data

The preceding simple problem was only executed in DIF3D and demonstrates that the SFEDIT data is correct. Given the peak values reported by DIF3D-FD and DIF3D-VARIANT were already verified as part of the DIF3D verification [14], the focus of this section is to follow how the peaking factors are used by REBUS to compute the peak fast fluence and peak burnup output edits. The problem selected for this was shown earlier in Figure 3-79. From the set of problems associated with that section, the primary zone assignment equilibrium problem is chosen as the study case. The only change made is to alter the energy boundaries consistent with the other two problems in this section such that the fast flux is a simple sum of group 1 and 2. Only the DIF3D-VARIANT calculation is displayed in this section for brevity.

Because the SFEDIT file is not stored in the stated file format in REBUS (both mesh-wise and region-wise data are stored in the same file and the conventional file name is not used), a separate DIF3D execution will be used at each time point to provide the SFEDIT output details. In the regular output, the peak power density details along with the peak fast flux details from DIF3D should match between these calculations. Figure 3-118 provides the primary DIF3D output sections of interest for this work extracted from the REBUS output. Because the BOEC and EOEC calculations in a equilibrium problem make heavy use of restarted DIF3D calculations, one can see relatively few outer iterations required to obtain convergence. The excerpt of the BOEC recalculation using the binary interface files from REBUS is provided in Figure 3-119 while the EOEC excerpt is provided in Figure 3-120. Because the restart capability was not used, the number of outer iterations required to converge the problem is significantly larger than that observed in the equivalent REBUS calculation. The slight difference in

convergence leads to a slight difference in the answer which propagates to all of the power and fast flux tables in Figure 3-119 and Figure 3-120.

```

BOEC State
...
OUTER ITERATIONS COMPLETED AT ITERATION 5, ITERATIONS HAVE CONVERGED
K-EFFECTIVE = 0.78624930
DIF3D 11.3114 04/10/20 ADIF3D: Hexagonal 3D Test Problem PAGE 286
...
REGION ZONE ZONE VOLUME INTEGRATION(1) POWER POWER DENSITY PEAK DENSITY PEAK TO AVG. POWER
NO. NAME NO. NAME (CC) WEIGHT FACTOR (WATTS) (WATTS/CC) (WATTS/CC) (2) POWER DENSITY FRACTION
1 CENT 1 CENT 1.03923E+04 1.00000E+00 9.56589E-04 9.20478E-08 1.98111E-07 2.15226E+00 9.56589E-11
2 REFL 2 REFL 1.12237E+06 1.00000E+00 1.68982E-01 1.50559E-07 6.37210E-07 4.23231E+00 1.68982E-08
3 CORE1 3 CORE1 3.11769E+04 1.00000E+00 2.42161E+06 7.76731E+01 1.05394E+02 1.35689E+00 2.42161E-01
4 CORE2 4 CORE2 3.11769E+04 1.00000E+00 1.91287E+06 6.13553E+01 1.00580E+02 1.63930E+00 1.91287E-01
5 CORE3 5 CORE3 3.11769E+04 1.00000E+00 2.09740E+06 6.72741E+01 1.03192E+02 1.53391E+00 2.09740E-01
6 CORE4 6 CORE4 3.11769E+04 1.00000E+00 1.00186E+06 3.21346E+01 6.54412E+01 2.03647E+00 1.00186E-01
7 CORE5 7 CORE5 3.11769E+04 1.00000E+00 1.28314E+06 4.11566E+01 7.82446E+01 1.90114E+00 1.28314E-01
8 CORE6 8 CORE6 3.11769E+04 1.00000E+00 1.28314E+06 4.11566E+01 7.82446E+01 1.90114E+00 1.28314E-01
TOTALS 1.31982E+06 0.00000E+00 1.00000E+07 7.57678E+00 1.05394E+02 1.39101E+01 1.00000E+00
...
DIF3D 11.3114 04/10/20 ADIF3D: Hexagonal 3D Test Problem PAGE 289
0 REGION AND AREA REAL FLUX INTEGRALS FOR K-EFF PROBLEM WITH ENERGY RANGE (EV) =(4.140E-01,1.000E+07)
...
REGION ZONE ZONE VOLUME TOTAL FLUX PEAK FLUX (1) TOTAL FAST FLUX PEAK FAST FLUX(1)
NO. NAME NO. NAME (CC) (NEUTRON-CM/SEC) (NEUTRON-CM2-SEC) (NEUTRON-CM/SEC) (NEUTRON-CM2-SEC)
1 CENT 1 CENT 1.03923E+04 3.32862E+19 7.02238E+15 2.42256E+19 5.20209E+15
2 REFL 2 REFL 1.12237E+06 5.42104E+20 2.10491E+15 3.69769E+20 1.49930E+15
3 CORE1 3 CORE1 3.11769E+04 1.64721E+20 7.17228E+15 1.23415E+20 5.38152E+15
4 CORE2 4 CORE2 3.11769E+04 1.24155E+20 6.53726E+15 9.33538E+19 4.94218E+15
5 CORE3 5 CORE3 3.11769E+04 1.38482E+20 6.82003E+15 1.04221E+20 5.15173E+15
6 CORE4 6 CORE4 3.11769E+04 5.98154E+19 3.93066E+15 4.38648E+19 2.95590E+15
7 CORE5 7 CORE5 3.11769E+04 7.85907E+19 4.81259E+15 5.82819E+19 3.63010E+15
8 CORE6 8 CORE6 3.11769E+04 7.85907E+19 4.81259E+15 5.82819E+19 3.63010E+15
TOTALS 1.31982E+06 1.21974E+21 7.17228E+15 8.75414E+20 5.38152E+15
...
BOEC State
...
OUTER ITERATIONS COMPLETED AT ITERATION 3, ITERATIONS HAVE CONVERGED
K-EFFECTIVE = 0.78921715
DIF3D 11.3114 04/10/20 ADIF3D: Hexagonal 3D Test Problem PAGE 349
...
REGION ZONE ZONE VOLUME INTEGRATION(1) POWER POWER DENSITY PEAK DENSITY PEAK TO AVG. POWER
NO. NAME NO. NAME (CC) WEIGHT FACTOR (WATTS) (WATTS/CC) (WATTS/CC) (2) POWER DENSITY FRACTION
1 CENT 1 CENT 1.03923E+04 1.01453E-03 9.76231E-08 2.10127E-07 2.15243E+00 1.01453E-10
2 REFL 2 REFL 1.12237E+06 1.00000E+00 1.79444E-01 1.59880E-07 6.76123E-07 4.22895E+00 1.79444E-08
3 CORE1 3 CORE1 3.11769E+04 1.00000E+00 2.36518E+06 7.58630E+01 1.02953E+02 1.35709E+00 2.36518E-01
4 CORE2 4 CORE2 3.11769E+04 1.00000E+00 1.90754E+06 6.11843E+01 1.00325E+02 1.63972E+00 1.90754E-01
5 CORE3 5 CORE3 3.11769E+04 1.00000E+00 2.07636E+06 6.65994E+01 1.02181E+02 1.53426E+00 2.07636E-01
6 CORE4 6 CORE4 3.11769E+04 1.00000E+00 1.03211E+06 3.31050E+01 6.74332E+01 2.03695E+00 1.03211E-01
7 CORE5 7 CORE5 3.11769E+04 1.00000E+00 1.30941E+06 4.19992E+01 7.98671E+01 1.90163E+00 1.30941E-01
8 CORE6 8 CORE6 3.11769E+04 1.00000E+00 1.30941E+06 4.19992E+01 7.98671E+01 1.90163E+00 1.30941E-01
TOTALS 1.31982E+06 0.00000E+00 1.00000E+07 7.57678E+00 1.02953E+02 1.35879E+01 1.00000E+00
...
DIF3D 11.3114 04/10/20 ADIF3D: Hexagonal 3D Test Problem PAGE 352
0 REGION AND AREA REAL FLUX INTEGRALS FOR K-EFF PROBLEM WITH ENERGY RANGE (EV) =(4.140E-01,1.000E+07)
...
REGION ZONE ZONE VOLUME TOTAL FLUX PEAK FLUX (1) TOTAL FAST FLUX PEAK FAST FLUX(1)
NO. NAME NO. NAME (CC) (NEUTRON-CM/SEC) (NEUTRON-CM2-SEC) (NEUTRON-CM/SEC) (NEUTRON-CM2-SEC)
1 CENT 1 CENT 1.03923E+04 3.53956E+19 7.46907E+15 2.58236E+19 5.54679E+15
2 REFL 2 REFL 1.12237E+06 5.76143E+20 2.23658E+15 3.93569E+20 1.59674E+15
3 CORE1 3 CORE1 3.11769E+04 1.75187E+20 7.62921E+15 1.31578E+20 5.73857E+15
4 CORE2 4 CORE2 3.11769E+04 1.32019E+20 6.95352E+15 9.94702E+19 5.26884E+15
5 CORE3 5 CORE3 3.11769E+04 1.47266E+20 7.25454E+15 1.11073E+20 5.49284E+15
6 CORE4 6 CORE4 3.11769E+04 6.35782E+19 4.17913E+15 4.66966E+19 3.14822E+15
7 CORE5 7 CORE5 3.11769E+04 8.35468E+19 5.11766E+15 6.20641E+19 3.86764E+15

```

Figure 3-118. REBUS Output Excerpt of DIF3D for the Equilibrium Problem

This issue is not a concern for the verification as the total error in both the power density and fast flux results between the three figures is small for every region. Looking at the BOEC peak power density in CORE1, in Figure 3-118 it is 1.05394E+02 which identically matches the peak power density for this region in Figure 3-119. Similarly, the peak fast fluence for this region is 5.38152E+15 which identically matches the result in Figure 3-120. Both of these values should be findable in the SFEDIT output excerpts.

Figure 3-121 provides the SFEDIT excerpts of the region-wise data. The values from Figure 3-119 and Figure 3-120 are highlighted in Figure 3-121. Note that the region ordering is identical between all three figures as the region order is defined by the user's DIF3D input. For the CENT region, it should be clear that all six surfaces have the same peak value because of the symmetry of the problem and

that the peak occurs at the center of the domain. The remaining regions have different locations of the peak also consistent with the flux shape in the problem. For the peak fast flux, the same peak value can occur on two adjacent regions as is the case for regions CORE5 and CORE6. Because of symmetry, the peak values also occur multiple times in the domain and the region/surface chosen in Figure 3-121 are just one of the cases.

```
...
    OUTER ITERATIONS COMPLETED AT ITERATION 17, ITERATIONS HAVE CONVERGED
    K-EFFECTIVE = 0.78624930
DIF3D 11.3114 04/10/20          ADIF3D: Hexagonal 3D Test Problem          PAGE 27
...
0          REGION AND AREA POWER INTEGRALS FOR K-EFF PROBLEM WITH ENERGY RANGE (EV)      =(4.140E-01,1.000E+07)
0
    REGION   ZONE   ZONE   VOLUME   INTEGRATION(1)   POWER   POWER DENSITY   PEAK DENSITY   PEAK TO AVG.   POWER
    NO.     NAME   NO.     NAME   (CC)     WEIGHT FACTOR   (WATTS)   (WATTS/CC)   (WATTS/CC) (2)   POWER DENSITY   FRACTION
1 CENT     1 CENT     1.03923E+04 1.00000E+00 9.56591E-04 9.20480E-08 1.98111E-07 2.15226E+00 9.56591E-11
2 REFL     2 REFL     1.12237E+06 1.00000E+00 1.68982E-01 1.50559E-07 6.37210E-07 4.23231E+00 1.68982E-08
3 CORE1    3 CORE1    3.11769E+04 1.00000E+00 2.42161E+06 7.76731E+01 1.05394E+02 1.35689E+00 2.42161E-01
4 CORE2    4 CORE2    3.11769E+04 1.00000E+00 1.91287E+06 6.13553E+01 1.00580E+02 1.63930E+00 1.91287E-01
5 CORE3    5 CORE3    3.11769E+04 1.00000E+00 2.09740E+06 6.72741E+01 1.03192E+02 1.53391E+00 2.09740E-01
6 CORE4    6 CORE4    3.11769E+04 1.00000E+00 1.00186E+06 3.21346E+01 6.54412E+01 2.03647E+00 1.00186E-01
7 CORE5    7 CORE5    3.11769E+04 1.00000E+00 1.28314E+06 4.11566E+01 7.82446E+01 1.90114E+00 1.28314E-01
8 CORE6    8 CORE6    3.11769E+04 1.00000E+00 1.28314E+06 4.11566E+01 7.82446E+01 1.90114E+00 1.28314E-01
TOTALS          1.31982E+06 0.00000E+00 1.00000E+07 7.57678E+00 1.05394E+02 1.39101E+01 1.00000E+00
...
    REGION   ZONE   ZONE   VOLUME   TOTAL FLUX   PEAK FLUX (1)   TOTAL FAST FLUX PEAK FAST FLUX(1)
    NO.     NAME   NO.     NAME   (CC)     (NEUTRON-CM/SEC) (NEUTRON/CM2-SEC) (NEUTRON-CM/SEC) (NEUTRON/CM2-SEC)
1 CENT     1 CENT     1.03923E+04 3.32863E+19 7.02239E+15 2.42256E+19 5.20209E+15
2 REFL     2 REFL     1.12237E+06 5.42104E+20 2.10491E+15 3.69769E+20 1.49930E+15
3 CORE1    3 CORE1    3.11769E+04 1.64721E+20 7.17228E+15 1.23415E+20 5.38152E+15
4 CORE2    4 CORE2    3.11769E+04 1.24155E+20 6.53726E+15 9.33538E+19 4.94218E+15
5 CORE3    5 CORE3    3.11769E+04 1.38482E+20 6.82003E+15 1.04221E+20 5.15173E+15
6 CORE4    6 CORE4    3.11769E+04 5.98154E+19 3.93067E+15 4.38648E+19 2.95590E+15
7 CORE5    7 CORE5    3.11769E+04 7.85907E+19 4.81259E+15 5.82819E+19 3.63010E+15
8 CORE6    8 CORE6    3.11769E+04 7.85907E+19 4.81259E+15 5.82819E+19 3.63010E+15
TOTALS          1.31982E+06 1.21974E+21 7.17228E+15 8.75414E+20 5.38152E+15
...
```

Figure 3-119. BOEC DIF3D Output Excerpt for the Equilibrium Problem

```
...
    OUTER ITERATIONS COMPLETED AT ITERATION 17, ITERATIONS HAVE CONVERGED
    K-EFFECTIVE = 0.78921715
DIF3D 11.3114 04/10/20          ADIF3D: Hexagonal 3D Test Problem          PAGE 27
...
0          REGION AND AREA POWER INTEGRALS FOR K-EFF PROBLEM WITH ENERGY RANGE (EV)      =(4.140E-01,1.000E+07)
0
    REGION   ZONE   ZONE   VOLUME   INTEGRATION(1)   POWER   POWER DENSITY   PEAK DENSITY   PEAK TO AVG.   POWER
    NO.     NAME   NO.     NAME   (CC)     WEIGHT FACTOR   (WATTS)   (WATTS/CC)   (WATTS/CC) (2)   POWER DENSITY   FRACTION
1 CENT     1 CENT     1.03923E+04 1.01453E-03 9.76233E-08 2.10127E-07 2.15243E+00 1.01453E-10
2 REFL     2 REFL     1.12237E+06 1.00000E+00 1.79444E-01 1.59880E-07 6.76123E-07 4.22894E+00 1.79444E-08
3 CORE1    3 CORE1    3.11769E+04 1.00000E+00 2.36518E+06 7.58630E+01 1.02953E+02 1.35709E+00 2.36518E-01
4 CORE2    4 CORE2    3.11769E+04 1.00000E+00 1.90754E+06 6.11843E+01 1.00325E+02 1.63972E+00 1.90754E-01
5 CORE3    5 CORE3    3.11769E+04 1.00000E+00 2.07636E+06 6.65994E+01 1.02181E+02 1.53426E+00 2.07636E-01
6 CORE4    6 CORE4    3.11769E+04 1.00000E+00 1.03211E+06 3.31050E+01 6.74332E+01 2.03695E+00 1.03211E-01
7 CORE5    7 CORE5    3.11769E+04 1.00000E+00 1.30941E+06 4.19992E+01 7.98671E+01 1.90163E+00 1.30941E-01
8 CORE6    8 CORE6    3.11769E+04 1.00000E+00 1.30941E+06 4.19992E+01 7.98671E+01 1.90163E+00 1.30941E-01
TOTALS          1.31982E+06 0.00000E+00 1.00000E+07 7.57678E+00 1.02953E+02 1.35879E+01 1.00000E+00
...
    REGION   ZONE   ZONE   VOLUME   TOTAL FLUX   PEAK FLUX (1)   TOTAL FAST FLUX PEAK FAST FLUX(1)
    NO.     NAME   NO.     NAME   (CC)     (NEUTRON-CM/SEC) (NEUTRON/CM2-SEC) (NEUTRON-CM/SEC) (NEUTRON/CM2-SEC)
1 CENT     1 CENT     1.03923E+04 3.53957E+19 7.46908E+15 2.58236E+19 5.54679E+15
2 REFL     2 REFL     1.12237E+06 5.76143E+20 2.23658E+15 3.93569E+20 1.59674E+15
3 CORE1    3 CORE1    3.11769E+04 1.75187E+20 7.62921E+15 1.31578E+20 5.73857E+15
4 CORE2    4 CORE2    3.11769E+04 1.32019E+20 6.95352E+15 9.94702E+19 5.26884E+15
5 CORE3    5 CORE3    3.11769E+04 1.47266E+20 7.25454E+15 1.11073E+20 5.49284E+15
6 CORE4    6 CORE4    3.11769E+04 6.35782E+19 4.17913E+15 4.66966E+19 3.14822E+15
7 CORE5    7 CORE5    3.11769E+04 8.35468E+19 5.11766E+15 6.20641E+19 3.86764E+15
8 CORE6    8 CORE6    3.11769E+04 8.35468E+19 5.11766E+15 6.20641E+19 3.86764E+15
TOTALS          1.31982E+06 1.29668E+21 7.62921E+15 9.32339E+20 5.73857E+15
...
```

Figure 3-120. EOEC DIF3D Output Excerpt for the Equilibrium Problem

Given the calculation of the peak values were verified in the previous section, and the display of the peak values in this section show that these peak values are similarly obtained, the next step is to understand how REBUS uses these values to compute the peak burnup and peak fast fluence.

This problem is simple and has all CORE regions lumped into a single PATH. REBUS still treats each region separately in the depletion scheme (i.e. 6 regions that all have X stages of burnup), such that

there are six possible discharge burnup values and six possible peak fast fluence values. The REBUS output excerpt is taken from the cumulative edits section of the REBUS output and provided in Figure 3-122. The average burnup of each stage of each path/region was also provided for clarity on how the peak discharge burnup is calculated.

```
BOEC State
...
[SFEDIT] (5D) Cell and surface averaged power density (w/cc)
[SFEDIT] ...|Region|Cell|Sample| Surface data ->
[SFEDIT] ...| 1| 3| 6| 1.975075E-07 1.981113E-07 1.981113E-07 1.981113E-07 1.981113E-07
[SFEDIT] ...| 2| 1| 11| 5.800157E-07 5.254212E-07 5.468563E-07 5.993097E-07 6.372103E-07 5.993097E-07 5.468563E-07
[SFEDIT] ...| 3| 8| 6| 1.035951E+02 1.001332E+02 9.598595E+01 1.001332E+02 1.053936E+02 1.038424E+02 1.053936E+02
[SFEDIT] ...| 4| 9| 6| 8.184731E+01 9.042616E+01 7.002093E+01 6.076111E+01 7.002093E+01 9.042616E+01 1.005798E+02
[SFEDIT] ...| 5| 9| 6| 9.000039E+01 1.031924E+02 8.893244E+01 7.301186E+01 8.893244E+01 1.031924E+02
[SFEDIT] ...| 6| 8| 6| 4.101834E+01 2.740430E+01 2.257074E+01 2.740430E+01 4.967311E+01 6.544121E+01 4.967311E+01
[SFEDIT] ...| 7| 11| 6| 5.353786E+01 5.498198E+01 7.824463E+01 7.379976E+01 4.860986E+01 2.912202E+01 3.100222E+01
[SFEDIT] ...| 8| 8| 6| 5.353786E+01 5.498198E+01 3.100222E+01 2.912202E+01 4.860986E+01 7.379976E+01 7.824463E+01
...
[SFEDIT] (6D) Cell and surface averaged fast flux (n/cm^2/sec)
[SFEDIT] ...|Region|Cell|Sample| Surface data ->
[SFEDIT] ...| 1| 3| 6| 5.167342E+15 5.202092E+15 5.202092E+15 5.202092E+15 5.202092E+15 5.202092E+15
[SFEDIT] ...| 2| 1| 11| 1.358363E+15 1.224939E+15 1.277308E+15 1.405478E+15 1.499295E+15 1.405478E+15 1.277308E+15
[SFEDIT] ...| 3| 10| 6| 5.306296E+15 5.220645E+15 5.381516E+15 5.155782E+15 4.947210E+15 5.155782E+15 5.381516E+15
[SFEDIT] ...| 4| 9| 6| 4.015869E+15 4.441969E+15 3.426791E+15 2.964339E+15 3.426791E+15 4.441969E+15 4.942185E+15
[SFEDIT] ...| 5| 9| 6| 4.494756E+15 5.151731E+15 4.442991E+15 3.637197E+15 4.442991E+15 5.151731E+15
[SFEDIT] ...| 6| 8| 6| 1.812591E+15 1.165311E+15 9.429161E+14 1.165311E+15 2.216662E+15 2.955904E+15 2.216662E+15
[SFEDIT] ...| 7| 11| 6| 2.450742E+15 2.518509E+15 3.630096E+15 3.420887E+15 2.219158E+15 1.272793E+15 1.359392E+15
[SFEDIT] ...| 8| 8| 6| 2.450742E+15 2.518509E+15 1.359392E+15 1.272793E+15 2.219158E+15 3.420887E+15 3.630096E+15
...
EOEC State
...
[SFEDIT] (5D) Cell and surface averaged power density (w/cc)
[SFEDIT] ...|Region|Cell|Sample| Surface data ->
[SFEDIT] ...| 1| 3| 6| 2.094890E-07 2.101273E-07 2.101273E-07 2.101273E-07 2.101273E-07 2.101273E-07
[SFEDIT] ...| 2| 1| 11| 6.151448E-07 5.574891E-07 5.802286E-07 6.358890E-07 6.761227E-07 6.358890E-07 5.802286E-07
[SFEDIT] ...| 3| 8| 6| 1.011971E+02 9.781754E+01 9.376470E+01 9.781754E+01 1.029528E+02 1.014288E+02 1.029528E+02
[SFEDIT] ...| 4| 9| 6| 8.163225E+01 9.019315E+01 6.983018E+01 6.058913E+01 6.983018E+01 9.019315E+01 1.003253E+02
[SFEDIT] ...| 5| 9| 6| 8.911248E+01 1.021806E+02 8.805499E+01 7.228190E+01 8.805499E+01 1.021806E+02
[SFEDIT] ...| 6| 8| 6| 4.226156E+01 2.822884E+01 2.324956E+01 2.822884E+01 5.118169E+01 6.743319E+01 5.118169E+01
[SFEDIT] ...| 7| 11| 6| 5.464119E+01 5.611495E+01 7.986707E+01 7.532889E+01 4.960844E+01 2.971159E+01 3.163020E+01
[SFEDIT] ...| 8| 8| 6| 5.464119E+01 5.611495E+01 3.163020E+01 2.971159E+01 4.960844E+01 7.532889E+01 7.986707E+01
...
[SFEDIT] (6D) Cell and surface averaged fast flux (n/cm^2/sec)
[SFEDIT] ...|Region|Cell|Sample| Surface data ->
[SFEDIT] ...| 1| 3| 6| 5.509736E+15 5.546792E+15 5.546792E+15 5.546792E+15 5.546792E+15 5.546792E+15
[SFEDIT] ...| 2| 1| 11| 1.446405E+15 1.304161E+15 1.359980E+15 1.496646E+15 1.596736E+15 1.496646E+15 1.359980E+15
[SFEDIT] ...| 3| 10| 6| 5.658149E+15 5.566617E+15 5.738572E+15 5.497179E+15 5.274221E+15 5.497179E+15 5.738572E+15
[SFEDIT] ...| 4| 9| 6| 4.279633E+15 4.734536E+15 3.650731E+15 3.157228E+15 3.650731E+15 4.734536E+15 5.268844E+15
[SFEDIT] ...| 5| 9| 6| 4.791013E+15 5.492843E+15 4.735629E+15 3.875234E+15 3.875234E+15 4.735629E+15 5.492843E+15
[SFEDIT] ...| 6| 8| 6| 1.929788E+15 1.240230E+15 1.003461E+15 1.240230E+15 2.360348E+15 3.148216E+15 2.360348E+15
[SFEDIT] ...| 7| 11| 6| 2.610102E+15 2.682297E+15 3.867643E+15 3.644420E+15 2.363014E+15 1.354670E+15 1.446930E+15
[SFEDIT] ...| 8| 8| 6| 2.610102E+15 2.682297E+15 1.446930E+15 1.354670E+15 2.363014E+15 3.644420E+15 3.867643E+15

```

Figure 3-121. DIF3D SFEDIT Output Excerpts for the Equilibrium Problem

```
AVERAGE BURNUP (MWD/MT) OF EACH STAGE OF EACH PATH
...
STAGE/REGION 1/CORE1 2/CORE1 3/CORE1 4/CORE1 5/CORE1 6/CORE1 5.546792E+15
9.68035E+03 1.94709E+04 2.93468E+04 3.92861E+04 4.92694E+04 5.92796E+04
STAGE/REGION 1/CORE2 2/CORE2 3/CORE2 4/CORE2 5/CORE2 6/CORE2 5.546792E+15
7.29536E+03 1.46551E+04 2.20683E+04 2.95250E+04 3.70161E+04 4.45332E+04
STAGE/REGION 1/CORE3 2/CORE3 3/CORE3 4/CORE3 5/CORE3 6/CORE3 5.546792E+15
8.14351E+03 1.636494E+04 2.46493E+04 3.29833E+04 4.13548E+04 4.97529E+04
STAGE/REGION 1/CORE4 2/CORE4 3/CORE4 4/CORE4 5/CORE4 6/CORE4 5.546792E+15
3.48124E+03 6.98204E+03 1.05009E+04 1.40365E+04 1.75874E+04 2.11524E+04
STAGE/REGION 1/CORE5 2/CORE5 3/CORE5 4/CORE5 5/CORE5 6/CORE5 5.546792E+15
4.59545E+03 9.22139E+03 1.38747E+04 1.85524E+04 2.32519E+04 2.79704E+04
STAGE/REGION 1/CORE6 2/CORE6 3/CORE6 4/CORE6 5/CORE6 6/CORE6 5.546792E+15
4.59545E+03 9.22139E+03 1.38747E+04 1.85524E+04 2.32519E+04 2.79704E+04
FCC004 11.3114 04/10/20 ABURN: Hexagonal 3D Test Problem PAGE 373
...
CUMULATIVE PEAK BURNUP AND FAST FLUENCE AFTER 1 BURNUP SUBSTEPS, FROM 0.000000000E+00 DAYS TO 1.000000000E+02 DAYS.
...
PEAK DISCHARGE BURNUP (MWD/MT) OF EACH PATH
PATH PATH1 PATH1 PATH1 PATH1 PATH1 PATH1
8.04416E+04 7.30128E+04 7.63251E+04 4.30814E+04 5.31826E+04 5.31826E+04
...
PEAK DISCHARGE FAST FLUENCE (N/CM^2) OF EACH PATH
PATH PATH1 PATH1 PATH1 PATH1 PATH1 PATH1
2.88233E+23 2.64670E+23 2.75907E+23 1.58219E+23 1.94341E+23 1.94341E+23
FCC004 11.3114 04/10/20 ABURN: Hexagonal 3D Test Problem PAGE 374
...
```

Figure 3-122. REBUS Peak Burnup and Fluence Output Excerpts for the Equilibrium Problem

By definition, the peak discharge burnup is the peak burnup of a given path at EOEC. From the average burnup part of Figure 3-122, the discharge burnup will be the last stage of each path and thus 59279, 44533, 49753, 21152, and 27970 MWd/MT for the six fuel regions (CORE5 and CORE6 have the same value of 27970). It is easy to compare this directly to the peak discharge burnup values of 80442, 73013, 76325, 43081, and 53183 and realize that there is a significant difference in the average and peak. The ratio of peak to average is easy to calculate as 1.3570, 1.6395, 1.5341, 2.0367, and 1.9014. Comparing these to the values in Figure 3-119 and Figure 3-120 they are similar to the peak to average values reported in the EOEC region. Looking specifically at CORE3, the BOEC peak to average ratio is 1.53391 while the EOEC value is 1.53426. The average of these two values is 1.5341 which exactly matches the CORE3 value computed using the peak discharge burnup and average burnup. The same result occurs with the other regions. From the REBUS manual, the peak to average power density ratio,  $f_{k,j}^n$ , is computed using

$$f_{k,j}^n = \frac{S_{k,j}^n + S_{k,j}^{n-1}}{P_k^n + P_k^{n-1}}, \quad j = 1, 2, \dots, N_k^S. \quad (72)$$

In this equation the index  $k$  represents the  $k$ th mesh in the region,  $n$  represents the time node index, and  $j$  represents the sample point on all surface  $s$ . The variable  $S_{k,j}^n$  is the sample/surface power density while  $P_k^n$  is the cell averaged power density. For CORE3, the peak power densities were provided in Figure 3-121 for BOEC and EOEC and it is important to note that in this case, the peaks occur on the same surface of the same mesh in each region. In more realistic problems this is not likely to occur and thus the hand calculation shown above will not work in practice as the reported values in each DIF3D output section is not concerned with the location. Because the actual calculation in REBUS follows the equation above, the verification of the peak burnup table of output can be done for CORE3 as

$$f_{k,j}^n = \frac{102.1806 + 103.1924}{66.5994 + 67.2741} = 1.5341. \quad (73)$$

The numerator values are taken from Figure 3-121 while the denominator values are taken from Figure 3-119 and Figure 3-120 and the resulting ratio exactly matches the computed value using the output from REBUS. As stated, since the mesh and sample/surface number are identical at each time point on this problem, the preceding hand calculation of the peak to average is identical to the actual formula used by REBUS. It is important to note, as shown in a previous verification problem, that the average burnup calculated by REBUS in MWD/MT is not the correct approach, but itself an approximation based upon the burnup in atom percent. In this sense, the peak burnup can also be somewhat erroneous.

The peak discharge fast fluence is a bit easier to hand calculate as REBUS. Looking again at Figure 3-121, one can see that the peak of the fast flux occurs at the same spatial mesh location and surface for both time points. In practice, REBUS just averages the peak fast flux over a given time node for each sample/surface of each mesh in each region and multiplies by the time step size. This result is summed over all time steps for the given mesh and surface and the maximum value of all meshes is reported in the REBUS output excerpt. To hand calculate this for CORE1, the peak fast flux value ( $\text{n/cm}^2/\text{sec}$ ) at BOEC of  $5.381516 \cdot 10^{15}$  and EOEC value of  $5.738572 \cdot 10^{15}$  lead to the average value of  $5.560044 \cdot 10^{15}$ . Multiplying by the 100 day time step size leads to  $4.80387802 \cdot 10^{22}$  ( $\text{n/cm}^2$ ) which is a factor of 6 off of the REBUS reported value of  $2.88233 \cdot 10^{23}$  ( $\text{n/cm}^2$ ). This factor of 6 is needed to account for the total residence time (number of cycles) that the fuel is in the given position. Using the peak power density and fast flux values reported in Figure 3-119 and Figure 3-120, the peak discharge burnup and fast fluence were calculated and are tabulated in Table 3-76. As can be seen,

the hand calculation of the peak discharge burnup and peak fast fluence exactly match the REBUS reported results.

**Table 3-76. Peak Burnup and Fluence Hand Calculation for the Equilibrium Problem**

|       | BOEC                |                         | EOEC             |                       |
|-------|---------------------|-------------------------|------------------|-----------------------|
|       | Power Density       | Peak Power Density      | Power Density    | Peak Power Density    |
| CORE1 | 7.767E+01           | 1.054E+02               | 7.586E+01        | 1.030E+02             |
| CORE2 | 6.136E+01           | 1.006E+02               | 6.118E+01        | 1.003E+02             |
| CORE3 | 6.727E+01           | 1.032E+02               | 6.660E+01        | 1.022E+02             |
| CORE4 | 3.213E+01           | 6.544E+01               | 3.311E+01        | 6.743E+01             |
| CORE5 | 4.116E+01           | 7.824E+01               | 4.200E+01        | 7.987E+01             |
| CORE6 | 4.116E+01           | 7.824E+01               | 4.200E+01        | 7.987E+01             |
|       | Power Peak/Average  | Reported Average Burnup | Hand Calculation | Reported Peak Burnup  |
| CORE1 | 1.3570              | 59280                   | 80442            | 80442                 |
| CORE2 | 1.6395              | 44533                   | 73013            | 73013                 |
| CORE3 | 1.5341              | 49753                   | 76325            | 76325                 |
| CORE4 | 2.0367              | 21152                   | 43081            | 43081                 |
| CORE5 | 1.9014              | 27970                   | 53183            | 53183                 |
| CORE6 | 1.9014              | 27970                   | 53183            | 53183                 |
|       | BOEC Peak Fast Flux | EOEC Peak Fast Flux     | Hand Calculation | Reported Fast Fluence |
| CORE1 | 5.38152E+15         | 5.73857E+15             | 2.88233E+23      | 2.88233E+23           |
| CORE2 | 4.94218E+15         | 5.26884E+15             | 2.64670E+23      | 2.64670E+23           |
| CORE3 | 5.15173E+15         | 5.49284E+15             | 2.75907E+23      | 2.75907E+23           |
| CORE4 | 2.95590E+15         | 3.14822E+15             | 1.58219E+23      | 1.58219E+23           |
| CORE5 | 3.63010E+15         | 3.86764E+15             | 1.94341E+23      | 1.94341E+23           |
| CORE6 | 3.63010E+15         | 3.86764E+15             | 1.94341E+23      | 1.94341E+23           |

While this same approach can be carried out for a more complicated geometry with more time nodes and a burnup where the peak power density and flux change mesh position, the preceding verification work is sufficient to demonstrate that the stated equations used by REBUS are working as expected for equilibrium problems. It is important to point out that using the equilibrium mode of REBUS involves an approximation and it should be no surprise that the peak fast fluence in a equilibrium problem has similar approximations and errors with respect to a real fuel shuffling result.

### 3.7.1.7 REBUS Non-Equilibrium Problem Used to Verify the SFEDIT Data

The preceding problem verified the REBUS outputs for peak discharge burnup and fast fluence for an equilibrium problem. This section is focused on doing the same verification for a non-equilibrium problem with fuel shuffling. It relies upon the previous experience that the SFEDIT data results provided by DIF3D are correct. The problem selected is the non-equilibrium case with 6 time steps discussed earlier with Figure 3-79. The same change to the energy boundaries was made such that the fast flux is a simple sum of group 1 and 2. Only the DIF3D-VARIANT calculation is displayed in this section for brevity.

For non-equilibrium problems, REBUS reports the peak discharge burnup and fluence at the end of each time step along with the cumulative burnup of all active paths. Unlike the equilibrium case, the path output for a non-equilibrium case is assigned to a single composition as it transitions through the domain. To unscramble the output, one must know which region the composition is assigned to as the output edits from REBUS are done with respect to the REGION name and no indication is given for the composition name. The output is extensive given there are seven time points and only part of it is provided in Figure 3-123 for the first two time steps. It is very important to point out that the region density error criteria was reduced to 1.0E-12 (instead of the typical 1.0E-4) on this calculation as the latent binary files caused substantial errors in the peak burnup and fluence calculations. By doing this, the maximum number (5) of region density iterations is always used.

```

Time Step 1
...
AVERAGE BURNUP (MWD/MT) OF EACH REGION
REGION    CORE1      CORE2      CORE3      CORE4      CORE5      CORE6
          8.28121E+03  6.25116E+03  6.97380E+03  2.99044E+03  3.94414E+03  3.94414E+03
FCC004  11.3114 04/10/20          ABURN: Hexagonal 3D Test Problem          PAGE    202
...
PEAK BURNUP (MWD/MT) OF EACH REGION
REGION    CORE1      CORE2      CORE3      CORE4      CORE5      CORE6
          1.12321E+04  1.02383E+04  1.06890E+04  6.08589E+03  7.49249E+03  7.49249E+03
...
PEAK FAST FLUENCE (N/CM**2) OF EACH REGION
REGION    CORE1      CORE2      CORE3      CORE4      CORE5      CORE6
          4.09003E+22  3.75968E+22  3.91758E+22  2.25545E+22  2.76691E+22  2.76691E+22
FCC004  11.3114 04/10/20          ABURN: Hexagonal 3D Test Problem          PAGE    205
...
CUMULATIVE PEAK BURNUP AND FAST FLUENCE AFTER 1 BURNUP SUBSTEPS, FROM 0.00000000E+00 DAYS TO 1.00000000E+02 DAYS.
...
PEAK BURNUP (MWD/MT) OF EACH REGION
REGION    CORE1      CORE2      CORE3      CORE4      CORE5      CORE6
          1.12321E+04  1.02383E+04  1.06890E+04  6.08589E+03  7.49249E+03  7.49249E+03
...
PEAK FAST FLUENCE (N/CM**2) OF EACH REGION
REGION    CORE1      CORE2      CORE3      CORE4      CORE5      CORE6
          4.09003E+22  3.75968E+22  3.91758E+22  2.25545E+22  2.76691E+22  2.76691E+22
FCC004  11.3114 04/10/20          ABURN: Hexagonal 3D Test Problem          PAGE    212
...
SUMMARY OF FUEL DISCHARGED
REGION
      U235      U238      PU239      PU240      PU241      PU242      LFPPS      DUMP
CORE6   1.1756E+01  2.4511E+02  7.0734E+00  4.9370E+00  3.5931E+00  1.2760E+00  1.1428E+00  5.9791E-03
...
THIS FUEL WAS THE 1ST BATCH TO BE LOADED INTO THE REACTOR.
ITS REGION-AVERAGED DISCHARGE BURNUP IS 4.1768E-01 ATOM % OR 3.9441E+03 MWD/MT.
ITS PEAK DISCHARGE BURNUP IS 7.4925E+03 MWD/MT.
ITS PEAK DISCHARGE FAST FLUENCE IS 2.7669E+22 N/CM**2

Time Step 2
...
PEAK BURNUP (MWD/MT) OF EACH REGION
REGION    CORE2      CORE3      CORE4      CORE5      CORE6      CORE1
          1.07810E+04  1.12166E+04  6.40677E+03  7.84661E+03  7.85558E+03  1.16756E+04
...
PEAK FAST FLUENCE (N/CM**2) OF EACH REGION
REGION    CORE2      CORE3      CORE4      CORE5      CORE6      CORE1
          3.91822E+22  4.07968E+22  2.35574E+22  2.88715E+22  2.88739E+22  4.25277E+22
FCC004  11.3114 04/10/20          ABURN: Hexagonal 3D Test Problem          PAGE    330
...
CUMULATIVE PEAK BURNUP AND FAST FLUENCE AFTER 1 BURNUP SUBSTEPS, FROM 1.00000000E+02 DAYS TO 2.00000000E+02 DAYS.
...
PEAK BURNUP (MWD/MT) OF EACH REGION
REGION    CORE2      CORE3      CORE4      CORE5      CORE6      CORE1
          2.20131E+04  2.14550E+04  1.70958E+04  1.39325E+04  1.53481E+04  1.16756E+04
...
PEAK FAST FLUENCE (N/CM**2) OF EACH REGION
REGION    CORE2      CORE3      CORE4      CORE5      CORE6      CORE1
          8.00825E+22  7.83936E+22  6.27331E+22  5.14260E+22  5.65430E+22  4.25277E+22
FCC004  11.3114 04/10/20          ABURN: Hexagonal 3D Test Problem          PAGE    337
...
THIS FUEL WAS THE 1ST BATCH TO BE LOADED INTO THE REACTOR.
ITS REGION-AVERAGED DISCHARGE BURNUP IS 8.5566E-01 ATOM % OR 8.0799E+03 MWD/MT.
ITS PEAK DISCHARGE BURNUP IS 1.5348E+04 MWD/MT.
ITS PEAK DISCHARGE FAST FLUENCE IS 5.6543E+22 N/CM**2
...
```

**Figure 3-123. REBUS Peak Burnup and Fluence Excerpts for the Non-Equilibrium Problem**

For the first time point, the average burnup reported by REBUS is provided along with the time point peak burnup and peak fast fluence. After the detail by time point is provided, a cumulative edit of each path is provided which repeats the peak burnup and fast fluence in Figure 3-123 as this is the first time point. At each shuffling point, which occurs after each time point in this problem, REBUS provides a summary of the fuel that is discharged as seen. In this summary, the discharge mass of each active isotope is given along with the peak discharge burnup (7492.5 MWd/MT) and fast fluence (2.7669E+22 n/cm<sup>2</sup>). This process repeats for each time step in the calculation.

The methodology behind the way REBUS calculates the average burnup for a given path has already been discussed in previous sections and does not need to be displayed again. As a consequence, the average burnup values reported by REBUS will simply be used in the hand calculations that follow. The discharge mass in this case is reported as the material loaded into CORE6 (Z0006 in the input) which is only present in the problem for a single cycle. The peak discharge burnup is calculated similarly to the way the peak discharge burnup was calculated in the equilibrium problem shown in the previous section. The peak power density for this region (CORE6) at the beginning and end of the first time step are obtained from the DIF3D section of the REBUS output as 74.52 W/cc and 75.8735 W/cc. Similarly, the average power density for this region at the beginning and end of the first time step are 39.2416 W/cc and 39.9273 W/cc. Using the formula shown in the previous section this produces the peak to average factor of 1.89965 for the time step and region. Applying this factor to the average burnup for this region of 3944.14 MWd/MT produces 7492.49 MWd/MT which is identical to the value reported by REBUS of 7492.49 MWd/MT above. This hand calculation was displayed in this manner using the DIF3D output excerpts after checking that the SFEDIT output did not change locations. As stated, the peak power density result in the regular DIF3D output cannot be reliably used if the location of the peak power changes.

The peak fast fluence result can be also be hand calculated. From the reconstructed time point DIF3D outputs, the peak fast flux for the beginning and end of the time step are 3.11405E+15 and 3.29085E+15 (n/cm<sup>2</sup>/sec). Using the formula described in the previous section, the average peak fast fluence over the time step is 2.76692E+22. The REBUS reported peak fast fluence, 2.76691E+22 which is within round-off error of the hand calculation.

The time step 2 result is more complicated as fuel shuffling has occurred on the fuel that is to be discharged (Z0005). Z0005 is loaded into CORE5 for time step 1 and CORE6 for time step 2. In this situation, both the average and peak burnup are simple sums of the burnup that occurred to the zone in each time point. The fast fluence is the same. This methodology was built on the concept that the shuffling scheme assumes the zone is a part of the assembly that does not imply mixing. In this particular problem, multiple assembly positions are assigned the same zone/path and thus the true peak burnup is not being calculated by REBUS. This is a mistake on the user side and not a problem with REBUS.

The hand calculation of all six time steps is quite involved and it is broken into two tables for convenience. The first task is to compute the peak to average factor for each region at each time point. The tabulated results of these hand calculations are provided in Table 3-77. Also included in this table is the REBUS reported average burnup of each region. This is the total burnup integrated over all time steps. To understand, Z0001 is loaded into regions CORE1, CORE2, CORE3, CORE4, CORE5, and CORE6 in the six time steps respectively. In the REBUS reported average burnup, this zone has an average burnup of 8281, 14867, 22513, 25910, 30484, and 35126. As can be seen, the shuffling pattern follows a diagonal path from the top left of the table to the bottom right. The third set of average burnup data provided is the back-calculated average burnup that occurred during the time step for

each region. This data is required to be able to properly hand calculate the peak burnup and it has a relatively consistent burnup for each time step even though different fuel is loaded in each region.

**Table 3-77. Power Peaking Factor and Average Burnup for the Non-Equilibrium Problem**

| Time Step  | Calculated Peak to Average Power Density Factors |        |        |        |        |        |
|--|--|--------|--------|--------|--------|--------|
|  | 1  | 2      | 3      | 4      | 5      | 6      |
| CORE1  | 1.3563   | 1.3560 | 1.3559 | 1.3557 | 1.3556 | 1.3555 |
| CORE2  | 1.6378   | 1.6369 | 1.6363 | 1.6352 | 1.6346 | 1.6343 |
| CORE3  | 1.5327   | 1.5320 | 1.5315 | 1.5307 | 1.5302 | 1.5300 |
| CORE4  | 2.0351   | 2.0354 | 2.0357 | 2.0360 | 2.0363 | 2.0365 |
| CORE5  | 1.8997   | 1.8994 | 1.8993 | 1.8990 | 1.8992 | 1.8994 |
| CORE6  | 1.8997   | 1.8994 | 1.8992 | 1.8989 | 1.8991 | 1.8995 |
| Reported Total Average Burnup (MWD/MT)           |  |        |        |        |        |        |
| CORE1  | 8281   | 8610   | 8897   | 9103   | 9265   | 9367   |
| CORE2  | 6251   | 14867  | 15426  | 15882  | 16219  | 16464  |
| CORE3  | 6974   | 13573  | 22513  | 23258  | 23862  | 24292  |
| CORE4  | 2990   | 10122  | 16856  | 25910  | 26721  | 27365  |
| CORE5  | 3944   | 7121   | 14437  | 21311  | 30484  | 31350  |
| CORE6  | 3944   | 8080   | 11423  | 18883  | 25870  | 35126  |
| Calculated Average Burnup (MWD/MT) Per Time Step |  |        |        |        |        |        |
| CORE1  | 8281   | 8610   | 8897   | 9103   | 9265   | 9367   |
| CORE2  | 6251   | 6586   | 6816   | 6985   | 7116   | 7199   |
| CORE3  | 6974   | 7322   | 7646   | 7833   | 7980   | 8073   |
| CORE4  | 2990   | 3148   | 3283   | 3396   | 3462   | 3504   |
| CORE5  | 3944   | 4131   | 4315   | 4455   | 4574   | 4629   |
| CORE6  | 3944   | 4136   | 4301   | 4446   | 4559   | 4643   |

Given the calculated average burnup per time step, it can be merged with the peaking factor to produce the peak burnup that occurred in that region for that time step. This calculated result is tabulated in Table 3-78 where the REBUS reported result for the peak burnup is also shown. As can be seen, the two calculations are a match indicating that the formula discussed in the previous section is being used in the expected manner. In the cumulative edits section, REBUS sums the burnup by zone, not by region, even though it reports it by region as shown in Figure 3-123. The hand calculated result for each zone, ordered by region, is also provided in Table 3-78 along with the REBUS reported result for the peak burnup. The results are again identical within round off error. This work verifies that the procedure described in the REBUS manual for calculating the peak burnup and peak discharge burnup is correctly being applied within REBUS. For this specific problem, it is important to point out that the “PEAK DISCHARGE BURNUP” line that appears in Figure 3-123 always corresponds to region CORE6 as that is the only place where fuel material is discharged from the domain. This is the bottom line of each table and one can easily find the values 7493 and 15348 match the reported values of 7492.5 and 15348 in Figure 3-123.

The last part to verify is the peak fluence. Much like the peak burnup, it begins by obtaining the peak fast flux reported by REBUS in the DIF3D output. As was the case with the peak burnup results, the SFEDIT data was checked to ensure that the position of the peak did not change. The average peak

fast flux over the time step was calculated using the DIF3D reported output and is tabulated in Table 3-79. This fast flux is easily converted to a peak fast fluence for each region in each time step as seen. This detail is also provided in the regular REBUS output and the hand calculation matches but the output data is not included for brevity. The time-wise peak fluence can be summed by zone to reproduce the REBUS reported peak fast fluence result at each time point. This data was collected from the REBUS output and is provided in Table 3-79. Comparing the REBUS result with the hand calculated results shows an exact match for every number. This work verifies that the peak fast fluence calculation described in the REBUS manual is consistently applied in the software itself.

**Table 3-78. Peak Burnup Calculation for the Non-Equilibrium Problem**

|           | Calculated Peak Burnup (MWD/MT) by Time Step     |       |       |       |       |       |
|-----------|--|-------|-------|-------|-------|-------|
| Time Step | 1  | 2     | 3     | 4     | 5     | 6     |
| CORE1     | 11232  | 11676 | 12064 | 12340 | 12559 | 12697 |
| CORE2     | 10238  | 10781 | 11153 | 11421 | 11632 | 11766 |
| CORE3     | 10689  | 11217 | 11710 | 11989 | 12210 | 12351 |
| CORE4     | 6086   | 6407  | 6683  | 6915  | 7050  | 7135  |
| CORE5     | 7493   | 7847  | 8195  | 8459  | 8687  | 8792  |
| CORE6     | 7493   | 7856  | 8169  | 8443  | 8657  | 8818  |
|           | REBUS Reported Peak Burnup (MWD/MT) By Time Step |       |       |       |       |       |
| CORE1     | 11232  | 11676 | 12064 | 12340 | 12559 | 12697 |
| CORE2     | 10238  | 10781 | 11153 | 11421 | 11632 | 11766 |
| CORE3     | 10689  | 11217 | 11710 | 11989 | 12210 | 12351 |
| CORE4     | 6086   | 6407  | 6684  | 6915  | 7050  | 7135  |
| CORE5     | 7492   | 7847  | 8195  | 8459  | 8688  | 8792  |
| CORE6     | 7492   | 7856  | 8169  | 8443  | 8658  | 8818  |
|           | Time Integrated Peak Burnup (MWD/MT) by Region   |       |       |       |       |       |
| CORE1     | 11232  | 11676 | 12064 | 12340 | 12559 | 12697 |
| CORE2     | 10238  | 22013 | 22828 | 23485 | 23972 | 24325 |
| CORE3     | 10689  | 21455 | 33723 | 34817 | 35695 | 36323 |
| CORE4     | 6086   | 17096 | 28138 | 40638 | 41867 | 42830 |
| CORE5     | 7493   | 13932 | 25291 | 36598 | 49325 | 50659 |
| CORE6     | 7493   | 15348 | 22101 | 33734 | 45255 | 58143 |
|           | REBUS Reported Cumulative Peak Burnup (MWD/MT)   |       |       |       |       |       |
| CORE1     | 11232  | 11676 | 12064 | 12340 | 12559 | 12697 |
| CORE2     | 10238  | 22013 | 22828 | 23485 | 23972 | 24325 |
| CORE3     | 10689  | 21455 | 33723 | 34817 | 35695 | 36323 |
| CORE4     | 6086   | 17096 | 28139 | 40637 | 41867 | 42830 |
| CORE5     | 7492   | 13933 | 25291 | 36598 | 49325 | 50660 |
| CORE6     | 7492   | 15348 | 22102 | 33734 | 45255 | 58143 |

As was the case with the peak burnup, the peak discharge fast fluence result is simply the CORE6 result in Table 3-79 at each time point. Looking at Figure 3-123, the reported discharge fast fluence numbers are 2.7669E+22 and 5.6543E+22 which exactly match the CORE6 detail in Table 3-79 for the time integrated portion of data. Overall, the preceding hand calculation work verifies that the

SFEDIT data is correct and that it is being used by REBUS as stated by the REBUS manual. As a consequence, the category 5 verification work dealing with burnup and fluence is completed.

None of the preceding examples considered whether the REBUS results were accurate, but only that they are consistent with the stated algorithm used by REBUS. In that regard, the use of REBUS requires the user to make their input conform to the capabilities of the REBUS methodology. Also not shown was a case where the peak power or fast flux location changes in a given region during a time step. This is not a required aspect of the verification work as it simply involves looking directly at the SFEDIT output data instead of the easier to access DIF3D output data. Given the SFEDIT verification work demonstrated how the DIF3D output data is generated, this aspect is left off of the verification work. The existing displayed algorithm should be sufficient to guide any user on how to hand calculate those numbers as desired.

**Table 3-79. Peak Fast Fluence Calculation for the Non-Equilibrium Problem**

| Time Step   | Average Fast Flux (n/cm <sup>2</sup> /sec) |            |            |            |            |            |
|---|--|------------|------------|------------|------------|------------|
|   | 1  | 2          | 3          | 4          | 5          | 6          |
| CORE1   | 4.7338E+15                                 | 4.9222E+15 | 5.0874E+15 | 5.2037E+15 | 5.2958E+15 | 5.3543E+15 |
| CORE2   | 4.3515E+15                                 | 4.5350E+15 | 4.6919E+15 | 4.8030E+15 | 4.8906E+15 | 4.9460E+15 |
| CORE3   | 4.5342E+15                                 | 4.7219E+15 | 4.8855E+15 | 4.9997E+15 | 5.0900E+15 | 5.1472E+15 |
| CORE4   | 2.6105E+15                                 | 2.7266E+15 | 2.8256E+15 | 2.9011E+15 | 2.9580E+15 | 2.9936E+15 |
| CORE5   | 3.2025E+15                                 | 3.3416E+15 | 3.4640E+15 | 3.5530E+15 | 3.6238E+15 | 3.6670E+15 |
| CORE6   | 3.2025E+15                                 | 3.3419E+15 | 3.4632E+15 | 3.5524E+15 | 3.6228E+15 | 3.6678E+15 |
| Fast Fluence (n/cm <sup>2</sup> ) for the Time Step   |  |            |            |            |            |            |
| CORE1   | 4.0900E+22                                 | 4.2528E+22 | 4.3955E+22 | 4.4960E+22 | 4.5756E+22 | 4.6261E+22 |
| CORE2   | 3.7597E+22                                 | 3.9182E+22 | 4.0538E+22 | 4.1498E+22 | 4.2254E+22 | 4.2733E+22 |
| CORE3   | 3.9176E+22                                 | 4.0797E+22 | 4.2211E+22 | 4.3197E+22 | 4.3977E+22 | 4.4472E+22 |
| CORE4   | 2.2554E+22                                 | 2.3557E+22 | 2.4413E+22 | 2.5065E+22 | 2.5557E+22 | 2.5865E+22 |
| CORE5   | 2.7669E+22                                 | 2.8872E+22 | 2.9929E+22 | 3.0698E+22 | 3.1310E+22 | 3.1682E+22 |
| CORE6   | 2.7669E+22                                 | 2.8874E+22 | 2.9922E+22 | 3.0693E+22 | 3.1301E+22 | 3.1690E+22 |
| Time Integrated Fast Fluence (n/cm <sup>2</sup> )     |  |            |            |            |            |            |
| CORE1   | 4.0900E+22                                 | 4.2528E+22 | 4.3955E+22 | 4.4960E+22 | 4.5756E+22 | 4.6261E+22 |
| CORE2   | 3.7597E+22                                 | 8.0083E+22 | 8.3066E+22 | 8.5452E+22 | 8.7214E+22 | 8.8489E+22 |
| CORE3   | 3.9176E+22                                 | 7.8394E+22 | 1.2229E+23 | 1.2626E+23 | 1.2943E+23 | 1.3169E+23 |
| CORE4   | 2.2554E+22                                 | 6.2733E+22 | 1.0281E+23 | 1.4736E+23 | 1.5182E+23 | 1.5529E+23 |
| CORE5   | 2.7669E+22                                 | 5.1426E+22 | 9.2662E+22 | 1.3350E+23 | 1.7867E+23 | 1.8350E+23 |
| CORE6   | 2.7669E+22                                 | 5.6543E+22 | 8.1348E+22 | 1.2336E+23 | 1.6481E+23 | 2.1036E+23 |
| REBUS Reported Peak Fast Fluence (n/cm <sup>2</sup> ) |  |            |            |            |            |            |
| CORE1   | 4.0900E+22                                 | 4.2528E+22 | 4.3955E+22 | 4.4960E+22 | 4.5756E+22 | 4.6261E+22 |
| CORE2   | 3.7597E+22                                 | 8.0083E+22 | 8.3066E+22 | 8.5452E+22 | 8.7214E+22 | 8.8489E+22 |
| CORE3   | 3.9176E+22                                 | 7.8394E+22 | 1.2229E+23 | 1.2626E+23 | 1.2943E+23 | 1.3169E+23 |
| CORE4   | 2.2554E+22                                 | 6.2733E+22 | 1.0281E+23 | 1.4736E+23 | 1.5182E+23 | 1.5530E+23 |
| CORE5   | 2.7669E+22                                 | 5.1426E+22 | 9.2662E+22 | 1.3351E+23 | 1.7867E+23 | 1.8350E+23 |
| CORE6   | 2.7669E+22                                 | 5.6543E+22 | 8.1348E+22 | 1.2336E+23 | 1.6481E+23 | 2.1036E+23 |

### 3.7.1.8 Verification of the Mass and Power Edits

As stated in Table 3-56, the remaining tasks to satisfy the category 5 verification work are the mass and power edits. These edits are specifically looking at outputs related to card type 29 and 30 inputs. Card type 29 allows the user to define area names applying to specific parts of the reactor such as inner core, middle core, blanket, control rods. Card type 30 impacts the mass balance tables which are typically not used by VTR but have been setup by some users. For testing purposes, the equilibrium problem from the previous section is modified to include the necessary inputs and the differences in the outputs are discussed here. The modifications to the base input are shown in Figure 3-124.

```
...
UNFORM=A.NIP3
...
07 CORE CORE1 CORE2 CORE3 CORE4 CORE5 CORE6
07 IICORE CORE1 CORE2
07 IOCORE CORE3
07 IIBLKT CORE4
07 IRBLKT CORE5
07 RBLKTO CORE6
07 CNTRL CENT
...
UNFORM=A.BURN
...
  ICORE MCORE OCORE IBLKT MBLKT OBLKT RBLKT ABLKT CONTRL ORBLKT
29 IICORE "" IOCORE IIBLKT "" "" IRBLKT "" CNTRL RBLKTO
30 5 U235
30 7 U238
30 11 PU239
30 12 PU240
30 13 PU241
30 14 PU242
31      2 U238 PU242
31      1 U235 PU239 PU241
31      3 DUMP
31      4 LFPPS
...
```

**Figure 3-124. Card Type 29 and 30 Modifications to the Equilibrium Problem**

The first aspect to note is that many area names were added to the A.NIP3 which are later used in A.BURN to map into the recognized core parts. Note that "" is used in card type 29 to signify a blank meaning that that particular feature is not present in the current reactor. The card type 30 data is relatively straightforward, and, if the active isotope names match the default ones, REBUS will sometimes display partial data in the affected output tables. The card type 31 data was already present and is only used for the neutron balance edits. This output is also by default exported and this input only corrects any mistakes in the ISOTXS data file for the given isotopes.

The mass balance output is the first one to check and an excerpt of that output is provided in Figure 3-125. In the input without card type 29, the mass balance output is not filled, unless the user names areas in A.NIP3 consist with the recognized names: ICORE, MCORE, OCORE, IBLKT, etc.... If this occurs, the mass balance data will be filled out using the partial names. These area names are commonly used in VTR and thus erroneous output can occur. In many cases, the "CORE" header is mistaken to be CORE by users instead of the mass balance defined header. Also included in Figure 3-125 is the reactor loading specification of the active isotopes which is produced by REBUS for all areas in the domain.

With the displayed input modification, the domain is properly setup such that the mass balance edits should make sense in Figure 3-125, not that the radial and axial blankets are actually present. In the equilibrium problem, there are two sections of output for the mass balance. The first one occurs at BOEC while the second is produced at the end of EOEC. For a problem with more time steps, it will be produced after each intermediate time step where the EOC result is updated incrementally. The

output produced in the mass balance table is simply the total mass of a given isotope loaded in the various areas specified on card type 29.

Starting with the U235 mass in "CORE" of 30.687 kg, the "CORE" region is composed of ICORE, MCORE, and OCORE which in this input example is only areas IICORE and IOCORE. From the reactor loading by area summary section also included in Figure 3-125, the U235 mass of 20.4122 kg and 10.2743 kg are combined to produce 30.6865 kg which is with the round off error of the reported REBUS result. Looking at the input earlier, no areas were assigned to the axial blanket recognized name and thus the mass summary output is all zero for this section of output. For the radial blanket, the U235 mass of 22.071 kg is reported by REBUS. From the card type 29 input, the IRBLKT and RBLKTO areas were assigned to the RBLKT and ORBLKT names. Taking the mass of 11.0354 kg and 11.0354 kg for these two areas from the reactor loadings section of the output one obtains 22.0708 kg which is within the round off error reported by REBUS. Finally, the internal blanket is defined to consist of the IBLKT, MBLKT, and OBLKT regions from card type 29 of which only IIBLKT was assigned. It is easy to see that all of the active isotopes in the "INTERNAL BLANKET" column match the masses reported for the IIBLKT area.

| REACTOR LOADINGS (IN KG) BY AREA OVER THE SUBINTERVAL |             |             |             |             |             |             |             |
|---|-------------|-------------|-------------|-------------|-------------|-------------|-------------|
| AREA:   | CORE        | IICORE      | IOCORE      | IIBLKT      | IRBLKT      | RBLKTO      | CNTRL       |
| AVG. BURNUP, MWD/MT: 0.00000E+00                      | 0.00000E+00 | 0.00000E+00 | 0.00000E+00 | 0.00000E+00 | 0.00000E+00 | 0.00000E+00 | 0.00000E+00 |
| AVG. FISSION POWER, MW: 1.02097E+02                   | 4.59326E+01 | 2.20171E+01 | 9.37185E+00 | 1.23876E+01 | 1.23876E+01 | 0.00000E+00 | 0.00000E+00 |
| ISOTOPE   |             |             |             |             |             |             |             |
| U235  | 6.40489E+01 | 2.04122E+01 | 1.02743E+01 | 1.12917E+01 | 1.10354E+01 | 1.10354E+01 | 0.00000E+00 |
| U238  | 1.44560E+03 | 4.78121E+02 | 2.39375E+02 | 2.43338E+02 | 2.42382E+02 | 2.42382E+02 | 0.00000E+00 |
| PU239   | 5.51775E+01 | 2.01125E+01 | 9.91911E+00 | 8.06260E+00 | 8.54165E+00 | 8.54165E+00 | 0.00000E+00 |
| PU240   | 2.94245E+01 | 9.79941E+00 | 4.89376E+00 | 4.91838E+00 | 4.90646E+00 | 4.90646E+00 | 0.00000E+00 |
| PU241   | 1.93471E+01 | 6.14203E+00 | 3.09246E+00 | 3.42883E+00 | 3.34189E+00 | 3.34189E+00 | 0.00000E+00 |
| PU242   | 7.97299E+00 | 2.69893E+00 | 1.34622E+00 | 1.30147E+00 | 1.31319E+00 | 1.31319E+00 | 0.00000E+00 |
| LFPPS   | 2.76474E+01 | 1.24367E+01 | 5.96195E+00 | 2.53876E+00 | 3.35501E+00 | 3.35501E+00 | 0.00000E+00 |
| DUMP  | 1.45713E-01 | 6.54792E-02 | 3.11478E-02 | 1.36304E-02 | 1.77278E-02 | 1.77278E-02 | 0.00000E+00 |

|                  |                  |                                  |                |                  |
|------------------|------------------|----------------------------------|----------------|------------------|
| FCC004           | 11.3114 04/10/20 | ABURN: Hexagonal 3D Test Problem | PAGE           | 331              |
| MASS BALANCE, KG |                  |                                  |                |                  |
|                  | CORE             | AXIAL BLANKET                    | RADIAL BLANKET | INTERNAL BLANKET |
|                  | BOC              | EOC                              | BOC            | EOC              |
| U235             | 30.687           | 0.000                            | 0.000          | 0.000            |
| U238             | 717.496          | 0.000                            | 0.000          | 0.000            |
| PU239            | 30.032           | 0.000                            | 0.000          | 0.000            |
| PU240            | 14.693           | 0.000                            | 0.000          | 0.000            |
| PU241            | 9.234            | 0.000                            | 0.000          | 0.000            |
| PU242            | 4.045            | 0.000                            | 0.000          | 0.000            |

|                  |                  |                                  |                |                  |
|------------------|------------------|----------------------------------|----------------|------------------|
| FCC004           | 11.3114 04/10/20 | ABURN: Hexagonal 3D Test Problem | PAGE           | 401              |
| MASS BALANCE, KG |                  |                                  |                |                  |
|                  | CORE             | AXIAL BLANKET                    | RADIAL BLANKET | INTERNAL BLANKET |
|                  | BOC              | EOC                              | BOC            | EOC              |
| U235             | 30.687           | 28.529                           | 0.000          | 0.000            |
| U238             | 717.496          | 708.772                          | 0.000          | 0.000            |
| PU239            | 30.032           | 34.081                           | 0.000          | 0.000            |
| PU240            | 14.693           | 14.683                           | 0.000          | 0.000            |
| PU241            | 9.234            | 8.525                            | 0.000          | 0.000            |
| PU242            | 4.045            | 4.143                            | 0.000          | 0.000            |

**Figure 3-125. Mass Balance Output for the Equilibrium Problem**

The end of cycle results are also easily verified by summing the area mass summary details according to the card type 29 input. This concludes the mass balance verification work from category 5.

The power aspect of category 5 refers to the output tables shown in Figure 3-126. These tables give a breakdown of the power being delivered by each stage of a path and can be used to indicate how much power drift will occur with burnup. The output itself is relatively easy to verify as it is simply the power conversion factor for each stage composition multiplied by the region averaged flux. For

the peak/average ratio, the instant power results are divided by the average power of the region taken from DIF3D (PWDINT).

In this problem, the U235 isotope is the only one that has a power conversion factor (1.0E-11 w-sec/fission) so only the U235 atom density matters with regard to the power calculation. The integrated flux magnitudes were collected from the DIF3D output and tabulated in Table 3-80. Also included is the U235 isotope fission cross sections. Combining these quantities gives the microscopic reaction rate in each region at BOEC and EOEC as seen. The stage atom density details were extracted from the REBUS output and are tabulated for BOEC in Table 3-81. The calculation of the instant power result is simply the U235 atom density multiplied by the region reaction rate in Table 3-80 and the stated power conversion factor.

```

    ...
    INSTANTANEOUS TOTAL POWER IN MW AT TIME = 0.000000000E+00 DAYS
    INSTANT POWER OF EACH STAGE OF EACH PATH

    STAGE/REGION 1/CORE1    2/CORE1    3/CORE1    4/CORE1    5/CORE1    6/CORE1
    4.93431E-01  4.53430E-01  4.16671E-01  3.82893E-01  3.51853E-01  3.23329E-01
    STAGE/REGION 1/CORE2    2/CORE2    3/CORE2    4/CORE2    5/CORE2    6/CORE2
    3.71618E-01  3.48695E-01  3.27186E-01  3.07004E-01  2.88067E-01  2.70298E-01
    STAGE/REGION 1/CORE3    2/CORE3    3/CORE3    4/CORE3    5/CORE3    6/CORE3
    4.14410E-01  3.86007E-01  3.59550E-01  3.34907E-01  3.11952E-01  2.90571E-01
    STAGE/REGION 1/CORE4    2/CORE4    3/CORE4    4/CORE4    5/CORE4    6/CORE4
    1.80115E-01  1.74643E-01  1.69337E-01  1.64192E-01  1.59203E-01  1.54366E-01
    STAGE/REGION 1/CORE5    2/CORE5    3/CORE5    4/CORE5    5/CORE5    6/CORE5
    2.36042E-01  2.26688E-01  2.17704E-01  2.09077E-01  2.00791E-01  1.92834E-01
    STAGE/REGION 1/CORE6    2/CORE6    3/CORE6    4/CORE6    5/CORE6    6/CORE6
    2.36042E-01  2.26688E-01  2.17704E-01  2.09077E-01  2.00791E-01  1.92834E-01
    FCC004 11.3114 04/10/20          ABURN: Hexagonal 3D Test Problem          PAGE 333

    INSTANTANEOUS TOTAL POWER/AVERAGE POWER AT TIME= 0.000000000E+00 DAYS
    POWER/AVG. POWER OF EACH STAGE OF EACH PATH

    STAGE/REGION 1/CORE1    2/CORE1    3/CORE1    4/CORE1    5/CORE1    6/CORE1
    1.22257E+00  1.12346E+00  1.03238E+00  9.48692E-01  8.71784E-01  8.01111E-01
    STAGE/REGION 1/CORE2    2/CORE2    3/CORE2    4/CORE2    5/CORE2    6/CORE2
    1.16564E+00  1.09373E+00  1.02627E+00  9.62965E-01  9.03566E-01  8.47831E-01
    STAGE/REGION 1/CORE3    2/CORE3    3/CORE3    4/CORE3    5/CORE3    6/CORE3
    1.18550E+00  1.10424E+00  1.02856E+00  9.58064E-01  8.92399E-01  8.31234E-01
    STAGE/REGION 1/CORE4    2/CORE4    3/CORE4    4/CORE4    5/CORE4    6/CORE4
    1.07869E+00  1.04592E+00  1.01414E+00  9.83326E-01  9.53449E-01  9.24481E-01
    STAGE/REGION 1/CORE5    2/CORE5    3/CORE5    4/CORE5    5/CORE5    6/CORE5
    1.10374E+00  1.06000E+00  1.01799E+00  9.77652E-01  9.38908E-01  9.01699E-01
    STAGE/REGION 1/CORE6    2/CORE6    3/CORE6    4/CORE6    5/CORE6    6/CORE6
    1.10374E+00  1.06000E+00  1.01799E+00  9.77652E-01  9.38908E-01  9.01699E-01
    FCC004 11.3114 04/10/20          ABURN: Hexagonal 3D Test Problem          PAGE 334
    ...

    AVERAGE POWER OF EACH STAGE OF EACH PATH

    STAGE/REGION 1/CORE1    2/CORE1    3/CORE1    4/CORE1    5/CORE1    6/CORE1
    4.43505E+00  4.48554E+00  4.52465E+00  4.55370E+00  4.57385E+00  4.58615E+00
    STAGE/REGION 1/CORE2    2/CORE2    3/CORE2    4/CORE2    5/CORE2    6/CORE2
    3.34237E+00  3.37187E+00  3.39636E+00  3.41628E+00  3.43203E+00  3.44399E+00
    ...

```

**Figure 3-126. Instant Power Output Excerpt for the Equilibrium Problem**

As an example, the stage 1 instant power of CORE1 is  $1.0007E-03 * 2.9586E+20 * 1.0E-11 = 2.9607$  MW. Because this stage only accounts for 1/6<sup>th</sup> of the volume, the instant power is  $2.9607/6=0.49345$  MW as seen in the table. The total power produced from all stages for each region is provided in the table. For CORE1, the power is 2.42162 MW which matches the DIF3D reported power for this region. The average stage power is  $2.42162/6=0.403603$  MW. The last section of the table is simply the instant power result divided by the total power from each stage. For CORE1, this is  $0.49345/0.403603=1.2226$ . Inspecting the tabulated results in Table 3-81 with the REBUS output excerpt in Figure 3-126, one finds that all of the region/stage results match. A similar hand calculation of the EOEC result also matches. Finally, in the REBUS output excerpt of Figure 3-126, a portion of the average power table is provided. This table is not simply the average of the instant power results at the beginning and end of the time step but instead is a converted value from the average burnup result. Because the input was manipulated to only have a single isotope produce power, the power

conversion used by REBUS is not appropriate and thus the average power is not consistent with regard to the reported instant power results.

**Table 3-80. U235 Micro Reaction Rate Calculation for the Equilibrium Problem**

| Group | U235<br>Fission XS | CORE1                                   | CORE2      | CORE3      | CORE4      | CORE5      | CORE6      |
|-------|--------------------|---|------------|------------|------------|------------|------------|
|       |                    | BOEC Flux (n/cm <sup>2</sup> /sec)      |            |            |            |            |            |
| 1     | 1.83896            | 3.3010E+19                              | 2.5114E+19 | 2.8057E+19 | 1.1512E+19 | 1.5508E+19 | 1.5508E+19 |
| 2     | 1.55634            | 9.0405E+19                              | 6.8240E+19 | 7.6165E+19 | 3.2353E+19 | 4.2774E+19 | 4.2774E+19 |
| 3     | 2.28678            | 4.1306E+19                              | 3.0801E+19 | 3.4261E+19 | 1.5951E+19 | 2.0309E+19 | 2.0309E+19 |
|       |                    | EOEC Flux (n/cm <sup>2</sup> /sec)      |            |            |            |            |            |
| 1     |                    | 3.5256E+19                              | 2.6796E+19 | 2.9947E+19 | 1.2263E+19 | 1.6531E+19 | 1.6531E+19 |
| 2     |                    | 9.6322E+19                              | 7.2674E+19 | 8.1127E+19 | 3.4433E+19 | 4.5534E+19 | 4.5534E+19 |
| 3     |                    | 4.3609E+19                              | 3.2548E+19 | 3.6193E+19 | 1.6882E+19 | 2.1483E+19 | 2.1483E+19 |
|       |                    | U235 Micro Reaction Rate (fissions/sec) |            |            |            |            |            |
|       | BOEC               | 2.9586E+20                              | 2.2282E+20 | 2.4848E+20 | 1.0800E+20 | 1.4153E+20 | 1.4153E+20 |
|       | EOEC               | 3.1447E+20                              | 2.3681E+20 | 2.6410E+20 | 1.1475E+20 | 1.5039E+20 | 1.5039E+20 |

**Table 3-81. BOEC Instant Power Table Calculation for the Equilibrium Problem**

|            | BOEC U235 Atom Densities      |            |            |            |            |            |
|------------|-------------------------------|------------|------------|------------|------------|------------|
| Stage      | CORE1                         | CORE2      | CORE3      | CORE4      | CORE5      | CORE6      |
| 1          | 1.0007E-03                    | 1.0007E-03 | 1.0007E-03 | 1.0007E-03 | 1.0007E-03 | 1.0007E-03 |
| 2          | 9.1954E-04                    | 9.3894E-04 | 9.3208E-04 | 9.7026E-04 | 9.6101E-04 | 9.6101E-04 |
| 3          | 8.4500E-04                    | 8.8102E-04 | 8.6820E-04 | 9.4078E-04 | 9.2292E-04 | 9.2292E-04 |
| 4          | 7.7650E-04                    | 8.2668E-04 | 8.0869E-04 | 9.1220E-04 | 8.8635E-04 | 8.8635E-04 |
| 5          | 7.1355E-04                    | 7.7569E-04 | 7.5326E-04 | 8.8448E-04 | 8.5122E-04 | 8.5122E-04 |
| 6          | 6.5570E-04                    | 7.2784E-04 | 7.0163E-04 | 8.5761E-04 | 8.1749E-04 | 8.1749E-04 |
|            | Instant Power (MW)            |            |            |            |            |            |
| 1          | 4.9345E-01                    | 3.7163E-01 | 4.1442E-01 | 1.8012E-01 | 2.3605E-01 | 2.3605E-01 |
| 2          | 4.5343E-01                    | 3.4869E-01 | 3.8601E-01 | 1.7464E-01 | 2.2669E-01 | 2.2669E-01 |
| 3          | 4.1667E-01                    | 3.2718E-01 | 3.5955E-01 | 1.6934E-01 | 2.1770E-01 | 2.1770E-01 |
| 4          | 3.8289E-01                    | 3.0700E-01 | 3.3491E-01 | 1.6419E-01 | 2.0908E-01 | 2.0908E-01 |
| 5          | 3.5185E-01                    | 2.8807E-01 | 3.1195E-01 | 1.5920E-01 | 2.0079E-01 | 2.0079E-01 |
| 6          | 3.2333E-01                    | 2.7030E-01 | 2.9057E-01 | 1.5437E-01 | 1.9283E-01 | 1.9283E-01 |
| Total (MW) | 2.42162                       | 1.91288    | 2.09741    | 1.00186    | 1.28314    | 1.28314    |
|            | Instant Power / Average Power |            |            |            |            |            |
| 1          | 1.22260                       | 1.16567    | 1.18553    | 1.07872    | 1.10378    | 1.10378    |
| 2          | 1.12345                       | 1.09373    | 1.10424    | 1.04591    | 1.06000    | 1.06000    |
| 3          | 1.03238                       | 1.02626    | 1.02856    | 1.01413    | 1.01798    | 1.01798    |
| 4          | 0.94869                       | 0.96296    | 0.95806    | 0.98332    | 0.97765    | 0.97765    |
| 5          | 0.87178                       | 0.90356    | 0.89239    | 0.95344    | 0.93890    | 0.93890    |
| 6          | 0.80110                       | 0.84783    | 0.83122    | 0.92448    | 0.90169    | 0.90169    |

No effort is taken to check this table of output noting that in most normal REBUS executions with proper fissionable isotope energy conversion factors, the average power results are more reasonable. As discussed previously, the same issue occurs when REBUS does a conversion of the atom % burnup into MWD/MT burnup. Much like that earlier case, the verification of the calculation by REBUS is rather difficult to check. In that regard, this table of output is not recommended for engineering work unless checked against the simple average power from the two DIF3D states associated with the time step.

This concludes the category 5 verification work. As displayed, the SFEDIT file and how it is used to compute the peak burnups and peak fast fluence was discussed. The instantaneous power edits were also displayed along with the mass balance edits. While the average power output table is not a mathematical representation of the average power over the time step, but an approximation based upon the atom % burnup, its verification is pointless and is not included in this report.

## 3.8 SUMRY File Verification Work

The preceding sections verified all categories of Table 2-1. In addition to the REBUS regular output, REBUS generates nine auxiliary output files listed in Table 3-82. They are merely the collapsed information already provided in the regular output. As an example, SUMRY3 provides the DIF3D  $k_{eff}$  solution and power level for each time point for both the preliminary, intermediate, final search, and final pass sections. In several of the other SUMRY files, such as SUMRY7, the file is rewound such that the file only contains the output produced during the “FINAL PASS” section. This section works through each SUMRY file and displays the output from REBUS that verifies it is a simple dump of the regular REBUS output. The problem selected is the equilibrium case discussed earlier with Figure 3-79.

**Table 3-82. REBUS Auxiliary “SUMMARY” Files**

| File Name | File Purpose  |
|-----------|---|
| SUMRY1    | Isotopic mass summary data from REBUS                           |
| SUMRY2    | Conversion, Breeding Ratio, and fissile atoms created/destroyed |
| SUMRY3    | $k_{eff}$ and power history data                                |
| SUMRY4    | Region volume, power, and peak power density                    |
| SUMRY5    | Region volume, peak flux, peak fast flux                        |
| SUMRY6    | Region burnup data in atom % and MWD/MT                         |
| SUMRY7    | Region volume, total flux, total fast flux                      |
| SUMRY8    | Isotopic atom density summary                                   |
| SUMRY9    | Stage/Region burnup (MWD/MT)                                    |

### 3.8.1 SUMRY1 File Verification

As stated in Table 3-82, the SUMRY1 file provides the isotopic mass for each region in the domain at each time point. An output excerpt from the SUMRY1 is provided in Figure 3-127. As can be seen, the output consists of six columns of data. For an equilibrium problem, the first column is the batch index number where 0 is used to indicate that it is an area. The second column is the region or area name while the third column is the active isotope name defined in the depletion chain. It is important to note that the isotope name is not one from ISOTXS, but the depletion chain alias. The fourth column gives the mass (kg) of the isotope in the stage of each region. The fifth column is the current time step

which for the chosen example problem is either 0.0 days or 100 days. Finally, the sixth column is the atomic mass of each isotope used by REBUS in calculating the mass from the atom density.

The associated REBUS output is the stage density information which must be combined with the region volume to get to mass. A small excerpt of the CORE1 region stated output is given in Figure 3-128. The volume of CORE1 from the DIF3D output in REBUS is 31176.9 cm<sup>3</sup> and the Avogadro number used in this REBUS calculation is 6.022141E+23. The mass reported in the SUMRY1 file for stage 1 of U235 is simply the U235 stage density of multiplied by 1/6<sup>th</sup> of the volume 1.0007E-03 \*31176.9/6/0.6022141\*235.117=2030.106 g. Converting to kg, one finds that this number is consistent with the reported 2.03004 kg within the round off error (both volume and atom density are approximate numbers in this hand calculation). The area edits are not produced by REBUS in the regular output unless the SUMMAR module of DIF3D is used. A simple hand calculation suffices in verifying the area edit. From the input, area IOCORE only consists of CORE3 and thus is the simple sum of all U235 isotopes in CORE3. The sum of CORE3 atom densities in Figure 3-128 is 5.0646E-03 which is identically converted to mass as the U235 example above to produce 10274.40 g. This result is identical to the 1.02743 kg result from Figure 3-127 within round off error.

```
...
1 CORE1      U235      2.03004E+00  0.000000000E+00  2.35117E+02
1 CORE1      U238      4.10897E+01  0.000000000E+00  2.38125E+02
1 CORE1      PU239     1.03233E+00  0.000000000E+00  2.39127E+02
1 CORE1      PU240     8.29322E-01  0.000000000E+00  2.40129E+02
1 CORE1      PU241     6.24589E-01  0.000000000E+00  2.41132E+02
1 CORE1      PU242     2.09062E-01  0.000000000E+00  2.42134E+02
1 CORE1      LFPPS     2.04629E-09  0.000000000E+00  2.37000E+02
1 CORE1      DUMP      2.03766E-09  0.000000000E+00  2.36000E+02
2 CORE1      U235      1.86547E+00  0.000000000E+00  2.35117E+02
2 CORE1      U238      4.05114E+01  0.000000000E+00  2.38125E+02
2 CORE1      PU239     1.36934E+00  0.000000000E+00  2.39127E+02
2 CORE1      PU240     8.16534E-01  0.000000000E+00  2.40129E+02
2 CORE1      PU241     5.65579E-01  0.000000000E+00  2.41132E+02
2 CORE1      PU242     2.17570E-01  0.000000000E+00  2.42134E+02
2 CORE1      LFPPS     4.67335E-01  0.000000000E+00  2.37000E+02
2 CORE1      DUMP      2.40293E-03  0.000000000E+00  2.36000E+02
...
6 CORE1      LFPPS     2.37857E+00  0.000000000E+00  2.37000E+02
6 CORE1      DUMP      1.27856E-02  0.000000000E+00  2.36000E+02
1 CORE2      U235      2.03004E+00  0.000000000E+00  2.35117E+02
1 CORE2      U238      4.10897E+01  0.000000000E+00  2.38125E+02
1 CORE2      PU239     1.03233E+00  0.000000000E+00  2.39127E+02
1 CORE2      PU240     8.29322E-01  0.000000000E+00  2.40129E+02
...
0 CORE      U235      6.06737E+01  1.00000E+02  2.35117E+02
0 CORE      U238      1.43230E+03  1.00000E+02  2.38125E+02
0 CORE      PU239     6.16902E+01  1.00000E+02  2.39127E+02
...
0 IOCORE     U235      1.02743E+01  0.00000E+00  2.35117E+02
...
0 RBLKTO     DUMP      1.77279E-02  0.00000E+00  2.36000E+02
0 CNTRL     U235      0.00000E+00  0.00000E+00  2.35117E+02
...
```

Figure 3-127. SUMRY1 Output Excerpt

```
FCC004 11.3114 04/10/20
PAGE 322

ATOM DENSITIES (IN ATOMS/BARN-CM.) OF ACTIVE ISOTOPES IN EACH STAGE OF EACH PATH
PATH PATH1

STAGE REGION      U235      U238      PU239      PU240      PU241      PU242      LFPPS      DUMP
+
1 CORE1  1.0007E-03  1.9998E-02  5.0033E-04  4.0026E-04  3.0020E-04  1.0007E-04  1.0007E-12  1.0007E-12
2 CORE1  9.1954E-04  1.9717E-02  6.6367E-04  3.9409E-04  2.7184E-04  1.0414E-04  2.2853E-04  1.1800E-06
3 CORE1  8.4500E-04  1.9439E-02  8.0768E-04  3.9124E-04  2.4687E-04  1.0764E-04  4.5967E-04  2.4038E-06
4 CORE1  7.7650E-04  1.9166E-02  9.3433E-04  3.9120E-04  2.2496E-04  1.1064E-04  6.9282E-04  3.6650E-06
5 CORE1  7.1355E-04  1.8896E-02  1.04548E-03  3.9352E-04  2.0577E-04  1.1320E-04  9.2746E-04  4.9582E-06
6 CORE1  6.5570E-04  1.8630E-02  1.1425E-03  3.9780E-04  1.8901E-04  1.1538E-04  1.1632E-03  6.2788E-06
...
1 CORE3  1.0007E-03  1.9998E-02  5.0033E-04  4.0026E-04  3.0020E-04  1.0007E-04  1.0007E-12  1.0007E-12
2 CORE3  9.3208E-04  1.9762E-02  6.3788E-04  3.9475E-04  2.7618E-04  1.0350E-04  1.9225E-04  9.8184E-07
3 CORE3  8.6820E-04  1.9529E-02  7.6168E-04  3.9161E-04  2.5459E-04  1.0653E-04  3.8634E-04  1.9944E-06
4 CORE3  8.0869E-04  1.9299E-02  8.7291E-04  3.9054E-04  2.3521E-04  1.0919E-04  5.8192E-04  3.0351E-06
5 CORE3  7.5326E-04  1.9071E-02  9.7267E-04  3.9125E-04  2.1785E-04  1.1152E-04  7.7867E-04  4.0995E-06
6 CORE3  7.0163E-04  1.8846E-02  1.0620E-03  3.9351E-04  2.0232E-04  1.1356E-04  9.7630E-04  5.1850E-06
...
```

Figure 3-128. REBUS Output Excerpt to Verify SUMRY1

It should be no surprise that the remaining values in SUMRY1 are all as consistent as the U235 hand calculations shown here. For non-equilibrium problems, the results at each time point are given and the stage index value is always one. As an additional note, the sum over the entire domain is also provided at the beginning of the area edits at each time point where no area name is provided (not shown for brevity).

### 3.8.2 SUMRY2 File Verification

From Table 3-82, the SUMRY2 file provides the conversion ratio, breeding ratio, and fissile isotopic masses for each region in the domain at each time point. An output excerpt from the SUMRY2 is provided in Figure 3-129. As can be seen, the output consists of six columns of data. The first column is the region or area name where a blank name is the sum over the entire domain. The second and third columns are the conversion ratio and breeding ratio. The fourth and fifth columns are the fissile atoms formed and destroyed over the time step. The sixth column is the time point. The REBUS output excerpt is provided in Figure 3-130.

|        |             |             |             |             |  |
|--------|-------------|-------------|-------------|-------------|--|
| CENT   | 0.00000E+00 |             | 0.00000E+00 |             |  |
| REFL   | 0.00000E+00 |             | 0.00000E+00 |             |  |
| CORE1  | 7.48154E-02 |             | 0.00000E+00 |             |  |
| CORE2  | 6.96597E-02 |             | 0.00000E+00 |             |  |
| CORE3  | 7.12384E-02 |             | 0.00000E+00 |             |  |
| CORE4  | 6.36154E-02 |             | 0.00000E+00 |             |  |
| CORE5  | 6.52435E-02 |             | 0.00000E+00 |             |  |
| CORE6  | 6.52435E-02 |             | 0.00000E+00 |             |  |
| CORE   | 6.96296E-02 | 6.96296E-02 | 0.00000E+00 |             |  |
| IICORE | 7.25929E-02 | 3.22521E-02 | 0.00000E+00 |             |  |
| IICORE | 7.12384E-02 | 1.51648E-02 | 0.00000E+00 |             |  |
| IIBLK  | 6.36154E-02 | 6.06525E-03 | 0.00000E+00 |             |  |
| IRBLKT | 6.52435E-02 | 8.07377E-03 | 0.00000E+00 |             |  |
| RBLKTO | 6.52435E-02 | 8.07377E-03 | 0.00000E+00 |             |  |
| CNTRL  | 0.00000E+00 | 0.00000E+00 | 0.00000E+00 |             |  |
|        |             | 6.96296E-02 | 0.00000E+00 |             |  |
| CENT   | 0.00000E+00 | 0.00000E+00 | 0.00000E+00 | 1.00000E+02 |  |
| REFL   | 0.00000E+00 | 0.00000E+00 | 0.00000E+00 | 1.00000E+02 |  |
| CORE1  | 7.87985E-02 | 7.15786E-01 | 9.08375E+00 | 1.00000E+02 |  |

Figure 3-129. SUMRY2 Output Excerpt

|        |                  |                      |                                  |                         |     |
|--------|------------------|----------------------|----------------------------------|-------------------------|-----|
| FCC004 | 11.3114          | 04/10/20             | ABURN: Hexagonal 3D Test Problem | PAGE                    | 324 |
|        |                  |                      |                                  |                         |     |
| CENT   | 0.00000E+00      |                      |                                  |                         |     |
| REFL   | 0.00000E+00      |                      |                                  |                         |     |
| CORE1  | 7.48154E-02      |                      |                                  |                         |     |
| CORE2  | 6.96597E-02      |                      |                                  |                         |     |
| CORE3  | 7.12384E-02      |                      |                                  |                         |     |
| CORE4  | 6.36154E-02      |                      |                                  |                         |     |
| CORE5  | 6.52435E-02      |                      |                                  |                         |     |
| CORE6  | 6.52435E-02      |                      |                                  |                         |     |
| TOTAL  | 6.96296E-02      |                      |                                  |                         |     |
|        |                  |                      |                                  |                         |     |
| AREA   | CONVERSION RATIO | BREEDING RATIO       | FISSILE ATOMS FORMED             | FISSILE ATOMS DESTROYED |     |
| CORE   | 6.96296E-02      | 6.96296E-02          | 0.00000E+00                      | 0.00000E+00             |     |
| IICORE | 7.25929E-02      | 3.22521E-02          | 0.00000E+00                      | 0.00000E+00             |     |
| IICORE | 7.12384E-02      | 1.51648E-02          | 0.00000E+00                      | 0.00000E+00             |     |
| IIBLK  | 6.36154E-02      | 6.06525E-03          | 0.00000E+00                      | 0.00000E+00             |     |
| IRBLKT | 6.52435E-02      | 8.07377E-03          | 0.00000E+00                      | 0.00000E+00             |     |
| RBLKTO | 6.52435E-02      | 8.07377E-03          | 0.00000E+00                      | 0.00000E+00             |     |
| CNTRL  | 0.00000E+00      | 0.00000E+00          | 0.00000E+00                      | 0.00000E+00             |     |
|        |                  |                      |                                  |                         |     |
| FCC004 | 11.3114          | 04/10/20             | ABURN: Hexagonal 3D Test Problem | PAGE                    | 396 |
|        |                  |                      |                                  |                         |     |
| REGION | CONVERSION RATIO | FISSILE ATOMS FORMED | FISSILE ATOMS DESTROYED          |                         |     |
| CENT   | 0.00000E+00      | 0.00000E+00          | 0.00000E+00                      |                         |     |
| REFL   | 0.00000E+00      | 0.00000E+00          | 0.00000E+00                      |                         |     |
| CORE1  | 7.87985E-02      | 7.15786E-01          | 9.08375E+00                      |                         |     |
| CORE2  | 7.28067E-02      | 5.01927E-01          | 6.89397E+00                      |                         |     |

Figure 3-130. REBUS Output Excerpt to Verify SUMRY2

Because the conversion ratio and breeding ratio are not part of the verification work, no additional effort is required to check the accuracy of these numbers. Similarly, the fissile atoms formed and destroyed are not part of the verification work. All four of these values are difficult to hand calculate as it requires the ability to separately integrate the production and destruction terms of the depletion equation for each isotope. For future verification, these outputs should be checked using one of the verification test problems with an analytical solution shown earlier in this manuscript. From the displayed results, the SUMRY2 output is consistently defined with respect to the REBUS output and no further effort is made to verify the accuracy of the data itself.

### 3.8.3 SUMRY3 File Verification

From Table 3-82, the SUMRY3 file provides the  $k_{\text{effective}}$  and power history data. An output excerpt from the SUMRY3 is provided in Figure 3-131. The output consists of four columns of data. The first column is the calculated  $k_{\text{effective}}$  from every DIF3D call. For equilibrium problems this includes all steps of the preliminary, intermediate, and final search procedures. The second column is the reactivity while the third column is the power level. The fourth column is the time point. The excerpt of the REBUS output is provided in Figure 3-132 which is significantly truncated to only focus on the  $k_{\text{effective}}$  results. As can be seen, the SUMRY3  $k_{\text{effective}}$  results are identical outputs for the values taken from the REBUS output. The reactivity is a simple conversion of each  $k_{\text{effective}}$  result such as  $1/0.776106-1 = 0.288484$  for the first point. The power level is that given as input and the time step results are the two possible values for the equilibrium problem. It is important to note that the region density iteration causes the EOEC  $k_{\text{effective}}$  result to repeat several times in the output stream.

```
7.76106E-01 -2.88484E-01 1.00000E+07 0.00000E+00
7.81030E-01 -2.80360E-01 1.00000E+07 1.00000E+02
7.85860E-01 -2.72491E-01 1.00000E+07 0.00000E+00
7.89011E-01 -2.67410E-01 1.00000E+07 1.00000E+02
7.89169E-01 -2.67156E-01 1.00000E+07 1.00000E+02
7.86218E-01 -2.71912E-01 1.00000E+07 0.00000E+00
7.89172E-01 -2.67151E-01 1.00000E+07 1.00000E+02
7.86243E-01 -2.71871E-01 1.00000E+07 0.00000E+00
7.86243E-01 -2.71871E-01 1.00000E+07 0.00000E+00
7.89183E-01 -2.67133E-01 1.00000E+07 1.00000E+02
7.89213E-01 -2.67084E-01 1.00000E+07 1.00000E+02
7.89214E-01 -2.67083E-01 1.00000E+07 1.00000E+02
7.86249E-01 -2.71861E-01 1.00000E+07 0.00000E+00
7.86249E-01 -2.71861E-01 1.00000E+07 0.00000E+00
7.89186E-01 -2.67128E-01 1.00000E+07 1.00000E+02
7.89216E-01 -2.67080E-01 1.00000E+07 1.00000E+02
7.89217E-01 -2.67078E-01 1.00000E+07 1.00000E+02
7.86250E-01 -2.71860E-01 1.00000E+07 0.00000E+00
```

Figure 3-131. SUMRY3 Output Excerpt

```
=VARIANT| 17| 0.0|001| 7.761061E-01|1.1E-08| F | 3.00E-08, 3.98E-08| T | 0 | 0.17 | 0.07 | 0.0 | 0.0 | 0.0 |
OUTER ITERATIONS COMPLETED AT ITERATION 17, ITERATIONS HAVE CONVERGED
K-EFFECTIVE = 0.77610613
DIF3D 11.3114 04/10/20 ADIF3D: Hexagonal 3D Test Problem PAGE 96
...
K-EFFECTIVE = 0.78103037
K-EFFECTIVE = 0.78586031
K-EFFECTIVE = 0.78901057
K-EFFECTIVE = 0.78916896
K-EFFECTIVE = 0.78621765
K-EFFECTIVE = 0.78917190
K-EFFECTIVE = 0.78624308
K-EFFECTIVE = 0.78624308
K-EFFECTIVE = 0.78918336
K-EFFECTIVE = 0.78921335
K-EFFECTIVE = 0.78921449
K-EFFECTIVE = 0.78624930
K-EFFECTIVE = 0.78624930
K-EFFECTIVE = 0.78918611
K-EFFECTIVE = 0.78921602
K-EFFECTIVE = 0.78921715
K-EFFECTIVE = 0.78625019
...
```

Figure 3-132. REBUS Output Excerpt to Verify SUMRY3

None of the displayed values in SUMRY3 are derivative values of those produced by DIF3D and thus no verification beyond that shown is required. The SUMRY3 file is a consistent output with respect to the REBUS output.

### 3.8.4 SUMRY4 File Verification

The SUMRY4 file provides the region volume, power, and peak power density at each time point. An output excerpt from the SUMRY4 is provided in Figure 3-133. The output consists of six columns of data. The first column is an index number which is for internal use to ARC and for users can simply be used to identify between regions (1) or areas (0) in their problems. The second column is the region or area name where a blank name indicates the sum over the entire domain. The third, fourth, and fifth columns are the volume, the power (Watts), and power density (W/cc), respectively. The sixth column is the time point index (0.0 or 100 days for this problem).

The excerpt of the REBUS output is provided in Figure 3-134 which is just the power table from the DIF3D section of output in the first time step. It should be clear that none of the values in SUMRY4 are derivative values, but simply duplicates of existing output. In this case, the DIF3D volumes, power, and power density are all seen to identically match the SUMRY4 results and the SUMRY4 file is therefore verified to be accurate.

```

1 CENT      1.03923E+04  9.56589E-04  1.98111E-07  0.00000E+00
1 REFL      1.12237E+06  1.68982E-01  6.37210E-07  0.00000E+00
1 CORE1     3.11769E+04  2.42161E+06  1.05394E+02  0.00000E+00
1 CORE2     3.11769E+04  1.91287E+06  1.00580E+02  0.00000E+00
1 CORE3     3.11769E+04  2.09740E+06  1.03192E+02  0.00000E+00
1 CORE4     3.11769E+04  1.00186E+06  6.54412E+01  0.00000E+00
1 CORE5     3.11769E+04  1.28314E+06  7.82446E+01  0.00000E+00
1 CORE6     3.11769E+04  1.28314E+06  7.82446E+01  0.00000E+00
0          1.31982E+06  1.00000E+07  1.05394E+02  0.00000E+00
0 CORE      1.87061E+05  1.00000E+07  1.05394E+02  0.00000E+00
0 IICORE    6.23538E+04  4.33448E+06  1.05394E+02  0.00000E+00
0 IOCORE    3.11769E+04  2.09740E+06  1.03192E+02  0.00000E+00
0 IIBLKT    3.11769E+04  1.00186E+06  6.54412E+01  0.00000E+00
0 IRLKLT    3.11769E+04  1.28314E+06  7.82446E+01  0.00000E+00
0 RBLKTO    3.11769E+04  1.28314E+06  7.82446E+01  0.00000E+00
0 CNTRL     1.03923E+04  9.56589E-04  1.98111E-07  0.00000E+00
1 CENT      1.03923E+04  1.01453E-03  2.10127E-07  1.00000E+02
1 REFL      1.12237E+06  1.79444E-01  6.76123E-07  1.00000E+02
1 CORE1     3.11769E+04  2.36518E+06  1.02953E+02  1.00000E+02
1 CORE2     3.11769E+04  1.90754E+06  1.00325E+02  1.00000E+02
1 CORE3     3.11769E+04  2.07636E+06  1.02181E+02  1.00000E+02
1 CORE4     3.11769E+04  1.03211E+06  6.74332E+01  1.00000E+02
1 CORE5     3.11769E+04  1.30941E+06  7.98671E+01  1.00000E+02
1 CORE6     3.11769E+04  1.30941E+06  7.98671E+01  1.00000E+02
0          1.31982E+06  1.00000E+07  1.02953E+02  1.00000E+02
0 CORE      1.87061E+05  1.00000E+07  1.02953E+02  1.00000E+02
0 IICORE    6.23538E+04  4.27271E+06  1.02953E+02  1.00000E+02
0 IOCORE    3.11769E+04  2.07636E+06  1.02181E+02  1.00000E+02
0 IIBLKT    3.11769E+04  1.03211E+06  6.74332E+01  1.00000E+02
0 IRLKLT    3.11769E+04  1.30941E+06  7.98671E+01  1.00000E+02
0 RBLKTO    3.11769E+04  1.30941E+06  7.98671E+01  1.00000E+02
0 CNTRL     1.03923E+04  1.01453E-03  2.10127E-07  1.00000E+02

```

Figure 3-133. SUMRY4 Output Excerpt

```

DIF3D 11.3114 04/10/20      ADIF3D: Hexagonal 3D Test Problem      PAGE      313
0      REGION AND AREA POWER INTEGRALS FOR K-EFF PROBLEM WITH ENERGY RANGE (EV)      =(4.140E-01,1.000E+07)
      NO. NAME      NO. NAME      VOLUME      INTEGRATION(1)      POWER      POWER DENSITY      PEAK TO AVG.      POWER
      NO. NAME      NO. NAME      (CC)      WEIGHT FACTOR      (WATTS)      (WATTS/CC)      (WATTS/CC)(2)      POWER DENSITY      FRACTION
1 CENT      1 CENT      1.03923E+04  1.00000E+00  9.56589E-04  9.20478E-08  1.98111E-07  2.15226E+00  9.56589E-11
2 REFL      2 REFL      1.12237E+06  1.00000E+00  1.68982E-01  1.50559E-07  6.37210E-07  4.23231E+00  1.68982E-08
3 CORE1     3 CORE1     3.11769E+04  1.00000E+00  2.42161E+06  7.76731E+01  1.05394E+02  1.35689E+00  2.42161E-01
4 CORE2     4 CORE2     3.11769E+04  1.00000E+00  1.91287E+06  6.13553E+01  1.00580E+02  1.63930E+00  1.91287E-01
5 CORE3     5 CORE3     3.11769E+04  1.00000E+00  2.09740E+06  6.72741E+01  1.03192E+02  1.53391E+00  2.09740E-01
6 CORE4     6 CORE4     3.11769E+04  1.00000E+00  1.00186E+06  3.21346E+01  6.54412E+01  2.03647E+00  1.00186E-01
7 CORE5     7 CORE5     3.11769E+04  1.00000E+00  1.28314E+06  4.11566E+01  7.82446E+01  1.90114E+00  1.28314E-01
8 CORE6     8 CORE6     3.11769E+04  1.00000E+00  1.28314E+06  4.11566E+01  7.82446E+01  1.90114E+00  1.28314E-01
TOTALS     TOTALS     1.31982E+06  0.00000E+00  1.00000E+07  7.57678E+00  1.05394E+02  1.39101E+01  1.00000E+00

```

Figure 3-134. REBUS Output Excerpt to Verify SUMRY4

### 3.8.5 SUMRY5 File Verification

The SUMRY5 file provides the region volume, peak flux, and peak fast flux at each time point. An output excerpt from the SUMRY5 file is provided in Figure 3-135. The output consists of six columns of data. The first column is an index number which is for internal use to ARC and for users can simply be used to identify between regions (1) or areas (0) in their problems. The second column is the region or area name where a blank name indicates the sum over the entire domain. The third, fourth, and fifth columns are the volume, the peak total flux (n\*cm/sec), and peak fast flux (n/cm<sup>2</sup>/sec), respectively. The sixth column is the time point index (0.0 or 100 days for this problem).

The excerpt of the REBUS output is provided in Figure 3-136 which is just the flux table from the DIF3D section of output in the first time step. It should be clear that none of the values in SUMRY5 are derivative values, but simply duplicates of existing output. In this case, the DIF3D results are all seen to identically match the SUMRY5 results and the SUMRY5 file is therefore verified to be accurate.

```

1 CENT      1.03923E+04  7.02238E+15  5.20209E+15  0.00000E+00
1 REFL      1.12237E+06  2.10491E+15  1.49930E+15  0.00000E+00
1 CORE1     3.11769E+04  7.17228E+15  5.38152E+15  0.00000E+00
1 CORE2     3.11769E+04  6.53726E+15  4.94218E+15  0.00000E+00
1 CORE3     3.11769E+04  6.82003E+15  5.15173E+15  0.00000E+00
1 CORE4     3.11769E+04  3.93066E+15  2.95590E+15  0.00000E+00
1 CORE5     3.11769E+04  4.81259E+15  3.63010E+15  0.00000E+00
1 CORE6     3.11769E+04  4.81259E+15  3.63010E+15  0.00000E+00
0          1.31982E+06  7.17228E+15  5.38152E+15  0.00000E+00
0 CORE      1.87061E+05  7.17228E+15  5.38152E+15  0.00000E+00
0 IICORE    6.23538E+04  7.17228E+15  5.38152E+15  0.00000E+00
0 IOCORE    3.11769E+04  6.82003E+15  5.15173E+15  0.00000E+00
0 IIBLKT    3.11769E+04  3.93066E+15  2.95590E+15  0.00000E+00
0 IRBLKT    3.11769E+04  4.81259E+15  3.63010E+15  0.00000E+00
0 RBLKTO    3.11769E+04  4.81259E+15  3.63010E+15  0.00000E+00
0 CNTRL    1.03923E+04  7.02238E+15  5.20209E+15  0.00000E+00
1 CENT      1.03923E+04  7.46907E+15  5.54679E+15  1.00000E+02
1 REFL      1.12237E+06  2.23658E+15  1.59674E+15  1.00000E+02
1 CORE1     3.11769E+04  7.62921E+15  5.73857E+15  1.00000E+02
1 CORE2     3.11769E+04  6.95352E+15  5.26884E+15  1.00000E+02
1 CORE3     3.11769E+04  7.25454E+15  5.49284E+15  1.00000E+02
1 CORE4     3.11769E+04  4.17913E+15  3.14822E+15  1.00000E+02
1 CORE5     3.11769E+04  5.11766E+15  3.86764E+15  1.00000E+02
1 CORE6     3.11769E+04  5.11766E+15  3.86764E+15  1.00000E+02
0          1.31982E+06  7.62921E+15  5.73857E+15  1.00000E+02
0 CORE      1.87061E+05  7.62921E+15  5.73857E+15  1.00000E+02
0 IICORE    6.23538E+04  7.62921E+15  5.73857E+15  1.00000E+02
0 IOCORE    3.11769E+04  7.25454E+15  5.49284E+15  1.00000E+02
0 IIBLKT    3.11769E+04  4.17913E+15  3.14822E+15  1.00000E+02
0 IRBLKT    3.11769E+04  5.11766E+15  3.86764E+15  1.00000E+02
0 RBLKTO    3.11769E+04  5.11766E+15  3.86764E+15  1.00000E+02
0 CNTRL    1.03923E+04  7.46907E+15  5.54679E+15  1.00000E+02

```

Figure 3-135. SUMRY5 Output Excerpt

```

DIF3D 11.3114 04/10/20      ADIF3D: Hexagonal 3D Test Problem      PAGE      316
0      REGION AND AREA REAL FLUX INTEGRALS FOR K-EFF PROBLEM WITH ENERGY RANGE (EV)      = (4.140E-01, 1.000E+07)
      NO. NAME      NO. NAME      VOLUME      TOTAL FLUX      PEAK FLUX (1)      TOTAL FAST FLUX      PEAK FAST FLUX (1)
      REGION  ZONE  ZONE      (CC)      (NEUTRON-CM/SEC)      (NEUTRON/CM2-SEC)      (NEUTRON-CM/SEC)      (NEUTRON/CM2-SEC)
1 CENT      1 CENT      1.03923E+04  3.32862E+19  7.02238E+15  2.42256E+19  5.20209E+15
2 REFL      2 REFL      1.12237E+06  5.42104E+20  2.10491E+15  3.69769E+20  1.49930E+15
3 CORE1     3 CORE1     3.11769E+04  1.64721E+20  7.17228E+15  1.23415E+20  5.38152E+15
4 CORE2     4 CORE2     3.11769E+04  1.24155E+20  6.53726E+15  9.33538E+19  4.94218E+15
5 CORE3     5 CORE3     3.11769E+04  1.38482E+20  6.82003E+15  1.04221E+20  5.15173E+15
6 CORE4     6 CORE4     3.11769E+04  5.98154E+19  3.93066E+15  4.38648E+19  2.95590E+15
7 CORE5     7 CORE5     3.11769E+04  7.85907E+19  4.81259E+15  5.82819E+19  3.63010E+15
8 CORE6     8 CORE6     3.11769E+04  7.85907E+19  4.81259E+15  5.82819E+19  3.63010E+15
TOTALS          1.31982E+06  1.21974E+21  7.17228E+15  8.75414E+20  5.38152E+15

```

Figure 3-136. REBUS Output Excerpt to Verify SUMRY5

### 3.8.6 SUMRY6 File Verification

The SUMRY6 file provides the burnup in atom % and MWD/MT at each time point. An output excerpt from the SUMRY6 file is provided in Figure 3-137. The output consists of four columns of data. The first column is the PATH name from the user input. The second column is the burnup in atom % while

the third column is the burnup in MWD/MT. The fourth column is the time point index which does not include the first time point in an equilibrium or non-equilibrium problem but is included for all follow-on time points.

The excerpt of the REBUS output is provided in Figure 3-138 which is just the burnup table from the REBUS output in the first time step. It should be clear that none of the values in SUMRY6 are derivative values, but simply duplicates of existing output. In this case, the SUMRY6 results are all seen to identically match the REBUS output results and the SUMRY6 file is therefore verified to be accurate.

```

CORE1      1.02515E+00  9.68035E+03  1.00000E+02
CORE1      1.03682E+00  9.79055E+03  1.00000E+02
CORE1      1.04586E+00  9.87592E+03  1.00000E+02
CORE1      1.05258E+00  9.93932E+03  1.00000E+02
CORE1      1.05723E+00  9.98331E+03  1.00000E+02
CORE1      1.06008E+00  1.00101E+04  1.00000E+02
CORE2      7.72580E-01  7.29536E+03  1.00000E+02
CORE2      7.79399E-01  7.35975E+03  1.00000E+02
CORE2      7.85059E-01  7.41320E+03  1.00000E+02
...
CORE5      4.99689E-01  4.71850E+03  1.00000E+02
CORE6      4.86659E-01  4.59545E+03  1.00000E+02
CORE6      4.89887E-01  4.62593E+03  1.00000E+02
CORE6      4.92786E-01  4.65330E+03  1.00000E+02
CORE6      4.95374E-01  4.67775E+03  1.00000E+02
CORE6      4.97670E-01  4.69942E+03  1.00000E+02
CORE6      4.99689E-01  4.71850E+03  1.00000E+02

```

**Figure 3-137. SUMRY6 Output Excerpt**

```

FCC004 11.3114 04/10/20          ABURN: Hexagonal 3D Test Problem          PAGE 404
                                         AVERAGE BURNUP OVER THE PRECEDING 1.00000000E+02 DAY SUBINTERVAL
                                         NOTE - ALL ISOTOPES UNDERGOING FISSION ARE INCLUDED IN THE CALCULATION OF THE FOLLOWING BURNUP FIGURES.

                                         AVERAGE BURNUP (ATOM %) OF EACH STAGE OF EACH PATH
STAGE/REGION 1/CORE1      2/CORE1      3/CORE1      4/CORE1      5/CORE1      6/CORE1
1.02515E+00  1.03682E+00  1.04586E+00  1.05258E+00  1.05723E+00  1.06008E+00
STAGE/REGION 1/CORE2      2/CORE2      3/CORE2      4/CORE2      5/CORE2      6/CORE2
7.72580E-01  7.79399E-01  7.85059E-01  7.89664E-01  7.93305E-01  7.96070E-01
STAGE/REGION 1/CORE3      2/CORE3      3/CORE3      4/CORE3      5/CORE3      6/CORE3
8.62399E-01  8.70647E-01  8.77320E-01  8.82572E-01  8.86543E-01  8.89358E-01
STAGE/REGION 1/CORE4      2/CORE4      3/CORE4      4/CORE4      5/CORE4      6/CORE4
3.68664E-01  3.70735E-01  3.72651E-01  3.74418E-01  3.76043E-01  3.77531E-01
STAGE/REGION 1/CORE5      2/CORE5      3/CORE5      4/CORE5      5/CORE5      6/CORE5
4.86659E-01  4.89887E-01  4.92786E-01  4.95374E-01  4.97670E-01  4.99689E-01
STAGE/REGION 1/CORE6      2/CORE6      3/CORE6      4/CORE6      5/CORE6      6/CORE6
4.86659E-01  4.89887E-01  4.92786E-01  4.95374E-01  4.97670E-01  4.99689E-01
...
                                         AVERAGE BURNUP (MWD/MT) OF EACH STAGE OF EACH PATH
STAGE/REGION 1/CORE1      2/CORE1      3/CORE1      4/CORE1      5/CORE1      6/CORE1
9.68035E+03  9.79055E+03  9.87592E+03  9.93932E+03  9.98331E+03  1.00101E+04
STAGE/REGION 1/CORE2      2/CORE2      3/CORE2      4/CORE2      5/CORE2      6/CORE2
7.29536E+03  7.35975E+03  7.41320E+03  7.45668E+03  7.49107E+03  7.51718E+03
...

```

**Figure 3-138. REBUS Output Excerpt to Verify SUMRY6**

### 3.8.7 SUMRY7 File Verification

The SUMRY7 file provides the region volume, average total flux, and average total fast flux at each time point. An output excerpt from the SUMRY7 file is provided in Figure 3-139. The output consists of six columns of data and is very similar to the SUMRY5 file earlier. The difference from SUMRY5 is that the fourth column here is the average total flux ( $n/cm^2/sec$ ) and the fifth column is the average total fast flux ( $n/cm^2/sec$ ).

```

1 CENT      1.03923E+04  3.20297E+15  2.33111E+15  0.00000E+00
1 REFL      1.12237E+06  4.83000E+14  3.29454E+14  0.00000E+00
1 CORE1     3.11769E+04  5.28341E+15  3.95854E+15  0.00000E+00
...
1 CORE5     3.11769E+04  2.52080E+15  1.86939E+15  0.00000E+00
1 CORE6     3.11769E+04  2.52080E+15  1.86939E+15  0.00000E+00
0          1.31982E+06  9.24173E+14  6.63281E+14  0.00000E+00
0 CORE      1.87061E+05  3.44461E+15  2.57359E+15  0.00000E+00
0 IICORE    6.23538E+04  4.63284E+15  3.47643E+15  0.00000E+00
...
0 CNTRL     1.03923E+04  3.20297E+15  2.33111E+15  0.00000E+00
1 CENT      1.03923E+04  3.40595E+15  2.48487E+15  1.00000E+02
1 REFL      1.12237E+06  5.13328E+14  3.50660E+14  1.00000E+02
1 CORE1     3.11769E+04  5.61912E+15  4.22036E+15  1.00000E+02
...

```

**Figure 3-139. SUMRY7 Output Excerpt**

The REBUS excerpt from SUMRY5 in Figure 3-136 is sufficient to verify the output. For the first time point of region CENT, the average total  $3.20297E+15$  is the total flux from Figure 3-136 of  $3.32862E+19$  divided by the region volume of  $1.03923E+04$ . Similarly, the average total fast flux of  $2.33111E+15$  is the total fast flux from Figure 3-136 of  $2.42256E+19$  divided by the region volume  $1.03923E+04$ . Since these values are simply modifications of the existing DIF3D outputs available in the REBUS output, no additional work is required for verification.

### 3.8.8 SUMRY8 File Verification

The SUMRY8 file provides the isotopic stage densities and only presently works for equilibrium problems. An output excerpt from the SUMRY8 file is provided in Figure 3-140. The output does not have a consistent column structure but it organized by cards. The first card lists the number of materials (6 for CORE1, CORE2, CORE3, CORE4, CORE5, CORE6), the number of active isotopes (8) and then the number of stages for each material (6 in this equilibrium problem). The second card output is the active isotope labels in the depletion chain. The third card output is the stage atom densities for the active isotopes ordered by isotope, then stage, then material. No additional REBUS output excerpt is needed as this output is fundamentally similar to SUMRY1 and thus Figure 3-128 can be used.

```

6      8      6      6      6      6      6      6
U235   U238   PU239   PU240   PU241   PU242   LFPPS   DUMP
9.19518E-04 1.97169E-02 6.63718E-04 3.94091E-04 2.71828E-04 1.04140E-04
2.28609E-04 1.18042E-06
8.44975E-04 1.94394E-02 8.07719E-04 3.91242E-04 2.46865E-04 1.07641E-04
4.59744E-04 2.40414E-06
7.76476E-04 1.91658E-02 9.34363E-04 3.91203E-04 2.24949E-04 1.10641E-04
6.92895E-04 3.66535E-06
7.13529E-04 1.88961E-02 1.04543E-03 3.93523E-04 2.05760E-04 1.13202E-04
9.27542E-04 4.95863E-06
6.55685E-04 1.86301E-02 1.14251E-03 3.97803E-04 1.89008E-04 1.15381E-04
1.16323E-03 6.27923E-06
6.02530E-04 1.83679E-02 1.22705E-03 4.03694E-04 1.74432E-04 1.17228E-04
1.39955E-03 7.62305E-06
9.38920E-04 1.97864E-02 6.24558E-04 3.95220E-04 2.78530E-04 1.03171E-04
1.72285E-04 8.80375E-07
...

```

**Figure 3-140. SUMRY8 Output Excerpt**

The REBUS excerpt indicates that the output provided in SUMRY8 is only for the EOEC and does not include the BOEC result. Therefore, inspection of the stage 2 output from Figure 3-128 shows an identical match, line by line for the first five output lines in Figure 3-140. The remaining data for the other regions can also be identified easily in the SUMRY8 file. Since this data is not a derivative manipulation of the regular REBUS output, no additional verification is needed and the SUMRY8 is complete.

### 3.8.9 SUMRY9 File Verification

The SUMRY9 file provides the stage burnup in MWD/MT for each material and only presently works for equilibrium problems. An output excerpt from the SUMRY9 file is provided in Figure 3-141. The output has a consistent column structure but it organized by cards. The first card lists the number of materials (6 for CORE1, CORE2, CORE3, CORE4, CORE5, CORE6) followed by the number of stages for each material (6 in this equilibrium problem). The next line of output is the stage burnup values for the first material. The remaining lines go through the other 5 materials. It should be very clear that the burnup values are not meaningful. As an example, for the first stage of the first material has a burnup of 80442 MWD/MT while the second stage has a burnup of 2.8E23 MWD/MT and the third is 9.76E-08 MWD/MT.

| 6           | 6           | 6           | 6           | 6           | 6           | 6 | 6 |
|-------------|-------------|-------------|-------------|-------------|-------------|---|---|
| 8.04416E+04 | 2.88233E+23 | 9.76231E-08 | 4.19992E+01 | 6.65994E+01 | 3.81959-313 |   |   |
| 7.30128E+04 | 2.64670E+23 | 1.59880E-07 | 4.19992E+01 | 3.31050E+01 | 3.81959-313 |   |   |
| 7.63251E+04 | 2.75907E+23 | 7.58630E+01 | 9.76231E-08 | 4.19992E+01 | 0.00000E+00 |   |   |
| 4.30814E+04 | 1.58219E+23 | 6.11843E+01 | 1.59880E-07 | 4.19992E+01 | 1.27320-313 |   |   |
| 5.31826E+04 | 1.94341E+23 | 6.65994E+01 | 7.58630E+01 | 1.10768-311 | 1.27320-313 |   |   |
| 5.31826E+04 | 1.94341E+23 | 3.31050E+01 | 6.11843E+01 | 3.81959-313 | 1.27320-313 |   |   |

**Figure 3-141. SUMRY9 Output Excerpt**

This indicates a bug in the REBUS software which was confirmed and not updated as no user could justify making use of the SUMRY9 file instead of the regular REBUS output. The actual data being printed by REBUS is a mixture of stored quantities such as the material peak burnup, the peak discharge fast fluence, the region power density (not aligned by material), and the labels of the regions printed as real values. The ordering of the data is not consistent as the number of materials and regions changes and thus no attempt should be made to use the SUMRY9 file.

## 4 Summary of the Preceding Verification Work

The preceding work verified all categories of Table 2-1 and all SUMRY files produced by REBUS. The set of test problems is summarized in Table 4-1 along with cross referencing for the section of this report it is discussed in and the category that it satisfies. In the REBUS distribution, there are 86 benchmarks and, as can be seen, only some apply to the work detailed in this report (27 through 86). Some of the test work detailed in this report for the SFEDIT file is not dependent upon REBUS and thus those tests can be found with the DIF3D distribution (includes the EvaluateFlux utility). The preceding verification work checked the accuracy of the Bateman equation solver in REBUS for which it was demonstrated that the underlying methodology was accurate. Numerous analytic solutions were created for a variety of complicated depletion chains and REBUS was used successfully to match the analytic solutions. Because powered transmutation problems are very difficult to define due to the coupled nature of the neutron transport equation and the Bateman equations, only a simple coupled analytic solution was displayed which REBUS solved correctly. It is noted that the DIF3D verification report ensures the accuracy of the DIF3D solution [14].

In addition to the analytic verification test problems, each aspect of the REBUS input methodology was checked. As an example, REBUS allows for equilibrium and non-equilibrium fuel cycle analysis with fuel fabrication. The input for the equilibrium analysis capability was displayed and verified in this work to be accurate and consistent with the expected behavior. The fuel fabrication aspects using external feeds was also displayed and verified to be accurate. Fuel shuffling and the non-equilibrium fuel cycle modeling aspects was displayed and verified to be accurate. Control rod movements were verified to be working along with burnup constraints on the cycle length and the enrichment search features. A calculation was also done to verify that the equilibrium state of the reactor is consistent with the non-equilibrium approach.

**Table 4-1. Verification Test Problems and Cross Referencing to Category and Section.**

| Index ID  | Verification Section | Verification Category   |
|---|----------------------|-------------------------|
| 27, 28, 29, 30                                    | 3.1                  | 1. a) b) c) d)          |
| 31  | 3.2 & 3.3            | 1. a) b) c) d) e)       |
| 32, 33, 34  | 0                    | 2. a) b) f) g)          |
| 35, 36  | 3.4.2                | 2. a) b) c) d) e) f) g) |
| 37, 38, 39, 40, 41, 42                            | 3.4.3 & 3.5.1        | 2. a) b) c) d) e) f) g) |
| 43, 44  | 3.4.4                | 2. a) b) c) d) e) f) g) |
| 45, 46  | 3.4.5                | 2. a) b) c) d) e) f) g) |
| 47, 48, 49  | 3.5.2.1              | 3. a)                   |
| 50, 51, 52, 53                                    | 3.5.2.2              | 3. a)                   |
| 54, 55, 56, 57, 58, 59, 60, 61                    | 3.5.2.3              | 3. a)                   |
| 62, 63, 64, 65, 66, 67, 68, 69, 70, 71            | 3.5.2.4              | 3. a) b)                |
| 72, 73, 74, 75, 76                                | 3.5.2.5              | 3. a) c)                |
| 77, 78, 79, 80, 81                                | 3.6.1.1 & 3.6.1.2    | 4. a) b) c)             |
| DIF3D: 51, 52, 53, 54, 55, 56<br>EvaluateFlux: 13 | 3.7.1                | 5. a)                   |
| 82, 83  | 3.7.1                | 5. a)                   |
| 84, 85, 86  | 3.8                  | SUMRY files             |

The SFEDIT output from DIF3D is used by REBUS to compute region-wise peaking factors for burnup and fast fluence. This manuscript displayed the SFEDIT file and verified it to be consistent with expectations. It is noted that the DIF3D-Nodal peaking methodology applied to the DIF3D-VARIANT solution scheme does not produce the true maximum as the corner points of the hexagon are not calculable with the DIF3D-Nodal scheme. The mass and power edits produced by REBUS were verified along with the peak burnup and peak fast fluence.

In the REBUS requirements report [11] there were numerous tables of output produced by REBUS that needed to be verified. The preceding work displays all of those tables and discusses how they are calculated. In almost all of the verification work, a hand calculation of an output from REBUS was displayed and an EXCEL based computation of the tabulated data is provided. For the analytic solutions, the MathCAD documents that were used to evaluate the solution were provided.

The only exceptions in accuracy can be identified as 1) the burnup values reported in MWD/MT, 2) the peaking factors for DIF3D-VARIANT, and 3) the SUMRY9 file. The stated burnup values are calculated in REBUS using a power conversion factor rather than the stated methodology in the literature. While this power conversion factor can be accurate, it is not guaranteed to be consistent with the conventional definition. The REBUS reported burnup in atom % is correct and there is sufficient information in the REBUS output to manually calculate the burnup in MWD/MT using the correct formula in the literature as desired by the user. The peaking factors are a minor issue for DIF3D and a provided utility program can be used, as needed, to verify and correct the accuracy of the peaking values reported by REBUS. Finally, the SUMRY9 file is not working properly and should not be used.

## References

1. R. P. Hosteny, "The ARC System Fuel Cycle Analysis Capability, REBUS-2," ANL-7721, Argonne National Laboratory (1978).
2. B. J. Toppel, "A User's Guide to the REBUS-3 Fuel Cycle Analysis Capability," ANL-83-2, Argonne National Laboratory (1983).
3. W. S. Yang, M. A. Smith, "Theory Manual for the Fuel Cycle Analysis Code REBUS," ANL/NE-19/21, Argonne National Laboratory (2020).
4. R. D. Lawrence, "Progress in Nodal Methods for the Solution of the Neutron Diffusion and Transport Equations," *Prog. Nucl. Energy*, 17, 271 (1986).
5. M. R. Wagner, "Three-Dimensional Nodal Diffusion and Transport Theory for Hexagonal-z Geometry," *Nucl. Sci. Eng.*, 103, 377-391 (1989).
6. K. L. Derstine, "DIF3D: A Code to Solve One-, Two-, and Three-Dimensional Finite-Difference Diffusion Theory Problems," ANL-82-64, Argonne National Laboratory (1984).
7. R. D. Lawrence, "The DIF3D Nodal Neutronics Option for Two- and Three-Dimensional Diffusion Theory Calculations in Hexagonal Geometry," ANL-83-1, Argonne National Laboratory, (1983).
8. Palmiotti, G., Lewis, E. E., Carrico, C. B., "VARIANT: VARIational Anisotropic Nodal Transport for Multidimensional Cartesian and Hexagonal Geometry Calculation," Argonne National Laboratory ANL-95/40 (1995).
9. M. A. Smith, E. E. Lewis, E. R. Shemon, "DIF3D-VARIANT 11.0, A Decade of Updates," ANL/NE-14/1 (2014).
10. L. C. Just, H. Henryson II, A. S. Kennedy, S. D. Sparck, B. J. Toppel and P. M. Walker, "The System Aspects and Interface Data Sets of the Argonne Reactor Computation (ARC) System," ANL-7711, Argonne National Laboratory (1971).
11. M. A. Smith and A. G. Nelson, "Requirements Description of the REBUS Software for the Versatile Test Reactor," ANL-VTR-50 (2020).
12. M. A. Smith, C. Adams, W. S. Yang, and E. E. Lewis, "VARI3D & PERSENT: Perturbation and Sensitivity Analysis," ANL/NE-13/8 Rev. 3 (2020).
13. M. A. Smith, C. H. Lee, and R. N. Hill, "GAMSOR: Gamma Source Preparation and DIF3D Flux Solution," ANL/NE-16/50 Rev. 1 (2017).
14. A. G. Nelson and M. A. Smith, "Verification of the DIF3D Software to Support Fast Reactor Analysis," ANL/NSE-20/3 (2020).
15. F. Heidet and T. Fei, "Updated Reference VTR Core for CD-1," ECAR 4647, (2019).
16. PTC Corporation, accessed 08/2020, <https://www.mathcad.com>
17. Microsoft Corporation, accessed 08/2020 <https://www.microsoft.com>



## **Nuclear Engineering Division**

Argonne National Laboratory  
9700 South Cass Avenue, Bldg. 208  
Argonne, IL 60439

[www.anl.gov](http://www.anl.gov)



Argonne National Laboratory is a U.S. Department of Energy  
laboratory managed by UChicago Argonne, LLC